Aircraft Loading and Structural Layout

Denis Howe

PROFESSIONAL ENGINEERING PUBLISHING

Aircraft Loading and Structural Layout

Denis Howe
PhD (Cranfield), SM (MIT), FRAeS, FIMechE
Professor Emeritus and formerly Head of the College of Aeronautics, and Dean of Engineering, Cranfield University, UK

Professional Engineering Publishing Limited,
London and Bury St Edmunds, UK

Acknowledgements

The contributions of many past students and former colleagues at Cranfield University are gratefully acknowledged. Particular mention must be made of Professor J J Spillman, Dr F M Burrows and the late Mr K H Griffin for some of the material in Chapters 9, 15. and 16.

This edition published 2004 hy Professional Engineering Publishing, UK.
Published in USA by American Institute of Aeronautics and Astronautics. Inc

ISBN 1 86058 432 2
ISSN 1743-386X

A CIP catalogue record for this book is available from the British Library.

Dedication

This volume is dedicated to the memory and achievements of Wilber and Orville Wright on the centenary of the first sustained, controlled flight at Kitty Hawk on December 17th, 1903.

A cord of three strands is not quickly broken....

Ecclesiastes, Chapter 4, *verse 12*

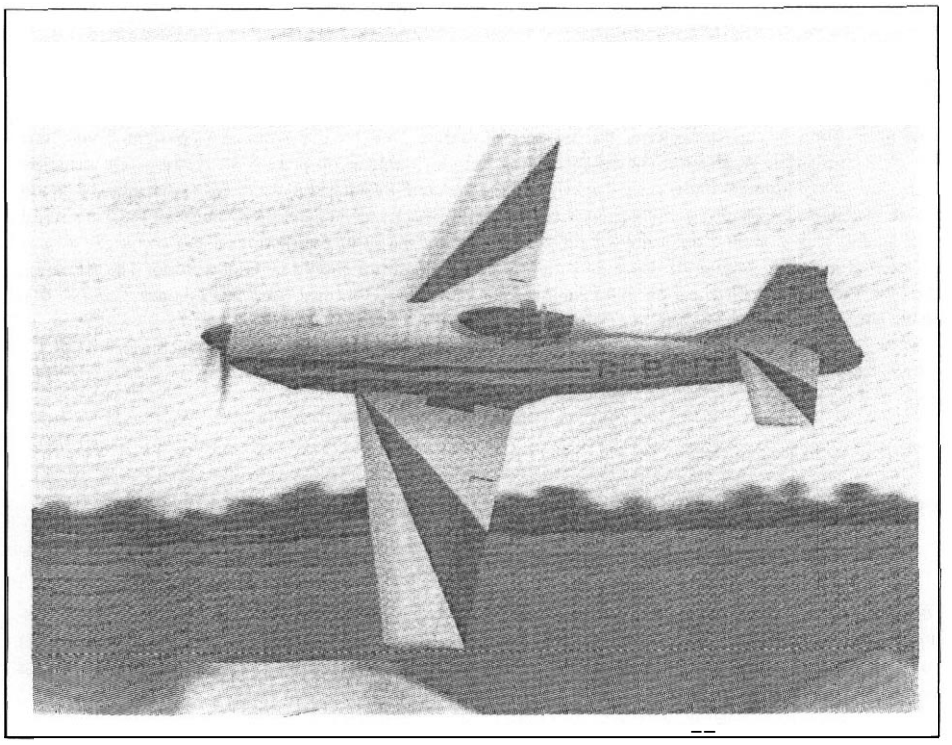

Cranfield A1 Aerobatic Aircraft, see Addendum AD1

Series Advisors' Foreword

The field of aerospace is wide ranging and covers a variety of disciplines and domains, not merely engineering but many related supporting activities. all combining to produce exciting and technologically challenging products.

The Aerospace Series aims to be a practical and topical series of books aimed at engineering professionals. operators and users in the aerospace industry. The range of topics is intended to be wide ranging covering design and development, manufacture. operation and support of aircraft as well as topics such as infrastructure operations. and developments in research and technology. The intention is to provide a source of relevant information that will be of interest and benefit to all those people working in aerospace

Aircraft Loading and ***Structural*** *Layout* is an invaluable source of information for students and practitioners in the field of aircraft structural loading. Based on many years of practical teaching by a distinguished professor, the text covers both ground and airborne loading cases. Commercial and military aircraft types are presented with their widely differing operating requirements. As well as providing a source book for undergraduate and postgraduate students, this book is also a reference book for practising engineers. The text is straightforward and comprehensive and practical examples are given. This volume nicely complements the other book in this series.

Ian Moir
Allan ***Seabridge***

Contents

Contents

Preface

All engineering design is an iterative process although for the purposes of discussion and analysis it is helpful to consider it as a series of discrete phases, each to be repeated sequentially as the concept is developed. Aircraft design is no exception to this generalization and the processes involved are outlined in the previous work by the author ***Aircraft Conceptual Design Synthesis.*** That text was primarily concerned with the initial phase of thedesign of fixed-wing aircraft, namely the interpretation of a written requirement or specification into a reasonably well-defined concept described in some detail. In order that this initial concept may provide a valid basis for further analysis it is necessary to give a qualitative consideration to the major features of the structure of the airframe.

The initial concept phase, as outlined in ***Aircraft Conceptual Design Synthesis,*** involves the making of many assumptions and once the outline of the aircraft has been established it is necessary to analyse it, especially from the point of view of aerodynamic and mass characteristics. A likely consequence of this analysis is the need to revise the concept in various ways since almost inevitably certain of the initial assumptions will be found to be inadequate, at least to some degree.

Once the external shape of the aircraft has been established with a sufficientdegree of confidence it is necessary to consider the design of the airframe quantitatively. This is also a synthesis process but before it can be undertaken the applied loading conditions must be established, whether they be a consequence of operations in Right and on the ground or of atmospheric turbulence. Essentially the loading actions analysis consists of the interpretation of established codes of requirements in the context of a particular design of aircraft. In flight an aircraft possesses six degrees of freedom of motion and thus the determination of the applied loads is more complex than that of a fixed structure and, indeed, some other forms of transport. Some texts on aircraft structures make passing reference to this aspect of aircraft design but few consider it in detail. When they do it is usually in the context of a statement of the requirements of the codes rather than covering the processes involved in their interpretation and analysis. This present text seeks to remedy this situation. In passing it should be pointed out that loading actions analysis is also an iterative process since the application of loads to the airframe causes a distortion of the structure which may well result in a change in the loading. In the present text the analysis is mainly based on the initial assumption that the airframe is

rigid but, where relevant, the impact of the likely effect of structural distortion is commented upon. The material presented covers the historical basis of the various design codes, their current provisions, and their interpretation in the context of the motion of the aircraft both in the air and on the ground. Relevant examples are given including the overall load and moment balancing which yields the stressing data.

Once the initial set of loads has been derived it is possible to proceed to the preliminary design of the airframe itself. There are two aspects of this. Firstly there is the need to determine the type of structure, the material of construction, and the location of the main structural memhers. As mentioned above some consideration should already have been given to these issues in the conceptual design phase. This aspect is largely a matter of experience and it is not unusual to compare a number of combinations of material and structural form. Secondly, having established the location of the primary members and the material. it is necessary to estimate the sizes needed to react the applied loading. There are numerous texts dealing with the analysis of aircraft structures but for the most pan they are based on the assumption that the component sizes have already been determined. In the present text this is not assumed to be the case and elementary structural theory is used in conjunction with simple 'rules of thumb' in order to invert the problem and enable a first estimate of the required sizes of the main structural members to be derived. However, since structural design and analysis is complex and dependent upon relatively small details of the configuration, such a procedure may, in some circumstances, be erroneous. This danger is recognized and covered by the inclusion of a chapter outlining the main areas where the simple approach is likely to be inadequate and providing suggestions for dealing with them.

Of course there are available so-called 'expert' programs capable of handling all aspects of the conceptual design phase in a seamless process. While these programs are extremely valuable they are dependent upon the data built into them and in some circumstances may he slow to converge to an acceptable solution. Further, it may be difficult to interpret the results without a good understanding of the detail of the program itself. It is the belief of the author that a preliminary structural design of the kind outlined in this text is always of considerable bcncfit in facilitating an understanding of the way in which the structure reacts the applied loading; it will provide an initial design of the airframe which should be reasonably close to the final solution and a datum against which to compare the output of a more advanced analysis. Having said this it is also essential to point out that, whatever initial method is used to determine the details of the airframe, it is necessary subsequently to undertake a detailed stress analysis using advanced techniques such as finite element/difference methods. This is beyond the aim and scope of the present volume but is adequately covered elsewhere.

As with *Aircraft* ***Conceptual Design*** Synthesis the present text is primarily intended for the use of graduate and post-graduate students and has been written as a consequence of the experiences of the author in teaching loading actions analysis and structural layout over a period of nearly half a century. Nevertheless, it is considered that it will provide a convenient reference for practicing aeronautical engineers and a means of undertaking simple, quick, checks on the outputs from advanced expert, and structural and analysis programs.

Notation

The notation is presented in alphabetical order with the following brackets containing the section number where the symbol is first used and defined. The letters a, b, c... and A, B, C... are used throughout the text as an algebraic shorthand for coefficients in equations and are defined locally as relevant.

a	Speed of sound in air (1.5.2)
a	Dimension used to define position of aerodynamic centre on the chord (9.4.2)
a	Length of short side of a structural panel (15.4.2)
a_1	Lift curve slope due lo incidence (3.2)
a_2	Lift curve slope due to control or Rap deflection (4.2.2)
$\bar{a}$	Average value of lift curve slope due to incidence (9.3.1)
$\tilde{a}$	Kussner attenuation factor (6.4.4)
A	Aspect ratio of lifting surface $= b^2/S$ (9.3.2)
A	Enclosed area of torsion box (15.2.1)
A_i, A_{ii}	Enclosed area of individual segments of torsion box (15.2.1)
A_b	Area of boom (spar cap) needed to resist bending (15.2.4)
A_e	Area of edge (coaming) member at edge of cut-out (16.5.1)
A_S	Area of stringer (16.5.1)
A_α, A_δ	Terms used to define the fraction of pressure load on a chord due to incidence and control deflection, respectively (9.4.3)
$\mathcal{A}$	Term used in the solution of a second-order equation (A4.3)
$\bar{A}$	Response of aircraft to continuous turbulence (3.5.2)
$\bar{A}$	Material compression (overall buckling) strength factor (15.3.8)
b	Wing span (4.4.7)
b	Stringer (stiffener) pitch (16.2.3)
b_S	Overall length of a continuous beam (15.4.1)
b_o	Reference semi-chord length $= c/2$ (6.4.1)
b_1	Control hinge moment coefficient due to incidence (AD1.3.4)
b_2	Control hinge moment coefficient due to control deflection (9.4.4)
b_1, b_2	Constants used to define turbulence density (6.4.2)
B	Coefficient in the definition panel/stringer buckling (16.2.3)
B	Damping coefficient of a landing gear leg (A7.2.2)
B_{ij}	Coefficients used to define response of aircraft to continuous turbulence, $i = 1, 2\, j = 1, 2$ (6.4.4)
$B.M.$	Bending moment (AD2.5.1)
$\bar{B}$	Induced drag factor (A7.4)

$c, \bar{c}$	Mean chord of lifting surface (4.2.1, 9.3.1)
c_f	Chord of trailing edge flap or control aft of hinge line (9.4.3)
c_S	Chord at 70 per cent semi-span of lifting surface (11.3)
c_1	Mean chord of wing area outside the body (11.5)
C_d	Drag coefficient (4.6.2)
C_{do}	Zero lift drag coefficient (A7.4)
C_i	Material constant of a windscreen laminate (A8.2.1)
C_l	Rolling moment coefficient (4.3.3)
C_L	Lift coefficient (4.2.2)
C_M	Pitching moment coefficient (4.2.2)
C_{Mo}	Pitching moment coefficient at zero lift (3.3.3, 4.2.2)
$(C_{M\theta})_{le\ \ tail}$	Pitching coefficient due to pitching, less horizontal stabilizer effect (4.2.2)
C_n	Yawing moment coefficient (4.3.4)
C_N	Normal force coefficient (2.6.2)
CP	Centre of pressure (9.4.1)
d	Body (fuselage) diameter (9.7.1)
d	90 per cent of semi-span of a lifting surface (11.3)
d	Maximum depth of wing at the side of the body (15.2.4)
d_r	Depth of a rib (16.2.3)
D	Drag (4.2.1)
D	Diameter of a control wheel (yoke) (3.3.2)
D	Signifies a determinate (1.4.1)
$\bar{D}_1, \bar{D}_2$	Non-dimensional drag factors (A7.4)
$\mathcal{D}$	Differential operator
e	Chord-wise offset of aerodynamic axis from flexural axis as fraction of chord (11.2)
e	Location of reference in torsion box as a fraction of chard (15.2.1)
e_c	Chord-wise centroid of vertical webs of a torsion box as a fraction of chord (15.2.1)
E	Modulus of elasticity (13.3.1)
E_b	Brake energy (7.8)
E_E	Rcduccd elastic modulus in overall buckling (16.2.3)
E_L	Reduced elastic modulus in local buckling (16.2.3)
$E_T(\sigma)$	Tangent modulus (13.5.1. 16.2.3)
E_{xo}	Elastic modulus of unidirectional composite fibre (13.5.1)
f	Term determining the rate of return of a control to neutral (5.2.3)
f	Frequency (Hz) $= \omega/2\pi$ (6.4.1)
f	Fractional position of the inertia axis on the chord aft of the leading edge (11.5)
f	Linear acceleration (A12.1)
f	Dynamic factor on nose gear load in dynamic braking (75.2)
f_E	Direct stress ratio at comer of a cut-out (16.5.1)
$f(Mat)$	Material factor in bird strike evaluation (8.3.2)
$f(\sigma)$	Stress factor $= \sigma/E_T(\sigma)$ (16.2.3)
F	Gust alleviating factor (35.2)
F	Landing gear 'bump' factor (7.6.2)
F	Front spar vertical load reaction (15.2.1)
$F(\kappa)$	Control motivator forcing function (A41)
F_B	Buckling term dependent upon form of construction (13.5.3)
F_g, F_{gm}, F_{gz}	Flight profile terms in the definition of the design gust velocity (3.5.3)

F_{TOW} Fore and aft towing load (7.5.6)
$F(\eta)$ Control forcing function in the longitudinal motion (4.6.3)
$F(\kappa_M)$ Maximum value of a forcing function (A4.3)
$F(\zeta)$, $F'(\zeta)$ Control forcing functions in the lateral motion (4.7.5)
F.S. Front spar

Gravitational acceleration (2.6.1)
g_m Location of centre of mass aft of leading edge as a fraction of the chord (11.5)
G Coefficient defining boundary conditions in second-order equation (A4.2)
G Shear modulus (13.3.2)
G_{xyz} Shear modulus of a $\pm 45°$ composite laminate (13.5.1)

Location of aircraft centre of gravity aft of leading edge of mean chord, as a fraction of the chord (4.2.1)
Height of aircraft centre of gravity above main wheel axle (7.4.1)
Mean height of shear webs in a torsion box (15.2.1)
h_b Height of a runway bump (7.6.2)
h_f Location flexural axis aft of leading edge as a fraction of the chord (11.5)
h_F Height of rudder force above the longitudinal axis (4.7.2)
h_i Individual height of a shear web in a torsion box (15.2.1)
h_m Position of controls-fixed manoeuvre point aft of leading edge as a fraction of the chord (4.3.2)
Position of controls-fined neutral point aft of the leading edge as a fraction of the chord (4.3.1)
h_S Height of a stringer (15.2.7)
h_T Total depth of all the shear webs in a structural box (15.2.1)
H Frequency response function (6.4.1)
H Height of aircraft centre of gravity above the ground (7.5.2)
H_i Coefficients used in the derivation of the lateral acceleration. i = 2, 3 (5.5.5)
H_m Controls-fixed manoeuvre margin (4.3.2)
H_o Location of the aerodynamic centre aft of the leading edge of mean chord as a fraction of the chord (4.2.1)
H.L. Hinge-line

i Sample condition (6.4.1)
i_{ij} Non-dimensional moments and products of inertia. i = x, y, z, j = x, y, z (4.4.7)
I Second moment of area (15.4.1)
I_i, I_{ij} Moments and products of inertia, i = x, y, z, j = x, y, z (1.4.2, AD12.1)
I_W Moment of inertia of rotation of wheel (7.4.4)

Non-dimensional damped natural frequency, i = 1, 2 (4.6.3, 4.7.5)

k Term used to define the response of the aircraft in roll (4.7.4)
k Term defining rate of application of a control (A4.3, 5.2.2)
k Constant in the definition of the torsional stiffness of a lifting surface (15.2.2)
k_i Radius of gyration of aircraft, i = x, y, z (3.5.4. 4.4.7)
k_o Reduced frequency (6.4.1)
k_S Effective shear stress factor of a buckled panel (16.2.4)
k_S Stiffness of shock absorber strut (7.2.2)
k_T Stiffness of tyre (7.2.3)
k_t Allowance on panel thickness for stringer area (16.2.3)
K Lift correction factor for a close coupled canard configuration (4.8.2)

K	Windscreen glass strength factor (A8.2.1)
K	Non-dimensional lifting surface stiffness criterion (11.3)
K_b	Factor allowing for aerodynamic braking effect (7.8)
K_E	Effective overall buckling coefficient (16.2.3)
K_L	Effective local buckling coefficient (16.2.3)
K_n	Controls-fixed static margin (4.3.1)
K_{SB}	Dynamic factor in landing gear spring hack (7.4.4)
K_{SU}	Dynamic factor in wheel spin-up (7.4.4)
K_β	Tail-plane rolling moment coefficient (5.6)
K_σ	Gust magnitude (alleviation) factor (6.4.4)
K_1, K_2	Terms used in the definition of aerofoil pitching moment (9.4.2)
K_{1C}	Material fracture toughness (13.7.1)
ℓ	Length generally
ℓ	Gust gradient length (3.5.2)
ℓ	Length of a strut (162.2)
ℓ	Spacing between supports of a continuous beam (15.4.1)
ℓ_h	Overhang of end of beam (15.4.1)
ℓ_F	Distance of vertical stabilizer centre of pressure to centre of gravity (3.5.4)
ℓ_m	Position of main landing gear wheel aft of centre of gravity of aircraft (7.1.4)
ℓ_n	Position of nose-wheel forward of the aircraft centre of gravity (7.1.4)
ℓ_N	Distance from body nose to aircraft centre of gravity (AD3.3)
ℓ_o	Position of centre of body side force fonvard of the centre of gravity (AD3.3)
ℓ_T	Location of horizontal stabilizer centre of pressure aft of wing–hody aerodynamic centre (4.2.1)
ℓ'_T	Location of horizontal stabilizer centre of pressure aft of aircraft centre of gravity (4.2.1)
ℓ_η	Chord-wise distance between centres of lift due to incidence and control deflection (4.8.3)
ℓ_φ	Bcnding stiffness of lifting surface (11.3)
L	Rolling moment (1.4.1)
L	Scale of turbulence (6.4.2)
L	Spacing (pitch) of ribs and frames (13.5.3)
L, $\bar{L}$, $\bar{L}_T$, $\bar{\bar{L}}$, $\bar{\bar{L}}_T$	Load level (10.3) Non-dimensional lift term (A7.4)
L.E.	Leading edge
$\mathcal{L}$	Lift (4.3.2)
$\mathcal{L}_{To}$	Increment of horizontal stabilizer load due to control deflection to give a constant rate of pitch (5.3.3)
m	Longitudinal acceleration factor (4.2.1)
m	Mach number factor = (I $- M_N^2$) (9.3.2)
m	Mass of a bird (8.2.2)
m	Mass of an element of a lifting surface or control (11.2)
m_θ	Pitching moment coefficient due to pitching. less horizontal stabilizer effect (4.2.2)
m_θ	Torsional stiffness of a lifting surface (11.2)
M	Pitching moment (1.4.1)
M	Bending moment (15.2.4)
M_C	Bending couple on a frame (15.7.1)
M_C	Cruise Mach number (2.6.2)
M_D	Mach number at design speed (2.6.2)
M_N	Mach number (1.5.2)
M_o	Pitching moment at zero lift (4.2.1)

M_θ	Pitching moment due to rate of pitch (4.2.1)
m	Mass of aircraft (2.6.1)
m_L	Landing mass of aircraft (7.2.4)
m_T	Take-off (maximum) mass of aircraft (7.2.4)
n	Normal acceleration factor. positive up (2.6.1)
n	Number of supports of a continuous beam (15.4.1)
n	Ratio of long side to short side of a panel (15.4.2)
n	Shear stress factor (16.2.4)
n_G	Normal acceleration factor increment due to a aust (3.4.2)
n_i	Particular value of normal acceleration factor, $i = 1, \ldots,4$ (3.2.3)
n_i	Number of repetitions of a given stress level, S_i (10.3)
$\bar{n}$	Normal acceleration factor, positive down $= -n$ (4.4.2)
N	Yawing moment (1.4.1)
N	Number of samples in statistical analysis (6.4.1)
N_b	Number of braked wheels (7.8)
N_i	Number of repetitions at a given stress level, S_i, to cause failure (10.3)
N_o	Number of crossings of zero in unit time, in positive sense (6.4.2)
$N(y)$	Number of crossings at given value of y in unit time, in positive sense (6.4.2)
o	Lateral acceleration (4.4.2)
O	Origin of axes, usually the centre of gravity of the aircraft (1.4.1)
p	Rolling velocity (roll rate) (1.4.1)
p	Uniform normal pressure on a panel (15.4.2)
Δp	Differential pressure, relative to local atmospheric value (15.5.1)
p	Local static air pressure (9.6.1)
p_o	Free-sueam static air pressure (1.5.2)
$p(y)$, $p(\sigma_{rr})$	Probability distribution (6.4.1, 6.4.2)
P	Load on lifting surface due to incidence and control angle (5.5.4)
P	Load across the width of a panel or on a strut (13.5.3, 16.2.2)
P_C, P_T	Loads in the compression and tension flanges of a beam (16.2)
P_n, P_t	Radial and tangential loads on a circular irame (15.7.1)
P_r	Perimeter of a torsion box (15.2.2)
P_S	End load in a stiffener (16.2)
P_1, P_2	Constants used to define the turbulence density (6.4.2)
q	Pitch velocity (pitch rate) (1.4.1)
q	Shear stress (16.2.4)
q_E	Shear stress ratio at the comer of a cut-out (16.5.1)
q_i	Generalized co-ordinate (AD7.1)
q	Dynamic pressure (1.5.2)
Q_i	Generalized force (A7.1)
Q_T	Shear flow due to torsion load (15.2.3)
Q_V	Shear flow in vertical webs due to vertical force (15.2.6)
Q_W	Total shear flow in vertical webs (15.2.6)
r	Yawing velocity (yaw rate) (1.4.1)
r	Radius of the leading edge of a lifting surface (8.3.2)
r	Radius of a circular frame (bulkhead) (15.7.1)
r	Ratio of the bending to torsional stiffness of a lifting surface (11.3)
r	Instantaneous radius of motion in pitching manoeuvre (4.2.1)
R	Ratio of two-dimensional control surface derivatives $(-b_2)$ and a_2 (9.4.4)

R	Vertical load on the rear spar (15.2.1)
R	Reaction in the flanges at the root of a hinge rib (15.3)
R	Local radius of a circular shell (15.5.1)
R	Vertical load reaction on a landing gear leg (7.1.4)
R_m, R_f	Loads defining the landing gear shock strut deflection curve (A7.3)
R_{SB}	Vertical load at landing gear spring-back (7.4.4)
R_{SU}	Vertical load during wheel spin-up (7.4.4)
$R(\tau)$	Auto-correlation function (6.4.1)
R_i	Non-dimensional damping coefficient, i = 1, 2 (4.6.3, 4.7.5)
R_1, R_2	Ratios of landing and zero fuel masses to maximum mass (3.5.3)
R	Ratio of $\pm 45°$ plies to sum of 0" and 90° in a composite laminate (13.5.4)
R_i	Response integral. $i = 0, 2, 4, 6$ (6.4.4)
R.S.	Rear spar
s	Semi-span of a lifting surface (11.2.1)
s	Distance of penetration of an aircraft into a gust (3.5.2)
s	Relative scale nf turbulence $= 2L/c$ (6.4.4)
S	Lifting surface reference area (2.6.1)
S	Side load on a landing gear unit (7.5.3)
S_i	Stress level (10.3)
S_1	Wing area outside the body side (11.5)
S_1, S_2, S_3	Proponions of load on a trailing edge device due to incidence, control angle, and rate of roll (5.5.4)
S.F.	Shear force (AD2.5.1)
t	Time
t	Track of main landing gear wheels (7.5.3)
t	Aerofoil leading edge or panel thickness generally (8.3.2, 9.3.1, 15.4.2, 15.7.2)
t_i	Individual thickness of a laminate in a windscreen (8.2.1)
t_i	Time of a given sample, i (6.4.1)
t_b	Thickness of a panel skin required to resist bending load (152.4)
t_e	Effective thickness to resist bending (15.2.4)
t_n	Natural frequency in fore and aft bending of a landing gear leg (7.4.4)
t_q	Panel thickness to resist torsional shear loads (15.2.3)
t_R	Time for wheel to spin-up to maximum vertical reaction (7.4.4)
t_S	Stringer thickness (15.2.7)
t_{SU}	Wheel spin-up time (7.4.4)
t_θ	Thickness of panel to provide required torsional stiffness (15.2.2)
$\hat{t}$	Non-dimensional time (4.4.7)
T	Thrust (4.2.1)
T	Total time of a sample (6.4.1)
T	Kinetic energy (A7.1)
T	Coefficient used in the derivation of panel/stringer buckling (16.2.3)
T_C	Concentrated torque (15.2.2)
T.E.	Trailing edge
u	Velocity along the x axis (1.4.1)
u	Uniformly distributed load (15.4.1)
u_1, u_2	Gust velocities on forward and aft lifting surfaces in transient motion (6.3.1)
U	Overall forward velocity of the aircraft (1.4.1, 4.4.2)
U	Gust velocity at a distances into the gradient length (3.5.2)
U_{de}	Design gust velocity (3.5.2)

U_r, U_{ref}	Reference gust velocity (3.5.3)
U_σ	True r.m.s. (root mean square) value of gust velocity (3.5.2)
v	Velocity along they axis (1.4.1)
V	Overall lateral velocity of aircraft (1.4.1, 4.4.2)
V	Applied vertical load (15.2.1)
V	Potential energy (A7.1)
V_{ap}	Approach speed (7.4.4)
V_A	Manoeuvre speed (2.6.2)
V_B, V_{BMIN}	Speed used to define maximum gust condition (2.6.2)
V_{BL}	High lift device design speed for baulked landing (2.6.2)
V_{BR}	Airbrake limiting speed (8.3.7)
V_C, V_{CMIN}	Design and minimum design cruise speed (2.6.2)
V_D	Design (diving) speed (2.6.2)
V_{DD}	Design speed for full extension of an air brake (8.3.7)
V_{DIV}	Lifting surface divergence speed (11.2)
V_e	Design speed used to define the frequency of elevator application in a checked manoeuvre (5.3.4)
V_f	Forward speed in landing (A7.4)
V_F	Flap design speed (2.6.2)
V_{FL}	High lift device design speed for landing condition (2.6.2)
V_{FLU}	Lifting surface flutter speed (11.3)
V_G	Gust design speed, see V_B (2.6.2)
V_H	Maximum speed in horizontal flight (2.6.2)
V_M	Bird strike design speed (8.3.7)
V_{MC}	Minimum contml speed (3.3.3)
V_{NO}	Maximum normal operating speed (2.6.2)
V_S, V_{S0}, V_{S1}, $V_{S(in)}$, V_{SFL}	Stalling speeds in particular conditions (2.6.2, 85.3)
V_{TO}	Take-off speed (2.6.2)
V_o	General forward speed (1.5.2)
V_v	Vertical descent velocity at landing (7.2.5)
$\bar{V}$	Horizontal stabilizer volume coefficient (4.3.1)
$\bar{V}_v$	Vertical stabilizer volume coefficient (4.7.2)
w	Velocity along the z axis (1.4.1)
w	Loaded width of panel (13.5.3)
W	Overall vertical velocity of the aircraft (1.4.1, 4.4.2)
W	Weight $= m_g$ (2.6.2)
W_1, W_2	Weight terms used to define the density of a lifting surface (11.5)
x	Fore and aft axis fixed relative to aircraft, body axis (1.4.1)
x'	Fore and aft axis fixed relative to an initial flight direction, aerodynamic or stability axis (1.4.1)
	Fore and aft axis fixed in space or relative to the gmund, space or earth axis (1.4.1)
x_i	Chord-wise location of vertical web, i = 1, 2 ... (15.2.1)
x_w	Position of centre of pressure as a fraction of the chord of the load forward of the hinge-line due to control deflection (9.4.4)
	Chord-wise centre of pressure position (9.4.2)
X	Force along the x axis (1.4.1)
X	Generalized parameter (A4.1)

y	Lateral axis fixed relative to aircraft. body axis (l.4.1)
y'	Lateral axis fixed relative to an initial flight direction, aerodynamic or stability axis (1.4.1)
y''	Lateral axis fixed in space or relative to the ground. space or earth axis (1.4.1)
y	Stationary random function (6.4.1)
y	Term used in the definition of the design elevator angle in the checked case (5.3.4)
y_T	Lateral off-set of the thrust line (4.7.2)
y_{1-g}	Correction for level flight condition in gust response calculation (64.2)
$\bar{y}$	Span-wise centre of pressure position as a fraction of semi-span (9.3.2)
$\bar{y}$	Average value of a sample (6.4.1)
Y	Force along they axis (1.4.1)
Y_1. Y_2	Terms used in the delinition of the checked elevator angle (5.3.4)
Y_1	Side load on body (AD3.3)
z	Venical axis fixed relative to aircraft, body axis (1.4.1)
z'	Venical axis fixed relative to an initial flight direction, aerodynamic or stability axis (1.4.1)
z''	Vertical axis fixed in space or relative to the ground. space or eanh axis (1.4.1)
Z	Force along z axis (1.4.1)
Z_{mo}	Maximum altitude (ft) used in the determination of the design gust velocity (3.5.3)
Z_o	Term used to define the buckling of a composite panel (135.4)
α	Angular acceleration of a beam (A12.1)
α	Ratio of the width of a cut-out to the total width of a panel (16.5.1)
α	Angle of attack (incidence) relative to flight path (1.4.1)
α_B	Angle of attack of body axis relative to flight path (1.4.1)
α_{Bo}	Body angle of attack for no wing–body lift (4.2.2)
α_w	Wing root chord setting to body datum (4.2.2)
α_o	Angle of attack of an aerofoil at zero lift (4.2.2)
β	Sideslip angle, horizontal angle of body axis relative to flight path (1.4.1)
β	Non-dimensional measure of the cross section area of the edge member along a cut-out (16.5.1)
β_T	Angle of thrust to body datum (4.2.1)
β	Ratio of turbulence frequency to aircraft undamped natural frequency (6.4.4)
γ	Angle of flight path relative to earth axis invertical plane (climbangle) (1.4.1)
γ	Ratio of specific heats of air (1.5.2)
γ	Width of cut-out as a fraction of the cut-out length (16.5.1)
Γ	Term used in the definition of elevator application in a checked manoeuvre (5.3.4)
Γ	Circulation around an aerofoil (9.3.1)
Γ	Dihedral angle (ADl.3.3)
δ	Indicates a partial differential (4.6.2)
δ	Deflection of a beam or panel (15.4.1)
δ	Measure of the effective end load carrying material in a panel (16.5.1)
δ, δ'	Control forcing function coefficients in a longitudinal manoeuvre (4.6.3)
δ	Vertical deflection of the centre of gravity of the aircraft at landing (72.5)
δ_S	Vertical deflection of shock absorber (7.2.5)
δ_T	Vertical deflection of tyre (7.3.5)

Δ	An increment in a parameter (3.2.2)
ε	Angle of downwash at tail-plane (4.2.2)
ε_n	Elastic portion of strain, $= \sigma_n/E$ (16.2.3)
$\varepsilon(y)$	Angle of twist across the span of a lifting surface (9.3.1)
ζ	Rudder angular deflection (1.4.1)
ζ_{Di}	Damping ratio, $i = 1, 2$ (4.6.5, 4.7.5)
ζ_e	Maximum oscillatory deflection of the rudder (5.5.3)
ζ_o	Datum rudder angle in a prescribed manoeuvre (5.5.2)
¶	Effectiveness of a panel skin in resisting compression (16.5.1)
¶	Fraction of lifting surface semi-span $= y/s$ (9.3.2)
¶	Effective slope of the surface of an aerofoil in supersonic flow (9.6.1)
¶	Elevator angular deflection (1.4.1)
η_C	Maximum change of elevator angle in a checked manoeuvre (5.3.4)
η_{MS}, η_{NS}	Vertical efficiencies of main and nose shock absorbers (7.2.5)
η_{SS}	Increment in elevator angle required to give a constant pitching velocity (5.3.1)
θ	Aircraft angle of pitch (1.4.1)
θ	Inclination of a landing gear leg to the vertical (7.4.4)
θ	Inclination of a bird strike normal to the surface (8.3.2)
θ	Angle of twist of a structural box under torsion loading (15.2.2)
κ	General deflection of a control motivator (A4.1, 5.2.2)
κ	Control deflection in an unchecked manoeuvre (5.2.2)
κ	Ratio of lift to weight at landing impact (7.2.5)
	Radius of gyration of a strut (16.2.2)
	Equivalent spring stiffness (A4.1)
λ	Taper ratio of a lifting surface = tip/root chord (9.3.2)
λ	Vertical reaction factor at landing impact (7.2.5)
λ, λ'	Windscreen panel shape factors (A8.2.1. A8.2.3)
λ_E	Allowance for imperfections in overall buckling (16.2.5)
λ_L	Allowance for imperfections in local buckling (16.2.5)
Λ	Sweep of a lifting surface 0.25 chord line (9.3.2)
μ	Load diffusion coefficient (16.8.2)
μ	Fore and aft ground friction coefficient (7.3.3)
μ_G	Relative density used in aircraft response to a gust (3.5.2)
μ_i	Aircraft relative density, $i = 1.2$ (4.3.1, 4.4.7)
ξ	Aileron angular deflection (1.4.1)
ρ	Density generally
ρ	Air density (1.5.2)
σ	Ratio of air density at a given altitude relative to the value of sea level (1.5.2)
σ	Sidewash angle (5.3.1)
σ	Stress generally (16.1)
σ_a	Allowable stress (15.5.3)
σ_b	Bending or buckling stress (13.5.1)
σ_E	Overall buckling stress (16.2.3)
σ_n	Stress at optimum compression design (16.2.3)
σ_o	Average stress across a panel having a cut-out (16.5.1)

σ_p	Tensile stress in a circular shell subjected to pressure (13.5.1)
σ_s	Allowable shear stress (13.5.1)
σ_t	Tension stress in a tension field web (16.2.4)
σ_{sb}	Skin (panel) buckling stress (16.2.4)
σ_y	Yield (proof) stress (13.3.1)
σ_y	Root mean square, r.m.s., value of a parameter, e.g. aircraft response (3.5.2)
$\bar{\sigma}_w$	Relative structural density of a lifting surface (11.5)
Σ	Aircraft manoeuvre over-shoot ratio (5.3 3)
τ	Non-dimensional time coefficient (4.4.7)
τ	Time separation of points in a sampling process (6.4.1)
τ_i	Continuous turbulence translational response time (6.4.4)
φ	Aircraft angle in roll (1.4.1)
φ	Frequency of application of a control demand (5.3.4)
φ_{eff}	Angle of gust to horizontal in front elevation (3.5.4)
$\Phi(\omega_m)$	Power spectral density, PSD (6.4.1)
$\Phi(\Omega)$	Von Karman power spectral density (6.4.2)
Ψ	Aircraft angle in yaw (14 1)
Ψ_C	Term used in the definition of the elevator angle in a checked manoeuvre (5.3.4)
Ψ_C	Boundary condition coefficient in solution of second-order equation (A4.2)
ω	Frequency generally (6.4.1)
ω_i	Non-dimensional undamped natural frequency. i = 1, 2 (4.6.3, 4.7.5)
Ω	Spatial or reduced frequency $= \omega/V$ (6.4.1)
Ω_S	Spin rate (8.2.2)

Subscripts

In addition to those already defined above the following subscripts are used, sometimes in combination

a	Aerodynamic effects due to airframe configuration (4.4.5)
a	'Additional' lift distribution terms (9.3.1)
a. b...	Axis systems (1.4.1)
ad	Atmospheric turbulence effects (4.4.6)
A	Aerodynamic effect (11.2.1)
h	'Basic' lift distribution terms (9.3.1)
B	Body (fuselage) effect (4.2.1)
B	'Bump' landing case (7.6.5)
c. *C*	Control deflection effects (4.4.5)
D	Drag effects (4.2.1)
D	Design or datum value (5.3.3)
e	Velocity components along body axes (1.4.1)
e	'Elliptical' lift distribution terms (9.3.1)
eff	Effective (4.2.1)
E	Equilibrium condition (55.2)

E	Overall buckling (16.2.3)
EAS	Equivalent air speed (1.5.2)
F	Fin (vertical stabilizer) terms (3.5.4)
g	Gravitational effects (4.4.5)
G	Term due to a gust (3.5.4)
	Landing condition (7.2.5)
L	Local instability (16.2.3)
$M.MAX$	Maximum value of a term
M	Main landing gear terms (7.1.4, 7.2.5)
N	Nose landing gear terms (7.1.4, 7.2.5)
o	Root (centreline) (9.3.2)
o	Sea level or datum condition (2.6.2, 4.2.1)
p	Due to rolling (1.4.1, 3.2.2)
PP	Powerplant effects (4.4.6)
q	Due to pitching (1.4.1)
r	Due to yawing (1.4.1)
R	Return to initial condition (5.5.2)
s	Simulation output (AD1.10.3)
S	Maximum or required value of control deflection (5.2.3, 5.3.3)
S	Structural effect (11.2.1)
SS	Simply supported value (15.4.1)
St	Steady trimmed condition (4.4.4)
T	Tail-plane (horizontal stabilizer) terms (3.2.2)
T	Thrust (4.2.1)
T	Total effective angles (4.4.5)
TED	Trailing edge device (5.3.7)
TO	Take-off condition
TAS	True air speed (1.5.2)
u	Due to forward velocity (1.4.1)
	Due to lateral velocity (1.4.1)
w	Due to vertical velocity (1.4.1)
W	Wing terms (4.2.1)
WB	Wing–body terms (4.2.1)
X	Component along the x axis (1.4.1)
Y	Component along the y axis (1.4.1)
Z	Component along the z axis (1.4.1)
α	Due to angle of attack (9.4.3)
β	Due to sideslip (3.3.3)
δ	Due to control or flap deflection (9.4.3)
ζ	Due to rudder deflection (3.3.3)
η	Due to elevator deflection (4.6.2)
θ	Due to pitch angle (1.4.1)
ξ	Due to aileron deflection (3.3.2)
π, 2π, 3π	Denotes conditions at given points of response motion (5.5.2)
φ	Due to roll angle (1.4.1)
ψ	Due to yaw angle (1.4.1)
o	Sea level condition (2.6.2)
1,2	Control angles to initiate and return to initial conditions (5.3.3)
1,2	Conditions in development of full gust velocity (6.3.1)
1	Longitudinal motion (4.6.3)
	Lateral/directional motion (4.7.5)

Notes

A differential with respect to time is indicated by $\dot{\chi}$
A non-dimensional motion of the aircraft is indicated by $\hat{\chi}$

Equivalent units

The units used throughout the text are the SI (Standard International) system. except in those instances where the codes of requirements specifically use an alternative. The more common equivalent usages are stated below together with relevant standard numerical values.

Unit	SI	Alternative equivalent
Length	m	3.281 ft 39.3 in 0.000622 miles
Area	m^2	10.675 ft^2
Volume	m^3	35.32 ft^3
(Capacity)	m^3 (10^3 litres)	0.004 54 Imperial gallons 0.003 79 US gallons
Speed (velocity)	m/s	3.281 ft/s 2.237 mile/h 1.942 knots
Speed of sound at sen level	*340.3 m/s*	*1116.5 ft/s*
Acceleration	m/s^2	3.281 ft/s^2
Standard gravitational acceleration	*9.807 m/s^2*	*32.17 ft/s^2*
Mass	kg	(2.2046 lb) 0.0685 slug
Weight	N	0.2248 lb
Density	kg/m^3	(0.0624 lb/ft^3) 0.001 94 $slug/ft^3$
Standard air density at sea level	*1.225 kg/m^3*	*(0.0765 lb/ft^3)* *0.002 378 $slug/ft^3$*
Moment of inertia	kg m^2	23.75 lb ft^2
Force	N	0.2248 lb
Moment (torque)	N m	0.7375 lb ft
Power	kW	745.8 lb ft/s 1.356 HP
Pressure	bar (10^5 N/m^2) (10^5 Pascal)	14.5 lb/ft^2
Standard air pressure at sea level	1.013 *bar*	*14.7 lb/ft^2*
Wing loading	N/m^2 (0.102 kg/m^2)	0.020 88 lb/ft^2
Stress	MN/m^2 (10^6 Pascal)	145 lb/in^2
Kinematic viscosity	m^2/s	10.76 ft^2/s
Standard air ***value at sea level***		*1.461×10^{-5} m^2/s* *1.572×10^{-4} ft^2/s*

CHAPTER 1
Introduction

1 . The preliminary design of an airframe

Engineering design is an iterative process in which there must be a continual feedback of data as they become available in order to check the assumptions needed to initiate the procedure. The loading analysis and the preliminary structural layout of an aircraft are no exception to this generalization. The conceptual design phase cannot he satisfactorily concluded without some consideration having been given to the location of the primary structural members, as is considered in the previous hook hy the author Chapter 4, Section **4.3.2,** and Chapter 5, Section 5.4.[1] Experience enables this to be achieved without the necessity of specific reference to the loading requirements. However, the more detailed layout of the components of the airframe and, especially, the initial sizing of the individual members, can only be undertaken in conjunction with a detailed reference to the loading requirements. For the present purposes this phase of the total aircraft design process is taken to be the definition of the configuration of the primary structural members and their preliminary sizing; the description 'structural layout' is taken to cover both aspects of this procedure. It follows the establishment of the external configuration and its verification by appropriate analytical methods. The preliminary conceptual design involves assumptions concerning the airframe mass and the present phase of the process seeks to produce the factual data needed to give confidence to these assumptions. Once the preliminary structural layout has been established it is possible to proceed to a detail design, analysis, and stressing of the airframe.

Experience over the history of aviation has led to the specification of requirements intended to ensure the structural integrity of the aircraft throughout its life. The current

'Howe, D. *Aircraft Conceptual* **Design** *Synthesis.* Professional Engineering Publications Ltd., 2000.

requirements, which are outlined in Chapter 2 and amplified in Chapters 3 and 5 to 8, form the starting point for the preliminary structural design. It must be pointed out that, since these requirements are based on past experience, it is also necessary to consider the introduction of special new requirements in those cases where the concept of the aircraft is in any way unconventional. The interpretation andapplication of the structural design requirements may be defined as loading actions analysis. A knowledge of the basic aerodynamic and inertial characteristics of the design is essential to enable the loading analysis to be undertaken and it is presumed that these data have been derived during the conceptual design and analysis phases. The usual initial assumption is that the airframe is nominally rigid. This is not the true situation since application of load must inevitably cause certain distortions of the airframe and hence result in a loading distribution which may bc different to that derived by assuming the airframe to be rigid. Therefore, the derivation of the loading and consequent sizing of the preliminary structure are interrelated and the iterative feedback procedure mentioned above is essential in deriving an acceptable overall solution. The whole issue of static and dynamic distortion is the province of aeroelasticity. This is given preliminary consideration in Chapter 11, but see also paragraph 1.4.3.5(c).

With the availability of powerful computational facilities and the development of finite element and difference methods it is feasible to produce a loading analysis program which includes the preliminary design of the airframe and hence is able to apply corrections for the effects of structural distortions. It may be expected that such a program will be available to facilitate the design of a sophisticated aircraft. However. the understanding of the way in which the structural design procedure is undertaken and how such a program may be developed demands a more pragmatic approach. It is necessary to make some fundamental initial assumptions, the validity of which must be checked subsequently and corrections made where required. These initial assumptions and the implication of making them are discussed in the following sections.

1.2 Airworthiness targets

1.2.1 Introduction

It is impracticable to design, manufacture, and operate an absolutely safe aerospace vehicle. To attempt to do so would produce an unacceptably heavy design and it would be prohibitively expensive. It is necessary, therefore, to establish an airworthiness standard for normal design and operational purposes, although the possibility of a lower standard. which nevertheless confers a safe 'get home' capability. can be considered in respect of the design of the structure and the associated systems. Past experience has a major influence upon the setting of the airworthiness target.

1.2.2 Civil aircraft

In the context of civil operations it has been observed that the media and fare-paying public react adversely when catastrophic accidents occur, especially if there are several in close sequence. Over the years. a successful attempt has been made to reduce the accident rate so that. on average, the frequency of major disasters is more or less constant in spite of

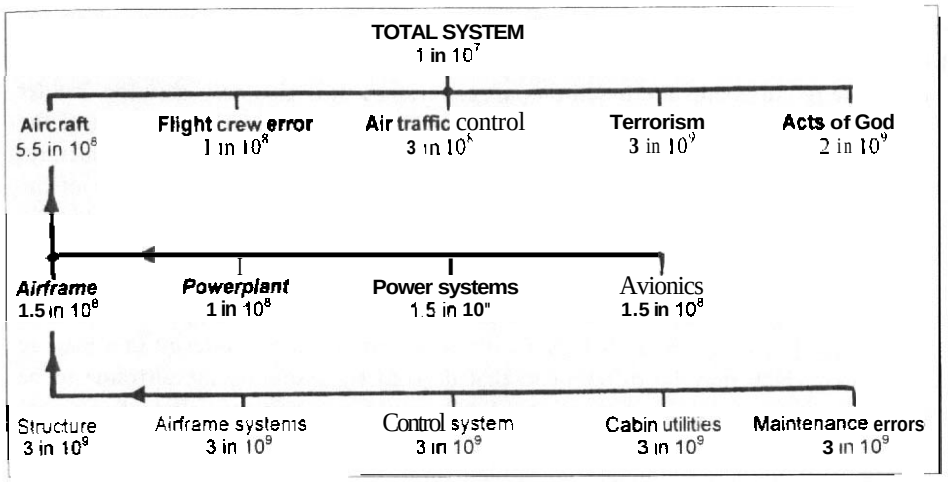

Fig. 1.1 *Breakdown of the risk of a fatal accident*

continually increasing traffic. Currently the fatal accident rate from all causes is about one for every 1 million (10^6) flying hours. On average this probably corresponds to about two passenger fatalities for every 100 million (10^8) kilometres flown. Approximately one in four of these accidents can be ascribed to airworthiness failings, the remainder being due to such things as human factors. air traffic control, the environment, and terrorism. This experience has led to the use of a notional airworthiness target of no more than one fatal accident in 10 million (10^7) hours due to airworthiness failures.

As the number of aircraft operations increases it becomes desirable to consider the implication of maintaining the rate of fatal accidents at the present level. This issue has been considered by Howard[2] who has suggested that it will be necessary to have a target of no more than one catastrophic incident from all causes in 10 million (10^7) flying hours. The possible implication of such a target is illustrated in Fig. 1.1 The numerical values shown are inevitably speculative and to a major extent depend upon the impact of technological development on the individual items of risk. For example, developments in automatic controls could well reduce the probability of crew error. Clearly air traffic control and the aircraft itself are the dominant contributors, but it must be stated that the allocation of equal risks to the airframe components is arbitray. Nevertheless the figure does indicate that the overall aircraft airworthiness achievement will require around a fivefold improvement. and it will need to be better than the present notional target of one loss in ten million flying hours. The individual target for the structure will have to be of the order of no more than one catastrophic failure in 1000 million (10^9) flying hours, see Section 1.2.4.

1.2.3 Military aircraft considerations

A similar philosophy is applied to the operation of military aircraft in peacetime and. at least to some degree, to guided weapons during the launch phase when personnel are

[2]Howard, R. W. Breaking through the 10^6 barrier. International Federation of Airworthiness Conference, October 1991.

involved. However, the airworthiness target for combat types may be somewhat less, possibly being an order of magnitude less than that of civil transport aircraft.

1.2.4 Definition of failure probabilities

A number of definitions have been made in an attempt to categorize the severity of incidents involving the safety of aircraft and the probability of their occurrence. For the purposes of overall system design it is useful to give definitions to the failure probability, especially for individually non-critical components and also when multiplexing is used to achieve the required overall safety level.

The accepted definitions of the effect of failure incidents for civil aircraft are:

(a) Minor effect, which covers normal operation. nuisance conditions and those where it becomes necessary to impose operating limitations or standard emergency procedures.

(b) Major effect, where there is significant reduction in safely margins. possible injuries to the occupants and adverse conditions which make it difficult for the crew to operate the aircraft.

(c) Hazardous effects, where there is a large reduction in the safety margins, possible fatalities to some of the occupants and unduly high workload for the crew.

(d) Catastrophic effect, when at least multiple occupant fatalities occur and most likely it will result in the loss of the aircraft.

These effects are related to the probability of occurrence and the European airworthiness requirements JAR-25. see Chapter 2. Section **2.2.3** and Chapter 17. Appendix A17, further allocate specific numerical values to them. The definitions are:

(a) Probable, which coincides with minor effects and is subdivided into:
  (i) Frequent: an event expected to occur often during the life of an aircraft. numerically taken to occur more often than once in 1000 hours (10^3);
  (ii) Reasonably Probable: an event which may occur several times in the life of an aircraft, that is once in 1000 (10^3) to 100 000 (10^5) hours.

(b) Improbable, which covers the major and hazardous effects being:
  (i) Remote (Major): Unlikely to occur to any given aircraft in its life, but which may occur several times in the total fleet of a given type, or once in 100 000 (10^5) to 10 million (10^7) hours:
  (ii) Extremely Remote (Hazardous): Unlikely to occur at all to any aircraft, but nevertheless it must be considered. This is usually taken as the one in 10 million (10^7) hours target but it covers the range up to one in 1000 million (10^9) hours.

(c) Extremely improbable, which coincides with the catastrophic effect and has a probability of no more than one in 1000 million (10^9) hours. Such an event does not need to be considered in isolation unless the overall aim for safety is increased beyond present targets.

1.3 Achievement of airworthiness targets – loads and factors

1.3.1 Requirements

The fundamental input data for loading action analysis are contained in the particular specification and the general requirements for an aircraft. Many years of experience have resulted in the formulation of definitive sets of requirements, sometimes referred to as requirements handbooks. These cover various types and classes of vehicle, such as manned aeroplanes (military and civil), helicopters, and guided weapons. They are issued by appropriate airworthiness authorities and are frequently updated in the light of both operating experience and technological developments. Specific details of the more important sets of requirements are outlined in Chapter 2.

It should be pointed out that the requirements contain much more than conditions to ensure structural strength and stiffness. Their scope ranges over performance, handling, general operating requirements and procedures, and the design of systems and installations. The latter have major relevance to the achievement of airworthiness targets.

1.3.2 Cause of loads

The loads experienced by a vehicle fall into two broad categories, see Fig. 1.2. One group consists of the loads resulting directly from the action of the pilot, or when appropriate, of the autopilot. These can be generally classified as manoeuvring loads since they occur as the vehicle carries out its intended role. For convenience they can be taken to include cabin pressure differential and the effects of kinetic heating at higher Mach number.

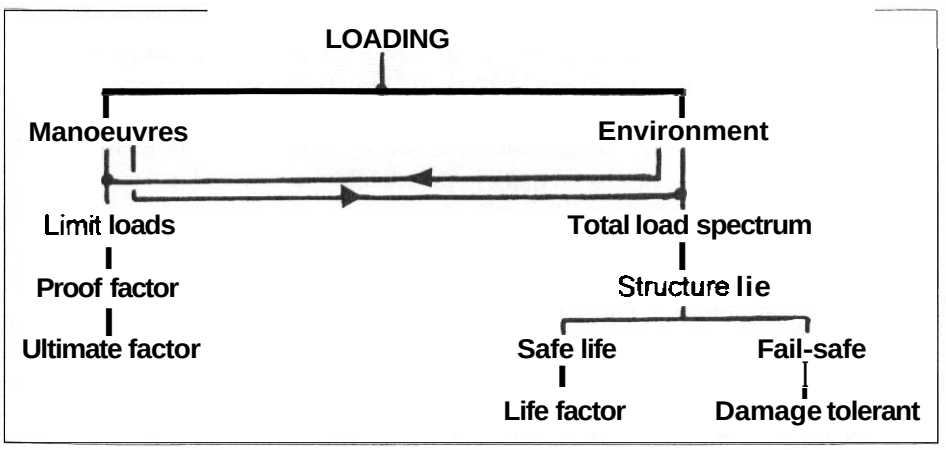

Fig. 7.2 Establishment of the integrity of the airframe

The second group of loads arise because of the imperfectness of the environment in which the vehicle operates. These may be due to such things as atmospheric turbulence or runway unevenness. Essentially this class of loading would not occur in an ideal situation but in practice has to be tolerated and appropriate provision made.

In each of the two categories there are a number of specific loading cases as explained in Chapter 2. Section 2.4.

1.3.3 Frequency of loads

Whether the loads are due to manoeuvres or to environmental effects, for the purposes of structural design they have to be dealt with in two ways.

(a) Firstly there is the limit load condition. The limit load is the actual maximum load of a particular case anticipated to occur in the prescribed operating conditions. A catastrophic failure due to the application of the limit load must be in the extremely remote category. That is. the limit load can be regarded as one which can be anticipated to be reached once. but not exceeded in, say. 10 million (10^7) flying hours. It is in fact the maximum load for a particular manoeuvre or environmental condition and represents the most severe isolated intensity of load appropriate to the particular case. It may occur at any time during the life of the aircraft.

(b) Secondly there is the load spectrum, or the total set of loads, of varying magnitude experienced by the airframe throughout its life and which arises in any given loading case. Often the majority of these loads are small in comparison with the limit value but each may reduce the ability of the structure to resist load and it is necessary to ensure that the total accumulated effect of all of them over the life of the airframe is within the capability of the structure. These loads may arise in a specific way and he of known magnitude and frequency as. for example, cabin pressurization, but unfortunately this is not usually the case. Some, especially those due to atmospheric turbulence or runway unevenness, are essentially random in nature.

1.3.4 Load factors

Conventional manned aerospace vehicle structures are designed using the concept of factors superimposed on the limit load. Two different factors are used for this purpose.

(a) The first of these is the proof factor which has a numerical value of 1.125 for military and 1.0 for civil aircraft. Under proof loading, that is the product nf the proof factor and the limit load, the airframe must not distort permanently more than a small specified amount, usually the equivalent of between 0.1 and 0.5 per cent permanent strain dependent upon the particular form of loading.

Clearly this factor is intended to ensure that the structure will effectively return to its original shape should the design limit load of a particular case be applied.

(b) Secondly there is an ultimate factor. In most cases it is 1.5 for both military and civil aircraft. The ultimate factor is effectively a safety factor on the limit load. It is related to the proof factor through the properties of typical airframe materials but the numerical value of 1.5 was established somewhat arbitrarily when it was realized that that factor of 2 used in the first 25 years or so of aviation was unduly severe. The ultimate factor is intended to cover such items as variation of material and structural properties outside the specified limits. deterioration in service, inadequacy of load and stress analysis, and possible flight of the aircraft just outside the stated design limitations. Attempts have been made to analyse these items statistically and for combat aircraft at least it would seem that a value of 1.5 may be somewhat high and a lower value of 1.4 is now used for some combat aircraft manoeuvre cases. Guided missile requirements introduce some variation in the value of the ultimate factor, it being only 1.33 except for the launch and initial flight phases when 1.5 is retained to safeguard the operating crews and installations. The structure must be capable of resisting the ultimate load, that is the product of the ultimate factor and the limit load, and the civil requirements specifically state that it must be possible to withstand this load for 3 seconds without collapse.

For some specific cases higher ultimate factors are stated. When this is so the value usually represents a special condition conveniently covered by means of an ultimate factor rather than implying a higher order of safety. One such example is the emergency alighting case where only ultimate conditions are relevant.

1.3.5 Structure life

1.3.5.1 Introduction

The application of proof and ultimate factors covers the limit load condition of a particular case but by itself is only adequate for a short-life vehicle. Other measures are necessary to safeguard the integrity of the structure when it is subjected to numerous repetitions of loads over the life of the vehicle. As is discussed in Chapter 10, Section 10.6, the life is usually defined in terms of the number of landings. It may be 6000–8000 landings for a combat aircraft rising to more than 80 000 landings for a short-haul transport aircraft. Further, flight in transonic and supersonic regimes introduces non-linearity of load distributions and possibly temperature effects due to kinetic heating, such as creep. Simple overall factors cannot effectively cover these contingencies.

Each individual load in the total load spectrum appropriate to a particular case has to be considered. The individual load is often relatively low and the strain resulting from it is elastic so that the effect of stress concentrations is of vital importance. The cumulative damage from all the loads must be evaluated to establish the satisfactory integrity of the structure at the end of its life. Unfortunately in the majority of cases the accurate

specification of the load spectrum and its application is very difficult and it is therefore necessary to incorporate safeguards to cover the unknowns. Chapter 10, Section 10.7. provides a further discussion of this issue but for completeness the philosophies used to ensure the continued airworthiness of the structure are outlined here.

1.3.5.2 Safe life – life factor

One approach is to ensure that the structure is able to continue to resist any design load for a substantially longer period than its design life. Thus the structure would be designed to have an estimated life, or safe life, of three or more times that actually intended in service. the ratio of the demonstrated life to that actually intended in operation being the life factor.

The actual numerical value of the life factor is determined by the statistical accuracy of the available design information. especially in relation to actual tests on both components of the structure and the whole airframe. The analysis is often based on unfactored loads. This is not necessarily entirely satisfactory and it might be better to consider factoring each individual load, or more reasonably the stresses resulting from it, before evaluating the safe life. This is a complex process but should enable a more reliable result to be obtained.

Further, it may well be that in some cases the loads are of high frequency but low magnitude and thus fall below the effective endurance limit of the component. In this case no theoretical damage is done. see Chapter 10. Sections 10.3 and 10.7, and a sensible result can only be achieved by reverting to a load factor, possibly of 2, on the individual loads in the spectrum to ensure that the effect of each load is included. This condition is met on rotorcraft transmissions and rotor heads.

Military combat aircraft are often designed using the safe life approach.

1.3.5.3 Fail-safe

A possible alternative philosophy is to accept that the accurate prediction of the loading and its effect upon the structure is difficult and that factors applied to ensure the integrity of the structure could imply a design penalty. Where possible it may be better to design the structure so that should a local failure or damage occur there is always an alternative load path to enable the vehicle to continue operating safely, see Chapter 10, Section 10.7.3. Any failure must be easily detectable on a subsequent inspection and repairable. If it is assumed that initially there are no flaws or damage present in the airframe this approach is known as fail-safe. Clearly such an approach requires early detection of a failure and assumes the existence of adequate structure life in the absence of any damage. Continued safe operation of the aircraft depends upon the assumption that after any single failure the residual strength is sufficient to meet the design loads. In practice there are initial flaws and damage in the airframe so that the fail-safe approach to structural design should also be accompanied by slow crack growth. The fail-safe concept is of considerable importance in system design where the consequences of a failure must be covered by redundancy in the form of multiplexing of components and channels, see Section 1.3.6.

1.3.5.4 Damage tolerant design

It is inevitable that some inherent flaws will be present in an airframe. The damage tolerance approach recognizes this and seeks to predict the rate of growth of such damage as well as incorporating design features to delay the propagation of cracks. Such an approach is obviously psychologically advantageous and can often be incorporated with little weight penalty. In practice the degree of tolerable damage is determined by the rate of crack propagation relative to inspection intervals.

Transport aircraft normally adopt a damage tolerant philosophy.

1.3.5.5 Practical structural life design procedure

Although the emphasis may vary it should be pointed out that any properly designed structure will possess both damage tolerance and safe life features as there are some parts of the aircraft where it is virtually impossible to incorporate fail-safe concepts. When this is the case, one possibility is to introduce a reliable means of failure warning which indicates the onset of a crack before it becomes catastrophic. This can sometimes be done on mechanical components, such as rotor blades, which are a particular problem in this respect.

It is undesirable for a structure to suffer numerous small failures and the difficulties of inspection must not he overlooked. Therefore any significant cracking must be considered as an exception rather than the rule and an overall life expectancy is still necessary. However, in a damage tolerant design the life before significant cracks occur can be less than would otherwise be the case. It is the practice for transport aircraft to have a specified life in the context of repairs and replacements.

1.3.5.6 Probabilistic design

A totally alternative approach to ensuring the continued integrity of a structure is the probabilistic design technique. This is based on an entirely statistical approach. The concept of factors superimposed on a limit load is replaced by a statistical demonstration of the required failure probability. It is particularly applicable in three circumstances:

(a) When the structure is very special both in concept and application such that there is inadequate past experience to be able to specify realistic factors.
(b) When there is high variability or randomness in the loading, material properties, construction techniques, and the like.
(c) When the design is a complex system having many components as, for example. in a flight control system.

The first two of these circumstances are encountered in nautical structures where each one may be different from every other and the wind and wave loadings are random. There is also likely to be **a** variability in materials and construction due to the use of production methods such as welding. For these reasons the technique of probabilistic design was extensively developed by offshore structures and ship designers. More recently it has been realized that a guided weapon system consists of many components,

most of which have to be designed on a statistical basis, and the airframe can he included in this. The concept has been applied to the design of military aircraft in the United Kingdom and it is accepted as one way of demonstrating compliance with structural design requirements. However, at the present time, in most cases the application of probabilistic design appears to result in a mass penalty relative to the traditional approach.

Basically, probabilistic design applied to structures involves a detailed statistical knowledge for each case of:

(i) the most adverse total loading spectrum on any structure of the type:
(ii) the maximum limit load to a stated probability:
(iii) the statistical hehaviour of the structure and its individual components and materials under both the limit load and the total loading spectrum.

The aim is to state the life of the structure with a given degree of confidence, or risk. There is no question of applying factors as they are replaced by the various probabilities and risk levels. **A** tremendous amount of information is needed before this approach can be used completely. One of the major unknowns is the behaviour of a complete structure because of the enormous variation possible in both design and manufacture. This problem may be reduced somewhat by identifying the critical members and then analysing them in sequence.

Damage tolerance remains an important design consideration.

1.3.6 Design of systems

Figure 1.1 shows that the airframe is only one component in a complex transport system. It must also be recognized that the integrity of advanced control systems which incorporate such features as load alleviation and flutter suppression has a direct impact upon the airworthiness of the airframe. While Section 1.3.5.3 explains the limited use of the true fail-safe concept in structural design, the reservations expressed there do not apply to the system as a whole or to the majority of its components. The continued satisfactory performance of a system subsequent to a failure is primarily dependent upon the use of the fail-safe philosophy. Aircraft have employed fail-safe concepts almost since the beginning of manned flight, sometimes in the airframe hut more often in the systems such as duplicated control cables and several powerplants. Howard[3] has reviewed the importance of fail-safe, where the term fail-safety is preferred.

Failure of a component in a fail-safe system usually results in a degradation of safety and often an accompanying reduction in performance. When the latter is not the case the design is sometimes referred to as fault tolerant or failure survivable. As with structural design a fail-safe system almost invariably relies upon the availability of a number of alternative paths, each being capable of performing the desired function. Very occasionally it may be satisfactory for a system to fail in a passive way, the consequent loss of performance being acceptable.

[3]Howard, R. W. Planning for super safety—the fail-safe dimension. Kings Norton Lecture. Journal of *the Royal* Aeronautical *Society*, 104 (1041). November 2000.

As electronic devices develop it is becoming possible to conceive the design of systems which are not only tolerant to the effects of failure of their components but can also adapt their operation so that in large measure their integrity is maintained.

It is important to understand that the design of sophisticated aircsaft relies upon the integration of the systems and the airframe. This is especially true of the use of the flight control system to provide load limitation or alleviation and clearly in these circumstances the design of the structure must allow for both the potential and the integrity of the system. The need for integrity has a major impact on system design which may accordingly include such techniques as redundancy, error monitoring, and separate channels having alternative hardware and software. Also system instabilities can result in structural oscillations and consequent fatigue loading.

1.4 Definitions and basic assumptions

1.4.1 Reference axes

1.4.1.1 Axes systems

Figure 1.3 illustrates the system of axes conventionally used to define both the aerodynamic and inertial characteristics of an aircraft in flight. In passing it should be pointed out that it may well be convenient to use different axes for the structural design process and this is discussed in Chapter 12, Section 12.5. As shown in Fig. 1.3 the origin of the axes is always the centre of gravity of the aircraft, O. The Ox axis extends

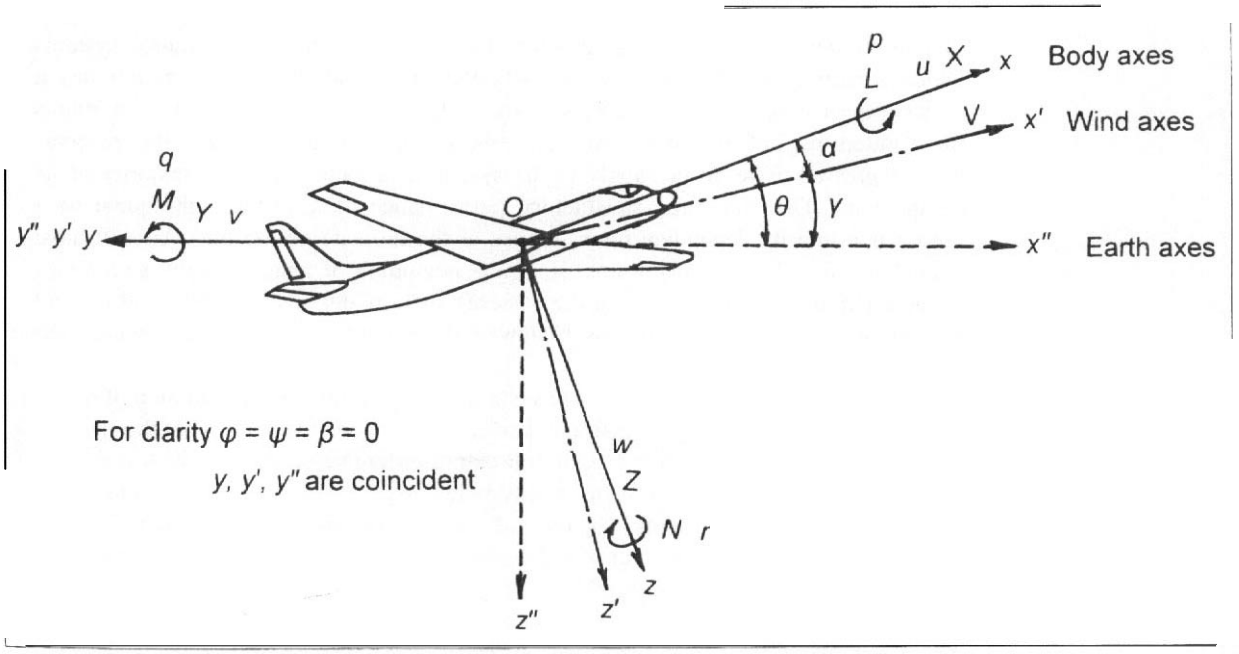

Fig. 1.3 *Aircraft* reference *awes*

forwards from the centre of gravity, the Oy axis to the right (or starboard) side and the Oz axis downwards to produce a right-handed set.

The actual orientation of the axes can vary and the usual possibilities are:

(i) fixed relative to the aircraft, so-called body axes, $Oxyz$;
(ii) fixed relative to an initial flight direction, known as wind, aerodynamic, or stability axes. $Ox'y'z'$;
(iii) fixed in spacc, or relative to the ground, space or earth axes, $Ox''y''z''$.

The use of axis systems requires careful consideration. An excellent discussion of the transformations which may be necessary is given by Cook[4].

For the purpose of loading action calculations it is often preferable to use body axes referred to an initial reference, possibly the earth axes. For structural design a modification of the body axis system is expedient.

The great majority of aircraft possess symmetry about the vertical fore and aft, Oxz, planc Some guided weapons also possess symmetry about the horizontal, Oxy, plane and have what is referred to as a doubly symmetric configuration.

Associated with the axis system $Oxyz$ are:

(a) Linear velocity perturbations of u, v, and w and the corresponding accelerations along the x, y, and z directions, respectively, together with forces X, Y, and Z.
(b) Angular velocity perturbations of p, q, and r and the corresponding accelerations about the x, y, and z axes together with moments L. M, and N, respectively.
(c) Angular displacements of the body axes relative to the initial reference axes about the point O, of ϕ (roll), θ (pitch), and ψ (yaw) together with the corresponding rates of angular displacement from the reference axes. It must be noted that the angular rates $\dot{\phi}$, $\dot{\theta}$, and $\dot{\psi}$ are only equal top, q, and r when all the perturbed displacement angles are small, see Fig. 1.4.
(d) Angular displacement of the wind axes as follows:
  (i) in the Oxz plane, relative to initial earth axes, γ, the angle of the flight path, and relative to the body axes $-\alpha$ where α is the angle of incidence of the body as illustrated in Fig. 1.3; in a symmetric flight situation, the motion king solely in the Oxz plane, γ, is equal to $(\theta - a)$;
  (ii) in the Oxy plane relative to the body axes $-\beta$, where β is the sideslip angle, and when the motion is solely in the Oxy plane β is equal to (dv/Vdt), where V is the velocity vector along the Ox' wind axis, see Fig.l.5.

1.4.1.2 Transformation of axes

It is frequently desirable to transform a parameter, for example velocity, from one set of reference axes to another. This is done by resolving the components of the parameter

[4]Cook, M. V. *Flight Dynamics Principles.* Arnold. 1997.

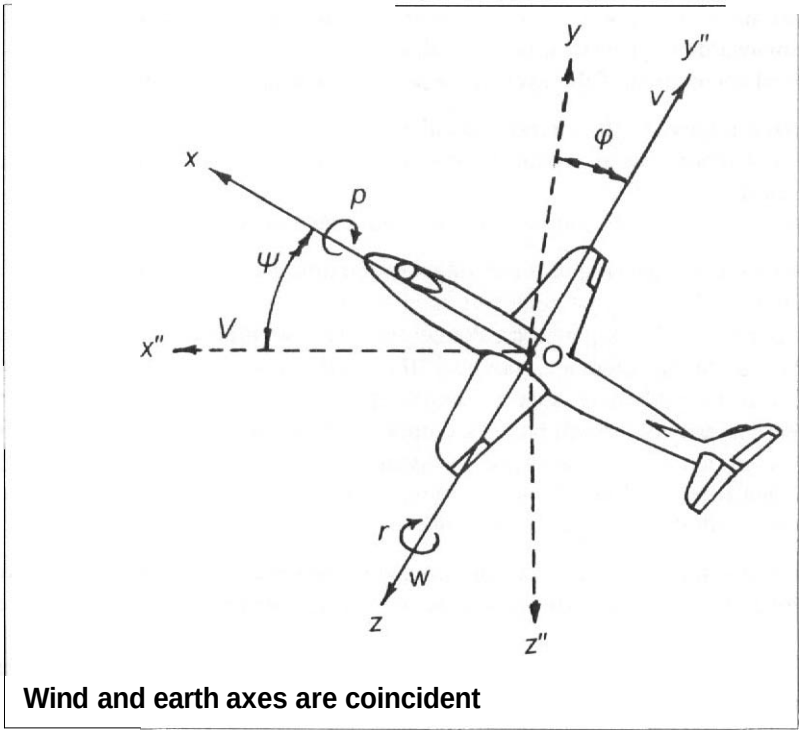

Fig. f.4 Axis system in asymmetric motion

from one axis system to another in sequence. It is important to do this in the correct order. Thus if a parameter is defined in the $Ox_a y_a z_a$ axis system and it is to be transformed into the $Ox_d y_d z_d$ axis system the procedure is:

(a) Apply a rolling motion about Ox, through an angle ϕ to transform to the $Ox_b y_b z_b$ system.
(b) Apply a pitching motion about Oy_b through an angle θ to transform to the $Ox_c y_c z_c$ axis system.
(c) Apply a yawing motion about Oz_c through an angle ψ to transform to the $Ox_d y_d z_d$ axis system.

The resulting transformation is conveniently expressed in matrix notation:

$$\begin{bmatrix} O_x \\ O_y \\ O_z \end{bmatrix}_a = \mathbf{D} \begin{bmatrix} O_x \\ O_y \\ O_z \end{bmatrix}_d \tag{1.1}$$

where

$$\mathbf{D} = \begin{bmatrix} \cos\theta\cos\psi & \cos\theta\sin\psi & -\sin\theta \\ \sin\phi\sin\theta\cos\psi - \cos\phi\sin\psi & \sin\phi\sin\theta\sin\psi + \cos\phi\cos\psi & \sin\phi\cos\theta \\ \cos\phi\sin\theta\cos\psi + \sin\phi\sin\psi & \cos\phi\sin\theta\sin\psi - \sin\phi\cos\psi & \cos\phi\cos\theta \end{bmatrix}$$

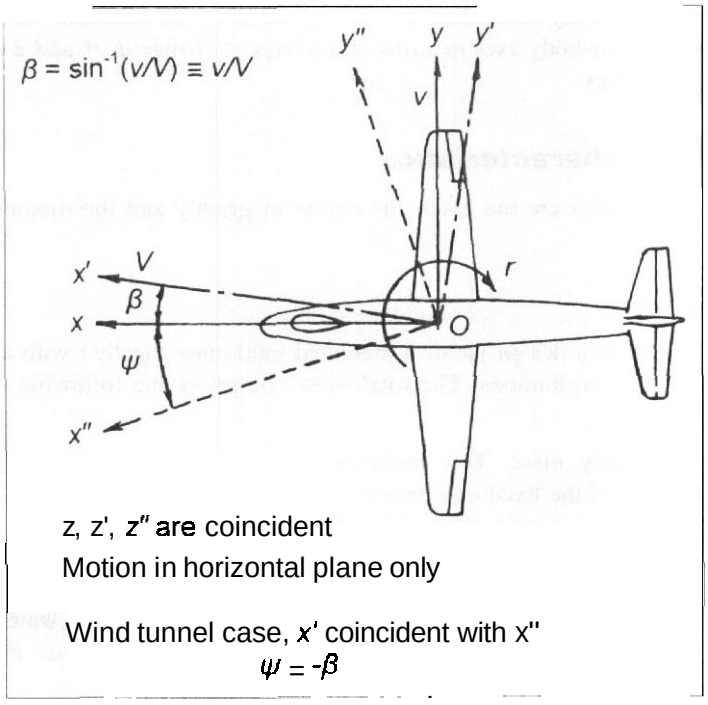

Fig. 1.5 *Axis system when motion is in the horizontal plane*

An important application of Eqn. (1.1) is the transformation of the forward velocity, V, defined in wind axes to the body axes when the aircraft has an angle of attack a and a sideslip angle β, noting that $\beta = (-\psi)$. In this case:

$$\phi = 0, \qquad \theta = \alpha, \qquad \psi = -\beta$$

The velocity components along the body axes $Oxyz$ are denoted by U_e, V_e, and W_e. Application of Eqn. (1.1) gives:

$$\begin{bmatrix} U \\ V \\ W \end{bmatrix}_e = \begin{bmatrix} \cos a \cos\beta & -\cos a \sin\beta & -\sin\beta \\ \sin\beta & \cos\beta & 0 \\ \sin\alpha\cos\beta & -\sin\alpha\sin\beta & \cos a \end{bmatrix} \begin{bmatrix} V \\ 0 \\ 0 \end{bmatrix} \tag{1.2}$$

or

$$U_e = V \cos a \cos\beta$$
$$V_e = V \sin\beta$$
$$W_e = V \sin\alpha \cos\beta$$

It is sometimes useful to use the inverse of the matrix D:

$$\mathbf{D}^{-1} = \begin{bmatrix} \cos\psi\cos\theta & \cos\psi\sin\theta\sin\phi - \sin\psi\cos\phi & \cos Q\sin\theta\cos\phi + \sin\psi\sin\theta \\ \sin\psi\cos\theta & \sin\psi\sin\theta\sin\phi + \cos\psi\cos\phi & \sin\psi\sin\theta\cos\phi - \cos\psi\sin\phi \\ -\sin\theta & \cos\theta\sin\phi & \cos\theta\cos\phi \end{bmatrix}$$

Similar transformations may be applied to other parameters, for example the angular rates p, q, and r about the body axes in terms of the rates of change $\dot{\phi}$, $\dot{\theta}$, and $\dot{\phi}$ defined in terms of the earth axes.

1.4.2 Inertial characteristics

The inenial characteristics are the mass, the centre of gravity and the moments and products of inertia.

1.4.2.1 Mass

The conceptual phase of a design yields a predicted total mass together with a break-down into individual contributions. The total mass comprises the following specific items:

(a) The basic empty mars. This includes the airframe, powerplant, systems. installations, and the fixed equipment.

(b) The operating items required to bring the aircraft to flight status hut with it otherwise being empty. These additional items are often specified by the operator and include crew, unusable fuel, removable equipment which may include some furnishings, and on board supplies such as food and water which have to be replenished after each flight. Together with the basic mass the operating items make up the operating empty mass.

(c) The disposable load. This consists of the payload and the fuel required to perform a specified operation or sortie. The sum of the disposable load and the operating empty mass is the total, or take-off, mass of the aircraft.

The basic empty mass may be assumed to be a fixed quantity for a given version of a design. The other items may he variable although the total can never exceed the maximum design mass. The magnitude of the variable components is determined both by the requirements of a particular flight and by their usage. Thus fuel mass reduces as it is consumed and the payload may he disposed of in combat operations.

To further complicate the matter the design mass may have more than one value. For example it is not unusual for military aircraft to have a specified 'overload' take-off mass associated with reduced performance requirements such as the allowable manoeuvres. In the case of some larger transport aircraft a 'ramp' mass is defined that is somewhat greater than the design take-off mass and allows for the fuel used between engine start-up and the commencement of the take-off run. The ramp mass has an impact upon the design of the landing gear.

1.4.2.2 Centres of gravity

The centre of gravity position of the basic empty mass is defined by the local centres of mass of the items which go to make it up. There will be a range of centre of gravity positions associated both with the operational items and the disposable load and, in general, there will be variation during the flight as the mass reduces.

The number of combinations of mass and centre of gravity is likely to be large and it is usual to define an 'envelope', the boundaries of which are used for both aircraft stability analysis and structural design, see Section 1.5.3.2.

The fore and aft centre of gravity is especially important. The specification of the fore and aft centre of gravity range is a matter of interaction between the desired operational characteristics. in that these determine the mass allocations. and the acrodvnamic characteristics. In a conventional configuration the size and location of the horizontal stabilizing surface is of particular significance. For an aircraft having a large disposable load the fore and aft centre of gravity range is likely to be of the order of 20 per cent of the aerodynamic mean chord of the wing. Typically it could be between 16 and 36 per cent of the chord aft of its leading edge.

1.4.2.3 Moments and products of inertia

In general for each mass and corresponding centre of gravity position there will be a set of three moments of inertia. I_x, I_y, and I_z about the Ox, Oy, and Oz axes, respectively. There will also be three corresponding products of inertia, I,,, I,,. and I_{zx}. However, for the usual case of an aircraft having nominal symmetry about the Oxy plane the products of inertia involving mass in the Oy direction are zero. The remaining product of inertia. I_{xz}, results from the mass coupling in the Ox and Oz planes and is only zero if the **Ox** and Oz axes happen to be principal axes. While this is not generally the case. it may be approximately true when the Ox and Oz body axes are very close to the **Ox'** and Oi' wind axes, that is, when the aircraft is flying at low angles of attack.

When undertaking loading analysis the moments and products of inertia must be consistent with the relevant mass and centre of gravity position.

1.4.3 Aerodynamic characteristics

1.4.3.1 Introduction

The geometric configuration of the aircraft is explicitly defined during the conceptual design phase. This includes such details as the type and extent of the high-lift devices and the sizes and locations of the aerodynamic surfaces used to confer the required stability and control. Indeed an important aspect of the conceptual design process is the determination of satisfactory stability and control characteristics whether the aircraft is designed to be naturally or artificially stable. To do this it is necessary to evaluate the aerodynamic derivatives for the defined configuration of the aircraft. While the derivation of these quantities is outside the scope of the present work it is useful to make some pertinent comments regarding their estimation as they are also essential for the loading analysis.

1.4.3.2 Standard aerodynamic data

Various standard reference sources are available for the evaluation of the aerodynamic derivatives, refer to the Bibliography in Chapter 17, Appendix A17. However, they are largely based on conventional aircraft configurations. When the proposed layout is in

any way unconventional it is important to recognize the limitations of the data and to make due allowances. This may imply a need for wind tunnel testing as well as the application of more advanced techniques such as computational fluid dynamics.

1.4.3.3 Problem derivatives and data

Even for conventional configurations there are some aerodynamic characteristics for which an accurate prediction is difficult. There are also some aspects of wind tunnel testing where accurate full-scale data are hard to achieve. For the purposes of stability and control analysis it may be acceptable to apply a sensitivity technique to ensure that satisfactory characteristics can be predicted across a numerical range of derivatives for which accurate prediction is difficult. The accurate derivation of loads requires a precise estimate of the significant values. Among the data critical for loading actions analysis are:

(a) Control hinge moment characteristics. On the one hand the use of too high a value can penalize the design of the control system and the control surfaces, and on the other hand it may have the effect that the motion of the aircraft consequent upon control deflection is less than would otherwise be the case.

(b) High-lift device characteristics, especially the associated pitching moments which have a major impact on the loads needed to trim the aircraft.

(c) The overall wing–body pitching moment in the zero-lift condition and the corresponding position of the aerodynamic centre. see Chapter 4, Section 4.2.1. As indicated above these values depend upon the deflection of the high-lift devices but are also affected by small, detail, aspects of the configuration such as the geometry of the wing–hody junction.

1.4.3.4 Airframe distortion

Although the airframe will distort under load, as discussed in Section 1.1, it is usually inevitable that the initial evaluation of the aerodynamic characteristics is based on the assumption that the airframe is rigid.

1.4.3.5 Aerodynamic data for loading calculations

Within the restrictions outlined in Sections 1.4.3.2 to 1.4.3.4 it may he assumed that all the aerodynamic data needed to undertake the loading analysis are available. However, in order to ensure that the structural design is adequate, although possibly somewhat conservative, it is necessary to consider making allowances for the difficulty of accurately predicting certain of the critical values.

(a) For the purposes of the initial design of the control surfaces, and parts of the control system where relevant, it is common to factor the predicted control hinge moments. **A** typical factor is 1.25 but this may he reduced or removed when flight test data become available. In some cases it is also necessary to assume a very severe distribution of air-load across the chord, especially when the surface incorporates a horn balance.

(b) It may be advisable to apply a factor to the predicted values of the wing–body zero-lift pitching moment coefficient in the various high-lift device configurations or to establish a minimum value for loading calculations. Associated with this it may be wise to include an adverse increment in the assumed position of the aerodynamic centre of the wing–body relative to the overall centre of gravity of the aircraft. Such allowances must be made with extreme caution since, while they may be desirable if not actually necessary, any undue allowance will result in an unjustifiably conservative and over-designed structure.

(c) The significance of the distortion of the airframe under the applied loading is worthy of further comment. When a load is applied to a lifting surface there is a tendency for the surface to both bend and twist. In the majority of cases the ohvious static bending deflection across the span of the surface is of negligible significance. The reason for the twisting of the wing is less clear and is due to the fact that the position of the local chord-wise centre of air-load is usually forward of the twisting axis of the structure. The implied additional lift lends to cause the local angle of attack to increase with a consequent further increase of the lift. The magnitude of the lift increase vanes across the span of the surface. being small in the root region and relatively larger at the tip where the wing is much more flexible in torsion. The net result is that there is a tendency for the span-wise centre of lift to be located further outboard than would be the case if the surface was rigid. The first direct consequence of this is an increase of the bending moment. In addition, excess local twisting may result in a form of static aeroelastic divergence. This is considered further in Chapter 11, Section 11.2.1. Nevertheless, in spite of the important effect of the distortion on the aerodynamic derivatives and the loads calculated by using them. there is no easy alternative to the assumption of a rigid airframe for the initiation of the loading analysis. Subsequent correction for the effects of distortion is essential.

1.5 Specification of design conditions

1.5.1 Operating and design flight envelopes

The structural integrity of the aircraft must be established at all points on, and within, its operating envelope with adequate allowance for possible excursions outside this envelope. Thus the structural design flight envelope represents more severe conditions than are specified for the operating envelope, especially in respect of the maximum design speed. The envelope is defined in terms of combinations of forward speeds and altitudes upon which are superimposed manoeuvres and the effects of atmospheric turbulence. The forward speeds and altitudes are determined by the performance requirements of the aircraft. Manoeuvre conditions may be determined by specific performance requirements or, like the effects of atmospheric turbulence, the general requirements for that class of aircraft. For higher subsonic, transonic, and supersonic flight it is usual to define the speeds in terms of Mach number.

1.5.2 Definition of speeds

The airloads experienced by the airframe are directly proportional lo the dynamic pressure. g, which may be defined in terms of either velocity or Mach number.

$$q = \rho(V_{oTAS})^2/2 = \gamma p_o(M_N)^2/2 \tag{1.3}$$

where

ρ	is the air density
p_o	is the local static pressure
V_{oTAS}	is the true. that is the actual. forward velocity
γ	is the ratio of the specific heats of air and is equal to 1.4

The Mach number is:

$$M_N = V_{oTAS}/a \tag{1.4}$$

where a is the local speed of sound at a given altitude.

However, it is important to note that the structural design speeds are specified as equivalent speeds, V_{oEAS}, that is the speed at zero altitude (sea level) that gives the same dynamic pressure as the true speed at a particular altitude.

$$V_{oEAS} = V_{oTAS}\sigma^{1/2} \tag{1.5}$$

where σ is the ratio of the density at the particular altitude corresponding to the true speed to that at sea level and thus $\sigma \leqslant 1$.

When the speed is defined as a Mach number at a particular altitude the equivalent structural design speed is deduced by first converting the Mach number to a true airspeed using Eqn. (1.4) and thence to an equivalent airspeed using Eqn. (1.5). It is common for aircraft operating at the higher Mach numbers referred to above to be limited by a maximum equivalent airspeed at low altitude and by Mach number above an altitude where the true speed derived from the design equivalent speed is equal to the limiting Mach number.

In passing it is worth commenting that the pilots' instruments show Mach number and indicated airspeed. The indicated airspeed differs only from the equivalent airspeed in respect of instrument errors.

When an aircraft only operates at low Mach number in what may be regarded as incompressible flow conditions the use of the equivalent airspeed enables the loading in static and quasi-static conditions to be calculated without reference to altitude. However, it must be pointed out that when the loading is a consequence of a dynamic disturbance of the aircraft the resulting motions, and hence loads, are dependent upon altitude in that the response of the aircraft is a function of the local air density. Atmospheric turbulence is also altitude dependent.

The situation is more complex when the aircraft operates in the transonic and supersonic flight regimes where compressibility effects are significant and therefore Mach number considerations are likely to be dominant. The complication arises

from the fact that the speed of sound vanes with altitude so that there is no simple relationship between Mach number and equivalent airspeed. A further difficulty is that the basic aerodynamic characteristics are also Mach number dependent.

The specification of actual design speeds and Mach numbers is covered in Chapter 2, Section 2.6.

1.5.3 Aircraft mass and centre of gravity

1.5.3.1 Mass

The structural design loads must he calculated for the complete range of masses appropriate to a given condition. The flight cases have to be considered for all masses in the range of the minimum flying mass to the maximum take-off mass, the minimum flying mass being the operating empty mass plus a minimum landing fuel reserve. The ground cases need to be considered for the range of masses from the basic empty mass to the ramp mass. In either case some operational limitations may he imposed. for example it is common to specify a maximum landing mass for ground cases which makes some allowance for the use of fuel during the Right.

It is important to examine mass conditions between the two extremes for a given case. This is necessary because of the effect of inertial forces in relieving the air-loads. For example, the wing structural loading may he higher than the take-off conditions when part of the fuel has been used and its relief effect reduced in greater proportion than the corresponding reduction of overall mass.

1.5.3.2 Centre of gravity

As mentioned in Section 1.4.2.2 the centre of gravity has a specified range. In practice specific combinations of empty mass, fuel, and payload will have corresponding centre of gravity positions. In some cases it may be possible to uniquely define these points but more usually the number of possible cases is large and, at least for the first set of loading calculations, it is conservative to apply the full range of masses at both the extreme fore and aft centre of gravity locations.

1.5.4 Engine conditions

The loads on the aircraft are influenced by the thrust of the powerplants, especially when they are located vertically above or below the centre of gravity and contribute to the overall pitching moment. A given operational performance case implies a certain thrust. As with other design conditions there is the possibility that a very large number of thrust cases must be considered. For initial work it is usually adequate either to use the engine condition appropriate to the particular case. for example steady level flight thrust is equal to the drag, or to examine the effect of the two extreme thrust settings for a given design case. Thus the engine conditions examined could be maximum and minimum thrust for that flight condition. the minimum possibly being the flight idling value unless it is an engine-failed case.

1.5.5 Altitude

The altitudes considered for structural design must cover the range from sea level to the maximum operating altitude, as mentioned in Section 1.5.2. Some considerations, for example Mach number and atmospheric turbulence, are a function of altitude. Further as the aircraft climbs to altitude fuel is used so that the mass at altitude is less than the take-off value. It is usual to specify a number of design altitudes based on the operational performance requirements of the aircraft. Almost certainly one case will be the lowest altitude at which the aircraft can reach its design maximum operating Mach number. This somewhat complex situation is simplified for those classes of aircraft where the operational altitude range is small, such as light general aviation types or combat aircraft which are required to achieve the maximum manoeuvre and Mach number performance immediately after take-off at nominally sea level conditions.

CHAPTER 2

Structural design requirements

2.1 Historical review

2.11 Introduction

A historical review of the development of structural design requirements is of interest. While the emphasis is placed on the United Kingdom and Europe, a similar process occurred in the United States and this will he referred to as appropriate. Although there has always been some interaction between military and civil requirements the impetus of the First World War placed emphasis on military aspects and for this reason these will he considered initially.

2.1.2 Development of requirements for military aircraft

2.1.2.1 Early contributions, 1907 to 1924

As early as 1907 an attempt was made to produce design data for military aircraft. This work began at the National Physical Laboratory in the United Kingdom and was continued at His Majesty's Balloon Factory at Famborough. The investigation naturally included lighter-than-air aircraft since at the time they were the subject of considerable research. By about 1910 the Superintendent of what by now had become the Royal Aircraft Factory introduced a scientific approach by encouraging his staff to publish technical papers on relevant aeronautical subjects. Perhaps the most significant of these was published in 'Flight' magazine in October 1913. Its title was 'The stresses in wings—the RAF method of investigation'. In that it covered design and not just a strength requirement it began a tradition and, to some extent, this has been continued in

British military airworthiness requirements. However, the first official British publication in the airworthiness field was a confidential Admiralty memorandum dated 1915. It was written by H. Booth and H. Bolas and was titled 'Some contributions to the theory of engineering structures with special reference to the problem of the aeroplane'

A summary of the existing knowledge appeared in 1916 when the Royal Aircraft Factory produced a six-page pamphlet. The next officially authorized publication was a classified document of 1918 written by A.J.S. Pippard and J.L. Pritchard. This was '*The **Handbook of Strength** Calculations*' and its contents were based on a case study of a single-engine biplane. It was issued by the British Ministry of Munitions – Aircraft Production and later formed the basis for a classical textbook '***Aeroplane** Structures*' published by these two authors in 1919. The 1918 Handbook. known as HB806. remained the official document for both military and civil aircraft for about six years.

2.1.2.2 The formative years, 1924 to 1939

The British Air Ministry had been established in 1919 and in 1924 it issued a revised version of document HB806 bearing the designation AP 970. The numerical pan of this designation has been retained to the present time. AP 970 was unclassified and could be purchased from His Majesty's Stationery Office for the price of one guinea, later reduced to three shillings! It was applicable to hoth military and civil single engined biplanes of conventional design. Some two years later a special civil version, AP 1208, appeared, see Section 2.1.3.3. A feature of AP 970 was the contributions made by industry and academia as well as the government departments through membership of the Load Factor subcommitlee of the Aeronautical Research Council. A new edition of AP 970 was issued in 1930 extending its coverage to monoplanes. The 1933 edition was given a new title '*Design Requirements for Aeroplanes **for the Royal Air Force'.*** Soon after the title was extended to include '***the Roval Navy'.*** The 1935 edition formed the basis of the British military design requirements for some 45 years, an amendment procedure keeping it up to date.

From time to time the work on strength requirements was undertaken by the Airworthiness Department of what by now was the Royal Aircraft Establishment, but there was a major change in policy in 1928 when many of the staff were dispersed around the aircraft industry as Resident Technical Officers in newly established 'Approved Organizations'. The strength requirements were supplemented by ones for structural stiffness based on the work of A. Pugsley and H. Roxbce-Cox (Lord Kings Norton). Additional requirements for such items as systems and installations were first issued in the form of Aircraft Design Memoranda (ADM), but were subsequently incorporated in AP 970.

During the years immediately preceding the Second World War there was doubt about the validity of certain of the requirements, especially in the industry. This led to discussions between the Society of British Aircraft Constructors (SBAC), and the Air Ministry and it was agreed that a procedure should be established whereby future changes resulted from co-operative efforts. The result was the formation of the Joint

Ainvonhiness Committee (JAC), which has shaped the nature of British military airworthiness requirements ever since. One of the aims of the JAC was to confine the documents to a clear statement of the purposes without attempting to define the detailed means of applying them. Another aim was to combine all the relevant documents into one volume for clarity and ease of reference.

2.1.2.3 Second World War. 1939 to 1947

During the wartime period it was essential for operational experience to be fed into the system very rapidly and this was done using ADMs. At the same time research produced new data and various IAC subcommittees were set up to handle issues of critical importance. New concepts of presenting strength requirements, such as the flight envelope proposed by A. Pugsley, were introduced and flight test requirements promulgated and added to AP 970 in 1945. There was an inevitable duplication of information in various documents so that one of the aims of the setting up of the JAC was not achieved. Consequently when the war ended the SBAC made a new representation to the Ministry of Aircraft Production and it was agreed that in future the design requirements should be separated from technical procedures and *'**Technical Requirements for Service** Aircraft*' was issued in 1947. It was later coded as AvP 25 and more recently as Def.Stan.05-123 under the title *'**Technical Procedures for the Procurement of Aircraft, Weapon** and **Electrical Systems'.***

A completely revised version of AP 970 was issued in 1947 at amendment 40 and an unclassified version made available to the public for 15 shillings.

2.1.2.4 Post the Second World War, 1947 to 1969

The JAC continued to be active during the two decades after the war in a period which saw major developments in aviation with the application of the jet engine and supersonic flight. Important changes included the introduction of a Volume 2 to AP 970 to cover advisory material and, in 1955, Volume 3 to cover *'Rotorcraft **Design Requirements'.*** After 1956 it was agreed that the Volume 2 material should be returned to Volume 1 but printed on distinctive green paper to emphasize its advisory nature. During this period the governmental authority changed first to the Ministry of Supply and then to the Ministry of Aviation, the designation following suit as SP 970 and then AvP 970. Towards the end of this period it was felt that AvP 970 was sufficiently well defined and that further upgrading was not required.

It was decided, therefore, that after amendment 109, 1st March 1969, no further alterations would be made to AvP 970, all new requirements being covered by the issue of Memoranda. After a period of some ten years the number of Memoranda was such that it became very difficult to use the requirements and there was concern over what action should be taken. Among the proposals made was the development of a pan-European set of military requirements and the complete replacement of AvP 970 by the Transport Supersonic Standards (TSS) requirements developed for Concorde, see Section 2.1.3.6. The JAC continued to meet and provided a degree of continuity.

By 1980 the situation had deteriorated to such an extent that urgent action was essential. The JAC proposed a complete review of the military design requirements. This was accepted and a completely new document prepared and given the code Def.Stan.00-970. This current document is discussed in Section 2.2.2.1

2.1.2.5 United States military requirements

There was a period of intense activity in the United States which coincided with that in the United Kingdom covered in Section 2.1.2.4. This led to the issue of a number of MIL-Specs covering various aspects of the structural design of US Air Force, Navy, and Marine aircraft. Unlike the British requirements there was no complete handbook or set of requirements and MIL-Specs cover many items other than aircraft structural design. Although there were some similarities with AvP 970 there were also many differences.

2.1.2.6 Joint European projects

In the case of collaborative European military aircraft projects the usual practice was to agree on a special set of structural design requirements based on those employed by the associated nations. This included elements of the ME-Specs as appropriate.

2.1.3 Civil aircraft requirements

2.1.3.1 Historical review

Civil aircralt operations in the United Kingdom commenced immediately after the end of the First World War in 1919. For some years the airworthiness requirements were common with those of military aircraft as mentioned in Section 2.1.2.1. At this time the military requirements were based on single-engined biplanes and there was concern among those involved in multi-engine civil operations that the imposed requirements were not applicable. An official approach was therefore made to the Air Ministry for civil aircraft to be considered in their own right.

The period after the First World War also saw rapid expansion of air transport operations in the United States. This led to the formation of the Bureau of Air Commerce and the production of a document entitled the 'Civil Aviation Manual'. The responsible authority changed names through the Civil Aviation Administration, the Civil Aernnautical Board (CAB), and ultimately the Federal Aviation Administration all of which in turn became responsible for the regulation and safety of civil operations. The governing documents also had title changes through 'Civil Aviation Regulations' (CAR) to 'Federal Aviation Regulations' (FAR). published as the 'Code of Federal Regulations', CFR-14.

2.1.3.2 The international scene up to 1960

As early as 1910 a somewhat premature attempt was made to develop a set of European aeronautical regulations. In 1919 an International Air Convention was prepared and by

1939 this had been ratified by some 33 states, a notable exception being the United States. A pan of this Convention was the establishment of an International Commission for Air Navigation (ICAN). A set of 'Regulations concerning the Minimum Requirements for Airworthiness Certificates' was approved in 1934 and adopted by the signatories as recommendations rather than mandatory requirements. Associated with this was an agreement that all participating states would accept 'Certificates of Airworthiness' from the other participating nations.

In 1944 the United States took an initiative by inviting some 52 nations to attend a convention on international civil aviation to bc held in Chicago. This now famous meeting formed the International Civil Aviation Organization (ICAO) and reiterated the ICAN concept of states accepting Certificates of Airworthiness from each other provided they conformed to minimum international standards. Perhaps not surprisingly the US delegates suggested that these minimum standards should be an international version of the US domestic Federal Aviation Requirements. While it was agreed that such a set of international standards was necessary, the US offer was not accepted, especially by the UK which cautioned a more considered approach.

In fact considerable difficulty was encountered in formulating a set of ICAO requirements. The first issue, in 1944, was accompanied by a statement encouraging member states to use it as a basis for certification. However, by 1952 this outlook had been reversed and member states were encouraged not to use ICAO as a basis for certification. A consequence of this was that a review undertaken in 1953 led to a decision that ICAO regulations were not a replacement of those of individual nations. The emphasis was therefore changed and in 1955 a short ICAO code of basic standards was accepted. This was supplemented by 'Acceptable Means of Compliance' (AMC) and later 'Provisional Acceptable Means of Compliance' (PAMC). The latter proved to be very valuable in establishing international guidelines for national codes of practice.

2.1.3.3 United Kingdom civil aircraft requirements in the period 1926 to 1946

A consequence of the representations made to the Air Ministry, referred to in Section 2.1.3.1, was that in 1926 a special document was issued with the code AP 1208 and the title 'Airworthiness Handbook for Civil Aircraft'. This consisted of two parts. The first was concerned with design and the second with inspection, and thereby it established the principles of initial and continuing airworthiness. Private flying was largely uncontrolled and this led to some degree of apprehension as the number of light aircraft increased. In 1933, the UK government set up a committee to examine the control of private flying, but in fact its report made recommendations concerning the whole field of civil aviation. While some notable members of the committee suggested an immediate separation of all civil aircraft activities from the Air Ministry, this was not implemented. For some years the Air Ministry retained responsibility for large civil aircraft. defined as those in excess of 10 000 lbs weight (4 536 kg). and AP 1208 still applied.

However, the basic recommendation that civil aircraft should be overseen by an independent organization was eventually accepted and the Air Registration Board (ARB) was established in 1937. The ARB was specifically charged with:

(i) controlling the airworthiness requirements for civil aircraft:
(ii) controlling the system of approved firms, which was the concept introduced for military aircraft in 1928;
(iii) the issue of Certificates of Airworthiness.

A transition period for the transfer of responsibility from the Air Ministry was envisaged and in fact this extended beyond the beginning of the Second World War in 1939. This had no immediate effect as there were virtually no civil operations during the wartime period.

2.1.3.4 The United Kingdom Air Registration Board. 1944 to 1972

When the Air Registration Board was formed one of its first tasks was to prepare a set of airworthiness and operational requirements to replace AP 1208 which was not amended after 1939. A fundamental principle of the new document was that it should be a code of practice rather than a set of absolute rules, thereby achieving a flexibility of application. The new document was modelled on AP 1208 with major emphasis on structural requirements, but covering also some performance and equipment stipulations. Work on it was stopped at the outbreak of the Second World War.

By 1944 it was clear that a new era of civil air transport was approaching and a fresh start was made on formulating the code of practice. This became known as British Civil Airworthiness Requirements (BCAR) and it was formally issued in 1948. Although the document conformed with the developing ICAO requirements it was more comprehensive in detail.

The Air Registration Board continued to operate until 1972 when the whole of UK civil aviation was reorganized with the formation of the Civil Aviation Authority (CAA). This was effectively an amalgamation of the Air Traffic Control operation with the ARB, the latter's activities becoming its Airworthiness Division. In fact the designation ARB was retained for an advisory committee known as the Airworthiness Requirements Board.

2.1.3.5 British Civil Airworthiness Requirements (BCAR)

Although BCAR has been superseded for new aircraft designs it is still current in the context of application to older aircraft which are still operating. It includes a section on procedures and has separate sections for individual classes of aircraft and their components. The layout partly stemmed from the original formation of the ARB and partly following the precedent of the US Federal Aviation Regulations. Each of the relevant individual sections covered all aspects of the design requirements for a given

class of aeroplane. Thus Section K applied to light aircraft and had the following subsections:

K1 General and Definitions
K2 Flight
K3 Structures
K4 Design and Construction
K5 Powerplant Installations
K6 Equipment Installation
K7 Operating Limitations Information

The inclusion of such a comprehensive set of topics was a major difference between the first versions of BCAR and its predecessors.

2.1.3.6 International developments and European co-operation

In parallel with these developments there was activity at the international level. In the United States the civil aeronautics authorities had made significant changes to the Federal Aviation Regulations, especially in respect of what is now known as field performance. Much of the performance section of the US requirements was adopted in the first issue of BCAR, but thereafter there was a divergence as research in the UK enabled new requirements for rate of climb to be specified in terms of atmospheric conditions.

The United Kingdom ARB began working on airworthiness requirements for supersonic airliners as early as 1959. With the decision that Concorde should be developed as a joint Anglo-French project there came the need to produce a single set of design requirements. The resulting 'Transport Supersonic Standards' (TSS) represented the first serious attempt to produce a detailed set of international requirements and it paved the way for future work in this context. The fundamental philosophy of the airworthiness aspect of the TSS requirements reflected the thinking which had already evolved round the certification of automatic systems, such as auto-land, for subsonic transport aircraft. This aimed at specifying acceptable rates of catastrophic failure to enable the appropriate reliability and multiplex system design to be undertaken meaningfully. The TSS requirements were the first to introduce the distinction between the three levels of hazard referred to in Chapter 1, Section 1.2.4. At the same time the four levels of probability were established: frequent, reasonably probable, remote, and extremely remote. By attaching numerical values to these a statistical design could be undertaken.

The advent of the Airbus consortium following on from the Anglo-French co-operation on the TSS standards gave the impetus for work to start on the formulation of a set of joint European airworthiness requirements for transport aircraft. The original aims of the 1944 Chicago convention were not overlooked and the first major decision was that the format of this code should exactly follow that of the US equivalent, FAR-25, and be designated JAR-25. The task was by no means easy. Each of the seven

or so European aeronautical nations initially involved already used their own set of requirements and the differences had to he taken into account. The question of the language used was of some significance, especially in relation to the interpretation in translation.

Apart from using FAR-25 as a basis for the format of the new document it was agreed that FAR-25 should be adopted as the 'Basic Code'. This has important ramifications. For example when the Federal Aviation Authority amended FAR-25, those amendments automatically applied to the European JAR-25 unless one of the participating countries gave notice of objection within a specified period.

In practice JAR-25 was produced by working through FAR-25 paragraph hy paragraph. Where acceptable to a11 the participating countries, the detail of FAR-25 was retained. Otherwise the attempt was made lo come to a common European agreement to replace the FAR-25 stipulations. In order to obtain a document having overall agreement it was necessary to allow for some national variations.

The first issue of the new code was limited to subparts: C – Structures. D – Design and Construction. and E – Powerplant installation. It appeared in 1974. However, it was several more years before the document had reached a more or less complete form, being changed to incorporate FAR-25 amendments, European amendments, and new material. Thus in this respect considerable progress has been made, albeit more than 30 years later, towards the aims of the Chicago convention.

Refinements over a period of several years resulted in a document in which all the basic requirements became common to the participating nations and this comprised Section 1. There was some variation in the means of compliance and this was covered by a supplementary Section 2. This used the terminology 'Advisory Circulars – Joint' (ACJ). It was agreed that none of the participating nations would introduce its own amendments without having first submitted them for general approval.

Subsequently the European Joint Airworthiness Requirements have been extended to cover all classes of aircraft and their components, as well as operational procedures.

2.2 Current airworthiness codes

2.2.1 Introduction

In recent years there has been a change of emphasis in the specification of requirements, especially in the case of those concerned with more sophisticated military and transport aircraft. Whereas at one time the aim was to provide a design handbook, outlining the calculation procedure to be used, it is the present policy to state the intended consequence of the code and to allow the design organization to use a 'rational analysis' of its own choice. As an example of this, comparison may be made between the transport aircraft requirements. FAR/JAR-25, and the light aircraft requirements. FAR/JAR-23. Although a cursory survey suggests that there is considerable similarity between the two. in practice the transport aircraft codes relegate 'design handbook' features to advisory information.

2.2.2 Military aircraft

2.2.2.1 United Kingdom

The proposal for a new version of AvP 970 referred to in Section 2.1.2.4 was that there should be a complete revision undertaken in three stages.

(a) *Phase* I. An immediate updating of AvP 970 amendment 109 to clarify the relationships between the Leaflets and Memoranda.

(b) ***Phase*** 2. To prepare a reprint of the whole document, edited to be consistent throughout and on A4 format. This was achieved by the end of 1983 with the issue of 'Design and airworthiness requirements for Service Aircraft' – Def.Stan.00-970.

(c) ***Phase*** **3.** To thoroughly update the technical content of the document, taking into account where appropriate the comparable civil requirements and the United States MIL-Specs. This was achieved by 1989.

The layout of the Def.Stan.00-970 Issue I followed closely that of its predecessor:

Volume 1: 3 books – Aeroplanes
Volume 2: 2 books – Rotorcraft

Some of the chapters are common to both Aeroplanes and Rotorcraft, but there is full duplication in the respective volumes so that cross-reference is not needed. Each volume consists of an Introduction, Reference to US MIL-Specs, an Index. and Parts 0 to 10 inclusive. Each part is subdivided into chapters, and each chapter into main text and leaflets. The parts are:

Part 0: Summaries of changes introduced by amendments
Part I: General and operational requirements
Pan 2: Structural strength and design for flight
Part 3: Structural strength and design for operation on specified surfaces
Pan 4: Detail design and strength of materials
Pan 5: Aeroelasticity
Part 6: Aerodynamics and flying qualities
Pan 7: Installations
Part 8: Maintenance
Pan 9: Flight tests – handling
Pan 10: Flight tests – installations and structures

One of the particular matters which had to be faced in the formulation of the requirements was that Volume 1 covers all classes of aeroplanes and Volume 2 all classes of rotorcraft. This is especially significant in the case of Volume 1 which includes coverage of all types from small trainers, through transports to supersonic combat aircraft. In some chapters it is necessary to distinguish between these and four specific classes of aircraft are identified. However, in most cases the requirements are written in such a way as to be general. The use of advisory leaflets gives the opportunity to record existing design and testing practice, and in some cases there is a parallel with the US MIL-Prime series of requirements, see Section 2.2.2.2.

Def.Stan.00-970 Issue 1 was updated to amendment AL 14. The original concept of a Design Handbook was formally abandoned over 50 years ago but the present document contains a large quantity of design information for the benefit of the future generations of designers.

At the end of 1999. Issue 2 of Def.Stan.00-970 was puhlished in part. The new version differs in that it is divided into pans each of which is appropriate to a given class of aircraft, or other topic, and is intended to be complete in itself. The parts are:

Part 1: Combat aircraft
Part 3: Small civil-type aircraft
Part 5: Large civil-type aircraft
Part 7: Rotorcraft
Part 9: Unmanned aircraft systems
Part 11: Engines
Part 13: Military common fit equipment
Part 15: Items with no specific military requirements

Each part consists of a number of sections which typically comprise:

Section 1: General
Section 2: Flight
Section 3: Structures
Section 4: Design and construction
Section 5: Powerplant
Section 6: Equipment
Section 7: Operating limits and information
Section 8: Gas turbine auxiliary power unit installations
Section 9: Military specific systems

The leaflet material is retained but is located at the end of each section as relevant.

The new issue is stated to he a replacement for:

Def.Slan.00-970 Issue 1, (12 December 1983)
AvP 970 (1959) (see Section 2.1.2.4)
AP 970, 2nd edition (1924) (see Section 2.1.2.2)
HB 806, 1st edition (1918) (see Section 2.1.2.1)

Until the publication of Issue 2 is complete, and in the event of any conflict of information. the provisions of Def.Stan.00-970 AL 14 take precedence.

2.2.2.2 United States

As mentioned in Section 2.1.2.5 the United States system of specifying military design requirements differs from that used in the United Kingdom in that there is no complete design handbook as such. Specific topics are covered hy individual Military Specifications in the MIL-Specs series. These cover all aspects of military operations. The more relevant requirements which were introduced in the period commencing at the

beginning of 1960 were:

MIL-A-8860: Airplane strength and rigidity – General specification
ASG (18 May 1960) and 008860A
USAF (31 March 1971)
MIL-A-8861: Airplane strength and rigidity – Flight loads
ASG (18 May 1960) and 008861A
USAF (31 March 1971)
MIL-A-8862: Airplane strength and rigidity – Landplane landing and ground handling loads
ASG (18 May 1960)
MIL-A-8863: Airplane strength and rigidity – Ground loads for Navy acquired airplanes
ASG (18 May 1960)
MIL-A-8865: Airplane strength and rigidity – Miscellaneous loads
ASG (18 May 1960)
MIL-A-8866: Airplane strength and rigidity – Reliability requirements, repeated loads, fatigue, and damage tolerance
ASG (18 May 1960) and 008866B
USAF (22 August 1975)
MIL-A-8867: Airplane strength and rigidity – Ground tests
ASG (18 May 1960) and 008867B
USAF (22 August 1975)
MIL-A-8870: Airplane strength and rigidity – Vibration, flutter, and divergence
ASG (18 May 1960) and 008870A
USAF (31 March 1971)
MIL-A-8871: Airplane strength and rigidity – Flight and ground operations testing
USAF (1 July 1971)
MIL-A-8892: Airplane strength and rigidity – Vibration
USAF (31 March 1971)
MIL-A-8893: Airplane strength and rigidity – Sonic fatigue
USAF (31 March 1971)
MIL-A-83444: Airplane damage tolerance requirements (2 July 1974)
MIL-F-8785: Flying qualities of piloted airplanes
MIL-F-9490: Flight control systems – Design, installation, and tests of piloted airplanes – General specification
MIL-F-18372: Flight control systems – Design, installation, and tests of piloted airplanes – General specification

The above specifications have now been replaced by a new series. These are of different format and make provision for the contractor to state the conditions appropriate to a given aircraft. Guidance notes based on the earlier specifications are included. Among this newer series, known as MIL-Prime, are:

AFGS(MIL-A)-87221: Airplane structures – General requirements
MIL-L-87139: Landing gear systems

2.2.2.3 Guided weapons

The current United Kingdom reference is Def.Stan.08-5, which is classified. This document replaces AvP 32 which was in existence for over 40 years. Until Def.Stan.08-5 is completed it is necessary to refer back to AvP 32.

2.2.3 Civil aircraft requirements

As indicated in Section 2.1.3.6 there is now considerable commonality between the European Joint Airworthiness Authority (JAA) requirements and the equivalent United States Federal Aviation Authority (FAA) requirements. In those cases where the FAA requirements have been used as a basis for the JAA requirements the format of the two is identical. The JAA requirements are arranged in such a way that the differences from the comparable FAA document are immediately apparent. This is done by:

(a) Underlining any textual details differing from the statements in the corresponding FAA document.
(b) Identifying all the FAA clauses but inserting the note 'Not required for' when the clause is not applicable in the JAA document.
(c) Introducing the letter 'X' in new clauses which do not appear in the equivalent FAA document

Further there is agreement on a harmonization process whereby as new or amended clauses are introduced they are agreed for both sets of documents so that, ultimately. there will be complete commonality.

The current JAA Joint Airworthiness Requirements, with the Basic Code from which they were derived and, where relevant, the corresponding sections of BCAR are:

JAR-I Definitions and Abbreviations (no Basic Code)
JAR-11 IAA Regulatory and Related Procedures (no Basic Code)
JAR-21 Certification Procedures for Aircraft and Related Parts (no Basic Code)
JAR-22 Sailplanes and Powered Sailplanes (German LFSM) (BCAR Section E)
JAR-23 Normal, Utility, Aerobatic, and Commuter Category Aeroplanes (up to 5700 kg mass except Commuter Aircraft up to 8618 kg mass) (FAR Part 23) (BCAR section K)
JAR-25 Large Aeroplanes, (FAR Part 25) (BCAR Section D)
JAR-26 Additional Airworthiness Requirements for Operations (no Basic Code)
JAR-27 Small Rotorcraft (FAR Part 27) (BCAR Section G)
JAR-29 Large Rotorcraft (FAR Part 29) (BCAR Section G)
JAR-36 Aircraft Noise (ICAO Annex 16) (BCAR Section N)
JAR-145 Approved Maintenance Organizations (no Basic Code)
JAR-147 Approved Maintenance/Training Examinations (no Basic Code)
JAR-APU Auxiliary power units (FAR Part 37-183-TSO-c77A)
JAR-E Engines (BCAR Section C)
JAR-P Propellers (BCAR Section C)
JAR-VLA Very Light Aeroplanes (no Basic Code) (BCAR Section S)

Further JAR standards cover such items as Standing Orders, All-Weather Operations, Commercial Operations, Licensing, Training Devices, and Simulators.

Some sections of BCAR are still current, such as Section Q, Non-Rigid Airships (CAP 471).

2.3 Categories of aeroplanes

2.3.1 Military aircraft

Def.Stan.00-970 Issue 1 divides aeroplanes into four main categories for requirements purposes (Chapter 600 paragraph 3 and Leaflet 600/1, and Chapter 606 paragraph 3):

Class I: Small light aeroplanes
Class II: Medium weight, low to medium manoeuvrability
Class III: Large, heavy, low to medium manoeuvrability
Class IV: High manoeuvrability,

Def.Stan.00-970 Issue 2 has different categories as listed in Section 2.2.2.1.

2.3.2 Civil aircraft

BCAR used the following groups based on performance:

A: Where the performance is such that an engine failure never requires forced landing procedure.
B: Where a forced landing is necessary if a failure occurs en *route* – multi-engine rotorcraft or small twin-engined aeroplanes having not more than 19 seats with a performance level such that a forced landing is unlikely to be necessary after an engine failure at any time.
F(i): Small twin-engined aeroplanes of not more that nine seats where engine failure may result in a forced landing just after take-off or before landing.
F(ii): Small single-engined aeroplanes having not more than nine seats.

The JAR requirements retain the categories A and B for rotorcraft.

2.4 Major categories of loading cases

2.4.1 Vehicle configuration and load cases

Virtually all vehicles are designed to possess symmetry about a vertical plane passing through the centreline of the body, see Fig. 2.1. However, manned aircraft are asymmetric with reference to a horizontal plane passing through the body centreline. Such an arrangement possessing single symmetry can be subjected to both symmetric and asymmetric loading cases. Certain guided missiles also come into this category and are known as 'polar' or 'twist and steer' missiles. However, many missiles are designed to be symmetric about both the vertical and horizontal planes through the body centreline. These doubly symmetric missiles are said to be of 'cartesian' or 'cruciform'

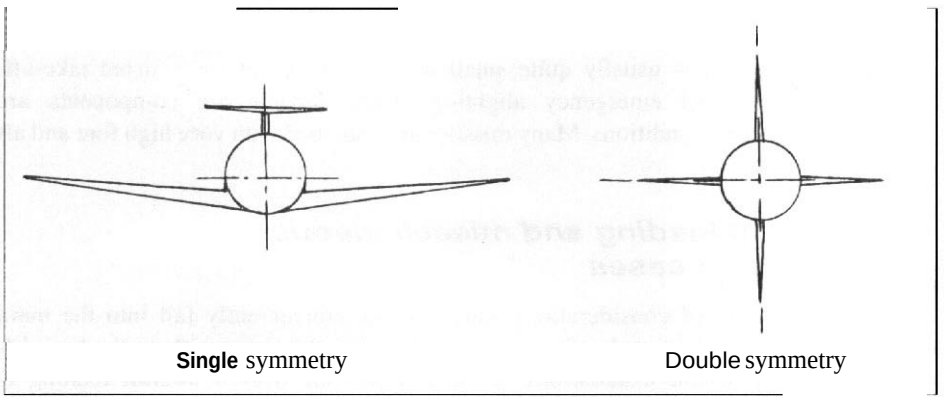

Fig. 2.1 Airframe configuration

configuration. They do not experience the usual asymmetric loading but are likely to be designed for special roll effects, such as roll stabilization.

2.4.2 Symmetric flight cases

Symmetric flight cases arise as a consequence of pilot- or autopilot-initiated manoeuvres solely in the longitudinal, or pitching plane. Uniform air turbulence in the vertical and head-on directions also gives rise to symmetric loading and may take the form of discrete gusts or continuous turbulence.

2.4.3 Asymmetric flight cases

Asymmetric loads arise when the controls are operated to initiate yawing or rolling motion. An engine failure has a similar effect. Asymmetric loads, particularly those due to rolling, are combined with symmetric ones. A cross-wind condition or a non-symmetric turbulence will also give rise to asymmetric loads.

2.4.4 Ground cases

From the point of view of landing gear design there are two types of requirement. The first of these covers the case of the aircraft while it is static or manoeuvring on the ground and is invariably associated with the maximum aircraft mass. The second is concerned with the absorption of vertical energy in a landing and may be associated with a reduced mass. The landing loads are the result of the vertical deceleration occurring when the aircraft lands or, for that matter, when it encounters a runway irregularity. There is an associated fore and aft deceleration and asymmetry of loading occurs due to side forces encountered in a crosswind landing. A 'one-wheel' landing case is introduced to ensure the integrity of the airframe between the main landing gear units.

2.4.5 Longitudinal load cases

Fore and aft loading is usually quite small on aircraft except for assisted take-off, arrester landings, and emergency alighting cases. Asymmetric components are associated with these conditions. Many missiles are launched with very high fore and aft accelerations.

2.4.6 Local loading and miscellaneous loading cases

There are a number of considerations which do not conveniently fall into the main categories. Many of these only affect local parts of the structure; such as the high-lift devices and powerplant installations. In these cases the overall aircraft loading is associated with local conditions. There are one or two of more general significance, for example cabin pressurization.

2.5 Interpretation *of* loading cases

The methods used for estimating the loads acting on a vehicle are complex and involve a knowledge of parameters which can only be determined accurately at the later stages of the design. The requirement handbooks have sometimes sought to overcome this difficulty by suggesting cases for loading that are based upon past experience with similar types of vehicle. These are relatively simple to apply and sometimes do not appear to have a very obvious theoretical backing. However, in the case of a conventional design they do enable a first indication of the loads to be obtained and hence allow the preliminary design to proceed. For an advanced design, particularly one of unconventional layout, it is essential to be more precise and because of this there has been a tendency in recent years for the specified requirements to be stated fundamentally, leaving the designer to interpret them. In fact it is now usually necessary to use more precise methods of analysis for all designs as soon as sufficient information is available.

It is essential to bear in mind certain points when interpreting the results of loading calculations and applying them to a design.

(a) An actual aircraft will not conform exactly to the ideal specification, and hence allowance must be made for the vehicle build to be at the most adverse tolerances. This is particularly important with regard lo wing–body setting, wing twist, horizontal and vertical stabilizer settings, and control angles.

(b) The accurate prediction of input data is very difficult for a design materially differing in either shape or operation from an existing type. Wind tunnel tests may be of limited accuracy, especially with regard to control hinge moments, which frequently play a significant part in overall load evaluation. In some cases computational fluid dynamics (CFD) analysis is of value.

(c) Since design codes are based on past experience there is no certainty that they will cover all the cases needing to be considered in the design of a vehicle. It is for the designer to introduce any new cases considered to be necessary,

especially when the design is unusual, and to obtain permission for the relaxation of ones which can he shown not to apply.

(d) Application of the details of the requirements should make allowance for physical and design limitations, such as the maximum lift coefficient. achievable tyre friction coefficient, and built-in features, especially in systems, which introduce load restricting characteristics.

(e) The complexity of a modem aircraft is such that it is often necessary to make some fairly drastic assumptions in the initial loading evaluation. The designer must use the best information available. On the other hand, an unduly severe assumption will penalize the design and must be avoided. The calculations must he continually updated as more accurate input information becomes available.

2.6 Design speeds

2.6.1 Introduction

The structural loading requirements are expressed in terms of a set of design speeds, complemented where appropriate by the corresponding Mach numbers. In the majority of cases the speeds are equivalent airspeeds, that is the speed is related to the sea level air density used to define the dynamic pressure, see Chapter 1, Section 1.5.2. In some circumstances, especially cases concerned with atmospheric turbulence, the effect of altitude is important and true speeds may be defined. hut unless this is specifically stated equivalent airspeed should be assumed.

It should be noted that the dynamic response of an aircraft to a disturbance is a function of its density relative to that of the local air. Since the air density is a function of altitude the dynamic response and the implied loading will be altitude dependent even though equivalent air speeds are being used.

2.6.2 Design speeds

2.6.2.1 **Stalling** speed, V_S

The stalling speed is defined as the minimum steady flight speed at which conmol can be maintained:

$$V_S = (2ngm/\rho_o SC_{NMAX})^{1/2} \tag{2.1}$$

where

ρ_o is the sea level density: so that
V_S is an equivalent airspeed, see Chapter I, equation (1.5)
S is the wing reference wing area
g is the gravitational acceleration
m is the appropriate mass
n is the normal acceleration factor and is one for level flight

C_{NMAX} is the maximum normal force coefficient at a Mach number corresponding to a true speed V at a given altitude, and with the appropriate setting of the high-lift devices. It should be noted that C_{NMAX} is a function of Mach number and this can materially alter the stall boundary for vehicles of high wing loading. The normal force coefficient is approximately equal to the lift coefficient in many cases.

There are some specific definitions of the stalling speed:

(a) V_{S1} is the stalling speed in a specified condition, typically with the high-lift devices, and undercarriage retracted and with the engines idling. However, the effect of engine power, high-lift devices, and dive brake positions must be investigated where appropriate.

(b) V_{S0} is the stalling speed in the landing configuration.

2.6.2.2 Manoeuvre speed. V_A

The manoeuvre speed is the lowest speed at which the aircraft can attain the prescribed maximum limit normal manoeuvre factor, n_1. Thus V_A is the speed defined by the intersection of the stall boundary, appropriate to the definition of V_{S1}, and the manoeuvre factor n_1. See Chapter 3, Section 3.2.3.

$$V_A = V_{S1}/(n_1)^{1/2} \tag{2.2}$$

V_A need not exceed the speed V_C, see below.

2.6.2.3 Design cruising speed, V_C

The definition of the speed V_C is somewhat complex as it is intended to cover the maximum normal operating condition, speed V_{NO}. On larger civil aircraft (JAR-25). V_C must be sufficiently greater than the gust design speed, V_B, to provide for inadvertent speed increases which may result from turbulence, see Section 2.6.2.6 for the definition of V_B. This may be taken as V_C is equal to $(V_B + 1.32U_{ref})$ providing that in doing so V_C does not exceed the maximum speed in level flight for the corresponding altitude. The definition of U_{ref} is to be found in Chapter 3, Section 3.5.3.3. Further, if the condition is at an altitude where the design speed V_D is limited by Mach number, V_C may also be Mach number limited. See Section 2.6.2.5 for the definition of V_D.

Far light civil aircraft (JAR-23) V_C (knots) is equal to $33(W/S)^{1/2}$ for W/S below 20 lb/ft^2 falling linearly to $28.6(W/S)^{1/2}$ for W/S of 100 lb/ft^2 (except for aerobatic aircraft where the value is $36(W/S)^{1/2}$ as a minimum value. W is the weight (lb), that is mg, and S is the reference wing area (ft^2).

In some military applications the speed V_H is used as an alternative, see the next section.

2.6.2.4 Maximum horizontal speed, V_H

The speed V_H is defined as the maximum speed attainable in level flight with powerplants set at the maximum continuous cruise condition. For a military type the aeroplane is assumed to he flying at the basic design mass with no external stores. For

aircraft designed for dive bombing or ground attack duties, V_H shall be assumed to be equal to V_D, see below.

2.6.2.5 Design (diving) speed, V_D

At one time the speed V_D was dehned as the maximum speed which the aircraft could attain in a dive of specified steepness. This is no longer a realistic definition due to the low drag characteristics of modem aircraft. In the case of civil aircraft designed to JAR-25 the definition depends on whether the aircraft is designed to operate into the transonic range or not. For an aircraft flying at relatively slow speed V_D may be set at $1.25V_C$ (or Mach number M_D at $1.25M_C$). However, this may well result in too large a margin for an aircraft designed to operate into the transonic speed range. In this case the value of V_D is estimated by either adding to V_C the speed increment resulting from a 7.5" dive from V_C sustained for 20 s and ending in a $1.5g$ total pull up, or providing sufficient margin to allow for contingences such as instrument errors and atmosphere variations. whichever is the greater. One critical atmospheric variation is a 15.2 m/s (50 ft/s) EAS horizontal, head-on, gust which implies a near instantaneous Mach number increment of about 0.05. Thus, even where compressibility effects limit the speed which can be achieved above the speed V_C, the value of M_D, cannot be less than $(M_C + 0.05)$ and the increment above M_C is more likely to be at least 0.07.

For light civil aircraft designed to JAR-23, V_D may not be less than 1.25 V_C (M_D not less than 1.25 M_C) or less than 1.4 V_{CMIN} for normal, 1.50 V_{CMIN} for utility, or $1.55V_{CMIN}$ for aerobatic category aircraft. V_{CMIN} is the minimum design cruising speed. For values of the wing loading, W/S, above 20 lb/ft^2 these multiplying factors are decreased linearly to 1.35 at W/S of 100 lb/ft^2. The method outlined above for larger aircraft may also be applied.

V_D is stated in the specification for military aircraft, its value being determined by the required operational characteristics as with civil aircraft.

2.6.2.6 Gust speed, V_B

The speed V_B is the design speed for the maximum gust intensity. V_B may be chosen to provide an optimum margin between the low- and the high-speed buffet boundaries, and it need not be greater than the speed V_C defined in Section 2.6.2.3. The civil aircraft requirements, JAR-25.335, at subparagraph (d) state that V_B may not be less than:

$$V_{BMIN} = V_{S1}(n_G + 1)^{1/2} \tag{2.3}$$

where n_G is the incremental load factor resulting from the aircraft encountering a gust of magnitude U_{ref} when flying at a speed V_C as estimated using an alleviated sharp-edged analysis, see Chapter 3, Sections 3.5.2 and 3.5.3. This is similar, but not identical. to the military speed V_G, see below.

V_{BMIN} need not exceed V_C. In order to determine V_{BMIN} the rough air gusting is assumed to be 20 m/s (66 ft/s) EAS between sea level and 6097 m (20 000 ft) then falling linearly to 11.6 m/s (38 ft/s) EAS at 15 240 m (50 000 ft). The possible overriding magnitude of 15.2 m/s (50 ft/s) EAS gust at speed V_C must be considered.

2.6.2.7 Gust speed, V_G (United Kingdom military aircraft requirements)

The definition of the speed V_G in Def.Stan.00-970 is somewhat similar to that of V_B but does depend on whether the maximum Mach number in horizontal flight is greater or less than unity:

(a) Aeroplanes where the speed V_H is equivalent to a Mach number of less than unity and other than weapon system aeroplanes; V_G shall be either the speed determined by the intersection of the line representing the maximum lift coefficient and the 20 m/s (66 ft/s) gust line on the $n-V$ diagram or $V_{SI}(n_G + 1)^{1/2}$ where here n_G is the incremental load factor resulting from a 15.2 m/s (50 ft/s) EAS alleviated sharp-edged gust when the aircraft is flying at speed V_H. See also Section 2.6.2.6 and Chapter 3, Section 3.2.3.

(b) Weapon system aeroplanes and others where the speed V_H is equivalent to a Mach number of one or greater; V_G shall be determined by the mission requirements, the permissibility of reducing speed and the slow-down speeds attainable, but V_G need not be greater than V_H.

2.6.2.8 Flap and high-lift device design speeds

A design flap speed. V_F, is defined in JAR-25 for each flap, or high-lift device. setting as not less than:

(i) 1.6 times the stalling speed at the maximum take-off mass with the high-lift devices in the take-off position; or

(ii) 1.8 times the stalling speed at the design landing mass with the high-lift devices in the approach (intermediate) position; or

(iii) 1.8 times the stalling speed at the landing mass with the high-lift devices in the landing position.

For military aircraft Def.Stan.00-970 gives the design speeds relevant for the various high-lift device settings. The speeds are:

(a) Retracted position: the design speed, V_D.

(b) Take-off position: the take-off speed, V_{TO}, which is the lesser of the speed attained before the high-lift devices can be retracted or 1.6 times the stalling speed at the maximum mass with the high-lift devices set at the take-off position.

(c) Intermediate position; the speed V_{BL}, which is the greater of the speed attained in a baulked landing before the high-lift devices can he retracted or 1.8 times the stalling speed at the landing mass with the high-lift devices in the intermediate condition.

(d) . Landing position; the speed V_{FL}, which is the greater of 1.8 times the stalling speed at the landing mass with the high-lift devices in the landing position or 1.4 times the stalling speed with the high-lift devices retracted.

CHAPTER 3

Flight loading cases

3.1 Introduction

The experience of a century of practical fixed-wing flight has resulted in comprehensive requirements for the safe design of aircraft structures. In many cases the individual provisions were made as a consequence of accidents in which aircraft encountered previously unrecognized flight conditions. There is now a substantial measure of consistency in the structural design codes for military and civil aircraft prescribed by the various relevant authorities. However, new or revised provisions are frequently introduced as a consequence of experience and research as well as for clarification of intent. It is essential that reference is made to the current issue of the relevant set of requirements for actual design calculations.

The following sections outline the loading cases prescribed for symmetric and asymmetric flight manoeuvers and atmospheric turbulence. Chapters 5 and *6* cover the interpretation and the application of the flight manoeuvre and atmospheric turbulence cases respectively.

3.2 Symmetric flight manoeuvres

3.2.1 Introduction

As implied by the title the symmetric flight cases are concerned with the design requirements for the strength of an airframe when it is subjected to loading in its plane of symmetry. In the case of **a** conventional aircraft or a twist and steer missile this loading is normal to the plane of the wings and in the case of a cruciform missile it also applies in the lateral direction.

3.2.2 Flight conditions in symmetric manoeuvres

The simplest case of a pilot- or auto-pilot induced manoeuvre is that of the vehicle changing from steady level flight to a climbing or diving path. In actual fact the greatest loads are likely to arise when the vehicle pulls out of a dive, or when it is in a correctly banked turn. The symmetric manoeuvre is a general case covering a number of specific loading conditions.

Consider the case of a conventional aircraft entering a dive from steady level flight as shown in Fig. 3.1. The pilot first moves the pitch motivator, usually the elevator or horizontal stabilizer, to induce a nose-down pitching acceleration. The resultant incremental loading is superimposed upon the steady condition. As the aircraft responds the motivator angle is reduced to stop the pitching acceleration. The aircraft gains a nose-down pitching velocity. q, causing it to fly on a circular path with a corresponding centrifugal load which has to be balanced by the lift. which in this case is negative rather than the usual upward lift. When the aircraft approaches the required angle of dive the pilot uses opposite motivator deflection to arrest the pitching velocity. At the end of the dive the reverse procedure is adopted.

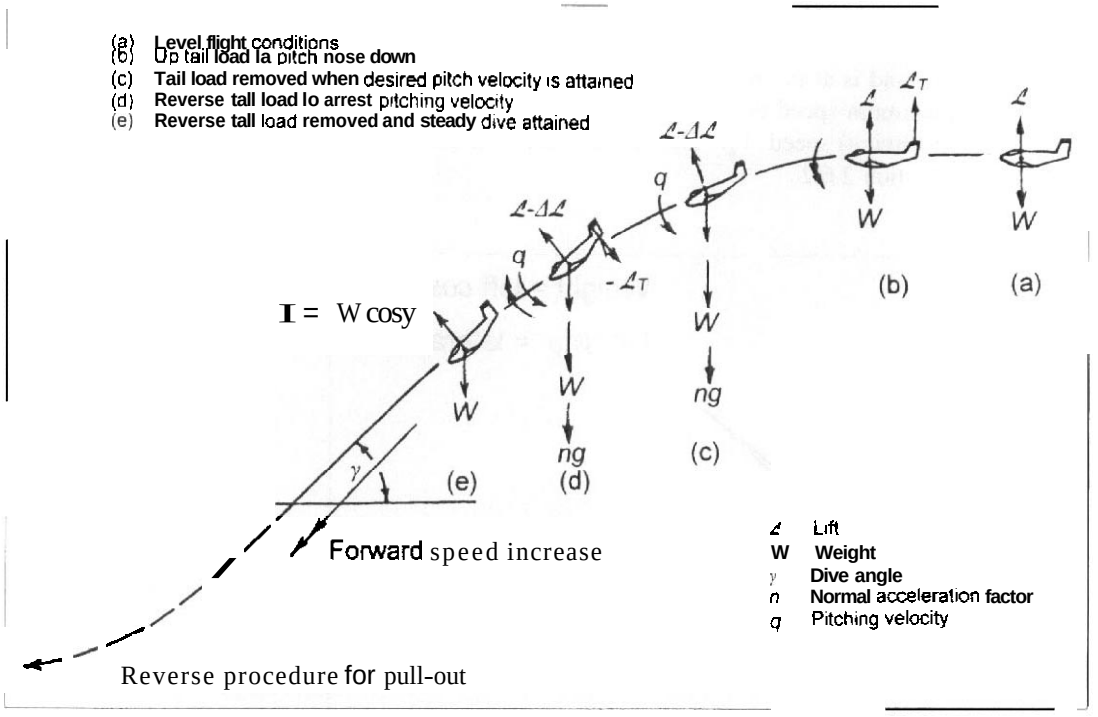

Fig. 3.7 *Sequence of a* symmetric *manoeuvre*

Thus, in general, the aircraft must be designed to withstand lifting loads greater or less than the weight, and with or without nose-up or nose-down pitching accelerations. Of course the speed will not necessarily remain constant and it is obvious that a very large number of possible cases can arise. As far as the lift on the wing is concerned the loading in a correctly banked turn is also effectively symmetric, see Fig. **3.2.**

3.2.3 The flight envelope or n–V diagram

A convenient way to describe the symmetric flight loading is to consider a Right envelope of forward velocity and acceleration perpendicular, or normal, to the flight path. The normal acceleration is simply the ratio of the lift to the mass in a given manoeuvre. This so-called 'n–V' diagram is illustrated in Fig. **3.3** and is arranged to give a set of cases that experience has shown are adequate for the design of the aircraft and its required performance. For convenience ***n,*** the normal acceleration factor. is specified in units of gravitational acceleration. In many operational circumstances the usual flight manoeuvre loads lie well within the boundaries of the envelope. However, in certain extremely improbable circumstances it may be possible to exceed the limits of the envelope and so, at least nominally, the 'n' boundaries are established by assuming that the probability of doing this is less than extremely remote, say no more than 1 in 10^7 to 1 in 10^8.

The left-hand comers of the $n–V$ diagram are determined by the stalling characteristics of the aircraft in both upright, that is normal, and inverted flight. The upper left-hand comer is the intersection of the stall line and the maximum normal acceleration factor, n_1, and is at the manoeuvre speed V_A. The right-hand comers are determined by the maximum speed conditions of the aircraft. the extreme right-hand side being the design (diving) speed. V_D. The actual definitions of the speeds may be found in Chapter 2, Section 2.6.2.

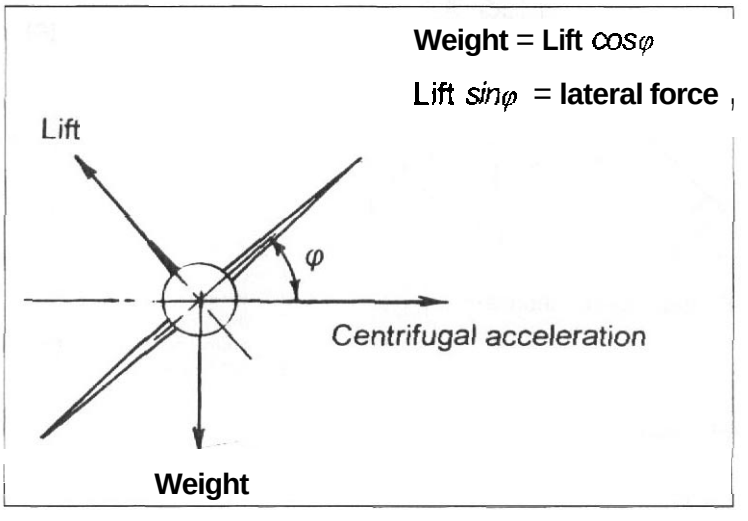

***Fig.* 3.2** *Correctly banked turn*

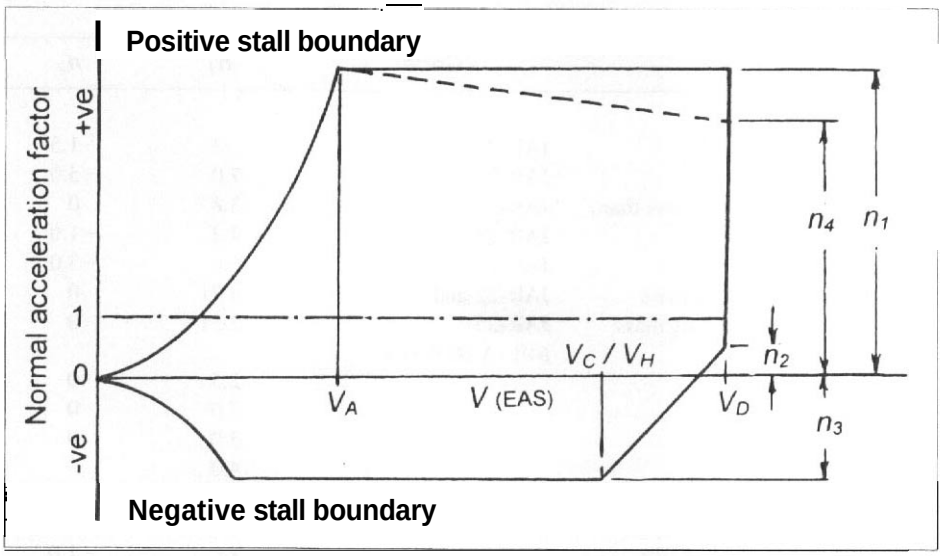

Fig. 3.3 A typical n–V diagram

There are potentially four definitive values of the normal acceleration factor in any given case although not all appear in all sets of requirements and the terminology sometimes differs. They are:

(i) n_1, the maximum positive, upright, value;
(ii) n_2, the lower normal acceleration factor at the speed V_D;
(iii) n_3, the maximum negative. inverted, value:
(iv) n_4, the maximum positive value at the speed V_D when it differs from n_1

In some structural design codes the values of the normal acceleration factors are specifically stated. In others, especially those relating to military aircraft, the value of the maximum normal acceleration factor, n_1, is quoted in the specification for the aircraft and the other values are determined from it. Table 3.1 is a summary of the normal acceleration factors to be found in the various design codes together with typical values where n_1 is given in the specification for the aircraft.

It should be noted that the speeds used in the diagram are equivalent airspeeds (EAS). This is because loads are directly proportional to the dynamic pressure which is half the product of the sea level air density and the square of the equivalent air speed, see Chapter 1 Section 1.5.2.

The $n–V$ diagram describes. all the points corresponding to every specified symmetric manoeuvre the vehicle is permitted to perform. The comers correspond to the maximum manocuvrcs permitted on the assumed probability of occurrence and consequently it is sufficient in general to examine only these comers when considering

Table 3.1 Limit normal acceleration factors (basic flight design mass)'

Class of aircraft	Code	n_1	n_2	n_3	n_4
Civil:					
Sailplane. normal utility	JAR-22	5.3	−1.5	−2.65	4.0
Sailplane. acrobatic	JAR-22	7.0	−5.0	−5.0	7.0
Very light aircraft (not less than)	JAR-VLA	3.8	0	−1.5	3.8
Utility	JAR-23	4.2	−1.0	−1.76	4.2
Aerobatic	JAR-23	6.0	−3.0	−3.0	6.0
Normal, up to 1860 kg mass	JAR-23 and	4.2†	0	−1.68‡	4.2
Normal, above 22665 kgmass	JAR-25	2.5†	0	−1.0	2.5
United States military:	MIL-A-008861A				
Strategic transport		2.5	0	−1.0	2.5
Assault transport		3.0	0	−1.0	3.0
Heavy bomber		3.0	0	−1.0	3.0
Medium bomber		4.0	0	−2.0	4.0
Trainer		6.0	−1.0	−3.0	6.0
Supersonic attack/interceptor		6.5	−1.0	−3.0	6.5
Subsonic attack/interceptor		8.0	−1.0	−3.0	8.0
United Kingdom military:	Def.Stan.00-970				
Strategic transport	(Typical specified	2.5	+0.25	−1.0	2.5
Tactical transport	values of n_1)	3.0	+0.1	−1.2	3.0
Medium bomber. in the range		4.0t05.0	+0.2 to −0.5	−1.8 to −2.4	4.0 to 5.0
Trainer		7.0	−1.1	−3.6	7.0
Supersonic interceptor		6.0	−0.8	−3.0	6.0
Subsonic ground attack		8.0	4 . 2	−4.2	8.0

'Reduced values of the acceleration factor are used for overload cases.
†For intermediate masses $n_1 = [2.1 + 24\,000/(10\,NO + 2.207\,m)]$ (m is mass in kg).
‡$n_3 = -0.4n_1$.

the loading cases. By this means the infinite number of possible manoeuvres to be considered can be reduced to a reasonable number of cases to be examined in detail.

It is, however, necessary to consider the possible variation of other parameters some of which may result in changes Io the boundary of the envelope. Among these are:

(a) Different engine conditions. Usually power on and power off is sufficient.
(b) All vehicle masses. Zero fuel or part fuel cases often design the inner wing structure of an aircraft with wing fuel tanks.
(c) All possible centre of gravity positions corresponding to a particular vehicle mass. It is usually adequate to consider the most forward and aft positions.
(d) All possible Mach number combinations relating to the equivalent airspeed condition considered. Mach number effects can alter not only the magnitude of the load but also the distribution of the load over the vehicle surfaces and may introduce the effects of temperature. In the case of supersonic aircraft it is

sometimes necessary lo specify a flight path to cover the effect of altitude change and to base the design of the aircraft on this.

(e) All positions of high-lift devices, undercarriage, and air brakes must be considered. Extension of high-lift devices changes the stall boundary.

(f) The effect of any boosting device must he investigated.

3.2.4 Pitching conditions

There are two aspects of the pitching conditions.

(a) *Steady pitching velocity.* A steady pitching velocity has to be considered at all points on and within the boundary of the flight envelope. The value to he used in any given condition is that appropriate to the relevant normal acceleration factor and forward speed.

(b) ***Pirching accelerarion.*** The specification of the pitching acceleration to be superimposed on the normal acceleration can be complex and, in general, requires a knowledge of the control, aerodynamic, and inertial characteristics of the vehicle. It may he specified in either of two ways:

(i) By specifying the control system demands made hy the pilot or autopilot. The movement may be in terms of control inputs, 'inceptor' signals, for example control column movement, or autopilot input.

(ii) By specifying the required pitching acceleration as a function of normal acceleration and speed, as appropriate. This is sometimes done for simple aircraft and is also appropriate for advanced aircraft with active controls where the control system is used to place boundaries on the manoeuvre parameters. A typical design envelope for an interceptor is shown in Fig. 3.4. See also Chapter 5, Section 5.3.2

The actual design conditions are considered in Chapter 5, Section 5.2.1, but one important ovemding case is the requirement to consider the loads which arise when the aircraft is in steady level flight at the manoeuvre speed, V_A, and the pitch motivators are moved suddenly to cause a positive (nose-up) or negative (nose-down) pitching acceleration, limited only by the available motivator deflection, pilot or actuator effort, or the design of the control system.

3.3 Asymmetric flight manoeuvres

3.3.1 Introduction

The loading cases in the asymmetric planes are concerned with rolling, yawing. and sideslip motions as well as combinations of these with symmetric loads. In general these loads arise from pilot-initiated manoeuvres or engine failure. The response of the vehicle in an asymmetric manoeuvre is treated in a way similar to that of a symmetric manoeuvre, hut may well be complicated by the coupling which can occur between all six degrees of freedom.

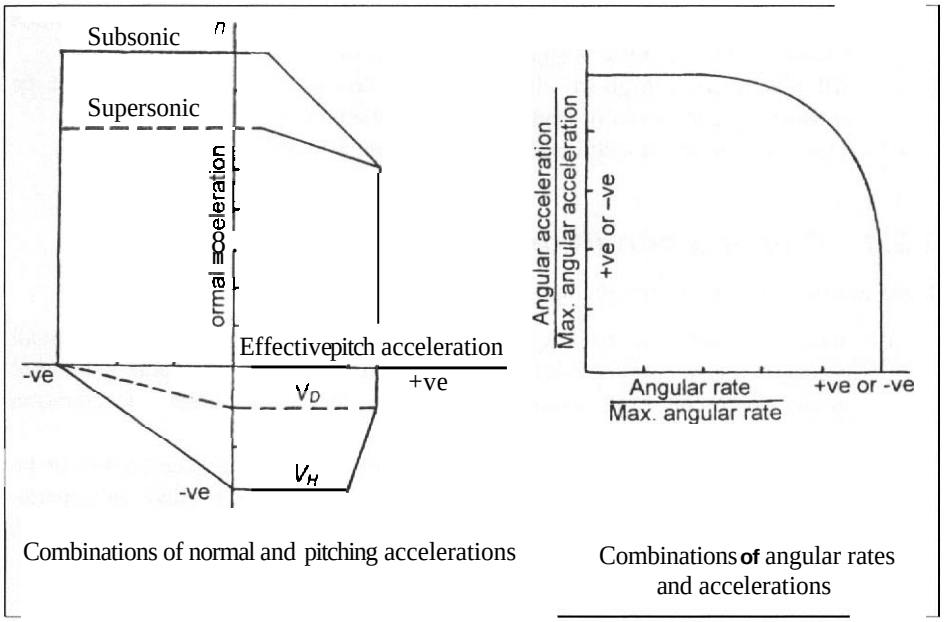

Fig. 3.4 Active *control* System symmetric ***manoeuvre*** *limits*

3.3.2 *Rolling cases*

3.3.2.1 Introduction

For an aircraft of conventional layout it is often acceptable for the roll performance and corresponding loads to be considered in isolation from the yawing motion. An exception to this is an aircraft having a low aspect ratio, highly swept, wing where the roll–yaw–pitch coupling demands a complete six degree of freedom analysis. In this case a first estimate of loads can be found by considering the roll–yaw interaction, and assuming pitch control is used to decouple the pitching motion. United Kingdom military requirements make specific provisions for this situation.

3.3.2.2 Roll considerations

There are no isolated roll loading cases as such, rolling load cases always being associated with symmetric loading conditions. It is necessary to refer to roll performance requirements to establish the capability of the roll motivators, typically the ailerons, to provide some basic design data. This is because the loads arising during rolling are a direct result of the roll motivator capability defined by the required roll performance.

Roll performance requirements can be divided into two main categories:

(a) ***Low-speed handling,*** especially the need to be able to rapidly lift a wing during approach to landing or in the event of a powerplant failure.

(b) ***High-speed handling.*** especially for combat aircraft. It should be noted that at high speed there is a significant aeroelastic distortion of a wing which results in a reduction of aileron effectiveness relative to the rigid condition. However, as the specified conditions relate to rates of roll, the overall loading is not affected by this unless there is a restriction on the motivator application force.

A summary of roll performance requirements is given in Appendix A3.

3.3.2.3 Rolling manoeuvre conditions

A rolling manoeuvre has to be analysed at three or four specific stages. These are illustrated in Fig. 3.5.

(a) Roll initiation due to an instantaneous or rapid roll motivator application, the resulting rolling moment being represented by L_ξ. The result is an initial roll acceleration at effectively zero roll rate.

(b) The steady roll rate state achieved when the roll damping moment of the aircraft. represented by L_{pp} is numerically equal to. and balances, the applied increment in rolling moment.

(c) The start of roll termination when the applied rolling moment, L_ξ, is removed so that a roll deceleration is imposed upon the steady roll rate as a consequence of the moment represented hy L_p.

(d) A reverse roll which is similar to case (c) except that the motivators are moved to give an equal rolling moment to the original value hut in the opposite sense. This case only applies to military combat types and results in a roll acceleration which is numerically twice that of the initial value due to algebraic sum of the representative moments L_p and $-L_\xi$.

3.3.2.4 Combined roll and pitch manoeuvre

Specific loading conditions are prescribed when a rolling manoeuvre is combined with a pitching manoeuvre. It is often assumed that the two effects can be analysed separately and the results superimposed in appropriate proportions. The symmetric part is analysed with a prescribed value of normal acceleration, the aircraft being assumed to be in a steady manoeuvring, zero pitching acceleration. condition. The additional effect of an appropriate application of roll motivators is then added.

The requirements usually specify that throughout the manoeuvre the yaw motivators are either held fixed in the position required to trim the aircraft wings level. or deflected to minimize any sideslip angle. When airbrakes are fitted the analysis should include

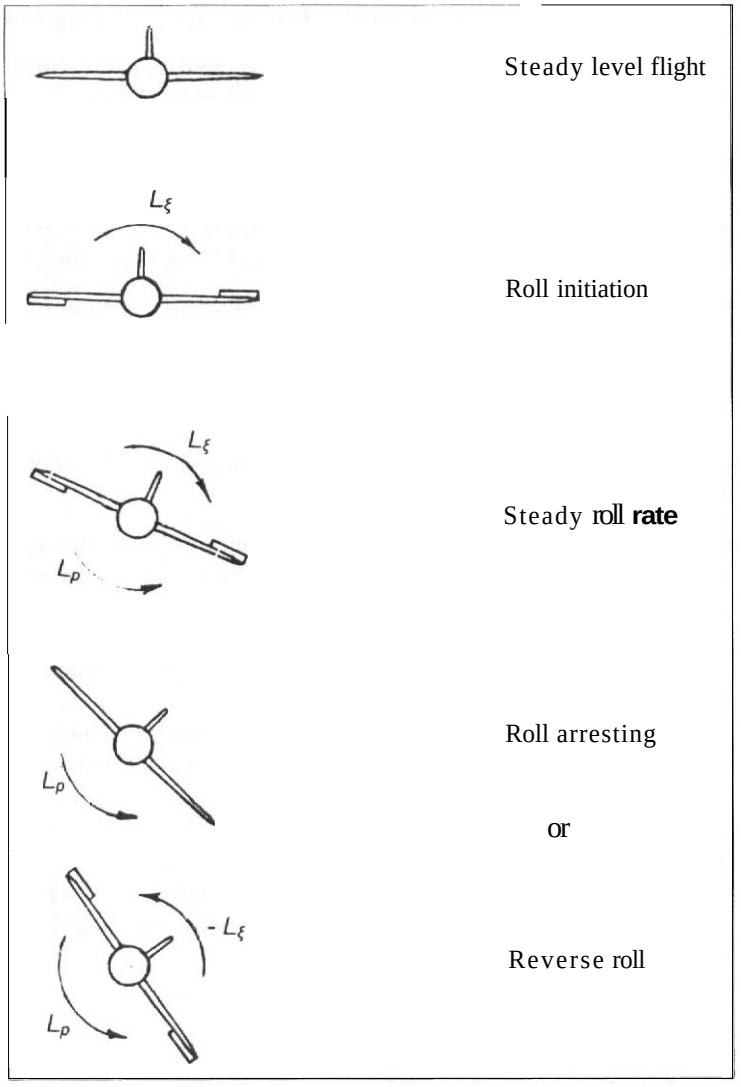

Fig.* 3.5 *Phases of a roll manoeuvre

both the open and closed settings. All flight speeds up to V_D and all altitudes must be covered.

The roll motivator deflections to be used are those corresponding to the most critical of:

(a) The deflection, or set of deflections, which results in one-and-a-third times the specified minimum rolling performance at that speed and altitude (see Appendix A3).

(b) The following deflections:
  (i) at speed V_A – the full available deflection(s) as defined in (a) ahove;
  (ii) at speed V_C/V_H – the deflection(s) required to give the steady roll rate which occurs in the condition at speed V_A;
  (iii) at speed V_D – the deflection(s) required to give one third of the steady roll rate which occurs in the condition at speed V_A.

(c) For combat aircraft the deflection, or set of deflections, given by whichever of the following is appropriate to the particular design:
  (i) that corresponding to the maximum output permitted by the flight control system by the power unit of a single roll motivator. or of the individual power units for a number of roll motivators used in combination;
  (ii) where the motivators are driven solely by the deflection of the pilot's stick or wheel, that corresponding to a control force of 267 N (60 lbf) for a stick control or 222 N (50 lbf) applied to the rim of a wheel of diameter D m or (D in), resulting in a couple of magnitude $222D$ N m or (50 D lbf in). In applying these conditions the accuracy with which the actual hinge moments of each individual motivator may be predicted may sometimes he such that doubts arise as to the magnitude of the deflections so defined. The assumed deflections are to he increased by 30 per cent in such cases:
  (iii) if the deflection (or any one deflection), so defined, exceeds that for full travel, it is replaced by the maximum available deflection.

For the roll motivator deflections prescribed above, a range of normal accelerations have to be considered:

(i) transport aircraft – 0 to $0.67n_1g$;
(ii) other aircraft – $1.0g$ to $0.67n_1g$ and in addition motivator deflections of one-half of those prescribed above are to be combined with a normal acceleration of $0.9n_1g$, with linear variation between $0.67n_1g$ and $0.9n_1g$.

In some requirements there is a statement of the need to allow for structural distortion resulting from aileron application.

In the case of the light aircraft requirements, JAR-23, there are somewhat different requirements. Similar roll/pitch conditions as those above are given as one design case. However, for wing design it is also required that a condition of 100 per cent load on one side of the aircraft should be combined with 75 per cent on the other side (60 per cent on aerobatic designs), which may override the more conventional condition.

3.3.3 Yawing/sideslip manoeuvres

3.3.3.1 General considerations

In the case of manned aircraft it is usual to assume that yaw motivator induced loading cases occur when the aircraft is initially, and remains, in steady level flight. The

exception of low aspect ratio, highly swept layouts is referred to in Section 3.3.2.1 where the pitch–yaw coupling may result in a departure from steady level flight.

The specified cases relate to the deflection of the rudder, or other yaw motivator, through angles which may be limited in some way by available travel or applied hinge moment. The actual motivator deflection required in a given condition is determined by performance requirements, such as handling in cross-winds, after powerplant failure at low speed or combat manoeuvre at high speed. Frequently the application of the full theoretically available deflection at high speed gives rise to manoeuvres which are more severe than is needed and consequently to unnecessarily high loads. Some form of limitation of the movement is then desirable. This can be done by limiting the available control motivator operating force, by introducing a gearing which is variable with speed or Mach number to reduce the allowed deflection appropriately, or by limiting the control demands in an active control system.

The determination of the necessary motivator deflection at high speed is not always easy. Considerations which may assist in determining rudder deflection limitation are:

(a) It must not be possible to stall the fin dynamically as a consequence of rudder application. The fin dynamic stall angle may be up to 1.5 times the static value. A dorsal fin assists in delaying fin stall if it is of consequence.

(b) Lateral manoeuvre acceleration is limited by occupant tolerance. A rather arbitrary figure sometimes used is that the maximum lateral acceleration at the head of the pilot should not exceed 2g. This applies only to a high-performance combat aircraft and is a severe condition.

(c) An automatic control system may incorporate some form of fin load limiting system. The value of this maximum limited load is a matter of design decision, but experience suggests that it is unlikely that operational requirements will require a load greater than about $(n_1 mg/8)$ where n_1 is the maximum normal acceleration factor and m is the normal take-off mass.

(d) In a fully active control system it is usual to specify appropriate combinations of normal acceleration with lateral and yaw rates and accelerations, as is illustrated in Fig. 3.6.

3.3.3.2 Instantaneous rudder deflection

One class of lateral loading case is associated with a step input of the rudder, or other yaw motivator.

In a way similar to that for the roll case, the resulting manoeuvre is evaluated for the following stages. as shown in Fig. **3.7.**

(a) Fin and rudder load, and corresponding lateral and yaw accelerations, at the instant the motivator is applied with the aircraft assumed to be initially in straight and level flight. This often gives the rudder design case. The side force due to the application of the rudder is represented by Y_ξ, and this results in a yawing moment represented by N_ξ.

(b) The corresponding loads and accelerations when the sideslip has reached the maximum 'over-swing' angle, β_{MAX}, in the resulting dynamic motion. This corresponds to a lateral velocity of v_{MAX}. The angle of attack of the fin gives

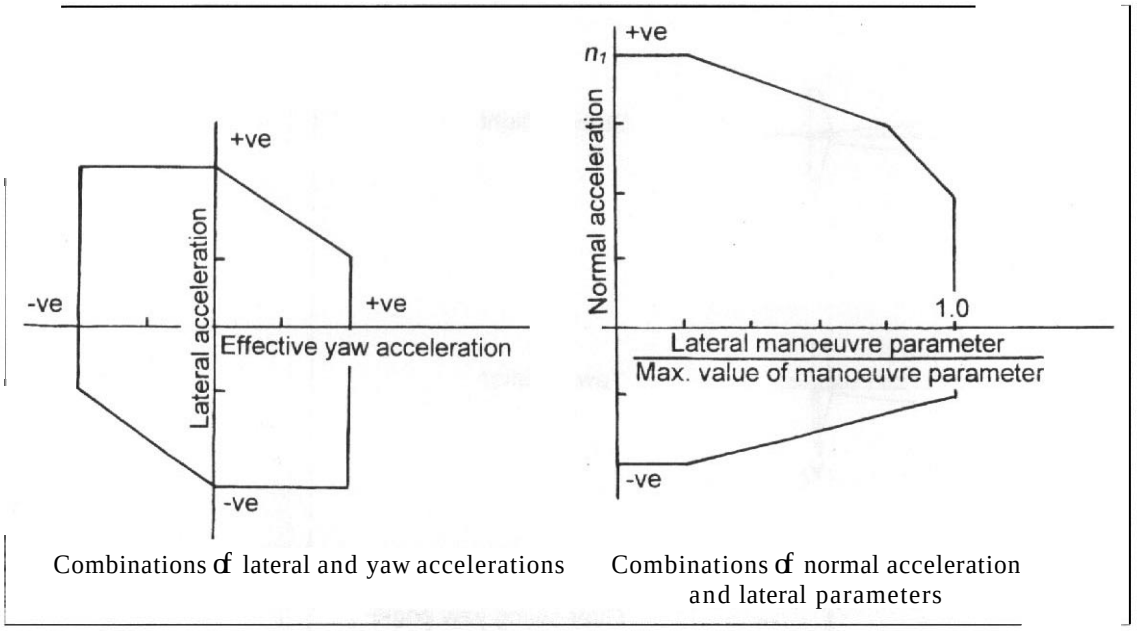

Fig. 3.6 Active *control system* directional manoeuvre limits

rise to a representative side force of $Y_{\beta MAX}$ and its associated yawing moment. It is sometimes assumed that β_{MAX} is 1.5 times the steady sideslip angle. β_E, which occurs when the moment about the centre of gravity due to the deflection of the rudder is equal, but of opposite sign, to that due to the resulting sideslip angle on the whole aircraft. However, the value is often somewhat less than 1.5 and it is not difficult to evaluate. This case may give a design vertical stabilizer load case and certainly is severe in torsion. Figure 3.8 illustrates the motion during a sideslip manoeuvre.

(c) The equilibrium condition referred to in (b) which does not usually give rise to a load case. The sideslip angle, β_E, corresponds to a lateral velocity, v_E, and the fin side load is represented by $Y_{\beta E}$. The overall aircraft yawing moment $N_{\beta E}$ balances the rudder imposed yawing moment of N_ξ.

(d) The yaw arresting case where the motivator deflection is returned to the neutral position and the aircraft starts to return to straight flight under the effect of the yawing moment $N_{\beta E}$. This may give the vertical stabilizer design case.

3.3.3.3 Oscillation of **yaw** motivator

A second case, which is especially, hut not exclusively, appropriate to military aircraft, is the loading which arises when the motivator is moved in oscillatory fashion at the damped natural frequency of the aircraft in yaw. This gives rise to a so-called 'fish-tail' aircraft

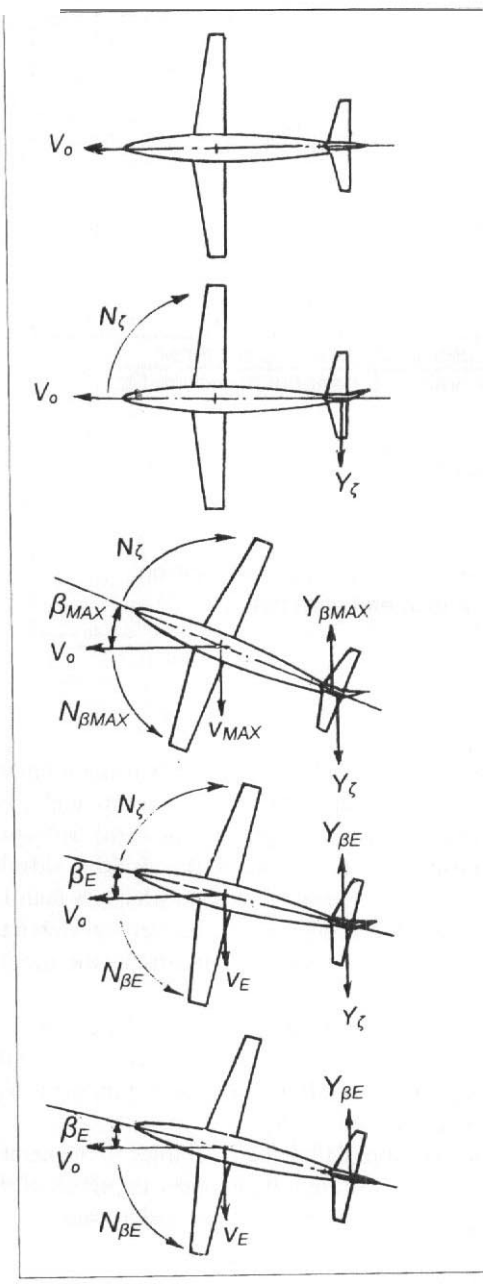

Straight flight

Yaw initiation

Over-swing yaw angle

Equilibrium sideslip angle

Yaw arresting

Fig. 3.7 ***Phases of a yawing manoeuvre***

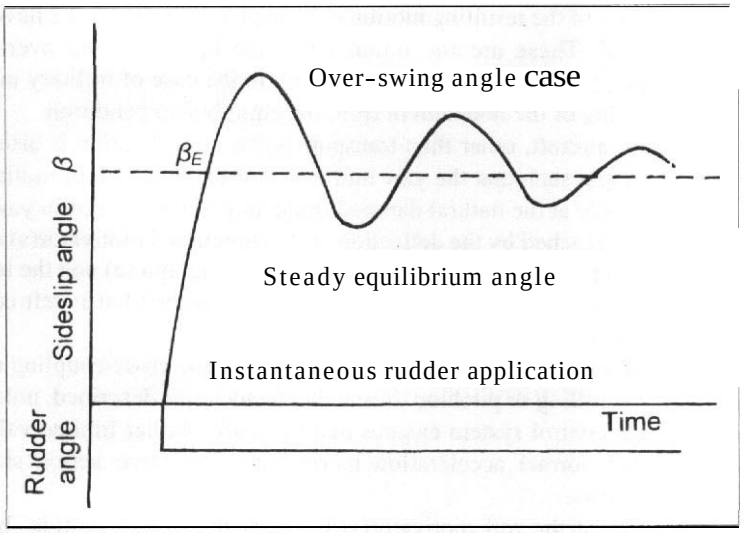

Fig. 3.8 Variation of sideslip angle in a yawing manoeuvre

manoeuvre which is used primarily as an evasive tactic in combat. Since the resulting vertical stabilizer and rudder loads and overall accelerations will continue to increase with time it is necessary to prescribe a limit to the motion. This limit is normally one-and-a-half cycles for combat aircraft. When it is required, this condition almost invariably gives rise to the maximum fin and rudder loads. See also Chapter 5, Section 5.5.1

3.3.3.4 Yaw motivator induced lateral manoeuvre cases

The initial flight is assumed to be steady and the bank and sideslip angles zero. The loading must be analysed at all altitudes and all speeds between the minimum control speed V_{MC}, and design speed V_D/M_D.

(a) The input from the pilot's inceptor shall be such that, in the absence of response of the aeroplane, it results in an effectively instantaneous application of the yaw motivator(s). The deflection(s) of the yaw motivator(s) is (are) determined by the following considerations, whichever yields the critical case for a particular aeroplane.

(i) that corresponding to the maximum output permitted by the flight control system by the power unit of each control motivator, or the maximum limited deflection at a given speed;

(ii) When the motivator(s) is (are) activated through the deflection of **pedals,** the specified deflection(s) shall be that corresponding to a total pedal force of 1334 N (300 lbf) from the minimum control speed, V_{MC}, to the manoeuvre speed, V_A, and 890 N (200 lbf) from the cruise speed, V_C/V_H, to the design speed, V_D, with linear variation between V_C/V_H and V_D.

The phases of the resulting motion described in Section 3.3.3.2 have to be considered. These are the initial zero sideslip angle, the over-swing condition, the equilibrium condition and, in the case of military aircraft, the arresting of the manoeuvre from the equilibrium condition.

(b) For all military aircraft, other than transport types, consideration is also to be given to pilot input such that the yaw motivator, or combination of motivators. moves sinusoidally at the natural damped frequency of the aircraft in yaw. The maximum value reached by the deflection of the directional motivator(s) during this process is to he two-thirds of that specified in paragraph (a) and the input is lo consist of one-and-a-half cycles of the pilot's inceptor (that is left-central-right-central-left-central).

(c) For those military aircraft where inertial or aerodynamic cross-coupling results in the aeroplane rolling or pitching during the manoeuvres described, unless the aeroplane flight control system ensures that there are smaller limited values of bank angle and normal acceleration increments, corrective action shall be assumed as follows:

(i) deflection of the roll motivator(s) to arrest the rolling motion, but not until the angle of bank has reached 15" or the maximum dynamic sideslip angle is achieved;

(ii) deflection of the pitch motivator to reduce the pitching response, hut not until the increment in normal acceleration has reached $0.25g$.

For light aircraft the equilibrium yaw angle condition is replaced by a 15" yaw angle condition, unless pilot effort is insufficient to maintain this angle.

3.3.3.5 Horizontal stabilizer loading in yawed flight

When the aircraft is in a sideslip condition or is subjected to a horizontal gust, see Section 3.5.4, the lift distribution on the horizontal tail surface becomes asymmetric. This arises because of the tendency of the vertical stabilizer and body to partially blank off one side of the horizontal stabilizer. This is particularly important when the tail-plane is mounted on the fin because the implied tail-plane rolling moment always adds to the fin bending moment. The condition is likely to give the critical rear fuselage torsion loading. Slipstream or jet efflux can give a similar asymmetric loading.

When the aircraft is in a sideslip the lateral component of the velocity affects the aerodynamic characteristics of the whole aircraft, not just the empennage. In particular it may be expected that the wing–body zero-lift pitching moment will be changed, resulting in a change in the horizontal stabilizer load relative to the level flight trimmed condition. see Chapter 4, Section 4.2.1. United Kingdom military requirements suggest that in evaluating the horizontal stabilizer loads required to trim the aircraft in a sideslipping manoeuvre the value of C_{M_0}, the pitching moment coefficient at zero lift, should be increased by (-0.0015) per degree of sideslip relative to the value for straight flight.

3.4 Engine failure cases

Failure of a powerplant on a multi-engined aircraft will generally give rise to a yawing moment which results in a sideslipping motion in just the same way as that due to yaw motivator deflection. It is essential to ensure that the loads resulting from the failure of one or more engines do not overload the airframe and that adequate rudder control is available to correct swing and maintain a straight path. With any one engine failure it is required that the rudder trim is capable of trimming the aircraft for straight flight. The sideslip angles resulting from a sudden engine failure can he estimated from a response calculation. The maximum sideslip, side gust, or cross-wind take-off cases are usually more critical than the engine failure cases, except possibly when the engine? are mounted well outboard. A general coverage of powerplant loads is to be found in Chapter 8, Section 8.5.

3.5 Atmospheric turbulence and gusts

3.5.1 Introduction

The cases considered in Sections 3.2 and 3.3 deal with the loading conditions where the manoeuvres have been imposed by the pilot or autopilot. However. accelerations are also experienced by a vehicle when it encounters variations in conditions in the air such as changes in wind direction, velocity, and general turbulence.

Sudden changes are known as discrete gusts, and velocity variations of over 20 m/s (66 ft/s) EAS have been measured. Discrete gusts are often encountered while flying low over mountainous country or through the tops of clouds, particularly of the cumulo-nimbus variety. Gusts of considerable intensity can be associated with the vehicle flying into a 'jet-stream' which is a region of air moving at a speed greater than the surrounding atmosphere. Apart from discrete gusts there is also the possibility of a general turbulence of the atmosphere.

Since gusts are natural phenomena and depend largely on the general weather conditions and the time of the year it is possible for a particular vehicle to operate for its complete lifetime without encountering any severe discrete gusts, say greater than 12 m/s (40 ft/s) EAS, in contrast, the next aircraft off the production line might meet a 15 m/s (50 ft/s) EAS gust during the initial flight trials. Even so, the cumulative effect of gusts and general turbulence in damaging the structure might well be more on the first aircraft during the whole life period. For this reason some of the design 'codes require that the aircraft is designed to he able to withstand the cumulative effects of both discrete gusting and continuous atmospheric turbulence.

The earliest design cases for discrete gusts were derived by 'reverse engineering' from measurements made on transport aircraft during normal operations. The result was expressed in terms of a 'sharp-edged' gust to which an 'alleviating factor' was incorporated to allow for the characteristics of individual aircraft. This required an assumption of the dynamic characteristics of the sample aircraft and was not entirely satisfactory. As the analysis was refined, provisions were added to the requirements to

ensure that the most critical case for a given gust intensity and particular aircraft was considered. This was achieved by deriving a 'tuned' gust, that is, one where the length of the gust build-up, or 'gradient', yields the most severe loads in a particular case.

3.5.2 Representation of gusts

3.5.2.1 *Discrete* gusts

Discrete gusts are assumed to build up from zero to a maximum intensity over the gradient distance in the form of a cosine function:

$$U = U_{de}\{1 - \cos(\pi s/\ell)\}/2 \qquad \text{for } 0 > s > 2\ell \tag{3.1}$$

where

U_{de} is a given design gust value which is a function of forward speed
ℓ is the gradient distance over which U_{de} builds up from zero to the maximum value
U is the gust velocity at a distance, s, into the gust

Figure 3.9 illustrates the motion of an aircraft as it encounters a discrete gust.

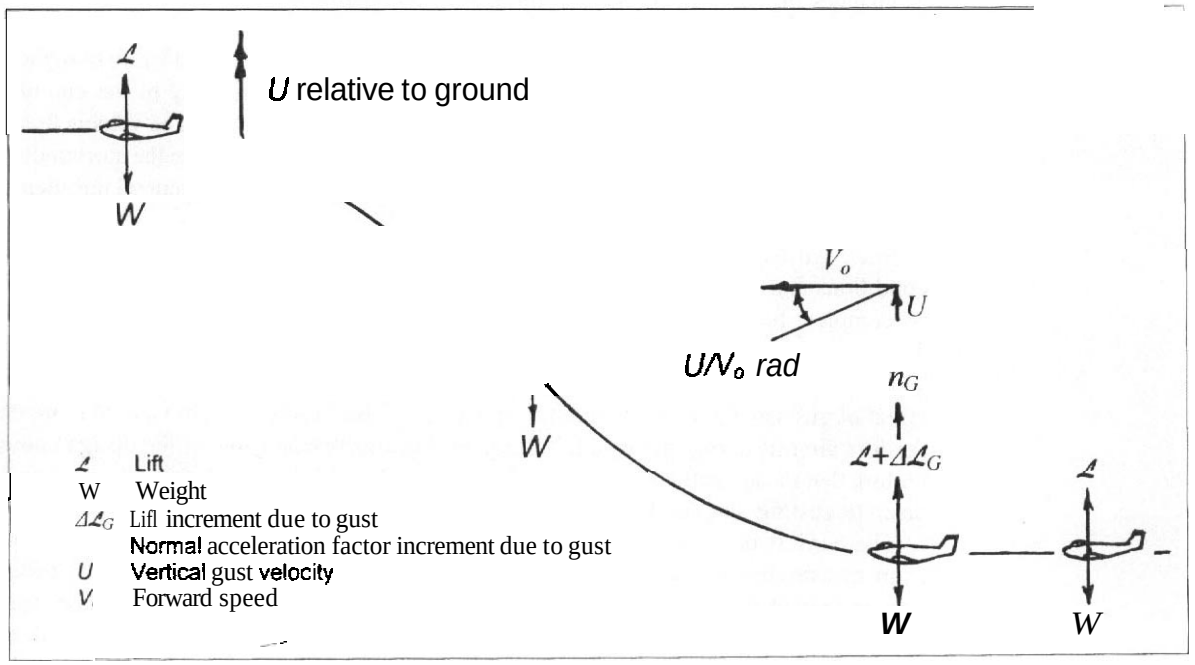

Fig. 3.9 Sequence of an encounter with a vertical gust

An approximate analysis can be used for some initial design work. The method is based upon the concept of the sharp-edged gust, that is. a gust arising from an instantaneous change in the velocity of the air. Such a gust may well induce bigger loads on the vehicle than the more gradual specified gust and consequently an alleviating factor is applied to the design gust velocities to compensate for this. The alleviating factor depends upon the response of the individual vehicle to the gust. The wing loading, mean chord, and lift curve slope are the main parameters in the case of a vertical gust. When an aircraft of unconventional layout, for example a canard configuration, enters a gust the loads may be greater than a sharp-edged analysis would indicate, so that the factor becomes a magnifying rather than an alleviating one.

The velocity of the alleviated sharp-edged gust is defined as FU_{de} where F is the alleviating factor. The alleviating factor for vertical gusts, F_1, is expressed as a function of a mass parameter:

$$\mu_{G1} = 2m/(\rho S c a_{1WB}) \tag{3.2}$$

where

c	is the wing mean chord
ρ	is the local air density at the altitude of flight, not the sea level value
a_{1WB}	is the lift curve slope of the wing-body combination (per radian). This is influenced by sweep and aspect ratio as well as Mach number
m	is the mass of the aircraft
S	is the reference wing area

Originally the values of F_1 were established by assuming that the critical value of the gradient length, ℓ, was $12.5c$ and then:

$$F_1 = 0.88\mu_{G1}/(5.3 + \mu_{G1}) \tag{3.3}$$

This assumption was associated with a statement of the design values of U_{de} as:

At the rough air speed (V_B or V_G), $U_{de} = 20$ m/s
At the normal operating speed (V_C or V_H), $U_{de} = 15.2$ m/s
At the design speed (V_D), $U_{de} = 7.6$ m/s

It may be erroneous to use these gust design values with methods of analysis other than the alleviated sharp-edged gust concept. In any case it only applies to aircraft of conventional layout. See Chapter 2, Section 2.6, for the definition of forward speeds.

The altitude and speed of the vehicle are assumed to remain constant during the time required for the gust to build up. The pilot is normally assumed to take no action to move the pitch motivator from the condition appropriate to steady level flight. The output of the alleviated sharp-edged gust analysis is the normal acceleration increment consequent upon the aircraft encountering the gust. It is possible to derive a gust

envelope to compare with the manoeuvre $n-V$ diagram as discussed in Chapter 6, Section 6.2.

3.5.2.2 The tuned gust approach

The response, or time history, of the vehicle when it encounters a discrete vertical gust is similar to that which occurs when the pilot or autopilot applies pitch control, see Fig. 3.9. The calculations needed to estimate the most severe loads are complex and lengthy. The analysis of the response of the vehicle involves the solution of the relevant equations of motion for the vehicle with the input conditions corresponding to the gust build-up shape and should include unsteady effects and airframe flexibility. It is necessary to consider discrete gusts having various gradient distances to ensure that the worst case is obtained, the worst case being the tuned gust appropriate to that aircraft and flight condition. The analysis is discussed in Chapter 6, Section 6.3, but in all cases the discrete gust is assumed to have a velocity contour as defined by Eqn. (3.1).

3.5.2.3 Continuous turbulence

The representation of continuous turbulence is more complex due to the random nature of the effects. One approach is to define a power spectral density to describe the turbulence. Two such definitions are used for aircraft, namely, the von Karman and Dryden expressions. The analysis required is described in FAA-ADS-53 and 54 and is summarized in JAR-25.ACJ 341. The background and the procedure for analysis are covered in Chapter 6, Section 6.4. The method is based on the prediction of the aircraft response to the power spectral density (PSD), this response being defined as:

$$\bar{A} = \sigma_y / U_\sigma \tag{3.4}$$

where

U_σ is the true root mean square (r.m.s) gust velocity
σ_y is the r.m.s value of the response of the aircraft, which can be one of various parameters such as acceleration, rate, or displacement

There are two ways of interpreting the results of the analysis:

(a) ***Design envelope analysis.*** This is equivalent to the alleviated sharp-edged or tuned gust approach in that the output is in the form of normal acceleration increments, and other relevant parameters, due to the turbulence in terms of the specified input conditions. The specified numerical design values of the gust differ from those used for the traditional analysis, but are related to them. The datum value of U_σ is defined as 25.91 m/s (85 ft/s) true speed in the altitude range up to 9144 m (30 000 ft) falling linearly to 9.14 m/s (30 ft/s) at 24 384 m (80 000 ft) altitude. These may be reduced to 22.86 and 9.14 m/s, respectively, if these lower values can be shown to he adequate. The datum value of U_σ is

applied at the forward speed V_C with $0.5U_\sigma$ at speed V_D and $1.32U_\sigma$ at speed V_B. See also Section 3.5.3.

(b) *Mission analysis.* One or more flight profiles have to be defined and each divided into segments having average values of such parameters as speed, altitude, and centre of gravity position. For each of these segments $\bar{A}$ and N_o are determined. N_o is the radius of gyration of the load power-spectral density function about zero frequency, see Chapter 6, Section 6.4.2.2. For each load and stress quantity selected, the frequency of exceedance is determined as a function of the load level. The limit gust loads are determined from the frequency of exceedance by selecting a design frequency of cxceedance of 2×10^{-5} exceedances per hour of flight for a civil transport. Both positive and negative loads have to be considered. When gust alleviation systems are used the flight profiles selected should allow for possible periods of system inoperation and the effects of stability augmentation have to be accounted for.

When the mission analysis approach is used it is also necessary to undertake a supplementary design envelope analysis, similar to that of paragraph (a) above, where the design gust values are reduced. The 25.91 and 9.14 m/s gust velocities are reduced to 18.29 and 7.62 m/s, respectively.

3.5.3 Gust and turbulence requirements

3.5.3.1 General

There are differences in the various design codes with regard to the specification of gust loading, in particular with respect to the requirement for continuous gust analysis.

Application of discrete gust cases is usually based on the assumption that the aircraft is in steady, level, unaccelerated flight when it encounters a vertical gust increasing from zero to the design value in accordance with Eqn. (3.1). An exception to this is the case of a terrain-following military aircraft when a gust of 7.6 m/s is assumed to occur at the same time as a manoeuvre of $0.6n_1$. Otherwise the following conditions apply, all speeds and velocities being equivalent airspeed (EAS).

3.5.3.2 Military requirements

The United Kingdom requirements are based exclusively on discrete gusts modified by the alleviating factor of Eqn. (3.3) and tuned gust analysis:

(a) At *speed* V_G. A gust velocity of 20.0 m/s (66 ft/s) between sea level and 6100 m (20 000 ft) and then decreasing linearly to 11.6 m/s (38 ft/s) at an altitude of 15 200 m (50 000 ft) being constant thereafter.

(b) *At speed* V_H. A gust velocity of 15.20 m/s (50 ft/s), between sea level and 6100 m (20 000 ft) and then decreasing linearly to 7.60 m/s (25 ft/s) at an altitude of 15 200 m (50 000 ft), being constant thereafter.

(c) *At* speed V_D. A gust velocity of 7.60 m/s (25 ft/s) between sea level and 6100 m (20 000 ft) and then decreasing linearly to 3.80 m/s (12.5 ft/s) at 15 200 m (50 000 ft), being constant thereafter.

The relevant flight speeds are defined in Chapter 2, Section 2.6. The effect of gusts occurring between the design speeds has to be considered, with linear variation of design gust velocity between them. The cases apply for all masses between the maximum mass at which the aircraft can reach the altitude considered and the minimum flying mass. Engine conditions must be appropriate to the design condition.

The United States MIL-Specs are similar but also allow for the application of continuous turbulence analysis where this is required by the contract and introduce a different alleviating factor at supersonic speed.

3.5.3.3 European transport aircraft requirements

For transport category aircraft the European requirements in JAR-25 are comprehensive. The following provisions apply:

JAR 25-341 is concerned with the definition of gust loading, subparagraph (a) of JAR 25-341 being concerned with discrete gust analysis and stating that a full dynamic analysis, the 'tuned gust' method, must be used. including unsteady aerodynamic effects. The specified gradient lengths vary from 106.7 m (350 ft) down to 9.15 m (30 ft).

(a) For gusts with 106.7 m (350 ft) gradient length the following reference discrete gust velocities are to be applied:
  (i) *aircraft* speed V_C. Positive and negative reference gust speed, U_{ref}, of 17 m/s (56 ft/s) EAS at sea level decreasing linearly to 13.4 m/s (44 ft/s) EAS at 4600 m (15 000 ft) altitude and then to 7 m/s (26 ft/s) EAS at 15 200 m (50 000 ft) altitude.
  (ii) *aircraft* speed V_D. 0.5 times that at speed V_C.

(b) For gusts with gradient lengths less than 106.7 m (350 ft) the reference gust velocities may be reduced below U_{ref} to a value U_r, proportional to the sixth root of the gradient distance, that is:

$$U_r = U_{ref}(\ell/350)^{1/6}$$

where ℓ is the gradient length (ft).

The design gust velocity U_{de} is related to the reference gust velocity by the flight profile alleviation factor, F_g:

$$U_{de} = F_g U_{ref} \quad \text{or} \quad F_g U_r \quad \text{as appropriate}$$

where

F_g $= 0.5\,(F_{gz} + F_{gm})$ at sea level and
$= 1.0$ at the operating altitude, with linear variation in between

F_{gz} $= 1 - Z_{mo}/250\,000$

F_{gm} $= [R_2 \tan(\pi R_1/4)]^{1/2}$;
R_1 is the ratio of the maximum landing to the maximum take-off mass
R_2 is the ratio of the maximum zero fuel to the maximum take-off mass
Z_{mo} is the maximum operating altitude in feet

Subparagraph (b) of JAR-25.341 states that in addition a continuous gust analysis should also be made. see Section 3.5.2.3.

3.5.3.4 European light aircraft requirements

In the case of light aircraft, JAR-23 retains the definition of discrete gust velocities to he applied at speeds V_C and V_D as given for military aircraft at speeds V_H and V_D respectively in Section **3.5.3.2.** Alleviated sharp-edged analysis is acceptable.

3.5.4 Asymmetric gust requirements

3.5.4.1 Introduction

The requirements associated with the encountering of gusts outside the plane of symmetry are essentially the same in magnitude as those stated in Section 3.5.3 for symmetric gusts. The civil requirements do not emphasize the application of discrete gusts, although the condition is quoted.

3.5.4.2 Lateral gust direction

In some cases the lateral gust is assumed to be horizontal only. The basis of this is that a gust occurring in any direction in the plane perpendicular to the flight path can be resolved into two components, horizontal and vertical, which can then bc dealt with separately. However, this assumption is not always sufficient and on certain advanced configurations and all cases where the tail-plane is mounted on the fin it is essential to consider the gust as coming from any direction. The reason for this is that the vertical and horizontal components interact on the tail-plane to give an asymmetric lift distribution which adds to the loading on the fin due to the horizontal component, see Fig. 3.10.

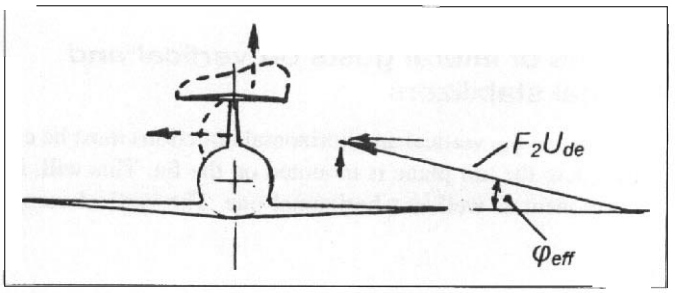

Fig. 3.10 Lateral gust case for high tail layout

3.5.4.3 Lateral gust alleviating factor

The concept of an alleviated sharp-edged gust load can be applied to the fin loading in a way similar to that for the horizontal surfaces subjected to vertical gust conditions. It should be pointed out that this approach may give unrealistic loads and continuous turbulence analysis is preferable.

Using F_2 to indicate the horizontal alleviating factor:

$$F_2 = 0.88\mu_{G2}/(5.3 + \mu_{G2}) \tag{3.5}$$

where

$$\mu_{G2} = 2m(k_z/\ell_F)^2/(\rho S_F c_F a_{1F}) \tag{3.6}$$

m aircraft mass
ρ is the local air density
a_{1F} is the fin lift curve slope based on a reference fin area S_F having a corresponding mean chord c_F
ℓ_F is the distance from the fin aerodynamic centre to the aircraft centre of gravity
k_z is the radius of gyration of the aircraft in yaw

A full dynamic response calculation using airframe flexibility is required eventually and Eqn. (3.5) only applies to conventional aircraft The effect of a high-mounted tail-plane can be evaluated by making the allowances discussed in Section 3.5.4.5.

3.5.4.4 Asymmetric vertical gust

There is a case for civil aircraft in which it is assumed that the vertical gust is not uniform across the span of the wing and therefore gives rise to a rolling effect. This involves modifying the gust loads appropriate to a vertical gust of 15.2 m/s at speed V_C so that while the load on one wing is unchanged, that on the opposite wing is only 80 per cent of the symmetric value. Alleviated sharp-edged analysis is acceptable in this case.

3.5.4.5 Directions of lateral gusts on vertical and horizontal stabilizers

Lateral gusts aligned between the vertical and horizontal directions must be considered, especially for aircraft where the tail-plane is mounted on the fin. This will, in general, result in a vertical component as well as a horizontal one. The vertical component is

$$U_{de} \sin \phi_{eff} \tag{3.7}$$

where

U_{de} is the design gust speed

ϕ_{eff} is the angle of gust direction, relative to the horizontal in the front elevation

The corresponding horizontal gust on the fin is

$$U_{de} \cos \phi_{eff} \tag{3.8}$$

When alleviated sharp-edged analysis is used. allowance should be made for the alleviating factor, F_2, given by Eqn. (3.5) in modifying the values of $(U_{de} \cos \phi_{eff})$ from Eqn. (3.8) but not $(U_d \sin \phi_{eff})$ from equation (3.7).

The horizontal component of the gust gives an effective sideslip angle:

$$\beta_G = F_2 U_{de} \cos \phi_{eff} / V_o \tag{3.9}$$

It is necessary to distribute the tail load asymmetrically as discussed in Section 3.3.3.5 using β_G as the effective sideslip angle.

Appendix A3 Roll performance requirements

A3.1 Military

The United Kingdom military requirements, Def.Stan.00-970, suggest suitable criteria for establishing handling and performance in roll.

(a) Low speed (terminal flight phase). This may be determined by the time taken to roll through a given change in bank angle:
   - (i) for small, light aircraft, the time should not exceed 1.3 s to achieve 30" bank angle;
   - (ii) for medium size and manoeuvrable aircraft. 2.5 s maximum to achieve 30" bank angle;
   - (iii) for heavy aircraft, 3.0 s maximum to achieve 30" bank angle;
   - (iv) for high manoeuvrability aircraft, 1.0 s maximum to roll through 30" hank.

(b) High speed (normal operating condition). The criterion is expressed in terms of time to roll through a given bank angle, which varies with type of aircraft:
   - (i) small light aircraft, 60" in not more than 1.3 s;
   - (ii) medium size aircraft, 45" in not more than 1.4 s;
   - (iii) heavy aircraft. 30" in not more than 1.5 s;
   - (iv) highly manoeuvrable aircraft, 30" in not more than 1.3 s, except for:
     - air combat. 90" in not more than 1.0 s and 360" in 2.5 s;
     - ground attack, with all stores carried the above figures may be relaxed.

(There are also suggestions as to how to specify roll performance in terms of roll rate.)

A3.2 Civil

No specific rates of roll are stated but in JAR-25 there are handling requirements, both with the most adverse engine failed and with all the engines operating:

(a) ***Critical engine inoperative.*** The roll control must be adequate for safety without demanding excess control forces. For four-engined aircraft at a speed of 1.4 times the stalling speed with the wing flaps in the take-off position and landing gear retracted it must be possible to roll the aircraft to a steady banked turn of 20°, both with and against the failed engine.

(b) ***All engines operating.*** At the approach speed, with wing flaps in the landing position and landing gear extended, the requirement is to complete a 60" reverse turn, that is to bank from 30" in one direction to 30' in the other direction. in not more than 7 s.

CHAPTER 4

Rigid airframe dynamics

4.1 Introduction

When in flight an aircraft is a free body within the gravitational field of the earth and therefore a rigid airframe has six degrees of freedom. A flexible airframe has an infinite number of degrees of freedom, or modes, although in practice only those of lower frequency are generally of significance. The six rigid body modes are identified by their zero frequency characteristics. This chapter is concerned only with the equations of motion of a rigid airframe.

The loading of an aircraft in flight may be placed into two general categories:

(a) The forces and moments present while the aircraft is in steady flight, these often being referred to as the trim conditions. In the case of a conventional aircraft having a vertical plane of symmetry the loading in the trim condition is limited to that plane, that is, to longitudinal forces and moments.

(h) The forces and moments consequent upon the departure of the aircraft from the trim conditions as a result of control inputs or atmospheric disturbances. This may be referred to as transient loading.

Associated with the trim conditions is the static stability of the aircraft. The static stability and the dynamic stability characteristics have an influence upon the loading when the aircraft performs manoeuvres or encounters atmospheric turbulence.

4.2 Longitudinal trim conditions

4.2.1 Forces and moments in symmetric flight

4.2.1.1 **Equilibrium** conditions

An aircraft in symmetric flight has its motion confined to the vertical plane of symmetry defined by the centreline, and it has three degrees of freedom. The degrees of freedom are translation in the flight direction, translation perpendicular to the flight direction, and rotation in pitch about the centre of gravity, see Chapter 1, Section 1.4.1. In general the forces and moments experienced by the aircraft arise from aerodynamic, power-plant, inertial, and atmospheric effects, and these are illustrated in Fig. 4.1. While this shows a conventional tailed layout the notation has been chosen so that equations derived may be also be applied to fore-plane and tailless layouts, see Sections 4.8.2 and 4.8.3, respectively.

The forward velocity along the flight path defined by the wind axis Ox' is V_o and it is inclined at a climb angle y relative to the earth axis *Ox"*. The body axis *Ox* is inclined at an angle of attack α_B relative to the wind axis. The aircraft is pitching relative to the earth axis with an angular velocity $d\theta/dt$. The acceleration along the flight path is ***mg*** and perpendicular to it the acceleration is ng, where m and n are acceleration factors and g is the gravitational constant. The notation used is:

$\mathcal{L}_{WB}$	lift on the aircraft, excluding the horizontal stabilizer contribution
$\mathcal{L}_T$	horizontal stabilizer (tail-plane) lift
D	total drag
T	net engine thrust

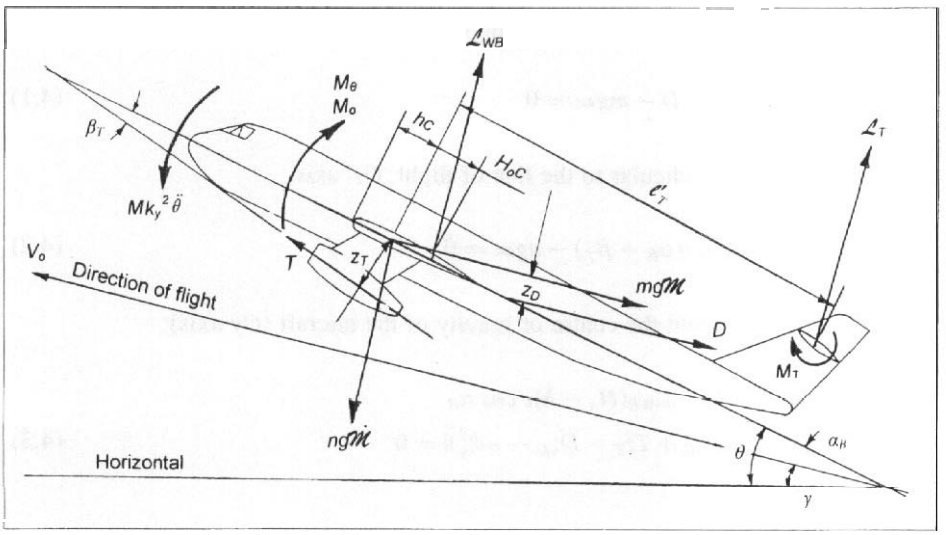

Fig. 4.1 Forces and moments in the longitudinal plane

m vehicle mass (weight/gravitational acceleration)
c mean aerodynamic chord of the wing (MAC). This is to be distinguished from the standard or geometric mean chord (SMC). The two are different for a swept wing. Care must be taken to ensure that all aerodynamic derivatives are based on the MAC and that all the analysis is consistent
hc distance of centre of gravity behind leading edge of aerodynamic mean chord
$H_o c$ distance of aerodynamic centre behind leading edge of aerodynamic mean chord, excluding tail effects. The aerodynamic centre is a reference point about which the pitching moment is constant, that is, it is independent of variation in wing-body lift
ℓ'_T distance along body from the centre of gravity to the point of application of $\mathcal{L}_T$
k_y radius of gyration of aircraft in pitch about the centre of gravity
z_D perpendicular distance of drag axis below the centre of gravity
z_T perpendicular distance of thrust axis below the centre of gravity
β_T angle of the thrust axis to the body axis
M_o pitching moment at zero lift, less the horizontal stabilizer contribution
M_T pitching moment due to the deflection of the elevator relative to the aerodynamic centre of the horizontal stabilizer
M_θ damping pitch moment, less that due to the horizontal stabilizer. This is the air load resistance to pitching motion of the aircraft excluding the contribution from the horizontal stabilizer
V_o velocity of the aircraft along the flight direction
ρ local density of the air

It should be noted that a dot notation is used to indicate differentiation with respect to either dimensional or non-dimensional time as appropriate. Thus if u is the increment in velocity along the longitudinal axis, $\dot{u}$ is the corresponding acceleration.

Resolving forces along the line of flight, ***Ox'*** axis:

$$T\cos(\alpha_B + \beta_T) - D - mgm = 0 \tag{4.1}$$

Resolving forces perpendicular to the line of flight, Oz' axis:

$$\mathcal{L}_{WB} + \mathcal{L}_T + T\sin(\alpha_B + \beta_T) - ngm = 0 \tag{4.2}$$

Resolving moments about the centre of gravity of the aircraft ***(Oy*** axis):

$$M_o + M_T + M_\theta - \mathcal{L}_{WB}(H_o - h)c\cos\alpha_B - \mathcal{L}_T\ell'_T\cos\alpha_B + Tz_T - Dz_D - mk_y^2\ddot{\theta} = 0 \tag{4.3}$$

where $\ddot{\theta} = d^2\theta/dt^2$.

Note that the acceleration factor, n, is positive upwards, see Section 4.4.2. It consists of two distinct components. First there is the component due to gravitational acceleration and second there is the effect of centrifugal acceleration due to the fact that, in general, the flight path is curved, that is, γ is not constant. If the instantaneous radius of the flight motion is 2, then this latter component is

$$An = \dot{\gamma})^2/g$$

hut

$$\dot{\gamma} = V_o$$

and

$$n = cosy + V_o\dot{\gamma}/g \tag{4.4a}$$

thus

$$An = V_o\dot{\gamma}/g$$

Likewise m consists of two components:

$$m = sin\gamma + dV_o/dt \tag{4.4b}$$

It is convenient to define a tail arm, ℓ_T, relative to the aerodynamic centre:

$$\ell_T = \ell'_T + (h - H_o)c \tag{4.5}$$

Using Eqn. ***(4.2)*** to eliminate $\mathcal{L}_{WB}$ in Eqn. ***(4.3):***

$$M_o + M_T + M_\theta - ngm(H_o - h)c\,cos\alpha_B - \mathcal{L}_T\ell_T\,cos_B + Tz_T + T(H_o - h)csin(\alpha_B + \beta_T)cos\alpha_B - Dz_D - mk_y^2\ddot{\theta} = 0$$

or

$$\mathcal{L}_T = [(M_o + M_T + M_\theta)sec\alpha_B + ngm(h - H_o)c + T\{z_T\,sec\alpha_B - (h - H_o)csin(\alpha_B + \beta_T)\} - Dz_D\,sec\alpha_B - mk_y^2\ddot{\theta}\,sec\alpha_B]/\ell_T \tag{4.6}$$

This is the tail load required to give a quasi-static balance of the aircraft $\mathcal{L}_T$ consists of two parts, that required for the initial trim of the aircraft and that arising as a result of the disturbance from the trim condition. Although $\mathcal{L}_{WB}$ has been eliminated in Eqn. ***(4.6)*** there are still terms in α_B. In fact $\mathcal{L}_{WB}$ and α_B are directly related and therefore a direct solution of Eqn. ***(4.6)*** is only possible when simplifying assumptions are made.

For an aircraft initially in level flight γ is zero and if the thrust is equal to the drag, m is unity. The drag force usually passes close to the centre of gravity so z_D may be neglected as may the wing–body damping term, M_θ, and the local tail moment term, M_T, in relation to the total moment due to the tail load for a conventional aircraft (see Sections 4.2.2.4 and 4.2.2.5). Note that both M_T and M_θ may he significant on tailless aircraft and should be included for this class of aircraft. Further, if the thrust is not specifically deflected β_T is usually negligible. Although α_B is not necessarily close to zero in all situations, if it assumed to be so, then Eqns (4.1) to (4.3) become:

$$\begin{aligned} &T - D - mgm = 0 \\ &\mathcal{L}_{WB} + \mathcal{L}_T - ngm = 0 \\ &M_o - \mathcal{L}_{WB}(H_o - h)c - \mathcal{L}_T\ell'_T + Tz_T - mk_y^2\ddot{\theta} = 0 \end{aligned} \tag{4.7}$$

In this case the horizontal stabilizer load is

$$\mathcal{L}_T = [M_o + ngm(h - H_o)c + Tz_T - k_y^2\ddot{\theta}]/\ell'_T \tag{4.8}$$

Thus $\mathcal{L}_T$ can be evaluated from Eqn. (4.8) and the corresponding value of $\mathcal{L}_{WB}$ found from Eqn. (4.7). Use of Eqn. (4.14d) enables the corresponding α_B to be evaluated and hence the analysis can be repeated using Eqn. (4.6) until convergence is achieved.

4.2.1.2 Trim conditions

The aircraft is said to be in trimmed flight when the conditions are steady. That is, the normal, or perpendicular, acceleration factor is unity, there is no acceleration along the flight path, and there is no pitching motion. In this situation with z_D and β_T assumed to be negligible, Eqn. (4.6) reduces to:

$$\begin{aligned} &M_o + M_T - gm(H_o - h)c\cos\alpha_B - \mathcal{L}_T\ell_T\cos\alpha_B + Tz_T \\ &\quad + T(H_o - h)c\sin\alpha_B\cos\alpha_B = 0 \end{aligned} \tag{4.9}$$

and

$$\begin{aligned} \mathcal{L}_T = [&(M_o + M_T)\sec\alpha_B + gm(h - H_o)c + T\{z_T\sec\alpha_B \\ &- (h - H_o)c\sin\alpha_B\}]/\ell_T \end{aligned}$$

For the case when α_B is relatively small:

$$\begin{aligned} &M_o + M_T - gm(H_o - h)c - \mathcal{L}_T\ell_T + Tz_T = 0 \\ &\mathcal{L}_T = [(M_o + M_T) + gm(h - H_o)c + Tz_T]/\ell_T \end{aligned} \tag{4.10}$$

4.2.2 Definition of aerodynamic terms

4.2.2.1 Wing–body lift, $\mathcal{L}_{WB}$

Here the dynamic pressure. Chapter 1 Section 1.5.2, is defined as:

$$q = (\rho_o V_{o\,EAS}^2)/2 \tag{4.11}$$

hence the wing–body lift is

$$\mathcal{L}_{WB} = qS\{a_{1W}\alpha_{eff} + a_B S_B \alpha_B / S\} \tag{4.12}$$

where

suffix 'B'	refers to body characteristics
S_B	is the reference area upon which the body lift curve slope a_B is based
a_{1W}	is the wing lift curve slope, based on the wing area S
α_{eff}	is the effective wing incidence

The definition of α_{eff} demands some care as several effects occur together, see Fig. 4.2 The total effective angle of attack is:

$$\alpha_{eff} = \alpha_B - \alpha_{Bo} \tag{4.13}$$

α_{Bo} is the body angle relative to the airflow for which the wing–body lift is zero and it is usually negative. It consists of two effects: firstly the angle of setting of the wing

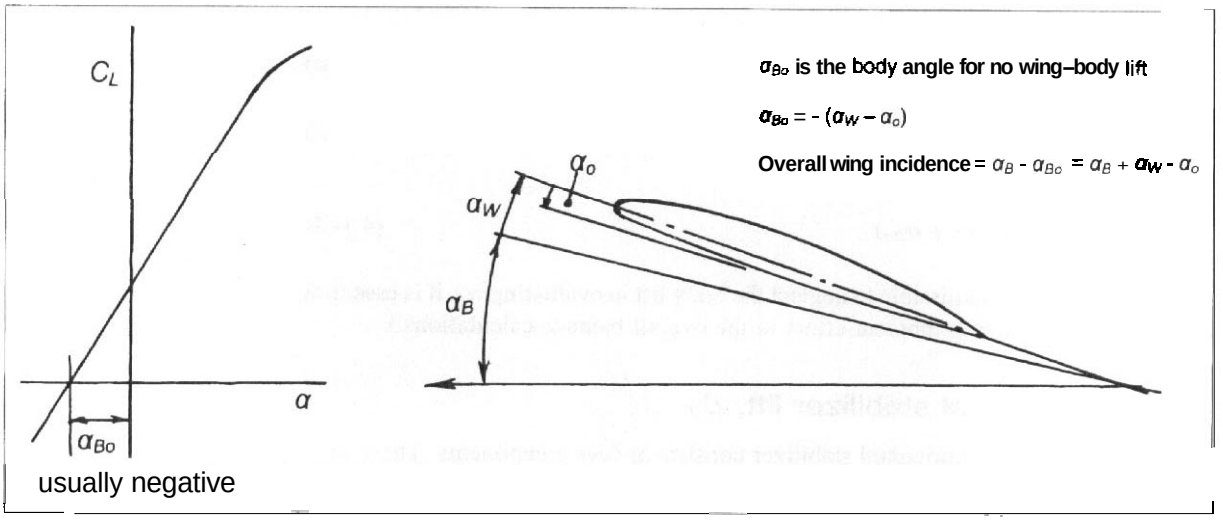

Fig. 4.2 The effective angle of attach of the wing

chord-line relative to the body datum, $a_{,,}$ and secondly a,, the wing no-lift angle. This latter is defined as the angle of attack that the chord-line of the wing must be set at to give zero wing lift. It is zero for an uncambered aerofoil hut is usually negative for a cambered aerofoil and may have a large negative value when high-lift devices are deployed.

Thus:

$$\alpha_{Bo} = -(\alpha_w - \alpha_o)$$

and hence

$$\alpha_{eff} = \alpha_B + \alpha_w - \alpha_o = \alpha_B(1 - \alpha_B/\alpha_{Bo})$$

Then

$$\mathcal{L}_{WB} = \varphi S\{\alpha_{1W}(1 - \alpha_{Bo}/\alpha_B) + \alpha_B S_B/S\}\alpha_B = \varphi S a_{1WB}\alpha_B \tag{4.14a}$$

where a_{1WB} is the effective wing–body lift curve slope given by

$$a_{1WB} = a_{1W}(1 - \alpha_{Bo}/\alpha_B) + a_B S_B/S \tag{4.14b}$$

Note that if $a_{,,}$ is negligibly small compared with a then a_{1WB} is independent of α_B. α_{Bo} may be negligible when the aircraft is manoeuvring at speeds close to V_A with high-lift devices retracted, since a is then large. It is not negligible when flaps are deployed. It may well not be negligible at higher speeds due to the implied lower values of a. When α_{Bo} is not negligible α_{1WB} must be calculated for each value of α_B:

$$\begin{aligned}\alpha_B &= \mathcal{L}_{WB}/[\varphi\{Sa_{1W}(1 - \alpha_{Bo}/\alpha_B) + \alpha_B S_B\}] \\ &= [\mathcal{L}_{WB}/(a_{1WB}\varphi S) + \alpha_{Bo}]/[1 + \alpha_B S_B/(a_{1W}S)]\end{aligned} \tag{4.14c}$$

For many aircraft, especially subsonic ones. $(a_B S_B)$ is small in comparison with $(a_{1W}S)$ and it may be neglected, from where:

$$\alpha_B = (\mathcal{L}_{WB}/a_{1WB}\varphi S + \alpha_{Bo}) \tag{4.14d}$$

(Note: While it may he admissible to neglect the body lift in evaluating a,, it is essential to retain the corresponding moment effect in the overall balance calculations.)

4.2.2.2 Horizontal stabilizer lift, $\mathcal{L}_T$

In general the lift on the horizontal stabilizer consists of four components. These are:

(a) The steady lift on the surface with the elevator neutral.
(b) The lift due to the pitching velocity. This has the effect of changing the angle of attack of the horizontal stabilizer. Refer to Fig. **4.3.**

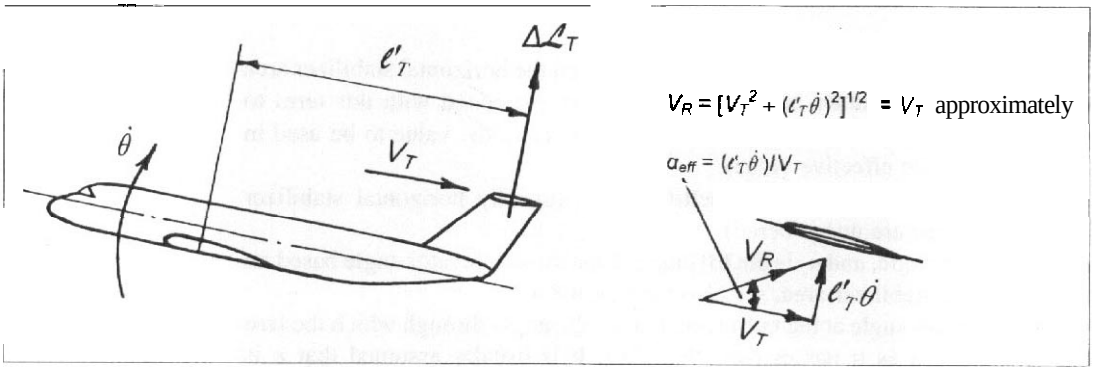

Fig. 4.3 The effective *incidence* of *the horizontal stabilizer* due to *pitching*

(c) The lift on a tail-plane due to the time lag in wing downwash effect at the tail.
(d) The lift due to the deflection of the elevator or the corresponding control.

The second of these terms is the major contribution to the aerodynamic damping of the aircraft in pitch for a conventional tailed or fore-plane layout.

In general the dynamic pressure at the tail will be different from that at the wing due to the additional effect of the pitching velocity and possibly other effects. Using the suffix 'T' to denote the effects at a tail-plane, the effective velocity at the tail, V_R, is:

$$V_R = [V_T^2 + (\ell'_T\dot{\theta})^2]^{1/2} \tag{4.15a}$$

where $(\ell'_T\dot{\theta})$ is the velocity at the tail normal to the wind velocity, V_T, due to the pitching motion, so that:

$$q_T = (\rho V_R^2)/2 \approx (\rho V_T^2)/2 \tag{4.15b}$$

and the angle of attack due to this effect, see Fig. 4.3, is:

$$(\ell'_T\dot{\theta})/V_T \tag{4.15c}$$

The total lift on a tail-plane is

$$\begin{aligned}\mathcal{L}_T = q_T S_T[&a_{1T}(\alpha_B + \alpha_T - \varepsilon) + a_{1T}(\ell'_T\dot{\theta})/V_T \\ &+ a_{1T}\{\ell'_T + c(h - H_o)\}(d\varepsilon/dt)/V_o + a_2\eta]\end{aligned} \tag{4.16}$$

where

a_{1T} is the horizontal stabilizer lift curve slope based on the horizontal stabilizer area S_T. (Note that sometimes an efficiency factor is associated with this term to allow for fuselage and other interference effects. Here the value to be used in Eqn. (4.16) is the effective value)

a_B is the horizontal stabilizer-body setting angle (usually horizontal stabilizer aerofoil sections are uncamhered)

η is the elevator angle, and a_2 is the lift curve slope due to elevator angle based on the horizontal stabilizer area, see also Section 4.8.4

ε is the downwash angle at the tail-plane, that is, the angle through which the free stream is turned as it passes over the wing. It is usually assumed that ε is directly proportional to the wing angle of attack:

$$\varepsilon = \alpha(d\varepsilon/d\alpha) \tag{4.17}$$

Let the effective angle of attack of the horizontal stabilizer in the steady case be:

$$\alpha_{Teff} = \alpha_B + \alpha_T - \varepsilon$$

Then

$$\begin{aligned}\alpha_{Teff} &= \alpha_B + \alpha_T - \alpha(d\varepsilon/d\alpha)\\ &= \alpha_B + \alpha_T - (\alpha_B - \alpha_{Bo})(d\varepsilon/d\alpha)\\ &= \alpha_B(1 - d\varepsilon/d\alpha) + \alpha_{Bo}(d\varepsilon/d\alpha) + \alpha_T\end{aligned} \tag{4.18}$$

where use has been made of Eqn. (4.13).

The third term in Eqn. (4.16) is the downwash lag term, point (c) in text above. It allows for the change in downwash angle with time, the downwash being referred to the wing aerodynamic centre. This term, which only applies to a conventional tail-plane layout, arises when the vehicle is in angular accelerated flight and is due to the time taken for a particle of air to flow from the wing to the tail. During this time the wing conditions will have changed and this term corrects for it. Now:

$$d\varepsilon/dt = (d\varepsilon/d\alpha)(d\alpha/dt)$$

Hence:

$$\begin{aligned}\mathcal{L}_T = q_T S_T[&a_{1T}\{\alpha_B(1 - d\varepsilon/d\alpha) + \alpha_{Bo}(d\varepsilon/d\alpha) + \alpha_T\} + a_{1T}(\ell'_T\dot{\theta})/V_T\\ &+ a_{1T}\{\ell'_T + (h - H_o)c\}(d\varepsilon/d\alpha)(d\alpha/dt)/V_o + a_2\eta]\end{aligned} \tag{4.19}$$

where the term in the square brackets is effectively the overall horizontal stabilizer lift coefficient, C_{LT}.

4.2.2.3 The zero lift pitching moment, M_o

The zero-lift pitching moment of the wing–body is:

$$M_o = qScC_{Mo} \tag{4.20}$$

where C_{Mo} is the zero-lift pitching moment coefficient due to the body, wing, nacelles, and interaction and distortion effects.

4.2.2.4 The horizontal stabilizer pitching moment term, M_T

There are two possible contributions to the horizontal stabilizer pitching moment. The first of these is present only when the aerofoil section is cambered, which is unusual. The second arises from elevator deflection and is due to the chord-wise offset of the increment in lift due to the elevator from the nominal aerodynamic centre of the basic aerofoil section. The effect is shown in Fig. 4.4.

The contribution from the elevator is:

$$M_T = q_T S_T C_T (dC_M/d\eta)\eta \tag{4.21}$$

where c_T is the aerodynamic mean chord of the horizontal stabilizer.

In overall aircraft terms M_T is small. It must not be confused with the hinge moment which is that part of the moment, M , due to the load on the control itself referred to the hinge-line.

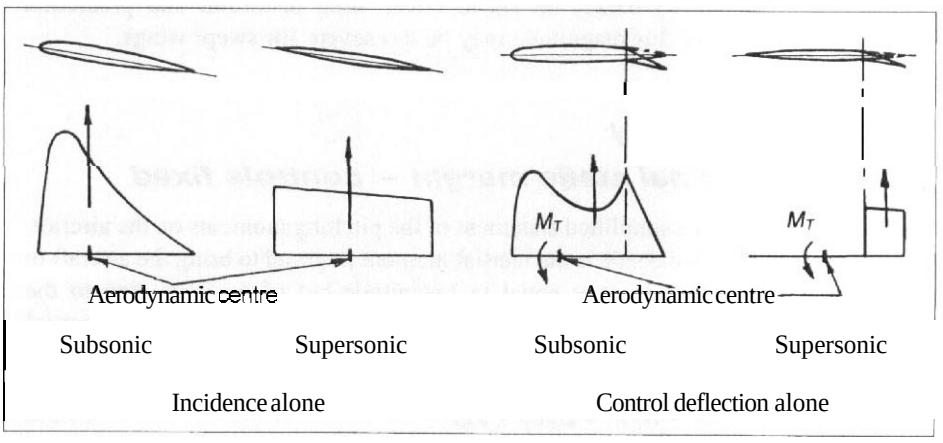

Fig. 4.4 *Origin* **of** *horizontal* Stabilizer pitching ***moment***

4.2.2.5 Pitch damping moment (less horizontal stabilizer), M_θ

The pitch damping moment on the aircraft excluding the tail effect is:

$$M_\theta = \rho Sc(C_{M\theta})_{less\ tail} \tag{4.22a}$$

where

$$(C_{M\theta})_{less\ tail} = dM/d\{c\dot{\theta}/V_o\}$$

It is convenient to write:

$$m_\theta \dot{\theta} = (V_o/c)(C_{M\theta})_{less\ tail} \tag{4.22b}$$

m_θ is equivalent to the wing–body contribution to M_q in standard aerodynamic derivative notation, see Section 4.6.2. Since the largest component in the pitching damping of a conventional tailed or canard aircraft is due to the horizontal stabilizer, this term is usually negligible except in the case of a tailless aircraft.

4.2.2.6 Estimation of aerodynamic forces and moments

The aerodynamic derivatives for the vehicle must be determined from the best possible data, allowing for distortion, limits on aircraft rigging angles, effects of propellen, slipstream, or jet efflux. These remarks apply particularly to the estimation of the pitching moment coefficient tail off, C_{Mo}, and the aerodynamic centre position (less tail), $H_o c$. It should be noted that both C_{Mo} and $H_o c$ vary considerably with change in Mach number, particularly in the transonic speed range. The United Kingdom military aircraft requirements suggest that on unswept wings an allowance should be made of (± 0.0075) on C_{Mo} and (± 0.025) on H_o to cover wing distortion and prediction tolerances. Allowances of this magnitude may be too severe for swept wings.

4.3 Static stability

4.3.1 Longitudinal static margin – controls fixed

The third of Eqns (4.7) is a simplified statement of the pitching moments on the aircraft. The last term on the left-hand side is the inertial moment required to bring the aircraft to a quasi-static balance, that is, it is equal in magnitude but of opposite sign to the algebraic sum of the aerodynamic and thrust effects. Thus, replacing the inertial moment by M, the equation may be rewritten in the form:

$$M = M_o + \mathcal{L}_{WB}(h - H_o)c - \mathcal{L}_T \ell'_T + Tz_T \tag{4.23}$$

Expressed in coefficient form this becomes:

$$\varphi ScC_M = \varphi ScC_{Mo} + \varphi ScC_{LWB}(h - H_o) - \varphi_T S_T C_{LT} \ell'_T + Tz_1$$

or if the dynamic pressure at the tail is assumed to be the same as that at the wing:

$$C_M = C_{Mo} + C_{LWB}(h - H_o) - C_{LT}(S_T \ell'_T / Sc) + Tz_T/(\varphi Sc)$$

The horizontal stabilizer volume coefficient is defined as:

$$\bar{V} = (S_T \ell'_T / Sc) \tag{4.24}$$

so that

$$C_M = C_{Mo} + C_{LWB}(h - H_o) - C_{LT}\bar{V} + Tz_T/(\varphi Sc) \tag{4.25}$$

Now

$$C_{LT} = \mathcal{L}_T/(\varphi_T S_T)$$

For steady conditions and with the dynamic pressure at the tail equal to that at the wing, from Eqn. *(4.19):*

$$C_{LT} = a_{1T}\{\alpha_B(1 - d\varepsilon/d\alpha) + \alpha_{Bo}(d\varepsilon/d\alpha) + \alpha_T\} + a_2\eta \tag{4.26}$$

This may be substituted into Eqn. *(4.25)* to give:

$$C_M = C_{Mo} + C_{LWB}(h - H_o) - [a_{1T}\{\alpha_B(1 - d\varepsilon/d\alpha) + \alpha_{Bo}(d\varepsilon/d\alpha) + \alpha_T\} + a_2\eta]\bar{V} + Tz_T/(\varphi Sc) \tag{4.27a}$$

Equation *(4.26)* can be rearranged to state the elevator angle required to trim the aircraft, that is to achieve $C_M = 0$:

$$\eta = [C_{Mo} + C_{LWB}(h - H_o)]/(a_2\bar{V}) - a_{1T}\{\alpha_B(1 - d\varepsilon/d\alpha) + \alpha_{Bo}(d\varepsilon/d\alpha) + \alpha_T\}/a_2 + Tz_T/(\varphi Sca_2\bar{V}) \tag{4.27b}$$

The condition for longitudinal static stability is that the rate of change of the pitching moment with lift should be negative. Noting that T, C_{Mo}, α_T, and α_{Bo} are constant and that $\alpha_B = C_{LWB}/a_{1WB}$, differentiation of Eqns *(4.26)* with respect to C_L gives.

$$dC_M/dC_L = (h - H_o) - \bar{V}\{a_{1T}(1 - d\varepsilon/d\alpha)/a_{1WB} + a_2(d\eta/dC_L)\} \tag{4.28}$$

Different stability conditions arise when the elevator angle is fixed, known as the controls-fixed case, as opposed to when it is free to move, the controls-free case. The controls-free condition is dependent upon the elevator hinge moment characteristics hut the controls-fixed condition follows directly from Eqn. *(4.28)* since $(d\eta/dC_L)$ is zero:

$$dC_M/dC_L = (h - H_o) - \bar{V}\{a_{1T}(1 - d\varepsilon/d\alpha)/a_{1WB}\} \qquad (4.29)$$

Many references cover the controls-free condition. for example Cook.[1] Let the controls-fixed static margin be defined as:

$$K_n = -dC_M/dC_L = (h, - h) \qquad (4.30)$$

where h_n is the position on he aerodynamic mean chord of the controls-fixed neutral point. From Eqn. *(4.29):*

$$h_n = H_o + \bar{V}\{a_{1T}(1 - d\varepsilon/d\alpha)/a_{1WB}\} \qquad (4.31)$$

Equation *(4.30)* shows that controls-fixed static stability is present when K_n is positive and that stability increases with increase of the distance of the centre of gravity ahead of the neutral point. Thus the controls-fixed neutral point defines the aft-most centre of gravity position consistent with inherent, natural, controls-fixed static stability. For aircraft with conventional control systems it is usually considered that the value of K_n should not be less than about $+0.05$. The forward centre of gravity limit is determined by the need to ensure that K_n is not so large as to create a situation where the control force required to manoeuvre the aircraft is unacceptably high. The actual control force required is a function of the characteristics of the control system.

Aircraft equipped with advanced control systems may be designed to allow for the possibility that the static margin becomes negative, artificial stability being achieved by means of automatic control deflection. Reference to Eqns *(4.28)* and *(4.30)* shows that K_n may be written in the form:

$$K_n = (H_o - h) + \bar{V}\{a_{1T}(1 - d\varepsilon/d\alpha)/a_{1WB}\} + a_2\bar{V}(d\eta/dC_L) \qquad (4.32)$$

Thus a negative numerical value of the sum of the first two terms on the right-hand side of the equation may be compensated for by an appropriate movement of thc pitch control, η. Since such an automatic control system is invariably designed to be irreversible the controls-fixed condition still applies.

[1]Cook, M.V. *Flight Dynamics* Principles. Arnold, 1997.

4.3.2 Longitudinal manoeuvre margin – controls fixed

When the aircraft is in a steady pitching manoeuvre the body angle, α_B, and the rate of change of pitching moment, $\dot{\theta}$, are both constant so that ($\dot{\theta} = \dot{\gamma}$).

The increment in the normal acceleration is given by Eqn. (4.4a) as:

$$\Delta n = V_o \dot{\gamma}/g = V_o \dot{\theta}/g \tag{4.33a}$$

Also the increment in the wing–body lift may be written as:

$$\Delta C_{LWB} = \Delta n C_{LWB} \tag{4.33b}$$

The increment in the angle of attack of the horizontal stabilizer is due both to the increase in the body angle consistent with Eqn. (4.33b) and the steady rotational effect given by the second term in the [ ] brackets on the right-hand side of Eqn. (4.19). When V_T is equal to V_o the latter term becomes:

$$(\Delta\alpha_T)_{pitching} = a_{1T}(\ell'_T \dot{\theta})/V_o = \Delta n g \ell'_T / V_o^2 \tag{4.34a}$$

In the steady level flight trimmed condition:

$$V_o^2 = 2mg/(\rho S C_{LWB})$$

and

$$(\Delta\alpha_T)_{pitching} = \Delta n \ell'_T \rho S C_{LWB}/(2m) = \Delta C_{LWB} \ell'_T \rho S/(2m)$$

or

$$(\Delta\alpha_T)_{pitching} = \Delta C_{LWB} \ell'_T/(\mu_1 c) \tag{4.34b}$$

where

$$\mu_1 = 2m/\rho S c \tag{4.35}$$

μ_1 is the longitudinal relative density, see Section 4.4.7.

The pitching moment equation, Eqn. (4.25). applies to this condition with modified values of the variable parameters and, for completeness, the inclusion of the M_θ term:

Write:

$$(C_M)' = C_{Mo} + (C_{LWB})'(h - H_o) - (C_{LT})' \bar{V} + (C_{M\theta})_{less\ tail} + T z_T/q S c$$

where

$$(C_M)' = C_M + \Delta C_M$$
$$(C_{LWB})' = C_{LWB} + \Delta n C_{LWB} = nC_{LWB}$$
$$(C_{LT})' = C_{LT} + \Delta C_{LT}$$

From Eqns (4.22b) and (4.33a):

$$(C_{M\theta})_{less\ tail} = cm_\theta \dot{\theta}/V_o = \Delta ng/V_o^2$$
$$= cm_\theta \Delta C_{LWB}\rho S/(2m) = m_\theta \Delta C_{LWB}/\mu_1$$

Now from Eqns (4.19) and (4.26):

$$(C_{LT})' = a_{1T}[\{\alpha'_B(1 - d\varepsilon/d\alpha) + \alpha_{Bo}(d\varepsilon/d\alpha) + \alpha_T\} + (\Delta\alpha_T)_{pitching}]$$
$$+ a_2(\eta + \Delta\eta) + m_\theta \Delta C_{LWB}/\mu_1$$
$$= a_{1T}[\{\alpha'_B(1 - d\varepsilon/d\alpha) + \alpha_{Bo}(d\varepsilon/d\alpha) + \alpha_T\} + \Delta C_{LWB}\ell'_T/(\mu_1 c)]$$
$$+ a_2(\eta + \Delta\eta) + m_\theta \Delta C_{LWB}/\mu_1$$

where use has been made of Eqn. (4.34b). Hence:

$$(C_M)' = C_{Mo} + (C_{LWB})'(h - H_o) - \bar{V}\{a_{1T}[\{\alpha'_B(1 - d\varepsilon/d\alpha) + \alpha_{Bo}(d\varepsilon/d\alpha) + \alpha_T\}]$$
$$+ \Delta C_{LWB}\ell'_T/(\mu_1 c)] + a_2(\eta + \Delta\eta)\} + m_\theta \Delta C_{LWB}/\mu_1 + Tz_T/\varphi Sc \tag{4.36}$$

and noting that $\alpha'_B = (C_{LWB})'/a_{1WB}$, collecting like terms:

$$(C_M)' = C_M + \Delta C_M$$
$$= [C_{Mo} + (C_{LWB})(h - H_o) - \bar{V}\{a_{1T}[\{(C_{LWB})'(1 - d\varepsilon/d\alpha)/a_{1WB}$$
$$+ \alpha_{Bo}(d\varepsilon/d\alpha) + \alpha_T\}] + a_2\eta\} + Tz_T/\varphi Sc] + [(\Delta C_{LWB})(h - H_o)$$
$$- \bar{V}\{a_{1T}[\{(\Delta C_{LWB})(1 - d\varepsilon/d\alpha)\}/a_{1WB} + \Delta C_{LWB}\ell'_T/(\mu_1 c)] + a_2\Delta\eta\}]$$
$$+ m_\theta \Delta C_{LWB}/\mu_1$$

The first of the terms on the right-hand side of the equation is the steady flight pitching moment and, as initial trim is assumed. it is zero. Therefore:

$$\Delta C_M = (\Delta C_{LWB})(h - H_o) - \bar{V}\{a_{1T}[\{(\Delta C_{LWB})(1 - d\varepsilon/d\alpha)\}/a_{1WB}$$
$$+ \Delta C_{LWB}\ell'_T/(\mu_1 c)] + a_2\Delta\eta\} + m_\theta \Delta C_{LWB}/\mu_1$$

For stability $d(C_M)'/dC_{LWB} < 0$ and for a steady pitching manoeuvre $(C_M)' = 0$.

Write Eqn. (4.36) in the form:

$$(C_M)' = C_{Mo} + (C_{LWB})'(h - H_o) - \bar{V}\{a_{1T}[\{(C_{LWB})'(1 - d\varepsilon/d\alpha)/a_{1WB} + \alpha_{Bo}(d\varepsilon/d\alpha) + \alpha_T\} + \{(C_{LWB})' - C_{LWB}\}\ell_T'/(\mu_1 c)] + a_2(\eta + \Delta\eta)\} + Tz_T/\varrho Sc + \{(C_{LWB})' - C_{LWB}\}m_\theta/\mu_1$$

When the controls are fixed:

$$d(\eta + \Delta\eta)/d(C_{LWB})' = 0$$

and then. since C_{LWB}, α_{Bo}, and α_T are constant:

$$d(C_M)'/d(C_{LWB})' = (h - H_o) - \bar{V}a_{1T}[(1 - d\varepsilon/d\alpha)/a_{1WB} + \ell_T'/(\mu_1 c)] + m_\theta/\mu_1$$

The controls-fixed manoeuvre margin, H_m is defined as:

$$H_m = -d(C_M)'/dC_{LWB} = h_m - h \tag{4.37a}$$

where, using Eqn. (4.31):

$$\begin{aligned} h_m &= H_o + \bar{V}a_{1T}[\{(1 - d\varepsilon/d\alpha)/a_{1WB}\} + \ell_T'/(\mu_1 c)] - m_\theta/\mu_1 \\ &= h_n + \bar{V}[a_{1T}\ell_T'/(\mu_1 c)] - m_\theta/\mu_1 \end{aligned} \tag{4.37b}$$

Hence from Eqn. (4.30):

$$H_m = K_n + \bar{V}a_{1T}\ell_T'/(\mu_1 c) - m_\theta/\mu_1 \tag{4.37c}$$

It follows from Eqn. (4.37c) that the controls-fixedmanoeuvre margin is greater than the controls-fixed static margin providing that $\bar{V}$ is positive. but see Section 4.8.2.

4.3.3 Lateral static stability

The tendency of an aircraft to return to a wings level condition after a disturbance about the **Ox,** rolling. axis is defined as lateral static stability. For an aircraft with the usual vertical plane of symmetry along the **Ox** axis ideally there are no forces or moments in the lateral trim condition.

Lateral static stability requires that:

$$dC_\ell/d\varphi < 0 \tag{4.38}$$

where dC_ℓ is the rolling moment coefficient and pis the hank angle. Although a number of effects contribute to the value of dC_ℓ including the vertical position of the wing on the body, the most significant ones are the dihedral and sweep of the wing. Positive dihedral, that is when the wing tips are above the root. and sweepback both give negative

contributions to the rolling moment coefficient, that is confer lateral static stahility. Thus less dihedral. or even anhedral, is associated with swept hack wings. See also Section 4.7.2.

4.3.4 Directional static stability

The tendency of an aircraft to align itself, or weathercock. into the wind direction is defined as directional static stability. The required condition is:

$$dC_n/d\psi > 0 \tag{4.39a}$$

where C_n is the yawing moment coefficient and ψ is the yaw angle. When the wind and earth axes coincide the sideslip angle. β, is equal to $(-\psi)$ the required stability condition may be written as:

$$dC_n/d\beta < 0 \tag{4.39b}$$

The main positive contribution to the static directional stability arises from the vertical stabilizing surface, or fin. The inclusion of a dorsal extension to the fin is advantageous in delaying the fin stall and thus ensures directional stability up to higher yaw angles. See also Section 4.7.2.

4.4 General equations of motion

4.4.1 Introduction

The general equations of motion of a rigid body are obtained by applying Newton's second law of motion to the three translational and three rotational degrees of freedom relative to the body axis system $Oxyz$. The point of origin of the system, 0 , is the centre of gravity of the aircraft. Thus the resultant force in each of the three translational modes must be balanced by the products of the acceleration in that direction and the masses of the local components. Similarly the resultant component of moment abouteach of the axes must be balanced by the product of the angular acceleration, about that axis, and the moments of inertia of the local components. As the aerodynamic characteristics are defined relative to the wind axes it is generally convenient to transform the equations of motion to the $Ox'y'z'$ axis system.

4.4.2 Components of acceleration

It is necessary to define the resultant acceleration at any point within the rigid aircraft in terms of the general motion relative to the body axis system. The aircraft, and therefore the body axes $Oxyz$, are assumed to be moving relative to the initial reference axes system. for example the earth axis system $Ox''y''z''$, see Chapter 1, Section 1.4.1. An arbitrary reference point within the body has co-ordinates (x, y, z) relative to the centre of gravity, O. The local components of the velocity and the acceleration of the reference point are u, v, and w and $\dot{u}$, $\dot{v}$ and $\dot{w}$ respectively relative to the three axis directions. Note that $\dot{w}$ is used here rather than n to distinguish it from the normal acceleration factor referred to in Chapter 3, Section 3.2.3, which is of opposite sign. As the body is rigid

there is no motion of the reference point relative to the origin, O. The resultant absolute velocities of the reference point as a consequence of the angular motion are:

$$\begin{aligned} u' &= -ry + qz \\ v' &= -pz + rx \\ w' &= -qx + py \end{aligned} \tag{4.40a}$$

Each term on the right-hand side represents the linear velocity at the reference point due to its displacement from the axis system. The absolute velocities of the reference point are obtained by adding the overall velocities of the aircraft:

$$\begin{aligned} u &= u' + U = U - ry + qz \\ v &= v' + V = V - pz + rx \\ w &= w' + W = W - qx + py \end{aligned} \tag{4.40b}$$

The acceleration components of the reference point each consist of three terms. The first is the linear acceleration along a given reference direction. The other two terms are a consequence of the centrifugal acceleration components of the angular velocities at the reference point. Thus. for example, in the Oxz plane the angular velocity about they axis is q and at the reference point it has a component $(-qx)$ in the **O:** direction. The corresponding centrifugal acceleration is $(-q^2x)$ in the x direction. From Eqn. (4.40a), in the Oxz plane when y is zero, w' is also equal to $(-qx)$. Substituting to eliminate $(-qx)$ from $(-q^2x)$ gives the acceleration component due to q parallel to the axis **Ox** as (qw').

In general:

$$\begin{aligned} m' &= \dot{u} - rv' + qw' \\ o' &= \dot{v} - pw' + ru' \\ \bar{n}' &= w - qu' + pv' \end{aligned} \tag{4.41a}$$

Substitution of Eqns (4.40b) into Eqns (4.41a) gives:

$$\begin{aligned} m &= \dot{u} - rv - qw \\ o &= \dot{v} - pw + ru \\ \bar{n} &= \dot{w} - qu + pv \end{aligned} \tag{4.41b}$$

Differentiation of Eqns (4.40b) gives, with respect to time:

$$\begin{aligned} \dot{u} &= \dot{U} - \dot{r}y + \dot{q}z \\ \dot{v} &= \dot{V} - \dot{p}z + \dot{r}x \\ \dot{w} &= \dot{W} - \dot{q}x + \dot{p}y \end{aligned} \tag{4.42}$$

Using Eqns (4.40b) and *(4.42):*

$$\begin{aligned} m &= \dot{U} - \dot{r}y + \dot{q}z - r(V - pz + rx) + q(W - qx + py) \\ &= \dot{U} - rV + qW - x(q^2 + r^2) + y(pq - \dot{r}) + z(pr + \dot{q}) \\ o &= \dot{V} - \dot{p}z + \dot{r}x - p(W - qx + py) + r(U - ry + qz) \\ &= \dot{V} - pW + rU + x(pq + \dot{r}) - y(p^2 + r^2) + z(qr - \dot{p}) \\ \bar{n} &= \dot{W} - \dot{q}x + \dot{p}y - q(U - ry + qz) + p(V - pz + rx) \\ &= \dot{W} - qU + pV + x(pr - \dot{q}) + y(qr + \dot{p}) - z(p^2 + q^2) \end{aligned} \tag{4.43}$$

Note that if the disturbance from the initial condition is considered for a point on the ***Ox*** axis, so that both y and z are zero, the acceleration components reduce to:

$$\begin{aligned} \mathbf{Am} &= \dot{U} - x(q^2 + r^2) \\ \Delta o &= \dot{V} + x(pq + \dot{r}) \\ \Delta\bar{n} &= \mathbf{W} + x(\dot{q} - pr) \end{aligned} \tag{4.44}$$

Thus for a point on the ***Ox*** axis the lateral acceleration due to the angular velocities is a function of $(\dot{r} + pq)$ while the normal acceleration is a function of $(\dot{q} - pr)$. These terms are the effective yawing and pitching accelerations referred to in Chapter 3, Figs ***3.6*** and ***3.4,*** respectively. When the motion is solely in the vertical plane the pitching acceleration is simply $\dot{q} = \ddot{\theta}$, and when it is solely in the horizontal plane the yawing acceleration is simply $(\dot{r} + \ddot{\psi})$.

4.4.3 Generalized force and moment equations

4.4.3.1 Forces

Since the origin used to define the acceleration components given in Eqn. *(4.43)* is the centre of gravity of the aircraft, the components of force acting on the aircraft as a whole may be written as:

$$\begin{aligned} X &= m_m = m(\dot{U} - rV + qW) \\ Y &= o_m = m(\dot{V} - pW + rU) \\ Z &= \bar{n}_m = m(\dot{W} - qU + pV) \end{aligned} \tag{4.45}$$

where m is the mass of the aircraft.

4.4.3.2 Moments

The moments actingon the aircraft are balanced by the summation of the products of the local masses and accelerations as follows:

About the x axis the rolling moment L is balanced by:
$\Sigma\Delta m(y\bar{n} - zo)$
About they axis the pitching moment M is balanced by:
$\Sigma\Delta m(zm - x\bar{n})$ (4.46)
About the z axis the yawing moment N is balanced by:
$\Sigma\Delta m(xo - ym)$

Am is a local item of mass located at x, y, z and subjected to accelerations m. o, and $\bar{n}$. Only angular effects are present and, from Eqn. ***(4.43)***. for the pitching moment equation:

$$M = \Sigma\Delta m[z\{-x(q^2 + r^2) + y(pq - \dot{r}) + z(pr + \dot{q})\} - x\{x(pr - \dot{q}) + y(qr + \dot{p}) - z(p^2 + q^2)\}]$$

Expanding and collecting like terms:

$$M = \Sigma\Delta m\dot{q}(x^2 + z^2) - \Sigma\Delta m(\dot{p} + rq)xy + \Sigma\Delta mpr(z^2 - x^2) + \Sigma\Delta m(pq - \dot{r})zy + \Sigma\Delta m(p^2 - r^2)xz \quad (4.47)$$

By definition the moments and products of inertia are:

Moment of inertia about x axis: $I_x = \Sigma\Delta m(y^2 + z^2)$
Moment of inertia about y axis: $I_y = \Sigma\Delta m(x^2 + z^2)$
Moment of inertia about z axis: $I_z = \Sigma\Delta m(x^2 + y^2)$
Product of inertia in the xy plane: $I_{xy} = \Sigma\Delta mxy$ (4.48)
Product of inertia in the xz plane: $I_{xz} = \Sigma\Delta mxz$
Product of inertia in the yz plane: $I_{yz} = \Sigma\Delta myz$

Using these definitions, Eqn. ***(4.47)*** becomes:

$$M = I_y\dot{q} + (I_x - I_z)pr + I_{yz}(pq - \dot{r}) + I_{xz}(p^2 - r^2) - I_{xy}(\dot{p} + rq) \quad (4.49a)$$

Similarly:

$$L = I_x\dot{p} - (I_y - I_z)qr + I_{xy}(pr - \dot{q}) - I_{xz}(pq + \dot{r}) - I_{yz}(p^2 + q^2) \quad (4.49b)$$

$$N = I_z\dot{r} - (I_x - I_y)pq - I_{yz}(pr + \dot{q}) + I_{xz}(qr - \dot{p}) + I_{xy}(q^2 + p^2) \quad (4.49c)$$

The products of inertia I_{xy} and I_{yz} are theoretically zero for an aircraft having conventional symmetry about the Oxz plane. Hence the moment equations reduce to:

$$\begin{aligned} L &= I_x\dot{p} - (I_y - I_z)qr - I_{xz}(pq + \dot{r}) \\ M &= I_y\dot{q} + (I_x - I_z)pr + I_{xz}(p^2 - r^2) \\ N &= I_z\dot{r} - (I_x - I_y)pq + I_{xz}(qr - \dot{p}) \end{aligned} \quad (4.50)$$

4.4.4 Initial steady trimmed conditions

In the initial steady trimmed condition the velocity components along the body axes Ox and Oz are U_{st} and W_{st}, respectively, while that along the Oy axis, V_{st}, is zero. The body Ox axis is inclined to the earth reference at a pitch angle of θ_{st} but the initial roll and yaw angles φ_{st} and ψ_{st} are both zero.

The force and moment balance in the trimmed case is analysed in Section 4.2.1.2.

4.4.5 Disturbed forces and moments

4.4.5.1 Introduction

When the motion of the aircraft is disturbed from the trimmed condition the velocity components along the Ox, Oy and Oz axes, respectively, are:

$$\begin{aligned} U &= U_{st} + u \\ V &= V_{st} + v = v \\ W &= W_{st} + w \end{aligned} \quad (4.51a)$$

and the total angles, denoted by the suffix T, relative to the same axes are:

$$\begin{aligned} \varphi_T &= \varphi_{st} + \varphi = \varphi \\ \theta_T &= \theta_{st} + \theta \\ \psi_T &= \psi_{st} + \psi = \psi \end{aligned} \quad (4.51b)$$

The rates of change of the velocity components with time are:

$$\begin{aligned} dU/dt &= du/dt = \dot{u} \\ dV/dt &= dv/dt = \dot{v} \\ dW/dt &= dw/dt = \dot{w} \end{aligned} \quad (4.51c)$$

Substituting Eqns (4.51) into the force equations (4.45) yields:

$$\begin{aligned} X &= m[\dot{u} - rv + q(W_{st} + w)] \\ Y &= m[\dot{v} - p(W_{st} + w) + r(U_{st} + u)] \\ Z &= m[\dot{w} - q(U_{st} + u) + pv] \end{aligned} \tag{4.52}$$

4.4.5.2 Disturbance forces and moments

The applied, or disturbance, forces and moments may arise from one or more of five causes:

(a) Gravity forces due to the movement of the hody axes relative to the initial reference. earth, axes and are denoted by the suffix g. There are no gravity disturbance moments when the origin of the axis system is the centre of gravity of the aircraft.
(h) Aerodynamic forces and moments on the airframe due to the disturbance of the aircraft from the initial trimmed condition, denoted by the suffix a.
(c) Pilot, or autopilot, inputs to the control motivators, denoted by the suffix, ***c***.
(d) Atmospheric disturbances in the form of gusting or continuous turhulcnce, denoted by the suffix ***ad***.
(e) Powerplant effects which arise as a consequence of changes in engine thrust as occurs. for example, when an engine fails. denoted by the suffix pp.

Thus for example:

$$X = X_g + X_a + X_c + X_{ad} + X_{pp} \tag{4.53}$$

4.4.5.3 Gravitational effects

The gravitational effects are sometimes included with the inertial terms on the right-hand side of Eqns (4.45). Since in the trimmed condition the body axis **Ox** is inclined at an angle θ_{st} to the earth reference axis Ox'':

$$\begin{aligned} X_g &= -mg\sin\theta_{st} \\ Y_g &= 0 \\ Z_g &= mg\cos\theta_{st} \end{aligned} \tag{4.54a}$$

When the aircraft is disturbed through the angles φ, θ, and ψ in roll, pitch, and yaw, respectively, the use of the axis transformation equation [Chapter 1, Eqn. (1.1)] gives:

$$\begin{bmatrix} X_g \\ Y_g \\ Z_g \end{bmatrix} = \mathbf{D} \begin{bmatrix} -(Mass)g\sin\theta \\ 0 \\ (Mass)g\cos\theta \end{bmatrix} \tag{4.54b}$$

4.4.5.4 Airframe aerodynamic effects

The aerodynamic force and moment contributions to the disturbed motion equations are a consequence of the linear and angular velocities and accelerations imposed upon the airframe. Thus, in addition to a possible constant tenn, there are potentially twelve contributions to each of the force and moment equations although in practice certain of the effects are likely to be insignificant. In addition to the twelve contributions due to the perturbed motion there may also be the constant term derived from the initial steady trimmed conditions. Thus, for example:

$$X_a = (X_a)_{const} + (X_a)_u + (X_a)_v + (X_a)_w + (X_a)_p + (X_a)_q + (X_a)_r + (X_a)_{\dot{u}} + (X_a)_{\dot{v}} + (X_a)_{\dot{w}} + (X_a)_{\dot{p}} + (X_a)_{\dot{q}} + (X_a)_{\dot{r}} \quad (4.55a)$$

where the suffixes indicate the cause of the effect.

Comparableequationsapply to the other forcesand to themoments. In fact, as theconstant terms refer to the trimmed flight condition, the only terms actually arising are due to the components of the lift, relative to the earth axes, which initially balance the weight. Thus:

$$(X_a)_{const} = mg\sin\theta_{st}$$
$$(Z_a)_{const} = -mg\cos\theta_{st} \quad (4.55b)$$

It is commonpractice to express eachof the individual effects as apower series, for instance:

$$(X_a)_u = (X_a)_{const} + (\partial X/\partial u)u + (\partial^2 X/\partial u^2)(u^2/2!) + (\partial^3 X/\partial u^3)(u^3/3!) + \text{etc.} \quad (4.55c)$$

and similar terms for the other parameters.

4.4.5.5 Control effects

The forces and moments consequential upon the operation of the controls are similar to those of the aerodynamic terms described in the previous paragraph. They arise from the three control inputs, namely ξ, η, and ζ in roll, pitch, and yaw, respectively. Thus:

$$X_c = (X_c)_\xi + (X_c)_\eta + (X_c)_\zeta \quad (4.56)$$

and similarly for the other terms.

4.4.5.6 Atmospheric disturbances

The terms in the force and moments equations which arise as a result of disturbances in the atmosphere may be represented in a similar way to those of the airframe aerodynamic effects. They are normally neglected in control and stability analysis

but are of considerable importance in loading calculations. These effects are further discussed in Chapter 6.

4.4.5.7 Powerplant effects

The contributions to the equations of motion which are a consequence of the changes in powerplant output relative to the trimmed case can also be expressed in a similar way to the airframe aerodynamic terms. They are further considered in Sections 4.6.2 and 4.7.2.

4.4.6 Rearrangement of the equations of motion and linearization

4.4.6.1 Rearrangement of the equations of motion

It is not unusual to rearrange the six equations of motion so that the right-hand sides represent the disturbing forces and moments, the left-hand sides being the basic characteristics of the aircraft. The latter can conveniently include the gravitational terms since the gravity field is constant. Using Eqns (4.52) and (4.53) the force equations (4.45) become:

$$\begin{aligned} m[\dot{u} - rv + q(W_{st} + w)] - X_g - X_a &= X_c + X_{ad} + X_{pp} \\ m[\dot{v} - p(W_{st} + w) + r(U_{st} + u)] - Y_g - Y_a &= Y_c + Y_{ad} + Y_{pp} \\ m[\dot{w} - q(U_{st} + u) + pv] - Z_g - Z_a &= Z_c + Z_{ad} + Z_{pp} \end{aligned} \tag{4.57a}$$

Likewise the moment equations, Eqns (4.50). become:

$$\begin{aligned} [I_x\dot{p} - (I_y - I_z)qr - I_{xz}(pq + \dot{r})] - L_a &= L_c + L_{ad} + L_{pp} \\ [I_y\dot{q} + (I_x - I_z)pr + I_{xz}(p^2 - r^2)] - M_a &= M_c + M_{ad} + M_{pp} \\ [I_z\dot{r} - (I_x - I_y)pq + I_{xz}(qr - \dot{p})] - N_a &= N_c + N_{ad} + N_{pp} \end{aligned} \tag{4.57b}$$

4.4.6.2 Linearization of the equations of motion

As derived the equations of motion, Eqns (4.57), are complex and non-linear. This renders them difficult to handle and for many purposes it is adequate to simplify the equations by linearizing them. To do this it is necessary to make certain assumptions:

(a) That all the disturbance effects are small so that powers and products of them are negligible. For example $(\sin\varphi \sin\theta)$ is negligible.

(b) In the case of the angular disturbances the cosine values may be taken as unity and the sine values are equal to the angle in radians. Thus, for example, the transformation matrix referred to in Section 4.4.5.3, see Chapter I, Eqn. (1.1),

simplifies to:

$$\mathbf{D} = \begin{bmatrix} 1 & \psi & -\theta \\ -\psi & 1 & \theta \\ \theta & -\phi & 1 \end{bmatrix} \tag{4.58a}$$

(c) The aerodynamic, control, atmospheric disturbances, and powerplant effects may all be represented by the constant and the first, linear, term in their power series expansion. see Eqn. (4.55c). Thus, for example:

$$(X_a)_u = (X_a)_{const} + (\partial X/\partial u)u \tag{4.58b}$$

(d) The disturbance terms are independent of the disturbed motion of the aircraft. This is true for the conventional control effects and for atmospheric disturbance. However, in the case of the effects of thrust changes the assumption may be invalid, see Section 4.6.2.

(e) The equations represent only the disturbances from the trimmed condition. Thus for example the application of Eqn. (4.54b) using Eqn. (4.58a) gives:

$$\begin{aligned} X_g &= -mgsin\theta_{st} - mg\theta cos\theta_{st} \\ Y_g &= mg\psi sin\theta_{st} + mg\varphi cos\theta_{st} \\ Z_g &= mg cos\theta_{st} - mg\theta sin\theta_{st} \end{aligned}$$

It will be noted that the first terns in the X_g and the Z_g expressions are equal, but of opposite sign, to the $(X_a)_{const}$ and $(Z_a)_{const}$ values defined in Eqn. (4.55b) and therefore cancel out. Further, when the aircraft is in initial steady Right the reference wind axes $Ox'y'z'$ coincide with the earth reference $Ox''y''z''$ axes, so that W_{st} is equal to zero and θ_{st} is small, being equal to α_B. In this case the forces in the disturbed motion reduce to:

$$\begin{aligned} X_g &= -mg\theta \\ Y_g &= mg\varphi \\ Z_g &= -mg\theta\theta_{st} \end{aligned} \tag{4.58c}$$

Z_g is approximately zero when θ_{st} $(=\alpha_B)$ is vety small.

It is convenient to write the disturbed airframe aerodynamic terms in the form:

$$X_a = \sum_{i=u}^{i} X_i i \tag{4.58d}$$

where

$$i = u, v, w, p, q, r, \dot{u}, \dot{v}, \dot{w}, \dot{p}, \dot{q} \text{ and } \dot{r}$$

since any constant terms relate to the initial trimmed condition. In practice not all of the effects represented by i are significant and in particular the only acceleration term of importance is w.

Likewise the control terms can take the form:

$$X_c = \sum_{i\equiv\xi}^{\zeta} X_i i \tag{4.58e}$$

where $i = \xi, \eta,$ and ζ.

The atmospheric disturbance effect may he written as:

$$X_{ad} = X_{ad}(ad) \tag{4.58f}$$

The thrust term becomes:

$$X_{pp} = X_T(T) \tag{4.58g}$$

Equations **(4.57)** now become:

$$\begin{aligned}
&m[\dot{u}] + mg\theta - \sum_{i\equiv u}^{r} X_a i = \sum_{i\equiv\xi}^{\zeta} X_c i + X_{ad}(ad) + X_T(T)\\
&m[\dot{v} + rU_{st}] - mg\varphi - \sum_{i\equiv u}^{r} Y_a i = \sum_{i\equiv\xi}^{\zeta} Y_c i + Y_{ad}(ad) + Y_T(T)\\
&m[\dot{w} - qU_{st}] + mg\theta\theta_{st} - \sum_{i\equiv u}^{r} Z_a i = \sum_{i\equiv\xi}^{\zeta} Z_c i + Z_{ad}(ad) + Z_T(T)\\
&[I_x\dot{p} - I_{xz}\dot{r}] - \sum_{i\equiv u}^{r} L_a i = \sum_{i\equiv\xi}^{\zeta} L_c i + L_{ad}(ad) + L_T(T)\\
&[I_y\dot{q}] - \sum_{i\equiv u}^{r} M_a i = \sum_{i\equiv\xi}^{\zeta} M_c i + M_{ad}(ad) + M_T(T)\\
&[I_z\dot{r} - I_{xz}\dot{p}] - \sum_{i\equiv u}^{r} N_a i = \sum_{i\equiv\xi}^{\zeta} N_c i + N_{ad}(ad) + N_T(T)
\end{aligned} \tag{4.59}$$

4.4.7 Non-dimensionalization of the equations of motion

Equations **(4.59)** are in dimensional form. This is the most suitable for some applications. However, the non-dimensional form of the equations is frequently used for the purpose of loading calculations as well as for the classical stability and control analysis as is illustrated by the static stability conditions covered in Section **4.3.**

Non-dimensionalization is accomplished by dividing the equations by:

Force equations: $\rho S V_o^2/2$

Roll and yaw moment equations: $\rho S V_o^2 b/2$ (4.60)

Pitching moment equation: $\rho S V_o^2 c/2$

Note that $(U_{st} = V_o \cos\theta_{st})$ from paragraph 4.4.6.2(e). The following definitions are also used to simplify the format of the final equations:

(a) When the aircraft is in initial steady flight the lift coefficient is:

$$C_L = 2mg/(\rho S V_o^2) \tag{4.61a}$$

(b) Non-dimensional time, $\hat{t}$, is derived by dividing real time, t, by:

$$\tau = 2m/(\rho V_o S) \tag{4.61b}$$

(c) Non-dimensional velocities and accelerations are defined as:

$$\begin{aligned}
\hat{u} &= u/V_o \qquad \hat{\dot{u}} = \dot{u}\tau/V_o \\
\hat{v} &= v/V_o \qquad \hat{\dot{v}} = \dot{v}\tau/V_o \\
\hat{w} &= u/V_o \qquad \hat{\dot{w}} = \dot{w}\tau/V_o \\
\hat{p} &= p\tau \qquad \hat{\dot{p}} = \dot{p}\tau^2 \\
\hat{q} &= q\tau \qquad \hat{\dot{q}} = \dot{q}\tau^2 \\
\hat{r} &= r\tau \qquad \hat{\dot{r}} = \dot{r}\tau^2
\end{aligned} \tag{4.61c}$$

(d) Relative density factors:

Longitudinal, pitch: $\mu_1 = 2m/(\rho S c)$
Lateral and directional, roll and yaw: $\mu_2 = 2m/(\rho S b)$ (4.61d)

where b is the wing span

(e) Non-dimensional moments of inertia:

$$\begin{aligned}
&\text{Roll:} && i_x = I_x/(mb^2) = (k_x/b)^2 \\
&\text{Pitch:} && i_y = I_y/(mc^2) = (k_y/c)^2 \\
&\text{Yaw:} && i_z = I_z/(mb^2) = (k_z/b)^2 \\
&\text{Product of inertia:} && i_{xz} = I_{xz}/(mb^2)
\end{aligned} \tag{4.61e}$$

where k_x, k_y and k_z are the respective radii of gyration.

The form of the non-dimensional equations is derived from Eqns **(4.59):**

$$\begin{aligned}
&\hat{\dot{u}} + C_L\theta - \{2/(\rho SV_o^2)\}\Big[\sum_{i\equiv u}^{\dot{w}} X_a i\Big] \\
&\quad = \{2/(\rho SV_o^2)\}\Big[\sum_{i\equiv\xi}^{\zeta} X_c i + X_{ad}(ad) + X_T(T)\Big] \\
&\hat{\dot{v}} + \hat{r} - C_L\varphi - \{2/(\rho SV_o^2)\}\Big[\sum_{i\equiv u}^{\dot{w}} Y_a i\Big] \\
&\quad = \{2/(\rho SV_o^2)\}\Big[\sum_{i\equiv\xi}^{\zeta} Y_c i + Y_{ad}(ad) + Y_T(T)\Big] \\
&\hat{\dot{w}} - \hat{q} + C_L\theta\theta_{st} - \{2/(\rho SV_o^2)\}\Big[\sum_{i\equiv u}^{\dot{w}} Z_a i\Big] \\
&\quad = \{2/(\rho SV_o^2)\}\Big[\sum_{i\equiv\xi}^{\zeta} Z_c i + Z_{ad}(ad) + Z_T(T)\Big] \\
&(i_x\hat{\dot{p}} - i_{xz}\hat{\dot{r}})/\mu_2 - \{2/(\rho SV_o^2 b)\}\Big[\sum_{i\equiv u}^{\dot{w}} L_a i\Big] \\
&\quad = \{2/(\rho SV_o^2 b)\}\Big[\sum_{i\equiv\xi}^{\zeta} L_c i + L_{ad}(ad) + L_T(T)\Big] \\
&i_y\hat{\dot{q}}/\mu_1 - \{2/(\rho SV_o^2 c)\}\Big[\sum_{i\equiv u}^{\dot{w}} M_a i\Big] \\
&\quad = \{2/(\rho SV_o^2 c)\}\Big[\sum_{i\equiv\xi}^{\zeta} M_c i + M_{ad}(ad) + M_T(T)\Big] \\
&(i_z\hat{\dot{r}} - i_{xz}\hat{\dot{p}})/\mu_2 - \{2/(\rho SV_o^2 b)\}\Big[\sum_{i\equiv u}^{\dot{w}} N_a i\Big] \\
&\quad = \{2/(\rho SV_o^2 b)\}\Big[\sum_{i\equiv\xi}^{\zeta} N_c i + N_{ad}(ad) + N_T(T)\Big]
\end{aligned} \tag{4.62}$$

where now $i = u$, v, w, p, q, r, and $\dot{w}$ or $i = \xi$, η, and ζ

Further development of the equalions requires the expansion of the terms within the summation signs on both the right- and left-hand sides. Thus for example:

$$\{2/(\rho SV_o^2)\}\left[\sum_{i\equiv u}^{\dot{w}} X_i\ i\right] = \{2/(\rho SV_o^2)\}[X_u u + X_v v + X_w w + X_p p + X_q q + X_r r + X_{\dot{w}}\dot{w}]$$

$$= 2X_u(u/V_o)/(\rho SV_o) + 2X_v(v/V_o)/(\rho SV_o) + 2X_w(w/V_o)/(\rho SV_o) + 2X_p p/(\rho SV_o^2) + 2X_q q/(\rho SV_o^2) + 2X_r r/(\rho SV_o^2) + 2X_{\dot{w}}(\dot{w}/V_o)(\rho SV_o)$$

$$= 2X_u\hat{u}/(\rho SV_o) + 2X_v\hat{v}/(\rho SV_o) + 2X_w\hat{w}/(\rho SV_o) + 2X_p(\hat{p}/\mu_1)/(\rho SV_o c) + 2X_q(\hat{q}/\mu_1)(\rho SV_o c) + 2X_r(\hat{r}/\mu_1)/(\rho SV_o c) + 2X_{\dot{w}}(\hat{\dot{w}}/\mu_1)/(\rho Sc) \quad (4.63a)$$

and

$$2/(\rho SV_o^2)\left[\sum_{i\equiv\xi}^{\zeta} X_i\ i\right] = 2/(\rho SV_o^2)[X_\xi\xi + X_\eta\eta + X_\zeta\zeta]$$

$$= 2X_\xi\xi/(\rho SV_o^2) + 2X_\eta\eta/(\rho SV_o^2) + 2X_\zeta\zeta/(\rho SV_o^2) \quad (4.63b)$$

The terms in the denominators of these expressions are used to define the non-dimensional derivatives. For example:

$$X_u = X_u/(\rho SV_o/2) \qquad X_p = X_p/(\rho SV_o^2 c/2)$$

$$X_{\dot{w}} = X_{\dot{w}}/(\rho Sc/2) \qquad X_\xi = X_\xi/(\rho SV_o^2/2) \quad (4.64)$$

$$X_{ad} = X_{ad}/(\rho SV_o^2/2) \qquad X_T = X_T/(\rho SV_o^2/2) \qquad \text{etc.}$$

Thus finally the equation of motion along the Or' wind axis becomes:

$$\hat{\dot{u}} - X_u\hat{u} - X_v\hat{v} - X_{\dot{w}}\hat{\dot{w}}/\mu_1 - X_w\hat{w} - X_p\hat{p}/\mu_1 - X_q\hat{q}/\mu_1 - X_r\hat{r}/\mu_1 + C_L\theta = X_\xi\xi + X_\eta\eta + X_\zeta\zeta + X_{ad}(\text{func.}ad) + X_T(\text{func.}T) \quad (4.65a)$$

Similar development of the other five equations of motion leads to:

$$\hat{\dot{v}} - Y_u\hat{u} - Y_v\hat{v} - Y_w\hat{w} - Y_p\hat{p}/\mu_2 - Y_q\hat{q}/\mu_2 - Y_r\hat{r}/\mu_2 + \hat{r} - C_L\varphi = Y_\xi\xi + Y_\eta\eta + Y_\zeta\zeta + Y_{ad}(\text{func.}ad) + Y_T(\text{func.}T) \quad (4.65b)$$

$$-Z_u\hat{u} + \dot{w} - Z_v\hat{v} - Z_{\dot{w}}\hat{\dot{w}}/\mu_1 - Z_w\hat{w} - Z_p\hat{p}/\mu_1 - Z_q\hat{q}/\mu_1 - Z_r\hat{r}/\mu_1 - \hat{q} + C_L\theta\theta_{st} = Z_\xi\xi + Z_\eta\eta + Z_\zeta\zeta + Z_{ad}(\text{func.}ad) + Z_T(\text{func.}T) \quad (4.65c)$$

$$-L_u\hat{u} - L_v\hat{v} - L_w\hat{w} + i_x\hat{\dot{p}}/\mu_2 - L_p\hat{p}/\mu_2 - L_q\hat{q}/\mu_2 - i_{xz}\hat{\dot{r}}/\mu_2 - L_r\hat{r}/\mu_2 = L_\xi\xi + L_\eta\eta + L_\zeta\zeta + L_{ad}(\text{func}.ad) + L_T(\text{func}.T) \quad (4.65d)$$

$$-M_u\hat{u} - M_v\hat{v} - M_w\hat{\dot{w}}/\mu_1 - M_w\hat{w} - M_p\hat{p}/\mu_1 + i_y\hat{\dot{q}}/\mu_1 - M_q\hat{q}/\mu_1 - M_r\hat{r}/\mu_1 = M_\xi\xi + M_\eta\eta + M_\zeta\zeta + M_{ad}(\text{func}.ad) + M_T(\text{func}.T) \quad (4.65e)$$

$$-N_u\hat{u} - N_v\hat{v} - N_w\hat{w} - i_{xz}\hat{\dot{p}}/\mu_2 - N_p\hat{p}/\mu_2 - N_q\hat{q}/\mu_2 + i_z\hat{\dot{r}}/\mu_2 - N_r\hat{r}/\mu_2 = N_\xi\xi + N_\eta\eta + N_\zeta\zeta + N_{ad}(\text{func}.ad) + N_T(\text{func}.T) \quad (4.65f)$$

where the $\dot{w}$ effects are assumed to be negligible in the lateral equations

4.4.8 Decoupling of the equations of motion

4.4.8.1 Introduction

Clearly for an aircraft having symmetry about the Oxz plane a motion in that plane will not result in any disturbance out of that plane. Thus in this case ***v, p, r,*** v, p, and $\dot{r}$ will all be zero. However, the reverse is not necessarily true in that disturbances in roll and yaw may give rise to changes in the longitudinal plane, that is u, ***w,*** q, $\dot{u}$, w, and q will not necessarily he zero. For example, an angular yawing velocity, r. may result in changes to the lift of the wing and horizontal stabilizer thereby inducing longitudinal motion.

Nevertheless for many aircraft of conventional layout, especially where the wing is of moderate to high aspect ratio, it is adequate to simplify the equations and their solution by isolating the pitching from the rolling and yawing effects. This includes the control inputs. It is also convenient at this stage to defer consideration of the effect of atmospheric disturbance effects to later, see Chapter 6.

4.4.8.2 Longitudinal equations of motion

The assumption is made that v, p, and r and their derivatives with respect to time are negligible and that the only control input is from the horizontal stabilizer/elevator cornhination. The equations which describe the motion in the plane of symmetry become from Eqns (4.65a), (4.65c), and (4.65e):

$$\hat{\dot{u}} - X_u\hat{u} - X_{\dot{w}}\hat{\dot{w}}/\mu_1 - X_w\hat{w} - X_q\hat{q}/\mu_1 + C_L\theta = X_\eta\eta + X_T(\text{func}.T) \quad (4.66a)$$

$$-Z_u\hat{u} + \dot{w} - Z_{\dot{w}}\hat{\dot{w}}/\mu_1 - Z_w\hat{w} - Z_q\hat{q}/\mu_1 - \hat{q} + C_L\theta\theta_{st} = Z_\eta\eta + Z_T(\text{func}.T) \quad (4.66b)$$

$$-M_u\hat{u} - M_{\dot{w}}\hat{\dot{w}}/\mu_1 - M_w\hat{w} + i_y\hat{\dot{q}}/\mu_1 - M_q\hat{q}/\mu_1 = M_\eta\eta + M_T(\text{func}.T) \quad (4.66c)$$

4.4.8.3 Lateral/directional equations of motion

In this case the terms in u. ***w,*** and q and their derivatives with respect to time are assumed to be negligible and there are no inputs from the pitch controls. The lateral/

directional equations of motion from Eqns (4.65b), (4.65d), and (4.65f) are now:

$$\hat{\dot{v}} - Y_v\hat{v} - Y_p\hat{p}/\mu_2 - Y_r\hat{r}/\mu_2 + \hat{r} - C_L\varphi = Y_\xi\xi + Y_\zeta\zeta + Y_T(\text{func.}T) \tag{4.67a}$$

$$-L_v\hat{v} + i_x\hat{\dot{p}}/\mu_2 - L_p\hat{p}/\mu_2 - i_{xz}\hat{\dot{r}}/\mu_2 - L_r\hat{r}/\mu_2 = L_\xi\xi + L_\zeta\zeta + L_T(\text{func.}T) \tag{4.67b}$$

$$-N_v\hat{v} - i_{xz}\hat{\dot{p}}/\mu_2 - N_p\hat{p}/\mu_2 - i_z\hat{\dot{r}}/\mu_2 - N_r\hat{r}/\mu_2 = N_\xi\xi + N_\zeta\zeta + N_T(\text{func.}T) \tag{4.67c}$$

4.5 Solution of the equations of motion

4.5.1 Introduction

The full six degree of freedom non-linear equations of motion represented by Eqns (4.57) are complex and are not amenable to analytical treatment. When the characteristics of the aircraft are such that it is necessary to deal with the non-linear equations of motion the recourse must be to a simulation of the problem. Solution of the equations using simulation techniques is now common practice and may readily be applied to the simpler linearized and decoupled formats as well as the more complex representations. A discussion of simulation techniques is beyond the scope of the present text and it suffices to comment that relevant software is commercially available in addition to purpose-built simulators. While for many aspects of loading calculations the use of simulation is not essential, it is always advantageous to employ the technique when it is available.

The linearized form of the equations of motion. Eqns (4.59), can be solved using analytical techniques since they are effectively a set of simultaneous linear differential equations with constant coefficients. As they are presented the terms on the right-hand side represent the external inputs to the motion, with the terms on the left-hand side describing the basic characteristics of the aircraft. Equations of this form, which represent a dynamic system, may be interpreted in terms of a solution which consists of two parts. The first part, the Complementary Function, is obtained by equating the terms on the left-hand side to zero. and this describes the transient motion subsequent to a disturbance. The second pan of the solution is a Particular Integral which is derived by equating the two sides of the equations, assuming, for example, that a given parameter is constant. The Particular Integral represents the final steady state of the system.

Among the techniques available for an analytical solution are the use of Laplace transforms and the differential operator. A treatment of the Laplace transform approach may be found in various references, for example Babister.[2] The approach adopted here is the application of the differential operator to the non-dimensional, decoupled, equations of motion as stated in Eqns (4.66) and (4.67).

[2] Babister. A. W. *Aircraft Dynamic Stability and Response*. Pergamon Press, 1980

4.5.2 Solution of the decoupled equations of motion using the differential operator

The application of the differential operator to the equations of motion enables linear simultaneous equations having constant coefficients to be dealt with as simple algebraic simultaneous equations. Since the perturbation parameters in the longitudinal equations, Eqns (4.66). and the lateral/directional equations, Eqns (4.67), are functions of non-dimensional time the differential operator takes the form:

$$\mathcal{D}(j) = dj/d\hat{t} \tag{4.68}$$

where j represents a non-dimensional linear or angular displacement or velocity as appropriate. Note that the second-order differential operator is required when the acceleration of a displacement parameter has to be dealt with. Thus, for example:

$\dot{\theta} = d\theta/d(\hat{t})$ and is represented by $\mathcal{D}(\theta)$

$\ddot{\theta} = d^2\theta/d(\hat{t})^2$ and is represented by $\mathcal{D}^2(\theta)$

4.6 Analysis of the longitudinal equations for loading actions calculations

4.6.1 Introduction

Application of the differential operator, $\mathcal{D}$, to Eqns (4.66) and the collection together of the terms dependent upon the individual parameters gives:

$$\begin{aligned}
&(\mathcal{D} - X_u)\hat{u} - (\{X_{\dot{w}}/\mu_1\}\mathcal{D} + X_w)\hat{w} - (\{X_q/\mu_1\}\mathcal{D} - C_L)\theta \\
&\quad = X_\eta\eta + X_{ad}(\text{func}.ad) + X_T(\text{func}.T) \\
&\{-Z_u\}\hat{z} + (\{1 - Z_{\dot{w}}/\mu_1\}\mathcal{D} - Z_w)\hat{w} - [(\{Z_q/\mu_1 + 1\}\mathcal{D}) - C_L\theta_{st}]\theta \\
&\quad = Z_\eta\eta + Z_{ad}(\text{func}.ad) + Z_T(\text{func}.T) \\
&\{-M_u\}\hat{u} - (\{M_{\dot{w}}/\mu_1\}\mathcal{D} + M_w)\hat{w} + (\{i_y/\mu_1\}\mathcal{D}^2 - \{M_q/\mu_1\}\mathcal{D})\theta \\
&\quad = M_\eta\eta + M_{ad}(\text{func}.ad) + M_T(\text{func}.T)
\end{aligned} \tag{4.69}$$

where use has been made of:

$$\hat{q} = q\tau = \dot{\theta} \tag{4.70}$$

It should be noted that the terms on the right-hand side of Eqns (4.69) are represented as constant inputs but in practice this may not be the case and they may vary with time. In particular the atmospheric turbulence terms require special consideration. This is defcrrcd until Chapter 6 and the relevant terms will he omitted in the subsequent development of the equations in this paragraph.

Manipulation of the equations is facilitated by writing them in the form:

$$\begin{bmatrix} A_1 & B_1 & C_1 \\ F_1 & G_1 & H_1 \\ K_1 & L_1 & M_1 \end{bmatrix} \begin{Bmatrix} \hat{u} \\ \hat{w} \\ \hat{\theta} \end{Bmatrix} = \begin{bmatrix} D_1 & E_1 \\ I_1 & J_1 \\ N_1 & P_1 \end{bmatrix} \{ \eta \text{ func.} T \} \tag{4.71}$$

where:

$$\begin{aligned}
A_1 &= (\mathcal{D} - X_u) \\
B_1 &= -(\{X_{\dot{w}}/\mu_1\}\mathcal{D} + X_w) \\
C_1 &= -(\{X_q/\mu_1\}\mathcal{D} - C_L) \\
D_1 &= X_\eta \\
E_1 &= X_T \\
F_1 &= \{-Z_u\} \\
G_1 &= (\{1 - Z_{\dot{w}}/\mu_1\}\mathcal{D} - Z_w) \\
H_1 &= -[(\{Z_q/\mu_1 + 1\}\mathcal{D}) - C_L\theta_{st}] \\
I_1 &= Z_\eta \\
J_1 &= Z_T \\
K_1 &= \{-M_u\} \\
L_1 &= -(\{M_{\dot{w}}/\mu_1\}\mathcal{D} + M_w) \\
M_1 &= (\{i_y/\mu_1\}\mathcal{D}^2 - \{M_q/\mu_1\}\mathcal{D}) \\
N_1 &= M_\eta \\
P_1 &= M_T
\end{aligned}$$

Consider the case when the disturbance is a consequence of the application of elevator deflection. Write:

$$[A] \begin{Bmatrix} \hat{u} \\ \hat{w} \\ \hat{\theta} \end{Bmatrix} = \begin{bmatrix} D_1 \\ I_1 \\ N_1 \end{bmatrix} (\eta) \tag{4.72}$$

where [A] is identical to the first matrix in Eqn. (4.71).

Equation (4.72) may be solved by the use of Cramer's rule. This states that for a system of n unknowns and n equations, providing the determinant $|A|$ is not zero, the values of a given parameter are obtained by dividing a determinant $|B|$ by $|A|$ where $|B|$ is formed by replacing the column in $|A|$ relevant to that parameter by the column on the right-hand side of the equation. Thus, for example:

$$\hat{w} = \begin{vmatrix} A_1 & D_1 & C_1 \\ F_1 & I_1 & H_1 \\ K_1 & N_1 & M_1 \end{vmatrix} (\eta) \div |A| \tag{4.73a}$$

or

$$|A|\,\hat{w} = \begin{vmatrix} A_1 & D_1 & C_1 \\ F_1 & I_1 & H_1 \\ K_1 & N_1 & M_1 \end{vmatrix} (\eta) \tag{4.73b}$$

where:

$$|A| = [A_1\{G_1M_1 - H_1L_1\} - B_1\{F_1M_1 - H_1K_1\} - C_1\{F_1L_1 - G_1K_1\}] \tag{4.73c}$$

The coefficients in Eqn. (4.73c) may be replaced by the terms given in Eqn. (4.71) but the consequence is complex algebraically, see also Section 4.6.4.

When the right-hand side of Eqn. (4.73b) is set to zero the solution obtained represents the basic dynamics of the aircraft and determines the transient motion subsequent to a disturbance. In practice there are four roots to the equation which, in general. make up two pairs of complex terms. These two terms define the periodicity and damping in the two fundamental dynamic longitudinal motions, the so-called short-period oscillation and the long-period, or phugoid, motion. A full treatment of the solution and the implications of the modes may be found in Babister[2]. The former motion is primarily an oscillation in angle of attack with the forward velocity remaining more or less constant. The latter motion is primarily a variation in the forward speed and the climb angle of the aircraft with the angle of attack remaining sensibly constant.

The loading on the aircraft is largely determined by the perturbations in angle of attack and pitching velocity for a given design speed and hence the critical motion is the short-period one. Considerable simplification of Eqns (4.71) may be accomplished by assuming that the phugoid motion is not relevant, that is by assuming that the forward speed is constant throughout the disturbance. Thus in Eqns (4.71) the terms in $\hat{u}$ may be deleted. The solution of the simplified equations is to be found in Section 4.6.3.

4.6.2 Definition of the non-dimensional longitudinal derivatives

The non-dimensional longitudinal derivatives used in Eqns (4.70) and (4 71) may he expressed in terms of the lift, drag, moment coefficients, and thrust. Using the non-dimensionalizing relations of Section 4.4.7 the relevant expressions follow.

(a) X_{u}, longitudinal force due to forward velocity

$$X_u = -2C_D - V_o(\delta C_D/\delta V) + 2(\delta T/\delta V)/(\rho V_o S) \tag{4.74a}$$

where C_D is the overall aircraft drag coefficient.

For the case where the drag coefficient and thrust are independent of velocity X_u is usually less than -0.1.

(b) X_w, longitudinal force due to the effect of incidence change:

$$X_w = C_L - (\delta C_D/\delta\alpha) \tag{4.74b}$$

where C_L is the overall aircraft lift coefficient.

For the case when the drag coefficient is independent of the incidence, X_w is of the order of unity.

(c) X_q, longitudinal force due to rate of pitch:

$$X_q = -\bar{V}(\delta C_D/\delta\alpha)_T \tag{4.74c}$$

where $\bar{V}$ is the volume coefficient of the horizontal stabilizer, see Eqn. (4.24), and **suffix** 'T' refers to the horizontal stabilizer. In most instances X_q is negligibly small.

(d) $X_{\dot{w}}$, longitudinal force due to the lag in wing downwash at the tail:

$$X_{\dot{w}} = X_q(d\varepsilon/d\alpha) \tag{4.74d}$$

where $(d\varepsilon/d\alpha)$ is the rate of change of downwash with wing angle of attack. As a consequence of the negligible value of X_q, and the fact that $(d\varepsilon/d\alpha)$ is typically less than 0.5, $X_{\dot{w}}$ is also negligible.

(e) Z_u, normal force due to forward velocity:

$$Z_u = -2C_L - V_o(\delta C_L/\delta V) \tag{4.74e}$$

This term has a typical value of -2 or less.

(f) Z_w, normal force due to change in effective incidence:

$$Z_w = -C_D - a_{1WB} \tag{4.74f}$$

where a_{1WB} is the wing–body lift curve slope.

The C_D term is usually negligible and the derivative has a typical value in the range of -2 to -6.

(g) Z_q, normal force due to rate of pitch:

$$Z_q = -a_{1T}\bar{V} \tag{4.74g}$$

where a_{1T} is the horizontal stabilizer lift curve slope. A typical value for Z_q is -2.

(h) $Z_{\dot{w}}$, normal force due to downwash lag:

$$Z_{\dot{w}} = Z_q(d\varepsilon/d\alpha) = -a_{1T}\bar{V}(d\varepsilon/d\alpha) \tag{4.74h}$$

A typical value for this term is of the order of unity

(i) M_u, pitching moment due to forward velocity:

$$M_u = V_o(\delta C_M/\delta V) \tag{4.74i}$$

At low speed where the pitching moment coefficient, C_M, is largely independent of forward speed this term is negligible. It may be significant in compressible flow.

(j) M_w, pitching moment due to change in effective incidence:

$$M_w = (\delta C_M/\delta\alpha) = -a_{1WB}K_n \tag{4.74j}$$

where K_n is the controls fixed static margin, see Eqn. (4.30). If compressibility is present the expression for K_n is more complex than that given in Eqn. (4.30) see, for example, Babister[2]. A typical value of M_w for a statically stable aircraft is of the order of -1 or rather less.

(k) M_q, pitching moment due to pitch rate, see also Section 4.2.2.5:

$$M_q = Z_q(\ell_T'/c) + m_\theta = -a_{1T}\bar{V}(\ell_T'/c) + m_\theta \tag{4.74k}$$

where

(ℓ_T'/c) is the ratio of the horizontal stabilizer moment arm to the wing aerodynamic mean chord

m_θ is the pitch damping effect of the wing–body combination. This term is usually relatively small when the aircraft employs a horizontal stabilizing surface but it is significant on tailless designs

$$m_\theta\dot{\theta} = (M_\theta)_{WB}/(\rho S V_o c^2/2)$$

where $(M_\theta)_{WB}$ is the absolute value of the pitching moment due to rate of pitch of the wing–body combination. Note m_θ is the same as $(M_q)_{WB}$.

For a conventional tailed design M_q has a typical value of the order of ten.

(l) Mw, pitching moment due to downwash lag:

$$M_{\dot{w}} = (M_q)_T(d\varepsilon/d\alpha) = -a_{1T}\bar{V}(\ell_T'/c)(d\varepsilon/d\alpha) \tag{4.74l}$$

So that for a conventional design Mw is typically around -2.

(m) X_η, longitudinal force due to pitch control deflection:

$$X_\eta = -(S_T/S)(\delta C_D/\delta\eta) \tag{4.74m}$$

where

(S_T/S) is the ratio of the horizontal stabilizer to wing areas
$(\delta C_D/\delta\eta)$ is the rate of change of the drag of the horizontal stabilizer with control deflection, η, and is normally negligible

For a tailless design the pitch control characteristics are based on the wing area since the horizontal stabilizer is not present and S_T is effectively zero, see Section 4.8.3.

(n) Z_η, normal force due to pitch control deflection:

$$Z_\eta = -a_2/(S_T/S) \tag{4.74n}$$

where a_2 is the lift curve slope due to the control deflection, η.

Z_η may have a typical value of less than one. In the case of a tailless design. $Z_\eta = -a_2$.

(p) M_η pitching moment due to pitch control:

$$M_\eta = -a_2(\ell_T'/c)(S_T/S) = -a_2\bar{V} \tag{4.74p}$$

M_η has a typical value of -2 or less. As mentioned in subparagraph (m) above, in the case of a tailless design a_2 is based on the wing area so that for this class of aircraft:

$$M_\eta = -a_2(\ell_\eta/c)$$

where ℓ_η is the chord-wise distance between the centre of pressure due to elevator deflection and the centre of gravity of the aircraft, see Section 4.8.3.

(q) X_T, longitudinal force due to increment in thrust. Assuming that the thrust is normally aligned along the Ox direction:

$$X_T = 2\Delta T/(\rho S V_o^2) \tag{4.74q}$$

where AT is the increment in thrust.

(r) Z_T, normal force due to the effective incidence change of the thrust:

$$Z_T = -2\Delta T\theta/(\rho S V_o^2) \tag{4.74r}$$

It is to be noted that this term depends upon the angle, 8, of the disturbed motion. This introduces a complexity in the solution of the equations unless it is justified to assume that the term is negligible, see Section **4.6.4.**

(s) M_T, pitching moment due to the change in thrust:

$$M_T = 2\Delta T(z_T/c)/(\rho S V_o^2) \tag{4.74s}$$

where z_T is the vertical offset of the thrust line from the **Ox** axis (positive down).

4.6.3 Response of the aircraft to pitch control input

4.6.3.1 Aircraft having inherent static stability

As discussed in Section 4.6.1 it is acceptable for the purpose of loading calculations to neglect the effect of any change in forward speed when analysing the response to pitch control of an inherently statically stable aircraft. The motion of the aircraft is now described by the latter two of Eqns (4.69) namely the normal force and the pitching moment equations. Eqn. (4.71) reduces to:

$$\begin{bmatrix} G_1 & H_1 \\ L_1 & M_1 \end{bmatrix} \begin{Bmatrix} \hat{w} \\ \theta \end{Bmatrix} = \begin{bmatrix} I_1 \\ N_1 \end{bmatrix} (\eta) \tag{4.75}$$

The terms are defined at Eqn. (4.71) and some simplification is possible. The longitudinal relative density factor, μ_1, has a magnitude of the order of 100 and when this is considered with the typical values of the relevant derivatives as given in Section 4.6.2 it is reasonable to assume that:

$$Z_q/\mu_1 \ll 1.0 \qquad \text{and} \qquad Z_{\dot{w}}/\mu_1 \ll 1.0$$

Further it is acceptable to assume that θ_{s1} is negligibly small. Thus, approximately:

$$\begin{aligned} G_1 &= (\mathcal{D} - Z_w) \\ H_1 &= -\mathcal{D} \end{aligned} \tag{4.76}$$

Applying Cramer's rule to Eqn. (4.75), see Eqn. (4.73). gives the solution for $\hat{\omega}$ as:

$$\hat{w} = \begin{vmatrix} I_1 & H_1 \\ N_1 & M_1 \end{vmatrix} \eta \div \begin{vmatrix} G_1 & H_1 \\ L_1 & M_1 \end{vmatrix} \tag{4.77a}$$

where

$$\begin{vmatrix} I_1 & H_1 \\ N_1 & M_1 \end{vmatrix} = (I_1 M_1 - H_1 N_1) \tag{4.77b}$$

$$\begin{vmatrix} G_1 & H_1 \\ L_1 & M_1 \end{vmatrix} = (G_1 M_1 - H_1 L_1) \tag{4.77c}$$

Substitution from Eqn. (4.71) with the simplifications of Eqn. (4.76) gives the expression for the first of the above determinants as:

$$[Z_\eta(\{i_y/\mu_1\}\mathcal{D}^2 - \{M_q/\mu_1\}\mathcal{D}) + M_\eta\mathcal{D}]$$
$$= \{i_y/\mu_1\}[Z_\eta\mathcal{D} - Z_\eta M_q/i_y + M_\eta\mu_1/i_y]\mathcal{D} \tag{4.78a}$$

Likewise the second of the determinants is:

$$[(\mathcal{D} - Z_w)(\{i_y/\mu_1\}\mathcal{D}^2 - \{M_q/\mu_1\}\mathcal{D}) - \mathcal{D}(\{M_{\dot w}/\mu_1\}\mathcal{D} + M_w)]$$
$$= [\{i_y/\mu_1\}\mathcal{D}^3 - \{M_q/\mu_1\}\mathcal{D}^2 - \{Z_w i_y/\mu_1\}\mathcal{D}^2 + \{Z_w M_q/\mu_1\}\mathcal{D}$$
$$- \{M_{\dot w}/\mu_1\}\mathcal{D}^2 + M_w\mathcal{D}]$$
$$= \{i_y/\mu_1\}[\mathcal{D}^2 - (M_q/i_y + Z_w + M_{\dot w}/i_y)\mathcal{D}$$
$$+ (Z_w M_q/i_y - M_w\mu_1/i_y)]\mathcal{D} \tag{4.78b}$$

Substituting these expressions into the determinants of Eqn. (4.77a) gives $\hat{w}$:

$$\hat{\dot w} - (M_q/i_y + Z_w + M_{\dot w}/i_y)\hat{\dot w} + (Z_w M_q/i_y - M_w\mu_1/i_y)\hat{w}$$
$$= Z_\eta\hat{\dot\eta} - (Z_\eta M_q/i_y - M_\eta\mu_1/i_y)\eta \tag{4.79}$$

where $\hat{\dot\eta} = d\eta/d(\hat{t})$.

Further development of Eqn. (4.79) is achieved by substituting the expressions for the aerodynamic derivatives given in Section 4.6.2. Noting that, from Eqn. (4.61e), i_y is equal to $(k_y/c)^2$ and neglecting C_D in comparison with a_1 in the Z_w term the coefficient of $\hat{w}$ becomes:

$$-[(c/k_y)^2\{-a_{1T}\bar V(\ell'_T/c) + m_\theta\} - a_{1WB} + (c/k_y)^2\{-a_{1T}\bar V(\ell'_T/c)(d\varepsilon/d\alpha)\}]$$
$$= [a_{1WB} + a_{1T}\bar V(\ell'_T/c)(c/k_y)^2\{1 + (d\varepsilon/d\alpha)\} - (c/k_y)^2 m_\theta]$$
$$= [a_{1WB} + a_{1T}(S_T/S)(\ell'_T/k_y)^2\{1 + (d\varepsilon/d\alpha)\} - (c/k_y)^2 m_\theta] \tag{4.80a}$$

The coefficient of $\hat{w}$ becomes:

$$(c/k_y)^2[a_{1WB}a_{1T}\bar V(\ell'_T/c) - a_{1WB}m_\theta + 2ma_{1WB}K_n/(\rho Sc)]$$
$$= [2ma_{1WB}K_n c/(\rho Sk_y)^2 + a_{1WB}a_{1T}\bar V(\ell'_T/c)(c/k_y)^2 - a_{1WB}m_\theta(c/k_y)^2]$$
$$= 2ma_{1WB}c[K_n + a_{1T}\bar V(\ell'_T/c)/\mu_1 - m_\theta/\mu_1]/(\rho Sk_y{}^2)$$
$$= 2ma_{1WB}cH_m/(\rho Sk_y{}^2) \tag{4.80b}$$

where use has been made of Eqn. (4.37c).

The coefficient of $\hat{\dot{\eta}}$ is $(-a_2 S_T/S)$ (4.80c)

The coefficient of η becomes:

$$(c/k_y)^2[-(a_2 S_T/S)\{-a_{1T}\bar{V}(\ell'_T/c) + m_\theta\} + 2\mu a_2 \bar{V}/(\rho S c)]$$
$$= -[2\mu a_2 S_T \ell'_T/(\rho S^2 k_y{}^2) + a_{1T} a_2 (S_T/S)^2 (\ell'_T/k_y)^2 - a_2 m_\theta (S_T/S)(c/k_y)^2] \quad (4.80d)$$

Therefore:

$$\hat{\ddot{w}} - [a_{1WB} + a_{1T}(S_T/S)(\ell'_T/k_y)^2\{1 + (d\varepsilon/d\alpha)\} - (c/k_y)^2 m_\theta]\hat{\dot{w}} + [2\mu a_{1WB} c H_m/(\rho S k_y{}^2)]\hat{w}$$
$$= (-a_2 S_T/S)\hat{\dot{\eta}} - [2\mu a_2 S_T \ell'_T/(\rho S^2 k_y{}^2) + a_{1T} a_2 (S_T/S)^2 (\ell'_T/k_y)^2 - a_2 m_\theta (S_T/S)(c/k_y)^2]\eta \quad (4.81)$$

Finally $\hat{w} = w/V_o = a$, where here a is the increment in the body angle due to the departure from the trimmed condition. Hence:

$$\hat{\ddot{\alpha}} + 2R_1\hat{\dot{\alpha}} + (R_1{}^2 + J_1{}^2)\alpha = \delta'\hat{\dot{\eta}} + \delta\eta \quad (4.82a)$$

where

$$\hat{\dot{\alpha}} = d\alpha/d(\hat{t})$$
$$R_1 = [a_{1WB} + a_{1T}(S_T/S)(\ell'_T/k_y)^2\{1 + (d\varepsilon/d\alpha)\} - (c/k_y)^2 m_\theta]/2 \quad (4.82b)$$

R_1 is the damping coefficient in the short-period motion

$$J_1 = [2\mu a_{1WB} c H_m/(\rho S k_y{}^2) - R_1{}^2]^{1/2} \quad (4.82c)$$

J_1 is the natural damped frequency in the short-period motion.

$$\delta' = -(a_2 S_T/S) \quad (4.82d)$$

δ' is the forcing function due to the rate of change of the pitch control and may often be taken as zero.

$$\delta = -[2\mu a_2 S_T \ell'_T/(\rho S^2 k_y{}^2) + a_{1T} a_2 (S_T/S)^2 (\ell'_T/k_y)^2 - a_2 m_\theta (S_T/S)(c/k_y)^2] \quad (4.82e)$$

An alternative form of Eqn. (4.82e) is:

$$\delta = -a_2\mu_1(S_T/S)(c/k_y)^2[(\ell'_T/c) + a_{1T}(S_T/S)(\ell'_T/c)^2/\mu_1 - m_\theta/\mu_1] \qquad (4.82f)$$

where δ is the forcing function due to pitch control deflection. The term in m_θ is negligible except, possibly, for a tailless aircraft. The first term in Eqn. (4.82e) is comparable in value to the relative density factor, μ_1, and is likely to be an order of magnitude greater than the middle term so that this latter also may often be neglected. Thus approximately:

$$\begin{aligned}\delta &= -2ma_2S_T\ell'_T/(\rho S^2k_y{}^2) = -a_2\mu_1(S_T/S)(\ell'_T/c)(c/k_y)^2 \\ &= -a_2\mu_1(c/k_y)^2\bar{V} \qquad (4.82g)\end{aligned}$$

The natural undamped frequency of the short-period motion, ω_1, is given by:

$$\omega_1 = (R_1{}^2 + J_1{}^2)^{1/2} \qquad (4.83a)$$

and the damping ratio is:

$$\begin{aligned}\zeta_{D1} &= R_1/\omega_1 \\ &= R_1/(R_1{}^2 + J_1{}^2)^{1/2} \qquad (4.83b)\end{aligned}$$

Thus Eqn. (4.82a) may be written in the form:

$$\hat{\hat{\alpha}} + 2\omega_1\zeta_{D1}\hat{\alpha} + \omega_1{}^2\alpha = F(\eta) \qquad (4.84)$$

where $F(\eta)$ is the right-hand side of Eqn. (4.82a) and is given either by Eqns (4.82e) or (4.82f) or, approximately, by Eqn. (4.82g).

The effect of the value of the damping ratio, ζ_{D1}, is considered in Appendix A4. Suffice it to note that if ζ_{D1} is negative, the system is unstable in the short-period mode.

The solution in terms of the non-dimensional pitching velocity, $\dot{\theta}$, is derived from Eqn. (4.75) as:

$$\begin{vmatrix} G_1 & H_1 \\ L_1 & M_1 \end{vmatrix}(\theta) = \begin{vmatrix} G_1 & I_1 \\ L_1 & N_1 \end{vmatrix}(\eta) \qquad (4.85a)$$

The expansion of the determinate on the left-hand side of this equation is given by Eqn. (4.78b). The expansion of the determinate on the right-hand side is:

$$\begin{aligned}\begin{vmatrix} G_1 & I_1 \\ L_1 & N_1 \end{vmatrix} &= (G_1N_1 - I_1L_1) \\ &= [(\mathcal{D} - Z_w)M_\eta + (\{M_{\dot{w}}/\mu_1\}\mathcal{D}^2 - \{M_q/\mu_1\}\mathcal{D})(Z_\eta)] \\ &= [\{M_{\dot{w}}Z_\eta/\mu_1\}\mathcal{D}^2 - (\{M_qZ_\eta/\mu_1\} - M_\eta)\mathcal{D} - Z_wM_\eta] \\ &= (i_y/\mu_1)[\{M_{\dot{w}}Z_\eta/i_y\}\mathcal{D}^2 - (\{M_qZ_\eta/i_y\} \\ &\quad - \{M_\eta\mu_1/i_y\})\mathcal{D} - Z_wM_\eta\mu_1/i_y] \end{aligned} \tag{4.85b}$$

In this case the left-hand side of Eqn. (4.85a), the equivalent of Eqn. (4.79). becomes:

$$[\mathcal{D}^2 - (M_q/i_y + Z_w + M_{\dot{w}}/i_y)\mathcal{D} + (Z_wM_q/i_y - M_w\mu_1/i_y)](\mathcal{D}\theta)$$

or

$$\dddot{\hat{\theta}} - (M_q/i_y + Z_w + M_{\dot{w}}/i_y)\ddot{\hat{\theta}} + (Z_wM_q/i_y - M_w\mu_1/i_y)\dot{\hat{\theta}} \tag{4.86a}$$

where the expressions for the coefficients in terms of the aerodynamic derivatives are given in Eqns (4.80a) and (4.80b).

The right-hand side of Eqn. (4.85a) becomes:

$$\{M_{\dot{w}}Z_\eta/i_y\}\ddot{\hat{\eta}} - (\{M_qZ_\eta/i_y\} - \{M_\eta\mu_1/i_y\})\dot{\hat{\eta}} - (Z_wM_\eta\mu_1/i_y)\eta \tag{4.86b}$$

It will be seen that the coefficient of $\dot{\hat{\eta}}$ is identical to that of the coefficient of η in Eqn. (4.79).

When the expressions for the derivatives are substituted, the coefficient of $\ddot{\eta}$ is:

$$a_{1T}a_2(S_T/S)^2(\ell'_T/k_y)^2(d\varepsilon/d\alpha) \tag{4.86c}$$

This term is similar to the middle term in the expression for δ given in Eqn. (4.82e) except for the $(d\varepsilon/d\alpha)$. From the comments made there it may he concluded that this term is negligible in comparison with the $\dot{\eta}$ term except, possibly, when the pitch control is applied rapidly.

The coefficient of η is:

$$-[2m(c/k_y)^2\{-a_2(\ell'_T/c)(S_T/S)\}(-a_{1WB})]/(\rho Sc)$$
$$= -a_{1WB}\{2ma_2S_T\ell'_T/(\rho S^2k_y{}^2)\} = a_{1WB}\delta \qquad (4.86d)$$

where use has been made of the approximate expression for δ from Eqn. (4.82g).

Therefore, using the same development as for the left-hand side of Eqn. (4.79). the solution of the equations in terms of the non-dimensional pitching velocity is:

$$\hat{\ddot{\theta}} + 2R_1\hat{\ddot{\theta}} + (R_1{}^2 + J_1{}^2)\hat{\dot{\theta}} = \delta\hat{\dot{\eta}} + a_{1WB}\delta\eta \qquad (4.87)$$

It should be noted that when the deflection of the pitch control is constant and the aircraft has reached a steady state condition such that the increment in the body angle, a. and the pitching velocity, $\dot{\theta}$, are both constant:

$$(\alpha)_{SS} = \delta(\eta)_{SS}/(J_1{}^2 + R_1{}^2)$$
$$(\hat{\dot{\theta}}_{SS}) = a_{1WB}\delta(\eta)_{SS}/(J_1{}^2 + R_1{}^2) \qquad (4.88)$$

and

$$(\dot{\theta}_{SS}) = a_{1WB}(\alpha)_{SS}$$

where the suffix SS refers to the steady state condition

4.6.3.2 Statically unstable aircraft

While Eqns (4.81). (4.82). and (4.84) apply to a statically or dynamically unstable system they are of little value for loading calculations due to the fact that the response of the aircraft to a pitch control input will cause it to depart from naturally restrained flight. In practice, an inherently unstable aircraft has to have the stability augmented through the control system as briefly mentioned in Section 4.3.1. The characteristics of the airframe and the control system become parts of a closed loop system utilizing feedback of the motion of the aircraft unlike the open loop system described by Eqn. (4.84). For a further discussion of this matter refer, for example, to Cook[1]

However, for the purpose of loading actions, it is not usually necessary to consider the closed loop dynamic characteristics of the aircraft since the control system is used to place limits on the displacements, velocities, and accelerations achieved by the aircraft. This enables limits to he placed on the parameters which determine the loads as discussed in Chapter 3, Section 3.2.4.

4.6.4 Response of the aircraft to changes in the thrust

It is clearly inevitable that a change in thrust will result in a disturbance of the motion in the flight direction and thus the simplifying assumption used to derive the response to pitch control input is not valid. The analysis of the effect of thrust change must involve all three degrees of longitudinal freedom. In this case using Eqn. (4.71) and Cramer's rule the equivalent of Eqn. (4.73b) is:

$$|A|\hat{w} = \begin{vmatrix} A_1 & E_1 & C_1 \\ F_1 & J_1 & H_1 \\ K_1 & P_1 & M_1 \end{vmatrix} (\text{func}.T) \tag{4.89a}$$

where the expansion of $|A|$ is given at Eqn. (4.73c). The expansion of the right-hand side of Eqn. (4.89a) is:

$$[A_1\{J_1M_1 - H_1P_1\} - E_1\{F_1M_1 - H_1K_1\} - C_1\{F_1P_1 - J_1K_1\}] \tag{4.89b}$$

While Eqn. (4.89b) may be further developed by substituting in the definition of the coefficients from Eqn. (4.71). the result is complex and it is usually easier to substitute the numerical values appropriate to a particular case. The expression is simpler when the normal offset of the thrust, z_T, is negligible since then P_1 is zero. In practice it is very unlikely that changes in thrust. inclusive of engine failure, will result in any critical loading condition. The further development of Eqns (4.89) is not therefore justified.

4.7 Analysis of the lateral/directional equations

4.7.1 Introduction

As mentioned in Section 4.4.8.1, when the aircraft has a wing of low aspect ratio the coupling between the lateral and longitudinal freedoms may be such that a full six degrees of freedom analysis is required. However. in the majority of cases it is sufficient to employ the decoupled lateral/directional equations for loading calculations. These are to be found in Eqns (4.67) where they are mainly expressed in terms of the non-dimensional linear and angular velocities $\hat{v}$, $\hat{p}$, and $\hat{r}$. It is convenient to write them in terms of the angles, β, ϕ, and ψ in sideslip, roll, and yaw, respectively. Hence:

$$\begin{aligned} \hat{v} &= v/V_o = \beta \\ \hat{p} &= d\varphi/d(\hat{t}) = \hat{\phi} \\ \hat{r} &= d\psi/d(\hat{t}) = \hat{\psi} \end{aligned} \tag{4.90}$$

Application of the differential operator $\mathcal{D}$ to Eqns (4.67) then yields:

$$
\begin{aligned}
&(\mathcal{D} - Y_v)\beta - (\{Y_p/\mu_2\}\mathcal{D} + C_L)\varphi - (\{Y_r/\mu_2\} - 1)\mathcal{D}\psi \\
&\quad = Y_\xi\xi + Y_\zeta\zeta + Y_T(\text{func.}T) \\
&-L_v\beta + (\{i_x/\mu_2\}\mathcal{D}^2 - \{L_p/\mu_2\}\mathcal{D})\varphi - (\{i_{xz}/\mu_2\}\mathcal{D}^2 + \{L_r/\mu_2\}\mathcal{D})\psi \\
&\quad = L_\xi\xi + L_\zeta\zeta + L_T(\text{func.}T) \\
&-N_v\beta - (\{i_{xz}/\mu_2\}\mathcal{D}^2 + \{N_p/\mu_2\}\mathcal{D})\varphi + (\{i_z/\mu_2\}\mathcal{D}^2 - \{N_r/\mu_2\}\mathcal{D})\psi \\
&\quad = N_\xi\xi + N_\zeta\zeta + N_T(\text{func.}T)
\end{aligned}
\tag{4.91}
$$

where the atmospheric disturbance terms have been omitted and the remarks made at Eqn. (4.70) concerning the terms on the-right hand side of the equations apply.

Writing Eqns (4.91) in matrix notation:

$$
\begin{bmatrix} A_2 & B_2 & C_2 \\ G_2 & H_2 & I_2 \\ M_2 & N_2 & O_2 \end{bmatrix} \begin{Bmatrix} \beta \\ \phi \\ \psi \end{Bmatrix} = \begin{bmatrix} D_2 & E_2 & F_2 \\ J_2 & K_2 & L_2 \\ P_2 & Q_2 & R_2 \end{bmatrix} \{\zeta\xi \ \text{func.}T\} \tag{4.92}
$$

where:

$$
\begin{aligned}
A_2 &= (\mathcal{D} - Y_v) \\
B_2 &= -(\{Y_p/\mu_2\}\mathcal{D} + C_L) \\
C_2 &= -(\{Y_r/\mu_2\} - 1)\mathcal{D} \\
D_2 &= Y_\xi \\
E_2 &= Y_\zeta \\
F_2 &= Y_T \\
G_2 &= -L_v \\
H_2 &= (\{i_x/\mu_2\}\mathcal{D}^2 - \{L_p/\mu_2\}\mathcal{D}) \\
I_2 &= -(\{i_{xy}/\mu_2\}\mathcal{D}^2 + \{L_r/\mu_2\}\mathcal{D}) \\
J_2 &= L_\xi \\
K_2 &= L_\zeta \\
L_2 &= L_T \\
M_2 &= -N_v \\
N_2 &= -(\{i_{xy}/\mu_2\}\mathcal{D}^2 + \{N_p/\mu_2\}\mathcal{D}) \\
O_2 &= (\{i_z/\mu_2\}\mathcal{D}^2 - \{N_r/\mu_2\}\mathcal{D}) \\
P_2 &= N_\xi \\
Q_2 &= N_\zeta \\
R_2 &= N_T
\end{aligned}
$$

Equation (4.92) may be solved by the application of Cramer's rule as described in Section 4.6.1 with reference to Eqn. (4.71). For example. considering only the control input due to the rudder deflection, ζ, and solving for β:

$$|C|\beta = \begin{bmatrix} E_2 & B_2 & C_2 \\ K_2 & H_2 & I_2 \\ Q_2 & N_2 & O_2 \end{bmatrix} (\zeta) \tag{4.93a}$$

where $|C|$ is the determinant of the first matrix in Eqn. (4.92) and may be expressed as:

$$|C| = [A_2\{H_2O_2 - I_2N_2\} - B_2(G_2O_2 - I_2M_2\} - C_2\{H_2M_2 - G_2N_2\}] \tag{4.93b}$$

The expansion of $|C|$ requires the substitution of the values of the coefficients given in Eqn. (4.92). Although some of the terms are small and often may be neglected the result is complex algebraically.

When the right-hand side of Eqn. (4.92) is set to zero, the solution of the equations describes the basic lateral/directional stability characteristics of the aircraft. There are four roots, usually two real ones and a complex pair. One of the real roots is invariably negative, and therefore represents a stable motion, and it is the subsidence in roll. The other real root is often positive and thus describes an unstable motion. Typically it represents a slow spiral motion, often divergent, and is of no consequence in loading analysis. The complex pair of roots describe the lateral oscillation of the aircraft in yaw and it is usually associated with some rolling motion. It is sometimes referred to as the 'Dutch Roll'. It is comparable to the longitudinal short-period mode and is the primary factor in determining the loading occurring during yawing/sideslipping manoeuvres. For aircraft of conventional design the yaw Right loading cases are based on the premise that the aircraft remains in level flight achieved, if necessary, by appropriate application of the roll control motivators. This leads to the assumption that the calculation of the loads occurring during yawing motion may be evaluated without consideration of any associated roll effects. Thus the yawing loads may be analysed by neglecting the coupling between the rolling equation on the one hand and the sideslipping and yaw equations on the other.

4.7.2 Definition of lateral/directional non-dimensional derivatives

The longitudinal derivatives given in Section 4.6.2 are primarily dependent upon the aerodynamic characteristics of the wing and the horizontal stabilizer and therefore may be expressed concisely. The lateral/directional aerodynamic characteristics are dependent upon relatively complex interactions of all the main airframe componcnts, namely the wing, body, vertical stabilizer and, to a lesser extent, the horizontal stabilizer. For most purposes it is simplest to retain the non-dimensional derivative format bearing in mind that, for a given case, each one has a simple numerical value. An exception to this generalization is the non-dimensional derivatives relating to the

application of directional control, usually the rudder, and the effect of change in powerplant thrust.

The following comments are included to indicate the major contributions to each of the lateral/directional derivatives and their relative importance. The actual numerical values may be derived by reference to a number of sources such as the relevant ESDU Data Sheets, see Chapter 17. Appendix A17.

(a) Y_v, ***sideforce due to side (lateral) velocity.*** The two main contributions are from the body and the vertical stabilizer (fin).The former is usually destabilizing and the latter has to be sufficiently great to more than offset this effect. There are also contributions from powerplant nacelles and deployed high-lift systems.

(b) L_v, ***rolling moment due to side velocity.*** This is the lateral static stability term and is primarily dependent upon the effective dihedral of the relevant components of the aircraft. The contributions arise from:

(i) wing dihedral, which is often the most important;
(ii) wing sweepback, which increases the lateral stability;
(iii) fin, which usually increases the lateral stability;
(iv) lateral flow across the junction of the wing and body, a high wing conferring stability and vice-versa for a low wing;
(v) powerplant nacelles;
(vi) deployed high lift devices.

An example of these effects in combination is the relatively large dihedral associated with an unswept low wing arrangement as compared with little dihedral, or even anhedral, on a swept-hack, high, wing layout.

(c) $N_{,,}$, ***yawing moment due to side velocity.*** This term determines the natural directional, or weathercock, stability. The largest contribution in a naturally stable aircraft arises from the fin but its effect is offset by the destabilizing component from the body. Propellers and powerplant nacelles located forward of the centre of gravity are also destabilizing and vice versa.

(d) Y_p, ***side force due to rate of roll.*** The fin and, possibly wing dihedral and sweep. are the main contributors to this term. It is often small and negligible.

(e) $L_{,,}$, ***rolling moment due to rare of roll.*** This term determines the damping in the rolling motion. While there are contributions from both the vertical and horizontal stabilizing surfaces and wing–body interference, the dominant effect arises from the wing plan-form and dihedral. It is always negative.

(f) N_p, ***yawing moment due to rate of roll.*** The fin makes some contribution but the greatest effect is from the wing. It depends upon the dihedral, lift. and drag characteristics. Overall it is usually negative hut may become positive for a highly swept. low aspect ratio, configuration.

(g) Y_r, ***side force due to rate of yaw.*** This term is often negligible. There arc contributions from the body, fin, and wing sweep.

(h) L_r, ***rolling moment due to rate of yaw.*** This effect can be important. There are contributions from the fin and the wing, the latter being dependent upon the spanwise lift distribution. Deployed high-lift devices also contribute to the term.

(i) N_r, *yawing* ***moment due to rare of yaw.*** This is a significant term in the lateral/directional stability of the aircraft as it represents the damping in yaw and is normally negative. The wing contribution is dependent upon the span-wise drag distribution and the body and deployed high-lift devices also make contributions. However, the biggest effect is likely to be from the vertical stabilizer.

(j) Y_ξ, ***side force dire to roll*** *motivator* ***(aileron) deflection.*** This term is usually small and negligible. Any effect is due to the dihedral component of the aileron force.

(k) L_ξ, ***rolling*** *moment* ***due*** *to* ***roll motivator*** *deflection.* This is the primary roll control effect and is dependent upon the geometry and aerodynamic characteristics of the roll controls relative to the wing.

(l) N_ξ, *yawing moment due to* ***roll*** *motivator* ***deflection.*** This term results from the relative drag of the up-going and down-going ailerons. In some aircraft the ailerons are deliberately designed to eliminate the difference. In any case the numerical value is usually small.

(m) Y_ζ, ***side force*** *due* ***to lateral*** *motivator* ***(rudder) deflecrion.*** This is simply:

$$Y_\zeta = a_{2F} S_F / S \tag{4.94a}$$

where

a_{2F} is the lift curve slope of the vertical stabilizer based on its area S_F.
S is the wing reference area

(n) L_ζ, ***rolling moment due to*** *lateral* ***motivator deflecrion.***

$$L_\zeta = a_{2F} h_F \bar{V}_v / \ell_F \tag{4.94b}$$

where

$\bar{V}_v$ is the vertical stabilizer volume coefficient, $\{\ell_F S_F/(bS)\}$
ℓ_F is the distance of the chord-wise load on the vertical stabilizer aft of the centre of gravity of the aircraft. For simplicity no distinction is made between loads due to angle of attack and control deflection
h_F is the height of the centre of pressure of the rudder force above the longitudinal axis
b is the wing span

(p) N_ζ, ***yawing moment due to lateral*** *motivator* ***deflection.***

$$N_\zeta = -a_{2F} \bar{V}_v \tag{4.94c}$$

(q) Y_T, ***side force*** *due* ***to*** *change* ***in the*** *thrust*. The side force which results from change in the thrust, AT. maybe expressed as:

$$Y_T = -2\Delta T \psi / (\rho S V_o^2) \tag{4.94d}$$

Note this term is a function of the disturbed yaw angle, ψ

(r) L_T, ***rolling moment due to change in thrust.*** The only rolling moment resulting from thrust changes is that due to the normal force effect, Z_T, Eqn. (4.74r), when the powerplant involved is offset from the rolling axis. The term is zero if there is no change in the pitch angle, θ.

(s) N_T, ***yawing moment due to change in thrust.*** This is likely to be the most significant effect of a change in thrust, especially when a powerplant has failed.

$$N_T = -2\Delta T(y_T/b)/(\rho S V_o^2) \tag{4.94e}$$

where y_T is the lateral offset of the thrust line of the effected powerplant from the centreline of the aircraft.

4.7.3 Decoupling of the lateral/directional equations of motion

The summary of the lateral/directional stability characteristics given in Section 4.7.1 leads to the conclusion that for the purposes of the loading calculations for conventional aircraft it is acceptable to consider the roll cases in isolation from those involving sideslipping/yawing motions. This results in a considerable simplification in the analysis.

It is further presumed that the aircraft is inherently stable in these two Right conditions. This assumption is fully justified for the rolling motion. Directional stability is usually present. although not infrequently stability augmentation is employed to increase the damping in the motion. This does not change the loading conditions providing the actuator used for augmentation is safeguarded against a run-away. In those cases where inherent lateral stability is not present, the design loading cases are prescribed in the same way as for the pitching conditions by using the control system to place limits on the manoeuvres allowed. see Section 4.6.3.2 and Chapter 3, Section 3.3.1.

4.7.4 Response of the aircraft to roll control input

When the rolling motion is decoupled from the other lateral modes, the second of Eqns (4.91) with only roll control input becomes:

$$H_2(\varphi) = J_2(\xi) \tag{4.95a}$$

and substituting for the coefficients:

$$\{i_x/\mu_2\}\mathcal{D}^2\varphi - \{L_p/\mu_2\}\mathcal{D}\varphi = L_\xi\xi$$

or

$$\hat{\ddot{\phi}} - \{L_p/i_x\}\hat{\dot{\phi}} = \{L_\xi\mu_2/i_x\}\xi \tag{4.95b}$$

and since $\hat{p} = \phi$:

$$\hat{\dot{p}} - \{L_p/i_x\}\hat{p} = \{L_\xi \mu_2/i_x\}\xi \tag{4.95c}$$

The solution of this equation takes the general form

$$\hat{p} = \text{Const.}e^{-k} + \hat{p}'$$

where

$$k = \int (-L_p/i_x)d(\hat{t}) = (-L_p/i_x)\hat{t}$$

For the case when the control input is held constant, a steady rolling state is reached where $\dot{p}$ is zero. From Eqn. (4.95c) in this condition:

$$\hat{p}' = \hat{p} = -\{L_\xi \mu_2/L_p\}\xi \tag{4.96a}$$

Also initially at $\hat{t} = 0$, $\hat{p} = 0$. and k = 0 therefore:

$$\text{Const.} = -\hat{p}' \tag{4.96b}$$

Hence

$$\hat{p} = \hat{p}'\{1 - \exp(L_p/i_x)\hat{t}\}$$

or:

$$\hat{p} = -\{L_\xi \mu_2/L_p\}\{1 - \exp(L_p/i_x)\hat{t}\}\xi \tag{4.97a}$$

Convening from non-dimensional to real time, t:

$$p\{2m/(\rho S V_o)\} = -\{2m/(\rho S b)\}\{L_\xi/L_p\}\{1 - \exp[\{\rho S V_o/(2m)\}(L_p/i_x)]t\}\xi$$
$$p = -(V_o/b)(L_\xi/L_p)\{1 - \exp[(V_o/b)\{L_p/(\mu_2 i_x)\}]t\}\xi \tag{4.97b}$$

Note that since L_p is always negative, as the time, t, tends to infinity the exponential term will tend to zero as would be expected from the particular integral of the solution, $\hat{p}'$.

4.7.5 Response of the aircraft to yaw control input

If it is assumed that there is no rolling motion, either naturally or as a consequence of the appropriate application of roll control, the lateral/directional response to yaw control

input is derived from Eqn. (4.91) as

$$\begin{bmatrix} A_2 & C_2 \\ M_2 & O_2 \end{bmatrix} \begin{Bmatrix} \beta \\ \psi \end{Bmatrix} = \begin{bmatrix} E_2 \\ Q_2 \end{bmatrix} (\zeta) \tag{4.98}$$

Using Cramer's rule the solution of Eqn. (4.98) for the sideslip angle, β, is:

$$\begin{vmatrix} A_2 & C_2 \\ M_2 & O_2 \end{vmatrix} (\beta) = \begin{vmatrix} E_2 & C_2 \\ Q_2 & O_2 \end{vmatrix} (\zeta) \tag{4.99a}$$

where

$$\begin{aligned} \begin{vmatrix} A_2 & C_2 \\ M_2 & O_2 \end{vmatrix} &= [A_2 O_2 - C_2 M_2] \\ &= (\mathcal{D} - Y_v)(\{i_z/\mu_2\}\mathcal{D}^2 - \{N_r/\mu_2\}\mathcal{D}) - (\{Y_r/\mu_2\} - 1)\mathcal{D}(N_v) \\ &= \{i_z/\mu_2\}\mathcal{D}^3 - \{Y_v i_z/\mu_2\}\mathcal{D}^2 - \{N_r/\mu_2\}\mathcal{D}^2 + \{Y_v N_r/\mu_2\}\mathcal{D} \\ &\quad - \{N_v Y_r/\mu_2\}\mathcal{D} + N_v\mathcal{D} \\ &= \{i_z/\mu_2\}[\mathcal{D}^2 - (Y_v + \{N_r/i_z\})\mathcal{D} + \{Y_v N_r/i_z\} \\ &\quad - \{N_v Y_r/i_z\} + \{N_v\mu_2/i_z\}]\mathcal{D} \end{aligned} \tag{4.99b}$$

$$\begin{aligned} \begin{vmatrix} E_2 & C_2 \\ Q_2 & O_2 \end{vmatrix} &= [E_2 O_2 - C_2 Q_2] \\ &= Y_\zeta(\{i_z/\mu_2\}\mathcal{D}^2 - \{N_r/\mu_2\}\mathcal{D}) + N_\zeta(\{Y_r/\mu_2\} - 1)\mathcal{D} \\ &= (i_z/\mu_2)(Y_\zeta\mathcal{D}^2 - \{Y_\zeta N_r/i_z\}\mathcal{D} + \{N_\zeta Y_r/i_z\}\mathcal{D} - \{N_\zeta\mu_2/i_z\}\mathcal{D}) \\ &= (i_z/\mu_2)(Y_\zeta\mathcal{D} - \{Y_\zeta N_r/i_z\} + \{N_\zeta Y_r/i_z\} - \{N_\zeta\mu_2/i_z\})\mathcal{D} \end{aligned} \tag{4.99c}$$

Hence. from Eqn. (4.99a):

$$\begin{aligned} &\ddot{\beta} - (Y_v + \{N_r/i_z\})\dot{\beta} + (\{Y_v N_r/i_z\} - \{N_v Y_r/i_z\} + \{N_v\mu_2/i_z\})\beta \\ &\quad = Y_\zeta\dot{\zeta} - (\{Y_\zeta N_r/i_z\} - \{N_\zeta Y_r/i_z\} + \{N_\zeta\mu_2/i_z\})\zeta \end{aligned}$$

or writing in the form:

$$\ddot{\beta} + 2R_2\dot{\beta} + (J_2^2 + R_2^2)\beta = F(\zeta) \tag{4.100a}$$

$$R_2 = -(Y_v + \{N_r/i_z\})/2 \tag{4.100b}$$

$$J_2 = (\{Y_v N_r - N_v Y_r + N_v\mu_2\}/i_z - R_2^2)^{1/2} \tag{4.100c}$$

$$F(\zeta) = Y_\zeta\dot{\zeta} - (\{Y_\zeta N_r - N_\zeta Y_r + N_\zeta\mu_2\}/i_z)\zeta \tag{4.100d}$$

R_2 and J_2 are the damping coefficient and natural damped frequency in the motion, respectively and $F(\zeta)$ is the forcing function, compare with Eqns (4.82) for the longitudinal case.

The terms involving Y_r are likely to be of negligible magnitude. Further, $(Y_\zeta N_r)$ may be expected to be small in comparison with $(N_\zeta \mu_2)$ so that approximately:

$$F(\zeta) = Y_\zeta \dot{\hat{\zeta}} - (N_\zeta \mu_2 / i_z)\zeta \tag{4.100e}$$

Substituting the derivatives from Eqns (4.94a) and (4.94c):

$$F(\zeta) = (a_{2F} S_F / S)\dot{\hat{\zeta}} + (a_{2F} \bar{V}_v \mu_2 / i_z)\zeta = F_{21}\dot{\hat{\zeta}} + F_{22}\zeta \tag{4.100f}$$

Equation (4.100a) may be expressed in the alternative form, see Eqn. (4.841 for the longitudinal motion:

$$\ddot{\hat{\beta}} + 2\omega_2 \zeta_{D2} \dot{\hat{\beta}} + \omega_2^2 \beta = F(\zeta) \tag{4.101a}$$

where the undamped frequency of the motion is:

$$\omega_2 = (J_2{}^2 + R_2^2)^{1/2} \tag{4.101b}$$

and the damping ratio in the motion is:

$$\zeta_{D2} = R_2 / \omega_2 \tag{4.101c}$$

The alternative solution of Eqn. (4.98) is in terms of the yaw angle. ψ

$$\begin{vmatrix} A_2 & C_2 \\ M_2 & O_2 \end{vmatrix} (\psi) = \begin{vmatrix} A_2 & E_2 \\ M_2 & Q_2 \end{vmatrix} (\zeta) \tag{4.102a}$$

The determinant on the right-hand side of this equation is:

$$\begin{aligned} \begin{vmatrix} A_2 & E_2 \\ M_2 & Q_2 \end{vmatrix} &= [A_2 Q_2 - E_2 M_2] \\ &= (\mathcal{D} - Y_v) N_\zeta + Y_\zeta N_v \\ &= N_\zeta \mathcal{D} - Y_v N_\zeta + Y_\zeta N_v \end{aligned} \tag{4.102b}$$

Hence, from Eqns (4.99) and (4.102b), the determinant is:

$$[\mathcal{D}^3 - (Y_v + \{N_r/i_z\})\mathcal{D}^2 + (\{Y_v N_r/i_z\} - \{N_v Y_r/i_z\} + \{N_v \mu_2/i_z\})\mathcal{D}]\psi$$
$$= (\mu_2/i_z)[N_\zeta \dot{\hat{\zeta}} - (Y_v N_\zeta - Y_\zeta N_v)\zeta]$$

Therefore, using Eqns (4.100):

$$\dddot{\hat{\psi}} + 2R_2 \ddot{\hat{\psi}} + (J_2^2 + R_2^2)\dot{\hat{\psi}} = F'(\zeta) \tag{4.103a}$$

where R_2 and J_2 are defined in Eqns (4.100b) and (4.100c) and:

$$F'(\zeta) = (\mu_2/i_z)[N_\zeta \dot{\hat{\zeta}} - (Y_v N_\zeta - Y_\zeta N_v)\zeta] \tag{4.103b}$$

Also the non-dimensional rate of yaw, $\hat{r}$, is equal to $\dot{\psi}$ and thus Eqn. (4.103a) may be written as:

$$\ddot{\hat{r}} + 2R_2 \dot{\hat{r}} + (J_2^2 + R_2^2)\hat{r} = F'(\zeta) \tag{4.104}$$

4.7.6. Response of the aircraft to changes in thrust

The lateral/directional response of the aircraft to changes in thrust is derived from Eqn. (4.92) as:

$$\begin{bmatrix} A_2 & B_2 & C_2 \\ G_2 & H_2 & I_2 \\ M_2 & N_2 & O_2 \end{bmatrix} \begin{Bmatrix} \beta \\ \phi \\ \psi \end{Bmatrix} = \begin{bmatrix} F_2 \\ L_2 \\ R_2 \end{bmatrix} (\text{func.}T) \tag{4.105}$$

By comparison with Eqn. (4.93a) the solution in terms of the sideslip angle, β, using Cramer's rule is:

$$|C|\beta = \begin{vmatrix} F_2 & B_2 & C_2 \\ L_2 & H_2 & I_2 \\ R_2 & N_2 & O_2 \end{vmatrix} (\text{func.}T) \tag{4.106a}$$

The expansion of $|C|$ is given by Eqn. (4.93b). The expansion of the determinant on the right-hand side of the equation is:

$$\begin{vmatrix} F_2 & B_2 & C_2 \\ L_2 & H_2 & I_2 \\ R_2 & N_2 & O_2 \end{vmatrix} = [F_2\{H_2O_2 - I_2N_2\} - B_2\{L_2O_2 - I_2R_2\} - C_2\{H_2R_2 - L_2N_2\}] \tag{4.106b}$$

From paragraph 4.7.2(r) it will be noted that when there is no disturbance in the pitch angle of the aircraft, the derivative L_T is zero, that is, the coefficient L_2 in Eqn. (4.106b) is zero. Thus Eqn. (4.106b) is simplified to:

$$\begin{vmatrix} F_2 & B_2 & C_2 \\ L_2 & H_2 & I_2 \\ R_2 & N_2 & O_2 \end{vmatrix} = [F_2\{H_2O_2 - I_2N_2\} + B_2I_2R_2 - C_2H_2R_2] \qquad (4.106c)$$

However, it will also be noted that the derivative Y_T is a function of the yaw angle, ψ, and thus a simple analytical solution to Eqn. (4.105) is not possible. Preferably a simulation technique should be used. Even if this term is assumed to be zero so that F_2 becomes zero in Eqns (4.106b) and (4.106c) there is still coupling between the rolling motion and the other lateral/directional modes since the yawing derivative due to the change in thrust. N_T, will cause a disturbance in both the sideslip and yaw rate with a consequent rolling effect through the derivatives L_v and L_r coefficients G_2 and I_2 respectively.

It is unlikely that the change in thrust consequent upon the failure of an outboard powerplant will result in a critical structural loading case. An approximate estimation of the loads occurring during such an event may be obtained by assuming:

(i) that the roll interaction may be neglected;
(ii) that the side force effect, Y_T, is zero;
(iii) that the change in thrust is instantaneous.

Then, replacing the control term, N_ζ, in Eqn. (4.100c) by N_T and with the equivalent of Y_ζ being zero. Eqn. (4.100a) becomes:

$$\ddot{\beta} + 2R_2\dot{\beta} + (J_2^2 + R_2^2)\beta = -N_T\mu_2/i_z \qquad (4.107)$$

4.8 Comments on special configurations of aircraft

4.8.1 *General*

The development of the equations thus far in this chapter is based on the assumption that the aircraft is of conventional configuration. This is defined as a layout having aft-located horizontal and vertical stabilizing/control surfaces. There are other possibilities deserving comment.

Very few aircraft dispense with the conventional aft vertical stabilizing surface as this is required to confer directional stability. Vertical surfaces may be located at the extremities of a swept-back wing but this does not basically alter the analysis developed in Section 4.7. A few more recent designs do dispense with the vertical surfaces for reasons of low observability and the control system is used to confer artificial stability. In this, comparatively rare, situation the comments in Section 4.7.3 are applicable.

The major variations are in the longitudinal arrangement of the auxiliary lifting surfaces and the notation introduced in Section 4.2.1.1 was chosen to enable the alternatives to be covered by simple adaptation.

The following sections are concerned only with the changes necessary to adapt the analysis for variations in the longitudinal layout, Inherent stability is assumed. Should this not be the case the remarks made in Section 4.6.3.2 are relevant.

4.8.2 Aircraft employing fore-plane layouts

4.8.2.1 Introduction

It is possible to place fore-plane, or canard, layouts into two nominal categories:

(a) Long coupled, where the aerodynamic centre of the fore-plane is four or more wing mean chords ahead of the centre of gravity of the aircraft.

(b) Close, or short, coupled, where the aerodynamic centre of the fore-plane is no more than three wing mean chords ahead of the centre of gravity of the aircraft. In this configuration the fore-plane is usually located above the wing. The fore-plane arm is unlikely to be less than 80 per cent of the wing mean chord.

4.8.2.2 Long coupled fore-plane layout

In a fore-plane layout the centre of gravity of the aircraft is usually between the fore-plane and the wing aerodynamic centre. The numerical sign of ***hc.*** as shown in Fig. 4.1, is only changed if the centre of gravity is ahead of the leading edge of the wing aerodynamic mean chord reference. However, the previously used tail-plane arm, ℓ'_T, is now the fore-plane arm and is negative. Appropriate changes must be made in the analysis including changing the sign of the volume coefficient, $\bar{V}$, Eqn. (4.24).

Unlike a conventional arrangement, the wing is in the wash from the fore-plane which will be a down-wash over the inner part of the wing but an up-wash outboard. In a long coupled configuration the wash effect will he small due to the distance between the two surfaces. For simplicity, therefore, it may he assumed that these flow effects are small or self-cancelling, as far as the wing is concerned. As there are negligible wash effects on the fore-plane all that is required is for all the down-wash terms, $(d\varepsilon/d\alpha)$, in the various equations to be deleted.

Thus, in summary, the analysis may be applied to a long coupled fore-plane layout by:

(a) Changing the sign of the centre of gravity location, ***hc,*** if necessary.

(b) Changing the sign of the location of the horizontal stabilizer arm relative to the centre of gravity of the aircraft, ℓ'_T, including the volume coefficient, $\bar{V}$.

(c) Deleting all the down-wash terms. $(d\varepsilon/d\alpha)$.

It will be noted from Eqn. (4.37c) that the definition of the manoeuvre margin, H_m, is unchanged since the sign of the product $(\ell'_T\bar{V})$ is unchanged. As a consequence of

this the damped short-period frequency, J_1, defined in Eqn. (4.82c) is unchanged. From Eqn. (4.82b):

$$R_1 = [a_{1WB} + a_{1T}(S_T/S)(\ell'_T/k_y)^2 - (c/k_y)^2 m_\theta]/2 \tag{4.108}$$

where the sign of the middle term is also unchanged

4.8.2.3 Close coupled fore-plane layout

In a closecoupled fore-plane configuration both the lifting surfaces are in the wash from the other. With an appropriate geometric arrangement, and providing that the fore-plane is less than two wing mean chords ahead of the wing, the total lift of the combination can be greater than the sum of the individual contributions. The interaction between the surfaces is complex and it is not possible to make accurate simple generalizations. A possible approach for the purposes of initial design is to:

(a) Neglect the wash effects as such, so that the $(d\varepsilon/d\alpha)$ terms may be deleted as in the long coupled case.
(b) Change the sign of the fore-plane arm relative to the centre of gravity of the aircraft as discussed in Section 4.8.2.2 above.
(c) Assume that the favourahle interaction effects may he represented by increases in the lift curve slopes of the wing and fore-plane.

Howe,[3] suggests that the favourable lift effects are equally allocated to the two lifting surfaces and that they may be estimated from:

$$a'_1 = (1 + KS_T/S)a_{1WB} \tag{4.109a}$$

$$a'_{1T} = (1 + K)a_{1T} \tag{4.109b}$$

where a'_1 and a'_{1T} are the enhanced values of the wing–body and fore-plane lift curve slopes, respectively. and:

$$K = \{0.11(\ell_T/c)^2 + 0.73(\ell_T/c) + 1.02\} \tag{4.109c}$$

for $0.8 < (\ell_T/c) < 2.0$.

Note that in this case ℓ_T, the aerodynamic fore-plane arm, is numerically negative.

4.8.3 Tailless aircraft

4.8.3.1 Introduction

A tailless aircraft is defined as one having a layout which does not include a horizontal stabilizing surface. It is presumed that pitch control is provided by an elevator, or equivalent, located at the trailing edge of the wing. It is also assumed that the usual

[3] **Howe.** D. *Aircraft Conceptual* Design Synthesis. Professional Engineering Publishing Ltd, 2000.

vertical stabilizing surface is present so that the special features are limited to the longitudinal arrangement.

4.8.3.2 Response of a statically stable tailless aircraft to pitch control input

The airframe aerodynamic derivatives given in Section 4.6.2 are expressed in such a way that the contributions of the horizontal stabilizer may be directly derived for the tailless case. In the absence of a horizontal stabilizer, the ratio (S_T/S) is taken to be unity and the terms containing the derivative a_{1T} and the volume coefficient, $\bar{V}$, are zero.

Hence, from Eqns (4.82) for the tailless case:

$$R_1 = [a_{1WB} - (c/k_y)^2 m_\theta]/2 \tag{4.110a}$$

$$J_1 = [2ma_{1WB}cH_m/(\rho Sk_y^2) - R_1^2]^{1/2} \tag{4.110b}$$

where now:

$$H_m = K_{,} - m_\theta/\mu_1 = (H_o - h) - m_\theta/\mu_1 \tag{4.110c}$$

The control derivatives for a tailless aircraft are defined in terms of the wing area as explained in paragraphs 4.6.2(m) to (p). Referring to Eqns (4.82). the coefficient of the $\dot{\hat{\eta}}$ term is simply $(-a_2)$ where here the derivative refers to the pitch control motivator. The coefficient of the η term becomes:

$$\begin{aligned}\delta &= -(c/k_y)^2[-a_2 m_\theta + 2ma_2(\ell_n/c)/(\rho Sc)] \\ &= -[-a_2 m_\theta (c/k_y)^2 + 2ma_2(\ell_\eta/c)c/(\rho Sk_y^2)] \\ &= -2ma_2 c[(\ell_\eta/c) - m_\theta \rho Sc/(2m)]/(\rho Sk_y^2) \\ &= -a_2\mu_1(c/k_y)^2[(\ell_\eta/c) - m_\theta/\mu_1]\end{aligned} \tag{4.110d}$$

where ℓ_η is the chord-wise distance between the centre of pressure of the air-load due to the deflection of the pitch control and the centre of gravity. It will be seen that Eqn. (4.110d) is comparable to Eqn. (4.82f) where (S_T/S) is unity and a_{1T} in the middle term is zero.

4.8.4 All-moving horizontal stabilizer

When the pitch control of the aircraft is obtained by adjusting the angle of attack of the whole horizontal stabilizer, rather than by the use of an elevator, the load due to the operation of the control is:

$$\mathcal{L}_T = \rho V_o^2 S_T a_{1T}(\Delta\alpha_T)/2 \tag{4.111}$$

where $(\Delta\alpha_T)$ is the change in the angle of the horizontal stabilizer due to the control input, and is equivalent to η for a conventional elevator. Thus throughout the analysis it is necessary to replace $(a_2\eta)$ by $\{a_{1T}(\Delta\alpha_T)\}$. For example. the simplified form of the coefficient of the pitch control forcing function, Eqn. (4.82g), becomes:

$$\delta = -a_{1T}\mu_1(c/k_Y)^2(\bar{V}) \tag{4.112}$$

and the input parameter is $\Delta\alpha_T$ rather than η.

Appendix A4 Characteristics of second-order linear differential equations

A4.1 Introduction

The equations which define both the longitudinal short-period motion and the lateral/directional oscillation. Eqns (4.84) and (4.101), are of the form:

$$\ddot{X} + 2\zeta_D\omega\dot{X} + \omega^2 X = F(\kappa) \tag{A4.1}$$

where the undamped natural frequency of the motion is:

$$\omega = (J^2 + R^2)^{1/2} \tag{A4.2a}$$

and the damping ratio is:

$$\zeta_D = R/\omega \tag{A4.2b}$$

κ represents an angular control input such as η or ζ and $\{J = \omega(1 - \zeta_D^2)^{1/2}\}$.

The damping coefficient. R, the damped natural frequency, J. and the forcing function. F, are defined at the relevant equations. The solution of Eqn. (A4.1) has two parts, namely the Complementary Function and the Particular Integral.

The form of the equation is typical of systems which may be represented by a damped spring-mass mechanism. In the simple case of a spring supporting a mass the variable, X, is the deflection. The coefficient of the $\ddot{X}$ term is effectively the mass m but it has been normalized in Eqn. (A4.1). The coefficient of the X term is the spring stiffness, say k. If there is no damping the $\dot{X}$ term is zero and the natural frequency of vibration is then simply $\omega = (k/m)^{1/2}$. The damping term is 90° out of phase relative to the stiffness term.

A4.2 The Complementary Function

The Complementary Function part of the solution of the equation represents the transient motion of the system. It is described by placing the right-hand side of

Eqn. **(A4.1)** to zero,

$$\ddot{X} + 2\zeta_D \omega \dot{X} + \omega^2 X = 0 \tag{A4.3a}$$

and applying the differential operator:

$$(\mathcal{D}^2 + 2\zeta_D \omega \mathcal{D} + \omega^2 \mathcal{D})X = 0 \tag{A4.3b}$$

Providing that they are not equal the general roots of this equation are:

$$\boldsymbol{X} = (-\zeta_D \omega \pm i2\omega(\zeta_D^2 - 1)^{1/2}) \tag{A4.3c}$$

The physical meaning depends upon the value of the damping ratio, ζ_D.

If $-1 < \zeta_D < 1$ the roots are $\{-\zeta_D \omega \pm i2\omega(1 - \zeta_D^2)^{1/2}\}$ and the Complementary Function can be written as:

$$X = e^{(-\zeta_D \omega \hat{t})}[A sin\omega(1 - \zeta_D^2)^{1/2}\hat{t} + B cos\omega(1 - \zeta_D^2)^{1/2}\hat{t}] \tag{A4.4}$$

where A and B are coefficients determined by system boundary conditions.

When ζ_D is negative this represents an oscillation of increasing magnitude. but if ζ_D is positive the oscillation decays.

For $\zeta_D = 0$, the solution becomes:

$$X = [A sin\omega\hat{t} + B cos\omega\hat{t}] \tag{A4.5}$$

When $\zeta_D = 1$ the roots are equal and in this special case the solution is:

$$X = e^{(-\omega\hat{t})}[A + B\hat{t}] \tag{A4.6}$$

and the system is said to be critically damped.

When $\zeta_D > 1$ the system is over-damped:

$$X = e^{(-\zeta_D \omega \hat{t})}[A sinh\omega(\zeta_D^2 - 1)^{1/2}\hat{t} + B cosh\omega(\zeta_D^2 - 1)^{1/2}\hat{t}] \tag{A4.7}$$

The system is convergent in this case, while if $\zeta_D < -1$ the form of the equation is similar but the system is divergent.

An alternative form of expressing the Complementary Function for $(-1 \leqslant \zeta_D \leqslant 1)$ is:

$$X = Ge^{(-\zeta_D \omega \hat{t})} sin\{(1 - \zeta_D^2)^{1/2} \omega \hat{t} + \psi_c\} \tag{A4.8}$$

where G and ψ_c are coefficients determined by the boundary conditions, and are equivalent to A and B of Eqns (A4.4) to (A4.7) which are $Gsin\psi_c$ and $Gcos\psi_c$, respectively. Although mathematically identical to Eqn. (A4.4), Eqn. *(A4.8)* is more convenient to use in some circumstances and is of value in understanding the physical interpretation of the transient motion.

A4.3 The Particular Integral

The Particular Integral represents the steady state condition of the system and is defined as a given solution to the left-hand and right-hand sides of Eqn. (A4.1). It is thus dependent upon the expression of the forcing function $F(\kappa)$.

A4.3.1 Exponential forcing function

Write the equation of motion in the form:

$$\ddot{X} + 2\zeta_D \omega \dot{X} + \omega^2 X = F(\kappa_M)\omega^2(1 - e^{-k\hat{t}})$$

where

$F(\kappa_M)$ gives the maximum value of the forcing function
κ is the measure of rate of application of the control

For this case the Particular Integral is of the form:

$$F(\kappa_M)\omega^2[1/\omega^2 - e^{-k\hat{t}}/(\omega^2 - 2k\zeta_D\omega + k')] \tag{A4.9}$$

This may be verified by differentiation and substitution into Eqn. (A4.1). The complete solution then becomes:

$$X = e^{(-\zeta_D \omega \hat{t})}[Asin\omega(1 - \zeta_D^2)^{1/2}\hat{t} + Bcos\omega(1 - \zeta_D^2)^{1/2}\hat{t}] + F(\kappa_M)\omega^2[1/\omega^2 - e^{-k\hat{t}}/(\omega^2 - 2k\zeta_D\omega + k^2)] \tag{A4.10}$$

The coefficients *A* and *B* areevaluated by assuming initial rest conditions. *At* time $\hat{t} = 0$, $X = 0$ and $\dot{X} = 0$ and then:

$$X = 0 = B + F(\kappa_M)\{1 - \omega^2/(\omega^2 - 2k\zeta_D\omega + k^2)\}$$

and:

$$B = -F(\kappa_M)\{1 - \omega^2/(\omega^2 - 2k\zeta_D\omega + k^2)\}$$

Note the term in { } brackets tends to unity as k tends to infinity.

Using this and differentiating Eqn. (A4.10):

$$\begin{aligned}\dot{X} = &-\zeta_D\omega[A sin\omega(1-\zeta_D^2)^{1/2}\hat{t} - F(\kappa_M)\{1 - \omega^2/(\omega^2 - 2k\zeta_D\omega + k^2)\}\\ &\times cos\omega(1-\zeta_D^2)^{1/2}\hat{t}] + e^{(-\zeta_D\omega\hat{t})}[A\omega(1-\zeta_D^2)^{1/2}cos\omega(1-\zeta_D^2)^{1/2}\hat{t}\\ &+ F(\kappa_M)\omega(1-\zeta_D^2)^{1/2}\{1 - \omega^2/(\omega^2 - 2k\zeta_D\omega + k^2)\}sin\omega(1-\zeta_D^2)^{1/2}\hat{t}]\\ &+ F(\kappa_M)k\omega^2 e^{-k\hat{t}}/(\omega^2 - 2k\zeta_D\omega + k^2)\end{aligned}$$

and for $\boldsymbol{X} = 0$ at $\hat{t} = 0$:

$$\begin{aligned}0 = &F(\kappa_M)\{1 - \omega^2/(\omega^2 - 2k\zeta_D\omega + k^2)\}\zeta_D\omega + A\omega(1-\zeta_D^2)^{1/2}\\ &+ F(\kappa_M)k\omega^2/(\omega^2 - 2k\zeta_D\omega + k^2)\end{aligned}$$

where $\boldsymbol{A}$ is given by:

$$A = -F(\kappa_M)[\zeta_D - (\zeta_D\omega^2 - k\omega)/(\omega^2 - 2k\zeta_D\omega + k^2)]/(1-\zeta_D^2)^{1/2}$$

Note that as k tends to infinity the term in the [] brackets tends to ζ_D

Finally:

$$\begin{aligned}X = &-F(\kappa_M)e^{(-\zeta_D\omega\hat{t})}[\{\zeta_D - (\zeta_D\omega^2 - k\omega)/(\omega^2 - 2k\zeta_D\omega + k^2)\}\\ &\times sin\,\omega(1-\zeta_D^2)^{1/2}\hat{t}/(1-\zeta_D^2)^{1/2}\\ &+ \{1 - \omega^2/(\omega^2 - 2k\zeta_D\omega + k^2)\}cos\omega(1-\zeta_D^2)^{1/2}\hat{t}]\\ &+ F(\kappa_M)\omega^2[1/\omega^2 - e^{-k\hat{t}}/(\omega^2 - 2k\zeta_D\omega + k^2)]\end{aligned} \tag{A4.11}$$

A4.3.2 Step function

This is a special case of the exponential forcing function where the rate of application, k, tends to infinity so that $e^{-k\hat{t}}$ tends to zero. In this case Eqn. (A4.11) becomes:

$$X = F(\kappa_M)[1 - e^{(-\zeta_D\omega\hat{t})}\{\zeta_D sin\omega(1-\zeta_D^2)^{1/2}\hat{t}/(1-\zeta_D^2)^{1/2} + cos\omega(1-\zeta_D^2)^{1/2}\hat{t}\}] \tag{A4.12}$$

Since X is directly proportional to $F(\kappa_M)$, it is convenient to examine the implications of Eqn. (A4.12) in terms of a unit step input, that is by assuming $F(\kappa_M) = 1$. See Fig. A4.1.

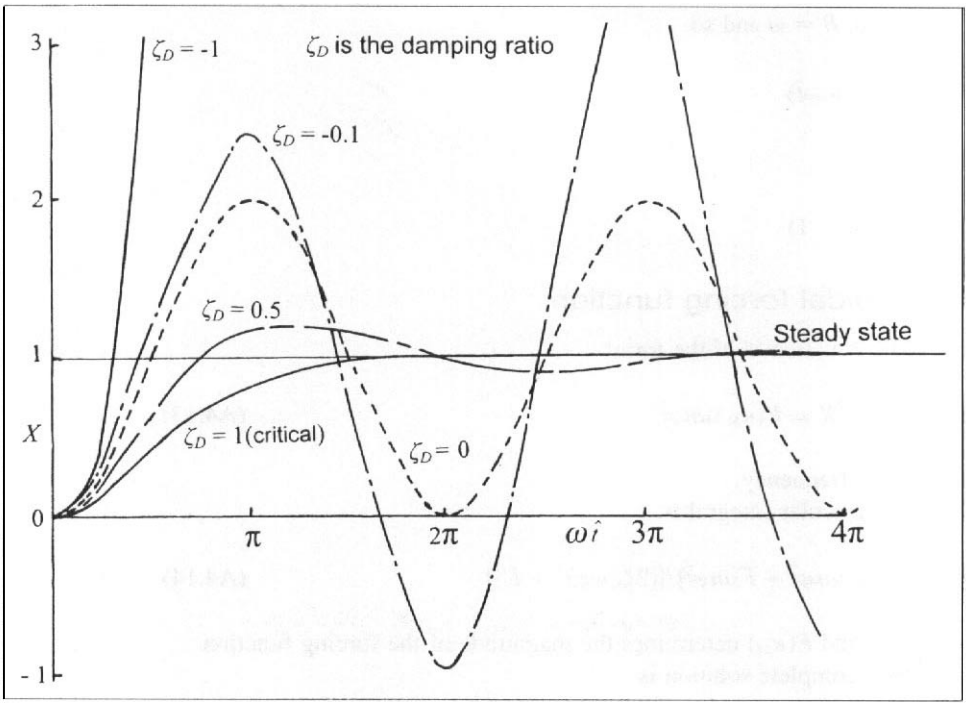

Fig. A4.1 ***Response*** of a ***second-order linear system to a unit step input***

For $-1 < \zeta_D < 1$:

$$X = 1 - e^{(-\zeta_D \omega \hat{t})}[\zeta_D sin\omega(1-\zeta_D^2)^{1/2}\hat{t}/(1-\zeta_D^2)^{1/2} + cos\omega(1-\zeta_D^2)^{1/2}\hat{t}]$$

Similarly for $\zeta_D = 0$:

$$X = 1 - cos\omega\hat{t}$$

For $\zeta_D = 1$, the special critically damped case:

$$X = 1 - e^{-\omega t}(A + B\hat{t})$$

At $\hat{t} = 0, X = 0$ and A = 1 hence:

$$\dot{X} = -\omega e^{-\omega\hat{t}}(B\hat{t} + 1) + e^{-\omega\hat{t}}B$$

and for $X = 0$ at $\hat{t} = 0$, $B =$ wand so:

$$X = 1 - e^{-\omega\hat{t}}(1 + \omega\hat{t})$$

For $\zeta_D = -1$:

$$X = 1 + e^{-\omega\hat{t}}(\omega\hat{t} - 1)$$

A4.3.3 Sinusoidal forcing function

In this case the basic equation is of the form:

$$\ddot{X} + 2\zeta_D\omega\dot{X} + \omega^2 X = F(\kappa_M)sin\varphi\hat{t} \tag{A4.13}$$

where φ is the forcing frequency.

One form of the Particular Integral is:

$$-F(\kappa_M)[2\zeta_D\omega\varphi cos\varphi\hat{t} + \Gamma sin\varphi\hat{t}]/[(2\zeta_D\omega\varphi)^2 + \Gamma^2] \tag{A4.14}$$

where $\Gamma = (\varphi^2 - \omega^2)$ and $F(\kappa_M)$ determines the magnitude of the forcing function.

The corresponding complete solution is:

$$\begin{aligned} X = {} & e^{(-\zeta_D\omega\hat{t})}[Asin\omega(1 - \zeta_D^2)^{1/2}\hat{t} + Bcos\omega(1 - \zeta_D^2)^{1/2}\hat{t}] \\ & - F(\kappa_M)[2\zeta_D\omega\varphi cos\varphi\hat{t} + \Gamma sin\,\varphi\hat{t}]/[(2\zeta_D\omega\varphi)^2 + \Gamma^2] \end{aligned} \tag{A4.15}$$

If the forcing function is assumed to be applied to a static condition at $\hat{t} = 0$, then X is zero at this time, from where:

$$B = 2F(\kappa_M)\zeta_D\omega\varphi/[(2\zeta_D\omega\varphi)^2 + \Gamma^2] \tag{A4.16}$$

The specification of a second boundary condition is less straightforward since $\dot{X}$ is not necessarily zero at time $\hat{t} = 0$. However, $\dot{X}$ will be zero when X is a maximum but due to the interaction between the two frequencies, w and φ, the time at which X is a maximum is not directly apparent.

A special case of particular importance is when the forcing frequency coincides with the undamped natural frequency, ω. In this case Γ is zero and using Eqn. (A4.16), Eqn. (A4.15) reduces to:

$$X = -F(\kappa_M)[cos\omega\hat{t} - e^{(-\zeta_D\omega\hat{t})}\{Asin\omega(1 - \zeta_D^2)^{1/2}\hat{t} + cos\omega(1 - \zeta_D^2)^{1/2}\hat{t}\}]/(2\zeta_D\omega^2) \tag{A4.17a}$$

where $A = 2A\zeta_D\omega^2/F(\kappa_M)$

In this case the second derivative of X with respect to $\hat{t}$ is zero at time $\hat{t} = 0$ and this leads to $A = (R/J)$. The full solution of the equation then becomes:

$$X = -F(\kappa_M)[cos\omega\hat{t} - e^{(-\zeta_D\omega\hat{t})}\{(R/J)sin\omega(1-\zeta_D^2)^{1/2}\hat{t} + cos\omega(1-\zeta_D^2)^{1/2}\hat{t}\}]/(2\zeta_D\omega^2) \quad \text{(A4.17b)}$$

An alternative form of Eqn. (A15) is:

$$X = Ge^{(-\zeta_D\omega\hat{t})}[sin\{(1-\zeta_D^2)^{1/2}\omega\hat{t} + \psi_c\}] + F(\kappa_M)\{sin(\varphi\hat{t} - \psi)\}/\{(2\zeta_D\omega\varphi)^2 + \Gamma^2\}^{1/2} \quad \text{(A4.18)}$$

where use has been made of Eqn. (A4.8) and

$$tan\psi = 2\zeta_D\omega\varphi/\{1 - \varphi^2/\omega^2\}$$

The boundary condition of X = 0 at $\hat{t} = 0$ enables either G or ψ_c to be determined

$$0 = Gsin\psi_c - F(\kappa_M)sin\psi/\{(2\zeta_D\omega\varphi)^2 + \Gamma^2\}^{1/2}$$

$$G = F(\kappa_M)sin\psi/[sin\psi_c\{(2\zeta_D\omega\varphi)^2 + \Gamma^2\}^{1/2}$$

from where

$$X = F(\kappa_M)[sin\psi e^{(-\zeta_D\omega\hat{t})}sin\{(1-\zeta_D^2)^{1/2}\omega\hat{t} + \psi_c\}/sin\psi_c + sin(\varphi\hat{t} - \psi)]/\{(2\zeta_D\omega\varphi)^2 + \Gamma^2\}^{1/2} \quad \text{(A4.19)}$$

For the special case where $\Gamma = 0$, so that $\varphi = \omega$, $tan\psi$ is infinity and hence ψ is 90":

$$X = -F(\kappa_M)[cos\omega\hat{t} - e^{(-\zeta_D\omega\hat{t})}sin\{(1-\zeta_D^2)^{1/2}\omega\hat{t} + \psi_c\}/sin\psi_c]/(2\zeta_D\omega^2) \quad \text{(A4.20)}$$

Again equating the second derivative of X with respect to $\hat{t}$ to zero gives $tan\,\psi_c = (J/R)$ and when this is substituted into Eqn. (A4.20) it yields the same solution as that given by Eqn. (A4.17b).

A further special case is when the forcing frequency, φ, is equal to the natural damped frequency, J. Here Γ is pow equal to $(-R^2)$. It is convenient to express the Particular Integral in the form:

$$-F(\kappa_M)J[2\,cos(1-\zeta_D^2)^{1/2}\omega\hat{t} - (R/J)\,sin(1-\zeta_D^2)^{1/2}\omega\hat{t}]/[R(4J^2 + R^2)] \quad \text{(A4.21)}$$

Following the same procedure as used above for the case when $\Gamma = 0$:

$$B = 2F(\kappa_M)J/[R(4J^2 + R^2)]$$

and (A4.22)

$$A = 2F(\kappa_M)/(4J^2 + R^2)$$

Substitution of these expressions for A and B and the Particular Integral from Eqn. *(A4.21)* **into Eqn.** (A4.15) **gives the *full* solution for this case as:**

$$X = F(\kappa_M)J[e^{(-\zeta_D\omega\hat{t})}\{2cos\omega(1-\zeta_D^2)^{1/2}\hat{t} + (R/J)\,sin\omega(1-\zeta_D^2)^{1/2}\hat{t}\}$$
$$- 2\,cos\omega(1-\zeta_D^2)^{1/2}\hat{t} + (R/J)\omega(1-\zeta_D^2)^{1/2}\hat{t}]/[R(4J^2 + R^2)] \qquad \text{(A4.23)}$$

CHAPTER 5

Flight manoeuvre loads

5.1 Introduction

5.11 General comments

For each of the flight design conditions outlined in Chapter 1, Section 1.5 it is necessary to interpret the relevant flight manoeuvre load cases, specified in Chapter 3, in terms of the equations of motion of the aircraft, derived in Chapter 4. In general the total loading consists of two parts, namely:

(a) The steady flight loading in the initial trimmed condition. This is nominally zero in the lateral/direction degrees of freedom for aircraft of a conventional symmetric configuration.

(b) The increment in loading consequent upon the movement of the appropriate control motivator. There may be several phases of the resulting motion that require analysis.

It should he noted that in terms of a conventional fin/rudder control the loads are those arising only from the imposed motion. However, in the case of a horizontal stabilizer and/or elevator, as relevant. there is the initial load in the trim condition. Likewise rolling loads on the wing caused by deflection of the ailerons must be superimposed upon those already present in trimmed flight.

5.1.2 Trimmed flight

The trimmed longitudinal flight loads are defined in Chapter 4, Section **4.2.1.**Eqns (4.6) and/or (4.9)enable the horizontal stabilizer load to be calculated and then, using Eqns **(4.2)** and/or (4.7), the corresponding wing–body load may he derived. In addition to

these loads being the basis for the pitch manoeuvre conditions they provide the initial load conditions for the rolling cases and the initial loads on the horizontal lifting surfaces in yawing motion.

5.1.3 Manoeuvre loads

In the absence of coupling between the pitching, rolling, and yawing motions the behaviour of the aircraft in response to the application of the relevant control motivator may he simplified so that it can he described by the classical second-order linear differential equation:

$$\ddot{X} + 2\zeta_D \omega \dot{X} + \omega^2 X = F(\kappa) \tag{5.1}$$

where the undamped natural frequency of the motion is:

$$\omega = (J^2 + R^2)^{1/2} \tag{5.2a}$$

and the damping ratio:

$$\zeta_D = R/\omega \tag{5.2b}$$

also:

$$J = \omega(1 - \zeta_D^2)^{1/2} \tag{5.2c}$$

κ represents an angular control input such as η or ζ. The damping coefficient. R, the damped natural frequency, J, and the forcing function, F, are defined appropriate to the longitudinal or directional condition.

The interpretation and solution of Eqn. (5.1) is discussed in Chapter 4, Appendix A4. In particular it is shown that while the transient motion is a function of the effective spring/mass/damping of the system, the final steady state condition depends upon both the magnitude and form of the control input as defined by $F(\kappa)$

5.2 Modes of control motivator movement

5.2.1 Introduction

There are three basic ways of moving a control motivator:

(a) Unchecked, where the device is moved from a neutral or trim position to a given deflection and then held at that deflection.
(b) Checked, where the motivator is moved to a given deflection and subsequently returned towards the original position.
(c) Excitation. where the motivator is moved in an oscillatory manner in both directions relative to the original setting. Since, under appropriate conditions,

the consequence of this mode is to cause a continuous increase in the response amplitude of the aircraft, the number of cycles applied is very limited.

5.2.2 Unchecked mode

As illustrated in Fig. 5.1 two mathematical models are commonly used to represent the unchecked mode of motivator application:

(a) *Ramp function*. Here it is assumed that the motivator instantaneously achieves a constant rate of application before it is brought instantaneously to zero when the required deflection is reached.

(b) *Exponential function*. Again it is assumed that thcrc is an instantaneous rate of application but thereafter the rate decreases continuously until it becomes zero at the time when the required deflection is achieved.

The step input is a special case of both the ramp and exponential representations and implies an initial infinite rate of control motivator application.

Analytically the exponential function is more readily dealt with since it is a continuous mathematical function. In non-dimensional time:

$$\kappa = \kappa_S(1 - e^{-k\hat{t}}) \tag{5.3}$$

where κ_S is the required final deflection of a representative control motivator, and it is achieved only as the non-dimensional time, $\hat{t}$, tends to infinity. k defines the rate of application of the motivator. In the limiting case of a step input, k is infinity so that $(e^{-k\hat{t}})$ is zero.

The value of κ_S may effectively be defined by the need for the aircraft to reach a given steady state manoeuvre, as for example in a normal acceleration case. Chapter 3, Section 3.2.3. Alternatively it may be specifically defined in the requirement for a given loading case, for example Chapter **3,** Section 3.3.2 which concerns rolling of the aircraft.

The choice of k is important in that it should represent a typical rate of control as applied by a pilot or control actuator and at the same time ensure that the required maximum deflection is approached with sufficient accuracy in an acceptably short time. In practice it is influenced by the response of the aircraft in relation to the rate of application of the motivator and for some situations it is acceptable to assume, albeit somewhat conservatively, that a step function representation is acceptable. The difficulty in choosing a value for ***k*** does not arise in a full simulation where an actual pilot or actuator is included in the loop. The problem in this latter situation is to ensure that the pilots employed in the study input the most severe practical rates of control application.

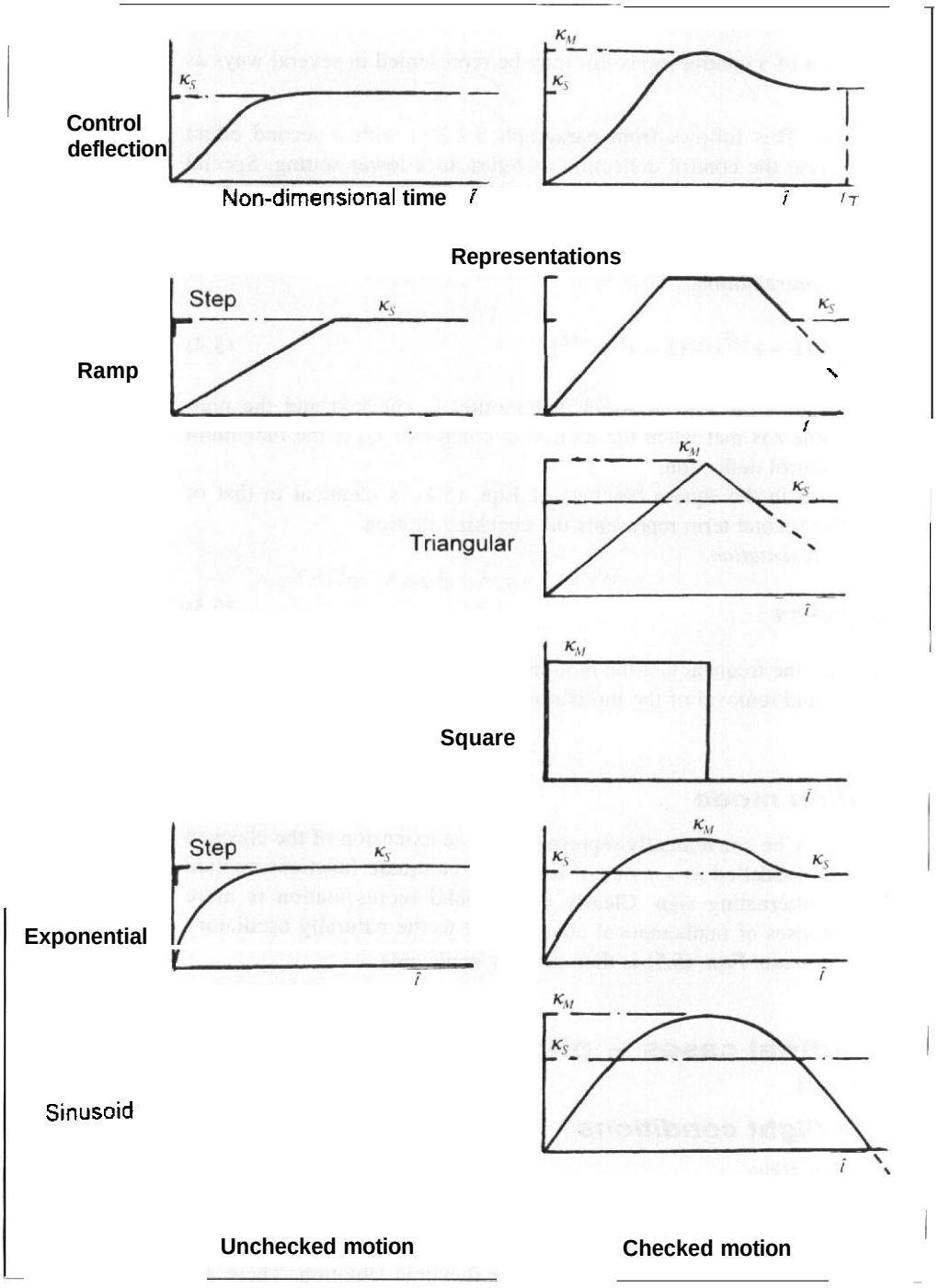

Fig. 5.1 ***Modes of control motivator movement***

5.2.3 Checked mode

The checked application of a control motivator may he represented in several ways as shown in Fig. 5.1.

(a) *Ramp function.* This follows from paragraph 5.2.2(a) with a second effect included to cause the control deflection to return to a lower setting. Special cases of the ramp representation are the triangular fonn and the square function. In the former there is no dwell time and in the latter the deflection is both applied and removed instantaneously.

(b) *Exponential representation.*

$$\kappa = \kappa_M[(1 - e^{-k\hat{t}}) + (1 - e^{f\hat{t}})e^{-f\hat{T}}] \tag{5.4}$$

where f determines the rate at which the motion is checked and the non-dimensional time $\hat{t}$ is that when the motion is complete. κ_M is the maximum value of the control deflection.

The first term in the square brackets of Eqn. (5.4) is identical to that of Eqn. (5.3). The second term represents the checking motion.

(c) *Sinusoidal representation.*

$$\kappa = \kappa_M \sin \varphi \tag{5.5}$$

where φ defines the frequency of the motion and therefore, effectively, the rate of application and removal of the motivator deflection.

5.2.4 Excitation mode

The excitation mode may be conveniently represented by an extension of the checked mode. Thus it could be modelled as a series of triangular or square functions applied with an amplitude of alternating sign. Clearly a sinusoidal representation is more convenient for the purposes of mathematical analysis due to the naturally oscillatory characteristic of the function. Eqn. (5.5) is then directly applicable.

5.3 Longitudinal cases – pitch motivator deflection

5.3.1 Steady flight conditions

5.3.1.1 Introduction

The equilibrium conditions for the longitudinal forces and moments are stated in Chapter 4, Section 4.2.1 and Eqns (4.6). These equations are general and enable the forces and moments to be evaluated for any particular dynamic situation. There are

certain special cases where particular terms are zero and consequently there is simplification of the equations.

5.3.1.2 Steady unaccelerated flight

In steady unaccelerated flight:

$$\dddot{\theta} = \ddot{\theta} = \dot{\theta} = \dot{\alpha} = \Delta m = \Delta n = 0$$
$$m = \sin\gamma \qquad (5.6a)$$
$$n = \cos\gamma$$

For this special case the horizontal stabilizer load is derived from Eqn. (4.6) by appropriate substitution. It should be noted that the trim condition used as a basis for calculating the total loads during a manoeuvre is a special case of Eqn. (5.6a) where the climb angle. γ, is zero so that:

$$m = 0 \qquad \text{and} \qquad n = 1 \qquad (5.6b)$$

This is the condition covered by Eqn. (4.9).The definition of the horizontal stabilizer load in terms of its component parts is derived from Eqn. (4.19) as:

$$\mathcal{L}_T = \varphi_T S_T[a_{1T}\{\alpha_B(1 - d\varepsilon/d\alpha) + \alpha_{Bo}(d\varepsilon/d\alpha) + \alpha_T\} + a_2\eta] \qquad (5.7)$$

The wing–body load. $\mathcal{L}_{WB}$, corresponding to this is found from Eqns (4.7) and (4.6) and it is defined by Eqn. (4.14a).

5.3.1.3 Steady symmetric manoeuvre

This is another special case defined as the condition when the normal acceleration factor. n, is greater or less than unity but the pitch velocity. $\dot{\theta}$, is zero. It is not a realistic case for horizontal stabilizer/elevator-initiated manoeuvres due to the pitching velocity implied hy the movement of a conventional pitch control. It can occur in two circumstances:

(i) on an aircraft utilizing direct lift control by means of the use of spoilers or high-lift devices in conjunction with the usual pitch control;

(ii) on a guided weapon where a normal or lateral manoeuvre is accomplished by adjusting the angle of attack of the main lifting surfaces, the moving wing concept.

The corresponding wing–body loading may be derived from Eqn. (4.6) with appropriate substitution, assuming level flight, of:

$$\dddot{\theta} = \ddot{\theta} = \dot{\theta} = \dot{\alpha} = m = 0 \qquad (5.8)$$

The horizontal stabilizer load is given by Eqn. (5.7).

5.3.1.4 Steady rotary motion, constant pitching velocity

For aircraft having a conventional form of longitudinal control the constant elevator angle, or equivalent, required to maintain the aircraft in a steady state of rotary motion is an important datum case. It is used both as a basis for the specification of the control angle required to initiate a manoeuvre and the initial condition as the termination of the manoeuvre is commenced. In practice it is a theoretical rather than practical situation due to the effect of gravitational acceleration. An exception to this is a cruciform guided missile manoeuvring in a horizontal plane where, for simplicity, it is usual for the manoeuvres to be defined in terms of lateral rather than normal accelerations.

In a steady rotary motion the pitching velocity. $\dot{\theta}$, is constant and the control deflection is not altered. From Eqns (4.88) the angle of attack of the aircraft is also constant. Thus:

$$\dddot{\theta} = \ddot{\theta} = \dot{\alpha} = \dot{\eta} = 0 \tag{5.9a}$$

Since $\dot{\theta} = \dot{\alpha} + \dot{\gamma}$ and $\dot{\alpha}$ is zero. the increment in the normal acceleration in a pitching manoeuvre is given by Eqn. (4.4a) as:

$$\Delta n = V_o \dot{\gamma}/g$$

and from Fig. **4.1.** with the angle of attack constant, $\dot{\gamma} = 0$. Hence, assuming that the aircraft is initially in steady level flight:

$$\Delta n = (n-1) = V_o \dot{\theta}/g$$

$$\dot{\theta} = (n-1)g/V_o \tag{5.9b}$$

For this case, from Eqn. (4.87):

$$(J_1^2 + R_1^2)\dot{\hat{\theta}} = a_{1WB}\delta\eta$$

Therefore the control angle. η_{SS}, required to give a constant pitching velocity is:

$$\eta_{SS} = (J_1^2 + R_1^2)\dot{\hat{\theta}}/a_{1WB}\delta \tag{5.10a}$$

Substitution for J_1 and R_1 from Eqns **(4.82)** and conversion to real time yields:

$$\eta_{SS} = 4\,m^2 c H_m \dot{\theta}/\{(\rho S k_y)^2 V_o \delta\}$$

and using Eqn. (5.9b):

$$\eta_{SS} = \{4m^2 cH_m(n-1)g\}/\{(\rho S k_y V_o)^2 \delta\} \tag{5.10b}$$

In the case of an aircraft with a horizontal stabilizer the coefficient of the forcing function, δ, is given by Eqns (4.82e) to (4.82g). Using the last of these, which is the simplified form, the control angle for a constant pitching velocity becomes:

$$\eta_{SS} = -\{2mH_m(n-1)g\}/\{a_2 \rho S V_o^2 \bar{V}\} \tag{5.11a}$$

where substitution has been made for μ_1.

When an all-moving horizontal stabilizer is employed, the increment in its angle of attack, $(\Delta\alpha_T)$, required to produce the manoeuvre is derived by using Eqn. (4.112) as the expression for 6 and it amounts lo replacing a_2 by a_1, in Eqn. (5.11a).

For a tailless layout the coefficient of the forcing function is given by Eqn. (4.110d) and in this case:

$$\eta_{SS} = -\{2mH_m(n-1)g\}/[a_2 \rho S V_o^2 \{(\ell_\eta/c) - m_\theta/\mu_1\}] \tag{5.11b}$$

For a conventional layout the load on the horizontal stabilizer due to η_{SS} is:

$$\begin{aligned} \mathcal{L}_{TSS} &= a_2 \rho V_o^2 S_T \eta_{SS}/2 \\ &= -mH_m c(n-1)g/\ell_T \end{aligned} \tag{5.12a}$$

The corresponding load on the wing of a tailless aircraft due to the control deflection is:

$$\mathcal{L}_{WSS} = -mH_m c(n-1)g/(\ell_\eta - cm_\theta/\mu_1) \tag{5.12b}$$

The load due to the angle of attack on the horizontal stabilizer and the wing load due to angle of attack are given in Eqns (5.20) and (5.21).

5.3.2 Pitching acceleration

5.3.2.1 Introduction

The design normal accelerations are specifically stated in the flight envelope described in Chapter 3. Section 3.2.3. The design wing–body loads are effectively given by these conditions when allowance is made for the horizontal stabilizer load required to trim the aircraft.

The pitching acceleration conditions have a major impact on the design of the horizontal stabilizer. In a conventional design, in addition to the trim loads, it is the increment in the load on this lifting surface which results in the pitching acceleration. The design pitching acceleration is directly proportional to the increment in the load

on the horizontal stabilizer. In the case of a tailless design the situation is less clear, due to the contribution of the pitch control motivator to the wing lift, but the principle is not changed. In practice it is the load on the horizontal stabilizer. or equivalent in a tailless design, which is of importance. The magnitude of the pitching acceleration is primarily required to evaluate the inertial relief effects.

Fundamentally the pitching acceleration is:

$$\ddot{\theta} = \mathcal{L}_T \ell_T' (m k_y^2) \tag{5.13a}$$

$$\mathcal{L}_T = m k_y^2 \ddot{\theta} / \ell_T' \tag{5.13b}$$

The various ways of specifying the incremental load on the horizontal stabilizer are outlined in the following sections.

5.3.2.2 Specification of the pitching acceleration in the requirements

In some cases the requirements for aircraft with a conventional tail specify the pitching acceleration directly. United States civil requirements tended towards this approach. Thus FAR-25:331 states that, unless pilot effect limits it, the elevator should be moved suddenly to the maximum angle while the aircraft is in steady level flight at V_A There is also a case at V_D. Minimum values of pitching acceleration to be used are quoted unless it can be shown by a rational analysis, such as that mentioned in Section 5.3.2.4, that a lower value cannot be exceeded. The prescribed minimum design pitching accelerations are:

(a) ***Nose-up,*** with the aircraft initially in steady level flight:

$$\ddot{\theta} = 39n(n - 1.5)/V \tag{5.14a}$$

where n is the maximum normal acceleration factor at a point on the flight envelope corresponding to the speed. V, in ***knots*** EAS and the pitching acceleration is in radians/s^2.

(b) ***Nose-down,*** applied with the aircraft initially at the maximum normal acceleration factor, which by implication is the steady rotary condition covered in Section 5.3.1.4.

$$\ddot{\theta} = 26n(n - 1.5)/V \tag{5.14b}$$

The light aircraft requirements. JAR/FAR-23.423 quote Eqn. (5.14a) as a minimum value for both the nose-up and nose-down conditions, with the rider that when V_D is

greater than 152 m/s (300 knots) a more rational approach. such as that of Section 5.3.2.4, must be used.

5.3.2.3 Aircrafl with advanced control systems

For aircraft with a fully automatic active control system the pitching acceleration is expressed in terms of system performance requirements by relating it to the normal acceleration and the pitching velocity. In practice it is convenient to use the effective pitching acceleration which makes allowance for the roll/yaw contributions. A typical design envelope is shown in Chapter 3, Fig. 3.4 and the effective acceleration is derived in Chapter 4, Section 4.4.2.

5.3.2.4 Specification in terms of control system characteristics

In the case of aircraft having conventional control systems with either manual or powered actuation, the United Kingdom requirements, both military and civil, have dealt with the issue by defining the motion and amplitude of the pitch control motivator in terms of the movement of the pilot's control column. Such an approach is applicable to the great majority of aircraft. the only exceptions being those referred to in the previous paragraph which incorporate automatic acceleration limitation. Sections 5.3.3 and 5.3.4 outline the procedure used in this approach. Such an approach is consistent with the European JAR requirements.

5.3.3 Analysis of the unchecked pitching manoeuvre

5.3.3.1 Introduction

While it is possible to envisage an unchecked control movement at any speed within the flight envelope, in practice the requirements limit the case to a condition at the manoeuvre speed, V_A. For example JAR-25.331(c) requires that at speed V_A the loads resulting from maximum attainable elevator movement, as limited by either angle or pilot effort, must be considered. Allowance may be made for the response of the aircraft and conditions giving a normal acceleration factor greater than the maximum design value, n_1, may be ignored. Similar cases are to be found in JAR-23/FAR-23.423 and Def.Stan.00-970, Chapter 202, paragraph 4.2.1. See also Chapter 3, Section 3.2.4, in this book.

Although the step input is a special case of the unchecked mode of control movement it is convenient to deal with it first as it results in datum values which are used Tor the specification of the more general case.

5.3.3.2 The step input

The step input is derived from Eqn. (5.3) with a value fork of infinity. Replacing κ by the pitch motivator deflection, η, so that:

$$7 = 'Is \tag{5.15}$$

where η_S is here the maximum value of the unchecked control deflection.

For this case the solution of the equation of motion given in Appendix **A4,** Section A4.3.2 is directly applicable. Using Eqns (5.1), (5.2), and (5.10a) and for the usual condition where the damping ratio lies between -1 and 1:

$$\hat{\dot{\theta}} = a_{1WB}\delta\eta_S[1 - e^{(-R_1\hat{t})}\{\cos J_1\hat{t} + (R_1 \sin J_1\hat{t})/J_1\}]/(J_1^2 + R_1^2) \tag{5.16a}$$

In a practical case the motion of the vehicle is limited and it is usually adequate to consider the worst design case as arising when it has completed the first half cycle of the damped motion. This coincides with the overshoot time shown in Fig. A4.1, and is when $\hat{t}$ is equal to (π/J_1). This may be confirmed by differentiating Eqn. (5.16a) with respect to $\hat{t}$ and equating the result to zero to obtain a maximum value of the nondimensional pitching velocity. Thus the design pitching velocity, $(\dot{\theta})_D$, is given by:

$$(\hat{\dot{\theta}})_D = a_{1WB}\delta\eta_S[1 + \exp(-\pi R_1/J_1)]/(J_1^2 + R_1^2) \tag{5.16b}$$

This may be written in the form:

$$(\hat{\dot{\theta}})_D = a_{1WB}\delta\eta_S/\Sigma(J_1^2 + R_1^2) \tag{5.16c}$$

where

$$\Sigma = [1 + \exp(-\pi R_1/J_1)]^{-1} \tag{5.16d}$$

Using Eqn. (5.16c):

$$\begin{aligned}\eta_S &= \Sigma(J_1^2 + R_1^2)(\hat{\dot{\theta}})_D/a_{1WB}\delta \\ &= \Sigma\eta_{SS}\end{aligned} \tag{5.17}$$

from Eqn. (5.10a) for the case when $(\dot{\theta})_D$ is the pitching velocity equivalent to the required increment in normal acceleration.

Thus, if the control is moved instantaneously from an initially trimmed, steady level, flight condition through an angle η_S, defined by Eqn. (5.17), then at the end of the first half cycle of the resulting motion the aircraft will be manoeuvring with an incremental normal acceleration of $(n - 1)g$. Note that if the motion is allowed to continue so that $\hat{t}$

tends to infinity, then Σ, as defined by Eqn. (5.16d), tends to unity as would be expected since the aircraft would now he in steady rotary motion, and η_S would he equal to η_{SS}. Σ may therefore be regarded as an inverse measure of the 'overshoot' which results in the first cycle of the transient motion of the aircraft following control application and it is usually less than unity. If the pitchinp motion is over-damped it will have a value greater than unity. The trend may be seen by comparing the curves for ζ_D equal to 0.5 and 1.0 in Appendix A4. Fig. A4.1.

When the control is moved through the angle η_S, defined by Eqn. (5.17), the change in the load on the horizontal stabilizer is:

$$\mathcal{L}_{To} = \rho V_o^2 S_T a_2 \eta_S/2 = \rho V_o^2 S_T a_2 \Sigma \eta_{SS}/2$$

Substitution from Eqn. (5.11a) for an aircraft having a horizontal stabilizer yields:

$$\mathcal{L}_{To} = -mH_m c(n-1)g\Sigma/\ell_T' \tag{5.18a}$$

In the case of a tailless layout the equivalent expression for the increment in wing load is:

$$\mathcal{L}_{Wo} = -mH_m c(n-1)g\Sigma/(\ell_\eta - cm_\theta/\mu_1) \tag{5.18b}$$

Equations (5.18) may he compared with Eqns (5.12)

If the conditions are assumed to be equivalent to the eventual steady situation, from Eqns (4.88) the increment in the angle of attack of the wing–body. a, is:

$$\alpha = \hat{\dot{\theta}}/a_{1WB}$$

and converting to real time:

$$\alpha = 2m\dot{\theta}/(\rho S V a_{1WB}) \tag{5.19a}$$

and using Eqns (5.9b):

$$\alpha = 2m(n-1)g/(\rho S V_o^2 a_{1WB}) \tag{5.19b}$$

The increment in the load on the horizontal stabilizer due only to the change in the overall angle of attack is obtained by substitution of a into Eqn. (4.19). where it is noted that the terms including $a_{,}$ and α_T are not present in the incremental motion as they are covered by the initial trim condition. Further. since the angle of attack is constant there is no downwash lag effect. Hence:

$$\begin{aligned}\mathcal{L}_{T\alpha} &= \rho V_o^2 S_T[a_{1T}(1 - d\varepsilon/d\alpha)\alpha + a_{1T}\ell_T'\dot{\theta}/V_o]/2 \\ &= \rho V_o^2 S_T a_{1T}\alpha[(1 - d\varepsilon/d\alpha) + \ell_T'\dot{\theta}/(\alpha_B V_o)]/2\end{aligned}$$

Now from Eqn. (5.19a):

$$\theta/\alpha = \rho S V_o a_{1WB}/2m$$

and using Eqn. (5.19b) for a:

$$\mathcal{L}_{T\alpha} = m(n-1)g(S_T/S)(a_{1T}/a_{1WB})[(1 - d\varepsilon/d\alpha) + \rho S a_{1WB}\ell_T'/(2m)]$$

or (5.20)

$$\mathcal{L}_{T\alpha} = m(n-1)g(S_T/S)(a_{1T}/a_{1WB})[(1 - d\varepsilon/d\alpha) + (a_{1WB}/\mu_1)(\ell_T'/c)]$$

The corresponding increment in wing lift, which applies to both conventional and tailless layouts is:

$$\begin{aligned}\mathcal{L}_{W\alpha} &= \rho V_o^2 S a_{1WB}\alpha/2 \\ &= m(n-1)g\end{aligned} \qquad (5.21)$$

The total load on a horizontal stabilizer at the end of the first half cycle of the motion resulting from an instantaneous application of a pitch control angle, η_s, is given by the algebraic sum of $\mathcal{L}_{To}$ and $\mathcal{L}_{T\alpha}$ as defined in Eqns (5.18) and (5.20), respectively plus the initial trim load. See also Section **5.3.6.** It will be noted that $\mathcal{L}_{To}$ and $\mathcal{L}_{T\alpha}$ are of opposite sign so that the effect of $\mathcal{L}_{T\alpha}$ is to first reduce the negative horizontal stabilizer term due to $\mathcal{L}_{To}$ and then, most likely, change the sign of the load. There are thus two maxima, one as the motion is initiated and the other when the aircraft reaches the first half cycle of the motion.

The step function loads are basic design values for the unchecked motion but may be unduly severe in that in practice the control deflection cannot be applied instantaneously. Nevertheless the two contributions. $\mathcal{L}_{To}$ and $\mathcal{L}_{T\alpha}$, are used as datum values for other representations of control movement.

5.3.3.3 Exponential control movement (conventional configuration)

The complete solution for the general unchecked exponential motion is derived directly from Chapter 4. Appendix A4. Eqn. (A4.11) by substituting the relevant values of J_1, R_1 and δ. It will be noted also that:

$$\zeta_{D1} = R_1/\omega \qquad \omega_1^2 = (J_1^2 + R_1^2)$$

$$\omega_1(1 - \zeta_{D1}^2)^{1/2} = J_1 \qquad (\zeta_{D1}\omega_1^2 - k\omega_1) = \omega_1(R_1 - k)$$

$$(\omega_1^2 - 2k\zeta_{D1}\omega_1 + k^2) = \{J_1^2 + (R_1 - k)^2\}$$

From where:

$$\alpha_B = \delta\eta_S[1 - e^{(-R_1\hat{t})}\{R_1(\sin J_1\hat{t})/J_1 + \cos J_1\hat{t}\}]/(J_1^2 + R_1^2)$$
$$- \delta\eta_S[e^{-k\hat{t}} - e^{(-R_1\hat{t})}\{(R_1 - k)(\sin J_1\hat{t})/J_1 + \cos J_1\hat{t}\}]/\{J_1^2 + (R_1 - k)^2)\} \quad (5.22)$$

The first of the terms in Eqn. (5.22) corresponds to the instantaneous case, Eqn. (5.16a).

The general solution of Eqn. (5.22) is lengthy. It was considered in the Aeronautical Research Committee's Research and Memoranda 3001 (R and M 3001)[1] and the results incorporated in Leaflet 201/1 of the earlier UK military requirements, AvP 970. The form of the Leaflet is suitable for analysis when all the numerical values of the parameters are defined and it includes graphs of some of the time-dependent terms. In R and M 3001 the definition of the non-dimensional time, $\hat{t}$, is twice that used in this text.

The value of k is dependent upon the actual rate of application of the pitch control, $d\eta/dt$:

$$k = 4m(d\eta/dt)/(\rho S V_o \eta_S) \quad (5.23a)$$

with a minimum suggested value of:

$$k = (4J_1 + R_1) \quad (5.23b)$$

The value for kgiven in Eqn. (5.23b) is somewhat arbitrary but it does provide a critical design condition which is somewhat less severe than the step input, and it does have the merit of considerably simplifying the analysis. It effectively assumes that the control is moved at rather more than four times the natural damped frequency of the longitudinal short-period oscillation. In certain cases there are clear overriding conditions. such as the maximum available rate of application. $(d\eta/dt)_M$, in a powered control system when k is defined by Eqn. (5.23a). The manoeuvre is in two stages:

(a) manoeuvre from steady level flight to ng:
(b) with the aircraft in a steady rotary motion, manoeuvre back towards level flight using the same magnitude of pitch control deflection as used in stage (a) but opposite in direction.

A further study of the problem was undertaken by Richards[2] and the results of his work were included as advisory information in the previous UK requirements for civil aircraft. BCAR Section D3. The results used Eqn. (5.23b) to define kexcept inasmuch as this is overridden by control system limitations. The solution was applied to a number of

[1]Czaykowski, J. Loading conditions of tailed aircraft in longitudinal manoeuvres. UK Aeronautical Research Committee, Reports and Memoranda 3001. 1957.
[2]Richards, L. W. *Aircraft Engineering* January. February, and March 1960

typical civil aircraft and the results interpreted to yield simple equations for design application. Whereas in the case of a step input of the control one of the design maxima occurs at the instant the control is applied, this is not so in the more general case since the aircraft begins to respond in angle of attack before the maximum control deflection has been reached. However, because the rate of application of the control is significantly greater than the response of the aircraft, it is to be expected that the initial maximum load will be experienced early in the subsequent motion. Richards defines the design horizontal stabilizer loads resulting from the manoeuvre in terms of that due to the movement of the control and the total rather than the contribution due to the angle of attack. Two conditions are identified, namely that when the manoeuvre is initiated from steady level flight (1 g towards ng), identified by the suffix '1', and that when the aircraft is returned to level flight from the steady rotary motion (ng towards 1 g), identified by the suffix '2'. In his analysis he used the same definition for non-dimensional time as that in R and M 3001, that is, twice the value used here. It was suggested, in line with R and M 3001, that if J_1 is numerically negative the value should be taken as zero.

The pitch control deflection required to initiate the manoeuvre is given as:

$$\eta_1 = \eta_{SS}\Sigma[1/(1 + 3.3R_1/k)]^{1/2} \tag{5.24a}$$

and that to return to level flight:

$$\eta_2 = \eta_{SS}\{1 - \Sigma[1/(1 + 3.3R_1/k)]^{1/2}\} \tag{5.24b}$$

In Eqns (5.24), η_{SS} is the angle required toachieve the steady rotary motion as defined in Eqn. (5.11a). The corresponding horizontal stabilizer loads due to the change in control angle only are:

$$\mathcal{L}_{T1\eta} = \mathcal{L}_{To}[1/(1 + 3.3R_1/k)]^{1/2} \tag{5.25a}$$

and

$$\mathcal{L}_{T2\eta} = \mathcal{L}_{To}\{1 - \Sigma[1/(1 + 3.3R_1/k)]^{1/2}\}/\Sigma \tag{5.25b}$$

where $\mathcal{L}_{To}$ is given in Eqn. (5.18a).

The corresponding total design horizontal stabilizer loads due to the manoeuvre, which include both the control and the angle of attack effect, are:

$$\mathcal{L}_{T1} = -\mathcal{L}_{T2} = \mathcal{L}_{To}[1/(1 + 10R_1/k)]^{1/2} \tag{5.26}$$

It should be noted that in Eqn. (5.26)the contribution due only to the control effect is not necessarily equal to the value given by Eqns (5.25). The total loads on the tail are those given by Eqn. (5.26) plus either the initial trim load or the load in the steady rotary motion, as appropriate, see also Section 5.3.6.

Since the values of the loads given in Eqns (5.25) and (5.26) are semi-empirical. in that they were derived from typical cases of tailed aircraft, it is not possible to apply them to a tailless concept. The values given hy Eqns (5.11b) and (5.21) for the control and angle of attack load contributions consequent upon a step input of the pitch control should be used in the absence of better information. such as may be derived from a simulator study, even though they are conservative.

5.3.4 Analysis of the checked pitching manoeuvre

5.3.4.1 Introduction

The solution of the checked motion based on the exponential form of control movement defined in Eqn. (5.4) is discussed fully in R and M 3001 [1] The application to real cases is somewhat complex and it was not reproduced in AvP 970 Leaflet 201/1. In his investigation, Richards[2] preferred the use of a sinusoidal representation fur the movement of the pitch control. This is more readily dealt with mathematically and has the additional merit that it reasonably represents the real situation in the case of powered control and auto-pilot malfunction.

Checked manoeuvre conditions have to be analysed at all speeds in excess of V_A, which by implication may be taken to include V_{μ}.

5.3.4.2 Sinusoidal application of pitch control

The solution of the equation of motion, Eqn (5.1), with a sinusoidal forcing function is discussed in Chapter 4, Appendix A4, Section A4.3.3. Substituting appropriate values into Eqn. (A4.19), noting the relationships detailed at Eqn. (5.22). gives:

$$\alpha = \delta\eta_C[\sin\psi e^{(-R_1\hat{t})}\{\sin(J_1\hat{t} + \psi_C)\}/\sin\psi_C + \sin(\varphi\hat{t} - \psi)]/\{(2R_1\varphi)^2 + \Gamma^2\}^{1/2} \quad (5.27a)$$

where η_C is the maximum control deflection applied at a frequency ϕ. ψ and ψ_C are phase angles associated with the motion. In particular:

$$\tan\psi = 2R_1\varphi/\{1 - \varphi^2/(J_1^2 + R_1^2)\} \quad (5.27b)$$

and

$$\Gamma = \varphi^2 - (J_1^2 + R_1^2) \quad (5.27c)$$

A special case is when the control application frequency. ϕ, coincides with the undamped natural frequency in the longitudinal short-period mode, $(J_1^2 + R_1^2)^{1/2}$, so that Γ becomes zero. From Eqn. (5.27b) *tan* \$is then infinity so that ψ is equal to $\pi/2$ (90").

In this situation Eqn. (5.27a) reduces to:

$$\alpha = -\delta\eta_C[cos\,(J_1^2 + R_1^2)\hat{t} - e^{(-R_1\hat{t})}\{sin\,(J_1\hat{t} + \psi_C)\}/sin\,\psi_C]/\{2R_1(J_1^2 + R_1^2)\}^{1/2} \tag{5.28a}$$

ψ_C depends on the boundary conditions and defines the non-dimensional time, $\hat{t}$, at which the increment in the wing–body angle. a. reaches its maximum value. Differentiation of Eqn. (5.28a) with respect to $\hat{t}$ and equating the result to zero yields:

$$tan\,\psi_C = (R_1 sin\,J_1\hat{t} - J_1 cos\,J_1\hat{t})/[\{(J_1^2 + R_1^2)sin\,(J_1^2 + R_1^2)\hat{t}\}/e^{(-R_1\hat{t})} - R_1 cos\,J_1\hat{t} - J_1\hat{t}\,sin\,J_1\hat{t}] \tag{5.28b}$$

Richards considered the general solution of Eqn. (5.27a) and used a graphical technique to derive the maximum forces and accelerations. As with the unchecked analysis a number of typical civil aircraft were used to enable semi-empirical formulae to be derived for design purposes.

The value of the control application frequency. ϕ, is taken as the greater **of:**

$$\varphi = (J_1^2 + R_1^2)^{1/2} \tag{5.29a}$$

or (in non-dimensional units):

$$\varphi = (V_e/V_A)\{m\pi/(\rho S V_o)\} \tag{5.29b}$$

where V_e is the appropriate speed for the design case, such as V_A, V_C, or V_D, and is thus effectively equal to V_o in a given case. Since ϕ is in non-dimensional time in Eqns (5.29a) and (5.29b), it is a so-called 'circular' frequency. and in real time Eqn. (5.29b) is:

$$(V_e\pi)/(2V_A) \tag{5.29c}$$

(see also JAR-25.ACJ331).

The maximum change in the deflection of the pitch control during the manoeuvre is given as:

$$\eta_C = \eta_{SS}[1 + 0.68(\varphi/R_1)^{1.7}\{R_1/(J_1 + R_1)\}^{(0.15 + 1.5J_1/R_1)}] \tag{5.30}$$

where η_{SS} is the control angle to give the steady rotary motion as defined in Eqn. (5.11a). The deflection angles to he associated with manoeuvring from (1 g to ng) and

(ng back to $1\ g$) are, respectively:

$$\eta_1 = \eta_C \sin[\pi\{2.0 + 2.8(R_1/\varphi)^{1.09}\}^{-1}] \tag{5.31a}$$

$$\eta_2 = \eta_C \sin[\pi/2 + \tan^{-1} y] \tag{5.31b}$$

where y is a complex function of the airframe characteristics and is defined for the interval $0 \leq \tan^{-1} y \leq \pi$ as:

$$y = -Y_1/Y_2 \tag{5.31c}$$

where:

$$\begin{aligned} Y_1 = {} & R_1\varphi a_{1T}\{1 - d\varepsilon/d\alpha + (a_{1WB}/\mu_1)(\ell_T'/c)\} \\ & + (\Gamma\varphi/4)\{(1 + d\varepsilon/d\alpha)(2a_{1T}/\mu_1)(\ell_T'/c)\} \end{aligned} \tag{5.31d}$$

$$\begin{aligned} Y_2 = {} & (\Gamma a_{1T}/2)\{1 - d\varepsilon/d\alpha + (a_{1WB}/\mu_1)(\ell_T'/c)\} \\ & - (R_1\varphi^2/2)(1 + d\varepsilon/d\alpha)(2a_{1T}/\mu_1)(\ell_T'/c) \\ & + a_{1WB}H_m[(\Gamma^2 + 4R_1^2\varphi^2)/\{2\bar{V}(J_1^2 + R_1^2)\}] \end{aligned} \tag{5.31e}$$

The corresponding horizontal stabilizer load increments due to the manoeuvre are then:

$$\mathcal{L}_{T1} = -\mathcal{L}_{To}(\varphi/R_1)^{1.2}[0.64/\{0.48(J_1/R_1)^{1.3} + 1\}] \tag{5.32a}$$

and

$$\mathcal{L}_{T2} = -\mathcal{L}_{To}(\varphi/R_1)^{1.38}[0.92/\{0.48(J_1/R_1)^{1.3} + 1\}] \tag{5.32b}$$

where $\mathcal{L}_{To}$ is given by Eqn. (5.18a).

The components of these horizontal stabilizer loads directly resulting from the deflection of the pitch control are:

$$\begin{aligned} \mathcal{L}_{T1\eta} &= (\mathcal{L}_{To}/\Sigma)(\eta_C/\eta_{SS})\sin[\pi\{2.0 + 2.8(R_1/\varphi)^{1.09}\}^{-1}] \\ &= (\mathcal{L}_{To}/\Sigma)(\eta_1/\eta_{SS}) \end{aligned} \tag{5.33a}$$

and

$$\mathcal{L}_{T2\eta} = -(\mathcal{L}_{To}/\Sigma)(\eta_C/\eta_{SS})\sin[\pi/2 + \tan^{-1} y] = (\mathcal{L})_{To}/\Sigma)(\eta_2/\eta_{SS}) \tag{5.33b}$$

The initial trim load must be added to the loads given in Eqns (5.32) to obtain the total load on the horizontal stabilizer, see also Section 5.3.6.

The above analysis is not applicable to a tailless configuration since the semi-empirical relationships were derived for conventional aircraft. A simulator investigation is really required for this class of aircraft.

5.3.5 Comparison of the loads resulting from unchecked and checked control movements

Although the unchecked mode of pitch control application has only to be applied at the speed V_A, see Section 5.3.3.1, a comparison of the loads arising with those in a checked manoeuvre is of interest. If k and ϕ are as given by Eqns (5.23b) and (5.29), respectively, then the checked motion will be found to give the greatest loads in all cases. This statement will not necessarily be true if the unchecked loads are derived from a step input of the pitch control.

5.3.6 Summary of the loads on the horizontal stabilizer

5.3.6.1 General

It must be recognized that the loads on the horizontal stabilizer, or for that matter the wing of a tailless configuration, during a pitching manoeuvre consist of two separate effects:

(a) The load due to the deflection of the control motivator both in the initial steady condition and due to the initiation of the manoeuvre.
(b) The load due to the angle of attack of the lifting surface, again both in the initial steady condition and as a consequence of the manoeuvre.

The chord-wise distribution of these two loads is different, as illustrated in Chapter 4, Fig. 4.4, and consequently this has an impact on the torque loading across the local sections of the surface. In general for a stable aircraft the load resulting from the angle of attack of the lifting surface is opposite in sign to that due to the deflection of the control. However, it does not necessarily follow that the maxima of each effect are coincident in terms of time.

5.3.6.2 Procedure for the evaluation of the loads

A summary of the procedure for the evaluation of the horizontal stabilizer loads in a pitching manoeuvre follows.

A. For all design cases establish the initial condition

This is either:

(a) Trimmed level flight using Chapter 4, Eqns (4.9), (4.14). and (4.19). Or
(b) The steady rotary motion in a manoeuvre using Eqns (4.19) and (5.11a) and including the initial level flight trim loads.

For each of the conditions the two components of load outlined in the above section will apply.

B. Establish the additional loads which are a consequence of the manoeuvre

There are several ways of doing this.

(a) By using a simplified semi-empirical method, such as may be found in an Appendix to the United States **FAR-23** requirements. Such an approach is simple but only really applicable to very basic conventional light aircraft and it is not recommended for any design where usual analysis will yield much more accurate design data.

(b) By directly defining the pitching acceleration required either for reasons of structural design or flight handling, see Section 5.3.2.3. Given the pitching acceleration, θ, and the moment of inertia of the aircraft in pitch, (mk_Y^2), the moment required to produce the initial acceleration follows from Eqn. (5.13). The required deflection of the pitch control is then:

$$\eta = 2\mathcal{L}_T / a_2 \rho S V_o^2 \tag{5.34}$$

This control angle may then be fed into the response equations using either an unchecked or checked representation, as relevant, in order to determine the angle of attack loads arising as the aircraft responds to the control input. The instantaneous unchecked analysis may he applied to tailless designs.

(c) By using a control response analysis such as outlined in Sections 5.3.3 and 5.3.4 for conventional aircraft. This requires a knowledge of the design normal acceleration factor, n, for each of the design speeds, the control input rate or frequency. and any limitations on the control force. The analysis yields both the loading due to the control deflection needed to initiate the manoeuvre and an estimate of the total load on the lifting surface. This method is preferable to those outlined in paragraphs (a) and (b) except for an aircraft having automatic limitation of overall aircraft rates of motion and accelerations.

(d) By employing a simulation study making use of the equations outlined in Chapter 4. At the very least these should be the decoupled short-period longitudinal equatinns and preferably a more cumprehensive representation. depending upon the class of aircraft. This approach is always preferable and in the case of unconventional designs, such as tailless layouts, it is really essential for more detailed design work.

5.3.6.3 Torque loads

The torque on a lifting surface results from the different chord-wise centre of pressure positions of the loads due to control deflection and angle of attack relative to the structural centre of twist. It is often convenient in loading analysis to use a reference datum for the evaluation of torques, such as the 35 per cent chord line. and to correct for the structural characteristics during detail stressing, see Chapter 12, Section 12.2 and Chapter 15, Section 15.2.

The initial trim load due to the deflection of the pitch control is derived directly from the $(\alpha_2 \eta)$ term in Eqn. (4.19), the remainder of the horizontal stabilizer load being related to the angle of attack, α_B, as defined in Eqns (4.2) or (4.7) with (4.14).

In the steady rotary motion the increment in the load due to the deflection of the control required to hold the aircraft in the manoeuvre is given by Eqn. (5.12a). The corresponding load increment due to the angle of attack is given by Eqn. (5.20).

In the case of a step input to the pitch control the two components of the incremental load due to the manoeuvre. $\mathcal{L}_{To}$ and $\mathcal{L}_{T\alpha}$, are given by Eqns (5.18) and (5.20), respectively. The incremental torque for this case is directly derived from the chord-wise distribution of these loads since both of them occur at the same time.

The exponential form of the unchecked motion is somewhat more complex due to the fact that the maximum values of the tail loads due to control deflection and angle of attack do not necessarily occur at the same time and also they are derived from semi-empirical formulae. The design torque in this case is the trim condition plus the greatest of either:

(i) that due to the loads implied by Eqns (5.25) and (5.26); or
(ii) that given by Eqn. (5.20) for the maximum control deflection and $\mathcal{L}_{To}/\Sigma$ from Eqn. (5.18a).

In the checked motion the design torque is the trim case plus the greatest of:

(i) that implied by the loads given in Eqns (5.32) and (5.33); or
(ii) the load due to the maximum deflection of the pitch control and an incidence load of $1.2\,\mathcal{L}_{T\alpha}$ as given by Eqn. (5.20). The maximum pitch control angle, η_C, is given by Eqn. (5.30).

5.3.7 Loads on trailing edge control devices

The loads on trailing edge control devices. such as elevators or ailerons, are derived from the chord-wise load distributions mentioned in the previous section. There are three possible components:

(i) the portion of the total due to the symmetric angle of attack of the lifting surface to which the device is attached;
(ii) the portion of the load due to the deflection of the device itself;
(iii) the portion of the load due to the anti-symmetric angle of attack such as is present when the aircraft is rolling, see Section 5.4.

The total of these components. $\mathcal{L}_{TED}$, may be written as:

$$\mathcal{L}_{TED} = S_1\mathcal{L}_{\alpha s} + S_2\mathcal{L}_k + S_3\mathcal{L}_{\alpha A} \tag{5.35}$$

where S_i are the ratios of the loads acting on the trailing edge device to those on the whole surface identified by the subscripts:

1 symmetric angle of attack. $\mathcal{L}_{\alpha S}$
2 trailing edge device deflection, $\mathcal{L}_\kappa$
3 anti-symmetric angle of attack, where present, $\mathcal{L}_{\alpha A}$

In practice the chord-wise load distributions due to each of the effects will vary across the span of a lifting surface or control device so that in order to obtain the value of $\mathcal{L}_{TED}$ it is necessary to use mean values of S_1, S_2 and S_3.

5.4 Lateral case – roll motivator deflection

The decoupled equation of motion in the lateral. rolling, mode is given in Chapter 4. Eqns (4.95). and its solution in Eqns (4.96) and (4.97).

It is usual to assume that the roll control motivator is applied instantaneously. In this case the maximum roll acceleration, $\dot{p}$, which occurs at the start of the manoeuvre, coincides with a zero rate of roll, p. Then from Eqns (4.95), in non-dimensional time:

$$\hat{\dot{p}} = L_\xi \mu_2 \xi / i_x \tag{5.36a}$$

where ξ is the deflection of the roll control motivator. Using Eqns (4.61c), in real time this becomes:

$$(\dot{p})_{\max} = (\rho V_o^2 S b L_\xi / 2)(m k_x^2) \tag{5.36b}$$

as would be expected since the numerator is the absolute value of the rolling moment and the denominator is the roll moment of inertia.

The rate of roll reaches its maximum value as the time tends to infinity when the rolling acceleration falls to zero. This is given by Eqn. (4.97b) as;

$$(p)_{\max} = -(V_o/b)(L_\xi/L_p)\xi \tag{5.37}$$

The wing load distributions implied by the movement of the roll controls to give the rolling acceleration, $(\dot{p})_{MAX}$, and that implied by the final steady rate of roll, $(p)_{MAX}$, have to be combined with the symmetric flight load distributions as specified in Chapter 3, Section 3.3.2.

The loads on the roll control device itself are covered by Section 5.3.7.

5.5 Directional case – yaw motivator deflection

5.5.1 Introduction

5.5.1.1 Equations of motion

When the yawing is isolated from the pitching and rolling motions, as discussed in Chapter 4, Sections 4.7.3 and 4.7.5, the lateral force and yawing moment equations may be derived from the first and third of Eqns (4.91). Noting that the sideslip angle, β, is equal to (v/V_o) and the non-dimensional rate of yaw, ϕ, is equal to $\hat{r}$, the equations

become:

$$\hat{\dot{\beta}} - Y_v\beta + \hat{r} = Y_\zeta\zeta \tag{5.38a}$$

$$\hat{\dot{r}} - (b/k_z)^2 N_r\hat{r} - \mu_2(b/k_z)^2 N_v\beta = \mu_2(b/k_z)^2 N_\zeta\zeta \tag{5.38b}$$

where I_z has been replaced by $(b/k_z)^2$.

The solution of Eqns (5.38) takes the form of Eqn. (5.1). for example in terms of the sideslip angle it is:

$$\hat{\ddot{\beta}} + 2R_2\hat{\dot{\beta}} + (J_2^2 + R_2^2)\beta = F(\zeta) \tag{5.39}$$

This may be compared with Eqn. (4.100a). Equations (4.100b) and (4.100c) define R_2 and J_2 $F(\zeta)$ is given in full in Eqn. (4 100d). In the great majority of cases the derivative Y_r is negligibly small, see paragraph 4.7.2(g). When this is assumed to be the case:

$$R_2 = -(Y_v + \{N_r/i_z\})/2 \tag{5.40a}$$

$$(J_2^2 + R_2^2) = (Y_vN_r + N_v\mu_2)/i_z \tag{5.40b}$$

$$F(\zeta) = Y_\zeta\hat{\dot{\zeta}} - (\{Y_\zeta N_r + N_\zeta\mu_2\}/i_z)\zeta \tag{5.40c}$$

Equation (5.40c) may be further simplified to the form given in Eqn. (4.100f):

$$F(\zeta) = (a_{2F}S_F/S)\hat{\dot{\zeta}} + (a_{2F}\bar{V}_v\mu_2/i_z)\zeta \tag{5.40d}$$

The alternative solution, in terms of the rate of yaw is:

$$\hat{\ddot{r}} + 2R_2\hat{\dot{r}} + (J_2^2 + R_2^2)\hat{r} = F'(\zeta) \tag{5.41a}$$

where

$$F'(\zeta) = (\mu_2/i_z)\{N_\zeta\hat{\dot{\zeta}} - (Y_vN_\zeta - Y_\zeta N_v)\zeta\} \tag{5.41b}$$

5.5.1.2 Loading requirements and yaw motivator movement

The loading requirements for directional/yaw manoeuvres are outlined in Chapter 3, Section 3.3.3 where the motion resulting from movement of the yaw motivator is described. The requirements identify two modes of yaw motivator input:

(a) An unchecked application of the control. that is, a step input. This mode of operation appears in all sets of requirements and the critical phases of consequent motion of the aircraft are outlined in Section 3.3.3.2.

(b) Sinusoidal application of the control at a frequency equal to that of the damped natural frequency in the yawing mode. This is an excitation motion and in the past was especially associated with military combat manoeuvres. However, a requirement to consider such a control input was included in the TSS code used for Concorde design and recent evidence suggests that it can result from pilot action when correcting for the effects of atmospheric turbulence, especially jet aircraft wake turbulence.[3]

As required by the United Kingdom military code. the sinusoidal application of the yaw motivator gives the greater design loads.

5.5.1.3 Loads on the vertical stabilizer

The total load on the vertical stabilizer during side slipping/yawing motion is:

$$\mathcal{L}_F = (\rho V_o^2 S_F/2)[-a_{1F}(1 - d\sigma/d\beta)\beta + a_{1F}r(\ell_F/V_o) + a_{2F}\zeta] \tag{5.42}$$

where

S_F is the reference area of the vertical stabilizer
a_{1F} is the lift curve slope of the surface due to the angle of attack. based on the area S_F, per radian
a_{2F} is the lift curve slope due to the deflection of the motivator. based on the area S_F, per radian
β is the sideslip angle, which is the angle of attack in this case
ζ is the deflection of the yaw motivator (radians)
r is the yaw rate (rad/s)
σ is the side-wash angle. This is similar to the downwash angle in the longitudinal plane and is the effective airflow angle over the vertical surface as a consequence of the airframe components ahead of the surface. It is usually small and negligible for loading calculations

The first term in the square brackets in Eqn. (5.42) is the load due to the angle of attack, the sideslip angle. and it is negative for positive control input. The term $\{a_{1F}r(\ell_F/V_o)\}$ is the damping in yaw and it always opposes the direction of motion, being comparable to the pitch damping in the symmetric equations. The last term in the square brackets is the load on the whole surface due to the motivator deflection.

When only the transient motion is considered and the right-hand side of Eqn. (5.38a) is set to zero:

$$\hat{r} = Y_v\beta - \hat{\dot{\beta}}$$

[3] Dornheim, M. A. Flight *587* probe shows tails have been overloaded before. *Aviation Week and Space Technology*, November 25th, 2002.

which when converted to real time is:

$$r = \rho S V_o Y_v \beta/(2m) - \dot{\beta} \tag{5.43}$$

This may be substituted into Eqn. (5.42) with $(d\sigma/d\beta)$ equal to zero to give:

$$\mathcal{L}_F = (\rho V_o^2 S_F/2)[-a_{1F}\{1 - (Y_v/\mu_2)(\ell_F/b)\}\beta + a_{1F}\dot{\beta} + a_{2F}\zeta] \tag{5.44a}$$

For the over-swing and equilibrium sideslip conditions after a step input, and at the end of each half-cycle in the case of a sinusoidal input, the rate of change of the angle with respect to time is zero. In these circumstances Eqn. (5.44a) simplifies to:

$$\mathcal{L}_F = (\rho V_o^2 S_F/2)[-a_{1F}\{1 - (Y_v/\mu_2)(\ell_F/b)\}\beta + a_{2F}\zeta] \tag{5.44b}$$

5.5.2 Step input to the yaw motivator

The motion of the aircraft in a horizontal plane as a consequence of a step input of the yaw motivator is illustrated in Chapter **3,** Figs 3.7 and 3.8. The aircraft passes through an 'over-swing' or maximum sideslip angle. β_{MAX}, before stabilizing at an equilibrium angle. β_E. The equilibrium angle is the Particular Integral of the solution of Eqn. (5.39):

$$\beta_E = F(\zeta_o)/(J_2^2 + R_2^2) \tag{5.45a}$$

where ζ_o is the deflection of the yaw control motivator ($\dot{\zeta}$ is zero).

Substituting from Eqns (5.40b) and (5.40d) gives:

$$\begin{aligned} \beta_E &= (a_{2F}\bar{V}_v\mu_2)\zeta_o/(Y_v N_r + N_v\mu_2) \\ \beta_E &= a_{2F}\bar{V}_v\zeta_o/(Y_v N_r/\mu_2 + N_v) \end{aligned} \tag{5.45b}$$

The complete solution of Eqn. (5.39) for the step input is derived from Chapter 4, Appendix A4. Section A4.3.2. For the case when thedamping ratio is between $+1$ and -1

$$\beta = \{F(\zeta_o)/(J_2^2 + R_2^2)\}[1 - e^{(-R\hat{t})}\{\cos J_2\hat{t} + (R_2/J_2)\sin J_2\hat{t}\}] \tag{5.46a}$$

$$= \beta_E[1 - e^{(-R_2\hat{t})}\{\cos J_2\hat{t} + (R_2/J_2)\sin J_2\hat{t}\}] \tag{5.46b}$$

Differentiation with respect to non-dimensional time yields:

$$\hat{\dot{\beta}} = \beta_E(J_2^2 + R_2^2)e^{(-R_2\hat{t})}\sin J_2\hat{t}/J_2 \tag{5.46c}$$

$$\hat{\ddot{\beta}} = \beta_E(J_2^2 + R_2^2)e^{(-R_2\hat{t})}(\cos J_2\hat{t} - (R_2/J_2)\sin J_2\hat{t}) \tag{5.46d}$$

The maximum. over-swing, sideslip angle occurs at the end of the first half-cycle of the damped motion when $\hat{t} = \pi/J_2$, that is when:

$$\beta_\pi = \beta_{MAX} = \beta_E[1 + \exp(-R_2\pi/J_2)] \tag{5.47}$$

Typically the term $\{\exp(-R_2\pi/J_2)\}$ has a value between 0.4 and 0.5. Some simple requirement codes allow the assumption of a value of 0.5 without requiring any further calculation.

The loads on the vertical stabilizer have to be evaluated at four stages in the response of the aircraft using Eqn. (5.44b). In each case $\dot{\beta}$ is found to be zero.

(a) ***The instant that the step input is applied,*** $\hat{t} = 0$. From Eqn. (5.44b) with $\beta = 0$:

$$\mathcal{L}_{F\beta o} = (\rho S_F V_o^2/2)a_{2F}\zeta_o \tag{5.48a}$$

In the case of a conventional rudder control, Eqn. (5.48a) gives the maximum design load on the rudder itself for the step input condition. See also Sections 5.3.7 and 5.5.4.

(b) ***The over-swing condition,*** $\hat{t} = \pi/J_2$. Here. with β defined by Eqn. (5.47). from Eqn. (5.44b):

$$\mathcal{L}_{F\beta\pi} = (\rho S_F V_o^2/2)[-a_{1F}\{1 - (Y_v/\mu_2)(\ell_F/b)\}\beta_{MAX} + a_{2F}\zeta_o]$$

Substituting for β_{MAX} using Eqns (5.45a) and (5.47):

$$\begin{aligned}\mathcal{L}_{F\beta\pi} &= (\rho S_F V_o^2/2)[-a_{1F}\{1 - (Y_v/\mu_2)(\ell_F/b)\} \\ &\quad \times \{F(\zeta_o)/(J_2^2 + R_2^2)\}\{1 + \exp(-R_2\pi/J_2)\} + a_{2F}\zeta_o] \\ \mathcal{L}_{F\beta\pi} &= (\rho S_F V_o^2/2)F(\zeta_o)[-a_{1F}\{1 - (Y_v/\mu_2)(\ell_F/b)\} \\ &\quad \times \{1 + \exp(-R_2\pi/J_2)\}/(J_2^2 + R_2^2) + a_{2F}\zeta_o/F(\zeta_o)]\end{aligned} \tag{5.48b}$$

(c) ***The equilibrium condition,*** $\hat{t}$ ***rending ro infinity.*** In this case β is the equilibrium angle defined in Eqn. (5.45b):

$$\begin{aligned}\mathcal{L}_{F\beta E} &= (\rho S_F V_o^2/2)F(\zeta_o)[-a_{1F}\{1 - (Y_v/\mu_2)(\ell_F/b)\}/(J_2^2 + R_2^2) \\ &\quad + a_{2F}\zeta_o/F(\zeta_o)]\end{aligned} \tag{5.48c}$$

(d) ***The start of return to straight flight.*** When the yaw control motivator is returned instantaneously to the neutral setting the aircraft begins to return to straight flight. The sideslip angle is the equilibrium value β_E given by Eqn. (5.45b) but the control angle is zero. Fmm Eqn. (5.44b):

$$\mathcal{L}_{F\beta R} = (\rho S_F V_o^2/2)F(\zeta_o)[-a_{1F}\{1 - (Y_v/\mu_2)(\ell_F/b)\}/(J_2^2 + R_2^2)] \tag{5.48d}$$

While the design maximum total load on the vertical surface is usually given by the over-swing condition. Eqn. (5.48b), it may be that the start of the return to straight flight, Eqn. (5.48d), results in a higher load and therefore this condition should be checked.

5.5.3 *Sinusoidal input to the yaw motivator*

5.5.3.1 General

The frequency of the excitation is required to be that of the natural damped yawing motion. J_2. Thus the solution given in Chapter 4, Appendix A4, Eqn. (A4.23) is appropriate with the Particular Integral as given by Eqn. (A4.21). Using J_2 to replace $[\omega(1 - \zeta_D^2)^{1/2}]$ enables the solution to be written as:

$$\beta = F(\zeta_e)J_2[e^{(-R_2\hat{t})}\{2\cos J_2\hat{t} + (R_2/J_2)\sin J_2\hat{t}\} - 2\cos J_2\hat{t} + (R_2/J_2)\sin J_2\hat{t}]/[R_2(4J_2^2 + R_2^2)] \quad (5.49a)$$

where ζ_e is the maximum deflection of the yaw control during the excitation.

In many cases it may be expected that (R_2^2) is very much less than $(4J_2^2)$ so that Eqn. (5.49a) may he simplified to:

$$\beta = F(\zeta_e)[e^{(-R_2\hat{t})}\{2\cos J_2\hat{t} + (R_2/J_2)\sin J_2\hat{t}\} - 2\cos J_2\hat{t} + (R_2/J_2)\sin J_2\hat{t}]/(4J_2R_2) \quad (5.49b)$$

Differentiation with respect to non-dimensional time gives:

$$\dot{\hat{\beta}} = F(\zeta_e)[e^{(-R_2\hat{t})}\{-R_2\cos J_2\hat{t} - ((R_2^2 + 2J_2^2)/J_2)\sin J_2\hat{t}\} + R_2\cos J_2\hat{t} + 2J_2\sin J_2\hat{t}]/(4J_2R_2) \quad (5.49c)$$

$$\ddot{\hat{\beta}} = F(\zeta_e)[e^{(-R_2\hat{t})}\{-2J_2^2\cos J_2\hat{t} + ((R_2^3 + 3R_2J_2^2)/J_2)\sin J_2\hat{t}\} + 2J_2^2\cos J_2\hat{t} - R_2J_2\sin J_2\hat{t}]/(4J_2R_2) \quad (5.49d)$$

The general solution to derive the maximum loads on the vertical surface including the yaw motivator is complex. The yaw motivator is zero at the end of each half-cycle of the motion and hence at these times the total load on the surface is due only to the angle of attack. This is the sideslip effect and the load follows directly from Eqns (5.44b) and (5.49b). The more difficult issue is the maximum load on the yaw motivator, presumed to be a rudder. The problem was investigated by Czaykowski,[4] and a summary of the

[4]Czaykowski, T. **Dynamic** fin **and rudder** loads **in yawing** manoeuvres. **UK RAE** Report Structures No. 76, **June** 1950.

work was included in the previous United Kingdom military requirements, Av P 970 as Leaflet 202/1.

It was noted that the maximum load on the control itself occurred at a somewhat later time than the maximum load on the vertical surface as a whole, and an approximate solution was adapted in order to predict this.

There are two possible situations as specified in the United Kingdom military requirements. For combat aircraft the loads have to be evaluated after 1.5 cycles of the motion while for some other types of aircraft the conditions at the end of one cycle are the design case.

5.5.3.2 Loads at the end of one cycle of the motion, $\hat{t} = 2\pi$

The sideslip angle at the end of the first cycle of the motion, as required for non-combat types of aircraft, is derived from Eqn. (5.49b) as:

$$\beta_{2\pi} = -F(\zeta_e)\{1 - \exp(-2\pi R_2/J_2)\}/(2J_2R_2) \tag{5.50a}$$

The maximum vertical surface load follows from Eqns (5.44b) and (5.50a) noting that at this condition the motivator deflection is zero:

$$\mathcal{L}_{F2\pi} = (\rho V_o^2 S_F/2)F(\zeta_e)a_{1F}\{1 - (Y_v/\mu_2)(\ell_F/b)\} \times \{1 - \exp(-2\pi R_2/J_2)\}/(2J_2R_2) \tag{5.50b}$$

The maximum load on a rudder for this case is given approximately as:

$$\mathcal{L}_{\zeta 2\pi} = [S_1^2(\mathcal{L}_{F2\pi})^2 + S_2^2(\mathcal{L}_{\zeta e})^2]^{1/2} \tag{5.50c}$$

where

$$\mathcal{L}_{\zeta e} = (\rho V_o^2 S_F/2)a_{2F}\zeta_e \tag{5.50d}$$

In Eqns (5.50). S_1 and S_2 are the proportions of the total surface load on the rudder itself relative to the loads on the whole vertical surface due to angle of attack and control deflection, respectively, see Sections 5.3.7 and 5.5.4.

5.5.3.3 Loads at the end of 1.5 cycles of the motion. $\hat{t} = 3\pi$

This is the combat aircraft case and the sideslip angle is:

$$B_{3\pi} = F(\zeta_e)\{1 - \exp(-3\pi R_2/J_2)\}/(2J_2R_2) \tag{5.51a}$$

The total surface load follows as:

$$\mathcal{L}_{F3\pi} = -(\rho V_o^2 S_F/2)F(\zeta_e)a_{1F}\{1-(Y_v/\mu_2)(\ell_F/b)\} \times \{1-\exp(-3\pi R_2/J_2)\}/(2J_2R_2) \quad (5.51b)$$

The design maximum rudder load is approximately:

$$\mathcal{L}_{\zeta 3\pi} = -[S_1^2(\mathcal{L}_{F3\pi})^2 + S_2^2(\mathcal{L}_{\zeta e})^2]^{1/2} \quad (5.51c)$$

5.5.4 Loads on the yaw control motivator

The loads on a trailing edge control surface, in this case usually a rudder, are described in general in Section 5.3.7. In the case of a step input to the motivator the load on the control itself is:

$$\mathcal{L}_{\zeta 0} = S_1 P_\beta + S_2 P_\zeta \quad (5.52)$$

where S_1 and S_2 are the proportions of the load on the control as a ratio of the total surface loads due to the sideslip load, P_β, and the control deflection, P_ζ, respectively. In Eqns (5.48) P_β is identified by the terms including a_{1F} and P_ζ by those including a_{2F}. P_ζ is identical to $\mathcal{L}_{F\beta o}$ as given by Eqn. (5.48a).

The loads on the motivator in the sinusoidal excitation case are given explicitly by Eqns (5.50c) and (5.51c) for the I and 1.5 cycles conditions, respectively.

5.5.5 Lateral and yaw accelerations

5.5.5.1 General

In the case of longitudinal motion the normal acceleration is specifically defined in the requirements and the consequent pitching acceleration follows from it. The normal acceleration is a statement both of the required manoeuvre performance and a recognition of the tolerance of a pilot. The requirements for asymmetric flight loads do not specify the associated lateral and yawing accelerations but they are implicitly defined by the motion occurring as a consequence of the deflection of the yaw motivator. The magnitude of these accelerations is needed in order to evaluate the inertial relief effects in the lateral motion. It is also desirable to consider the lateral accelerations experienced by a pilot to ensure that they fall within tolerable limits. It is possible that the need to limit the lateral acceleration for reasons of pilot tolerance may provide a corresponding limit to the allowable deflection of the yaw motivator at higher speeds and hence a limit upon the loads, see Chapter 3, paragraph 3.3.3.1(b).

The lateral acceleration at any point on the aircraft is given by Chapter 4, Eqns (4.43) as:

$$o = \dot{V} - pW + rU + x(pq + \dot{r}) - y(p^2 + r^2) + z(qr - \dot{p})$$

For motion only in the horizontal plane p, q. and Ware zero. U is the equivalent of V_o. Thus:

$$o = \dot{V} + rV_o + x\dot{r} - yr^2 \tag{5.53a}$$

For a point along the x axis:

$$o = \dot{V} + rV_o + x\dot{r}$$

and, since $\dot{\beta} = \dot{v}/V_o$:

$$o = (\dot{\beta} + r)V_o + x\dot{r} \tag{5.53b}$$

In non-dimensional time this becomes:

$$o = \rho SV_o^2(\hat{\beta} + \hat{r})/(2m) + \{x(\rho SV_o)^2/(2m)^2\}\hat{r} \tag{5.53c}$$

While it is usually acceptable for the Y_ζ term to be neglected in the calculation of loads, see Chapter 4, Eqn. (4.100e), it is necessary to retain it for the evaluation of accelerations. From Eqn. (5.38a):

$$\hat{\beta} + \hat{r} = Y_\zeta\zeta + Y_v\beta \tag{5.54a}$$

Rearranging and differentiating this equation gives:

$$\hat{r} = Y_\zeta\hat{\zeta} + Y_v\hat{\beta} - \hat{\hat{\beta}} \tag{5.54b}$$

Substitution for $(\beta + \hat{r})$ and $\hat{r}$ from Eqns **(5.54)** into Eqn. (5.53c) gives:

$$o = \rho SV_o^2(Y_\zeta\zeta + Y_v\beta)/(2m) + x\{(\rho SV_o)^2/(2m)^2\}(Y_\zeta\hat{\zeta} + Y_v\hat{\beta} - \hat{\hat{\beta}}) \tag{5.55a}$$

and, since $Y_\zeta = a_{2F}S_V/S$:

$$o = \{\rho S_F V_o^2 a_{2F}/(2m)\}[\zeta + SY_v\beta/(a_{2F}S_F) + \{\rho Sx/(2m)\}\{\hat{\zeta} + (S/(a_{2F}S_F))(Y_v\hat{\beta} - \hat{\hat{\beta}})\}] \tag{5.55b}$$

5.5.5.2 Instantaneous application of the yaw motivator

(a) Initially, at time $\hat{t} = 0$, $\zeta = \zeta_o$, and $\dot{\zeta} = 0$
From Eqns (5.46):

$$\beta = \dot{\beta} = 0 \qquad \ddot{\beta} = F(\zeta_o)$$

Note that from Eqn. (5.40d) for $\dot{\zeta} = 0$:

$$F(\zeta_o) = 2ma_{2F}S_F\ell_F\zeta_o/(\rho S^2k_z^2) \tag{5.56}$$

where substitution had been made for μ_2 and i_z.
Therefore. from Eqns (5.39). (5.46d), and (5.45a):

$$\ddot{\beta} = F(\zeta_o) = 2ma_{2F}S_F\ell_F\zeta_o/(\rho S^2k_z^2) \tag{5.57a}$$

and

$$\begin{aligned} o_o &= \{\rho S_F V_o^2 a_{2F}/(2m)\} \\ &\quad \times [\zeta_o - (\rho Sx/(2m))(S/(a_{2F}S_F))\{2ma_{2F}S_F\ell_F\zeta_o/(\rho S^2k_z^2)\}] \\ &= \{\rho S_F V_o^2 a_{2F}\zeta_o/(2m)\}[1 - (\ell_F x/k_z^2)] \end{aligned} \tag{5.57b}$$

and at the tail where $x = -\ell_F$:

$$(o_o)_{Tail} = \{\rho S_F V_o^2 a_{2F}\zeta_o/(2m)\}[1 + (\ell_F/k_z)^2] \tag{5.57c}$$

The first of the terms in the [] brackets is the lateral acceleration of the centre of gravity and the second is due to the effect of the rate of yaw.

(b) Over-swing condition at time $\hat{t} = \pi/J_2$, $\zeta = \zeta_o$, and $\dot{\zeta} = 0$.
In this case from Eqns (5.46) and (5.47):

$$\beta_{MAX} = \beta_E[1 + \exp(-R_2\pi/J_2)] \qquad \dot{\beta} = 0$$
$$\ddot{\beta} = -\beta_E(J_2^2 + R_2^2)[\exp(-R_2\pi/J_2)]$$

Hence:

$$\begin{aligned} o_\pi = \{\rho S_F V_o^2 a_{2F}/(2m)\}&[\zeta_o + S\beta_E Y_v\{1 + \exp(-R_2\pi/J_2)\}/(a_{2F}S_F) \\ &+ (\rho Sx/(2m))\{S\beta_E(J_2^2 + R_2^2)\}(\exp(-R_2\pi/J_2))/(a_{2F}S_F)] \end{aligned}$$

Noting that:

$$\begin{aligned}\beta_E S/(a_{2F}S_F) &= F(\zeta_o)S/\{a_{2F}S_F(J_2^2+R_2^2)\}\\ &= \ell_F b\mu_2\zeta_o/\{k_z^2(J_2^2+R_2^2)\}\end{aligned} \tag{5.58}$$

$$\begin{aligned}o_\pi =&\{\rho S_F V_o^2 a_{2F}\zeta_o/(2m)\}[1+\ell_F b\mu_2 Y_v\{1+\exp(-R_2\pi/J_2)\}/\\ &\{k_z^2(J_2^2+R_2^2)\}+(\ell_F x/(k_z^2)\{\exp(-R_2\pi/J_2)\}]\end{aligned} \tag{5.59a}$$

and at the tail where $x=-\ell_F$:

$$\begin{aligned}(o_\pi)_{Tail} =& \{\rho S_F V_o^2 a_{2F}\zeta_o/(2m)\}\\ &\times[1+\ell_F b\mu_2 Y_v\{1+\exp(-R_2\pi/J_2)\}/\{k_z^2(J_2^2+R_2^2)\}\\ &-(\ell_F/k_z)^2\{1+\exp(-R_2\pi/J_2)\}]\end{aligned} \tag{5.59b}$$

(c) Equilibrium condition, t tending to infinity. $\zeta=\zeta_o$, and $\dot\zeta=0$.

$$\begin{aligned}&\beta=\beta_E \qquad \dot{\hat\beta}=\ddot{\hat\beta}=0\\ &o_E = \{\rho S_F V_o^2 a_{2F}/(2m)\}[\zeta_o+S\beta_E Y_v/(a_{2F}S_F)]\\ &\quad = \{\rho S_F V_o^2 a_{2F}\zeta_o/(2m)\}[1+\ell_F b\mu_2 Y_v/\{k_z^2(J_2^2+R_2^2)\}]\end{aligned} \tag{5.60}$$

The same value applies at the tail.

(d) Return to straight flight, $\zeta=\dot\zeta=0$.

$$\beta=\beta_E \qquad \dot\beta=0$$

By definition from paragraph (a). Eqn. (5.57a):

$$\begin{aligned}&\ddot{\hat\beta} = -F(\zeta) = -2ma_{2F}S_F\ell_F\zeta_o/(\rho S^2k_z^2)\\ &o_R = \{\rho S_F V_o^2 a_{2F}/(2m)\}[SY_v\beta_E/(a_{2F}S_F)+(\rho Sx/(2m))\\ &\quad\times(S/(a_{2F}S_F))\{2ma_{2F}S_F\ell_F\zeta_o/(\rho S^2k_z^2)\}]\\ &o_R = \{\rho S_F V_o^2 a_{2F}\zeta_o/(2m)\}[\ell_F b\mu_2 Y_v/\{k_z^2(J_2^2+R_2^2)\}+(\ell_F x/k_z)]\end{aligned} \tag{5.61a}$$

At the tail where $x = -\ell_F$:

$$(o_R)_{Tail} = \rho S_F V_o^2 a_{2F} \zeta_o/(2m)[\ell_F b \mu_2 Y_v/\{k_z^2(J_2^2 + R_2^2)\} - (\ell_F/k_z)^2] \quad (5.61b)$$

5.5.5.3 Sinusoidal application of the yaw motivator

(a) Conditions at the end of the first cycle of the motion – non-combat aircraft case.

$$\hat{t} = 2\pi/J_2 \qquad \zeta_{MAX} = \zeta_e$$

From Eqns (5.49) and (5.50a), using H_2 to represent the terms in the { } brackets:

$$\beta_{2\pi} = -F(\zeta_e)\{1 - \exp(-2\pi R_2/J_2)\}/(2R_2J_2) = -H_2/(2R_2J_2) \quad (5.62a)$$

$$\hat{\beta} = F(\zeta_e)\{1 - \exp(-2\pi R_2/J_2)\}/(4J_2) = H_2/(4J_2) \quad (5.62b)$$

$$\hat{\hat{\beta}} = F(\zeta_e)J_2\{1 - \exp(-2\pi R_2/J_2)\}/(2R_2) = H_2J_2/(2R_2) \quad (5.62c)$$

$$\zeta = 0 \qquad \hat{\zeta} = J_2\zeta_e \quad (5.62d)$$

Hence. using Eqn. (5.55b):

$$\begin{aligned} o_{2\pi} &= \rho S_F V_o^2 a_{2F}[\{-SY_vH_2/(2R_2J_2a_{2F}S_F)\}/(2m) + (\rho Sx/(2m)^2) \\ &\quad \times \{J_2\zeta_e + (S/(a_{2F}S_F))(Y_vH_2/(4J_2) - H_2J_2/(2R_2))\}] \\ &= \{\rho S_F V_o^2 a_{2F}H_2/(2m)\}[-SY_v/(2R_2J_2a_{2F}S_F) \\ &\quad + (\rho Sx/(2m))\{J_2\zeta_e/H_2 + (S/(a_{2F}S_F))(Y_v/(4J_2) - J_2/(2R_2))\}] \\ &= -\{\rho S_F V_o^2 a_{2F}H_2/(2m)\}[SY_v/(2R_2J_2a_{2F}S_F) - \rho SxJ_2\zeta_e/(2mH_2) \\ &\quad - \{\rho S^2x/(2ma_{2F}S_F)\}\{Y_v/(4J_2) - J_2/(2R_2)\}] \end{aligned}$$

In practice the terms containing ζ_e and (xY_v) are found to he numerically small and may be assumed to he negligible. therefore approximately:

$$\begin{aligned} o_{2\pi} &= -\{\rho SV_o^2H_2/(2m)\}[Y_v/(2R_2J_2) + \{\rho Sx/(2m)\}\{J_2/(2R_2)\}] \\ &= -\{\rho SV_o^2H_2/(4mR_2J_2)\}[Y_v + \rho SxJ_2^2/(2m)] \end{aligned} \quad (5.63a)$$

Substituting for H_2:

$$\begin{aligned} o_{2\pi} &= -\{\rho SV_o^2/(4mR_2J_2)\}[Y_v + \rho SxJ_2^2/(2m)] \\ &\quad \times \{1 - \exp(-2\pi R_2/J_2)\}F(\zeta_e) \end{aligned} \quad (5.63b)$$

and at the tail where $x = -\ell_F$:

$$(o_{2\pi})_{Tail} = -\{\rho S V_o^2/(4mR_2J_2)\}[Y_v - \rho S\ell_F J_2^2/(2m)] \times \{1 - \exp(-2\pi R_2/J_2)\}F(\zeta_e)$$
$$= -\{\rho S V_o^2(4mR_2J_2)\}[Y_v - (\ell_F/b)J_2^2/\mu_2] \times \{1 - \exp(-2\pi R_2/J_2)\}F(\zeta_e) \quad (5.63c)$$

(b) Conditions at the end of 1.5 cycles of the motion – combat aircraft case

$$\hat{t} = 3\pi/J_2 \qquad \zeta_{MAX} = \zeta_e$$

From Eqns (5.49) and (5.51a) using H_3 to represent the terms in the { } brackets:

$$\beta_{3\pi} = F(\zeta_e)\{1 - \exp(-3\pi R_2/J_2)\}/(2R_2J_2) = H_3/(2R_2J_2) \quad (5.64a)$$

$$\dot{\beta} = -F(\zeta_e)\{1 - \exp(-3\pi R_2/J_2)\}/(4J_2) = -H_3/(4J_2) \quad (5.64b)$$

$$\hat{\beta} = -F(\zeta_e)J_2\{1 - \exp(-3\pi R_2/J_2)\}/(2R_2) = -H_3J_2/(2R_2) \quad (5.64c)$$

$$\zeta = 0 \qquad \hat{\zeta} = -J_2\zeta_e \quad (5.64d)$$

Hence:

$$o_{3\pi} = \rho S_F V_o^2 a_{2F}[\{SY_vH_3/(2R_2J_2a_{2F}S_F)\}/(2m) + (\rho Sx/(2m)^2)\{-J_2\zeta_e + (S/(a_{2F}S_F)) \times (-Y_vH_3/(4J_2) + H_3J_3/(2R_2))\}]$$
$$= \{\rho S_F V_o^2 a_{2F}H_3/(2m)\}[SY_v/(2R_2J_2a_{2F}S_F) + (\rho Sx/(2m))\{-J_2\zeta_e/H_3 + (S/(a_{2F}S_F)) \times (-Y_v/(4J_2) + J_2/(2R_2))\}]$$
$$o_{3\pi} = \{\rho S_F V_o^2 a_{2F}H_3/(2m)\}[SY_v/(2R_2J_2a_{2F}S_F) - \rho SxJ_2\zeta_e/(2mH_3) + \{\rho S^2x/(2ma_{2F}S_F)\}\{-Y_v/(4J_2) + J_2/(2R_2)\}]$$

The terms containing ζ_e and (xY_v) may be assumed to be negligible and therefore approximately:

$$o_{3\pi} = \{\rho SV_o^2H_3/(2m)\}[Y_v/(2R_2J_2) + \{\rho Sx/(2m)\}\{J_2/(2R_2)\}]$$
$$= \{\rho SV_o^2H_3/(4mR_2J_2)\}[Y_v + \rho SxJ_2^2/(2m)] \quad (5.65a)$$

Substituting for H_3:

$$o_{3\pi} = \{\rho S V_o^2/(4mR_2J_2)\}[Y_v + \rho S x J_2^2/(2m)]\{1 - \exp(-3\pi R_2/J_2)\}F(\zeta_e) \tag{5.65b}$$

and at the tail where $x = -\ell_F$:

$$\begin{aligned}(o_{3\pi})_{Tail} &= \{\rho S V_o^2/(4mR_2J_2)\}[Y_v + \rho S \ell_F J_2^2/(2m)] \\ &\quad \times \{1 - \exp(-3\pi R_2/J_2)\}F(\zeta_e) \\ &= \{\rho S V_o^2/(4mR_2J_2)\}[Y_v \\ &\quad + (\ell_F/b)J_2^2/\mu_2\{1 - \exp(-3\pi R_2/J_2)\}F(\zeta_e)\end{aligned} \tag{5.65c}$$

5.6 Asymmetric horizontal stabilizer load due to sideslip

This case is referred to in Chapter 3, Section 3.3.3.5. The rolling moment on the horizontal stabilizer due to the asymmetric distribution of the corrected trim load is:

$$(L)_\beta = 0.5\rho V^2 S_T b_T K_\beta \beta \tag{5.66}$$

where

- S_T is the tail-plane (including elevator) area
- b_T is the tail-plane (including elevator) span
- K_β is the slope of the curve of the tail-plane rolling moment coefficient against angle of sideslip in radians at the appropriate Mach number
- β is the sideslip angle, in radians

The evaluation of K_β is difficult due to the interaction of a number of effects, each critically dependent on geometric and aerodynamic detail. These effects have been discussed by Braun.[5] If possible K_β should be obtained from wind tunnel tests. A conservative value for a low set tail-plane is 0.14 per radian. K_β is critical for a fin-mounted tail-plane and Def.Stan.00-970 Leaflet 203/1, paragraph 6 suggests that it should be assumed that there is a lift coefficient difference on the two halves of the tail-plane of 1.0 or C_{LMAX} whichever is lower. If the span-wise centre of pressure on each half of the tail-plane is assumed to be at 40 per cent of the semi-span then this last

[5]Braun, W. Asymmetric tail-plane loads due to sideslip. RAE Technical Note 81 (C.P. No.119), 1952.

criterion gives:

$$K_\beta \beta = 0.1 \text{ or } 0.1 C_{LMAX} \qquad \text{whichever is least}$$

This approach is conservative and may give high loads. It is also suggested that the shear strength of the tail-plane inboard of its attachment fittings should not he less than that outboard.

5.7 Application of flight manoeuvre load analysis

Addendum AD1 includes an example of the flight manoeuvre load analysis of a particular aircraft using the analysis outlined in this chapter. The calculated values are compared with the results obtained from a simulation of the motion of the aircraft.

CHAPTER 6

Loads due to atmospheric turbulence

6.1 The nature of atmospheric turbulence

6.1.1 General comments

A brief introduction to the nature of atmospheric turbulence is given in Chapter 3, Sections 3.5.1 and 3.5.2, where it serves as an introduction to the specified requirements for horizontal and lateral gust loading conditions quoted in Sections 3.5.3 and 3.5.4. The purpose of the present chapter is to provide a more complete background to the subject and to deal more comprehensively with the derivation of the structural loading consequent upon an aircraft encountering turbulence.

In general, atmospheric turbulence consists of a random continuous variation in the condition of the atmosphere. This is usually of relatively low intensity hut it can include discrete gusts of relatively high intensity. In this context the intensity is defined in terms of some measure of the velocity of the gusting. The true root mean square (r.m.s.) gust velocity is used to define the intensity of continuous turbulence whereas the absolute maximum velocity is used for discrete gusts. The earlier requirements for gust loads were based on the discrete gust approach and this was used in conjunction with a gust spectrum to determine the fatigue loading conditions, see Chapter 10, Section 10.4.3. More recently the continuous turhulence approach has become of importance either to replace the discrete gust analysis or. in many cases. to supplement it.

Discrete gusts may he regarded as columns of air moving at some velocity relative to the ambient atmosphere. There is a boundary region between the nominally static air

and the moving column, the width of which has a significant effect upon the response of the aircraft as it encounters the gusl. The column of air may he oriented in any direction relative to the flight path of the aircraft although it is often assumed that its effect may be resolved into three components: along, laterally perpendicular to, and vertically perpendicular to the flight path. The discrete gust component along the flight path is covered by ensuring that there is an adequate margin on the structural design speed. V_D, see Chapter *2*, Section 2.6.2.5. The dynamic response of the airframe in a discrete gust encounter is an important consideration as it can significantly increase the structural stresses.

Continuous turhulence is specified in terms of a power spectral density (PSD), of the root mean square gust velocity. While it is not usually of importance, the head on, horizontal, PSD is defined differently to the lateral/vertical PSD.

A full consideration of the loading due to atmospheric turbulence may be found in Hoblit,[1] to which reference may he made for a fuller explanation than is included in the following sections.

6.1.2 Mathematical models of atmospheric turbulence

6.1.2.1 Discrete gusts

The simplest, and the earliest. representation of a discrete gust was the so-called 'sharp-edged' gust which is effectively a step change in the velocity conditions relative to the aircraft, see Chapter 3. Section 3.5.1. Clearly a sharp-edged gust is unrealistic as it does not represent the boundary effect referred to in the previous section and its application to an aircraft of conventional layout results in a higher acceleration increment than would occur in a practical situation.

In order to provide a more realistic, but simple, model of the variation of gust velocity in the boundary region it was assumed that the boundary velocity profile followed a (I-cosine) form as defined in Chapter 3. Eqn. (3.1). In this representation the gust is assumed to build-up from zero to the maximum value over the boundary region known as the gradient distance, ℓ, see Fig. 6.1. Experimental observation of the response of some transport aircraft to encounters with vertical gusts indicated that a typical value for the gradient distance is 12.5 times the wing mean chord. On this basis an 'alleviating' factor. F, was deduced as a correction factor to be applied to the normal acceleration increment derived from a sharp-edged analysis. see Chapter **3,** Eqns (3.3) and (3.5) and Section 6.2. The alleviating factor was intended to cover the lag in the build-up of the gust and the response of the aircraft as it entered the gust. In practice the design gust velocities were determined by the measurement of the incremental accelerations associated with actual flight into gust conditions and thus included the response of the aircraft. The reduction of the flight data included the ordinary alleviation

[1] Hoblit, *F. M. Gust Loads on Aircraft: Concepts and Applications* AIAA Education Series, 1988.

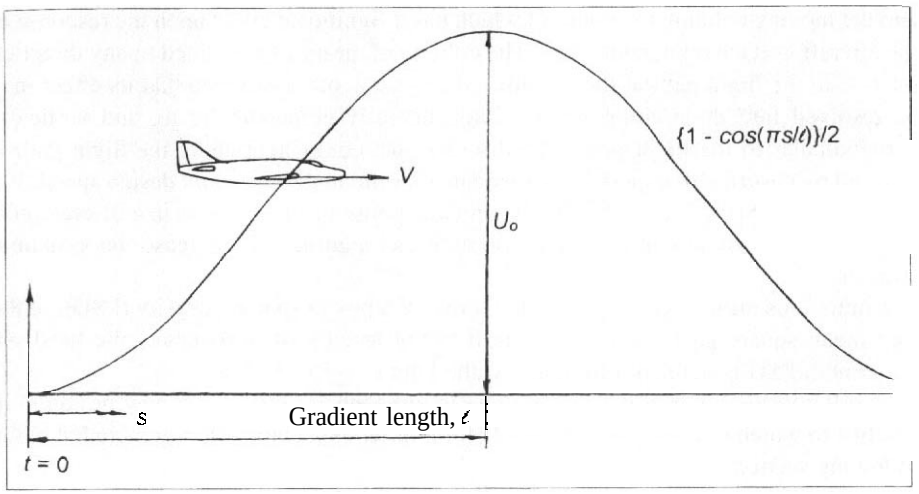

Fig. 6.1 *Passage of* ***an*** *aircraft into* ***a*** *(I-cosine) gust*

correction so that the derived design values were somewhat arbitrary in terms of the actual situation.

The alleviated sharp-edged gust concept using a gradient distance of 12.5 wing mean chords formed the basis for discrete gust load requirements for a considerable period and still appears in some design codes. However, it was realized that the assumption of a single, typical, gradient distance is an over-simplification and it is possible that some other gradient distance could result in a higher value of the acceleration increment due to the gust. This led to the 'tuned' gust concept, that is, one where the gradient distance used is that which gives the highest acceleration increment for a given design gust velocity. The application of the tuned gust concept requires the analysis of the response of the aircraft as the gust is encountered in much the same way as the analysis of the response of the aircraft to control input; see Section **6.3.** While the tuned gust concept is of importance it should be understood that, because of the way they were originally derived, it is not necessarily appropriate to apply the alleviated sharp-edged. gust velocities to a tuned gust analysis. Hence tbe gust design values may be different. This is recognized in the current European JAR-25 civil transport requirements.

In practice it has been found that the effect of variation in the gradient distance on the acceleration increments is not large, but it can have an important impact upon the consequent dynamic stresses in the structure.

6.1.2.2 Representation of continuous turbulence

One way of representing more general, continuous. turbulence in the atmosphere is to assume that it takes the form of a series of (1-cosine)-shaped velocity variations in sequence along the path of the aircraft. This is not really realistic since in practice there is a general variation of the magnitude. frequency, and effective gradient distance. It is

preferable to represent the turbulence as a stationary Gaussian random process. This leads to the specification of a pou'er spectral density, PSD, as discussed in Section 6.4. Two shapes of gust PSD have been used for aircraft gust analysis. These have become known as thr von Kármán and Dryden representations. Of the two, it has been found that the former provides a somewhat better agreement with observed data and it has now become the standard for use in design. The von Kármán PSD is stated in Eqns (6.21). An important parameter in the representation is the scale of the turbulence, L, which is typically an order of magnitude greater than the gradient distance, ℓ, associated with discrete gusts.

6.1.2.3 Orientation of gust gradients and turbulence

It is normally assumed that both the discrete gust gradient distance and the scale of the random turbulence are one-dimensional in form and are aligned along the flight path of the aircraft. In the case of vertical gusts this implies there is no variation of the gust intensity across the span of the wing of an aircraft. Clearly in practice there may well be a variation in gust velocity in the span-wise direction and at its extreme this could be assumed to take the form of a cosine shape having the maximum gust velocity at either wing tip with a zero velocity on the centreline of the aircraft. This is an extremely severe condition as well as being extremely improbable. In fact the majority of aircraft wings are relatively stiff structures and thus have the effect of averaging out. at least to some extent, the effect of span-wise variation of gust velocity. The possibility of the span-wise variation is recognized in the European JAR-25 civil transport aircraft requirements where it is necessary to investigate a condition such that the magnitude of a gust on one side of the aircraft is 80 per cent of that on the other, see Chapter 3, Section 3.5.4.4. Span-wise variation of gust velocity becomes much more significant in the case of an aircraft having a very flexible wing of large span. It is questionable whether the severe case of a span-wise discrete gust mentioned above is realistic and a better approach for design purposes is possibly the application of a two-dimensional form of the von Kármán PSD. This problem of large-span flexible wings has been considered by Lissaman and Brownlow.[2]

6.2 Analysis of the alleviated sharp-edged gust – the gust n–V diagram

6.2.1 The alleviating factor

The corrected design velocity of an alleviated sharp-edged gust is FU_{de} where U_{de} is the design gust velocity, as an equivalent airspeed. specified as a function of forward speed in Chapter 3, Section 3.5.2. F is the alleviating factor as defined in Chapter 3; Eqn. (3.3) defines F as a function of the mass parameter μ_{G1}, Eqn. (3.2). for symmetric vertical

[2]Lissaman. P. B. S and Brownlow, L. W. Torsional and flexural response of a large span wing to high altitude turbulence. *Aeronautical Journal*, 106 (1060). June 2002.

gusts while in Eqn. (3.5), F is defined as a function of the mass parameter, μ_{G2}, of Eqn. (3.6), for lateral gusts. The expression for F given in Eqn. (3.3) is an empirical equation found to closely approximate the alleviating factor deduced by considering only the vertical, that is the heave, degree of freedom as the wing of an aircraft encounters a (1-cosine) gust presumed to have a gradient length of 12.5 wing chords. This is discussed in Appendix A of Hoblit,[1] and in Fig. 6.5 in this chapter. In the analysis given in Hobilt,[1] allowance is made for two effects:

(a) The lag in the build-up of the lift consequent upon an instantaneous change of the angle of attack such as occurs with a sharp-edged gust, known as the 'Wagner' function.

(b) The lag due to the fact that the angle of attack across the chord does not change simultaneously, but gradually as it progresses into the gust, see Fig. 6.1. This is known as the 'Kussner' function.

For a given aircraft both of these effects are a function only of the distance the wing travels into the gust. The Kussner function results in a delay in the time the maximum gust effect occurs as well as somewhat reducing its magnitude.

It should be noted that in practice the aircraft also responds in pitch as a consequence of the effect of the gust on the auxiliary lifting surface, as shown in Chapter 3, Fig. 3.9. Thus the assumption that the response may be evaluated in terms only of the heave motion of the isolated wing is aconsiderable simplification of the true situation.

6.2.2 The gust n–V diagram

6.2.2.1 Assumptions

The effective change in the angle of attack of the lifting surface due to its encountering an alleviated sharp-edged gust may be used lo derive the corresponding increment in the normal or lateral acceleration of the aircraft, as relevant. In the case of a gust in the plane of symmetry the values obtained at the various design forward speeds may be used to construct an n–Vdiagram for comparison with that describing the normal manoeuvres, Chapter 3, Fig. 3.3. The usual assumptions made in the case of an aircraft of conventional tailed or tailless layout are that:

(i) the aircraft is in steady level flight at the time that the gust is encountered, but see Chapter 3. Section 3.5.3.1 for terrain-following military types;

(ii) the forward speed and the altitude of the aircraft are unchanged during the passage into the gust;

(iii) no action is taken by the pilot, such as movement of the pitch control, during the passage into the gust;

(iv) pitching moments developed during the passage of the aircraft into the gust are balanced by rotational inertia effects.

6.2.2.2 Wing–body lift

The change in angle of attack, α, due to an alleviated sharp-edged gust is given by:

$$\alpha = \tan^{-1}\left(\frac{F_1 U_{de}}{V_{oEAS}}\right) \quad \text{radians}$$
$$= \left(\frac{F_1 U_{de}}{V_{oEAS}}\right) \quad \text{for small angles} \tag{6.1}$$

where

F_1 is the gust alleviating factor
U_{de} is the specified gust velocity, EAS
V_{oEAS} is the vehicle flight speed, EAS

Thus the change in the load on the wing–body, $\mathscr{L}_G$, due to the gust is given by:

$$\mathscr{L}_G = \rho_o V_{o\,EAS}^2 S a_{1WB} \frac{F_1 U_{de}/V_{oEAS}}{2} \tag{6.2}$$

where

ρ_o is the sea level value of the air density
S is the reference area of the wing
a_{1WB} is the wing–body lift curve slope

It should be noted that the value of $\mathscr{L}_G$ may be limited by the implied wing angle of attack reaching the stall value. However, since it is a dynamic situation it is usual to assume that the allowable value of maximum lift coefficient is 1.25 times the static value. That is, the value of (FU_{de}/V_{oEAS}) applies unless it is greater than $1.25(C_{LMAX}/a_{1WB})$, this being the highest value required.

It will also be noted that the loads due to the gust increase directly in proportion to the equivalent speed of the vehicle, provided the lift curve slope, a_{1WB}, does not vary with speed. In the transonic or supersonic range a_{1WB} is dependent upon Mach number. The loads are also directly proportional to the gust velocity. The gust will also change the lift on the tail but this is not considered in the estimation of wing–body load when using the alleviated sharp-edged analysis.

The incremental gust accclcration factor, n_G, is given by:

$$n_G = \rho_o V_{o\,EAS}^2 S a_{1WB} \frac{F_1 U_{de}/V_{oEAS}}{2mg}$$

but in level flight the lift is equal to the weight, mg, thus:

$$mg = \rho_o V_{o\,EAS}^2 S C_L/2$$

Hence:

$$\begin{aligned} n_G &= 2\rho_o V_{o\,EAS}^2 S a_{1WB}(F_1 U_{de}/V_{oEAS})/(2\rho_o V_{o\,EAS}^2 S C_L) \\ &= (a_{1WB}/C_L)(F_1 U_{de}/V_{oEAS}) \end{aligned} \tag{6.3}$$

That is, n_G is equal to the change of angle of attack due to the gust divided by the angle of attack of the wing at the time of gust encounter. This is the usual alleviated sharp-edged gust formula. Note that n_G is an increment above or below level flight conditions, depending upon whether the gust is directed upwards or downwards.

Since the increment in the normal acceleration due to the gust is inversely proportional to the lift coefficient in level flight it is also inversely proportional to the wing loading.

The gust $n-V$ diagram may be drawn by plotting the function $(n_G + 1)$ against the forward speed, V_{oEAS}, for each of the specified gust velocities. The inclusion of 1 is necessary since the gust loads have to be superimposed on the level flight conditions. For a given gust velocity and constant aerodynamic derivatives, each condition results in a straight line. A typical n–V diagram for an aircraft flying in incompressible flow conditions is illustrated in Fig. 6.2. As shown. such an $n-V$ diagram can be superimposed upon that for symmetric manoeuvres to indicate which gives the highest normal accelerations. In general only the comers of the n–V diagram need to be investigated although the gust design cases apply throughout the speed range above the gust speed, V_G. The definitions of V_G and the other relevant flight speeds are to be found in Chapter 2. Section 2.6.2. It must be remembered that the wing–body load is $\{(n_G + 1)mg\}$ so that a high value of n_G, often associated with a low wing loading case, may not actually give a critical load.

When the vehicle is subjected to compressibility effects the gust normal acceleration factor is not directly linear with forward speed. At supersonic speeds the reduction of lift curve slope with increase in Mach number may cause a reduction in n_G in spite of the apparent direct increase due to higher Mach number which relates to higher true, not equivalent, speed.

6.2.3 Horizontal stabilizer load due to a symmetric gust

In a conventional tail layout the effect of the gust in changing the lift developed on the horizontal stabilizer is influenced by the change in downwash of the wing. Thus if $(d\varepsilon/d\alpha)$ is the rate of change of downwash angle with wing angle of attack at the horizontal stabilizer position, the actual change of angle of attack of the stabilizer. α_T,

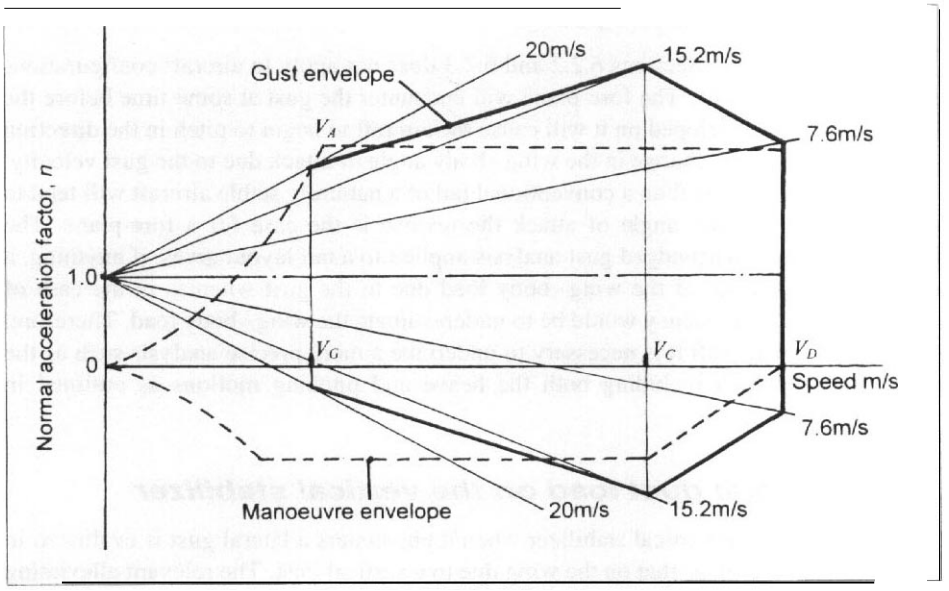

Fig. 6.2 Typical gust n – V diagram

due to the gust will be:

$$\alpha_T = \left\{\tan^{-1}\left(\frac{F_1 U_{de}}{V_o}\right)\right\}\left(1 - \frac{d\varepsilon}{d\alpha}\right) \quad \text{radians}$$
$$= \left(\frac{F_1 U_{de}}{V_o}\right)\left(1 - \frac{d\varepsilon}{d\alpha}\right) \quad \text{for small angles} \tag{6.4}$$

Note the value of the alleviating factor, F, is that evaluated for the wing since the wing characteristics are used for calculating the horizontal stabilizer load by this method.

The incremental load due to the gust. $\mathscr{L}_{GT}$, is then:

$$\mathscr{L}_{GT} = \rho_o V_{o\,EAS}^2 S_T a_{1T}\left(1 - \frac{d\varepsilon}{d\alpha}\right)\frac{F_1 U_{de}/V_{oEAS}}{2} \tag{6.5}$$

where

S_T is the reference area of the horizontal stabilizer
a_{1T} is the lift curve slope of the surface

$\mathscr{L}_{GT}$ is used only for the calculation of the load on the horizontal stabilizer and it has no influence upon the load on the wing or the gust acceleration increment, n_G.

6.2.4 Fore-plane layouts

The analysis given in Sections 6.2.2 and **6.2.3** does not apply to aircraft configurations which use a fore-plane. The fore-plane will encounter the gust at some time before the wing and the lift developed on it will cause the aircraft to begin to pitch in the direction of the gust before the change in the wing–body angle of attack due to the gust velocity. Thus, while the gust load on a conventional tail of a naturally stable aircraft will tend to reduce the wing–body angle of attack the reverse is the case for a fore-plane. The simple alleviated sharp-edged gust analysis applied to a tail layout gives. if anything. a conservative estimate of the wing–body load due to the gust whereas in the case of the fore-plane, the tendency would be to underestimate the wing–body load. Therefore, for this class of aircraft it is necessary to undertake a more precise analysis such as the tuned gust approach including both the heave and pitching motions as outlined in Section **6.3.**

6.2.5 Lateral gust load on the vertical stabilizer

The gust load on the vertical stabilizer when it encounters a lateral gust is evaluated in exactly the same way as that on the wing due to a vertical gust. The relevant alleviating factor, F_2, is given in Chapter **3,** Eqn. (3.5). this being expressed in terms of the mass parameter, μ_{G2}, given by Eqn. (3.6). The lateral alleviating factor was derived by a similar approach to that used for the symmetric factor described in Section **6.2.1** except that in this case it was based on the single degree of freedom yawing motion of the aircraft.

The fin load due to the gust on the isolated surface, $\mathscr{L}_{GF}$, is:

$$\mathscr{L}_{GF} = \rho_o V_{o\,EAS}^2 S_F a_{1F} \frac{F_2 U_{de}/V_{oEAS}}{2} \tag{6.6}$$

where

S_F is the reference area of the vertical stabilizer
a_{1F} is the corresponding lift curve slope

6.3 The tuned gust approach

6.3.1 Symmetric gusts

The assumptions outlined in Section 6.2.2.1 are also appropriate in this case. The gust is assumed to build up over a gradient distance which here is a variable over the range of values specified in the requirements, for example as in Chapter **3,** Section 3.5.2.3.

As a conventional aircraft enters an up-gust the first effect is to increase the effective wing incidence due to the change in direction of the resulting velocity and hence impart an upward acceleration. This is accompanied by a pitching acceleration, the direction of

which depends upon the relative positions of the wing aerodynamic centre and the centre of gravity. The magnitude is not likely to he large. At a later time, dependent upon the aircraft geometry and speed, the tail surface enters the gust adding a small increment to the vertical acceleration. Also, for a stable aircraft, it induces a relatively large nose-down pitching moment tending to reduce wing incidence and the vertical acceleration increment. Finally the. level attitude condition is restored but the aircraft is subjected to a vertical velocity equal to that of the gust.

The case of a canard aircraft is somewhat different since when the fore-plane enters the gust it causes a substantial nose-up pitching moment giving a vertical acceleration even before the wing enters the gust. It is quite possible for the wing to reach an incidence greater than that due to the vertical gust velocity alone. that is. for the gust acceleration to be greater than the *sharp-edged* value. Eventually, assuming natural static stability, the nose-down pitching moment due to the wing lift restores the aircraft to level flight

One of the main difficulties with gust response analysis is that the calculation must be carried out in a number of definite steps:

(i) wing (or canard fore-plane) experiencing the gust along gradient;
(ii) wing (or fore-plane) experiencing the full gust. or tail surface (or wing of a canard layout) entering the gust gradient. depending upon the speed and geometry of the aircraft and the gradient distance;
(iii) full gust on the wing (or fore-plane), with gradient on tail surface (or wing of a canard layout);
(iv) full gust on the tail surface (or on the wing of a canard layout) with a reduced gust on the forward surface;
(v) reducing gust on both surfaces, with the forward surface exiting the gust earlier than the rear one.

Only steps (i) and (ii) apply to a tailless design

For simplicity it may be assumed that the Wagner function referred to in Section 6.2.1 is unity, that is the chord of a given lifting surface immediately develops the lift coefficient appropriate to the gust velocity at a particular point into the gradient distance. Further, it may be assumed that the Kussner function is also unity, that is the lifting surface is represented by an unswept lifting line. This latter is a conservative assumption in that it will result in a tendency to overestimate the response of the lifting surface to the gust encounter. In the case of a longitudinally statically stable aircraft having two lifting surfaces there will be a degree of compensation for this as a consequence of the pitching effect when the aft surface encounters the gust.

Let u hc the gust velocity at a time t, and U_o the maximum value achieved at the end of the gradient distance, ℓ. The distance between the lift reference locations of the forward and rear surfaces is ℓ'_T. Using suffix '1' for the first lifting surface to enter the gust and suffix '2' for the second, and with a gust build-up of (1-cosine) form:

(a) At the wing or the fore-plane of a canard layout:
For the time $0 < t < 2\ell/V_o$ the gust velocity is:

$$u_1 = U_o \frac{\{1 - cos(\pi V_o t/\ell)\}}{2} \tag{6.7a}$$

For the time $t \geq 2\ell/V_o$:

$$u_1 = 0 \tag{6.7b}$$

(b) At the tail-plane or the wing of a canard layout:
For the time $0 < t < \ell'_T/V_o$:

$$u_2 = 0 \tag{6.7c}$$

For the time $\ell'_T/V < t < (\ell_T + 2\ell)/V_o$:

$$u_2 = U_o \frac{[1 - cos\{\pi(V_o/\ell)(t - \ell'_T/V)\}]}{2} \tag{6.7d}$$

For the time $t \geq (\ell'_T + 2\ell)/V_o$:

$$u_2 = 0 \tag{6.7e}$$

It is assumed that the effects due to the gust solely arise from the change in the incidence of a lifting surface implied by the gust velocity at any particular time as described in Eqns (6.7). The absolute terms are non-dimensionalized in accordance with Chapter 4, Section 4.4.7. Then for an aircraft of conventional tail layout encountering an up-gust:

(a) The increment of the normal force on the wing, opposite in sign to the lift increment. is:

$$Z_{G1} = -\mathcal{L}_{G1} = -\rho_o V_o^2 S a_{1WB} \frac{(u_1/V_o)}{2}$$

or non-dimensionally:

$$-a_{1WB}(\hat{u}_1) \tag{6.8a}$$

(b) The increment of lift on the rear horizontal surface is:

$$Z_{G2} = -\mathcal{L}_{G2} = -\rho_o V_o^2 S_T a_{1T} \frac{(u_2/V_o)}{2}$$

or non-dimensionally:

$$-a_{1T}(S_T/S)(\hat{u}_2) \tag{6.8b}$$

(c) The pitching moment due to the lift on the wing is:

$$M_{G1} = -\rho_o V_o^2 S a_{1WB}(u_1/V_o)(H_o - h)c/2$$

or non-dimensionally:

$$-a_{1WB}(H_o - h)(\hat{u}_1) \tag{6.8c}$$

(d) The pitching moment from the rear horizontal stabilizer is:

$$M_{G2} = -\rho_o V_o^2 S_T a_{1T}(u_2/V_o)\ell'_T/2$$

or non-dimensionally:

$$-a_{1T}(S_T/S)(\ell'_T/c)(\hat{u}_2) \tag{6.8d}$$

The equivalent terms for a canard layout follow directly from the above by exchanging the effects of the wing and horizontal stabilizer.

Chapter **4,** Eqns (4.69) are the basic equations of motion of the aircraft. If, as with the analysis of the response to pitch control input, it is assumed that the forward speed is constant during the passage into the gust, the first of Eqns (4.69) is decoupled and the remaining two, which represent the heave and pitch motions, may be written in the form of Eqns (4.75):

$$\begin{bmatrix} G_1 & H_1 \\ L_1 & M_1 \end{bmatrix} \begin{Bmatrix} \hat{w} \\ \theta \end{Bmatrix} = \begin{bmatrix} Q_1 \\ R_1 \end{bmatrix} (\hat{u}_{1,2}) \tag{6.9}$$

where the right-hand side has replaced the control input terms but the left-hand side is unchanged and represents the basic aircraft dynamic charactenstics. From Eqns (6.8):

$$Q_1 = -\{a_1(\hat{u}_1) + a_{1T}(S_T/S)(\hat{u}_2)\} \tag{6.10a}$$

$$R_1 = -\{a_1(H_o - h)(\hat{u}_1) + a_{1T}(S_T/S)(\ell'_T/c)(\hat{u}_2)\} \tag{6.10b}$$

The second term in the expression for Q_1 may usually be neglected in the case of a tail or tailless layout but it is essential to retain it when the configuration utilizes a fore-plane.

Using Cramer's rule the solution of Eqn. (6.9) is:

$$\hat{w} = \begin{vmatrix} Q_1 & H_1 \\ R_1 & M_1 \end{vmatrix} (\hat{u}_{1,2}) \div \begin{vmatrix} G_1 & H_1 \\ L_1 & M_1 \end{vmatrix} \tag{6.11a}$$

The determinant in the denominator is given by Eqn. (4.78b). The determinant in the numerator is:

$$\begin{vmatrix} Q_1 & H_1 \\ R_1 & M_1 \end{vmatrix} = (Q_1 M_1 - H_1 R_1) \tag{6.11b}$$

M_1 is defined at Eqn. (4.71) and the approximate form of H_1 by Eqn. (4.76). Using these in conjunction with Eqns (6.10) gives:

$$\begin{aligned} \begin{vmatrix} Q_1 & H_1 \\ R_1 & M_1 \end{vmatrix} &= \{i_y/\mu_1\}\mathcal{D}[-(\mathcal{D} - M_q/i_y)\{a_{1WB}(\hat{u}_1) + a_{1T}(S_T/S)(\hat{u}_2)\}] \\ &\quad + \mathcal{D}\{-a_{1WB}(H_o - h)(\hat{u}_1) - a_{1T}(S_T/S)(\ell'_T/c)(\hat{u}_2)\} \\ &= \{i_y/\mu_1\}\mathcal{D}\{-a_{1WB}(\hat{\dot{u}}_1) + (M_q/i_y)a_{1WB}(\hat{u}_1) \\ &\quad - a_{1T}(S_T/S)(\hat{\dot{u}}_2) + (M_q/i_y)a_{1T}(S_T/S)(\hat{u}_2) \\ &\quad - \{i_y/\mu_1\}\mathcal{D}\{a_{1WB}(\mu_1/i_y)(H_o - h)(\hat{u}_1) \\ &\quad - a_{1T}(\mu_1/i_y)(S_T/S)(\ell'_T/c)(\hat{u}_2)\} \\ &= \{i_y/\mu_1\}\mathcal{D}[-a_{1WB}(\hat{\dot{u}}_1) + (a_{1WB}/i_y)\{M_q - \mu_1(H_o - h)\}(\hat{u}_1) \\ &\quad - a_{1T}(S_T/S)(\hat{\dot{u}}_2) + (a_{1T}/i_y)(S_T/S)\{M_q - \mu_1(\ell'_T/c)\}(\hat{u}_2)] \end{aligned} \tag{6.11c}$$

In the last term in the above equation M_q is likely to be negligible in comparison with $\mu_1(\ell'_T/c)$. Substitution for μ_1 and i_y from Eqns (4.61d) and (4.61e) results in:

$$\begin{aligned} \begin{vmatrix} Q_1 & H_1 \\ R_1 & M_1 \end{vmatrix} &= \{i_y/\mu_1\}\mathcal{D}[-a_{1WB}(\hat{\dot{u}}_1) + 2ma_{1WB}c/(\rho S k_y^2) \\ &\quad \times \{M_q/\mu_1 - (H_o - h)\}(\hat{u}_1) - a_{1T}(S_T/S)(\hat{\dot{u}}_2) \\ &\quad + 2ma_{1T}c\bar{V}/(\rho S k_y^2)(\hat{u}_2)] \end{aligned} \tag{6.12}$$

Substituting for M_q from Eqn. (4.74k) and using Eqns (4.30), (4.31), and (4.37c) to define $H_{,,}$ yields:

$$\begin{vmatrix} Q_1 & H_1 \\ R_1 & M_1 \end{vmatrix} = \{i_y/\mu_1\}\mathcal{D}[-a_{1WB}(\hat{u}_1) + 2ma_{1WB}c/(\rho Sk_y^2) \times \{H_m - \bar{V}(a_{1T}/a_{1WB})(1 - d\varepsilon/d\alpha)\}(\hat{u}_1) - a_{1T}(S_T/S)(\hat{u}_2) + 2ma_{1T}c\bar{V}/(\rho Sk_y^2)(\hat{u}_2)] \quad (6.13)$$

Finally, Eqn. (6.13) is substituted into Eqn. (6.11a) in conjunction with Eqn. (4.78b) to give:

$$\hat{\ddot{\alpha}} + 2R_1\hat{\dot{\alpha}} + (R_1^2 + J_1^2)\alpha_B = [-a_{1WB}(\hat{u}_1) + 2ma_{1WB}c/(\rho Sk_y^2) \times \{H_m - \bar{V}(a_{1T}/a_{1WB})(1 - d\varepsilon/d\alpha)\}(\hat{u}_1) - a_{1T}(S_T/S)(\hat{u}_2) + 2ma_{1T}c\bar{V}/(\rho Sk_y^2)(\hat{u}_2)] \quad (6.14)$$

The difficulty with the use of this equation is the discontinuities of the functions $(\hat{u}_1)$ and $(\hat{u}_2)$ as given by Eqns (6.7). It is necessary to employ a stepped solution.

6.3.2 Lateral gusts

In the case of symmetric gusts it is acceptable to include the aerodynamic contributions from the fuselage in the wing terms. This is not possible in the lateral gust analysis. There are several possible approaches in the formulation of the lateral tuned gust equations of motion:

(a) The simplest is to neglect all the aerodynamic contributions except those of the vertical stabilizer. Apart from the opportunity to investigate the effect of gradient length, this is essentially similar to the alleviated sharp-edged approach using the alleviating factor, F_2.

(b) To include all the aerodynamic terms. This is very complex due to the many detail contributions to the lateral derivatives and the fact that there will be different Kussner function effects for each of these contributions.

(c) To compromise by including the primary aerodynamic effects assuming that they consist only of two contributions. namely those of the vertical stabilizer and those of the wing–body taken as a concentrated contribution located at the centre of gravity of the aircraft. In this, the first effect of the gust is on the wing–body at the centre of gravity, neglecting the Kussner contribution, followed at some later time by the vertical stabilizer encountering the gust. Thus, as with the symmetric tuned gust analysis of the previous section, the equations of motion must include two distinct gust representations. Furthermore it is necessary to isolate the fin contributions to the side force derivative, Y_v, and the moment derivative, $N_{,,}$ from those of the rest of the

aircraft. There is a considerable simplification if it is assumed that all the gust effects occur simultaneously but this is not a realistic approach and it is questionable if it would yield more reliable results than the simple method of (a) above.

On balance it may be concluded that the accurate application of the tuned gust approach to the lateral gust condition is fraught with difficulty. The alternative is the use of continuous turbulence analysis as discussed in Section 6.4, where the nature of the method is such that there is an overall averaging in terms of the natural frequency of the lateral sideslip/yaw equations of motion.

6.4 Continuous turbulence analysis

6.4.1 Basis of continuous turbulence analysis

6.4.1.1 Introduction

The definitive reference for continuous turbulence analysis is Federal Aviation Authority Technical Report FAA-ADS-~3.~

The continuous turbulence analysis of aircraft response is based on probability theory. As mentioned in Section 6.1.2.2, the turbulence profile is idealized as a stationary Gaussian random process. This formulation is chosen partly because it provides a good representation of empirical data and partly because of the availability of analysis techniques. The discussion here is limited to a statement of definitions necessary to apply the method. Further explanation may be had by reference to Hoblit.[1]

A stationary random function of time is one where the time history is considered to be of infinite duration and where the statistical properties are the same wherever the sample is taken. Three characteristics are required to define a stationary Gaussian random process, namely the magnitude, the probability distribution, and the frequency content.

6.4.1.2 The magnitude or intensity

If y is a stationary random function of time, such as the gust velocity or for that matter the aircraft response to it, then the magnitude of fluctuation of y as an increment about its mean value is evaluated from a time history in terms of its root mean square value. σ_y.

$$\sigma_y = (\bar{y}^2)^{1/2} = [\mathrm{Lim}(T \to \infty)\{(1/(2T))\} \int_{-T}^{T} \{y(t)\}^2\} \, dt]^{1/2} \qquad (6.15a)$$

[3]Hoblit, F. M., Paul, N., Shelton. J. D.. and Ashford, F. E. Development of power-spectral gust design procedure for civil aircraft. Federal Aviation Authority Technical Report FAA-ADS-53, January 1966.

where $\bar{y}$ is the average value obtained by taking the square of the individual values. to eliminate the effect of positive and negative variations about the mean, before averaging. T is the total time of the sample. Equation (6.15a) applies only when the mean value is zero as is the case of the gust velocity. If y is the aircraft response to a gust it represents the incremental response from the steady level flight condition.

In practice σ_y has to be evaluated numerically:

$$\sigma_y = (\bar{y}^2)^{1/2} = \left[\text{Lim}(N \to \infty) \left\{ \left(\frac{1}{N}\right) \sum_{i=1}^{N} \{y(t_i)^2\} \right\} \right]^{1/2} \tag{6.15b}$$

where i is a sample condition, N being the number of samples and t_i the time of a given sample.

6.4.1.3 The probability distribution

This gives a more detailed description of the magnitude of y. In a stationary Gaussian random process the Gaussian, or normal. probability distribution is defined by:

$$p(y) = \{1/(2\pi)\}^{1/2} [\exp\{-0.5(y/\sigma_y)^2\}]/\sigma_y \tag{6.16}$$

While a characteristic of a stationary Gaussian random process is that the probability density of v is Gaussian, as given by Eqn. (6.16). it is also a requirement that the rate of change of y with time. $\dot{y}$, is also Gaussian and that either it is independent of y or the process is what is known as 'joint Gaussian'. Gaussian joint probability is defined in terms of the autocorrelation function, see Eqn. (6.18a).

6.4.1.4 The frequency content and power spectral density

To complete the definition of a stationary Gaussian random process it is necessary to define its frequency content. This is done by use of the power spectral density or PSD. The concept is that the process can be considered as being made up of an infinite number of sinusoidal components, each having infinitesimal frequency differences. Each component has infinitesimal amplitude and phase relationships are random. This leads to:

$$y(t) = \sum_{m=1}^{\infty} \{\Phi(\omega_m)\Delta\omega\}^{1/2} \cos(\omega t + \psi_m) \tag{6.17a}$$

where m is a given sinusoid component of frequency ω_m, of phase ψ_m and infinitesimal amplitude $\Phi(\omega_m)\Delta\omega$. ω_m varies from a frequency of zero to infinity. $\Phi(\omega_m)$ is the power spectral density (PSD).

The relationship between σ_y and $\Phi(\omega)$ is:

$$\sigma_y = \left\{ \int_0^\infty \Phi(\omega) d\omega \right\}^{1/2} \tag{6.17b}$$

where $\Phi(\omega)$ is a 'one-sided' PSD, that is the frequency integration is only between 0 and infinity, not minus to plus infinity.

$$\Phi(\omega) = \mathrm{Lim}(T \to \infty)[\{1/(\pi T)\} | \int_{-T}^{T} y(t) e^{-i\omega t} dt|^2] \tag{6.17c}$$

The | | indicates the modulus of the complex number of the integral

6.4.1.5 The autocorrelation function – relationship between the PSD and the time history

In practice Eqn. (6.17c) cannot be integrated to infinity and it is necessary to use a finite time history As different durations will give different PSDs an alternative approach is to use an 'autocorrelation function' as an intermediate step in the process. This is defined as:

$$R(\tau) = \overline{y(t)y(t+\tau)} = \mathrm{Lim}(T \to \infty)[\{1/(2T)\} \int_{-T}^{T} y(t)y(t+\tau)dt] \tag{6.18a}$$

which expresses the correlation of the function $y(t)$ at points separated by various times, τ:

When $(\tau = 0)$. from Eqns (6.15a) and (6.18a):

$$R = (\bar{y})^2 = \sigma_y^2 \tag{6.18b}$$

In reality the autocorrelation function is better written in the normalized form of $R(\tau)/\sigma_y^2$. The PSD is then given by:

$$\Phi(\omega) = (2/\pi) \int_0^\infty R(\tau) cos(\omega t) d\tau \tag{6.18c}$$

and

$$R(\tau) = \int_0^\infty \Phi(\omega) cos(\omega t) d\omega \tag{6.18d}$$

In practice the PSD is derived from the time histories by using a fast Fourier transform technique (FIT).

6.4.1.6 Definitions of frequency

In the above equations the frequency. ω, is by implication defined in the usual form of rad/s. Other definitions of frequency are sometimes more useful.

(a) f_o, defined in Hz:

$$f_o = \omega/(2\pi) \tag{6.19a}$$

(b) Ω, defined in rad/unit length, sometimes referred to as a spatial frequency or reduced frequency:

$$\Omega = \omega/V = 2\pi f_o/V = k_o/b_o \tag{6.19b}$$

(c) k, defined as rad/semi-chord:

$$k_o = \omega b_o/V = \Omega b_o = 2\pi f_o b_o/V = \pi f_o c/V \tag{6.19c}$$

where b_o is a reference semi-chord and V is the true airspeed.

Numerical values of the PSD depend upon the definition of frequency used.

6.4.1.7 The frequency response function (transfer function)

The frequency response function, or transfer function, of a system is an important characteristic since it determines the output PSD in terms of the input PSD. The frequency response function is mathematically the same as the transfer function, except it is expressed in terms of $(i\omega)$ rather than, say, (s) of Laplace transform notation. In terms of complex vector notation, the frequency response function:

$$H = \text{Output/Input} = a + ib = |H|e^{i\psi} \tag{6.20a}$$

where $|H|$ is the modulus. that is amplitude ratio, and ψ is the phase angle.

In the case of gust analysis, if the input gust is defined as $U_o e^{i\omega t}$ and the output as q, then:

$$H = q_o e^{i\psi}/U_o = (q_o/U_o)e^{i\psi} \tag{6.20b}$$

In this case (q_o/U_o) is the amplitude ratio and ψ the phase angle as in Eqn. (6.20a). In terms of power spectral densities:

$$\Phi_o(f) = \Phi_i(f)|H(f)|^2 \tag{6.20c}$$

where Φ_o is the output PSD which will be Gaussian provided that the input PSD, Φ_i is Gaussian.

6.4.2 Application to aircraft gust response

6.4.2.1 Continuous turbulence PSD

Although the two forms of power spectral density mentioned in Section 6.1.2.2 have been used for aircraft design work that which is now more usually accepted, and which appears in the various requirements codes. is known as the von Kármán PSD.

For vertical and lateral gusts perpendicular to the flight path:

$$\Phi(\Omega) = \sigma_w^2(L/\pi)\{1 + 2.667(1.339L\Omega)^2\}/\{1 + (1.339L\Omega)^2\}^{11/6} \tag{6.21a}$$

where

, is the true r.m.s. gust velocity, the subscript *'w'* originally referring to vertical gust hut now used generally. (Note in JAR-25.ACJ 341, σ_w is replaced by σ)

L is a scale of turbulence, which is usually taken to be 762 m (2500 ft) but lesser values are proposed for low altitude flight in the United States military code MIL-A-008861A

For gusts along the flight direction:

$$\Phi(\Omega) = \sigma_w^2(2L/\pi)/\{1 + (1.339L\Omega)^2\}^{5/6} \tag{6.21b}$$

The validity of these representations and the selection of the value of L are discussed in Hoblit.[1]

In terms of other expressions of frequency:

$$\Phi(\omega) = \Phi(\Omega)/V \tag{6.22a}$$

$$\Phi(f) = (2\pi/V)\Phi(\Omega) \tag{6.22b}$$

$$\Phi(k) = \Phi(\Omega)/b_o \tag{6.22c}$$

6.4.2.2 Frequency of exceedance data

Unfortunately for load calculations the specification of σ_w and the probability distribution does not provide all the data needed to adequately define load magnitude.

The missing information is the probability of a given peak load being reached in a finite time interval. such as one flight, or the number of peaks exceeding a given value in this time. Frequency of exceedence data is needed for this. This is obtained from a time history by measuring each peak, counting the number of peaks in arbitrarily defined time bands and summating the counts from high to low values of y to give a result similar in form to a load spectrum. A theoretical way of producing similar, but not identical data, is to use Rice's equation:

$$N(y) = N_o \exp\{-0.5(y/\sigma_y)^2\} \tag{6.23a}$$

where

$N(y)$ is the number of crossings of a given level of y, per unit time with positive slope

N_o is the number of crossings of zero per unit time, with positive slope

Use of only positive slope crossings ensures that the number of crossings is approximately the same as the number of peaks. N_o can be thought of as being equivalent to the radius of gyration of the PSD about zero frequency:

$$N_0 = \left[\left\{\int_0^\infty f^2 \Phi(f) df\right\} \Big/ \left\{\int_0^\infty \Phi(f) df\right\}\right]^{1/2} = \{1/(2\pi)\}(\sigma_{dy/dt}/\sigma_y) \tag{6.23b}$$

6.4.2.3 Application of frequency of exceedance data

The application of frequency of exceedance data to gust load analysis involves a sequence of operations:

(1) Establish one. or more, mission (flight) profiles.

(2) Break each mission profile up into convenient segments for analysis. For each segment constant. mean, values of altitude. speed, and aircraft mass are assumed.

(3) For each segment account for the true r.m.s. gust velocity, σ_w, expected to be encountered. In practice this is done by first assuming that each segment is made up of a number of discrete patches of continuous turbulence of different σ_w intensities, and then replacing these by a model which has a continuously varying distribution of σ_w. In order for the stationary Gaussian random process to apply the continuously varying distribution is assumed to have a sufficiently low rate of variation with time, see paragraph 4 below.

(4) Calculate the dynamic response of the aircraft. A, to the gust model. This is defined as:

$$\bar{A} = \sigma_y/\sigma_w \tag{6.24a}$$

$\bar{A}$ is obtained from a dynamic analysis of the aircraft using the equations of motion and Eqns (6.17b) and (6.20c) to give $H(f)$. A single gust PSD, assumed to be independent of σ_w, is used. Inverting Eqn. (6.24a):

$$\sigma_y = A\sigma_w$$

and this may be substituted into Eqn. (6.23b) to give:

$$\begin{aligned} N(y) &= N_o \exp\{-0.5(y/\sigma_y)^2\} \\ &= N_o \exp\{-0.5y/(\bar{A}\sigma_w)^2\} \\ &= N_o \exp\{-0.5(y/\bar{A})^2/\sigma_w^2\} \end{aligned} \tag{6.24b}$$

This now enables the known probability distribution of σ_w to be used, Eqn. (6.24b) being used to superimpose the various turbulence patches described by different values of σ_w:

$$N(y) = \sum_{\sigma_{wi}} t_i N_o \exp\{-0.5(y/\bar{A})^2/\sigma_{wi}^2\} \tag{6.24c}$$

where t_i is the fraction of time that σ_w has the value σ_{wi}.

If now σ_w is considered to vary continuously Eqn. (6.24c) is replaced by:

$$N(y) = \int_{\sigma_w=0}^{\infty} N_o \exp\{-0.5(y/\bar{A})^2/\sigma_w^2\} p(\sigma_w) d\sigma_w \tag{6.24d}$$

where $(p(\sigma_w)d\sigma_w)$ is the probability density referred to time t_i. This implies that the probability that σ_w has a value between σ_w and $(\sigma_w + d\sigma_w)$ is equivalent to the fraction of time that σ_w is between σ_w and $(\sigma_w + d\sigma_w)$.

A convenient mathematical fonn for the probability density is:

$$\begin{aligned} p(\sigma_w) = {} & P_1(2/\pi)^{1/2}(1/b_1)\exp\{-0.5(\sigma_w/b_1)^2\} \\ & + P_2(2/\pi)^{1/2}(1/b_2)\exp\{-0.5(\sigma_w/b_2)^2\} \end{aligned} \tag{6.25}$$

This form of the equation is used only for $\sigma_w > 0$ and the two terms in P_1 and P_2 are such that the integration of $p(\sigma_w)$ with respect to σ_w is unity. P_1, P_2, b_1, and b_2 are constants dependent only upon altitude. P_1 and P_2 are the respective fractions of time in the different probable intensities of turbulence indicated by b_1 and b_2, respectively. P_1 is sometimes considered to cover non-storm turbulence and P_2 storm turbulence. Comparison of each of the two terms, excluding P_1 and P_2, with Eqn. (6.16) shows that b_1 and b_2 are the r.m.s. values of σ_w for the time spent in each of the two turbulence conditions. Figures 6.3

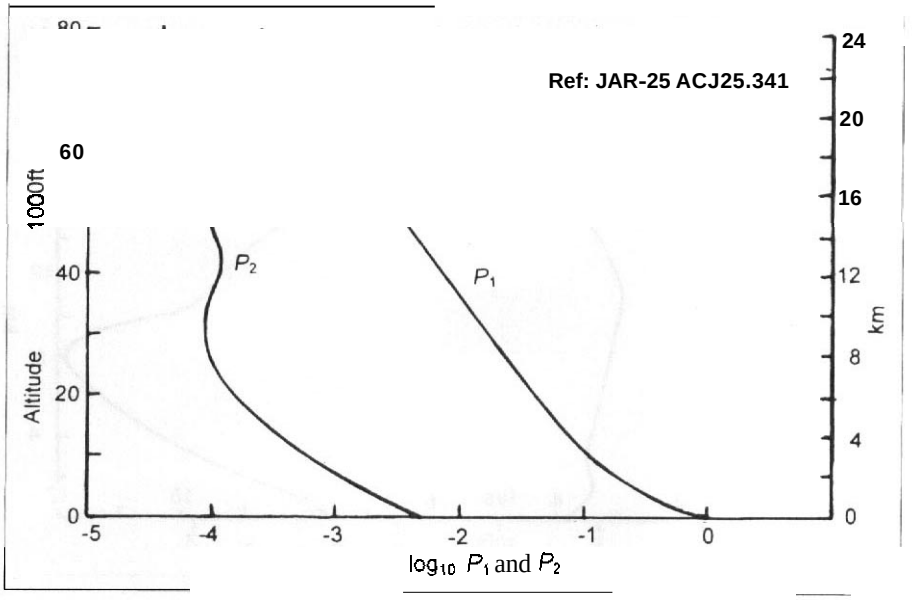

Fig. 6.3 Probability of turbulence intensifies, P_1 and P_2, as functions of altitude

and 6.4 give appropriate values of P_1 and P_2 and b_1 and b_2, respectively, as proposed in JAR-25 ACJ25.341.

Substitution of Eqn. (6.25) into Eqn. (6.24d), see Appendix ***G*** of Hoblit,[1] gives:

$$N(y)/N_o = P_1 \exp\{-(y/\bar{A})/b_1\} + P_2 \exp\{-(y/\bar{A})/b_2\} \tag{6.26}$$

(5) Individual mission segments are now superimposed to obtain the total exceedances:

$$N(y) = \sum t_i N_o [P_1\{-(y/\bar{A})/b_1\} + P_2\{-(y/\bar{A})/b_2\}] \tag{6.27a}$$

where t_i is the fraction of time spent in mission segment, i.

Note that because $\bar{A}$ and N_o differ from one segment to another, the variables which must be used are $N(y)$ rather than $[N(y)/N_o]$ and y rather than $(y/\bar{A})$.

(6) Finally when the exceedance values are to be used to determine limit loads it is necessary to allow for the level flight, Ig, condition and:

$$N(y) = \sum t_i N_o [P_1\{-((y - y_{1-g})/\bar{A})/b_1\} + P_2\{-((y - y_{1-g})/\bar{A})/b_2\}]$$

(6.27b)

where y_{1-g} is the corresponding load (or stress) in the level flight condition.

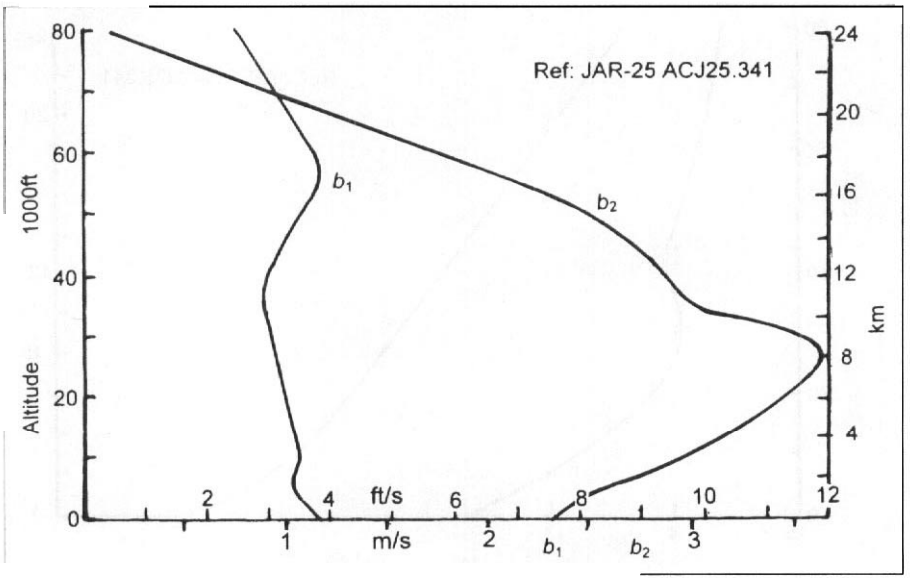

Fig. **6.4** *Turbulence r.m.s.* **intensifies,** b_1 *and* b_2, **as** *functions of altitude*

Equation (6.27b) is the form which is to be found for the mission analysis criterion in the various requirements codes, such as FAR-25, JAR-25 and MIL-A-008861A. Note that $(y/\bar{A})$ always has units of velocity.

6.4.3 Continuous turbulence gust design criteria

6.4.3.1 Design envelope analysis and mission analysis

Chapter 3, Section 3.5.2.3 outlines the alternative design criteria which may be used to interpret the continuous turbulence data into design information.

The first is the 'design envelope analysis' approach. which has some similarities to the derivation of the gust $(n-V)$ diagram but uses different values of gust velocity. These are specified in terms of a datum value, U_{ref} in Section 3.5.2.3 of Chapter 3. In order to apply the method it is necessary to evaluate the response parameter $\bar{A}$.

The second is the 'mission analysis' approach and it is based on the determination of exceedance values, Eqn. (6.27b). In some respects this approach has similarities with a load spectrum as used for fatigue evaluation. Both A and N_o, Eqns (6.23), are required for the application of this method. For a civil transport the limit gust loads are found by selecting a frequency of exceedance of **2** x 10^{-5} per hour of flight.

6.4.3.2 Comparison of alternative design criteria

There is considerable merit in the mission analysis approach because it can give a more realistic indication of the conditions likely to be encountered. However. the method is difficult to apply in that a complete statement of all aircraft operating conditions is needed before any results can he obtained. The back-up design envelope analysis required with this method is necessary to ensure that there is a defined minimum value of strength.

The design envelope method follows a more conventional approach to load derivation and enables anticipated critical cases to he analysed individually. Its use avoids some of the inevitable assumptions needed for the mission analysis method. On the other hand if it is to be used in isolation it is necessary to set the values of U_σ to a sufficiently high value to render any further analysis unnecessary, and this can lead to a tendency to an unduly conservative design.

Therefore, while the mission analysis method is preferable, it may not be expedient to apply it in the early stages of design.

6.4.4 Determination of functions A and N_o

6.4.4.1 General comments

It will be realized by reference to Eqn. (6.27b) and Section 6.4.3.1 that it is necessary to evaluate $\bar{A}$, the response function, before either a design envelope or mission analysis method may he used, and in addition N_o, the number of crossings of zero per unit time, is required for mission analysis evaluation. A is defined by Eqn. (6.24a) and N_o by Eqn. (6.23b), hut in practice both require the formulation and solution of the equations of motion of the aircraft, inclusive of any relevant elastic modes. There is some similarity with flutter analysis except that the rigid body modes of the airframe must also be considered. Such an analysis is extensive and in some circumstances it is useful to employ approximate techniques. **A** usual first assumption is that the airframe is rigid and that elastic effects may be covered by multiplying the derived values by an appropriate dynamic factor. The dynamic factor is often deduced by comparison with a similar type of aircraft for which the value is known, either as the result of a full analysis or by experimental measurement, see Section 6.4.5.

6.4.4.2 Single degree of body freedom – heave only

This is the simplest case and, in reality, has little value except for purposes of comparison with the alleviated sharp-edged analysis. In solving the heave equation of motion as the aircraft moves through the turbulence it is necessary to make allowance for the dynamic development of lift as is discussed in Section 6.2.1. When the heave equation is solved for the case of an aircraft passing into a discrete gust of a (I-cosine)

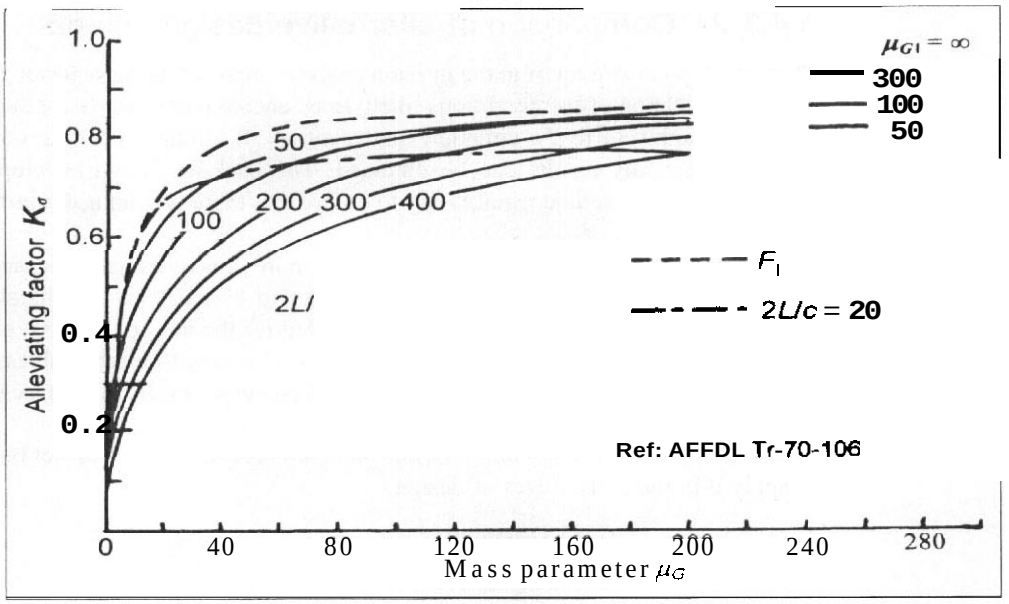

Fig. 6.5 Single degree** of **freedom** response to **gusting

build-up shape, the normal acceleration increment due to a vertical gust closely resembles the alleviated sharp-edged gust as explained in that section.

If the turbulence is defined as continuous using the von-Kármán representation of Eqn. (6.21a) the solution takes the form:

$$\bar{A} = \{\rho S V a_{1WB}/(2mg)\} K_\sigma \tag{6.28}$$

Here the term in { } brackets is effectively ***An*** due to a unit sharp-edged gust, so the coefficient K_σ is directly comparable to the gust alleviating factor, F_1. However, K_σ is also dependent upon the ratio of the scale of turbulence, L, to the chord of the wing. c. The curves of Fig. 6.5 are due to Hubolt.[4] In addition to showing the dependence on $(L/2c)$ the figure shows the comparison between F_1, which is based on $12.5c$, and K_σ.

Curves are also available for N_o for this case, but there is little merit in undertaking a mission analysis using such a simplistic approach to the response of the aircraft.

[4]Hubolt, J. C. Design **manual** for vertical gusts based on power-spectral-density techniques. Air Force Flight Dynamics Laboratory Technical Report. TR-70-106, December 1970.

6.4.4.3 Two degrees of body freedom – heave and pitch (lateral and yaw)

Hoblit,[1] refers to a graphical method for determining $\bar{A}$ derived from an internal Lockheed-California Company report. LR18382. While the method is straightforward to use it does not cover the derivation of N_o required for a mission analysis. NASA Report TN **D-6273** by Peele,[5] presents a semi-graphical method for the evaluation of both $\bar{A}$ and N_o. The procedure starts by identifying the dominant longitudinal and lateral characteristics of the rigid aircraft. The assumptions made in order to simplify the equations of motion are similar to those of Chapter 4, Sections 4.6.3 and 4.7.5. Hence the method applies either to the heave and pitch degrees of freedom or to the sideslip and yawing degrees of freedom. In the sequence below. the first set of terms is for the longitudinal motion and uses the suffix '1'. The second set of terms. for the lateral analysis, uses the suffix '2' to distinguish the values from the longitudinal ones. The format generally follows that presented in Chapter 8 of Hoblit's book.'

(a) Calculate the translational response distance constant, δ:

$$\delta_1 = 2m/(\rho S a_{1WB}) \qquad \delta_2 = 2m/(-\rho S Y_v) \tag{6.29a}$$

(Note that δ has units of length.)

(b) Calculate the translational time response, τ:

$$\tau_1 = \delta_1/V \qquad \tau_2 = \delta_2/V \tag{6.29b}$$

(V is true airspeed and the time response is in seconds.)

(c) Calculate the undamped natural frequency of the motion, f_o:

$$f_{o1} = \rho SV(J_1^2 + R_1^2)^{1/2}/(4\pi m)$$
$$f_{o2} = \rho SV(J_2^2 + R_2^2)^{1/2}/(4\pi m) \tag{6.29c}$$

J_1 (or J_2) and R_1 (or R_2) are the non-dimensional damped frequency and damping coefficient of the appropriate motion as derived in Chapter 4 Eqns (4.82) [or Eqns (4.100)]. Refer also to Section 6.4.4.4

[5] Peele, E.J. A method for estimating some longitudinal and lateral rigid-body responses to continuous turbulence. NASA Report TN D-6273, August 1971.

(d) Calculate the damping ratio, ζ_D:

$$\zeta_{D1} = R_1/(J_1^2 + R_1^2)^{1/2} \qquad \zeta_{D2} = R_2/(J_2^2 + R_2^2)^{1/2} \tag{6.29d}$$

See Section 6.4.4.4.

(e) Calculate the relative gust scale, s:

$$s = 2L/c \tag{6.29e}$$

(f) Calculate the reduced frequency, k:

$$k_{o1} = \pi f_{o1} c/V \qquad k_{o2} = \pi f_{o2} c/V \tag{6.29f}$$

(g) Calculate the product of the relative gust scale and the reduced frequency:

$$\begin{aligned}(sk_o)_1 &= 2\pi f_{o1} L/V = 2\pi f_{o1}\tau_1/(\delta/L)\\ (sk_o)_2 &= 2\pi f_{o2} L/V = 2\pi f_{o2}\tau_2/(\delta_2/L)\end{aligned} \tag{6.29g}$$

(sk_o is non-dimensional.)

(h) Calculate the product of the Kussner attenuation factor, $\tilde{a}$, and the reduced frequency:

$$(\tilde{a}k_o)_1 = (\pi f_o c/V)\tilde{a}_1 \qquad (\tilde{a}k_o)_2 = (\pi f_{o2} c/V)\tilde{a}_2 \tag{6.29h}$$

In the case of the longitudinal motion, $\tilde{a}_1$ is a function of wing geometry and Mach number and may be deduced from Fig. **6.6.** For the lateral motion $\tilde{a}_2$ lies in the range of 0 8 to 1.2 and a value of unity may he assumed in the absence of better information ($\tilde{a}k_o$ is non-dimensional).

(i) Use the values of ζ_D, $\tilde{a}k_o$, and sk_o as relevant to evaluate the values of the non-dimensional response integrals $(\bar{R})_0$, $(\bar{R})_2$, $(\bar{R})_4$, and $(\bar{R})_6$:

$$(\bar{R})_j = (sk_o/\pi)\int_0^\infty \frac{(\bar{\beta})^j \exp(-\tilde{a}k_o\bar{\beta})\{1 + 2.667(1.339sk_o\bar{\beta})^2\}}{\{(1-\bar{\beta})^2 + 4\zeta^2\bar{\beta}^2\}\{1 + (1.339sk_o\bar{\beta})^2\}^{1.8333}}\,d\bar{\beta} \tag{6.29i}$$

where $\bar{\beta}$ is the ratio of a given turbulence frequency, ω, to the undamped natural frequency of the aircraft, ω_1 or ω_2 as relevant, see Section 6.4.4.4. The units

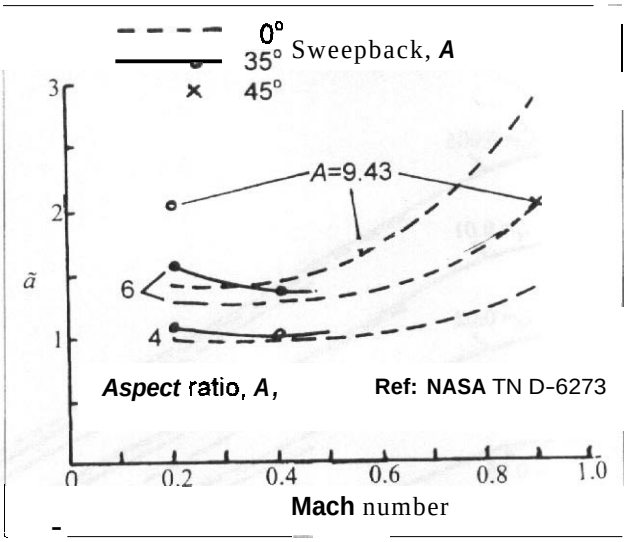

Fig. 6.6 Longitudinal values of the Kussner parameter, $\tilde{a}$

must he consistent, that is non-dimensional or dimensional. j is the appropriate function: 0. 2, 4, or 6.

The integral may be written in numerical form:

$$(\bar{R})_j\{\pi/(sk_o)\} = \sum_{i=1}^{n} \frac{(\bar{\beta}_i)^j \exp(-\tilde{a}k_o\bar{\beta}_i)\{1+2.667(1.339\,sk_o\bar{\beta}_i)^2\}}{\{(1-\bar{\beta}_i)^2+4\zeta^2\bar{\beta}_i^2\}\{1+(1.339\,sk_o\bar{\beta}_i)^2\}^{1.8333}} \tag{6.29j}$$

In practice i must cover the range of $\bar{\beta}$ from zero to a value n where the expression within the summation sign has effectively converged to a constant. The magnitude of the increment in $\bar{\beta}$ must be small enough to ensure an acceptable accuracy of the integration. Convergence is slow for the higher values of j, especially for low values of $\tilde{a}k_o$ and the equation may become ill-conditioned for certain values of the parameters.

NASA Report TN D-6271 contains a series of curves, reproduced in Figs 6.7(a) to (d). These enable the response functions to be read off as a function of the parameters ζ, $\tilde{a}k_o$, and sk_o. However, the range of parameters covered is limited and the curves are difficult to read accurately for values of sk_o less than about 10. The integral $(\bar{R})_6$ is especially difficult

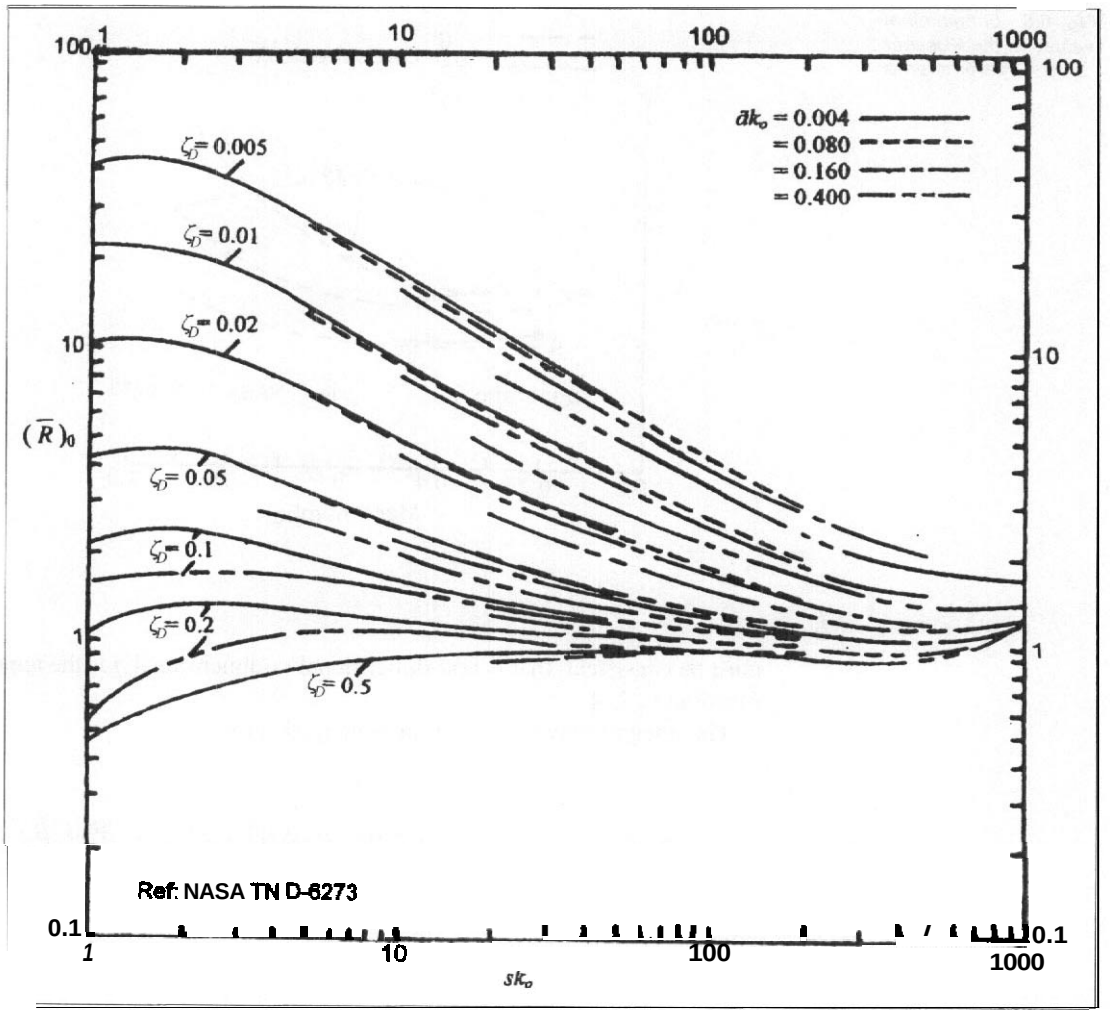

Fig. 6.7 *(a)* ***Response*** *integral* $(\bar{R})_0$ ***as a function of*** ζ_D, sk_a, ***and*** $\bar{a}k_o$

due to slow convergence and the information given in Fig. 6.7(d) was derived from an incomplete inte-gration. It is recommended that the parameter $\bar{a}k_o$ should be interpolated for a given value of sk_a before interpolation of the parameter ζ.

Although Eqns (6.29i) and (6.29j) are expressed in terms of the longitudinal parameters the lateral ones are identical using the appropriate lateral parameters.

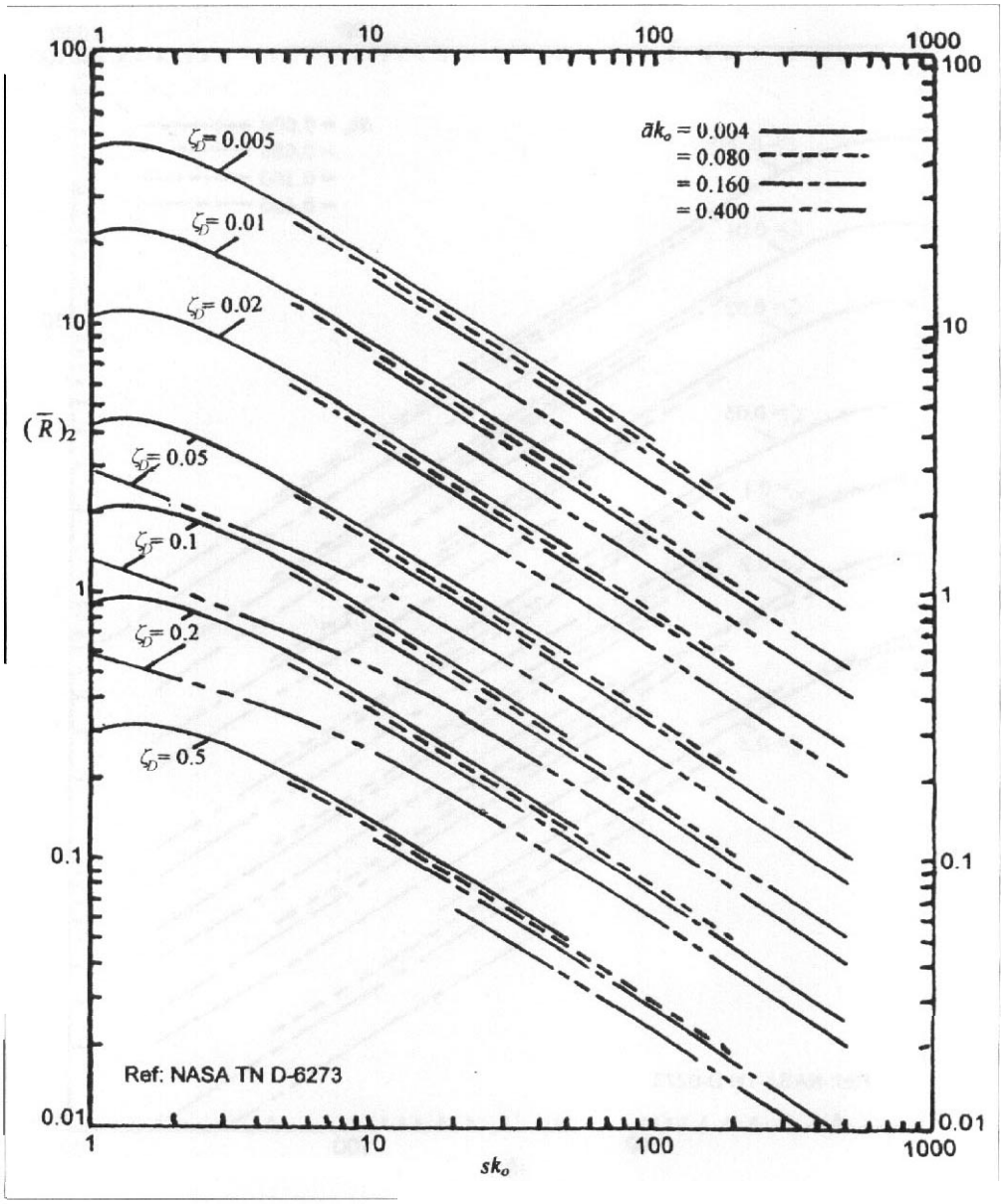

Fig. 6.7 **(b) Response integral (R), as a** *function of* ζ_D, sk_o, **and** $\bar{a}k_o$

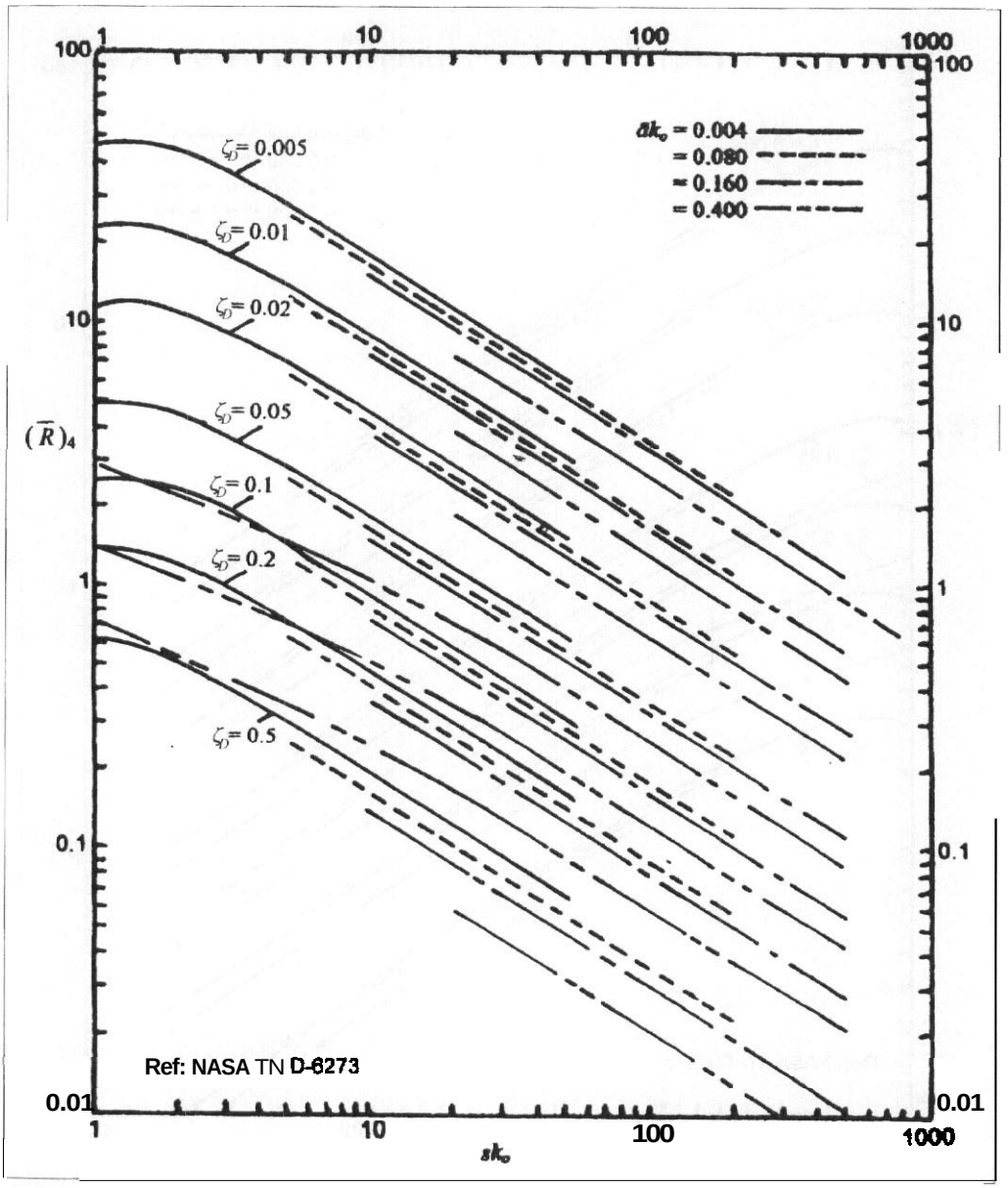

Fig. **6.7** *(c)* ***Response integral*** $(\bar{R})_4$ ***as a*** *function of* ζ_D, sk_o, ***and*** $\bar{a}k_o$

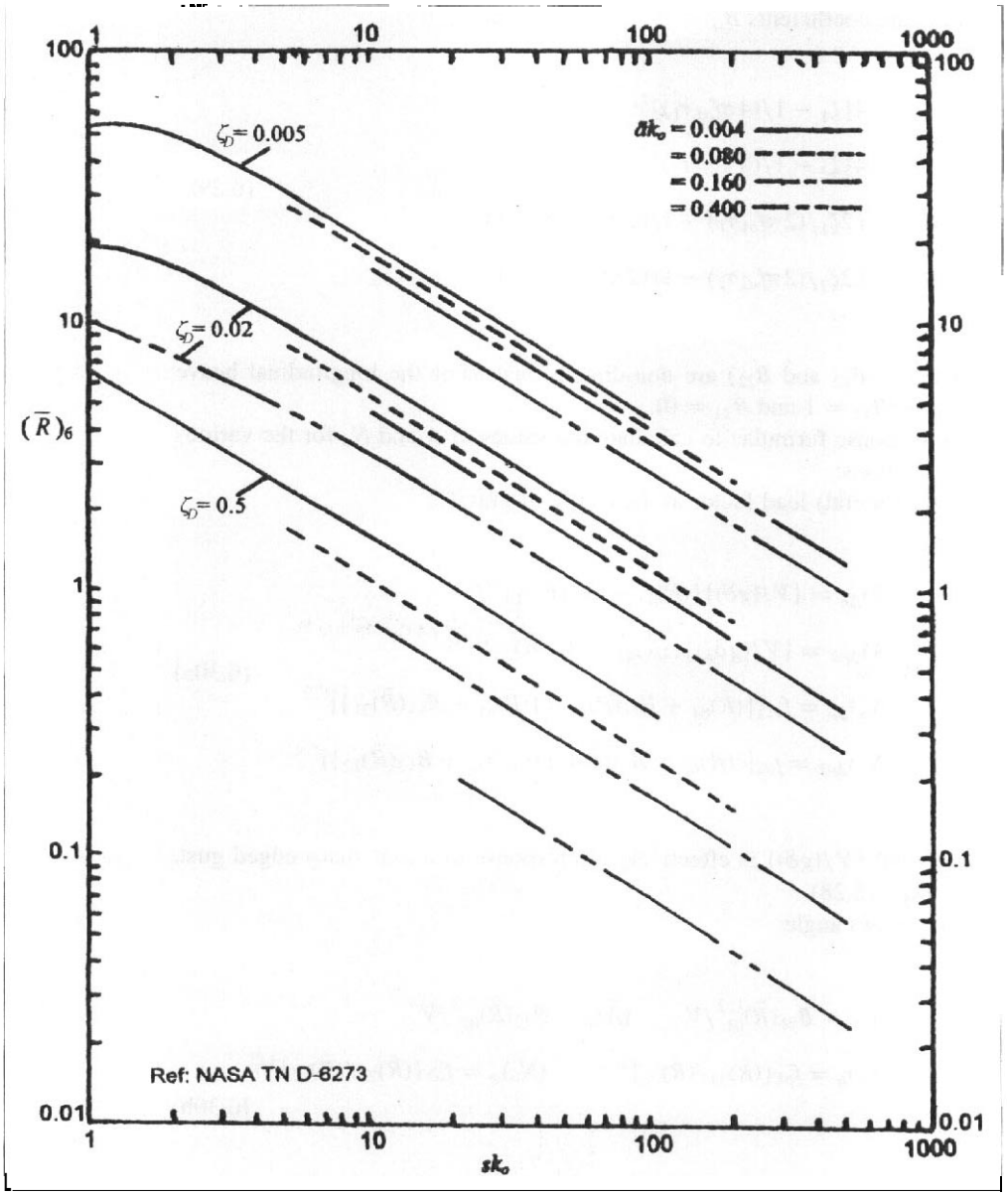

Fig. 6.7 (d) Response integral (R), as a function of ζ_D, sk_o, *and* $\grave{a}k_o$

(j) Calculate the coefficients B_{ij}:

$$
\begin{aligned}
B_{11} &= 4\{\zeta_1 - 1/(4\pi f_{o1}\tau_1)\}^2 \\
B_{12} &= 4\{\zeta_2 - 1/(4\pi f_{o2}\tau_2)\}^2 \\
B_{21} &= \{2\zeta_1/(2\pi f_{o1}\tau_1) - 1/(2\pi f_{o1}\tau_1)^2 - 1\} \\
B_{22} &= \{2\zeta_2/(2\pi f_{o2}\tau_2) - 1/(2\pi f_{o2}\tau_2)^2 - 1\}
\end{aligned}
\qquad (6.29k)
$$

B_{11} and B_{21} (B_{12} and B_{22}) are nun-dimensional, (For the longitudinal heave mode only. $B_{11} = 1$ and $B_{21} = 0$).

(k) Use the response formulae to calculate the values of $\bar{A}$ and N_o for the various output functions:

(i) Heave (lateral) load factor at the centre of gravity:

$$
\begin{aligned}
(\bar{A})_{\Delta n} &= \{V/(g\delta)\}\{(\bar{R})_{41} + B_{11}(\bar{R})_{21}\}^{1/2} \\
(\bar{A})_{\Delta n2} &= \{V/(g\delta_2)\}\{(\bar{R})_{42} + B_{12}(\bar{R})_{22}\}^{1/2} \\
(N_o)_{\Delta n} &= f_{o1}[\{(\bar{R})_{61} + B_{11}(\bar{R})_{41}\}/\{(\bar{R})_{41} + B_{11}(\bar{R})_{21}\}]^{1/2} \\
(N_o)_{\Delta n2} &= f_{o2}[\{(\bar{R})_{62} + B_{12}(\bar{R})_{42}\}/\{(\bar{R})_{42} + B_{12}(\bar{R})_{22}\}]^{1/2}
\end{aligned}
\qquad (6.30a)
$$

Note that $\{V/(g\delta)\}$ is effectively the response to a unit sharp-edged gust, see Eqn. (6.28).

(ii) Pitch (yaw) angle:

$$
\begin{aligned}
(\bar{A})_\theta &= B_{21}(\bar{R})_{01}^{1/2}/V \qquad (\bar{A})_\psi = B_{22}(\bar{R})_{02}^{1/2}/V \\
(N_o)_\theta &= f_{o1}\{(\bar{R})_{21}/(\bar{R})_{01}\}^{1/2} \qquad (N_o)_\psi = f_{o2}\{(\bar{R})_{22}/(\bar{R})_{02}\}^{1/2}
\end{aligned}
\qquad (6.30b)
$$

(iii) Pitch (yaw) rate:

$$
\begin{aligned}
(\bar{A})_{\dot\theta} &= (2\pi f_{o1}/V)B_{21}\{(\bar{R})_{21}\}^{1/2} \qquad (\bar{A})_{\dot\psi} = (2\pi f_{o2}/V)B_{22}\{(\bar{R})_{22}\}^{1/2} \\
(N_o)_{\dot\theta} &= f_{o1}\{(\bar{R})_{41}/(\bar{R})_{21}\}^{1/2} \qquad (N_o)_{\dot\psi} = f_{o2}\{(\bar{R})_{42}/(\bar{R})_{22}\}^{1/2}
\end{aligned}
\qquad (6.30c)
$$

(iv) Pitch (yaw) acceleration:

$$(\bar{A})_{\ddot{\theta}} = \{(2\pi f_{o1})^2/V\}B_{21}(\bar{R})_{41}^{1/2} \qquad (\bar{A})_{\ddot{\psi}} = \{(2\pi f_{o2})^2/V\}B_{22}(\bar{R})_{42}^{1/2}$$

$$(N_o)_{\ddot{\theta}} = f_{o1}\{(\bar{R})_{61}/(\bar{R})_{41}\}^{1/2} \qquad (N_o)_{\ddot{\psi}} = f_{o2}\{(\bar{R})_{62}/(\bar{R})_{42}\}^{1/2} \tag{6.30d}$$

(l) The $\bar{A}$ values may be used to factor U_{σ}, Sections 6.4.2.3 and 6.4.3.1, for the design envelope method. Alternatively the values of N_o may be used with the A values in Eqn. (6.27b) to derive the values of $N(y)$ for the mission analysis approach. For civil transport aircraft the limit strength frequency of exceedance is based on 2×10^{-5} per hour of flight. see Chapter 3. paragraph 3.5.2.3(b). A more severe case with a lower frequency of exceedance may be prescribed for certain military aircraft.

6.4.4.4 Summary of basic aircraft dynamic characteristics

Section 6.4.4.3. paragraphs (c) and (d), requires a knowledge of the basic dynamic characteristics of the aircraft in the relevant modes. Although these are derived in Chapter 4 Eqns (4.82). for the longitudinal, and Eqns (4.100) for the lateral modes. it is useful to restate them here in the form required.

(a) Frequency f_o (f_{o2})

$J_1(J_2)$ is the non-dimensional damped circular frequency
$R_1(R_2)$ is the non-dimensional damping coefficient

The non-dimensional undamped natural frequency:

$$\omega_1 = (J_1^2 + R_1^2)^{1/2} \qquad \omega_2 = (J_2^2 + R_2^2)^{1/2} \tag{6.31a}$$

From Eqn. (4.83a) for the longitudinal mode and Eqn. (4.101b) for the lateral mode, in non-dimensional time:

$$\omega_1 = \{2ma_1cH_m/(\rho Sk_y^2)\}^{1/2}$$
$$\omega_2 = \{(N_v\mu_2 + N_rY_v)(b/k_z)^2\}^{1/2} \tag{6.31b}$$

The dimensional frequency, in real time:

$$f_{o1} = \omega_1 \rho SV/(4\pi m) \qquad f''? = \omega_2 \rho SV/(4\pi m)$$

$$f_{o1} = \{\rho SV/(4\pi m)\}\{2m a_1 c H_m/(\rho S k_y^2)\}^{1/2} \tag{6.31c}$$

$$f_{o2} = \{\rho SV/(4\pi m)\}\{(N_v \mu_2 + N_r Y_v)(b/k_z)^2\}^{1/2}$$

(b) Damping ratio, ζ.

$$\zeta_{D1} = R_1/\omega_1 \qquad \zeta_{D2} = R_2/\omega_2 \tag{6.32a}$$

$$R_1 = a_1/2 + \{a_{1T} S_T/(2S)\}(\ell'_T/k_y)^2(1 - d\varepsilon/d\alpha) - m_\theta)(\ell'_T/k_y)^2 \tag{6.32b}$$

$$R_2 = -0.5[N_r\{b/(2k_z)\}^2 + Y_v]$$

ω_1 and ω_2 are given by Eqns (6.31a)

6.4.5 Structural response dynamic factors

6.4.5.1 Introduction

Without undertaking an analysis, the estimation of the values of dynamic factors is not straightforward unless data are available for a closely comparable type of aircraft. Although dynamic effects may be negligible on a small, relatively rigid, aircraft they are likely to be significant on a large one. The number of structural modes needed to get an accurate result can be large. Hoblit[1] include? some data for the Lockheed 1011 Tristar, and various versions of the earlier Lockheed Constellation. The following comments are made from consideration of this information.

6.4.5.2 Wing

There is considerable variation across the span, particularly in the region of powerplant attachment, and with fuel load condition. At the wing root typical values of dynamic factor are:

(i) shear force, 1.1 for zero fuel to 1.3 with full fuel;
(ii) bending moment, 1.1 for zero fuel to 1.2 with full fuel, although it was as high as 1.55 for one version of the Constellation.

Across the span of the wing the values are almost invariably greater and 1.5–1.6 is possible in a full fuel case.

6.4.5.3 Fuselage

Near to the centre of gravity the dynamic factor for both shear force and bending moment is likely to be no more than 1.1–1.2. However, it may be as high as 4 at the extremities of the fuselage. In the case of the Tristar, the dynamic factor at the rear end was less than 2, probably because of the stiffer fuselage and localized mass consequent upon the rear engine installation.

6.5 Concluding remarks

Continuous turbulence analysis is of considerable importance in the determination of both the limit design loads and the fatigue history of the airframe. The design envelope approach may be used to establish the limit loads, possibly in conjunction with a tuned gust analysis for the longitudinal conditions. In the case of the lateral gust analysis the design envelope method is probably preferable to a discrete or tuned gust calculation. The mission analysis approach is more complex and may he difficult to apply in the initial stages of a design but it is desirable to use it for fatigue calculations and it must be supplemented by the reduced gust intensity design envelope requirement.

The Peele two degree of freedom method described in Section 6.4.4.3 represents an acceptable first approach to continuous turbulence analysis but eventually it should be replaced by a full dynamic analysis including the structural modes.

In view of the importance of continuous turbulence analysis in the lateral case the application of the method is outlined for a particular aircraft in Appendix **A6.**

Appendix A6 Example application of lateral two degree of freedom continuous turbulence analysis

A6.1 Introduction

This example illustrates the derivation of the gust loading on the vertical stabilizer of a large freight aircraft using both the alleviated sharp-edged analysis and continuous turbulence analysis. The latter covers both the design envelope approach and mission analysis although for simplicity it is limited to one typical mission segment.

A6.2 Aircraft and case data

A6.2.1 Basic aircraft data, see also Addenda AD2 and AD3

Mass, m	101 500 kg		
Wing span, b	46 m	Wing area. S	193 m^2
Fin area, S_F	33 m^2	Fin mean chord. c_F	5.78 m
Fin arm, ℓ_F	19 m	Yawing radius of gyration, k_z	8.87 m
Fin lift course slope due to sideslip, a_{1F}	2.2/rad		
Side force due to sideslip, Y_V,	–1.0		

A6.2.2 Design case

Cruise speed, V_C, 217 m/s TAS (145 m/s EAS) at 7.62 km (25 000 ft) altitude where $\rho = 0.549\ \text{kg/m}^3$. For this condition the non-dimensional damped frequency, J_2, is 8.164 and the damping coefficient, R_2, is 1.302.

The turbulence scale factor, L, is taken to be 762 m.

A6.3 Alleviated sharp-edged gust analysis

Substitution of the above values into Eqn. (3.6) gives the lateral mass parameter:

$$\mu_{G2} = \{2m/(\rho S_F c_F a_{1F})\}(k_z/\ell_F)^2$$
$$= \{203\,000/(0.549 \times 33 \times 5.78 \times 2.2)\}(8.87/19)^2 = 192.04$$

and hence the lateral alleviating factor from Eqn. (3.5) is:

$$F_2 = 0.88\mu_{G2}/(5.3 + \mu_{G2}) = (0.88 \times 192.04)/(5.3 + 192.04) = 0.856$$

At 7.62 km altitude and at speed V_C the design gust velocity is 15.2 m/s EAS and therefore the isolated fin load from the alleviated sharp-edged analysis is:

$$\mathscr{L}_{FG} = 0.5 \times 1.225 \times 2.2 \times 33 \times (0.856 \times 15.2/145) = 83\,890\ \text{N}$$

A6.4 Calculation of $\bar{A}$ and N_o for continuous turbulence analysis

This calculation uses the Peele method as outlined in Section 6.4.4.3

$$\delta_2 = 2 \times 101\,500/\{0.549 \times 193 \times (-1.0)\} = 1916\ \text{m}$$
$$\delta_2/L = 1916/762 = 2.514$$
$$\tau_2 = 1916/217 = 8.829$$
$$\omega_2 = (J_2^2 + R_2^2)^{1/2} = (8.164^2 + 1.302^2)^{1/2} = 8.267$$
$$f_{o2} = \rho S V \omega_n/(4\pi m) = 0.549 \times 193 \times 217 \times 8.267/(4\pi \times 101\,500)$$
$$= 0.1489\ \text{Hz}$$
$$\zeta_{D2} = R_2/\omega_2 = 1.302/8.267 = 0.1574$$
$$f_{o2}\tau_2 = 0.147\,91 \times 8.829 = 1.315$$

From paragraph 6.4.4.3(h) for lateral gusts assume that $\tilde{a} = 1.0$:

$$\tilde{a}k_o = \pi f_{o2} c/V = \pi \times 0.1489 \times (193/46)/217 = 0.0091$$
$$sk_o = 2\pi f_{o2}\tau_2/(\delta_2/L) = 2\pi \times (1.315/2.514) = 3.287$$

Since $\tilde{a}k_o$ is low and sk_o is less than 10 in this case it is preferable to calculate the values of $(\bar{R})_{i2}$ using Eqn. (6.29j). However, interpolating from Fig. 6.7 for $sk_o = 3.287$, $\tilde{a}k_o = 0.0091$, and $\zeta_{D2} = 0.1574$ gives:

$$(\bar{R})_{02} = 1.65$$

$$(\bar{R})_{22} = 0.98$$

$$(\bar{R})_{42} = 1.17$$

$$(\bar{R})_{62} = 6.0 \text{ approximately}$$

The first three values have been confirmed by calculation but an incomplete numerical integration for $(\bar{R})_{62}$ suggested that the value should be somewhat higher.

$$B_{12} = 4\{\zeta_2 - 0.25/(\pi f_{o2}\tau_2)\}^2 = 4\{0.1574 - 1/(4\pi \times 1.315)\}^2 = 0.0375$$

$$B_{22} = 2\zeta_2/(2\pi f_{o2}\tau_2) - 1/(2\pi f_{o2}\tau_2)^2 - 1$$

$$= 2 \times 0.1574(2\pi \times 1.315) - 1/(2\pi \times 1.315)^2 - 1 = -0.9766$$

$$(\bar{A})_{\Delta n} = (V/g\delta)\{(\bar{R})_{42} + B_{12}(\bar{R})_{22}\}^{1/2}$$

$$= \{217/(9.81 \times 1916)\}(1.17 + 0.0375 \times 0.98)^{1/2}$$

$$= 0.0115 \times 1.099 = 0.0126 \qquad \text{(A6.1a)}$$

$$(N_o)_{\Delta n} = f_{o2}[\{(\bar{R})_{62} + B_{12}(\bar{R})_{42}\}/\{(\bar{R})_{42} + B_{12}(\bar{R})_{22}\}]^{1/2} = 0.1489[\{6 + 0.0375$$

$$\times 1.17\}/\{1.17 + 0.0375 \times 0.98\}]^{1/2} = 0.1489[6.0439/(1.17$$

$$+ 0.0368)]^{1/2} = 0.1489 \times 2.236 = 0.333 \qquad \text{(A6.1b)}$$

$$(\bar{A})_{\psi} = B_{22}\{(\bar{R})_{02}\}^{1/2}/V = -0.9766 \times 1.65^{1/2}/217 = -0.00578 \qquad \text{(A6.2a)}$$

$$(N_o)_{\psi} = f_{o2}\{(\bar{R})_{22}/(\bar{R})_{02}\}^{1/2} = 0.1489(0.98/1.65)^{1/2} = 0.1147 \qquad \text{(A6.2b)}$$

$$(\bar{A})_{\dot{\psi}} = 2\pi f_{o2}B_{22}\{(\bar{R})_{22}\}^{1/2}/V$$

$$= 2\pi \times 0.1489 \times (-0.9766) \times (0.98)^{1/2}/217 = -0.00417 \qquad \text{(A6.3a)}$$

$$(N_o)_{\dot{\psi}} = f_{o2}\{(\bar{R})_{42}/(\bar{R})_{22}\}^{1/2} = 0.1489(1.17/0.98)^{1/2} = 0.163 \qquad \text{(A6.3b)}$$

$$(\bar{A})_{\ddot{\psi}} = \{(2\pi f_{o2})^2/V\}B_{22}\{(\bar{R})_{42}\}^{1/2} = \{(2\pi \times 0.1489)^2/217\}$$

$$\times (-0.9766)\{1.17\}^{1/2} = -0.004\,03 \times 1.056 = -0.004\,26 \qquad \text{(A6.4a)}$$

$$(N_o)_{\ddot{\psi}} = f_{o2}\{(\bar{R})_{62}/(\bar{R})_{42}\}^{1/2} = 0.1489(6/1.17)^{1/2} = 0.3373 \qquad \text{(A6.4b)}$$

A6.5 Application to design envelope analysis

A6.5.1 Full design envelope condition

Chapter 3, Section 3.5.2.3 states that at altitudes below 9.144 km the datum gust velocity for continuous turbulence analysis, U_σ, is 25.91 m/s TAS. This is the datum gust velocity which applies at the speed V_C. The corresponding design conditions are given by $\bar{A}U_\sigma$. The appropriate aircraft response factors, A, are given by Eqns (A6.1a) to (A6.4a).

(a) Lateral acceleration increment:

$$\Delta n_G = (\bar{A})_{\Delta n} U_\sigma = 0.0126 \times 25.91 = 0.327g$$

(b) Sideslip angle:

$$\psi = (\bar{A})_\psi U_\sigma = -0.005\,78 \times 25.91 = -0.15 \text{ radians}$$

This sideslip angle implies a fin load of:

$$0.5 \times 1.225 \times 145^2 \times 33 \times 2.2 \times 0.15 = 140\,240 \text{ N}$$

This may be compared with the value of 83 890 N derived from the alleviated sharp-edge analysis in Section A6.3 (98 000 N if the alleviating factor is excluded). Part of the difference is explained by the fact that the value of U_σ is 17.33 m/s EAS, or 1.14 times that stated for the discrete analysis. Thus the two degree of freedom calculation suggests a magnification factor of 1.255 rather than an alleviation, presumably due to the over-swing effect. This casts doubt on the validity of the alleviated lateral gust approach.

(c) Yaw rate:

$$\dot{\psi} = (\bar{A})\dot{\psi} U_\sigma = -0.004\,17 \times 25.91 = -0.108 \text{ rad/s}$$

(d) Yaw acceleration:

$$\ddot{\psi} = (\bar{A})\ddot{\psi} U_\sigma = -0.004\,26 \times 25.91 = -0.110 \text{ rad/s}^2$$

A6.5.2 Supplementary Design Envelope Analysis

The supplementary design envelope analysis to be used in conjunction with the mission analysis approach allows the datum gust velocity to be reduced to 18.29 m/s, that is to

70.59 per cent of the value used in the previous section. The corresponding design conditions become:

(a) Lateral acceleration. $0.231g$.
(b) Sideslip angle. -0.106 radians (giving 99 100 N side force).
(c) Yaw rate, -0.076 rad/s.
(d) Yaw acceleration. $-0.078\,\text{rad/s}^2$.

A6.6 Application to mission analysis

The mission analysis technique requires the whole of a typical flight to be broken down into segments and analysed separately, the final result being the summation of the individual segment values. Here only one segment has been analysed, a typical cruise condition, and the values derived will simply be used to illustrate the procedure. It will also be limited to lateral acceleration conditions.

Assume the typical cruise segment applies for the whole of the flight, so that t is unity here. The number of exceedances is given by Eqn. (6.27b) and since this is a lateral case y_{1-g} is zero. For 7.52 km altitude (25 000 ft), Figs 6.3 and 6.4 give:

$P_1 = 0.0255$
$P_2 = 0.000\,112$
$b_1 = 3.13$ ft/s $= 0.954$ m/s
$b_2 = 11.89$ ft/s $= 3.63$ m/s

$$N(y) = N_o[0.0255\exp\{-y/(0.954\bar{A})\} + 0.000\,112\exp\{-y/(3.63\bar{A})\}]$$

The required values of $\bar{A}$ and N_o are to be found in Eqns (A6.1) to (A6.4).

For the lateral acceleration condition $\bar{A}$ and N_o are given by Eqns (A6.1a) and (A6.1b), respectively. The acceleration increments are evaluated as follows.

Assume. initially. that $y = \Delta n = 0.1g$. Then:

$$\begin{aligned} N(\Delta n) &= N(0.1) \\ &= 0.333[0.0255\exp\{-0.1/(0.954\times 0.0126)\} \\ &\quad + 0.000\,112\exp\{-0.1/(3.63\times 0.0126)\}] \\ &= 0.333[0.000\,000\,63 + 0.000\,126] = 0.63\times 10^{-5} \end{aligned}$$

Repeating the calculation for other values of An gives:

$\Delta n(g)$	$N(\Delta n)\times 10^5$
0.10	0.63
0.08	1.74
0.075	2.38
0.0778	2.0

If this one segment is representative of the whole flight then the design value of Δn is that where $N(\Delta n)$ is 2 x 10^{-5}, that is $0.0778g$. Although it is not a true comparison, because it only represents one flight segment, it may be compared with a design envelope value of $0.231g$ which results from the supplementary analysis required to be undertaken in conjunction with a mission analysis, see Section A6.5.2.

A similar analysis applied to the sideslip (yaw) angle indicated that the design value is 0.0285 rad in the cruise condition, which is lower than the 0.15 rad given by the design envelope analysis or the value of 0.106 rad given by the supplementary design envelope analysis.

CHAPTER 7
Ground loads

7.1 Introduction

7.11 General comments

As the title implies ground loads are those occurring when the aircraft is in contact, or makes contact with, the ground. For convenience ground may be taken to include water in the case of seaplanes and flying boats. Contact with the surface is generally described as alighting but more frequently for aircraft based on hard surfaces it is referred to as landing. Although the stipulation? of the various design codes are expressed in terms of the alighting gear units or their components there in an implicit effect upon the airframe as a whole.

For the most part the consideration of ground loading conditions in this chapter will be limited to hard surface, that is, land-based, aircraft.

There are two distinct aspects of the requirements for the design of the landing gear units of aircraft designed to operate from hard surfaces:

(a) The energy absorption characteristics associated with the vertical descent velocity of the aircraft at landing impact. The equivalent for water-borne aircraft is the displacement of the water on impact.

(b) The strength requirements for which loading cases may arise from:

(i) landing impact conditions, these being directly dependent on the energy absorption characteristics of (a) above; the aircraft mass is either the take-off or a reduced. landing. value see Section 7.1.3;

(ii) aircraft movement on the ground. always associated with the maximum or 'ramp' mass, see Section 7.1.3.

7.1.2 Scope of the requirement codes

There is some variation in the different design codes in respect of the coverage of various configurations of alighting gear:

(a) The European JAR-23, Light Aircraft. and JAR-25, Transport Aircraft, codes cover both nose-wheel and tail-wheel layouts and there are some provisions for water-borne aircraft. The corresponding United States FAR-23 and FAR-25 have the same coverage.

(b) The United Kingdom military requirements, Def.Stan.00-970, only make provision for nose-wheel, tricycle, landing gear arrangements.

(c) The United States military code MIL-A-8862. supplemented by MIL-L-87139, covers both nose- and tail-wheel configurations and also deals with ski landing gear. MIL-A-8862 is useful in that it includes a method for the analysis of the loads occumng during a high-drag landing.

None of the requirements specify design conditions for unusual wheel configurations, such as out-riggers on bicycle layouts, although flying boat wing tip floats are covered under (a) above.

7.1.3 Aircraft design mass conditions

It is necessary to distinguish between three separate mass conditions for landing gear design:

(a) Ramp mass, m_T. This is the maximum mass of the aircraft when fully loaded and before it begins to move to the take-off point.

(b) Take-off mass. This is often the same as the ramp mass, but may be somewhat less for a long-range aircraft. It allows for the fuel used in moving to the take-off point, and is primarily a performance consideration.

(c) Landing mass, m_L. This can allow for the fuel used during the shortest design flight and any stores disposed of. In the case of short-range aircraft it may be specified as the take-off value, but it can he significantly less for a combat type or less than the ramp mass for a long-range transport.

7.1.4 Aircraft attitude in the longitudinal plane

The distribution of energy between the nose or tail and main landing gear units depends upon the attitude of the aircraft at touchdown. Although there are detail differences between the various design codes the most important consideration is the sequence of contact of the main and auxiliary wheel units with the ground. In a so-called 'two-point' landing the main gear wheels contact the ground first with the auxiliary wheels well clear. This implies a tail-down attitude for a nose-wheel layout and a more or less horizontal one for a tail-wheel arrangement. On the other hand in a 'three point' landing all the wheels contact the ground at the same time and the attitude conditions of the aircraft are reversed relative to the two-point case. This is illustrated in Fig. 7.1.

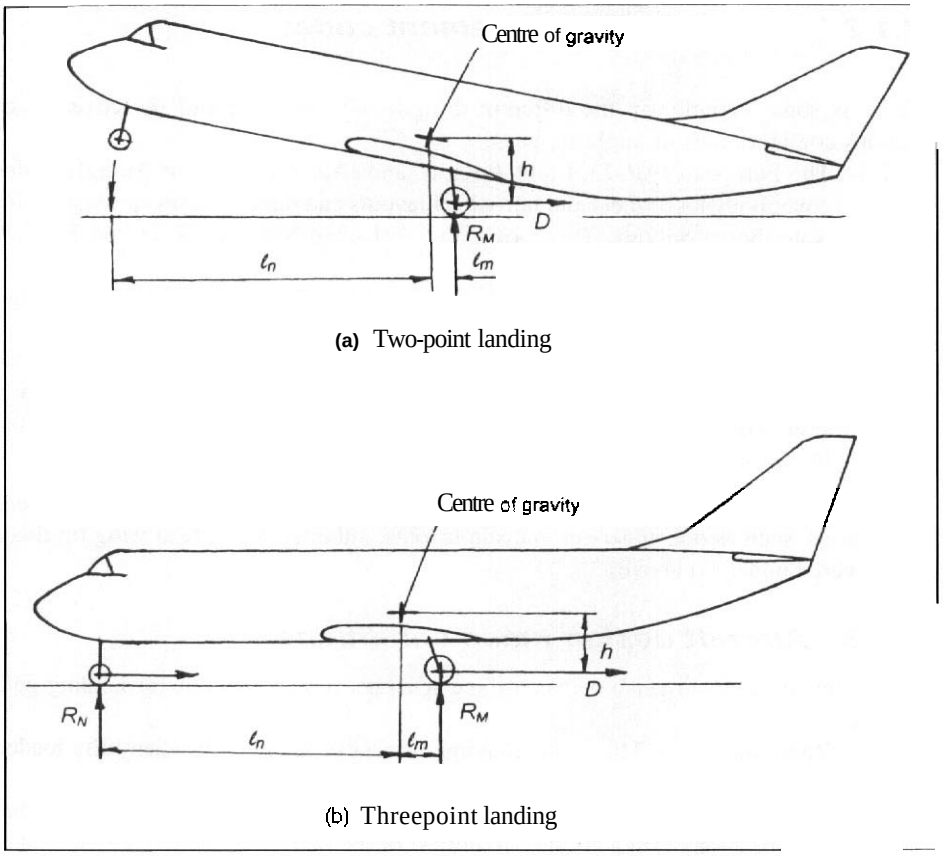

Fig. 7.7 *Aircraft* ***landing attitudes***

Def.Stan.00-970 distinguishes between aircraft that flare at touchdown and those that do not. The former implies that only the main gear units may be available to absorb the energy at touchdown, the two-point condition. In the latter case the nose gear can share in the process, the three-point case. For either case the attitude of the aircraft has to be varied over a range of $\pm$ 7" from the datum condition except where the higher angle limit is unobtainable because of overall lift or control reasons.

JAR-23 and JAR-25 specify a tail-down, two-point landing and a level, three-point landing for conventional tricycle landing gear layouts, as described above. When a tail-wheel layout is used, rather than the conventional nose gear arrangement, the two- and three-point conditions are reversed. That is. the flared landing gives a three-point case and a level landing a two-point case. Regardless of how many main gear units are actually employed, an attitude where only the main gear units initially touch down is always referred to as a two-point landing. Likewise a three-point landing describes the case when the nose, or tail, gear units touch down simultaneously with the main units.

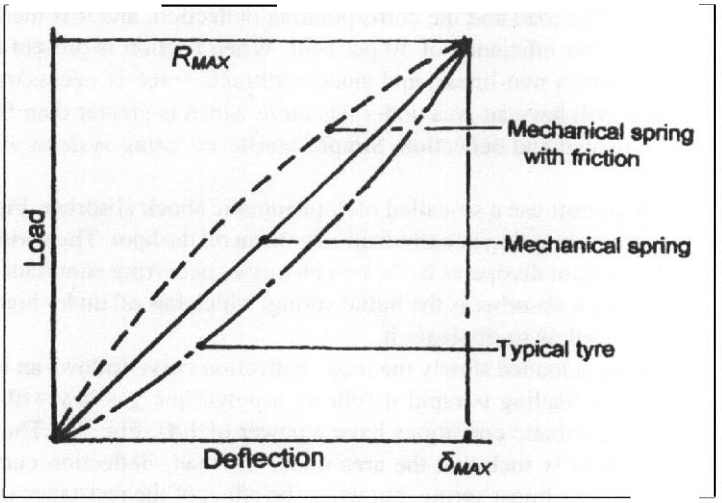

Fig. 7.2 Simple spring load–deflection characteristics

7.2 Summary of shock absorber design characteristics

7.2.1 Introduction

The loads developed when an aircraft lands are dependent upon the shock absorbing characteristics of the landing gear and the eventual dissipation of the vertical energy of touchdown. It is necessary, therefore. to include a brief discussion of this topic. A more complete coverage of landing gear design characteristics may be found in Addendum 1 of *Aircraft Conceptual Design Synthesis*.[1]

7.2.2 Shock absorber performance and efficiency

In a typical telescopic arrangement the shock absorber is attached to the wheel axle, or bogie unit, at its lower end and to the airframe at its upper end. Alternately a lever system can be used. The performance of a shock absorber is conveniently defined by a load–deflection diagram, such as is illustrated in Figs 7.2 to 7.4. The characteristics of such a unit depends upon:

(a) The type of shock absorber.
(b) The impact velocity and equivalent force due to the mass supported by it.
(c) The rate of closure, which is related to (b).

A simple mechanical spring having no associated friction, Fig. 7.2, has a linear load–deflection curve regardless of the rate of load application. The area under the line is half

[1]Howe, D. *Aircraft Conceptual Design Synthesis*, Professional Engineering Publications Ltd, 2000.

of the product of a given load and the corresponding deflection, and it is therefore said to have a shock absorber efficiency of 50 per cent. When friction is present the load–deflection curve becomes non-linear, and since additional force is necessary to overcome the friction, it will have an area under the curve which is greater than 50 per cent of the product of the load and deflection. Simple cantilever spring systems are used on some light aircraft.

The majority of aircraft use a so-called oleo-pneumatic shock absorber, Figs 7.3 and 7.4. This consists of an air spring in combination with an oil dashpot. The spring absorbs the energy and the dashpot dissipates it, the two processes occurring simultaneously. An alternative type of shock absorber is the liquid spring, which has oil under high pressure to absorb energy as well as to dissipate it.

When an air spring is loaded slowly the load–deflection curve follows an isothermal gas law, but when the loading is rapid it follows a polytropic gas law with a typical power of about 1.3 (adiabatic conditions have a power of 1.4). Fig. 7.3. The nature of either of these two laws is such that the area under the load–deflection curve is well below the 50 per cent of a linear spring, but when the effect of the resistance of the oil is included the characteristic shape changes significantly. Under rapid loading conditions. typical of a landing, it is possible to arrange for the initial rise of the load–deflection curve to be very steep, subsequently levelling out to give an area under the curve approaching the product of the load and deflection at higher values of deflection. A typical value of the area under the curve, or efficiency, is 85 per cent, but it is generally a function of the deflection in a given case. The liquid spring is somewhat less efficient, achieving a typical maximum of 80 per cent.

One disadvantage of a high efficiency of energy absorption is the implied high loads associated with small deflections, that is, small energy absorption requirements. This is

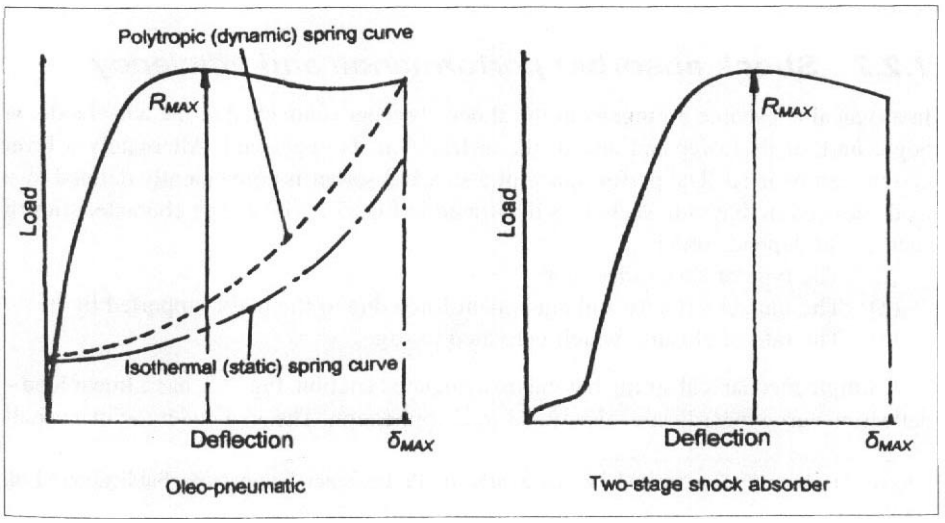

Fig. 7.3 *Oleo-pneumatic* ***shock absorber*** *characteristics*

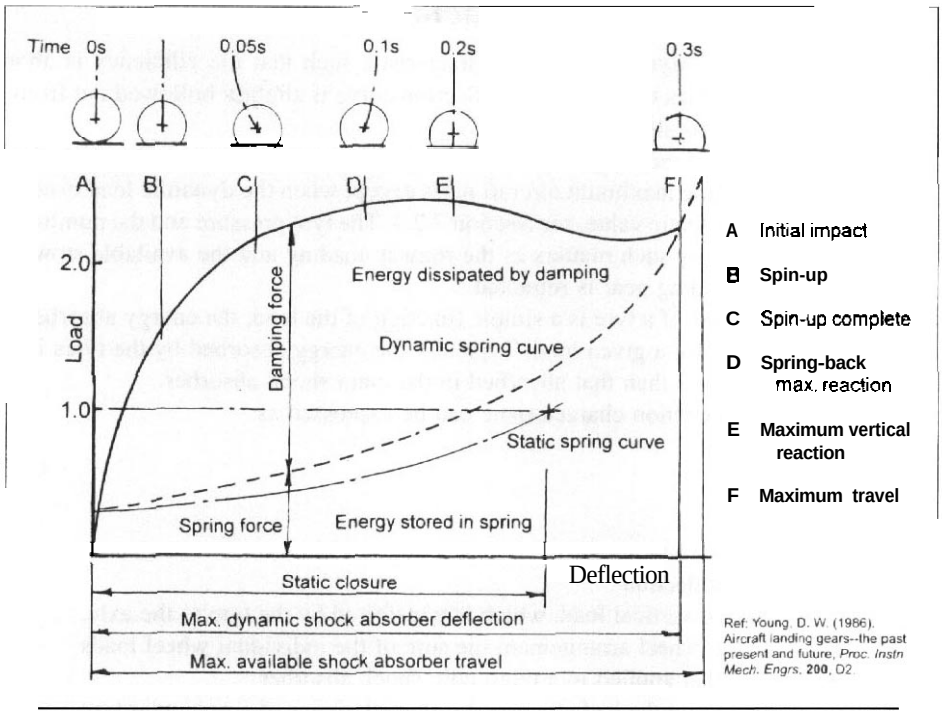

Fig. 7.4 *Oleo-pneumatic* ***shock absorber — high-drag landing sequence***

clearly disadvantageous from the fatigue aspect and may be overcome by using a two-stage shock absorber characteristic as shown in Fig. 7.3. The advantage of the 'soft' initial characteristic is that it results in a low load for small energy requirements. such as during taxiing. The penalty is a lower overall efficiency, perhaps only 60 per cent at the design energy absorption case. The implication of this is the need for a greater deflection, that is. a longer stroke.

Since the actual energy absorption requirement is vertical in the sense of aircraft centre of gravity movement, it is convenient to describe the characteristic of an aircraft landing shock absorber in terms of vertical load and vertical axle travel. The actual shock absorber characteristic may be modified by its inclination to the vertical, or by being incorporated in a lever mechanism.

In passing it is worth noting that an idealized shock absorber characteristic described by:

$$R = k_S \delta_S^{1/4} \tag{7.1}$$

always gives an 80 per cent efficiency. Here R is the vertical load, see also Section 7.2.3, δ_S is the vertical axle travel, and k_S is some constant.

7.2.3 Pneumatic tyre characteristics

Tyres have static and dynamic spring characteristic such that the efficiency is about 47 per cent. This implies that the load–deflection curve is slightly hollowed out from a linear characteristic, as shown in Fig. 7.2.

In the design of a landing gear unit the tyre size is determined by the static load carrying capacity at the maximum aircraft mass except when the dynamic load exceeds about three times the static value, see Section 7.2.4. The tyre pressure and the number of tyres are determined by such matters as the runway loading and the available stowage volume when the landing gear is retracted.

Since the deflection of a tyre is a simple function of the load, the energy absorbed is uniquely established for a given load. Typically the energy absorbed by the tyres is an order of magnitude less than that absorbed in the main shock absorber.

The tyre load–deflection characteristic can be expressed as:

$$R = k_T \delta_T^{1.1} \tag{7.2}$$

where

δ_T is the tyre deflection

R is the applied vertical load. which is transferred by the tyre to the axle. In any given wheel arrangement the sum of the individual wheel loads is equal to that applied to a telescopic shock absorber

k_T is some constant dependent upon the characteristics of a particular tyre

7.2.4 Shock absorber reaction factor and stroke

It is clear that for a given energy absorption requirement and shock absorber efficiency it is possible to choose an appropriate combination of maximum load and deflection. A high load corresponds to a small deflection and vice versa. It is convenient to define the maximum dynamic load non-dimensionally by dividing it by the equivalent load applied under static conditions. This ratio is known as the shock absorber reaction factor, **A**, and is equal to the vertical deceleration factor of the centre of gravity of the aircraft. Since the actual load is directly proportional to A in a given case, the choice of **A** is a fundamentally important design decision.

Generally speaking a short undercarriage is the lightest and hence within the limitations of ground geometry the closure, or stroke, should be made as small as possible to minimize the overall length of the unit. However. a short stroke will imply a relatively high value of the reaction factor, A, and since this implies also a higher load any mass saved by the use of a short unit may be more than offset by a heavier airframe construction and, in particular, the effects of fatigue. For the majority of aircraft the value of **A** corresponding to the limit vertical velocity varies between 1.3 and 2.5 with a definite tendency to lower values on aircraft designed with low normal flight manoeuvre factors and long life. A fighter-type aircraft has a high-strength airframe and can tolerate a value of **A** of 3.0 or more without undue penalty. Naval aircraft have to meet increased

energy absorption requirements due to deck motion. This is associated with severe size restrictions and reaction factors of the order of 4 or more are common in these circumstances. Strokes are frequently in the range of 0.25–0.5 m. They are rarely less than 0.18 m, hut may exceed 0.8 m.

Defining m_L as the design landing mass and m_T as the maximum, ramp, mass, when the value of the parameter $(\lambda m_L/m_T)$ exceeds about 3, the tyre size is determined by the dynamic landing condition. In practice this situation arises only on some high-performance military aircraft.

7.2.5 The energy absorption equation

The energy to he absorbed on impact is the sum of the kinetic energy due to the vertical velocity at the instant of impact and the potential energy. The potential energy is equal to the product of the weight and the vertical displacement of the unit occurring over the period of time from the instant of impact to that when the shock absorber and tyre have reached their maximum deflections. The latter of these is dependent upon the degree to which the lift on the wing of the aircraft off-sets the gravitational force. Although there are some exceptions many of the military and civil requirements allow the assumption that the weight of the aircraft is balanced by the lift throughout the touchdown and in this case only the vertical kinetic energy has to he considered.

For the landing mass condition at a vertical velocity of V_v, the total vertical kinetic energy is simply:

$$0.5m_L V_v^2 + m_L g\delta(1-\kappa)$$

where

δ is the vertical deflection of the centre of gravity in the initial impact
κ is the ratio of the lift to the weight at impact

The absorption of this energy will he shared between all the landing gear units touching down at the same time. The datum case is a two-point landing and the energy is assumed to be equally absorbed by each main unit. When there are only two main gears, as is usual, the energy absorbed by each main gear unit is:

$$0.25m_L V_v^2 + 0.5m_L g\delta(1-\kappa)$$

At the landing mass of the aircraft this corresponds to a vertical static load on that unit of $0.5m_L g$.

The reaction factor, A, is the ratio of the maximum vertical reaction in a given case to the static load on that unit in that case. If A is known. the maximum vertical landing load. $(R_M)_{MAXL}$, on one unit can be expressed in terms of the static condition:

$$(R_M)_{MAXL} = 0.5\lambda m_L g \tag{7.3}$$

The energy absorbed during the impact is the sum of the product of the shock absorber efficiency, its maximum load and maximum deflection, and the efficiency of the tyre, or tyre assembly, its maximum load and maximum deflection. Defining the shock absorber characteristics relative to the vertical, the load in both components is identical and the total energy absorbed is:

$$0.5\lambda m_L g(0.47\delta_{MT} + \eta_{MS}\delta_{MS})$$

where

δ_{MT}, δ_{MS}	are the maximum vertical deflections of the tyre and shock strut (effectively axle movement), respectively. Suffixes 'MT' and 'MS' refer to main tyre and shock absorber, respectively
η_{MS}	is the effective vertical efficiency of the shock absorber, defined in Section 7.2.2
0.47	is a typical tyre efficiency, defined in Section 7.2.3.

Equating the kinetic energy to the absorbed energy and noting that δ is equal to the sum of δ_{MT} and δ_{MS} gives:

$$0.25m_L V_v^2 + 0.5m_L g(\delta_{MT} + \delta_{MS})(1 - \kappa) = 0.5\lambda m_L g(0.47\delta_{MT} + \eta_{MS}\delta_{MS})$$

$$V_v^2 + 2g(1 - \kappa)(\delta_{MT} + \delta_{MS}) = 2\lambda g(0.47\delta_{MT} + \eta_{MS}\delta_{MS})$$

and

$$\lambda = \{V_v^2 + 2g(1 - \kappa)(\delta_{MT} + \delta_{MS})\}/\{2g(0.47\delta_{MT} + \eta_{MS}\delta_{MS})\} \quad (7.4a)$$

When the lift is equal to the weight, $\kappa = 1$, and Eqn. (7.4a) becomes:

$$\lambda = V_v^2/\{2g(0.47\delta_{MT} + \eta_{MS}\delta_{MS})\} \quad (7.4b)$$

From Eqn. (7.3) the maximum vertical load during impact is:

$$(R_M)_{MAXL} = m_L\{V_v^2 + 2g(1 - \kappa)(\delta_{MT} + \delta_{MS})\}/\{4(0.47\delta_{MT} + \eta_{MS}\delta_{MS})\} \quad (7.5a)$$

and when the lift is equal to the weight:

$$(R_M)_{MAXL} = m_L V_v^2/\{4(0.47\delta_{MT} + \eta_{MS}\delta_{MS})\} \quad (7.5b)$$

In some cases the reaction factor, A, may be assumed or otherwise fixed and it is required to establish the shock absorber stroke, δ_{MS}, for given tyre characteristics and an assumed shock absorber efficiency, η_{MS}.

Rearranging Eqn. (7.4a) gives:

$$\delta_{MS} = [V_v^2/(2\lambda g) - \{0.47 - (1 - \kappa)/\lambda\}\delta_{MT}]/[\eta_{MS} - (1 - \kappa)/\lambda] \quad (7.6a)$$

and for the case when the lift is equal to the weight:

$$\delta_{MS} = [V_v^2/(2\lambda g) - 0.47\delta_{MT}]/\eta_{MS} \quad (7.6b)$$

δ_{MT} is known in this case, since the corresponding maximum reaction is known. and η_{MS} will depend upon the shock absorber characteristics as described in Section 7.2.2.

7.2.6 Energy dissipation

As much as possible of the energy should be dissipated during the initial compression stroke. The United Kingdom military requirements. Def.Stan.00-970, specify that at least 67 per cent of the energy must be dissipated in the initial closure and the rest dealt with on the first rebound.

7.3 Energy absorption requirements

7.3.1 Introduction

The energy absorption requirements are defined in terms of the vertical velocity of the aircraft at impact and the extent to which the weight of the aircraft is balanced by the lift. In general the aircraft may be accelerating vertically at the instant the wheels contact the ground. As stated in Section 7.2.5 the acceleration depends upon the value of the lift relative to the weight and is clearly zero when the two are equal. While the majority of requirements specify this condition. there are exceptions. The main ones are the case of a naval aircraft intended to be stalled onto the deck of an aircraft carrier so that the lift is assumed to he zero, and light aircraft where JAR-23.473(e) specifies that the lift must not exceed two-thirds of the weight.

7.3.2 Landing vertical velocity requirements

7.3.2.1 General remarks

In general there are three conditions to be considered. These cover both limit and ultimate energy conditions as well as landing at the take-off and the design landing masses. The values of the vertical descent velocity specified by the requirement handbooks are not intended to represent the actual conditions encountered in normal operations. It has been found that in most landings the vertical velocity is less than

one-third of the specified value and, with the exception of naval operations, two-thirds is rarely exceeded. They do, however, result in a satisfactory design of the landing gear.

Neither the shock absorber nor the tyre must reach maximum deflection under the limit load or maximum reaction. One of the two may reach maximum deflection in the ultimate energy case.

7.3.2.2 Limit energy condition at the design landing mass, m_L

This is the basic case and the requirement codes quote a design vertical velocity, V_v, to be applied when the aircraft touches down at the design landing mass:

(a) United Kingdom military aircraft, Def.Stan.00-970 (fixed wing):

$V_v = 3.66$ m/s (12 ft/s) for combat aircraft
$= 3.96$ m/s (13 ft/s) for trainers

Higher values may be required for ship-home aircraft to allow for the motion of the ship as well as for the possibility that the landing is being made without a flaring of the descent path, when zero lift may be assumed

(b) United States military aircraft. MIL-A-8862:

$V_v = 3.05$ m/s (10 ft/s) generally but
$= 3.96$ m/s (13 ft/s) for land-based trainers

(c) JAR-25/FAR-25 (Civil transport aircraft):

$V_v = 3.05$ m/s (10 ft/s)

(d) JAR-23 (Light aircraft):

$$V_v = 4.4(mg/S)^{1/4} \text{ ft/s} \quad \text{hut} \quad 7 \text{ ft/s} < V_v < 10 \text{ ft/s}$$

where (mg/S) is the wing loading in lb/ft^2 and the wing lift is taken to be no more than two-thirds of the weight.

For light aircraft the design landing mass is often the same as the take-off mass but JAR-23.473(a) to (c) allows for a lower value in some cases.

7.3.2.3 Condition at the take-off mass, m_T

A reduced vertical velocity is specified in association with the take-off mass. Nevertheless it may result in a higher energy absorption requirement and design load when the landing mass is significantly less than the take-off value.

(a) United Kingdom military, Def. Stan.00-970:

$0.8V_v$ in all cases

(b) United State military aircraft, MIL-8862:

1.83 m/s (6 ft/s) generally, but 2.6 m/s (8.53 ft/s) for land-based trainers

(c) JAR-25:

1.83 m/s (6 ft/s)

(d) JAR-23: see Section 7.3.2.2

7.3.2.4 Ultimate energy condition

In many design codes the application of an ultimate vertical velocity of $1.2V_v$ is required at the landing mass condition. This will result in a requirement for a greater stroke than needed to meet the limit landing energy absorption requirement. It may, or may not, result in a higher shock absorber maximum load depending on the shape of the load–defection curve. However, since it is an ultimate case the load is factnred by unity, unlike the limit case where the usual proof and ultimate factors apply, see Chapter 1, Section 1.3.4. It is very unlikely that this case will result in a critical load.

There is no ultimate energy case as such in the United States military requirements. MIL-A-8862, but there is an overload landing case. This is at a mass of 1.15 times the design landing condition associated with a vertical velocity of 93 per cent of the corresponding design value.

No specific ultimate energy conditions are given for light aircraft in JAR-23.473 but it is stated that the limit ground reaction factor should not be less than 2.

7.3.3 Distribution of the vertical energy into the landing gear units

7.3.3.1 General

In the basic two-point landing case covered in Section 7.2.5 all the vertical energy at touchdown is absorbed in the main landing gear units. As a consequence of this the maximum vertical load during the impact is $(R_M)_{MAXL}$ as given by Eqns (7.3) and (7.5). There is a corresponding load at the take-off condition which may, or may not, be higher. The greater of these vertical loads are used as datum values in specifying the overall loading on the main landing gear units in a landing. It is, of course, also necessary to determine the energy absorbed and the corresponding loads on the auxiliary landing gear unit, usually the nose gear. There are two conditions associated with the landing of the aircraft, see Section 7.1.4:

(a) The two-point landing where there is no initial load on the nose gear. However, the main gear loads are almost inevitably located aft of the centre of gravity of the aircraft and there is also a fore and aft drag load at the ground. The consequence is a nose-down pitching moment. This results in the eventual impact of the nose-wheel so that the unit absorbs some of the rotational energy and a vertical load is developed; see Fig. 7.1(a).

(b) The three-point landing condition where the nose-%,heelcontacts the ground at the same time as the main wheels and the nose gear unit absorbs a share of the vertical energy. see Fig. 7.1(b).

In some cases it is necessary to carry out a full dynamic analysis of the landing behaviour in order to deduce an acceptable loading system. This may he so with a naval aircraft or when the configuration is unusual, for example a long slender aircraft having a high ratio of pitch to roll inertia. In practice it is desirahle to undertake such an analysis for any advanced subsonic or supersonic design. Appendix A7 outlines a method of approaching this analysis.

However, in many cases, especially for initial design calculation, it is adequate to use a quasi-static analysis and such an approach may be found in the United Kingdom military requirements, Def.Stan.00-970. The analysis is outlined in the following sections.

7.3.3.2 Loads in a two point landing case

This applies to a conventional aircraft where a tail-down landing is the usual situation.

The main landing gear unit load for the case when the lift is equal to the weight is derived from Eqn. (7.5b) as:

$$(R_M)_{MAXL} = (R_M)_L = \frac{m_L V_v^2}{4\eta_M \delta_M} \tag{7.7a}$$

where

η_M is the overall tyre and shock absorber efficiency

δ_M is the corresponding overall vertical deflection $\eta_M \delta_M = (0.47\delta_{MT} + \eta_{MS}\delta_{MS})$

where suffixes 'MT' and 'MS' refer to the main-wheel tyre and shock ahsorber, respectively.

As the aircraft impacts the ground the main wheels must rapidly 'spin-up' tn a rotational speed equivalent to rolling at the forward velocity of the aircraft. To achieve this a horizontal friction force, D, is developed at the ground and, coupled with the location of the vertical reaction force aft of the centre of gravity, results in the strong tendency to nose-down pitching, as shown in Fig. 7.1(a). If the ground friction coefficient is μ, so

that $D = \mu(R_M)_L$, a quasi-static analysis gives the nose-wheel load as:

$$(R_N)_L = \frac{2(R_M)_L\{\ell_m + \mu h\}}{[(\ell_m + \ell_n)(\ell_n - \mu h)]^{1/2}} \tag{7.7b}$$

where

ℓ_m and ℓ_n	are the horizontal distances of the main and nose ground contact points either side of centre of gravity of the aircraft, respectively
h	is the height of the centre of gravity above the axle of the main-wheel
μ	is quoted as 0.4 for military aircraft, by reference to landing Load Case (1c), (see Section 7.4.2 and Table 7.1) and 0.25 for transport aircraft. Load Case (1a)

The numerator in Eqn. (7.7b) is effectively the moment of the main-wheel vertical and corresponding horizontal loads about the centre of gravity. The denominator is effectively a mean value of nose unit moment arm about the main wheels making allowance for the drag force on the nose-wheel.

7.3.3.3 Loads in a three-point landing case

This applies to a conventional nose gear layout aircraft where a nominally horizontal landing is usual.

The following equations are based on the assumption that the shock absorber characteristics of the nose landing gear unit are such as to minimize the pitching during the absorption of the vertical energy. The reaction factor and stroke of the nose gear unit are usually determined by this condition but special considerations, such as the assisted take-off of **a** naval aircraft, may override this case.

The vertical reference load on each of two main landing gear units is:

$$(R_M)_L = \frac{m_L V_v^2(\ell_n - \mu h)}{\{4\eta_M \delta_M(\ell_m + \ell_n)\}} \tag{7.8a}$$

see Eqn. (7.7a) for the notation. This equation covers the two-point case and Eqn. (7.8a) may be compared with it.

The corresponding vertical nose landing gear load is:

$$(R_N)_L = \frac{m_L V_v^2(\ell_m + \mu h)}{\{2\eta_N \delta_N(\ell_m + \ell_n)\}} \tag{7.8b}$$

where suffixes 'NT' and '*NS*' refer to the nose-wheel tyre and shock absorber, respectively: $\eta_N\delta_N = \{0.47\delta_{NT} + \eta_{NS}\delta_{NS}\}$.

Unless the operation of the aircraft and its layout clearly preclude one of the above solutions, the greatest values of $(R_M)_L$ and $(R_N)_L$ from Eqns (7.7) and (7.8) should be used as the datum values for design limit loads during a landing.

7.4 Load cases resulting from landing conditions

7.4.1 Introduction

Although there are some differences between the military and civil transport requirement codes the categories of the primary loading cases are similar. In the main they apply only to operation from smooth runways. Where appropriate special conditions are prescribed for operation on uneven runway surfaces. see Section 7.6

The cases are summarized in Table 7.1 and. unless otherwise stated, apply to both nose- and main-wheel units.

The values to be used for the datum vertical load, R, are the maximum of those derived from Eqns (7.7a) and (7.8a) for main-wheel and Eqns (7.7b) and (7.8b) for nose-wheel units, respectively. All the conditions of Section 7.3.2 have to be covered. The values of R appropriate to the limit vertical velocity and the take-off mass vertical velocity cases are factored by 1.5 to obtain the ultimate loads. However. that resulting from the ultimate vertical velocity case is factored by 1.0 only to obtain the ultimate load value.

In general the vertical loads are associated with fore and aft, or drag. loads and side loads. The side loads are assumed to be applied at the point of contact with the ground and, except for braking and related loads, the drag loads act at the axle.

7.4.2 Landing with drag and side load – Load Case (7)

7.4.2.1 Landing with drag only – Load Case (1a)

This is the basic case, although it does not explicitly appear in the United Kingdom military aircraft requirements as it is covered by other conditions. In the civil aircraft requirements the maximum vertical reaction in the limit vertical velocity case is usually associated with a drag load which is 25 per cent of the vertical load. It effectively represents the conditions assumed in the analysis of Section 7.3.3.

The light aircraft requirements, JAR-23.479(b), state that the drag load must be at least 25 per cent of the maximum vertical ground reaction, see also Section 7.4.4.

The United States military requirements, ME-A-8862. require a maximum vertical load in combination with the drag load occurring at the instant the maximum vertical load is developed, but not less than 25 per cent of the vertical load. This corresponds to the JAR-25 case.

Table 7.1 Landing load cases

Case	No	Application'	Vertical load	Drag load	Side load – inward†	Side load – out†	Shock absorber closure
Combined drag and side load	(1a)	Civil	R	$0.25R$	*0*	*0*	As appropriate
	(1b)	Civil	$0.75R$	$0.4R$	$0.25R$	$0.25R$	Closure *at* $0.75R$
	(1c)	UK military	R	$0.4R$	$0.25R$	$0.25R$	$0.3\delta_S$
Side load	(2)	Military and civil	$0.5R$	*0*	$0.4R$	$0.3R$	$0.5\delta_S$
High drag and spring-back§	(3)	Military and civil	$0.8R$	$\pm 0.64R$	*0*	*0*	$0.15\delta_S$
One-wheel landings	(4)	Military and civil	As Case (1)	As Case (1)	As Case (1)	As Case (1)	As Case(1)
Rebound of unsprung parts (Mass m_{US})	*(5)*	Military and civil	$20\ m_{US}g$	*0*	*0*	*0*	Full closure

'UK military Def.Stan.00-970 and civil JAR-25 (not JAR-23 – see lent).
† At any one time inwards an one side and outwards on the other.
‡ Loads arc the maximum values which may be reduced by a dynamic analysis. see section 7.4.4.2
§ The loads *are* applied to only one of two main landing gear units.

7.4.2.2 Landing with drag and side load – Civil Load Case (Ib) and Military Load Case (Ic)

The specification of this case varies somewhat with different sets of requirements. Essentially it covers the case of the initial impact of the aircraft when landing at the design vertical velocity with a sideways drift. The combination of the full resulting vertical reaction and the side load is not always required. While Def.Stan.00-970, Chapter **304,** does prescribe that the full value of the vertical reaction should be used, other requirements allow a somewhat lower value, typically 75 per cent. The drag load is taken as **40** per cent of the maximum reaction and the side load 25 per cent.

7.4.3 Side load – Load Case (2)

This case is intended to cover the development of a side drift condition when the wheels are just rolling. Thus the drag load is assumed to be zero. Typically the vertical reaction is 50 per cent of the maximum with an inwards side load of **40** per cent of the vertical load on one landing gear unit and an outwards side load of 30 per cent of the vertical load on the other unit.

The light aircraft requirements, JAR-23.485, prescribe a side load of 50 per cent of the weight on one landing gear unit and simultaneously a side load of **33** per cent of the weight on the other, associated with a limit vertical load factor of 1.33 (that is a total vertical load on the main-wheels of 1.33 times the weight).

ML-A-8862 paragraph 3.2.9 specifies a drift landing condition, this being the equivalent to Case 2 of Table 7.1.

7.4.4 High-drag landing – Load Case (3)

7.4.4.1 Specification of spin-up loading conditions and spring-back

This is an important case and forms the basis of the United States MIL-A-8862 requirements which are further covered in the next section. The aircraft is assumed to touch down at the limit vertical velocity condition. possibly on an unprepared surface, so that the effective drag load is high. Typically the vertical reaction is taken to be 80 per cent of the datum value of Case (la). Section 7.4.2.1. The fore and aft force is dependent upon the time it takes for the wheel to 'spin-up' to a rotational velocity equivalent to the forward speed of the aircraft, in relation to the time it takes for the shock absorber to close. This is illustrated in Fig. 7.4, point C. In the absence of better information a ground drag coefficient of 0.8 has to be assumed. A method of evaluating the loads for this case, based on ML-A-8862, is given in the next section.

An important part of the case is that the drag, that is horizontal load, has to be considered as acting in either a forwards or an aft direction. This is to allow for the 'spring-back' effect as the wheel starts to roll freely before the brakes are applied, at the instant the maximum loads are developed, see Fig. 7.4, point D.

The JAR-23 light aircraft requirements specify that the spin-up and the spring-back must be covered with a ground friction coefficient of 0.8, the vertical reaction corresponding to that when the fore and aft load has reached the maximum value. JAR-23. Appendix D. presents a simple method for the evaluation of the ground frictior coefficient which is similar, but not identical, to that given in Section 7.4.4.2.

7.4.4.2 Analysis of spin-up and spring-back – MIL-A-8862 requirements

The major landing gear loading cases in the United States military requirements are expressed in a rather different form from either Def.Stan.00-970 or JAR-25, as has been noted where relevant in the previous section.

In addition to the side load case already covered and the ground manoeuvre cases stated in Section 7.5, MIL-A-8862 paragraph 3.2.1 requires that the landing conditions to bc investigated should include at least the following which correspond to Case (3) of Table 7.1 and also cover Case (1):

(a) Maximum spin-up load (drag) in combination with the vertical load occurring at the instant of maximum spin-up load, applied at the ground line but see Eqn. (7.12a).

(b) Maximum spring-back load in combination with the corresponding vertical load, applied at the axle.

The spring-back loads have to be calculated for ground friction coefficients of up to an avcragc value of 0.55 at touchdown speeds of at least 1.2 times the stalling condition, in conjunction with a dynamic factor. The inclusion of a dynamic factor may raise the maximum value of friction coefficient to as high as 0.85, see Eqns (7.12) and Fig. 7.5.

MIL-A-8862 paragraph 4 outlines a method for the evaluation of the loads during spin-up and spring-back.

A. *Maximum* spin-up

The venical load on the wheel is assumed to develop sinusoidally with respect to time. the average friction coefficient being 0.55. The basic maximum spin-up loads are a function of the relative values of the time required for the wheel circumferential velocity to reach the speed of the aircraft over the ground, t_{SU}, Eqns (7.11), and the time required to develop the maximum vertical reaction after the initial contact. t_R, Eqn. (7.10):

For $t_{SU} < t_R$:

$$R_{SU} = R_{MAX} \sin\left\{\frac{\pi t_{SU}}{2t_R}\right\}$$
$$D_{SU} = 0.55 R_{MAX} \sin\left\{\frac{\pi t_{SU}}{2t_R}\right\} \qquad (7.9a)$$

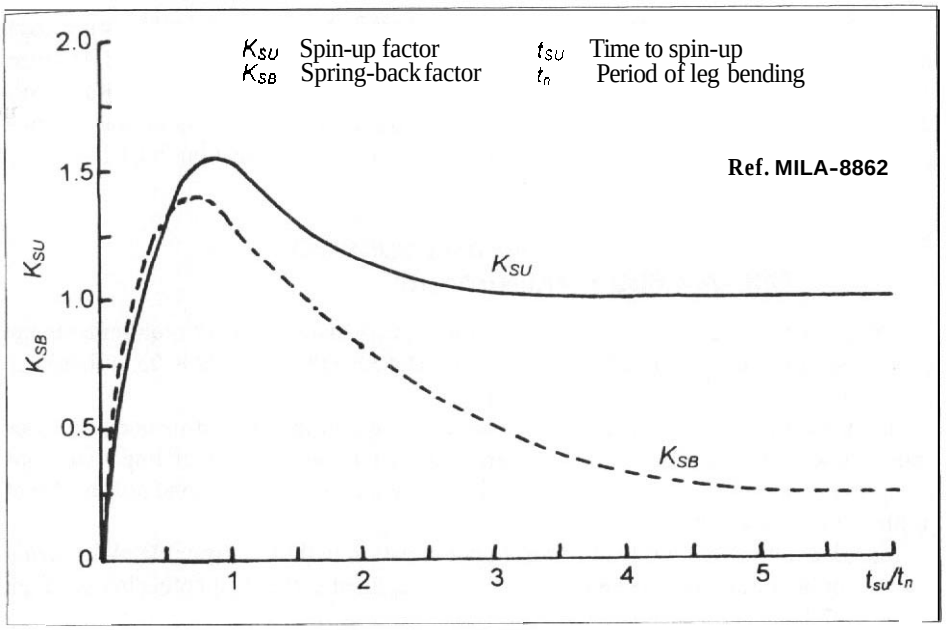

Fig. 7.5 *Spin-up and* ***spring-back dynamic*** factors

or for $t_{SU} > t_R$

$$R_{SU} = R_{MAX}$$
$$D_{SU} = 0.55R_{MAX} \tag{7.9b}$$

where

R_{SU} is the vertical load during spin-up
R_{MAX} is the maximum vertical load, see Eqns (7.5) in Section 7.2.5
D_{SU} is the drag (horizontal) load at the ground during spin-up

If appropriate experimental data are not available the values of t_R and t_{SU} can be taken as:

$$t_R = \frac{\{V_v - (V_v^2 - 9.08\delta_v\lambda)^{1/2}\}}{4.54\lambda} \tag{7.10}$$

where

δ_v is the total deflection and may be taken as the sum of the tyre deflection and half the total shock absorber stroke (m)
V_v is the vertical velocity in m/s
λ is the reaction factor corresponding to R_{MAX}

For $t_{SU} < t_R$:

$$t_{SU} = \left(\frac{2t_R}{\pi}\right) \cos^{-1} \left\{\frac{1 - (V_{ap} I_w \pi)}{1.1 t_R R_{MAX} r^2}\right\} \tag{7.11a}$$

or for $t_{SU} > t_R$:

$$t_{SU} = \frac{V_{ap} I_w}{0.55 R_{MAX} r^2} + 0.363 t_R \tag{7.11b}$$

where

V_{ap} is the approach (touchdown speed) (m/s)
r is the tyre rolling radius (m)
I_w is the polar mass moment of inertia of the rotating wheel assembly (kg m^2)

The loads R_{SU} and D_{SU} are then resolved parallel to and perpendicular to the axis of the shock absorber and modified to allow for dynamic magnification using a factor K_{SU}:

Normal to the shock absorber (aft) in this case applied at the axle:

$$\text{Load} = K_{SU}(D_{SU} \cos\theta - R_{SU} \sin\theta) \tag{7.12a}$$

Parallel to the shock absorber:

$$\text{Load} = R_{SU} \cos\theta + D_{SU} \sin\theta \tag{7.12b}$$

where

θ is the angle of inclination of the shock absorber (positive when the wheel is forward of the top attachment of the landing gear leg)
K_{SU} is a function of the ratio (t_{SU}/t_n) and is given in Fig. 7.5
t_n is the natural period of the landing gear in fore and aft bending vibration

I_w is best determined from vibration tests on the actual component. If static deflection information is available then for units where the inclination is within $\pm 20°$ of the normal to the horizontal aircraft datum, approximately:

$$t_n = 2.0(x)^{1/2} \quad \text{seconds} \tag{7.13}$$

where x (m) is the aft deflection at the axle resulting from a load normal to the leg equal to the total weight (N) of the wheel assembly and that part of the shock strut extending from the axle up a distance equal to one tyre radius. If t_n is unknown K_{SU} should be assumed to be 1.4.

B. Dynamic spring-back

Subsequent to the development of the maximum spin-up load and the aft deflection of the landing gear leg, the wheel rotational speed is assumed to have reached the forward rolling speed condition so that the sliding friction load reduces rapidly to zero. A direct consequence of this is that the bending strain energy in the leg causes a forward springing of the axle and wheel, known as the spring-back. At the instant of the maximum forward deformation it can he considered that there is a dynamic spring-back load which results from the inertia of the effective mass at the axle, acting forward and perpendicular to the shock absorber. It is assumed that at this instant the vertical reaction is at its maximum value. When allowance is made for dynamic magnification the components of load at the axle are:

Normal to the shock absorber (forward), at axle:

$$\text{Load} = K_{SB}(D_{SU}\cos\theta - R_{SU}\sin 8) + R_{SU}\left(0.9^{*} + \frac{R_{MAX}}{R_{SU}}\right)\sin\theta \qquad (7.14a)$$

Parallel to the shock absorber:

$$\text{Load} = R_{MAX}\cos\theta \qquad (7.14b)$$

K_{SB}, the dynamic magnification factor, is given in Fig. 7.5. If t_n is unknown K_{SB} should he assumed to he 1.25. ('Note that if 0 is negative then 0.9 is replaced by zero.)

7.4.5 One-wheel landing condition – Load Case (4)

The loads in this case are derived directly from those of Section 7.4.2 for a given main landing gear unit. Thus they are not normally a design case for the landing gear units themselves but may provide a critical loading case for the airframe structure between the main gear units.

However, when there are three of four main gear units it is necessary to consider whether the outermost units may have to react higher loads than those developed in a symmetric landing. It is possible for a pair of main landing gear units on one side of an aircraft having four main units to he interconnected such that the loads in an asymmetric landing are shared and are no higher than in the symmetric case. On the other hand when there are three main landing gear units an outer unit may have to be designed for a single wheel loading which allows for the additional load normally carried by the centre unit. A rational approach to this problem demands a dynamic analysis to ascertain what proportion of the centre unit loading must be added to that normally reacted by the outer gear. The method of Appendix A7 may be adapted for this purpose.

The light aircraft requirements are similar to those of transport aircraft.

7.4.6 Rebound of unsprung parts – Load Case (5)

The recoil of all moving parts must be damped such that the stresses caused by the parts coming to rest on their stops after a bounce at the limit vertical velocity are acceptably low. In this connection some requirements specify that the attachment of the unsprung mass, that is whccl, axle, and lower part of the shock absorber mechanism, should be designed to withstand a limit load factor of 20 along the direction of the shock absorber when the unit is fully extended.

7.5 Load cases resulting from ground manoeuvring conditions

7.5.1 Introduction

As with the landing cases there are some differences between the military and civil requirements. In particular the military requirements in Def.Stan.00-970 and the light aircraft requirements in JAR-23 require allowance to he made for uneven runway surfaces, see Section 7.6. Unless otherwise stated the prescribed conditions have to be applied at the maximum, or ramp, mass of the aircraft.

The side loads are assumed to act at the point where the tyre contacts the ground, as are the braking fore and aft loads.

7.5.2 Braking cases

7.5.2.1 Braked rolling/dynamic braking

This case deals with the loads which arise when the brakes are suddenly applied and cause a pitching down on lo the nose-wheel. There is a main-wheel as well as nose-whccl loading case.

(a) Main-wheel case. Def.Stan.00-970 Leaflet 302/2 paragraphs 2 and 4 and JAR-25.493. The aircraft is assumed to be in an attitude such that the nose-wheel is just clear of the ground with the main units at static deflection. The vertical load factor at the centre of gravity, used to calculate main-wheel vertical reaction is 1.2, at the design landing mass. m_L, or 1.0 at the maximum mass. m_T. The drag load at each wheel is taken as 80 per cent of the vertical reaction or the peak dynamic brake drag. whichever is the lower.

(b) Military aircraft nose-wheel case. The load to he applied to the nose-wheel is:

$$R_N = \frac{(m_T g \ell_m + 2HD)}{(\ell_m + \ell_n)} \tag{7.15a}$$

where H is the height of the centre of gravity of the aircraft above the ground and D is the lesser of total peak dynamic brake force, or:

$$D = 0.8 m_T g \ell_n / (\ell_m + \ell_n) \tag{7.15b}$$

Side load may be assumed to be zero.

(c) Civil nose-wheel case, JAR-25.ACJ493. This suggests:

$$R_N = m_T g \frac{\{\ell_m + f\mu\ell_n H/(\ell_m + \ell_n + \mu H)\}}{(\ell_m + \ell_n)} \tag{7.16}$$

f is a dynamic factor which may be taken as 2.0 unless a lower value can be established. If a high value of 0.8 is allocated to μ, the ground friction coefficient, the value of R_N is similar, but not identical, to that given by the military requirement of (b) above. Drag and side loads are zero on the nose-wheel.

(d) Main-wheel case, Light aircraft JAR-23.493. A total vertical reaction of 1.33 times the weight associated with a ground friction coefficient of 0.8 has to be applied to the main-wheels, except that it need not exceed the value determined by the limiting brake torque.

(e) Light aircraft nose-wheel case. JAR-23. See Section 7.5.5.

(f) United States, MIL-A-8862. The United States requirements, MIL-A-8862 paragraph 3.3.1, specify braked rolling cases which are similar to those outlined above.

7.5.2.2 Steady braking

The United Kingdom military requirements, Def.Stan.00-970. Leaflet 302/2, give steady braking cases which, apart from an asymmetric condition. are related to movement over uneven ground. These are covered in Section 7.6.3.

7.5.2.3 Reversed braking

This provision is intended to cover the case of the aircraft being moved backwards against the brakes or chocks. Thus the horizontal force acts forwards. Whether this case is more critical than Load Case (3), Section 7.4.4, depends upon the magnitude of the reaction factor. See also MIL-A-8862 paragraph 3.3.1.4.

(a) Military (Def.Stan.00-970 Leaflet 302/2 paragraph 4). The military requirement is for a case similar to that of Section 7.5.2.1(a) above, but with the horizontal force applied in a forwards direction. It only applies to the main-wheels.

(b) Civil (JAR-25.507). The civil case is somewhat different, prescribing a horizontal forward force of 55 per cent of the vertical reaction at each main leg. If the nose-wheel has brakes, the vertical reaction to be considered with

55 per cent of the horizontal load is:

$$R_N = \frac{m_T g \ell_m}{(\ell_n + \ell_m)} \tag{7.17}$$

7.5.3 Turning and pivoting

Turning cases can be divided into two categories:

(a) Overall loads on the aircraft due to turning while taxiing. The usual assumption is a lateral acceleration of $0.5g$ at the centre of gravity but no brake loads.

(b) Loads on local pans, such as nose-wheel steering and main leg bogie/torque links, when the aircraft is either manoeuvred or ground handled.

MIL-A-8862 paragraph 3.3.2 gives a ground turning condition where the total side load on both main units is taken as half the weight except that the value need not exceed the overturning situation. The United Kingdom military requirements (Def.Stan.00-970 Leaflet 302/2, paragraph 3) and the civil requirements (JAR-25.495) may he interpreted as follows:

(a) Main-wheel units:

$$R_M = 0.5 m_T g \left\{ \frac{\ell_n}{(\ell_m + \ell_n)} \pm \frac{H}{t} \right\} \tag{7.18a}$$

where t is the track of the main-wheels and the vertical load is $+(H/t)$ on one side and $-(H/t)$ on the other main unit.

The side load, inwards on one side and outwards on the other, is:

$$S_M = 0.5 R_M \tag{7.18b}$$

The drag load is assumed to be zero.

(b) Nose-wheel units:

$$R_N = \frac{m_T g \ell_m}{(\ell_m + \ell_n)} \tag{7.19a}$$

To cover the case where nose-wheel steering is not used the side load is:

$$S_{,,} = 0.5 R_N \tag{7.19b}$$

The drag load is zero.

In addition the main units must he designed to allow the aircraft to pivot about either of them at the mass, m_T, and a ground friction coefficient of 0.8.

7.5.4 Take-off cases

There is a take-off case to cover the condition when an obstacle or an unevenness of take-off surface is encountered. This is specified in Section 7.6.3.

7.5.5 Supplementary nose-wheel loads – steering

7.5.5.1 Nose-wheel steering – Def.Stan.00-970, Chapter 303, and JAR-25.499

Both the United Kingdom military aircraft and the civil transport aircraft requirements make similar provisions.

The civil transport requirements are detailed but essentially prescribe a side load of 80 per cent of the maximum vertical reaction on the nose-wheel when there is a vertical factor of unity at the centre of gravity of the aircraft and, separately, the application of maximum steering torque when the nose-wheel vertical reaction is 133 per cent of the maximum value.

Light aircraft steering requirements are covered in the following section.

7.5.5.2 Light aircraft supplementary conditions – JAR-23.499

A number of supplementary loading cases for light aircraft nose-wheel design are identified.

(a) Aft-wards acting load case. A drag component of 80 per cent of the vertical load acting with a vertical load of 225 per cent of the static load on the nose-wheel.

(b) Forwards acting load case. A forward component of 40 per cent of the vertical load as defined in (a) above.

(c) A side load of 70 per cent of the vertical load as defined in (a) above.

(d) Steering conditions are covered by assuming that a design steering torque of 133 per cent of the maximum steering torque is applied at the same time as 133 per cent of the maximum static reaction on the nose-wheel.

7.5.6 Towing loads

It is usual to tow aircraft from attachments made to the landing gear units:

(a) Military aircraft. Def.Stan.00-970 Chapter 308. Generally, the towing load, F_{TOW}, is 15 per cent of the take-off weight with side and drag load components all taken together. These latter are a side load of $(F_{TOW} \sin \theta)$ and a drag load of $(F_{TOW} \cos 0)$ where θ is up to 30" for main-wheel units and up to the maximum castoring angle for nose-wheel units.

Proof and ultimate factors of 1.5 and 2.0, respectively, are normally applied, although reduction to the usual values of 1.125 and 1.5 may be considered when the towing loads are critical and shear pins are incorporated in the design.

(b) Civil transport aircraft, JAR-25.509. The requirements are based on a towing force of:

For $m_T < 13\,600$ kg:

$$F_{TOW} = 0.3 m_T g$$

For 13 600 kg $< m_T <$ 453 300 kg:

$$F_{TOW} = \frac{6(m_T g + 2 \times 10^7)}{70} \tag{7.20}$$

For $m_T >$ 453 300 kg:

$$F_{TOW} = 0.15 m_T$$

The loads on the main undercarriage towing point have to be applied at $\pm 30'$ relative to the drag axis.

The nose unit case is $\pm F_{TOW}$ with the wheel in the fore and aft position, or $0.5F_{TOW}$ when the wheel is turned through 45^c. In each case the load direction is in the plane of the wheel.

(c) Light aircraft, JAR-23.509. The light aircraft requirements are somewhat different but require a swivelled maximum towing load of $0.3 m_T g$ an thc main gear unit and $0.15 m_T g$ on the nose gear unit.

7.6 Operation from uneven surfaces

7.6.1 Introduction

The United Kingdom military requirements, Def.Stan.00-970 Chapter 305. introduce conditions to cover the eventuality of the aircraft manoeuvring over both normal runways with steps or obstacles and runways repaired after battle damage. There are two cases, namely a steady hraked situation and the take-off.

The civil transport requirements. JAR-25.491, also deal with the take-off condition and the light aircraft requirements, JAR-23.473(g), provide for take-off over rough ground.

7.6.2 Definitions of runway unevenness and the bump factor, F

Def.Stan.00-970 Chapter 305, specifies design cases for the operation of aircraft off surfaces other than smooth, hard runways. Leaflet 305/2 defines four classes of runway surface and introduces appropriate factors to define the height of a bump. step, or repair condition, see Table 7.2. In addition, Def.Stan.00-970 Chapter 305 deals with the

Table 7.2 Classes of runway surface

Class	Description	Height factor	Bump height (mm)	Step height (mm)
A	Paved, stable base. well maintained	1	30	25
B	Poor quality paved or fully graded unpaved	1.5	45	40
C	Unpaved, partially graded	2.5	75	60
D	Unpaved on virgin soil	4	120	100

overall aircraft dynamics during operation on uneven surfaces and the conditions appropriate to operation from soft ground, such as sand and clay.

The conditions of Table 7.2 are related to aircraft operations from damaged and repaired runways. The shape of the runway unevenness is also defined mathematically. For preliminary design purposes the appropriate design case, as stated in paragraphs 7.6.3 and 7.6.4, can be derived by introducing a bump factor, F. This factor is a function of the tyre characteristics relative to the bump size.

For initial design purposes it may be assumed that when an aircraft suddenly contacts a bump or step the main shock absorber does not deflect. This is a severe assumption and some landing gear units are specifically designed to absorb energy in these circumstances. However, using this assumption the increment in load that results depends only upon the tyre characteristics. In particular the increase in vertical load is taken lo be that due to deflecting the tyre through an additional displacement equal in magnitude to the height of the bump.

From Section 7.2.3 Eqn. (7.2) the tyre stiffness characteristic is given by:

$$R = k_T \delta_T^{1.1}$$

$$\delta_T = \left(\frac{R}{k_T}\right)^{0.9}$$

Now if δ_{T1} is the tyre deflection appropriate to an initial load R_1, and h_b is the height of the bump, then:

$$F = \frac{R_2}{R_1} = (1 + h_b/\delta_{T1})^{1.1}$$

where R_2 is the increased vertical reaction due to the bump.

At one time the requirements quoted a value of F appropriate to operation off unprepared surfaces:

F = 2.33 for tyres up to 0.76 m (30 inch) diameter
= 1.80 for tyres of above 1.53 m (60 inch) diameter

with linear variation in between.

This appears to give some consistency with the above equation for tyres of moderate pressure having a width/diameter ratio of about 0.25, and using the Class C runway definition of Table 7.2.

7.6.3 Military aircraft steady braking cases – Def.Stan.00-970 Chapter 305

These cases cover steady braking conditions and include asymmetric effects on the main-wheels and encountering a runway bump during steady braking. Def.Stan.00-970 Leaflet 302/2, paragraphs 2, 3 and 4 require:

(a) Asymmetric case – main and nose wheels. An asymmetric case is specified where the aircraft is assumed to be in a static equilibrium condition at the maximum mass, m_T, and a drag force of 80 per cent of the vertical reaction acts on one main unit only. The out of balance moments are reacted by side loads on the main- and nose-wheels and an additional vertical reaction on the nose leg.

(b) Encountering a hump – main-wheels. The *total* load on the main landing gear units is to be taken as:

$$R_{TOTAL} = m_L{}^T g\left[\frac{l_n}{(\ell_m + \ell_n)} \quad \frac{H}{3(\ell_m + \ell_n)}\right] \tag{7.21a}$$

One wheel assembly encounters the bump and a bump factor, F (see Section 7.6.2), is used to calculate the vertical reaction on that unit. R_{MSB}, by multiplying the vertical reaction on that leg by F. The term $m_L{}^T$ represents any mass between the landing value, m_L, and the maximum, ramp, value of m_T.

Then the side and drag loads are to be taken as. respectively:

$$\begin{aligned} S_{MSB} &= 0.25R_{MSB} \\ D_{MSB} &= 0.4R_{MSB} \end{aligned} \tag{7.21b}$$

(c) Encountering a hump – nose wheels.

$$R_{NSB} = Fg\left[\frac{m_L{}^T \ell_m}{(\ell_m + \ell_n)} + \frac{m_T H}{3(\ell_m + \ell_n)}\right] \tag{7.22a}$$

$$D_{NSB} = S_{NSB} = 0.25R_{NSB} \tag{7.22b}$$

The nose-wheel has to be in a position up 20° from the central position with the maximum steering torque applied.

7.6.4 Take-off cases

7.6.4.1 Military aircraft – Def.Stan.00-970 Chapter 305

This case covers the forward movement of the aircraft and gets its name from the fact that the design mass is that appropriate to the take-off tun. It is only critical when a hump is encountered.

There are two conditions:

(a) With all wheels touching the ground, up to the rotation speed, the *total* vertical reaction on the main landing gear units is taken as:

$$R_{TOTAL} = m_T g \ell_n / (\ell_m + \ell_n) - \mathscr{L} \tag{7.23a}$$

where $\mathscr{L}$ is the total lift. As in paragraph 7.6.3(b) above, the bump factor, F, is used to calculate the vertical reaction on one main-wheel unit, R_{MTO}, and the associated side and drag loads are:

$$S_{MTO} = D_{MTO} = 0.25 R_{MTO} \tag{7.23b}$$

(b) With the nose-wheel clear of the ground, after the rotation speed has been reached the *total* vertical reaction on the main-wheel units is:

$$R_{TOTAL} = m_T g + (\mathscr{L}_T - \mathscr{L}) \tag{7.23c}$$

where $\mathscr{L}_T$ is the tail load required to rotate

7.6.4.2 Civil transport aircraft take-off requirements – JAR-25.491 (ACJ491)

It is suggested that the load on each main-wheel unit should be taken as $1.5 m_T g/2$ or alternatively $1.7 m_T g$ be shared between all the units at the most adverse position of the centre of gravity.

7.6.4.3 Light aircraft – JAR-23.473(g)

Unless it can he demonstrated that taxiing at speed over the roughest terrain anticipated in service gives rise to lower values, then a total vertical load factor of 2 should be combined with a fore and aft inertia factor of 2.67.

7.7 Supplementary loading conditions

7.7.1 General

These cover a number of specific matters which often affect only local parts of the aircraft or give overall conditions which result from the behaviour of the aircraft and its operation. They are not all direct load conditions. but can influence loads. Other than those covered in the following sections, matters dealt with include the effect of variations in the design parameters and fatigue considerations.

7.7.2 Directional control and nose-wheel castoring – Def.Stan.00-970 Chapters 300,302 and 303; JAR-25.499

It is usual to provide castoring of a nose-wheel unit through 360". There are also requirements regarding nose-wheel 'shimmy', see Def.Stan.00-970 Chapter 301, paragraph 5.

7.7.3 Forward speed at and after touchdown – JAR-25.479 and 481

JAR-25 specifies landing at up to 1.2 times the appropriate stall speed as part of the high-drag case.

7.7.4 Taxiing and take-off run

Def.Stan.00-970 Chapter 302, paragraph 2, specifies taxiing and ground manoeuvre in cross winds of 4.1 m/s (8 knots) for normal operation or up to 18 m/s (35 knots) with some degradation of performance. JAR-25.237 specifies taxiing in the range of 10.3–12.9 m/s (20–25 knots) unless 20 per cent of the stalling speed is less than 10.3 m/s (20 knots).

7.7.5 Unequal loads on wheels and tyres

Def.Stan.00-970, Leaflet 303/2, covers special considerations when tyres are deflated, while Chapter 301 states that pressure variations of up to ±10 per cent must he considered for individual tyres in multi-lyre units. JAR-25.511 specifics ±5 per cent variation but also requires a consideration of the curvature of the runway.

7.7.6 Tyre clearances

Tyres grow with age and rotational speed. Thus it is necessary to make an adequate clearance allowance of +5 per cent in width and +7 per cent in diameter relative to nominal sizes. With twin tyres on a common axle the clearance between them should be 25 per cent of the grown width.

7.7.7 Retraction and lowering

Def.Stan.00-970 Chapter 306 deals with this topic. Specific points are:

(a) Retraction to be complete in no more than 5 s and lowering in 10 s, Leaflet 306/1, paragraph 2.
(b) Maximum speed for gear extension. Leaflet 306/1, paragraph 6.
(c) Allowance must be made for aerodynamic and inertial loads and an ultimate factor of 2.0 applied.

7.8 Absorption of horizontal energy – brake considerations

Reference may be made to Def.Stan.00-970, Chapter 310.

For initial calculations the required energy absorption for each brake unit can be estimated from the following:

$$E_b = \frac{K_b m_L V^2}{(2N_b)} \tag{7.24}$$

where

N_b is the number of brakes on the main-wheels
m_L is the design landing mass
V is the speed from which a stop must be made
K_b is a factor which allows for the contribution of the aerodynamic drag

K_b may be taken to be as low as 0.7 for a tail-wheel aircraft but it is nearer 1.0 for a clean nose-wheel aircraft. However, it may be possible to use the drag effect of a nose-wheel aircraft by maintaining a high incidence until late in the landing run by delaying the dropping of the nose or by using flap effect and airbrakes. In this case K_b may be as low as 0.8.

Brakes have to be designed for the normal landing conditions and also for an emergency stop case at the take-off mass. Since the latter is a special case a higher brake temperature is permitted and it only becomes critical when the landing mass is considerably less than the take-off value or, possibly, when the field length requirements are determined by the accelerate/stop case.

7.9 Effect of airframe flexibility and other variables

Investigations have shown that for a conventional aircraft the effect of wing flexibility is not very critical in landing gear load estimation. Application of the stipulated loading cases without allowance for dynamic effects, including wing flexibility, may give rise to

an underestimation of the wing loads but when the dynamic effects are allowed for the results are likely to be conservative.

As discussed in Section 7.4.4.2 the ground friction coefficient, μ, varies during the spin-up phase, but the assumption of constant μ has been found to imply only a negligible error. The same is true when the unsprung mass effect is neglected.

7.10 Example calculation

A sample calculation illustrating the derivation of the landing loads from the energy absorption requirements and shock absorber characteristics is given in Addendum AD4.

Appendix A7 Dynamic analysis of landing

A7.1 Introduction

A7.1.1 General comments

In some circumstances it is desirable or necessary to undertake a full dynamic analysis of the motion of the aircraft during landing. For example this may be so when the aircraft is of unusual configuration or if the runway surface is uneven. The following method can fonn the basis for such a problem. When undertaking this type of dynamic analysis it is often more convenient to express it in terms of energy and work rather than by use of Newton's laws of motion. The formulation of the analysis is then in terms of Lagrange's equation, see the following section.

A7.1.2 Lagranges's equation

Lagrange's equation is a relationship between the energies and work of a system rather than the force and momentum change used in Newton's laws. When the system is complex the equations of motion are often derived more directly by the use of Langrange's equation. The technique consists of specifying the kinetic and potential energies and the external work in terms of so called 'generalized co-ordinates' which are usually in the form of displacements.

The generalized co-ordinates are the variables in the system and must be specified such that they are completely independent of one another. They are equal in number lo the degrees of freedom in the system. For example a simple pendulum is free only to rotate about its fulcrum through an angular displacement, 8, say, and this is the generalized co-ordinate. As an alternative it might be preferable to specify the motion in terms of the canesian displacements of the centre of gravity, say x and y. However. x and y are not independent, as they are related by the 'constraint' equation $(x^2 + y^2 = \ell^2)$, where ℓ is the length of the pendulum. Thus it is possible to specify a system of n degrees of freedom in terms of m coordinates providing that $(m - n)$ constraint equations are introduced.

As dealt with in Chapter 4, a rigid body with discrete dimensions has six degrees of freedom, three translations and three rotations. When constrained to move in one plane there are only three degrees of freedom. A flexible body will have additional freedoms,

the number of which depends upon the form of the assumed mass distribution and flexibility.

The general form of Lagrange's equation is:

$$\frac{d(\delta T/\delta \dot{q}_i)}{dt} - \frac{\delta T}{\delta q_i} + \frac{V}{q_i} = Q_i \qquad \text{(A7.1)}$$

where

q_i is a generalized co-ordinate, there being n equations for $i = 1, \ldots, n$
T is the kinetic energy of the system
V is the potential energy of the system
Q_i is the generalized force corresponding to the coordinate q_i, the work done being $Q_i \delta q_i$

In many systems the kinetic energy is a function only of the velocities of the generalized coordinates and in this case the second term in Eqn. (A7.1) is not present.

A7.2 The definition of the problem

A7.2.1 General

The general configuration of an aircraft dunng a symmetric landing is shown in Fig. A7.1. The mass of the aircraft is m. The motion of the aircraft is described by linear displacements relative to the orthogonal axes x forward and z vertically downward referred to the centre of gravity, and an angular displacement, that is a rotation, of a about the centre of gravity. These three displacements are the generalized co-ordinates in this system.

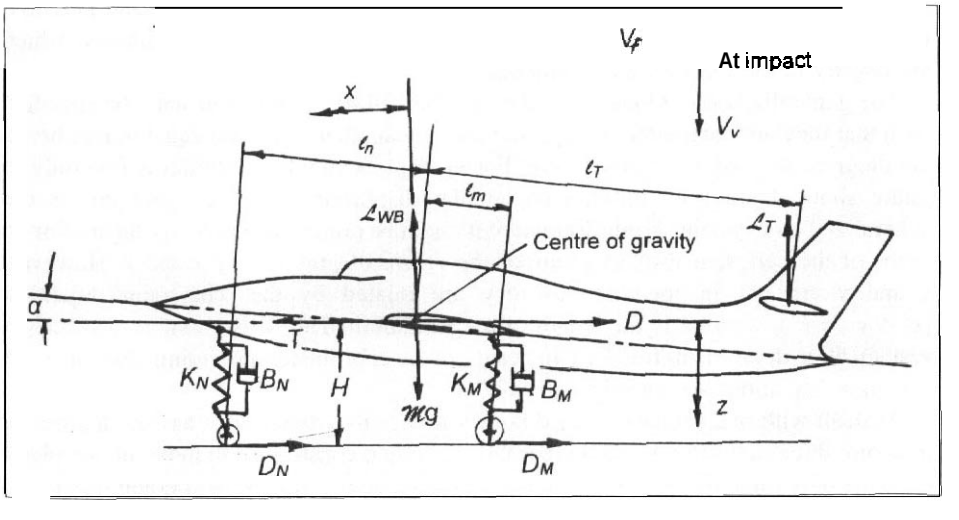

Fig. A7.i Configuration at landing impact

The vertical descent velocity, V_v, is assumed to he constant immediately before the wheels impact the ground, at which time the centre of gravity is at a height, H, above the ground.

The forward velocity at touchdown is V_f, and it is assumed that the trim of the aircraft is unchanged during the short period over which the maximum loads are developed, refer to Fig. 7.4.

A7.2.2 Notation

The notation used is:

$\mathscr{L}$	is the resultant trimmed lift, assumed to act at the centre of gravity of the aircraft.
$\mathscr{L}_T$	is the incremental lift on the horizontal stabilizer due to the changes of the vertical velocity and the pitch damping effects after the landing impact.
D	is the aerodynamic drag, assumed to act through the centre of gravity.
T	is the thrust (which may be reversed) assumed, for simplicity, to act through the centre of gravity.
D_M, D_N	are the drags due to contact of the wheels with the ground, suffix 'M' referring to the main-wheel and 'N' to the nose-wheel.
ℓ_m, ℓ_n	are the respective fore and aft distances of the main-wheels and the nose-wheels from the centre of gravity at the instant of touch-down.
ℓ_T	is the distance of the horizontal stabilizer lift to the centre of gravity.
k_y	is the radius of gyration of the aircraft in pitch about the centre of gravity.
μ	is the coefficient of ground friction, assumed to be constant during the period when maximum loads are developed. The chosen value must he evaluated from a wheel spin-up analysis, such as that suggested in MIL-A-8862 and given in Section 7.4.4.2.
K_M, K_N	are the stiffnesses of the main and nose shock absorber units respectively. These terms are assumed to be linear, see Section A7.3, and should include an allowance for the tyre stiffness. Note that K_M is the total value of all main units.
B_M, B_N	are the damping coefficients of the main and nose shock absorber units, respectively. They are assumed to be proportional to velocity, see Section A7.3. This assumption may not always be justified.

A7.3 Derivation of landing gear spring and damping characteristics

The analysis is based on the assumption that the effective overall spring characteristic of the shock absorber and the tyres of a given unit is linear. Likewise it is assumed that the damping characteristic of the unit is directly proportional to the velocity of closure. This paragraph suggests a method by which approximate values for the linear stiffness and

viscous damping coefficient may be derived given the actual, non-linear, landing gear characteristics.

It is necessary to assume that:

(a) The shape of the dynamic load–deflection curve is smooth and may be represented by the loads corresponding to the mid- and final deflections, $\delta_F/2$ and δ_F, respectively.

(b) The velocity of closure is zero at both ends of the stroke, that is both initially and finally, and it may be represented as a sine function.

The assumed form of the load–deflection curve is shown in Fig. *A7.2*

Let:

R_F be the final load corresponding to a deflection, δ_F

R_M be the load at mid-deflection. $\delta_F/2$

Also let:

$$R = K\delta + BV_v \tag{A7.2}$$

where V_v is the closure velocity (effectively I).

By assumption (b) V_v is zero when the deflection is δ_F and therefore:

$$K = \frac{R_F}{\delta_F} \tag{A7.3}$$

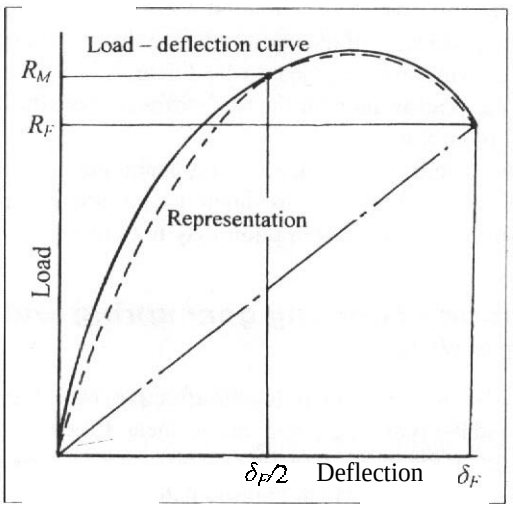

Fig. A7.2 Assumed form of the landing gear load–deflection curve

Further. let:

$$V_v = V_{vMAX} sin\ \pi\left(\frac{\delta}{\delta_F}\right) \tag{A7.4}$$

where V_{vMAX} is the maximum closure velocity, which is at the mid point of the deflection since the motion is assumed to be simple harmonic:

$$V_{vMAX} = 1.41 V_{vMEAN}$$

where V_{vMEAN} is the average velocity over the closure:

$$V_{vMEAN} = \frac{\delta_F}{t_F}$$

where t_F is the total time of the closure and thus:

$$V_{vMAX} = 1.41 \delta_F / t_F \tag{A7.5}$$

The load at mid-deflection is then, from Eqns (A7.2 to A7.5):

$$R_M = (R_F/\delta_F)\delta_F/2 + 1.41 B \delta_F / t_F$$

or

$$R_M/R_F = 0.5 + 1.41(B/R_F)\delta_F/t_F$$

and

$$B = R_F\{(R_M/R_F) - 0.5\}/(1.41\delta_F/t_F) \tag{A7.6}$$

Also:

$$\frac{R}{R_F} = \frac{\delta}{\delta_F} + \left\{\left(\frac{R_M}{R_F}\right) - 0.5\right\} sin\ \pi\left(\frac{\delta}{\delta_F}\right) \tag{A7.7}$$

Note that the load is independent of the velocity of closure. K is given by Eqn. (A7.3) and B by Eqn. (A7.6)

Example

$$\frac{R_M}{R_F} = 1.1 \quad t_F = 0.2\,\text{s}$$

then

$$K = \frac{R_F}{\delta_F} \quad \text{and} \quad B = \frac{0.0851 R_F}{\delta_F}$$

hence:

δ/δ_F	R/R_F
0	0
0.2	0.553
0.4	0.971
0.5	1.10
0.6	1.171
0.8	1.53
1.0	1.0

A7.4 Derivation of applied forces

A7.4.1 Aerodynamic lift terms

Initially the overall lift on the aircraft is assumed to he equal to the weight and this defines an initial angle of attack, α_o, hut as the pitch angle, α, changes after impact so will the lift. The lift coefficient is the product of the lift curve slope and the angle of attack, $(a_1\alpha)$, hence generally the lift is:

$$\mathscr{L} = \frac{a_1 \alpha \rho S V_f^2}{2} = \frac{a_1 \alpha \rho S \dot{x}^2}{2} = \bar{L}\alpha\dot{x}^2 \qquad \text{(A7.8a)}$$

since the forward velocity, V_f, is identical to $dx/dt = \text{x}$

where

S	is the wing reference area
a_1	is the lift curve slope of the aircraft as a whole in the **trimmed** condition
p	is the local air density

and

$$\bar{L} = a_1 \rho S/2 \qquad \text{(A7.8b)}$$

The initial angle of attack is:

$$\alpha_o = \frac{2mg}{(\rho a_1 S V_f^2)} \tag{A7.8c}$$

The effective angle of attack of the horizontal stabilizer due only to the vertical velocity and the pitching velocity increments subsequent to initial impact is:

$$\frac{(dz/dt)}{V_f} + \frac{\ell_T (d\alpha/dt)}{V_f}$$

Thus:

$$\mathscr{L}_T = a_{1T}\rho S_T(\dot{z} + \ell_T\dot{\alpha})\dot{x}/2 = \overline{L_T}(\dot{z} + \ell_T\dot{\alpha})\dot{x} \tag{A7.9a}$$

where

S_T is the reference area of the horizontal stabilizer
a_{1T} is the lift curve slope of the horizontal stabilizer

and

$$\overline{L_T} = a_{1T}\rho S_T/2 \tag{A7.9b}$$

Similarly the aerodynamic drag is:

$$D = C_d \rho S\dot{x}^2/2 \tag{A7.10a}$$

where C_d is the total drag coefficient:

$$C_d = C_{do} + \bar{B}C_L{}^2 = C_{do} + \bar{B}(a_1\alpha)^2$$

where C_{do} is the zero lift drag coefficient and $\bar{B}$ the induced drag factor.

Thus:

$$D = (\bar{D}_1 + \bar{D}_2\dot{\alpha}^2)\dot{x}^2 \tag{A7.10b}$$

and

$$\bar{D}_1 = \rho S C_{do}/2$$
$$\bar{D}_2 = \rho S \bar{B} a_1{}^2/2 \tag{A7.10c}$$

A7.4.2 Ground drag force

The total ground friction drag force is:

$$\begin{aligned} D_M + D_N &= \mu(mg - \mathscr{L} - \mathscr{L}_T) \\ &= \mu\{mg - \bar{L}\alpha\dot{x}^2 - \overline{L_T}(\dot{z} + \ell_T\dot{a})\dot{x}\} \end{aligned} \tag{A7.11}$$

A7.5 Kinetic energy terms

The total kinetic energy of the system expressed in terms of the three generalized coordinates is:

$$T = m(\dot{x}^2 + \dot{z}^2 + k_y{}^2\dot{\alpha}^2)/2 \tag{A7.12}$$

A7.6 Potential energy terms

It is assumed that the potential energy is due only to the linear landing gear stiffness effects, the damping effects being covered in the external work terms.

The effective vertical deflections of the main and nose landing gear springs are:

$$\delta_M = z + \ell_m(\alpha - \alpha_o) \quad \text{and} \quad \delta_N = z - \ell_n(\alpha - \alpha_o) \tag{A7.13}$$

The potential energy is thus:

$$\begin{aligned} V &= [K_M\{z + \ell_m(\alpha - \alpha_o)\}^2 + K_N\{z - \ell_n(\alpha - \alpha_o)\}^2]/2 \\ &= (K_M + K_N)z^2/2 + (K_M\ell_m - K_N\ell_n)(\alpha - \alpha_o)z \\ &\quad + (K_M\ell_m{}^2 - K_N\ell_n{}^2)(\alpha - \alpha_o)\}^2/2 \end{aligned} \tag{A7.14}$$

A7.7 External work

The total external work arises from the movement of the mass and the externally applied forces, together with the effects of landing gear damping which are included for convenience in this item. Thus the external work is:

$$\begin{aligned} \Sigma Q_i\delta q_i = {} & mg\delta z - \mathscr{L}\delta z - \mathscr{L}_T\delta(z + \ell_T\alpha) - B_M(\dot{z} + \ell_m\dot{\alpha})\delta(z + \ell_m\alpha) \\ & - B_N(\dot{z} - \ell_n\dot{\alpha})\delta(z - \ell_n\alpha) + T\delta x - D\delta x \\ & - (D_M + D_N)\delta\{x - (H - z)\alpha\} \end{aligned} \tag{A7.15a}$$

Substituting from Eqns (A7.8) to (A7.11) and collecting together the terms inx. z, and a gives:

$$\begin{aligned}\Sigma Q_i \delta q_i = {} & [mg - \bar{L}\alpha\dot{x}^2 - \overline{L_T}(\dot{z} + \ell_T\dot{\alpha})\dot{x} - B_M(\dot{z} + \ell_m\dot{\alpha}) - B_N(\dot{z} - \ell_n\dot{\alpha})]\delta z \\ & + [T - (\bar{D}_1 + \bar{D}_2\alpha^2)\dot{x}^2 - \mu\{mg - \bar{L}\alpha\dot{x}^2 - \overline{L_T}(\dot{z} + \ell_T\dot{\alpha})\dot{x}\}]\delta x \\ & - [\overline{L_T}(\dot{z} + \ell_T\dot{\alpha})\ell_T\dot{x} - B_M(\dot{z} + \ell_m\dot{\alpha})\ell_m - B_N(\dot{z} - \ell_n\dot{\alpha})\ell_n \\ & - \mu(H - z)\{mg - \bar{L}\alpha\dot{x}^2 - \overline{L_T}(\dot{z} + \ell_T\dot{\alpha})\dot{x}\}]\delta\alpha \qquad \text{(A7.15b)}\end{aligned}$$

A7.8 Derivation of the equations of motion

Applying Lagrange's equation to each of the three generalized co-ordinates x, z, and α in turn and making use of Eqns (A7.12), (A7.14), and (A7.15b) enables the three equations of motion to be derived:

$$m\ddot{x} = T - (\bar{D}_1 + \bar{D}_2\alpha^2)\dot{x}^2 - \mu\{mg - \bar{L}\alpha\dot{x}^2 - \overline{L_T}(\dot{z} + \ell_T\dot{\alpha})\dot{x}\}$$

$$\begin{aligned}m\ddot{z} + (K_M + K_N)z + (K_M\ell_m - K_N\ell_n)(\alpha - \alpha_o) = {} & mg - \bar{L}\alpha\dot{x}^2 \\ & - \overline{L_T}(\dot{z} + \ell_T\dot{\alpha})\dot{x} - B_M(\dot{z} + \ell_m\dot{\alpha}) - B_N(\dot{z} - \ell_n\dot{\alpha})\end{aligned}$$

$$\begin{aligned}mk_y^2\ddot{\alpha} + (K_M\ell_m^2 + K_N\ell_n^2)(\alpha - \alpha_o) + (K_M\ell_m - K_N\ell_n)z \\ = \overline{L_T}(\dot{z} + \ell_T\dot{\alpha})\ell_T\dot{x} - B_M(\dot{z} + \ell_m\dot{\alpha})\ell_m \\ - B_N(\dot{z} - \ell_n\dot{\alpha})\ell_n - \mu(H - z)\{mg - \bar{L}\alpha\dot{x}^2 - \overline{L_T}(\dot{z} + \ell_T\dot{\alpha})\dot{x}\}\end{aligned}$$

Collecting like terms:

$$m\ddot{x} + (\bar{D}_1 + \bar{D}_2\alpha^2 + \mu\bar{L}\alpha)\dot{x}^2 + \mu\overline{L_T}(\dot{z} + \ell_T\dot{\alpha})\dot{x} = T - \mu mg \qquad \text{(A7.16a)}$$

$$\begin{aligned}m\ddot{z} + (B_M + B_N + \overline{L_T}\dot{x})\dot{z} + (K_M + K_N)z + (\overline{L_T}\ell_T\dot{x} + B_M\ell_m - B_N\ell_n)\dot{\alpha} \\ + (K_M\ell_m - K_N\ell_n + \bar{L}\dot{x}^2)\alpha = mg + (K_M\ell_m - K_N\ell_n)\alpha_o \qquad \text{(A7.16b)}\end{aligned}$$

$$\begin{aligned}mk_y^2\ddot{\alpha} - [\overline{L_T}\dot{x}\{\ell_T^2 + \mu(H - z)\ell_T\} + B_M\ell_m^2 + B_N\ell_n^2]\dot{\alpha} \\ + \{K_M\ell_m^2 + K_N\ell_n^2 - \mu(H - z)\bar{L}\dot{x}^2]\alpha \\ - [\overline{L_T}\dot{x}\{\ell_T + \mu(H - z) + B_M\ell_m - B_N\ell_n]\dot{z} + (K_M\ell_m - K_N\ell_n)z \\ = (K_M\ell_m^2 + K_N\ell_n^2)\alpha_o - \mu(H - z)mg \qquad \text{(A7.16c)}\end{aligned}$$

Equations (A7.16) are a set of three simultaneous, non-linear, differential equations. Compete solution of these general equations requires a numerical analysis as would he the case anyway if the shock strut characteristics are more accurately represented.

One possible approach is to simplify the equations so that an analytic solution can be applied for a given, small. increment of time, followed by successive corrections until convergence is obtained. This is discussed in the next section.

A7.9 Simplification and solution of the equations of motion

A7.9.1 Decoupling of the longitudinal equation and linearization

Considerable simplification of the equations of motion is possible if it is assumed that during the short period of time between the initial impact and the development of the maximum vertical reaction the forward velocity, x, is constant. This effectively implies that the thrust is equal to the sum of the aerodynamic and ground friction drags. This is not likely to be the case but nevertheless the assumption may be justified for the short period of time involved. The consequence of it is that the longitudinal equation, (A7.16a), disappears and all the terms in x become constant in the other two equations. For simplicity write:

$$\begin{aligned} \bar{L}\dot{x}^2 &= \bar{\bar{L}} = \text{ a constant} \\ \bar{L}\dot{x} &= \bar{\bar{\mathrm{L}}} = \text{ another constant} \end{aligned} \tag{A7.17}$$

A further simplification may be made to complete the linearization of Eqns (A7.16b) and (A7.16c). This is that:

$$H \gg z \tag{A7.18}$$

when the two appear together in the term $(H - z)$.

Again this may not always be true but it is justified by the simplification implied. The vertical translation and pitch rotation equations now become:

$$\begin{aligned} &m\ddot{z} + (B_M + B_N + \bar{\bar{L}})\dot{z} + (K_M + K_N)z + (\bar{\bar{L}}_T\ell_T + B_M\ell_m - B_N\ell_n)\dot{\alpha} \\ &\quad + (K_M\ell_m - K_N\ell_n + \bar{\bar{L}})\alpha = mg + (K_M\ell_m - K_N\ell_n)\alpha_0 \end{aligned} \tag{A7.19}$$

$$\begin{aligned} &mk_y^2\ddot{\alpha} - \{\bar{\bar{L}}_T(\ell_T^2 + \mu H\ell_T) + B_M\ell_m^2 + B_N\ell_n^2\}\dot{\alpha} + (K_M\ell_m^2 + K_N\ell_n^2 - \mu H\bar{\bar{L}})\alpha \\ &\quad - \{\bar{\bar{L}}_T(\ell_T + \mu H) + B_M\ell_m - B_N\ell_n\}\dot{z} + (K_M\ell_m - K_N\ell_n)z \\ &= (K_M\ell_m^2 + K_N\ell_n^2)\alpha_0 - \mu Hmg \end{aligned} \tag{A7.20}$$

A7.9.2 Solution of linearized equations

Equations (A7.19) and (A7.20) are now linear simultaneous equations of similar form to those developed for the flightdynamics and discussed in Chapter 4, Section 4.6.1, and Appendix A4. They may he solved by use of the differential operator, $\mathscr{D}$. Inspection of either of the equations shows that the Particular Integral is $\mathrm{a} = \mathrm{a}$, since the lift is equal to the weight at the time of the impact.

It is convenient to write the equations in the simplified form:

$$(A\mathcal{D}^2 + B\mathcal{D} + C)z + (D\mathcal{D} + E)\alpha = F$$
$$(G\mathcal{D} + H)z + (J\mathcal{D}^2 + K\mathcal{D} + L)\alpha = M \qquad \text{(A7.21)}$$

where

$$A = m \qquad G = -\overline{\overline{L_T}}\{\ell_T + \mu H) + B_M\ell_m - B_N\ell_n$$
$$B = B_M + B_N + \overline{\overline{L}} \qquad H = K_M\ell_m - K_N\ell_n$$
$$C = K_M + K_N \qquad J = mk_y^2$$
$$D = \overline{\overline{L_T}}\ell_T + B_M\ell_m - B_N\ell_n \qquad K = \overline{\overline{L_T}}\{\ell_T^2 + \mu H\ell_T\} + B_M\ell_m^2 + B_N\ell_n^2$$
$$E = K_M\ell_m - K_N\ell_n + \overline{\overline{L}} \qquad L = K_M\ell_m^2 + K_N\ell_n^2 - \mu H\overline{\overline{L}}$$
$$F = mg + (K_M\ell_m - K_N\ell_n)\alpha_o \qquad M = (K_M\ell_m^2 + K_N\ell_n^2)\alpha_o - \mu Hmg$$

When the light-hand sides of Eqns (A7.21) are set to zero and the second equation is used to eliminate z, the Complementary Function solution in a becomes:

$$\{AJ\mathcal{D}^4 + (AK + BJ)\mathcal{D}^3 + (AL + BK + CJ - DG)\mathcal{D}^2$$
$$+ (BL + CK - EG - DH)\mathcal{D} + (CL - EH)\}\alpha = 0 \qquad \text{(A7.22)}$$

This equation may be solved with the following boundary conditions used to derive the values of the constants:

$$(\alpha)_{t=0} = a\,, \qquad (\dot{\alpha})_{t=0} = 0 \qquad (z)_{t=0} = 0 \qquad (\dot{z})_{t=0} = V_v$$

The analysis is directly applicable to a two-point landing on the main-wheels only by substituting $K_N = B_N = 0$ where necessary. However, at some time during the landing the nose-wheel will contact the ground, and there is a discontinuity in the analysis. From this time onward the values of K , and B_N must be included.

A7.10 Comments

The analysis presented in this appendix is limited to a symmetric landing condition, the motion out of the plane of symmetry not being considered. Nevertheless the approach may he readily adapted to include the three out of plane degrees of freedom. such as would be required if a one-wheel landing condition is to be investigated. Some simplification may well be possible, for example hy considering only the main landing gear loads and neglecting the pitching effects.

Analysis of unconventional landing gear configurations does not introduce any other effects.

CHAPTER 8

Loading on individual airframe components

8.1 Introduction

Chapters 5, 6, and 7 outline the derivation of the overall airframe loading consequent upon the application of the flight manoeuvre, atmospheric turbulence, and ground loading requirements, respectively. The aerodynamic and inertia forces have to be distributed appropriately across the various airframe components in order to derive the information needed to undertake the structural analysis. Air-load distribution is discussed in Chapter **9** and the derivation of the stressing data in Chapter 12.

In addition to the cases covered in the three previous chapters there are a number of other matters which may have to he considered. These may give rise to overall airframe loading or they may be specific conditions for particular components. This chapter outlines these additional issues, primarily in the context of the individual airframe components.

8.2 Additional overall considerations

8.2.1 Longitudinal acceleration and deceleration

8.2.1.1 General comments

In many respects longitudinal acceleration conditions do not cause a significant overall loading of the airframe but they do affect local components such as the attachments of point loads. For the majority of aircraft the maximum forward acceleration case derives from the thrust of the powerplant, often in the initial take-off condition. Likewise the most severe overall longitudinal deceleration condition occurs in the emergency braking case, typically no more than about $0.65g$. The important point in the interpretation of these

cases is the need to ensure that there is adequate strength in the connections between the individual airframe components, such as the drag loading of the wing–body joint.

More severe loading cases occur when the aircraft is required to operate under assisted take-off and arrested landing conditions. The overall acceleration values in these conditions depend upon the mass of the aircraft and the performance of the catapult and arresting gears, respectively. It is important to consider the dynamic effects arising from the rapid application of the loading. Typical arrester gear decelerations are of the order of 4–6g. The usual proof and ultimate factors apply.

8.2.1.2 Emergency alighting

Emergency alighting cases are sometimes, incorrectly, referred to as crash cases. These requirements are solely intended to protect the occupants in the event that the aircraft comes to an abrupt stop while on, or in close proximity to, the ground. That is, they only cover the eventuality of incidents during take-off and landing. In general the stipulations are applied to:

(i) occupant seats;
(ii) safety harnesses (seat belts);
(iii) seat attachments and local fuselage structure, especially floors;
(iv) items of equipment and components, 'such as engines, which should they become detached could inflict injury upon the occupants;
(v) fuel systems, which should they he ruptured may present a fire hazard to the occupants.

There are some differences in the requirements for combat aircraft as compared with transport and general aviation types.

A. United Kingdom military *aircraft – Def.Stan.00-970* Chapter 307

Details of the impulse conditions at crew stations are specified as well as overall deceleration conditions for the design of crew and passenger seats, harnesses, and local attachment fittings. These depend upon the category of the aeroplane:

A Aeroplanes with ejection seats
B Light aeroplanes without ejection seats
C Transport and other large aeroplanes without ejection seats.

The design deceleration factors are quoted in Table 8.1 and are ultimate conditions. It is also specified that fuel and other hazardous fluids must be contained in a crash. (Def.Stan.00-970 Leaflet 702/5).

B. Civil *aircraft – JAR-25.561* and *562*

The civil aircraft emergency alighting case specifies design requirements for critical structure, based on occupant conditions, as:

6.0*g* downward to 3.0*g* upwards
9.0*g* forward to 1.5*g* aft
Zero to 3.0*g* sideways, on the airframe and 4.0*g* sideways, on the seats

Table 8.1 Inertial factors for the static design of relevant components for military aircraft

Direction	Category A	Category B	Category C
Longitudinally forward	25g	9.0g	9.0g
Longitudinally aft	10g	5.5g	5.5g
Laterally	10g	5.5g	7.0g
Vertically down	25g	14.5g	12.5g
Vertically up	10g	4.52	3.5g

The derivation of the actual design cases for the seats and harnesses is complex, but is likely to result in deceleration conditions at the floor of the order of *14g* vertically and *16g* forward and aft, with the sideways component.

8.2.2 Spinning

Some aircraft must be designed for the loads experienced during spinning and recovery from spins. Design for spinning is primarily limited to light utility/aerobatic and training aircraft. The United Kingdom military requirements, at Def Stan.OO-970 Chapter 207, prescribe design loading cases. In the absence of better information these may he read across to relevant civil types. Spins usually occur at low forward speed and consequently the usual aerodynamic loads are small. However, secondary aerodynamic and inertial loading can be high.

The most adverse combinations of yaw, pitch, and roll rotations, allowing for unsteadiness during a spin, have to be considered. Leaflet 207/1 suggests a spin rate of:

$$\Omega_S = [18.3\bar{V}c/(k_z^2 - k_x^2)]^{1/2} \quad \text{rad/s} \tag{8.1}$$

where

c is the wing mean chord
$\bar{V}$ is the tail volume coefficient (see Chapter 4, Section 4.3.1)
k_x and k_z are the radii of gyration about the stability x' and z' axes, respectively

All the linear dimensions are in metres; Ω_s is based on the assumption that the aircraft descends with its longitudinal axis at *60°* to the vertical, and with its lateral axis horizontal.

During recovery from the spin the aircraft longitudinal axis is assumed to be vertical (nose-down) and the most adverse rate of rotation about the axis has to be considered. Leaflet 207/1 suggests a roll rate of 5 rad/s in the absence of better data.

The usual proof and ultimate factors apply.

8.2.3 Ground handling loading

8.2.3.1 General remarks

These cases cover the loads likely to be experienced during transport, maintenance, and ground operations generally.

8.2.3.2 Slinging

(a) ***United Kingdom military aeroplanes – Def.Stan.00-970 Chapter 308.*** The whole aircraft (when so required in the Specification) or any component of all aircraft shall be designed Io be lifted using proof and ultimate factors of 2.25 and 3.0, respectively. For naval aircraft the factors are **3.0** and 4.0. respectively.

(b) ***Civil aircraft.*** The above factors may be used if required.

8.2.3.3 Jacking

(a) ***United Kingdom military aeroplanes – Def.Stan.00-970 Chapter 308.*** The same factors apply as for slinging, with loads misaligned up to 10" from the nominal direction.

(b) ***Civil aircraft.*** Again the military factors are appropriate.

8.2.3.4 Towing and transportation

Aircraft are normally towed using attachments to the landing gear. For this reason the towing load cases are covered in Chapter 7, Section 7.5.6.

8.2.3.5 Parking – Def.Stan.00-970 Chapter 310

It is necessary to be able to park military aircraft and picket them at three points. These three points and the surrounding structure shall have an ultimate factor of 1.5 when the aircraft is held in a 40 m/s wind blowing from any direction. There are special loads for parking on aircraft carriers.

8.2.3.6 Maintenance and assembly

In certain cases parts of the structure are removed for maintenance. Sometimes special 'jury' structure is used to support the weight of the components during this operation. It is recommended that the jury structure and any associated parts of the main structure should have an ultimate factor of 3.0 vertically and 2.0 laterally under the component weights. Stiffness considerations may well override these strength requirements.

8.2.4 Crashworthiness

The primary aim of crashworthiness is to maximize the possibility of occupant survival in the event of an accident to an aircraft. For convenience the description may he

extended to cover the consequences of an in-flight incident, such as a mechanical failure of a powerplant or a bird strike. The main considerations are:

(a) The strength and distortion of occupant accommodation in an emergency alighting, see Section 8.2.1.2.
(b) The location of powerplants to minimize the impact of a failure on the occupants, aircraft systems, and other powerplants, see Section 8.5.5.
(c) Fuel tank location to minimize fire risk and damage from mechanical failures, see Section 8.3.3.
(d) Survivability in the event of a bird strike, see Sections 8.3.2, **8.4.4,** and **8.5.4.**

8.3 Lifting surfaces

8.3.1 Introduction

8.3.1.1 General

The major loads on the lifting surfaces are derived from the flight manoeuvre and atmospheric turbulence cases. In addition to these overall loads spinning may be of significance, where it is relevant, as may be the ground loads defined in Chapter **7,** Sections **7.4** to 7.7. There are also certain other, often local, loading conditions, which are outlined subsequently.

The primary cases for the lifting surfaces are defined in the following sections.

8.3.1.2 Wing

The design conditions derive from the superposition upon the loading in the trimmed condition, (Chapter 3, Section **3.2,** with a normal acceleration factor, n, having a value of unity), of the loads due to symmetric and rolling manoeuvres with the values of n given by Chapter **3,** Sections **3.2** and **3.3,** or the atmospheric turbulence conditions specified in Section **3.5.** The latter may he due to discrete gust requirements (Chapter **3,** Sections **3.5.2.1** and 3.5.2.2) or continuous turbulence (Section 3.5.2.3), as analysed in Chapter **6,** Sections **6.2** and **6.3** or 6.4, respectively.

8.3.1.3 Horizontal stabilizer and control

As is the case of the wing there is the basic trim load given in Chapter **4,** Section **4.2.** The additional loading due to manoeuvres depends upon the mode of operation of the control surface and is summarized in Chapter 5, Section **5.3.6.** Section **5.3.7** outlines the derivation of the manoeuvre loads on trailing edge control surfaces. The atmospheric turbulence case, whether a result of discrete gusting or continuous turbulence. is as given for the wing in the previous section. The asymmetric loads are detailed in Chapter **5.** Section 5.6.

8.3.1.4 Vertical stabilizer and control

Unlike the horizontal lifting surfaces it is usually assumed that there are no loads on the vertical surface in steady level flight conditions, although this may not be strictly true

when slipstream effects are present. The loads in manoeuvres are derived as described in Chapter 5. Section 5.5, the basic requirements being defined in Chapter 3, Sections 3.3 and 3.4. Preferably continuous turbulence conditions are applied for the atmospheric turbulence case as specified in Chapter 3, Section 3.5.4 and analysed in accordance with Chapter 6, Section 6.4. The loading of the yaw motivator, the rudder, is given by Chapter 5, Sections 5.3.7 and 5.5.4.

8.3.2 Bird strikes

8.3.2.1 Introduction

The leading edge of the wing, and possibly those of the other lifting surfaces, has to be designed to withstand the impact of a bird strike. There are some differences between the military and civil requirements in this respect.

8.3.2.2 United Kingdom military requirements – Def.Stan.00-970 Chapter 209

The requirements are intended to ensure that in the event of a single bird strike the aircraft will he able to complete its mission, albeit with some degradation of performance. The bird to be considered is of 1 kg mass. The analysis of forces resulting from the strike is assumed to he proportional to bird mass, impact footprint, and the square of the impact velocity. The bird strike design speed is defined as V_M where V_M is the lesser of 246 m/s (480 knots) true air speed or the maximum normal mission speed of the aircraft at altitudes up lo 762 m (2500 ft). The application of the requirement depends upon the airframe component being considered:

(a) Leading *edge fixed* structure. No damage which prevents the completion of the mission up to speed V_M.
(b) *Moveable* leading edge devices. When closed, no damage preventing mission completion up to 0.9 V_M and recovery of the aircraft at V_M. When open, recovery of the aircraft up to the lesser of V_M or the appropriate design speed for the devices.
(c) *Systems.* No damage to critical flight instruments, sensors, and fuel system, and no fire or failure to operate the landing gear up to V_M.

The cases are applied with the aircraft either in straight and level Right or at the maximum yaw and pitch angles associated with the mission.

8.3.2.3 Civil transport aircraft – JAR-25.631

The civil requirements are less specific and arc stated to apply to the aircraft in general. A 1.8 kg (4 lb) bird is specified to be encountered at the design cruising speed, V_C, at sea level, or 0.85 V_C at 2440 m (8000 ft) altitude, whichever is most critical. It is suggested that care should be taken to avoid the location of critical systems components immediately behind regions of a likely bird strike.

8.3.2.4 Compliance

Design for compliance with bird strike requirements is difficult. Ultimately it is usually based on direct testing or a read across from previous tests on comparable components. Some semi-empirical methods of analysis of fixed structure are available for initial design purposes. One such method, extracted from United Kingdom Royal Aerospace Establishment Report TR 72056 (1972). gives the required thickness of theleading edge as:

$$t = 0.02 V_M m^{1/3} f(Mat) \cos^{2/3} \theta / [\exp\{1230/(r^2 + 30r + 1000)\}] \qquad (8.2)$$

where

t is the thickness of the leading edge (mm)
r is the leading edge nose radius (mm)
m is the mass of the bird (kg)
V_M is the impact velocity (m/s)
θ is the inclination of the impact direction normal to surface
f (Mar) is a material factor defined as $0.8[f_1(\text{L73})/f_1(Mat)]$ where $f_1(Mat)$ is the 0.1% proof stress of the chosen material and $f_1(\text{L73})$ is that of the light alloy material specification L73.

8.3.3 *Fuel systems – integral and bag tanks*

8.3.3.1 Refuelling case

During refuelling substantial pressures may occur in the delivery lines and tanks, 3.45 bar (50 lb/in^2) being the accepted design value. Pressure relief valves are normally incorporated to avoid this case in as much of the system as possible.

8.3.3.2 United Kingdom military aircraft tank cases – Def.Stan.00-970 Chapter 702

Integral tanks and the structural compartments for bag tanks must be designed to proof and ultimate factors of 1.5 and 2.0, respectively, under loads resulting from internal pressure. Emergency alighting cases apply if a failure would affect the occupants.

Drop tanks must be designed to withstand the normal flight manoeuvre cases, unless special conditions are specified.

8.3.3.3 Civil transport tank cases – JAR-25.963, 965, and 967

General requirements for strength and installations are specified. A maximum test pressure of 0.24 bar (3.5 lb/in^2) is quoted.

8.3.3.4 Fuel tank location

The location of fuel tanks should allow for the possibility of tank rupture as a consequence of bird strike, mechanical damage. or emergency alighting. The aim must

be to minimize the chances of fuel leakage and the consequent fire hazard. Location may also be affected by aeroelastic considerations where it is usually desirable to keep large masses forward on the chord of a lifting surface, see Chapter 11, Section 11.6.

8.3.4 Loading of control surfaces and high-lift devices along the effective hinge-line

The civil requirements specify accelerations to he assumed parallel to the hinge-lines of auxiliary surfaces for the purpose of designing the hinge brackets. These are given in JAR-25.393:

(i) for vertical surfaces the acceleration is 24g;
(ii) for horizontal surfaces the acceleration is $12g$

8.3.5 Control surface tail to wind case

Trailing edge control surfaces have to he designed for a case where the aircraft is parked with the tail facing in the wind direction. The wing speed may he up to 40 m/s and the case can be severe due to the fact that the centre of pressure on the surface may be relatively far aft. The control stops are often designed by this case.

8.3.6 High-lift devices

8.3.6.1 Introduction

It is necessary to consider not only the loads on the high-lift devices themselves. but also the effect upon the structure as a whole. The stressing cases are numerous due to the large number of variables, such as flight conditions. speed, flap and slat position, and engine conditions. There is some similarity between the military and civil requirements. Alleviated sharp-edged gust analysis is acceptable for the evaluation of gust loads.

8.3.6.2 United Kingdom military requirements – Def.Stan.00-970 Chapter 205

The operating mechanism and high-lift devices are designed in relation to specified device positions and aircraft speeds. The positions are (references in { } are to paragraphs in Def.Stan.00-970 Chapter 205):

(i) retracted {paragraph 3.6.1};
(ii) take-off (paragraphs 3.2.1(a) and 3.6.2};
(iii) intermediate or 'baulked' approach position {paragraphs 3.2.1(b) and 3.6.2};
(iv) landing {paragraphs 3.2.1(c) and 3.6.2}.

The speeds are:

(i) retracted position, V_D;

(ii) take-off, V_{TO}, which is the lesser of 1.15 times maximum speed attained before the device can be retracted or 1.6 times stalling speed at the maximum mass with device at the take-off position;
(iii) intermediate, V_{BL}, which is the greater of the speed attained in a baulked landing before the device can be retracted or 1.8 times the stalling speed at the landing mass in this case;
(iv) landing. V_{FL}, which is the greater of 1.8 times the stalling speed at the landing mass. in this case, or 1.4 times the stalling speed with the device retracted.

The strength is determined in the following flight conditions:

(a) Retracted, full normal envelope.
(b) Devices used en route or in combat, full normal envelope, except that speeds V_A, V_C, V_D, V_G, and V_H can allow for the effect of the deployed high-lift device.
(c) Other positions, defined above, at appropriate speeds:
  (i) manoeuvring to $4g$ for combat aircraft and $2g$ for others;
  (ii) positive and negative gusts of 7.6 m/s (25 ft/s).

Allowance must he made for slipstream. jet efflux, and the effect of a head-on gust of 7.6 m/s (25 ft/s).

The proof and ultimate factors are 1.125 and 1.5, respectively, except for a training aircraft where factors of 1.5 and 2.0 are applied to a case at speed V_{BL} with the position of the device between intermediate and landing.

8.3.6.3 Civil aircraft: transport types – JAR-25.345

A design flap speed, V_F, is defined in JAR-25.335 for each flap setting as not less than:

(i) 1.6 times the stalling speed at the maximum take-off mass with the flaps in the take-off position; or
(ii) 1.8 times the stalling speed at the landing mass with flaps in the approach (intermediate) position; or
(iii) 1.8 times the stalling speed at the landing mass with landing flap position.

The strength requirements are similar to the military ones with a checked manoeuvre to $2g$ but there is an additional condition of a manoeuvre to $1.5g$ at the maximum mass with the high-lift devices in the landing configuration.

8.3.6.4 Civil aircraft: general aviation types – JAR-23.345

The requirements of JAR-23 are basically similar to those of JAR-25 except that the design flap speed is the greater of:

(i) 1.4 times the stalling speed at the take-off mass with the flaps retracted; or
(ii) 1.8 times the stalling speed at the take-off mass with landing flap position.

8.3.7 Wing-mounted spoilers and air-brakes

The wing design of many transport aircraft incorporates spoilers. some of which may also be used as air-brakes. The primary use of spoilers is to reduce lift at the instant of touchdown although they may he employed in some cruise conditions. Air-brakes are used to control speed throughout the flight envelope. but especially to increase drag at touchdown so that when they are used with spoilers the landing run is reduced. Air-brakes intended for use at higher speeds often incorporate a device in the actuator system to ensure that the load does not exceed a predetermined, limiting, value.

For military aircraft Def.Stan.00-970 Chapter 205. paragraph 4.2, specifies two design possibilities:

(a) Airbrake fully extended at speed V_D when no load limiter device is fitted; OR
(b) When a limiter device prevents full extension above a speed V_B:
  (i) airbrake extended as far as permitted by the device at V_D;
  (ii) airbrake fully extended at 1.15 V_B or V_D, whichever is less.

In the case of civil transport types, JAR-25.335 requires that the air-brake design speed with full air-brake extension is V_{DD}, where V_{DD} is appropriate to any load limiting condition except that it must not be less than V_D if the air-brake is to be used at high speed.

8.4 Fuselages

8.4.1 General comments

With the possible exception of the powerplant installation the loading conditions to be considered for the structural design of the fuselage are the most complex of any component. It is necessary to investigate all of the cases outlined in Chapters 5.6, and 7 and referred to in Section 8.1. The bending and torsion design of the rear fuselage is determined by the loads on the horizontal and vertical tail surfaces, although nearer to the rear wing attachments the main landing gear loads may prove to be more critical. The bending and torsion of the forward fuselage derives from the nose landing gear and, where relevant, the fore-plane. Loads transmitted from the wing and, possibly, the one-wheel landing case are major Factors in the loading of the centre fuselage. The matter is further complicated when the powerplants are mounted within, or on, the fuselage as the contribution from this source is then likely to be significant.

A loading condition associated with many aircraft is the pressurization of the payload volume, which often occupies much of the fuselage. This is dealt with in Section 8.4.3.

8.4.2 Deceleration cases

There is a general discussion of deceleration conditions in Section 8.2. Of special relevance to the design of the fuselage is the emergency alighting case, Section 8.2.1.2, to which reference may be made.

8.4.3 Pressurization

8.4.3.1 Introduction

In the case of some general aviation aircraft and military combat and training types the pressurized compartment may be limited to the region of crew occupancy. More usually when pressurization is a requirement it involves the greater part of the volume, and hence the structure, of the fuselage.

8.4.3.2 United Kingdom military requirements – Def.Stan.00-970 Chapter 716

Two standards of cabin pressurization are laid down, low differential and high differential pressure.

(a) ***Low differential pressure.*** The pressurization must start at an altitude of 1.5 km and the differential pressure must ensure that a cabin altitude not exceeding 6.7 km is maintained to the service ceiling or the maximum operating altitude. The differential pressure shall not be less than 0.276 bar (4 lb/in^2).

(b) ***High differential pressure.*** The differential pressure shall be the greater of that required to maintain a cabin altitude of 1.85 km to the maximum cruising altitude or 2.5 km to the service ceiling. The rate of change of pressure must not exceed 0.02 bar/min (0.3 lb/in^2 per min) for the transport aeroplanes and 0.07 bar/min (1 lb/in^2 per min) for other types.

Two strength cases are laid down:

(a) At any given height an ultimate factor of 1.5 shall be achieved under the combination of any pressure up to the most severe contingency at the maximum altitude, any local pressure due to airflow and the inertia and flight loads of the most severe case at that altitude. The pressure must allow for relief valve tolerances and blockages.

(b) An ultimate factor of 1.5 is required when the cabin pressure falls to 0.07 bar (1 lb/in^2) below atmospheric.

In both of these cases the aircraft speed is to be the design speed. V_D. Fatigue must be considered. At one time it was a requirement to test the cabin to twice the working differential pressure as part of the fatigue qualification procedure.

8.4.3.3 Civil aircraft – JAR-25.365 and JAR-23.365

The former United Kingdom civil requirements (BCAR Section D3-7), required the pressure cabin to be tested to twice the working differential pressure. In addition to compliance with static strength, a repeated loading test requirement was specified. It was also necessary to carry out a static acceptance test at 1.33 times the differential pressure with the flight loads. Tests had to be undertaken aimed at establishing either that any cracks did not result in catastrophic failure or that the cabin had an adequate life, inclusive of a life factor.

The current requirements in **JAR-25** are less specific about means of compliance but the static test to 1.33 times the working differential pressure is retained with various other cases.

8.4.4 Bird strikes

8.4.4.1 General comments

The overall requirements stipulated to cover the eventuality of bird strikes are outlined under the lifting surfaces at Section 8.3.2, to which reference should be made. The specific implications for fuselage components are dealt with in Sections 8.4.4.2 and 8.4.4.3.

8.4.4.2 United Kingdom military aircraft – Def.Stan.00-970 Chapter 209

(a) ***Forward facing transparencies.*** There should be no unacceptable loss of vision, no cracking, and no deflection resulting in contact with internal items up to the speed V_M. Further there should be no shattering or penetration up to 1.1 V_M (except for non-load carrying items).

(b) *Transparency supports.* At speeds up to V_M there must be no permanent deformation affecting airworthiness or resulting in debris likely to he ingested by the engines.

(c) *Forward fuselage.* There should be no appreciable damage up to 0.7 V_M and no penetration at V_M.

(d) *Systems.* No damage to critical flight instruments, sensors, fuel system, occupants. and no fires or failure to operate the landing gear up to V_M.

8.4.4.3 Civil aircraft

The requirements for the fuselages of civil aircraft are covered in Section 8.3.2.3

8.4.4.4 Design of transparencies to meet the bird strike requirements

Some design formulae relevant to the design of transparencies to meet the bird strike conditions are presented in Appendix A8.

8.4.5 Freight loading conditions

The United Kingdom military aircraft requirements include provisions for the design of freight loading and attachments, Def.Stan.00-970 Chapter 719.

Freight loads are very dependent upon the particular usage envisaged for the aircraft. Floors, doors. or structure loaded when the aircraft is standing on the ground during freight loading or unloading must have an ultimate factor of 3 under the loads developed.

Freight lashing and tie-down points must be designed to the following accelerations to cover normal acceleration and emergency landing cases:

(i) 1.5*g* forward to 3.0*g* aft;
(ii) 1.5*g* laterally, to he taken independently or in combination with (i) above;
(iii) 2.0*g* downwards (normal).

The ultimate factor is unity but the usual aircraft take-off and landing load cases also apply.

Tie-down points are usually arranged on a 0.51 m (20 in) grid system and attachment fittings are available for ultimate loads of 22 270 N, 44 540 N, and 111 250 N; 1 tonne webbing is also used. The disposition and combination of these loads on the grid will depend upon user requirements.

8.5 Powerplant installations – engine mounting loads

8.5.1 Introduction

As suggested in Section 8.4.1 the loading cases for powerplant installations are complex. In general it is necessary lo consider all the flight manoeuvre, gust, and ground load cases combined with engine thrust and torque and the gyroscopic effects due to the combination of aircraft and engine rotations.

The mountings of primary and auxiliary powerplants have to be designed for the combination of loads which arise from:

(i) thrust, forward and reverse;
(ii) engine torque, including the excess torque due to a malfunction;
(iii) gyroscopic couples due to the angular motion of the aircraft;
(iv) inertia forces, due to linear and angular accelerations including emergency alighting cases where appropriate;
(v) aerodynamic forces and moments due to propellers including the effect of their inclination to the air-stream;
(vi) air-loads on nacelles:
(vii) structural flexibility;
(viii) thermal effects.

8.5.2 United Kingdom military aircraft – Def.Stan.00-970 Chapter 200, paragraph 8 and Leaflet 200/3

Leaflet 200/3 gives guidance on the interpretation of the effects outlined in the previous section, especially in relation to the evaluation of torque, gyroscopic couples, and inertia loads. A summary of the recommended loading cases is given in Table 8.2.

Table 8.2 Summary of recommended loading cases

Case	Forward speed	Angular velocity	Normal acceleration coefficient	Engine conditions
1A Recovery from dive	$V_S n_1^{1/2}$	$gn_1^{1/2}/V_S$	n_1	Max. power
1B Recovery from inverted dive	$V_{S(in)} n_3^{1/2}$	$-gn_3^{1/2}/V_{S(in)}$	n_3	(with or without torque limit)
2 Flight in gusts	Appropriate to max. gust factor	Zero	Max. positive and negative values	Max. continuous cruise (thrust and torque)
3 Spinning				
a) Trainers and fighters	Zero	Rates of yaw and roll as given in Section 8.2.2	$3.33 < n < n_1$	Max. power and max. rotational speed
b) All others	Zero		$2.67 < n < n_1$	
4 Static (take-off)	Zero	Zero	1.0 ($\pm$ 1.5 Carrier aircraft)	As Case 1
5 Yawing manoeuvres	Max, appropriate speed	Zero, but with max sideslip from the lateral case	1.0	Max. power and limit torque
6 Propeller braking	$1.2V_{SFL}$	Zero	See note below	Man. power with reverse pitch
7 Landing	$1.2V_{SFl}$	Zero	See **note** below	Idling
8 Side load (see note below)	Zero	Zero	Zero	Not applicable
9 Excess torque	Max. climb speed	Zero	1.0	Max. power with excess torque

Notes:

Case 1. V_S is stalling speed in level Right. flaps retracted.

$V_{S(in)}$ is stalling speed in inverted flight. flaps retracted.

Cases 6 and 7: V_{SFL} is stalling speed in level flight with Raps at the landing setting.

The normal acceleration component in these cases should include dynamic effects where appropriate. Fare and aft and lateral deceleration effects should be included.

Case 8: The overriding side load limit load factor should not he less than the lower of 1.33 or $0.33n_1$. No other loads need be considered.

Case 9: The 'excess' torque case is severe md is usually that required to stop the main rotating assembly of the engine in 0 3 s. In the care of turbo-prop engines the inertia of the gearbox/propeller assembly is excluded from this requirement

8.5.3 *Civil aircraft – JAR-25 and JAR-23 paragraphs 361, 363, and 371*

The requirements are concerned with torque cases, and side and gyroscopic loads.

The torque cases have to be associated with flight loads at point A on the flight envelope (speed V_A and acceleration factor n_1). The design torque is dependent upon the type of engine and different factors are applied to cover dynamic effects. A likely critical case for a turbine engine is when there is a sudden stoppage due to seizure of the rotating parts. A somewhat high stopping time of 3 seconds is quoted for transport aircraft.

The side load is applied independently of the other conditions and must not be less than a load factor of 1.33 or 0.33 n_1, whichever is the greatest.

JAR-23.371 states that gyroscopic couples must be considered with symmetric and asymmetric manoeuvre and gust cases. Design aircraft rotation rates and accelerations are given. In addition to the usual manoeuvre and gust cases they include all the possible combinations of:

(i) a yaw velocity of 2.5 rad/s;
(ii) a pitch velocity of 1.0 rad/s;
(iii) a normal load factor of *2.5;*
(iv) maximum continuous thrust.

Aerohatic aircraft cases may override these

8.5.4 Bird strikes – Intakes

The United Kingdom military aircraft requirements for bird strike protection referred to in Section 8.3.2.2 stipulate that there should be no appreciable damage to intakes up to 0.7 V_M, and nothing resulting in any detraction of performance up to V_M, including the operation of moving parts.

8.5.5 Location of powerplants

The location of powerplants, especially in the case of multi-engined aircraft. must take account of the effect of a mechanical failure. such as a fan disc burst, and ensure that there is no consequent critical damage to the airframe, systems, and other powerplants or injury to the occupants. The various design codes give guidelines on the implication of this requirement. It can have a major impact upon the span-wise and chord-wise location of wing-mounted powerplants and clearly rules out the use of an adjacent pair of engines as has sometimes been used in the past. The provisions of Section 8.2.1.2. apply when the detachment of a powerplant in an emergency alighting could result in injury to the occupants.

Appendix A8 Design formulae for transparency design under bird strike conditions

A8.1 Introduction

A number of references are available which quote empirical formulae for the estimation of windscreen thickness as a function of bird size, impact speed, windscreen material, and geometry. Comparison between these is difficult, partly because of the use of different units and partly because of the numerous details in testing which influence the result. This latter is particularly true of panel dimensions and edge conditions. However, there are some general trends appearing from the work. The windscreen thickness is generally found to be proportional to bird mass to the power of 0.333 and the cosine of

the impact angle relative to the normal to the local tangent at the windscreen surface. While variations on these relationships appear, the effect is not significant over the range of values which have been tested.

There are two basic concepts of windscreen design:

(a) rigid, where the concept is that the bird is bounced off the windscreen.
(b) flexible, where the bird impact is absorbed and the debris caught by the windscreen material; this implies a laminated screen with flexible interlayers, usually of polyvinylbutyryl (PVB).

Three classes of material are available:

(i) toughened and tempered glass, possibly of high strength achieved by chemical addition or special treatment;
(ii) acrylic, usually employed in the stretched form for the windscreen, but sometimes cast for side panels;
(iii) polycarbonate.

A useful reference in relation to glass and acrylic windscreens is that by M. J. Mott contributed to the Society of British Aerospace Constructors (SBAC) Symposium on Optical Transparencies. June 1971. The value lies more in the detail of the test results than in the conclusions derived. These can be used as a check on various empirical formulae, the derivation of which is not given in detail. As always in testing there is considerable scatter and it is not easy to derive design criteria without being too conservative. Another reference on glass and acrylic is that by Poullain and Clamagirand, SBAC Symposium quoted above. Some work on polycarbonate is described by T. M. Young. Cranfield University, MSc Project Thesis, September 1988.

A8.2 Penetration formulae

A8.2.1 *Glass*

The formula proposed by Mott for glass windscreens, converted to SI units, becomes:

$$t = KV_M m^{1/3} \cos\theta \qquad \text{(A8.1)}$$

where

t is the thickness in mm
V_M is the impact velocity (m/s)
θ is the impact angle, as defined in Section 8.3.2.4
m is the bird mass (kg) (Note that Mott actually used a value of $m^{\frac{1}{3}}$, rather than $m^{\frac{1}{3}}$)

K is a material factor depending upon the actual glass, being 0.23 for conventional toughened/tempered glass and 0.18 for Triplex 'Ten-Twenty' glass. There is no significant difference between laminated and monolithic designs.

Clamagirand also quotes an empirical formula for glass windscreens. It is based on the use of a laminated screen and can be written in the form:

$$\Sigma(t_i C_i^{2/3}) = V_M^{1.33} m^{0.444} \lambda cos^{2/3}\theta \qquad \text{(A8.2a)}$$

where

t_i and C_i refer to the thickness and material constants for the various laminations
A is a panel shape factor, usually having a value of between 0.94 and 1.07
C is quoted as varying between about 260 for normal tempered glass to 300 for chemically strengthened glass, although it may be as low as 110 for annealed glass

When only tempered glass is used the equation may be written approximately as:

$$t = 0.03 V_M^{1.33} m^{1/3} cos\theta \qquad \text{(A8.2b)}$$

for a typical set of values of 0 and m.

This gives similar results to that derived by Mott, Eqn. (A8.1), at above 340 m/s, but predicts less thickness at lower speed. There appears to be little justification for the $V_M^{1.33}$ dependence from the tests carried out by Mott and hence the formula should be regarded with caution since it covers the higher of Mott's values, rather than the mean.

A8.2.2 Stretched acrylic

Mott's experimental results show a tendency for a non-linearity of the required thickness with variation of speed up to about 130 m/s. The variation is approximately linear at higher speeds. One definite conclusion from the results is that monolithic screens are of significantly lower strength than laminated ones in this material. The formula dehved by Mott has the form:

$$t = 0.015 V_M^{1.5} m^{1/3} cos\theta \quad \text{(adapted on the same basis as glass)} \qquad \text{(A8.3a)}$$

Alternatively the results suggest:

$$t = 0.35(V_M - 80) m^{1/3} cos\theta \qquad \text{(for } V_M > 130 \text{ m/s)} \qquad \text{(A8.3b)}$$

Clamagirand gives an expression of the form:

$$tC^{1/2} = V_M m^{1/3} \lambda cos^{1/2}\theta \qquad \text{(A8.4a)}$$

In this case C is quoted as 32 and A as unity for flat screens, hut as low as 0.6 for wrap-around screens. Use of 32 for C appears to give optimistic results in companson with Mott's experiments and it is possible that this may be explained by a difference in

edge conditions. Using a somewhat lower value of C and allowing for the correction of $(cos^{1/2}\theta)$ suggests for A of unity:

$$t = 0.27V_M m^{1/3} cos\theta \tag{A8.4b}$$

A8.2.3 Polycarbonate

Young quotes as a reference United States Air Force report AFWAL-TR-80-3003 and extracts from it a formula due to Inglese and Wintermute' derived from tests at about 230 m/s. This is expanded to give:

$$t = 0.11(V_M - 85)m^{1/3}(\lambda cos\theta)^{1/2} \tag{A8.5a}$$

where A is a shape factor, typically quoted as 1.75.

Using A = 1.75 and correcting for $(cos^{1/2}\theta)$:

$$t = 0.18(V_M - 85)m^{1/3} cos\theta \tag{A8.5b}$$

Young also quotes investigations by Bosik.[1] There are two formulae, one for clamped panels, which is not a realistic windscreen application, and the other for bolted ones. This latter case quotes the thickness as a function of the cube of the velocity, and while it gives reasonable comparison with Eqns (A8.5) for lower speeds, it appears to become quite unrealistic above 200 m/s.

A8.3 Deflection analysis

Another arpect of windscreen design is to ensure that the deflection consequent upon bird impact does not result in contact with internal items. Deflection prediction requires a finite element analysis. Two relevant papers were presented to the SBAC Conference on Aerospace Transparencies, September 1980. These were:

(a) The role of finite element analysis in the design of bird strike resistant transparencies, B. S. West.
(b) Aircraft transparency bird impact analysis using the MAGNA computer program, R. E. McCarty.

[1] YOU~ T.M. (MSc Thesis, Cranfield University UK, 1988)

CHAPTER 9

Air-load distributions

9.1 Introduction

The analysis of the loading cases dealt with in Chapters 5, 6, and 7 and summarized in Chapter 8 leads to the derivation of the overall air loads on the various components of the aircraft, namely the. wing–body, the stabilizing. and the control surfaces. In order to convert these overall loads into stressing information it is necessary to distribute each of them across the relevant component. In practice this implies the determination of the air pressure distribution, this being a matter of aerodynamic analysis. The process is accomplished by using various analytical techniques such as panel methods and, with the advent of powerful computational aids, computational fluid dynamics (CFD). Before the availability of these advanced techniques it was necessary to use more approximate methods backed up, as now, by wind tunnel and flight testing.

The application of the more recent computational methods is beyond the scope of the present text. This chapter, therefore, presents only the earlier. simpler, approaches in order to discuss the important parameters and characteristics. In many cases the assumptions needed to apply these simpler techniques are sufficiently justified for the purposes of initial loading action analysis.

Most of the following is concerned with the pressure distributions over lifting surfaces in both subsonic and supersonic flow. The air loads on bodies in subsonic Row are generally small but are of importance because of the large associated pitching moments. In supersonic flow the body may be expected to develop significant au-loads.

9.2 General comments concerning lifting surfaces

A typical pressure distribution over one-half of an unswept wing in subsonic flow is illustrated in Fig. 9.1. For this case it is possible to consider the overall air-load distribution as being described by separately identifiable span-wise and chord-wise loadings. The former directly defines overall shear force and bending moments, while the latter the overall torque distrihution and local rib shear and bending.

For forward speeds below that at which shock waves begin to form on the aerofoil. the non-dimensional form (or shape) of the span-wise loading is largely determined by:

(i) plan-form geometry;
(ii) variation of effective local angle of attack of the aerofoil across the span due to built-in or structural twist, change of aerofoil shape or deflection of auxiliary surfaces, such as flaps and controls.

In this case, the non-dimensional form of the chord-wise loading depends mainly upon:

(i) the shape of the aerofoil, especially the camber;
(ii) the local angle of the aerofoil to the air-stream.

It is usually sufficient to represent an unswept wing of moderate aspect ratio by a so-called 'lifting Line' located at the quarter chord, described, for example, by Glauert.[1] See Fig. 9.2.

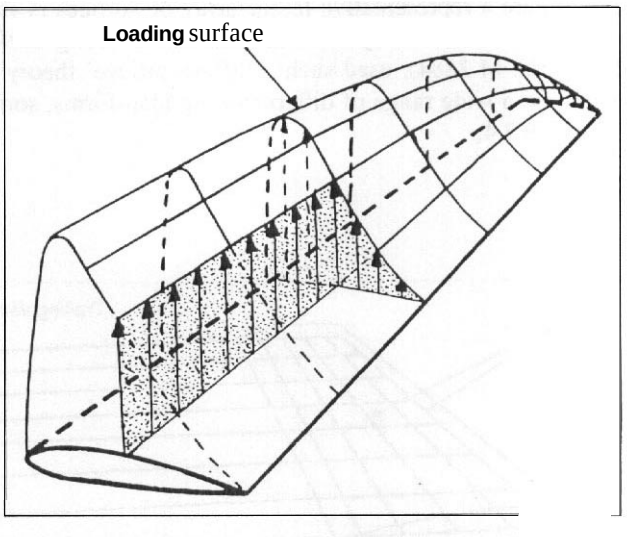

Fig. 9 . Span-wise and chord-wise loadings

[1] Glauert, H. The Elements of Aerofoil and Airscrew Theory. Cambridge University Press. 1948.

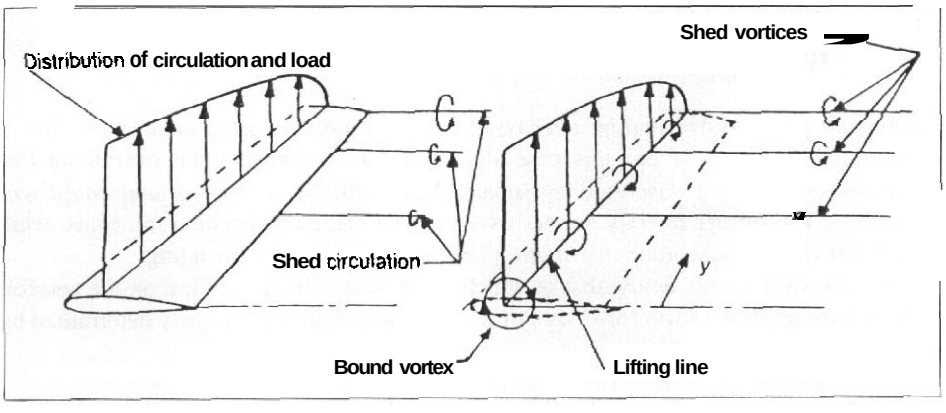

***Fig.* 9.2** *Representation of a wing by a lifling line*

When the wing is of lower aspect ratio. or if it is swept, it is necessary to consider the distribution of the effects over the whole surface. In particular swept wings introduce a complexity in that the obliquity between the chord-wise (stream-wise) direction and the structural (span-wise) direction results is an interaction implying that the two must be considered together. In this case the simplest approach is to use the so-called 'Wessinger' method (NACA Technical Memo 1120). This uses a second reference line aft of the lifting line to correct for the interaction. More rigorous than this is the 'Vortex-lattice' theory, described for example by Faulkner (United Kingdom Aeronautical Research Council, ARC, R and M 1910). illustrated in Fig. 9.3. In this figure a representative lattice array of vortices is shown and when the number of vortices in the array becomes infinite a lifting surface is formed. Multhopp, (ARC R and M 2884), used such a 'lifting surface' theory to evaluate the air-load distribution on a wide range of different wing plan-forms, some of which are discussed in Section 9.3.4.

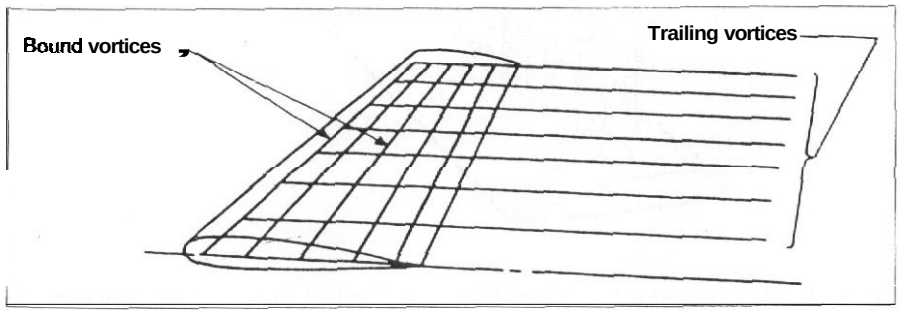

***Fig.* 9.3** *Vortex representation of the elements of a lifting surface*

9.3 Span-wise loading of lifting surfaces in subsonic flow

9.3.1 Un-swept lifting surfaces

9.3.1.1 General comments

In the case of an unswept wing of moderate to high aspect ratio, say above about 5, the span-wise loading can be evaluated with reasonable accuracy by the 'lifting line' theory referred to in the previous section and shown in Fig. 9.2. This method provides a way of estimating the local velocities across the span induced by the aerofoil so that the corresponding variation may be determined. The theory is based on the Kutta–Joukowski relation which is related to the circulation along the quarter chord line:

$$\text{Lift per unit span} = \rho V_o \Gamma \tag{9.1}$$

where

p is the air density
V_o is the free stream velocity
Γ is the circulation around the aerofoil

When the lift, $\mathcal{L}(y)$, is reduced to the non-dimensional form with y being the span-wise ordinate measured from the centreline, the local lift coefficient is given by:

$$C_L(y) = \rho V_o \Gamma / \{\rho V_o^2 c(y)/2\} = 2\Gamma / \{V_o c(y)\} \tag{9.2a}$$

where $c(y)$ is the local chord.

An important consequence of the theory is that the drag due to lift, the induced drag, is minimized when the overall span-wise lift distribution is of semi-elliptic shape, that is when $[c(y)C_L(y)]$ is of semi-elliptic distribution across the span.

Considering a two-dimensional situation. which is true on those pans of a three-dimensional wing where there is no locally induced span-wise flow:

$$C_L(y) = a_{1o}(y)\alpha(y) \tag{9.2b}$$

by definition, where $a_{1o}(y)$ and $\alpha(y)$ are the local two-dimensional lift curve slope and the angle of attack of the aerofoil, respectively. $(\Gamma/V_o c)$ is related to a_{1o} and a.

a_{1o} may well vary with y due to change of aerofoil section shape. a may vary gradually for a similar reason or due to twist and may change more suddenly due to the deflection of an auxiliary surface:

It should be noted that a is measured relative to the angle that the chord line has to be placed in the airflow to give an overall zero lift condition. the 'zero-lift' angle, see Section 9.3.1.2.

The airflow tends to smooth out discontinuities caused by geometric changes, that is, there is always a tendency towards the ideal, minimum drag, state. Thus, while the ideal semi-elliptic distribution may not be achieved, there is a tendency towards it. In practice. from Eqns (9.2):

$$\Gamma = V_o C_L(y)c(y)/2 = V_o a_{1o}(y)\alpha(y)c(y)/2 \qquad (9.2c)$$

It is convenient to calculate the total span-wise loading as the sum of two separate effects:

(a) The so-called 'basic' loading which corresponds to zero overall lift on the surface and arises due to the effective twist of the aerofoil across the span.

(b) The 'additional' loading which is due to the lift arising from an increment in angle of attack of the surface relative to that corresponding with the zero-lift condition.

9.3.1.2 Overall zero-lift angle of attack

In the particular case of a lifting surface which uses the same aerofoil section over the whole span. possesses no twist and has no auxiliary surfaces deflected, then the zero-lift angle is constant across the whole span. When the surface is placed at this zero-lift angle there will be zero load everywhere across the span. In general when there is effective twist, for whatever reason, this will not be the case. It is still possible, however, to define an overall zero-lift angle for the surface such that there is no net lift. There will be local lift across the span, some up and some down, giving zero overall. For the case when the twist varies continuously across the span, the local angle of attack at some point across the span may be written as:

$$\alpha = \alpha_o + \varepsilon(y) \qquad (9.3a)$$

where

α_o is the overall zero-lift angle for the wing, that is the angle of attack of the chord line of the aerofoil section at the centreline coinciding with no overall lift

$\varepsilon(y)$ is the angle of twist of a local section at a distance y out from the centreline, relative to the zero-lift line of the centreline aerofoil section, positive nose-up

The corresponding lift coefficient of the section is:

$$C_L(y) = a_{1o}(y)\{\alpha_o + \varepsilon(y)\} \qquad (9.3b)$$

Thus the overall lift on the lifting surface in this condition is:

$$2(\rho V_o^2/2)\int_0^{b/2} a_{1o}(y)\{\alpha_o + \varepsilon(y)\}c(y)dy$$

where b is the total span of the lifting surface.

For zero overall lift:

$$\int_0^{b/2} a_{1o}(y)\{\alpha_o + \varepsilon(y)\}c(y)dy = 0$$

or

$$\alpha_o \int_0^{b/2} a_{1o}(y)c(y)dy = -\int_0^{b/2} a_o(y)\varepsilon(y)c(y)dy$$

but

$$\int_0^{b/2} a_{1o}(y)c(y)dy = S\bar{a}/2 \tag{9.4a}$$

where $\bar{a}$ is the average lift curve slope for the whole surface and S is the plan area of the surface:

$$S = 2\int_0^{b/2} c(y)dy$$

Thus the zero-lift angle is:

$$\alpha_o = -2\left\{\int_0^{b/2} a_{1o}(y)\varepsilon(y)c(y)dy\right\}/(S\bar{a}) \tag{9.4b}$$

A continuous twist distribution is described as linear when $\varepsilon(y)$ varies linearly across the span, or uniform when the tip chord is twisted relative to the root chord and the leading and trailing edges are straight, that is $\varepsilon(y)c(y)$ varies linearly across the span. When the effective twist does not vary continuously, as when an auxiliary surface is deflected, the analysis must be performed in discrete span-wise steps.

9.3.1.3 Basic load distribution

If the twist is wholly effective then the local lift coefficient appropriate to no overall lift may be written as:

$$C_L(y) = \{\alpha_o + \varepsilon(y)\}a_{1o}(y, t) \tag{9.5a}$$

where $a_{1o}(t)$ refers to the effect of variation of thickness

In practice, the local induced flow field referred to previously tends to modify the effectiveness of the twist such that, typically:

$$C_L(y) = 0.5\{\alpha_o + \varepsilon(y)\}a_{1o}(y, t) = \{C_L(y)\}_b \tag{9.5b}$$

and the corresponding local air load distribution, the basic distribution, is:

$$\rho V_o^2 C_L(y)c(y)/2 = \rho V_o^2\{\alpha_o + \varepsilon(y)\}a_{1o}(y, t)/4 \tag{9.5c}$$

9.3.1.4 Additional load distribution

In general the lifting surface will not be placed at the zero-lift angle since the surface is normally required to produce a specified lift. The lift distribution consequent upon the angle of attack setting of the centreline aerofoil section relative to the zero-lift angle, a_o. Eqn. (9.4b) is the additional load distribution.

For the case of unswept wings of moderate to high aspect ratio Schrenk's method,[2] is appropriate. This employs the lifting line concept and proposes that the shape of the additional load distribution is the mean between that of the ideal semi-elliptic plan-form and that which would result directly from the wing plan-form geometry. That is, it assumes that the induced flow effectively corrects for half of the effect of the departure of the geometry from that which would result in the ideal.

A. The ideal semi-elliptical distribution

If a is the maximum ordinate of the ellipse at the centreline, as shown in Fig. 9.4, the area of the semi-ellipse is $(\pi ab/4)$ where, as previously, b is the span of the surface and a here is half of the minor axis.

If this area is taken to be equal to the plan-form area of the surface, S, then:

$$a = 4S/(\pi b)$$

The semi-ellipse may now be defined by the equation:

$$[\{c(y)_e\}/\{4S/(\pi b)\}]^2 + \{y/(b/2)\}^2 = 1 \tag{9.6a}$$

$$c(y)_e = \{4S/(\pi b)\}\{1-(2y/b)^2\}^{1/2} \tag{9.6b}$$

where $c(y)_e$ is the ideal local chord needed lo define the semi-ellipse.

[2] Schrenk, O. A simple approximate method for obtaining the span-wise lift distribution. NACA Technical Memo No. 948, 1940.

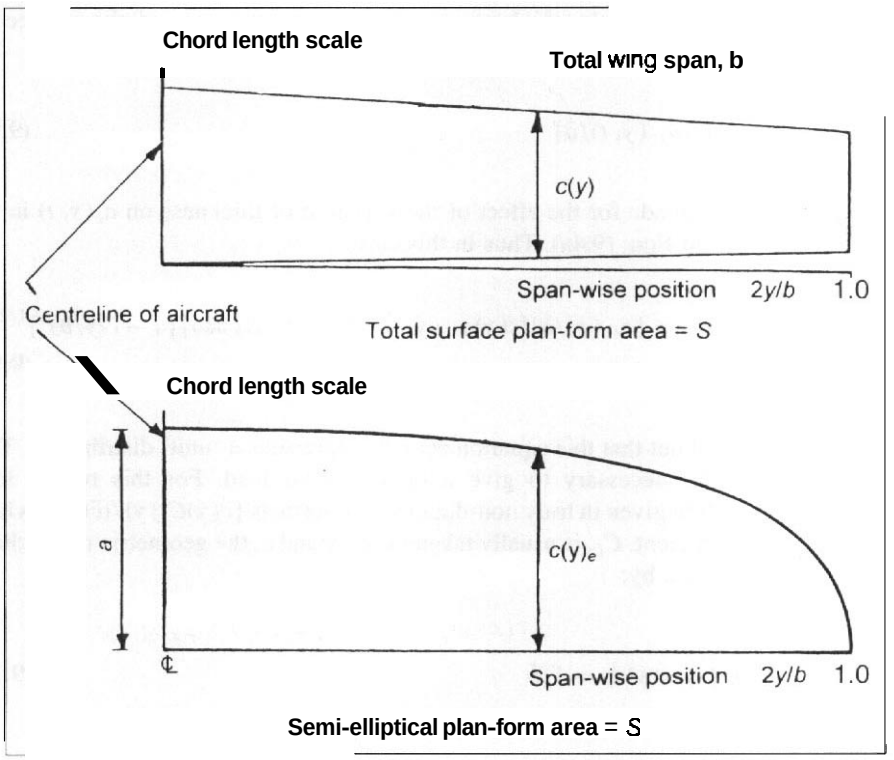

Fig. 9.4 Plan-form geometry for Schrenk's method

B. The Schrenk additional span-wise load distribution

The shape of the additional loading is given by the mean of the semi-elliptical equivalent chord, as defined above. and the actual geometric value:

$$c(y)_a = \{c(y)_e + c(y)\}/2 \tag{9.7a}$$

Therefore:

$$\{c(y)C_L(y)\}_a = \alpha a_{1o}(y)\{c(y)_e + c(y)\}/2 \tag{9.7b}$$

It is convenient to define the shape of the additional load distribution for the case of unit overall lift coefficient, that is when $(air) = 1$, from where:

$$\{c(y)C_L(y)\}_a = \{a_{1o}(y)/\bar{a}\}[c(y)/2 + \{2S/(\pi b)\}\{1 - (2y/b)^2\}^{1/2}] \tag{9.8}$$

It is possible to allow for the thickness variation across the span of the surface by introducing an effective geometric chord defined as:

$$c(y)_t = c(y)\{a_{1o}(y, t)/\bar{a}\} \tag{9.9a}$$

where allowance is made for the effect of the variation of thickness on $a_o(y, t)$ in the evaluation of $\bar{a}$ from Eqn. (9.4a). Thus in this case:

$$\{c(y)C_L(y)\}_a = \{a_{1o}(y)/\bar{a}\}[c(y)a_{1o}(y, t)/(2\bar{a}) + \{2S/(\pi b)\}\{1 - (2y/b)^2\}^{1/2}] \tag{9.9b}$$

It should be pointed out that this equation actually represents a 'unit' distribution. This may be factored as necessary to give a finite overall load. For this reason load distributions are often given in truly non-dimensional form as $\{c(y)C_L(y)/(\bar{c}C_L)\}$ where the overall lift coefficient. C_L, is usually taken as unity and $\bar{c}$, the geometric mean chord of the surface is given by:

$$\bar{c} = (2/b)\int_0^{b/2} c(y)dy = S/b \tag{9.10}$$

It follows from Eqn. (9.9b) that:

$$\{C_L(y)\}_a = \{a_{1o}(y)/(\bar{a}c(y))\}[c(y)a_{1o}(y, t)/(2\bar{a}) + \{2S/(\pi b)\}\{1 - (2y/b)^2\}^{1/2}] \tag{9.11}$$

9.3.1.5 The total span-wise loading

The total span-wise loading on the lifting surface is taken to be the algebraic sum of the basic and additional loads. For the unswept case under consideration this follows from Eqns (9.5) and (9.9):

$$\{c(y)C_L(y)/(\bar{c}C_L)\} = \{c(y)/(\bar{c}C_L)\}[\{C_L(y)\}_b + \{C_L(y)\}_a] \tag{9.12}$$

where $\{C_L(y)\}_b$ is given by Eqn. (9.5b) and $\{C_L(y)\}_a$ by Eqn. (9.11).

In low-speed Right where the overall lift coefficient is generally relatively high, the additional loading is the dominant term. However, at high equivalent airspeeds the additional lift coefficient is relatively low and hence the basic load distribution is likely to be significant.

9.3.2 *Span-wise loading of swept lifting surfaces*

9.3.2.1 General comments

As mentioned in Section 9.2, the evaluation of the span-wise load distribution for a swept wing requires consideration of effects over the whole surface, not just along a nominal lifting line.

9.3.2.2 Basic span-wise load distribution

The analysis of Section 9.3.1.3 is strictly only applicable to unswept wings of moderate aspect ratio, since it is based on the lifting line assumption. However, providing the basic lift is of small magnitude compared with the total lift in a given case, Eqns (9.5) may be used to give an approximate value for swept wings.

9.3.2.3 Additional load distribution on uncranked swept surfaces of moderate to high aspect ratio

A simple evaluation of the additional load distribution on uncranked swept wings may be made using the method of Stanton-Jones.? The method uses the Weissenger approach, referred to in Section 9.2, to interpret experimental results. The shape of the distribution is completely defined by the position of the span-wise centre of pressure of one-half of the surface, $\bar{y}$, which must lie between the limits $0.4 < \bar{y} < 0.5$ for the

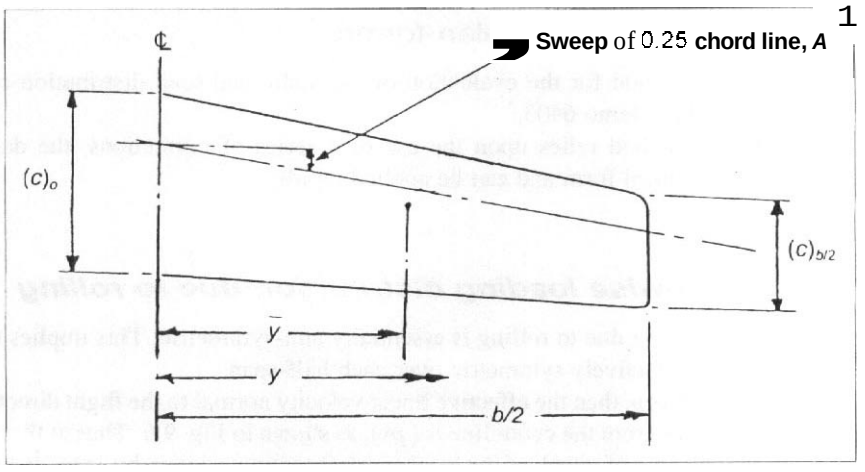

Fig. 9.5 Notation for Stanton-Jones swept wing analysis

[3]Stanton-Jones, R. The rapid estimation of span-wise loading of swept wings. CranfieldCollege *of* Aeronautics Report No. **32.** 1951.

method to give acceptable results. The notation is illustrated in Fig. **9.5** and the relevant formulae are:

$$\bar{y} = 0.42 + Am'\{(4.45 + 5\lambda)tan\,\Lambda/m' + 10.4\lambda^{1/2} - 6.7\} \times 10^{-3} \quad (9.13)$$

where

A	is the aspect ratio (b^2/S)
A	is the ratio of the tip to root chord
A	is the sweep of the 0.25 chord line
m' $= (1 - M_N^2)$	where M_N is the subsonic Mach number

Let $\eta = 2y/b$, then for $\eta < 0.7$:

$$\{c(y)C_L(y)/(\bar{c}C_L)\} = 1.28(1 - \eta^2)^{1/2} + (14.13\eta - 6.35)(\bar{y} - 0.425) \quad (9.14a)$$

and for $\eta \geqslant 0.7$:

$$\{c(y)C_L(y)/(\bar{c}C_L)\} = 1.28(1 - \eta^2)^{1/2} + \{4.25 - 53.8(\eta - 0.815)^2\}(\bar{y} - 0.425) \quad (9.14b)$$

The method is likely to he as accurate as the vortex-lattice approach for this restricted range of lifting surface plan-forms.

9.3.2.4 Additional span-wise load distribution on general swept plan-forms

A more general method for the evaluation of the additional load distribution can be found in ESDU TD Memo 6403.[4]

Although the method relies upon the use of a series of corrections, the data are provided in a graphical form and can he applied rapidly.

9.3.3 Span-wise loading distribution due to rolling

The span-wise loading due to rolling is essentially anti-symmetric. This implies that it can be treated as effectively symmetric over each half-span.

If the rate of roll isp, then the effective linear velocity normal to the flight direction at a point on the span y from the centreline is (py), as shown in Fig. 9.6. Thus at that value of y the effective angle of attack of the local aerofoil section is given by $\{tan^{-1}(py/V_o\}$ where V_o is the forward velocity. Assuming that this angle of attack is small, then the

[4]Transonic Data Memoranda TD 6403. Method for the rapid estimation of theoretical span-wise loading due to change of incidence. ESDU International plc, August 1983.

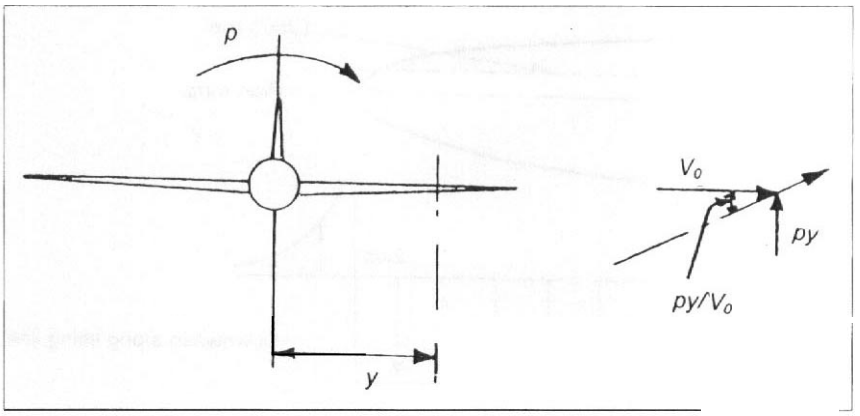

Fig. 9.6 Local angle *of attack* due *to rolling*

local lift coefficient due to the rate of roll is:

$$\{C_L(y)\}_p = (py/V_o)a_{1o}(y) \tag{9.15a}$$

Although this is actually a kind of aerodynamic twist it can be considered as a form of additional load except that the angle of attack varies linearly across the span rather than having a constant value. From Schrenk's hypothesis there will be an induced airflow tending to modify the consequent air-load distribution towards the equivalent ideal form. It is necessary, therefore, to correct the value of Eqn. (9.15a) by the factor implied by Eqns (9.7):

$$\{c(y)C_L(y)\}_p = (py/V_o)\{a_{1o}(y)\}[c(y)/2 + \{2S/(\pi b)\}\{1 - (2y/b)^2\}^{1/2}] \tag{9.15b}$$

9.3.4 General comments on the span-wise loading of lifting surfaces in subsonic flow

9.3.4.1 Elliptic plan-form

A fundamental case is an untwisted lifting surface of elliptic plan-form having similar cross-sections along the span, see Fig. 9.7. In this case the downwash along the lifting line is constant, that is $(\rho V_o \Gamma)$ is constant. Hence, the lift coefficient is also constant, see Eqns (9.2). However, since the chord varies in an elliptical manner, the additional lift loading is also semi-elliptic. **Thus** this can be considered as the ideal.

9.3.4.2 Tapered plan-forms

Consider two quite different plan-forms as shown in Fig. 9.8, both having an untwisted distribution of similar cross-sections and providing the same total lift.

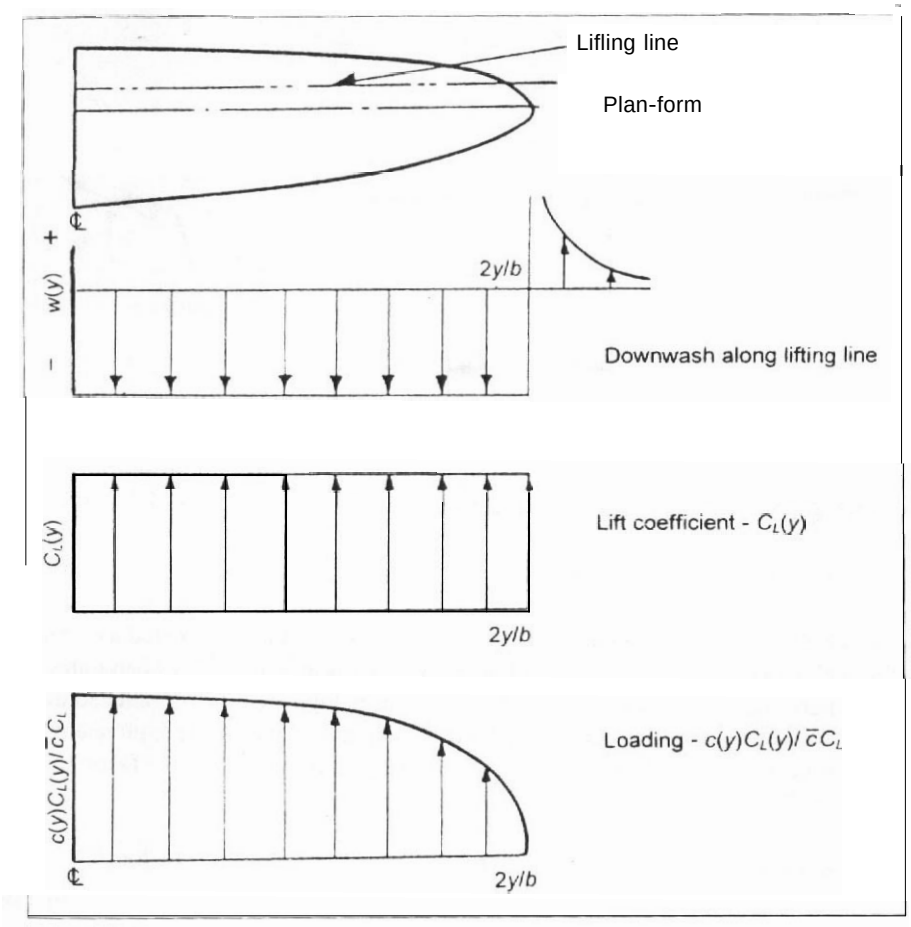

Fig. 9.7 *Lifting* ***line theory applied to an untwisted*** *elliptical* ***plan-form surface***

Compared with the surface of rectangular plan-form it is apparent that there will be a smaller root bending moment in the case of the alternative highly tapered surface. The possibility of a lighter structure is, however, outweighed by the increased induced drag which occurs as a result of the marked departure from semi-elliptic loading and by the tendency for relatively high values of lift coefficient to he attained in regions close to the wing tip. In the figure the relative variation of the maximum attainable lift coefficient along the span is shown. For a given wing section this variation depends on the local chord Reynolds number and the diagram shown corresponds only to a maximum value of overall C_L. The span-wise position at which the curve intercepts the loading curve is theoretically that at which wing stalling is initiated. Since, in many cases, a substantial amount of separated flow exists before the stalled condition is properly established, the span-wise position at which the stall is initiated on a wing should be arranged wherever possible so as not to be in stream-wise alignment with the lateral control surfaces.

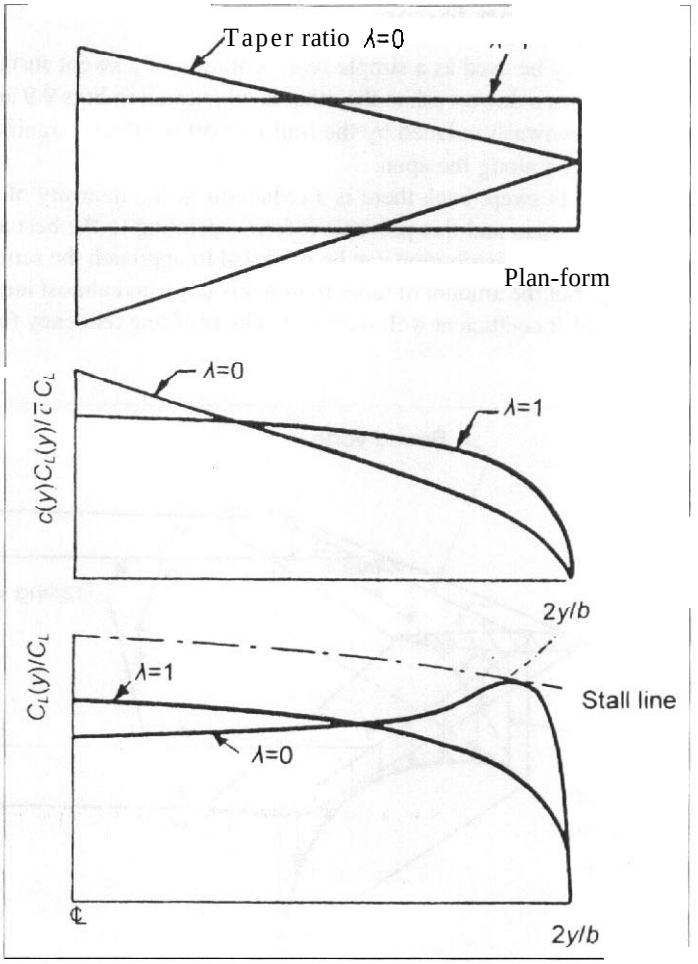

Fig. 9.8 The effect of taper of the plan-farm

Failure to do this results in a loss of control effectiveness and the inability to counteract wing drop at stall. Ideally stall should be initiated near the root, as it is in the case of the untapered wing.

Clearly the effect of taper is such that the load distribution can be substantially modified and hence a load distribution corresponding with moderate accuracy to the semi-elliptic optimum can be arranged by the appropriate choice of taper ratio. When considered in terms of the unswept lifting line, it is found that taper ratios in the region of $0.4 < \lambda < 0.6$ yield values of induced drag fairly close to that incurred with semi-elliptic loading for aspect ratios between 4 and 12. Geometrically a straight tapered surface is much simpler than one of elliptical plan-form

9.3.4.3 Swept plan-forms

A bent lifting line may be used as a simple representation of a swept surface. Each half of the bent line induces adownwash at the other as illustrated in Figs 9.9 and 9.10. This, together with the downwash induced by the trailing vortex effects, significantly affects the distribution of load along the span.

When the surface is swept back there is a reduction in the intensity of load over the middle portion of the span and this prevents it from operating to the best advantage. By introducing taper the load distribution can be modified to approach the semi-elliptical, as with straight wings, but the amount of taper required is large and almost inevitably places the higher values of lift coefficient well outboard. The resulting tendency for such a wing

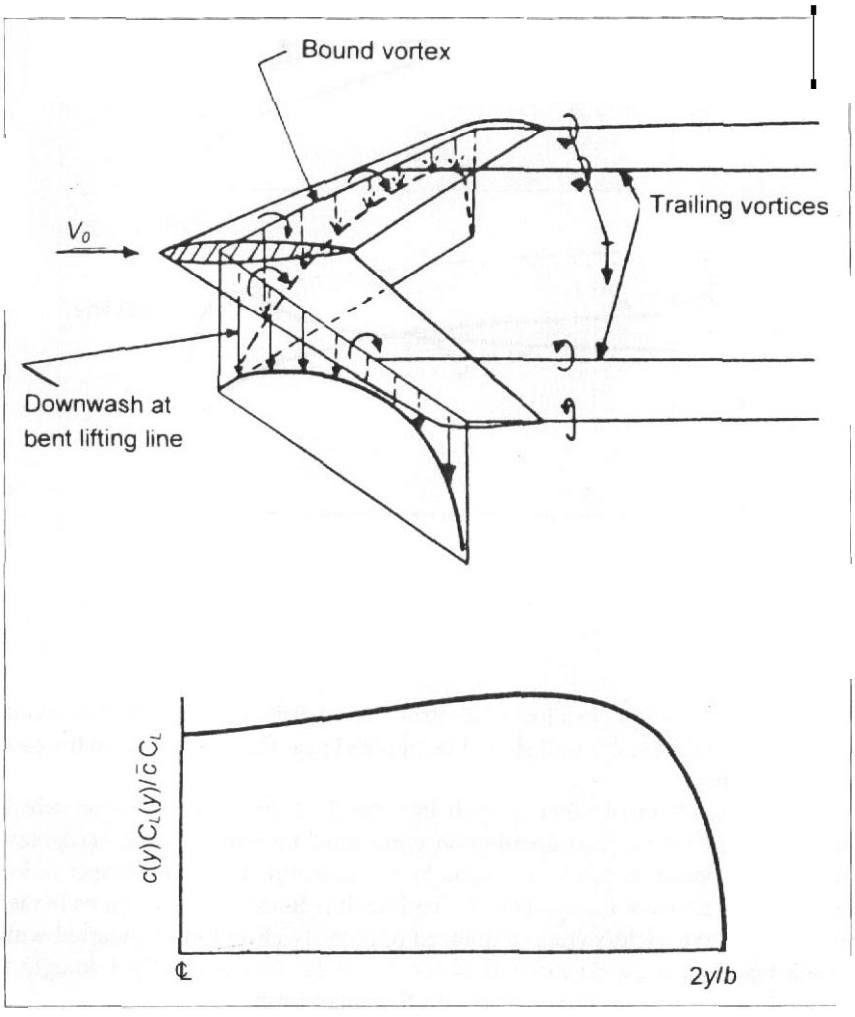

Fig. 9.9 Downwash and loading on a swept-back lifting surface

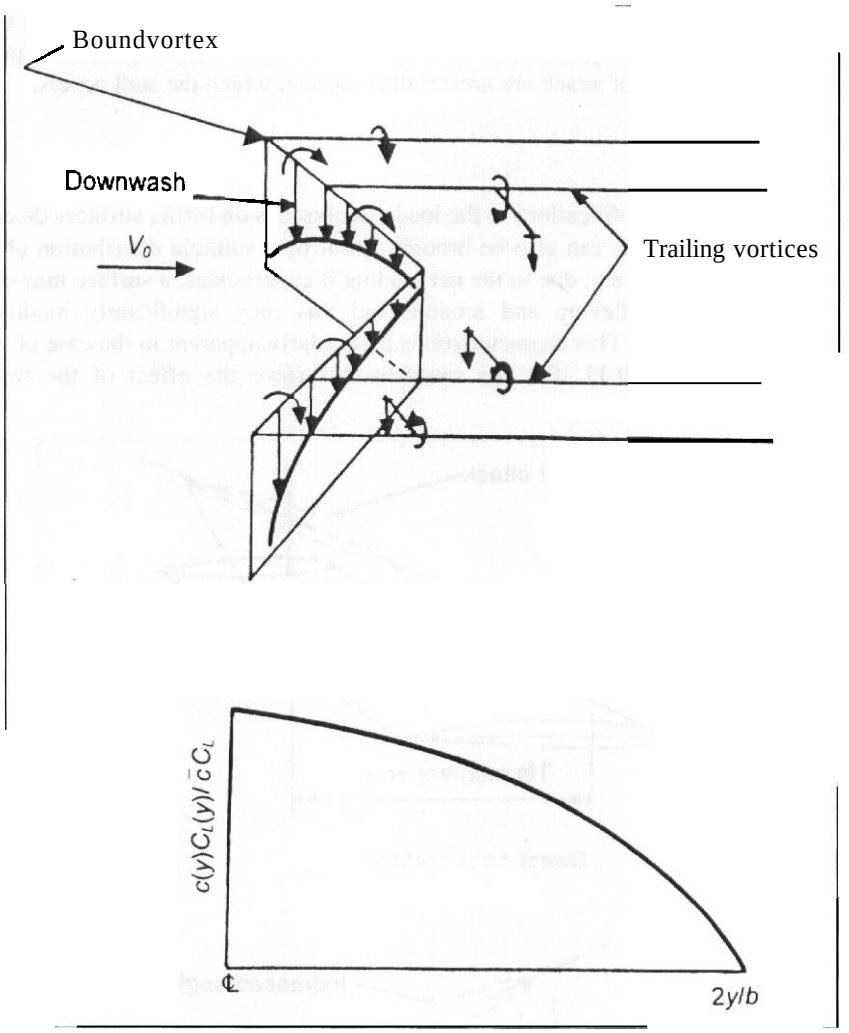

Fig. 9.10 Downwash and loading on a swept-forward lifting surface

to stall near the tip can be alleviated by reducing the angle of sweep back near to the tip; this can be done by twisting the wing so that the tip sections have lower angle than the mot, a so-called 'washed out' condition, or by using leading edge flaps or slats. Tip stalling results in 'pitch-up' due to loss of lift aft on the surface. This aggravates the consequences.

With forward sweep the induced velocities encourage a concentration of load towards the centreline, Fig. 9.10, but the possibility of a lighter structure cannot usually he realized because of the need to distribute the load as nearly as possible as a semi-ellipse. for which an inverse distribution of taper is suggested. There is still the problem of pitch-up since if the rwt stalls first the remaining lift is outboard and forwards. Further. in a sideslip at relatively low angles of attack a forward swept wing is different from the more usual

plan-forms in that it experiences a rolling moment of exactly the opposite sign to that required for lateral stability. This phenomenon only occurs on unswept and swept-back wings when the angles of attack are greater than those at which the stall occurs.

9.3.4.4 Twist

Most of the possible modifications to the load distributions on lifting surfaces discussed in the foregoing sections can also be brought about by a suitable distribution of twist along the span. Conversely, due to the net loading it experiences, a surface may distort as a consequence of flexure and torsion. and this may significantly modify the distribution of the load. This characteristic is particularly apparent in the case of wings with sweep, see Fig. 9.11. For the swept-back surface the effect of the twisting

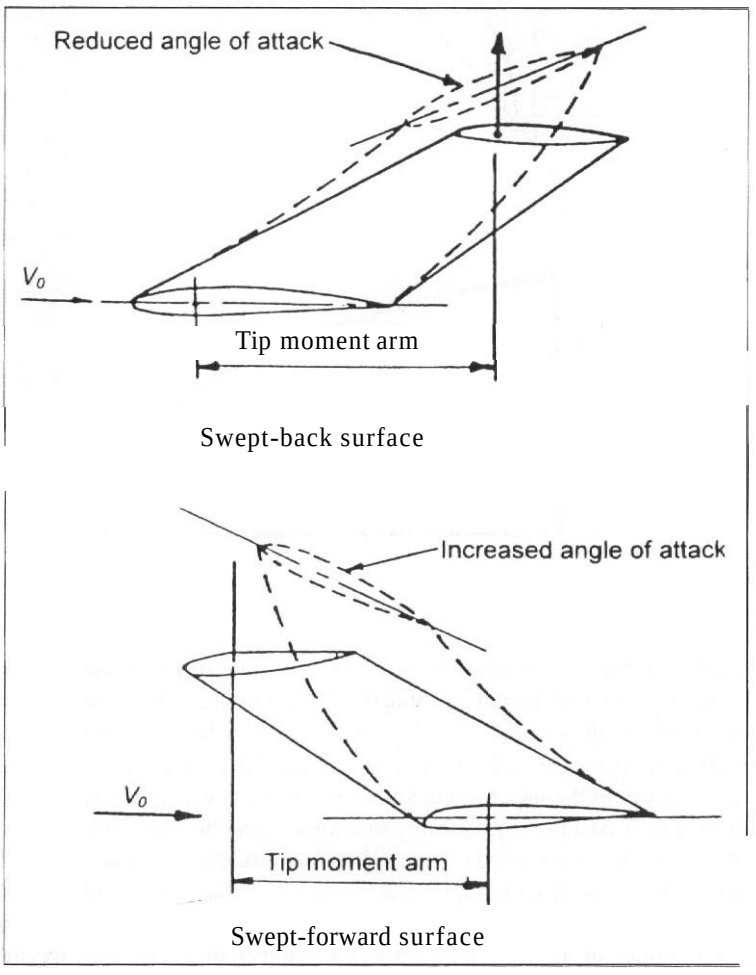

Fig. 9.11 *The flexure-induced torsion on swept lifting surfaces*

movement induced by the flexure is to tend to reduce that load. The opposite is true for surfaces having forward sweep so that the possibility of wing torsional divergence is very real. This is further discussed in Chapter 11 but it is worth noting that use of wings with significant forward sweep only became a practical proposition when computational techniques enabled anisotropic structures to be designed so that the coupled bending and torsion flexibilities act together in such a way as to modify both the span-wise load distribution and to offset the divergence tendency.

9.4 *Chord-wise loading of lifting surfaces in subsonic flow*

9.4.7 Components of loading

Along the chord of a wing section the distribution of load is principally defined by three factors, which are:

(i) the thickness distribution of the section;
(ii) the shape of the mean ordinate or camber line;
(iii) the angle of attack.

The components of a pressure distribution over a section contour are shown in Fig. 9.12. There is a resultant force from which the section lift and drag, which by definition are the forces acting perpendicular to and along the air-stream, respectively. may be determined. For stressing purposes it is often assumed that two-thirds of the load acts as a suction on the upper surface of the aerofoil and the remaining one-third as a pressure on the lower surface. This may be erroneous in the case of wings of low aspect ratio and high sweep back due to the formation of upper surface vortices.

The intersection of the line of action of the resultant and the chord line, or similar datum, in the aerofoil is defined as the centre of pressure. CP. This is the position about which the aerofoil experiences no pitching moment and is of fundamental importance in determining span-wise torsion loads. Because the movement of the centre of pressure with angle of attack can be quite large it is not the best choice as a reference point in an overall stability or loading assessment. It is thus seldom used except for the local evaluation of the air-loading on a rib.

9.4.2 Location of the chord-wise centre of pressure and the aerodynamic centre

The wide variation in the location of the centre of pressure with the angle of attack is illustrated in Fig. 9.13. This shows that for a cambered aerofoil the centre of pressure tends to infinity past the trailing edge (T.E.) as the angle of attack is reduced towards the zero-lift condition. and returns from infinity forward of the leading edge as the lift coefficient is increased from zero in a negative sense. Clearly, use of the centre of pressure as a reference creates difficulties at low values of lift coefficient. A more convenient, and usual, reference is the aerodynamic centre. This is a particular reference

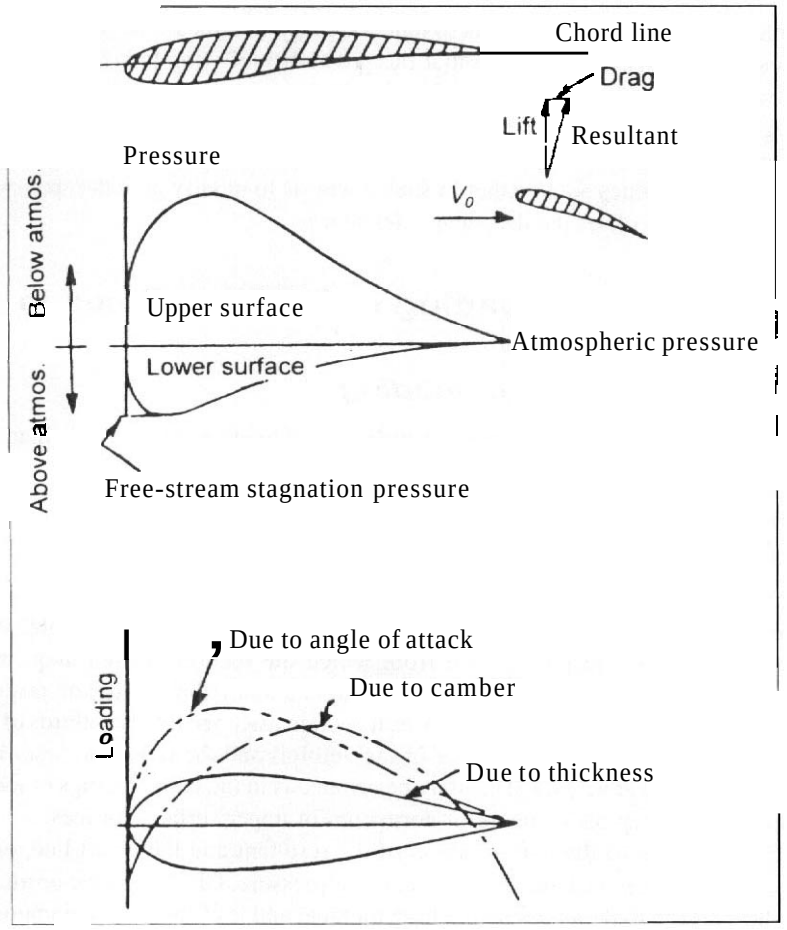

Fig. 9.12 Chord-wise load

point on the chord chosen so that there is no change of pitching moment about that point over the whole range of angles of attack.

As is shown in Fig. 9.14 on a cambered aerofoil there is a chord-wise lift distribution even when the overall lift on the section is zero. This gives rise to the zero-lift pitching moment coefficient. C_{Mo}, of the section.

Referring to Fig. 9.13, the non-dimensional pitching moment due to the lift about the leading edge may he written as:

$$(C_M)_{LE} = K_1 + K_2 C_L \tag{9.16a}$$

where K, and K_2 are constant on the assumption that the pitching moment is a linear function of lift. K_1 is the moment coefficient at zero lift, that is ($K_1 = C_{Mo}$).

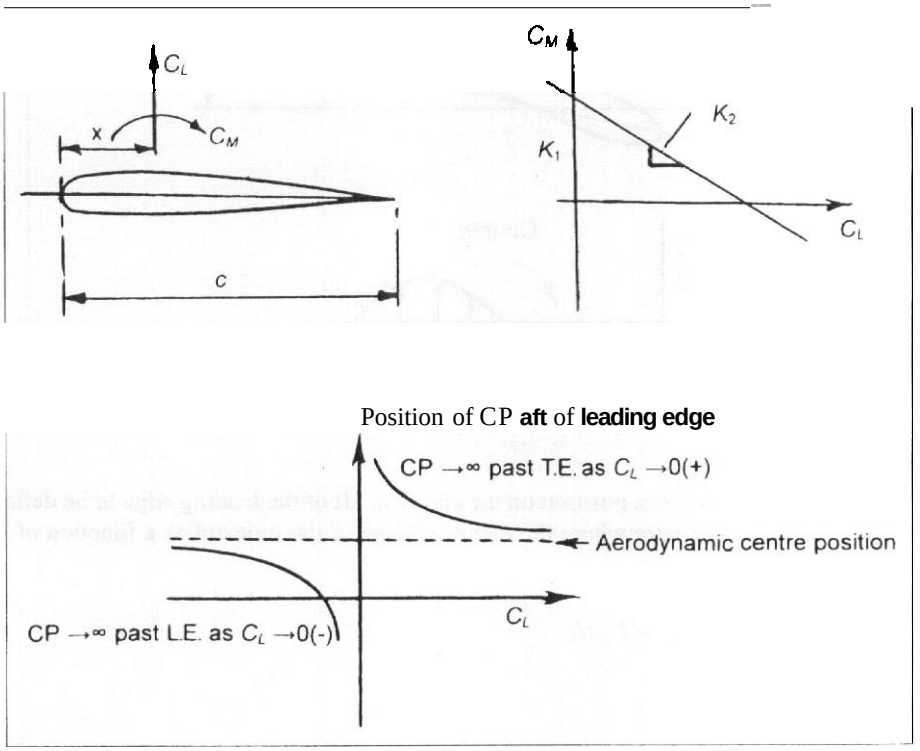

Fig. 9.13 Centre of pressure and aerodynamic ***centre***

If $\bar{x}$ is the location of the centre of pressure aft of the leading edge on a total chord length of c, then there is no moment about $\bar{x}$ by definition. Thus:

$$(C_M)_{\bar{x}} = (C_M)_{LE} - C_L\bar{x}/c = 0 \tag{9.16b}$$

Substituting from Eqn. (9.16a) for $(C_M)_{LE}$ gives:

$$C_{Mo} + K_2C_L + C_L\bar{x}/c = 0$$

and

$$K_2 = -C_{Mo}/C_L - \bar{x}/c = -(C_{Mo}/C_L + \bar{x}/c) = \text{constant} \tag{9.16c}$$

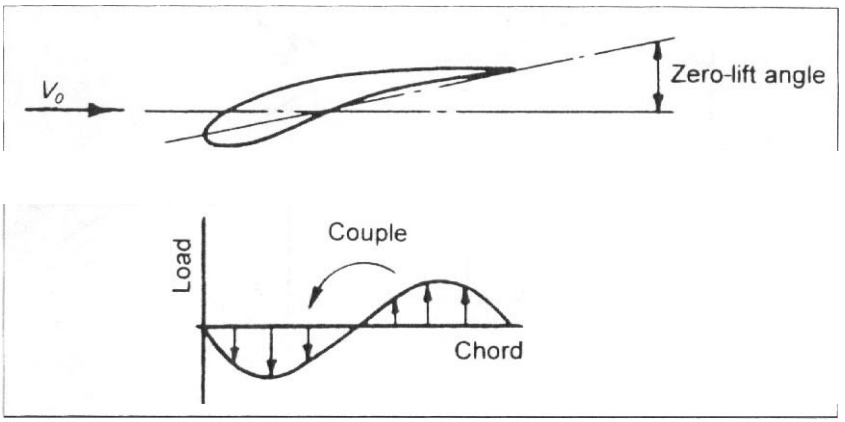

Fig. 9.74 *Zero-lift pitching couple*

It is possible to define a position on the chord, a, aft of the leading edge to be defined as the aerodynamic centre where the rate of change of the moment as a function of lift is zero:

$$(C_M)_a = (C_M)_{LE} - C_L a/c$$

therefore

$$(C_M)_a = C_{Mo} + K_2 C_L + C_L a/c$$

and

$$(dC_M/dC_L)_a = 0 = K_2 + a/c$$
$$a = -K_2 c \tag{9.17a}$$

as would be expected by definition. Hence:

$$a/c = \bar{x}/c + C_{Mo}/C_L \tag{9.17b}$$

In the notation used in Chapter 4, Section 4.2.1, the aerodynamic centre position is defined as being located at a fraction of the chord H_o aft of the leading edge. Thus:

$$H_o = \bar{x}/c + C_{Mo}/C_L \tag{9.17c}$$

or the centre of pressure position as a fraction of the chord aft of the leading edge is:

$$\bar{x} = H_o - C_{Mo}/C_L \tag{9.17d}$$

It should be noted that while the ahove analysis relates to a two-dimensional aerofoil the same principle applies more generally.

9.4.3 Overall chord-wise load and moment

9.4.3.1 Torque implications

The torque on a chord-wise section is the moment of the chord-wise air-load about a given reference point. Convenient structural reference lines are discussed in Chapter I?, Section 12.5. The chord-wisecentre of pressure due to a typical overall value of angle of attack is usually relatively forward on the aerofoil in incompressible flow, typically 0.25–0.28of the chord aft of the leading edge. In transonic conditions there is a general tendency for it move hack towards the 0.50 chord point, see Section 9.6.2. The chord-wise centre of pressure due to the deflection of a flap or control is usually further hack. and the smaller the control chord relative to the overall chord the further back it is.

It is often assumed that the total chord-wise load can he derived by superposition of the two separate distributions due to overall angle of attack and flap deflection, as illustrated in Chapter 4. Fig. 4.4. The local torque on the aerofoil is the algebraic sum of the products of the separate loads and their chord-wise distances to the reference point, see Chapter 5, Section 5.3.7, and Fig. 9.15 (L.E., leading edge).

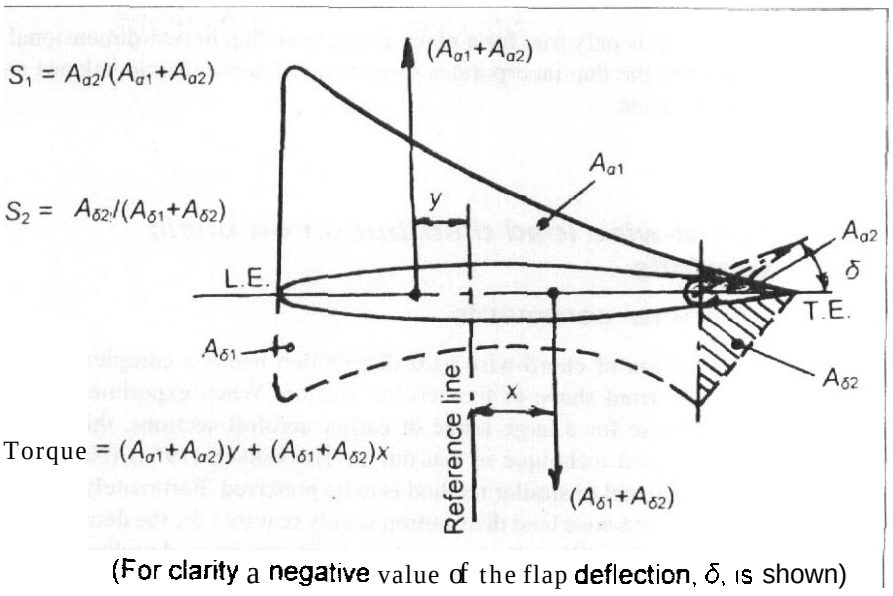

Fig. 9.15 Components of ***chord-wise*** load due lo angle of ***attack*** *and* flap *deflection*

9.4.3.2 Hinge moment on flaps and control surfaces

Care must be taken in distinguishing between the total pitching moment due to the chord-wise loading consequent upon the deflection of the flap and the flap hinge moment. In subsonic flow the air-load distribution on a flap due both to overall aerofoil incidence and flap deflection is approximately triangular over the flap chord, c_f, with the maximum value at the hinge-line falling to zero at the trailing edge. Thus the centre of pressure of the load on the flap itself is about one-third of the flap chord aft of the hinge-line. The resulting hinge moment due to this load about the hinge-line is only part of the total torque on the aerofoil section due to deflection of the flap, since there is also a load forward of the hinge-line. Chapter 5, Section 5.3.7 expresses the loads on a trailing surface in terms of S, where the S_i are the fractions of the total chord-wise load on the control itself. As defined subscripts '1', '2', and '3' refer to the loads due to symmetric angle of attack. control surface deflection, and anti-symmetric angle of attack, respectively.

For the condition of a symmetric angle of attack the total load on a unit span of the deflected flap may be written as:

$$\text{Total load on flap} = \rho V_o^2 c(S_1 a_1 \mathrm{a} + S_2 a_2 \delta)/2 \tag{9.18a}$$

where a_1 and a_2 are the lift curve slopes, based on overall chord, due to angle of attack, a, and flap deflection. δ, respectively.

Therefore assuming a triangular distribution of load over the flap, the hinge moment:

$$\rho c c_f V_o^2 (S_1 a_1 \alpha + S_2 a_2 \delta)/6 \tag{9.18b}$$

Note that this moment is only true for a plain, roundnose flap in two-dimensional flow and is modified when the flap incorporates some form of aerodynamic balance and by three-dimensional effects.

9.4.4 Chord-wise load distribution on basic aerofoils

9.4.4.1 General comments

The accurate estimation of chord-wise load distribution needs a complex calculation dependent upon the detail shape of the aerofoil section. When experimental data are available, as is the case for a large range of earlier aerofoil sections, this is the best approach. One analytical technique is that due to Theodorsen (1933) (NACA Report 411), but the use of a panel or similar method is to be preferred. Fortunately, for loading analysis, the actual chord-wise load distribution is only required for the details of rib and local skin panel stressing. Overall structural analysis can be undertaken with just a knowledge of the chord-wise centre of pressure position, as given by Eqn. (9.17d).

9.4.4.2 Simple estimation of chord-wise pressure distribution due to angle of attack

It is possible to derive certain very simple expressions for chord-wise pressure distribution due only to the angle of attack of the section. These depend only on the chord-wise centre of pressure. Such an expression, one of which follows, may well be applicable for initial design work. The pressure distribution across the chord of the aerofoil, as shown in Fig. 9.16, is represented by a second-order polynomial as:

$$p = ax^2 + bx + c \tag{9.19a}$$

where *a*, b and *c* are coefficients.

In Fig. 9.16, L.E. and T.E. refer to the leading and trailing edges. respectively. The coefficients may be evaluated by assuming that the pressure at the trailing edge is zero. the area under the curve for a unit chord is unity and the moment of the area about the leading edge for unit area is equal to the chord-wise centre of pressure position. $\bar{x}$. These assumptions lead to:

$$p = 6[1 - 2\bar{x} + (8\bar{x} - 3)x + 2(1 - 3\bar{x})x^2] \tag{9.19b}$$

9.4.4.3 Simplified chord-wise pressure distribution due to deflection of a plain flap

A similar approach to that of the previous section may be employed to estimate the chord-wise pressure distribution due only to the deflection of a plain flap. The assumed shape of the distribution is shown in Fig. 9.17 and the ratio of the flap chord aft of the hinge-line to the total is $(c_f/c = r)$. It is assumed that forward of the hinge-line the distribution given by Eqn. (9.19a) applies, and that aft of the hinge-line the distribution

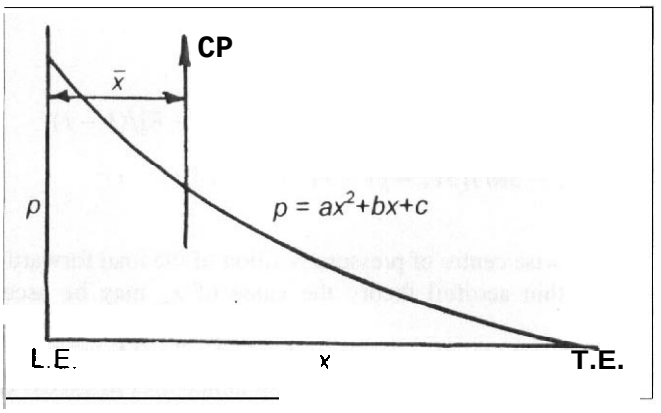

Fig. 9.16 *Simplified chord-wise pressure distribution due to angle of attack*

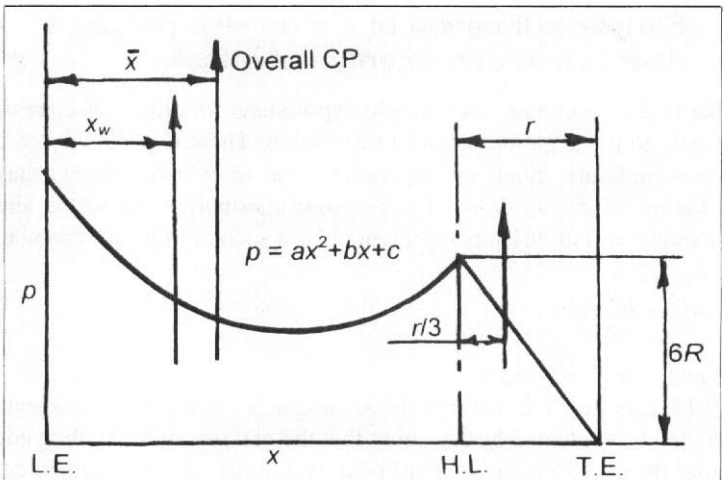

Fig. 9.17 Simplified chord-wise pressure distribution due to the deflection of a plain flap

is triangular in shape, falling to zero at the trailing edge. Let:

$$R = -b_2/a_2 \tag{9.20a}$$

where a_2 and b_2 are the lift curve slope and hinge moment coefficient, respectively, due to the deflection of the plain flap. Note that b_2 is based on the flap chord and is normally negative so that R is positive.

Since the distribution over the flap is triangular, the moment arm of the lift on the flap alone is one-third of the flap chord aft of the hinge-line, or $(r/3)$. It follows from this and the definitions of a_2 and b_2 that the area of the distribution aft of the hinge-line has an area equal to 3Rr and the value of p at the hinge-line is 6R. Thus the area forward of the hinge-line is $(1-3Rr)$. These data may be used in conjunction with Eqn. (9.19a) to evaluate the coefficients needed to define the distribution forward of the hinge-line:

$$\begin{aligned} a &= 6[R - 2(1 - 3Rr)\{x_w - (1 - r)/2\}/(1 - r)^2] \\ b &= 36[2(1 - 3Rr)\{2x_w/3 - (1 - r)/4\}/(1 - r)^2 - R]/(1 - r) \\ c &= 12[3R - (1 - 3Rr)\{3x_w - (1 - r)\}/(1 - r)^2]/(1 - r)^2 \end{aligned} \tag{9.20b}$$

where x_w is the chord-wise centre of pressure position of the load forward of the hinge-line only. Based on thin aerofoil theory the value of x_w may be ascertained from Table 9.1.

It should be noted that the analysis assumes that both a_2 and b_2 are linear functions of the flap deflection. This becomes less true for flap deflections in excess of about 20°.

Table 9.1 Chord-wise centre of pressure due to flap deflection

Flap chord ratio, r	Overall centre of pressure, x	Centre of pressure of load forward of hinge-line, x_w
0.2	0.436	$(0.436 - 0.519R)/(1 - 0.6R)$
0.25	0.42	$(0.42 - 0.624R)/(1 - 0.75R)$
0.3	0.405	$(0.405 - 0.72R)/(1 - 0.9R)$
0.35	0.39	$(0.39 - 0.804R)/(1 - 1.05R)$
0.4	0.376	$(0.376 - 0.878R)/(1 - 1.2R)$

9.5 Longitudinal air-load distribution on bodies in subsonic flow

The lift on a body in subsonic flow is small in comparison with that on the wing, being typically only 3–5 per cent of the total. It may be estimated from the lift curve slopes of the wing–body combination, a_{1WB}, and the wing in isolation. a_{1W}:

$$\text{Ratio of load on body to total load} = (a_{1WB} - a_{1W})/a_{1WB} \tag{9.21}$$

The distribution of this load along the length of the body cannot be accurately predicted without wind tunnel or advanced computational analysis. For initial loading calculations the simplest approach is to assume a distribution ensuring that it corresponds both with the additional lift on the body and the increment in pitching moment due to the body defined by the coefficient $(\Delta C_{Mo})_B$. This may be done by assuming that the load distribution consists of two components: one due to body incidence and the other due to a pitching couple. See also Section 9.8.4.

9.6 Pressure distribution on lifting surfaces in supersonic flow

9.6.1 Pressure distribution on a lifting surface of infinite aspect ratio in inviscid supersonic flow

Because of the assumption of infinite aspect ratio the flow is said to be two-dimensional. For the inviscid case the local pressure coefficient at any point on a surface in supersonic conditions is given by:

$$\begin{aligned} C_p = (p - p_0)/q_0 = {} & [2/(M_N^2 - 1)^{1/2}]\eta + [\{\gamma M_N^4 + (M_N^2 - 2)^2\}/\{2(M_N^2 - 1)^2\}]\eta^2 \\ & + [\{(\gamma + 1)M_N^8 + (2\gamma^2 - 7\gamma - 5)M_N^6 + 10(\gamma + 1)M_N^4 \\ & - 12M_N^2 + 8\}/\{6(M_N^2 - 1)^{3.5}\}]\eta^3 + \cdots \end{aligned} \tag{9.22}$$

where

p is the local static pressure
p_o is the free-stream static pressure
q_o is the free-stream dynamic pressure ($q_o = \rho V_o^2/2 = \gamma p_o M_N^2/2$)
M_N is the free-stream Mach numher corresponding to velocity V_o
y is the ratio of specific heats (C_p/C_v)
η is the slope of the surface of the aerofoil at any point relative to the stream direction. That is, η is the sum of the angle of the chord-line of the surface relative to the free-stream, a, and the local angle of the surface relative to the chord-line, η_a

For a thin flat plate, therefore, the pressure over the top surface is constant and equal and opposite to that over the bottom surface. Consequently there is a uniform load over the whole surface.

For an aerofoil section of finite thickness, η will not he equal and opposite on the top and bottom surfaces and hence equal and opposite pressure will not he generated on the top and bottom at the same point on the lifting surface. However. if the aerofoil section is very thin, η_a is small, and η will approximate to $\pm \alpha$, and therefore the pressure will he almost equal and opposite for thin sections with pointed edges. Also, for aerofoil sections with finite thickness, η_a must vary over the chord. Thus η will vary slightly over the top and bottom. and the second and subsequent terms in Eqn. *(9.22)* will result in the load distribution being non-uniform over the whole surface. However, for thin sections at all hut very large angles of attack, the first term in Eqn. *(9.22)* is large in comparison with the others, and consequently the load distrihution will not he far from uniform. The effect of finite thickness is usually to reduce the pressure at the trailing edge relative to that at the leading edge.

When the aspect ratio is less than about unity there is a cross-flow round the surface similar to that occurring on bodies, see Section 9.7.1. This modifies the pressure distrihution.

9.6.2 Pressure distribution on an unswept lifting surface of finite aspect ratio in inviscid supersonic flow

The only part of an unswept wing which does not normally experience two-dimensional flow is that part of the wing in the Mach cone generated from the leading edge of the tip region since, when the flow is inviscid, pressure disturbances caused by the tip region cannot be transmitted to any part of the wing outside of that region, see Fig. *9.18.* The semi-apex angle of the Mach cone is that whose cosecant is equal to the free-stream Mach numher. While this is strictly true only for a flat plate at zero angle of attack the result is a very close approximation for a thin aerofoil at all but very large angles of attack.

Inside the tip Mach cones the pressure falls away from the two-dimensional value at the edge of the Mach cone to zero at the tip in the manner illustrated in Fig. *9.18.* If the

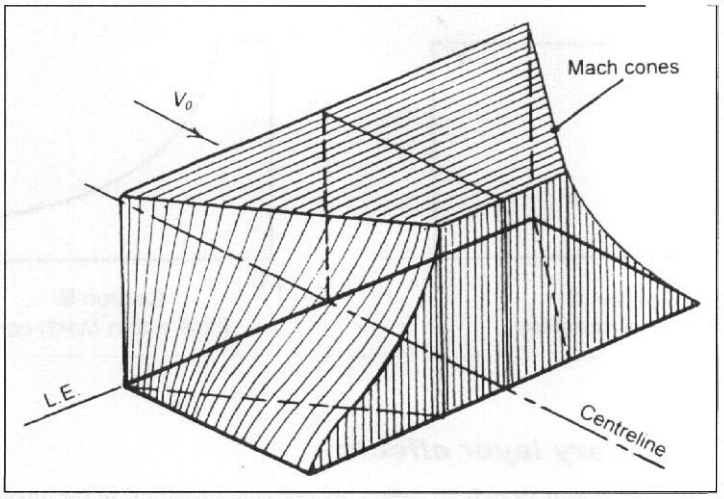

Fig. 9.18 Supersonic pressure distribution on unswept lifting surface

Mach number or the aspect ratio is so low that the Mach cones from the tip intersect on the surface, a very severe loss of load results. In some cases a negative loading can be obtained on the triangular part of the wing behind the line joining the points of intersections of the Mach lines and the opposite tips and the reflection waves from the tips.

Typical span-wise load distributions for wings with unswept leading edges are illustrated in Fig. 9.19. Typical theoretical chord-wise load distributions are shown in Fig. 9.20

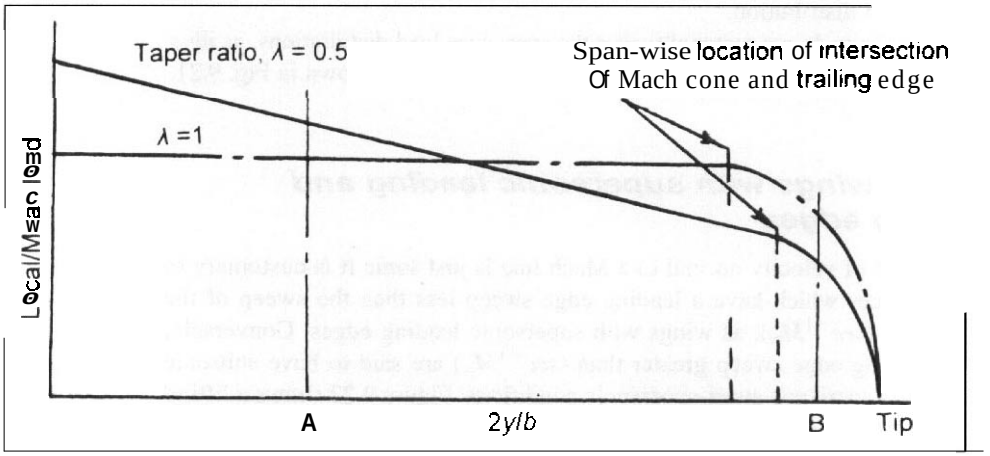

Fig. 9.19 Span-wise loading of surfaces with unswept leading edges in inviscid supersonic flow

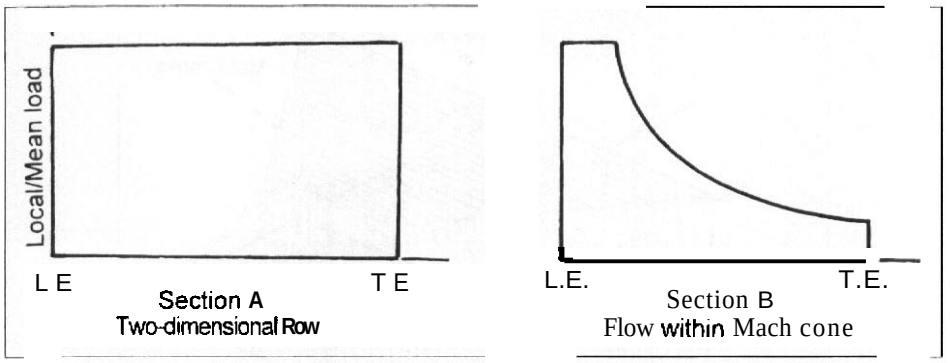

Fig. 9.20 Chord-wise pressure distribution in inviscid supersonic flow

9.6.3 Boundary layer effects

Equation (9.22) and Figs **9.18** to **9.20** define the pressure distribution for unswept lifting surfaces in inviscid flow conditions, that is, in the absence of skin friction effects and consequently of the boundary layer. The effects of the boundary layer must not be neglected, especially in regions near the trailing edge. As the boundary layer is a region of slower moving air relative to the surface, pressure changes can be transmitted through the houndary layer to regions outside the Mach cones, at least to some extent. Consequently, in practice, the sudden changes in slope of the loading curves occurring at the edges of the Mach cones and at the trailing edge are rounded. The extent of the rounding will depend upon the thickness of the boundary layer, this being a function of the load distribution itself and of the Reynolds number.

A further effect resulting from the presence of a houndary layer is that in regions where the chord-wise pressure increases steeply the houndary layer tends to separate from the surface. This effectively modifies the shape of the aerofoil section and consequently the load distribution.

Boundary layer effects do not materially alter the span-wise load distributions, as illustrated in Fig. 9.19 hut the chord-wise loading becomes more like that shown in Fig. 9.21.

9.6.4 Swept wings with supersonic leading and trailing edges

Since the component of velocity normal to a Mach line is just sonic it is customary to refer to lifting surfaces which have a leading edge sweep less than the sweep of the Mach line, which is $(sec^{-1}M_N)$, as wings with supersonic leading edges. Conversely, wings with the leading edge sweep greater than $(sec^{-1}M_N)$ are said to have subsonic leading edges, or to experience quasi-supersonic conditions. Figure **9.22** shows a lifting surface with supersonic leading edges in inviscid flow.

As shown, the trailing edge is also swept at an angle less than that of the Mach line and the trailing edge is also said to be supersonic. The only difference between the wing

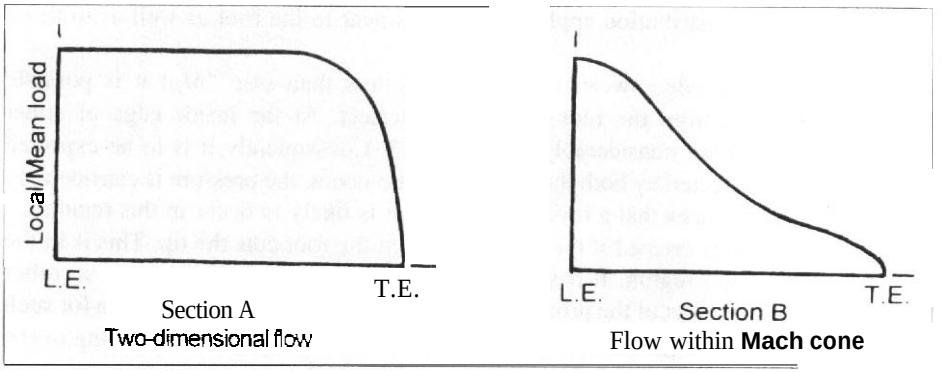

Fig. 9.21 Chord-wise *pressure* distribution *in viscous supersonic flow*

illustrated in Fig. 9.22 and the wing considered in Fig. 9.18 is that, due to the sweep, there is a kink in the pressure distribution at the centre. The leading edge of the centreline chord is the most forward part of the kink, and hence the region which is affected by the kink must he contained inside a Mach cone whose apex is at the leading edge of the centreline chord. **A** conical flow pattern exists in this region just as in the tip cone region. However, there is no condition necessitating that the pressure on the centreline should fall to zero and in practice it does not. The region outside the root and the tip Mach cones only experiences two-dimensional flow and consequently the pressure is approximately constant.

The span-wise load distribution is similar to that shown in Fig. 9.19 except that there is a reduction of load at the root because of the root cone effects. The chord-wise load distribution, allowing for viscous effects is similar to that shown in Fig. 9.21 but in this

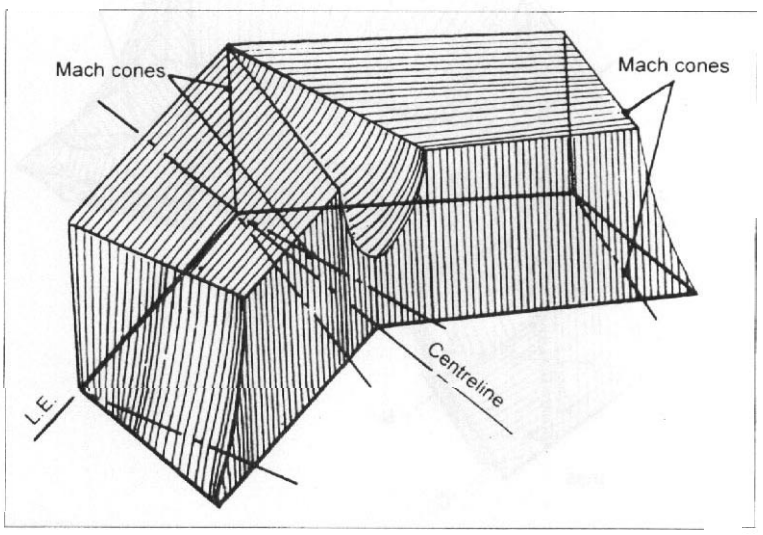

Fig. 9.22 *Lifting surface with* Supersonic leading and trailing edges

case the right-hand distribution applies to sections near to the root as well as to those near to the tip.

When the leading edge sweep is only slightly less than $(sec^{-1}M_N)$ it is possible for the Mach cones from the root and tip to intersect. At the inside edge of either cone the pressure drops considerably, see Fig. 9.23. Consequently it is to he expected that, in the region affected by both the root and the tip cones, the pressure is considerably reduced. Theory indicates that a reversal of pressure is likely to occur in this region.

A reflection cone is created if the Mach line from the root cuts the tip. This is in the form of an expansion region. It has the effect of decreasing the pressure or, in other words, reducing the effect of the primary Mach cones. The pressure distribution for such a case is illustrated in Fig. 9.23. The span-wise load distributions corresponding to the wings shown in Figs 9.22 and 9.23 are shown in Fig. 9.24.

The chord-wise pressure distributions for this class of surface. Fig. 9.23, are illustrated in Fig. 9.25.

9.6.5 Swept lifting surfaces with subsonic leading edges

In this case no part of the lifting surface experiences two-dimensional flow since the whole wing is in the conical flow field developed from the centreline leading edge. There are two forms of this type of condition. firstly the case when the trailing edge is

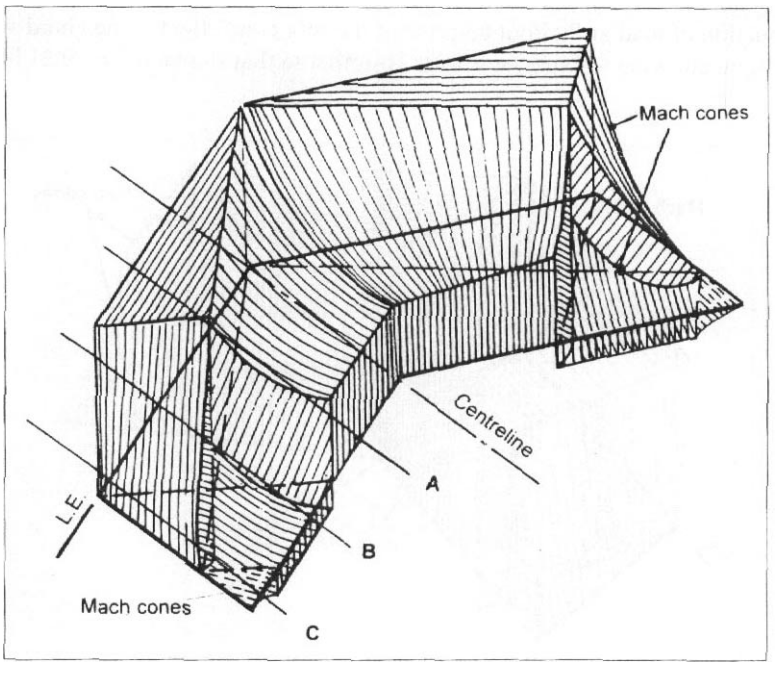

Fig. 9.23 *Pressure* distribution *an* lifting *surface* with just *sonic* leading edges

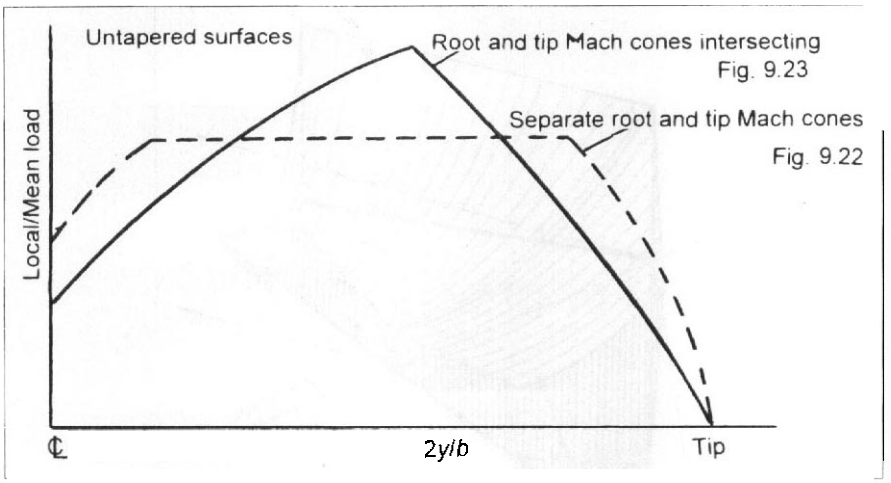

Fig. 9.24 Span-wise load distribution an lifting surfaces with sonic leading edges

supersonic, and secondly when hoth leading and trailing edges are subsonic. Figure 9.26 illustrates the pressure distribution for the case of a surface with subsonic leading edge and supersonic trailing edge. There is a reversal of load at the tip regions where hoth the root and tip cones interact.

The case in which both leading and trailing edges are subsonic is similar and differs only in the further, relatively small. reduction in pressure in the region influenced by the Mach cone from the centreline trailing edge. A series of reflections of this cone can occur from the tip and the trailing edge to give a fluctuating loading pattern in the tip trailing edge region. The magnitude of pressure in this region is usually quite small. The load distribution on a wing with hoth leading and trailing edges subsonic is shown in Fig. 9.27.

9.6.6 'Commentson the pressure distributions over lifting surfaces in supersonic flow

The pressure distributions over lifting surfaces in supersonic flow have been discussed under several categories dependent on the sweep of the leading and trailing edges

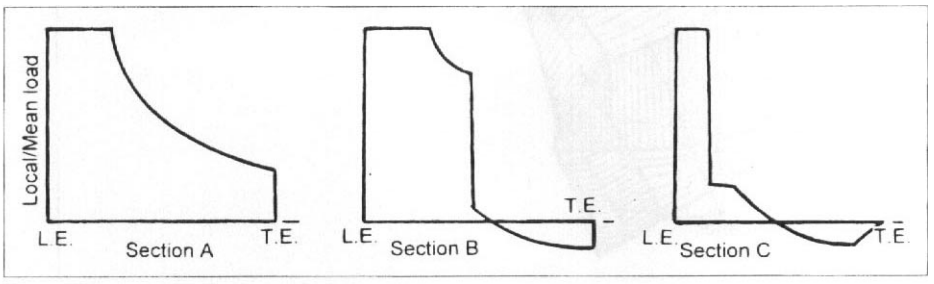

Fig. 9.25 *Chord-wise pressure distribution on a surface having supersonic leading and trailing edges in supersonic inviscid flow*

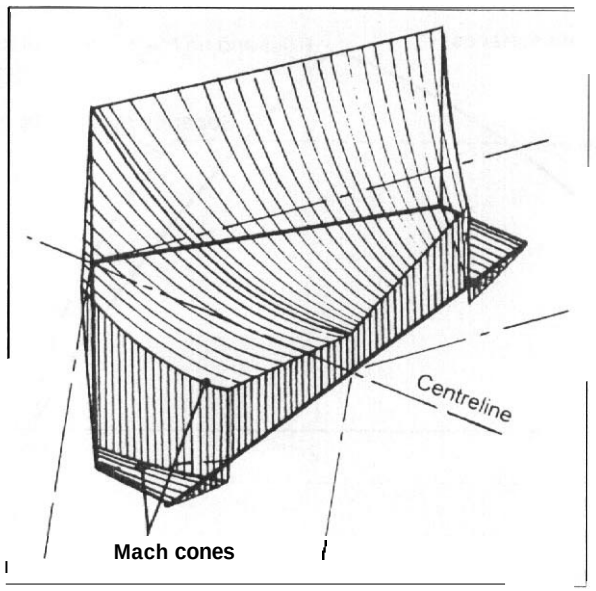

Fig. 9.26 *Lifting surface having a subsonic leading edge in inviscid supersonic flow*

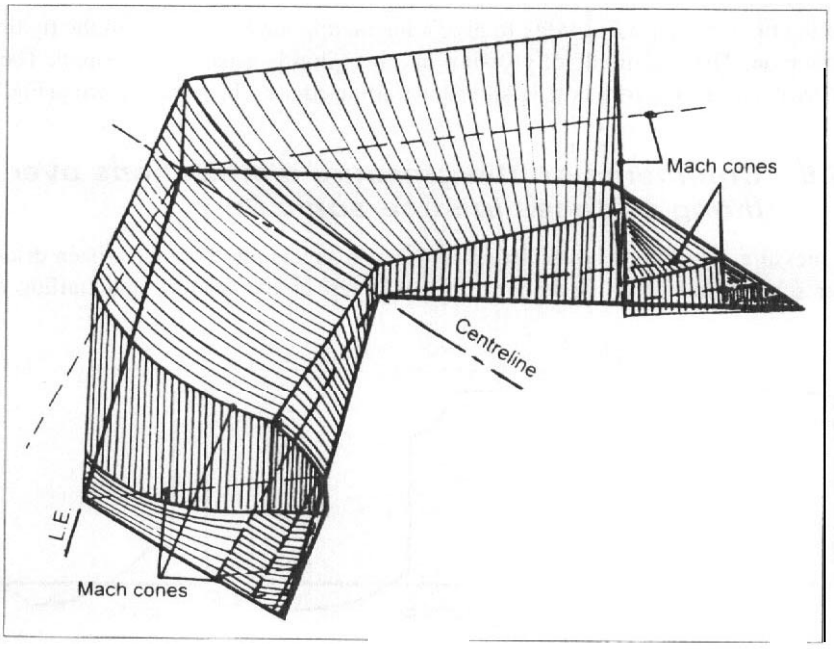

Fig. 9.27 *Lifting surface having both subsonic leading and trailing edges in inviscid supersonic flow*

relative to the Mach cones. An actual surface will pass from one category to another as the flight Mach number changes. For example a moderately swept, untapered, wing with stream-wise tips will have a pressure distribution similar to that shown in Fig. 9.27 at low supersonic speeds and it will change to that shown in Fig. 9.23 and then to that shown in Fig. 9.22 as the Mach number increases. Only in this latter phase is the tip making a significant contribution to the overall lift and even then to a lesser extent than the rest of the surface. It follows that a finite stream-wise tip contributes little to the lifting characteristics of the surface but it can have a considerable effect on the pitching moment. and hence on the position of the aerodynamic centre. This. as can be seen from the figures, will move backwards significantly with increase in Mach number due to the increase in the area of the lifting surface experiencing two-dimensional flow, especially over the tip region. Comparison of the local centres of pressure of the loading at the tip indicated by Fig. 9.25, Section C, with that of Fig. 9.20, Section B, illustrates this effect. It is logical to consider adopting means of reducing this undesirable characteristic. One method is to taper the surface to a point. Fig. 9.28(a), which leads to a true delta wing. Alternatively the tips can be cut along the Mach line corresponding to the highest flight Mach number, Fig. 9.28(b). An extreme example of this is when the tips are cut off normal to the centreline giving the plan-form as shown in Fig 9.28(c).

It can be seen from the load distributions that even with lifting surfaces having tips shaped such that they do not contribute to the shift of aerodynamic centre, there will still be a rearward shift in aerodynamic centre with increasing Mach number. This will be most rapid for wings with unswept leading edges and most gradual for highly swept wings. The aerodynamic centre in all cases will move from about 0.25 to 0.3 of the mean aerodynamic chord at low supersonic Mach number to 0.45 to 0.48 of the mean aerodynamic chord at high supersonic Mach number.

Although, with the exception of Fig. 9.21, the distributions are for inviscid flow conditions, it must be noted that the modifying effects of the boundary layer described previously apply in all cases. At high angles of attack the distributions suggest that quite large adverse pressure gradients can exist on the aerofoil. Consequently it is probable that some boundary layer separation will take place and cause a modification of the pressure distributions.

The distributions for wings with supersonic leading edges apply only to wings with effectively sharp leading edges. For wings with rounded leading edges. or wings at

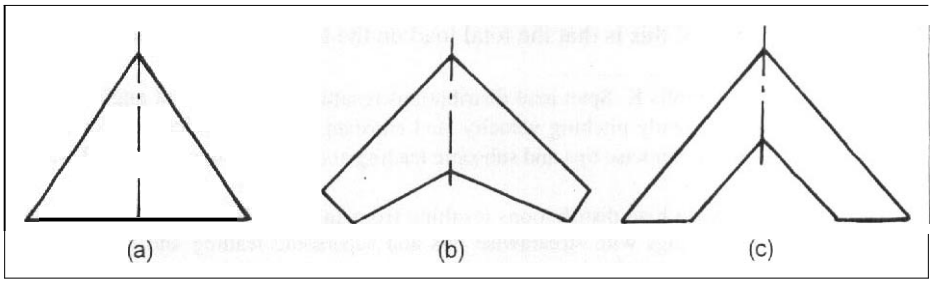

Fig 9 28 Methods of avoiding tip effects

relatively low supersonic speeds and at high angles of attack, the shock at the leading edge will not be attached and as a consequence a subsonic leading edge type of pressure distribution will occur.

Figures **9.29** and **9.30** have been extracted from reports by Hannah and Margolis[5] and Marlin and Jefferys.[6] These figures illustrate the effects of changes in Mach number, aspect ratio, sweepback and taper ratio on surfaces with subsonic and supersonic leading edges respectively. They show that the rate of change of magnitude of the span-wise loading with increase of angle of attack decreases with increasing Mach number and aspect ratio, but the shape of loading is not greatly affected. On the other hand increase of sweephack or taper ratio does not significantly affect the rate of change of the total load with increase of angle of attack but does have considerable effect in increasing the loading towards the tips of the surface. This effect is more marked for the case of a surface having supersonic leading edges. It is apparent from these figures that, with the exception of surfaces with little or no sweep, the loading towards the tip will be large in comparison with that at the root. This is likely lo result in very high loads in the structure, especially for highly tapered wings. Use of camber and twist to decrease the pressure towards the tip offsets this tendency.

Some surfaces have been designed such that the span-wise loading is uniform at a given lift coefficient. It should be realized, however, that if this is done a span-wise and chord-wise shift of centre of pressure position will result with change in angle of attack since $(M_N{}^2 C_L)$ is independent of change in Mach number for constant height and vehicle mass. This can lead to undesirable trim and stability characteristics.

The references from which Figs **9.29** and 9.30 have been extracted also give span-wise load distributions resulting from steady rolling velocity, steady pitching velocity, and constant vertical acceleration. These can be used to correct the load distributions for the effects of camber and twist, whether it is built-in or results from deformation of the wing under load.

9.6.7 *Effect of yaw on the pressure distribution in supersonic flow*

When a lifting surface at incidence is yawed in supersonic flight the Mach cones at the tips affect different extents of the span of the surface on either side. As can be seen from Fig. **9.31** the cone from the leading tip covers a larger region of the surface than when the surface is not yawed. while that from the trailing tip affects a smaller area. The obvious consequence of this is that the total load on the trailing side is greater than that

[5] Hannah M. E. and Margolis K. Span load distributions resulting from constant angle of attack, steady rolling velocity, steady pitching velocity, and constant vertical acceleration for tapered, sweptback wings with streamwise tips and subsonic leading and trailing edges. NACA Technical Note 2831. 1952.

[6] Martin and Jefferys.Span load distributions resulting from angle of attack, rolling and pitching for tapered sweptback wings with streamwise tips and supersonic leading and trailing edges. NACA Technical Note 2643, 1952.

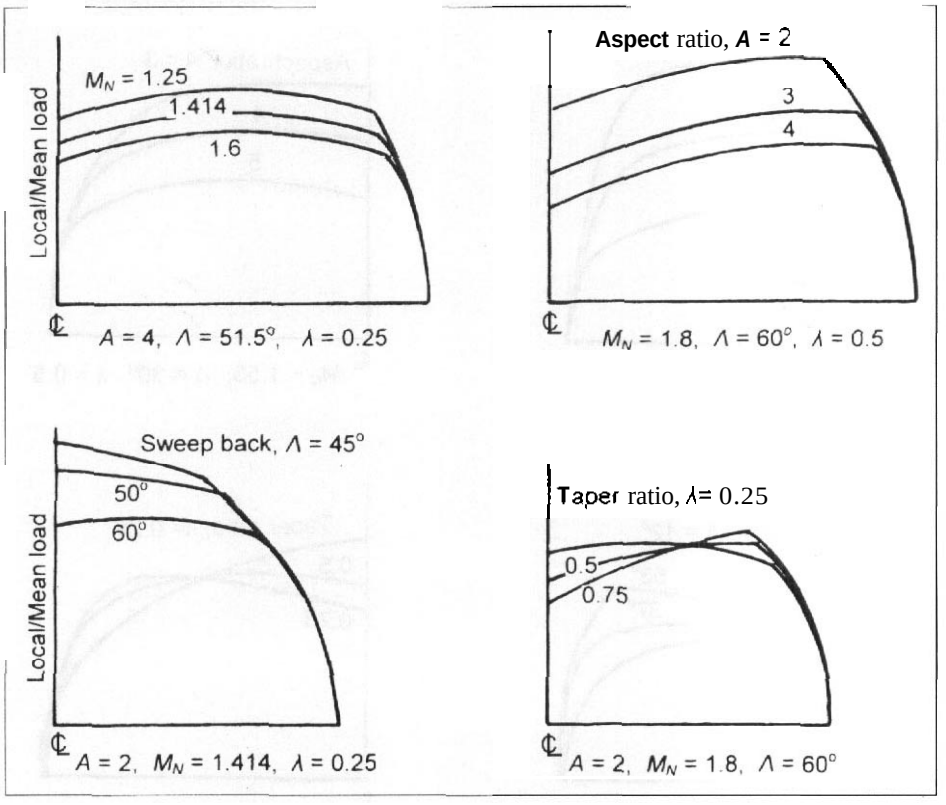

Fig. 9.29 Effect of Mach number and geometry on the span-wise loading of wings with subsonic leading and trailing edges

on the leading side and its centre of pressure acts nearer to the tip. Hence, there is a rolling moment developed in the sense of the trailing wing moving upwards.

This effect is considerably increased at all but small combinations of incidence and yaw by the effects of the trailing vortex core in the centre of the tip cone, which will separate from the surface and tend to follow the free-stream direction. The vortex core of the leading tip moves in towards the centre of the surface, while the vortex core of the trailing tip moves out from the tip. Since these tip vortices cause a substantial downwash effect, the result of the movement of the vortices relative to the surface is to decrease the lift on the leading tip and increase it on the trailing tip relative to the unyawed condition.

A wing rolling, in the sense of trailing wing up, is said to have a positive rolling moment due to sideslip, that is, the contribution to the derivative L_v is positive. **This** effect can be significantly reduced by cutting off the tips or fully tapering the wing as suggested in the previous section.

Figures 9.29 and 9.30 show that even when the effects of the tip cone are neglected, the effect of reducing the sweep of a surface is to move the span-wise centre of pressure in towards the centreline. Since the total load on the wing remains almost constant this will also tend to give a positive contribution to the derivative L,.

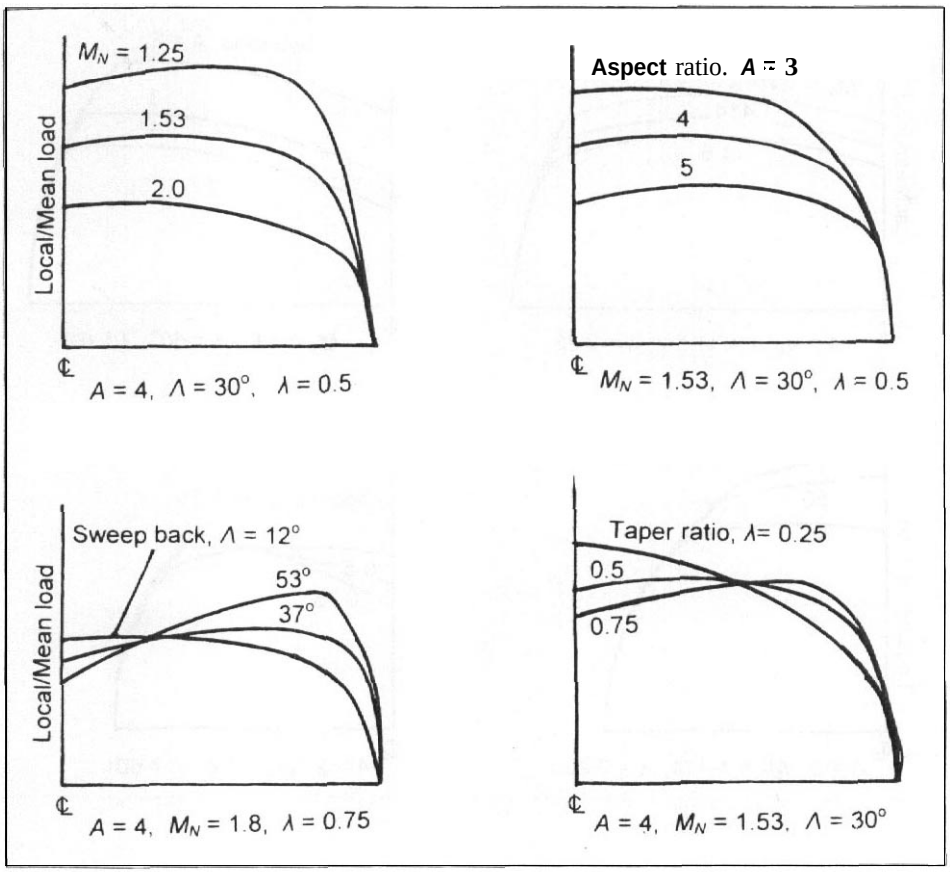

Fig. 9.30 Effect of Mach number and geometry on the span-wise loading of wings with supersonic leading and trailing edges

In the case of a vehicle with a doubly symmetric, cruciform, lifting surface layout an angle of attack in one plane is equivalent to yaw in the other. Consequently if the vehicle is manoeuvring in both planes, so that both pairs of surfaces are at angle of attack. there will be a rolling moment from each pair which will be additive. Hence, combined pitch and yaw on a cruciform winged vehicle causes a rolling moment. This effect is in addition to the rolling moment resulting from the interaction of the pressure fields of each set of surfaces.

9.6.8 Pressure distribution due to control deflection in supersonic flow

9.6.8.1 Isolated, all-moving. control surfaces

Isolated. all-moving, controls can be treated in exactly the same manner as fixed lifting surfaces. The only additional effect likely to arise is that the control may be in the

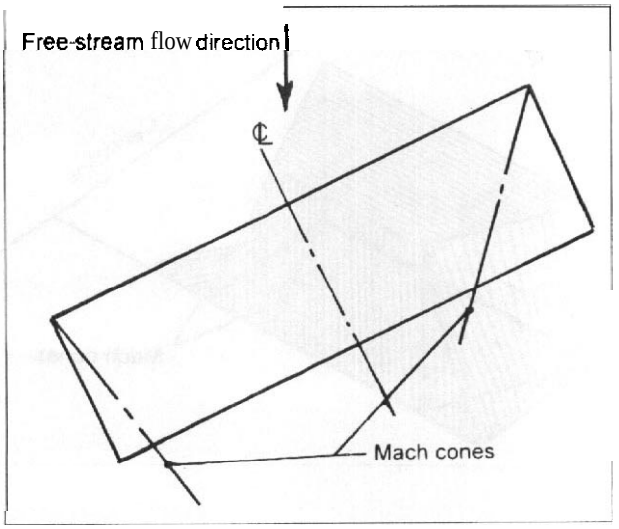

Fig. 9.31 Unswept and untapered surface yawed in supersonic flow

downwash field of a wing, in which case the wing pressure distribution must be determined and a correction made for it in a way similar to that for the twist effects due to distortion referred to in Section 9.6.6. Large downwash effects can result if the control is in the region of the vortex cone from a wing tip.

9.6.8.2 Trailing edge control surfaces with a supersonic hinge-line

Theoretically the pressure distribution on a control surface at the trailing edge of a lifting surface resulting from the deflection of the control is unaffected by the presence of the fixed surface ahead of it. Hence; it does not impose any load on that surface except, possibly, in the regions of the tip Mach cones emanating from the edges of the control. Consequently for the case of a supersonic hinge-line the load distribution due to control deflection is as shown in Fig. 9.32. The distribution is just the same as if the control were isolated, except for a small load on the adjacent fixed surface in the tip cones. The load on the control itself is additional to that on it due to angle of attack of the whole surface. Theoretically the additional loading due to control deflection is not affected by root and tip cone effects from the fixed surface. In practice viscous effects cannot be neglected, especially for trailing edge controls near to the tip. The boundary layer effect can he large even at relatively small angles of attack and small control deflections. It is worth noting that separation may occur at the trailing edge on the top surface at zero control deflection and that pressure is transmitted through the boundary layer on the lower surface. mainly at the hinge-line, associated with the strong shock pattern at this position. The theoretical estimation of loading on controls is difficult and it is probably best to rely upon wind tunnel testing at the relevant Reynolds numbers.

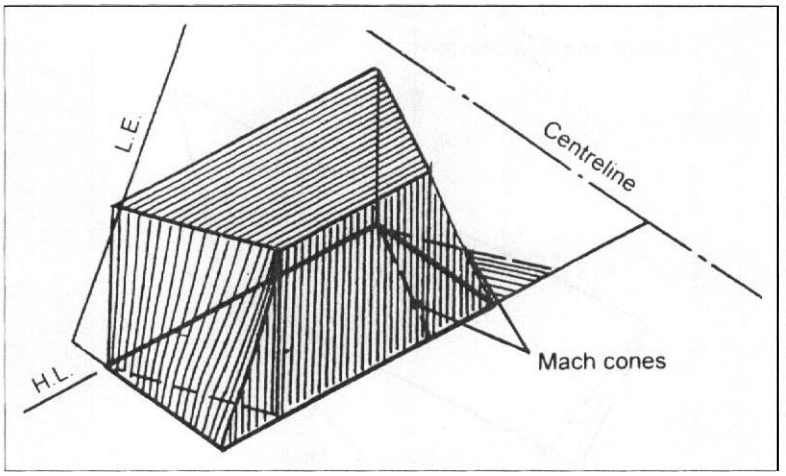

Fig. 9.32 ***Pressure*** distribution ***on*** a ***control surface*** with a supersonic hinge-line

Approximate estimates of the chord-wise load components and the hinge moment due to conuol or flap deflection in two-dimensional supersonic flow may be made by following the procedure outlined in Section 9.4.3.2 for subsonic flow conditions.

This is illustrated in Fig. 9.33. The total load on a flap, Eqn. (9.18a), is also applicable to this case. However, the distribution of the load across the flap chord in two-dimensional inviscid supersonic flow is theoretically uniform. Hence:

$$S_1 = c_f/c \qquad \text{and} \qquad S_2 = 1 \tag{9.23a}$$

Therefore on a unit span:

$$\begin{aligned}\text{The total hinge moment on flap} &= \{\rho V_o^2 c(S_1 a_1 \alpha + S_2 a_2 \delta)/2\}(c_f/2)\\ &= \{\rho V_o^2 c(c_f a_1 \alpha/c + a_2 \delta)\}(c_f/2)\\ &= \rho V_o^2 c c_f (a_1 \alpha c_f/c + a_2 \delta)/4 \qquad (9.23b)\end{aligned}$$

As in the subsonic case three-dimensional effects will change this simple analysis due to the influence of the Mach cones, as will the boundary layer in viscous flow.

9.6.8.3 Trailing edge control surfaces with a subsonic hinge-line

When the control surface or flap hinge-line is swept at a greater angle than the Mach line the hinge-line is said to be subsonic even though the overall flow is supersonic. Typical chord-wise pressure distributions for this case based on inviscid linearized theory are shown in Fig. 9.34. These are due to Frick.[7]

[7] Frick, C. W. Application of the linearised theory of supersonic flow to the estimation of control surface characteristics. NACA, Technical Note 1554. 1948.

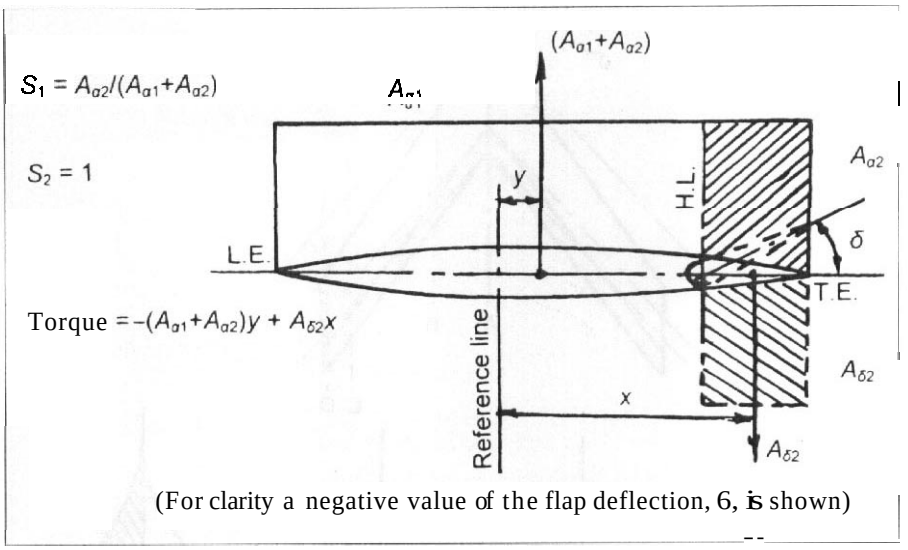

Fig. 9.33 Two-dimensional ***chord-wise*** *loading* in *inviscid supersonic flow*

The load on the surface due to control deflection is zero back to the point where the Mach cone from the inboard end of the hinge-line cuts a particular chord-wise section. The boundary layer effects are Likely to be less than for the supersonic hinge-line case. The main effects are probable reductions of the load at the inboard end and at the hinge-line. The tip effects reduce the load on the control by a much smaller amount than they do with angle of attack loading on a surface with stream-wise tips. This suggests that in the case of an aileron the rate of roll which can be attained on a wing with stream-wise tips will be greater than for a wing with cut-off tips since the latter has a relatively greater damping in roll.

9.7 Air-load distribution on bodies and wing–body combinations in supersonic flow

9.7.1 Isolated bodies

The load distribution on an isolated body at an angle of attack is determined both by the potential flow characteristics and the effects of viscosity. The flow over a body at incidence can be resolved into a flow parallel to the body centreline and a flow normal to the body centreline. as illustrated in Fig. 9.35. The analysis is similar to that for swept lifting surfaces when the velocity component normal to the sweep is considered in determining. for example, the critical Mach number of a yawed wing of infinite aspect ratio.

The component of velocity parallel to the body axis will not contribute directly to the normal force on the body. The component normal to the body is effectively flowing round the cross-sectional shape of the body, which in many cases is effectively circular.

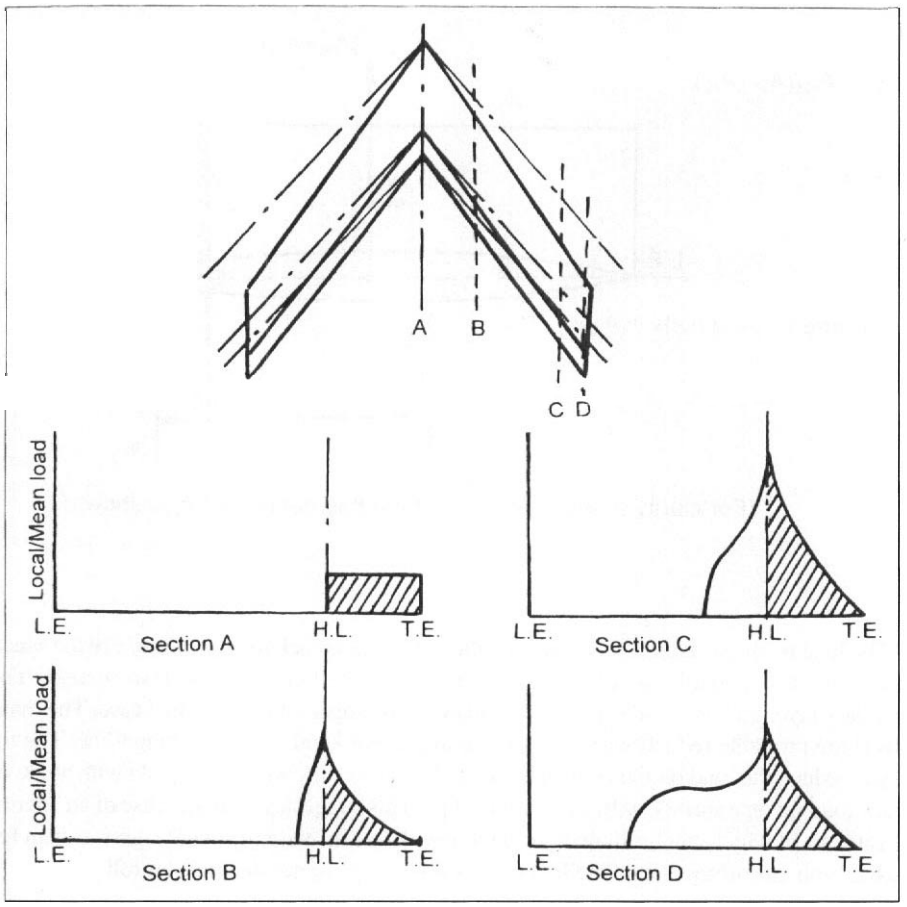

Fig. 9.34 ***Pressure distribution due to the deflection of a flap having a subsonic hinge-line in inviscid supersonic flow***

When the value of $(V_o \sin \alpha)$ corresponds to a subsonic Mach number it is to be expected that the flow pattern in this direction will be similar to that for a circular cylinder placed normal to a subsonic flow. In this case, for all but very low Reynolds numbers, the flow forms a pair of vortices on the aft side of the cylinder where they separate and flow downstream. Experiments on inclined bodies of revolution at supersonic speeds have shown that a pair of vortices do form at some point on the upper surface away from the nose, and that for all but very small incidences these vortices separate from the upper surface and follow an approximately free stream direction in a similar manner to the trailing vortices of a wing. The drag associated with this cross-flow velocity is effectively equivalent to the normal force on the body and, since drag is proportional to the square of the speed, it follows that normal force can be expected to be proportional to $(V_o \sin \alpha)^2$ or, for small incidences, in proportion to $(V_o \alpha)^2$.

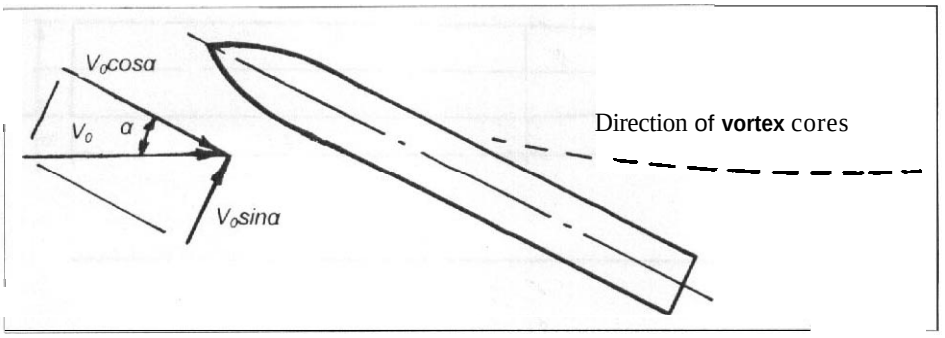

Fig. 9.35 Velocity components on a ***body*** *at* incidence in supersonic *flow*

The essentially viscous form of this normal force indicates that Reynolds number effects are important, since below the critical Reynolds number the separation will not occur. Consequently the extent of the length of the body experiencing this drag, or normal force, will increase as $(V_o \sin \alpha)$ increases, that is, as the angle of attack increases. At large angles of attack there will be separated flow over the whole of the top surface of the body and the centre of pressure will approximate to the centre of plan area. At low angles of attack the normal force on the body away from the nose will bc small and the majority of the normal force will result from the flow over the nose portion and may be assessed reasonably accurately by potential flow theories. Typical load distributions at various angles of attack are shown in Fig. 9.36, taken from work by Perkins and Huehn.[8]

Figure 9.36 shows the variation of lift and centre of pressure with change in angle of attack in supersonic flow. A similar cross-flow phenomenon is experienced on wings of low aspect ratio, as well as bodies. The angle of attack at which it becomes marked decreases with aspect ratio and increase of sweepback. see Section 9.6.1.

9.7.2 Air-load distribution on wing–body combinations in supersonic flow

In addition to the load distributions on the isolated lifting surface and on the body at angle of attack there are load distributions resulting from the effect of the body on the wing and the wing on the body. The effect of the body on the wing is due to two [actors. Firstly at the wing–body junction the body usually has a relatively thick boundary layer and this has the effect of reducing the pressure changes on the wing so that the resulting loading at the root of the wing is reduced considcrahly in the boundary layer region. The second effect is that the body usually induces an upwash field over the wing causing an increase in load. This increase may be as much as 10 per cent of the load on the isolated

[8]Perkins E. W. and Huehn. Comparison of the theoretical and experimental distributions of lift on a slender inclined body of revolution. NACA Technical Note 3715.

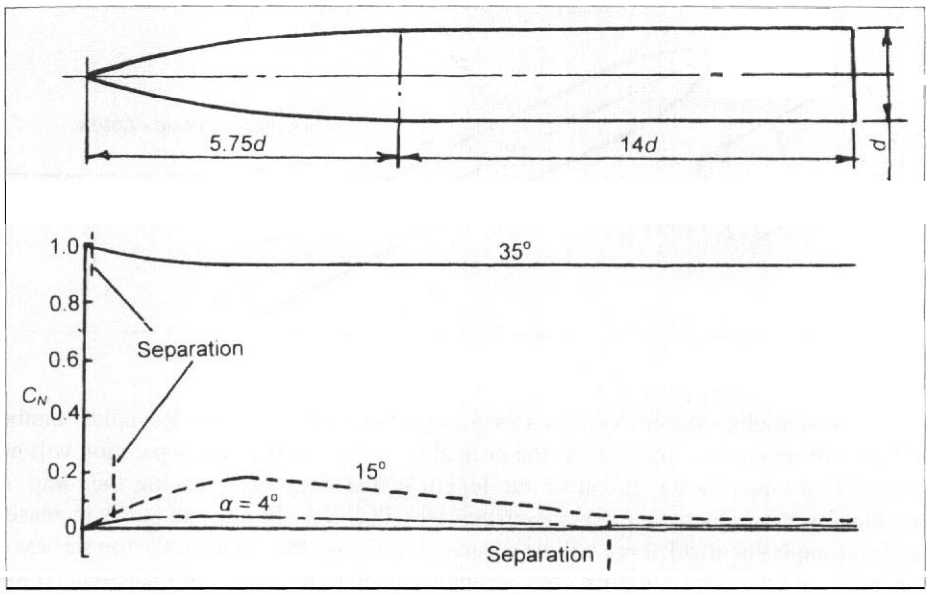

Fig. 9.36 Variation of load distribution along a body with increase of angle of attack

wing section. The distribution of these local increments is approximately similar to that for the angle of attack of the isolated wing.

The region of interference of a wing on a body can be determined by tracing the helices made by the Mach lines from the wing root chord on the body. In invicid flow the chord-wise pressure distribution at the root of the wing is transmitted to the body in the region aft of the position of the helices from the root leading edge and decreases in magnitude with the distance aft from the root chord. The effect of body boundary layer is to smooth out this effect, especially at some distance from the root, but the distribution of load is essentially similar for cases where there is no marked separation over the body in the region of the wing. The magnitude of the lift induced on the body will depend very largely upon the size of the body relative to the wing. A typical result for a guided missile configuration is that the lift induced on the body is half that on the net wing. It follows that, although the body blanks the wing, the overall lift on the wing–body combination is not very different from that on the isolated gross wing.

An important effect of the body is that the load induced by the wing acts over a region behind the root chord, as is clear from considering Fig. **9.37.** As the flight Mach number increases the position of the centre of pressure of the wing-induced body load moves aft. If the aft end of the body is close to the trailing edge of the root of the wing then the induced load will diminish rapidly with increasing speed. Figure 9.37 also shows that, if the body length is large, the downwash from the wing tip cones can cause a down-load near the aft end of the body. This load is usually small but acts at a large moment arm and consequently will change the overall pitching moment.

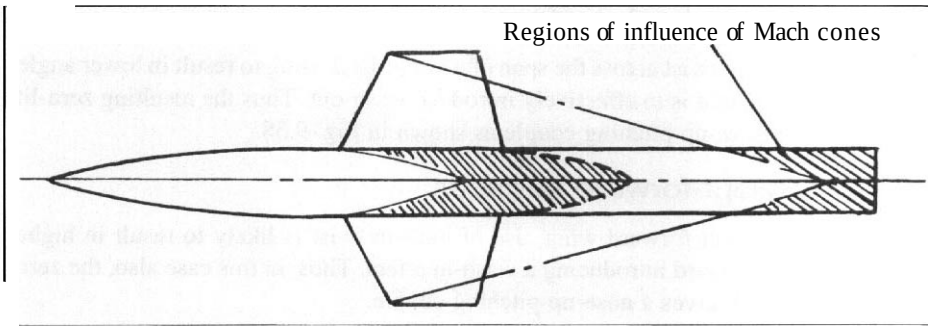

Fig.* 9.37** ***Zones of influence of the wing on the ***body in supersonic flow***

9.8 The contribution of overall loading at zero lift to the zero-lift pitching moment

9.8.1 Introduction

While the algebraic sum of all the local lift distributions on an aircraft may become zero, the local loading across the airframe is likely to produce couples. each of which contributes to the overall zero-lift pitching moment. The more significant of these effects are discussed in the following sections.

9.8.2 Wing aerofoil section camber

Aerofoil sections, other than those having symmetry about the chord-line, experience a pitching couple resulting from the distribution of pressure over the contour and the consequent chord loading, see Fig. 9.14. This couple corresponds to the term C_{Mo} for the local aerofoil. The accuracy of an aerofoil intended to be of symmetrical section is limited and the section may experience distortion under load. Hence, there will be a pitching moment of questionable magnitude and the design and manufacture must be controlled such that the resulting value of C_{Mo} is within the limits defined by the specification of the aircraft. When the aerofoil section is cambered the value of C_{Mo} is determined by a combination of the defined aerodynamic and the distortion characteristics. The effect is usually nose-down.

9.8.3 Lifting surface twist

9.8.3.1 Unswept surfaces

The span-wise loading of twisted wings at zero lift produces bending couples on each semi-span. When the lifting line is unswept these couples do not affect the pitching equilibrium of the system.

9.8.3.2 Swept-back surfaces

It is usual for built-in twist across the span of a swept-back wing to result in lower angles of attack outboard. that is to effectively introduce wash-out. Thus the resulting zero-lift load produces a nose-up pitching couple as shown in Fig. 9.38.

9.8.3.3 Swept-forward surfaces

In the case of a swept-forward wing, use of built-in twist is likely to result in higher angles of attack outboard introducing a wash-in effect. Thus, in this case also, the zero-lift load distribution gives a nose-up pitching couple.

9.8.4 Fuselage camber

Although, as mentioned in Section 9.5, at subsonic speed the lift contribution of the body is small it may well be made up of two relatively large components of opposite magnitude, as shown in Fig. 9.39. There is thus likely to he a large pitching effect, especially when the locus of the mid-depths of the body cross-section is curved to improve view over the nose and to give tail-down clearance. The resulting, usually nose-down, moment contributes to C_{M_0}. Powerplant nacelles often exhibit a similar effect although the magnitude of the contribution to C_{M_0} is usually much less.

9.8.5 Wing–body effect

The presence of a body considerably alters the wing loading over the intersection region such that locally at the centreline the lift may be as low as 40 per cent of that of an isolated wing. Outboard of the sides of the body the wing functions more or less

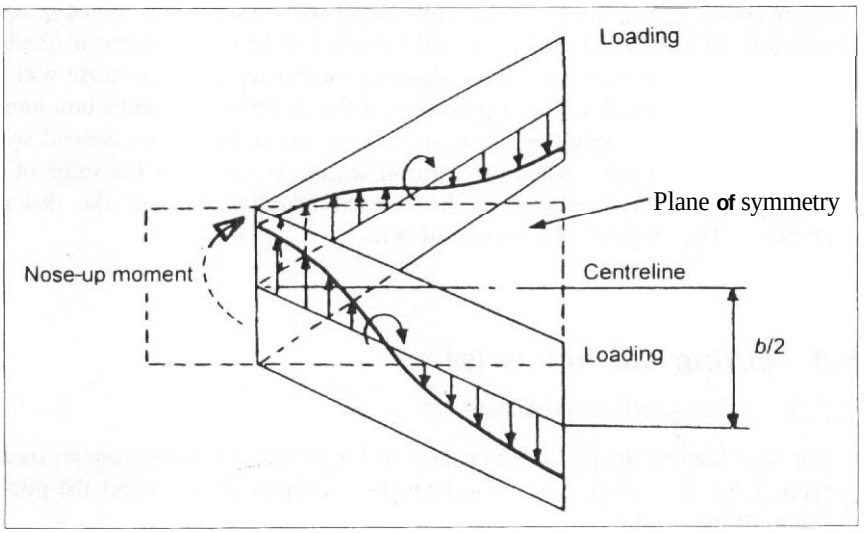

Fig. 9.38 Origin of the zero-lift pitching moment on a swept-back surface

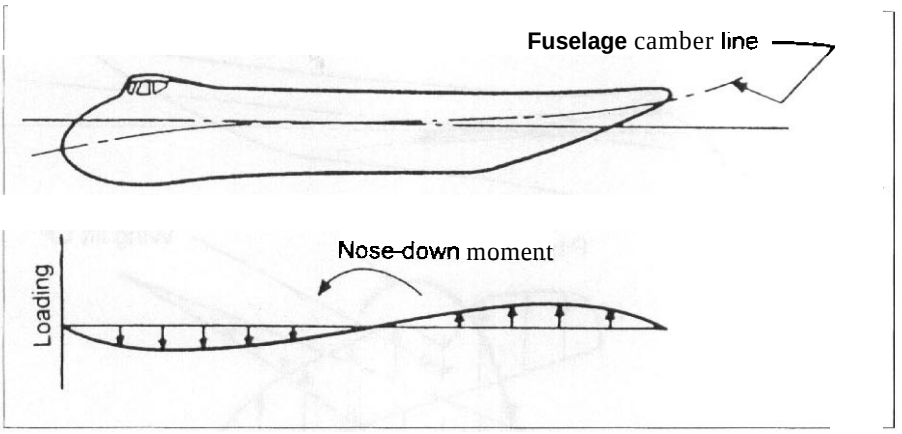

Fig. 9.39 Origin of fuselage zero-lift pitching moment

normally as is indicated in Fig. 9.40. Taken overall the lift on the body usually more than compensates for the local loss of wing lift.

The alignment of the body with the air-stream in cruise should be such that it is in its most streamlined position to ensure that the drag is as low as is possible. This usually implies that the wing is set at a positive angle of attack relative to the body. The zero-lift attitude tor such a combination is then as is shown in Fig. 9.41. From the figure it is seen that when the centres of pressure of the wing and of the body do not coincide a further pitching couple arises and again it is usually nose-down.

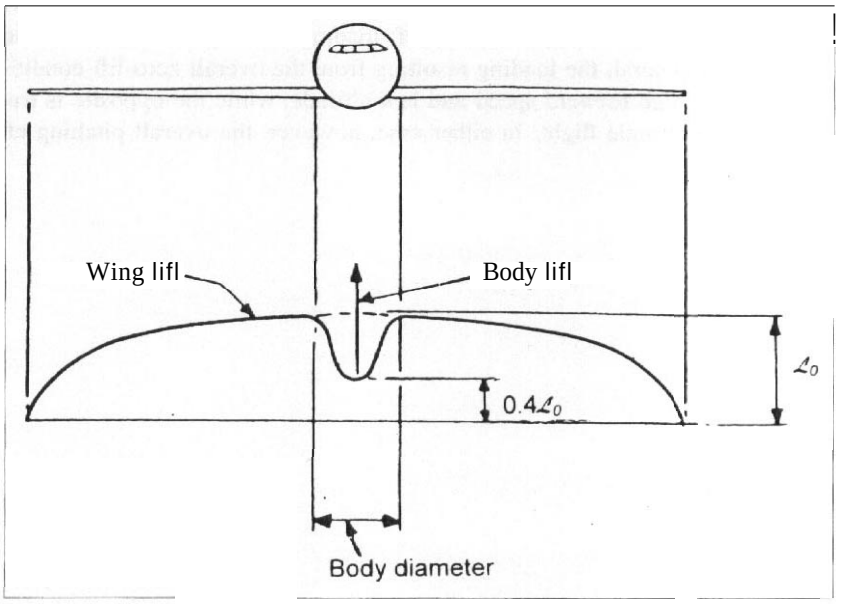

Fig. 9.40 Wing–fuselage interference effect

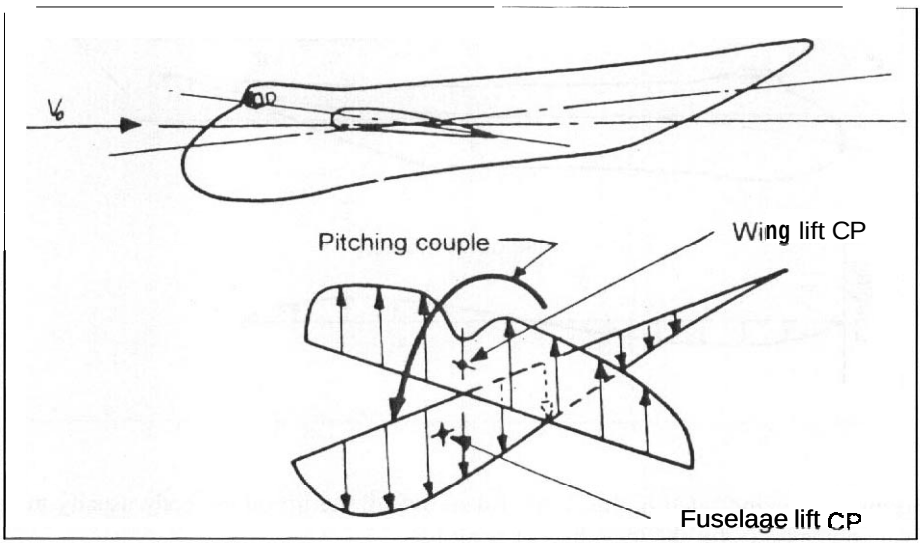

Fig. 9.41 Origin of the wing–fuselage pitching moment

9.8.6 Total zero-lift pitching moment

All the foregoing effects, together with similar contributions appropriate to special vehicle configurations, must be added to give the complete zero-lift loading and the zero-lift pitching couple, C_{Mo}, for the whole aircraft.

As mentioned in Section 9.3.1.5 when the wing is working at a high angle of attack the zero-lift loading components are small in comparison with the other loads; however, when the angle of attack is small the zero-lift loading forms a substantial fraction of the total. Thus, in general, the loading resulting from the overall zero-lift condition is most significant at high forward speed and low altitude, while the opposite is true for low-speed or high-altitude flight. In either case, however, the overall pitching effects are of importance.

CHAPTER 10

Specification and analysis of repeated loading

10.1 Introduction

The satisfactory behaviour of an airframe under a single occurrence of the maximum design load may be ascertained with an acceptable degree of accuracy by interpreting the information contained in the requirements handbooks. The appropriate limit load cases have been established by experience as the maximum expected to occur within the required probability. However, as was discussed in Chapter 1, Section 1.3, in order to establish the design life of the airframe it is essential to consider all the occurrences of load. In normal operations the aircraft encounters a very large number of loads in any given category each being lower in magnitude than the corresponding limit design case. Nevertheless, these lower loads are significant in the design of the structure since individually they cause 'fatigue damage' and hence collectively determine the life of the airframe. Fatigue damage manifests itself as the propagation of cracks in various members of the structure. These, if not detected and repaired, ultimately result in complete failure of those members.

The analysis of the conditions necessary to establish the life of an airframe is fraught with difficulty. The structural damage caused by a given increment in load is not only a function of its magnitude but depends also upon such factors as the previous loading history and the initial conditions to which the load increment is added. The damage is not always linearly dependent upon the magnitude of the load, such as when stress concentration effects give rise to local plasticity. The philosophies adopted to deal with these difficulties are outlined in Chapter 1, Section 1.3, and are further considered in this chapter in Section 10.7.

10.2 Fatigue design requirements

10.2.1 Introduction

The emphasis of the requirements specified to ensure the integrity of airframes under fatigue loading is on the methods of analysis and the means of demonstrating a satisfactory life. Only in United States military code is there a specification of the magnitude and frequency of the repeated loading and this is outlined in Section 10.2.4. Loading conditions for all categories of aircraft are discussed in Section 10.4.

10.2.2 Civil transport aircrafl

JAR-25.571 outlines the basic requirements for fatigue evaluation and damage tolerance design of transport aeroplanes. The paragraph outlines the general requirements for the analysis and the extent of the calculations. Amplification of the details is given in the associated 'acceptable methods of compliance' given in JAR-25.ACJ 25.571

10.2.3 United Kingdom military aircraft

The basic requirements for fatigue analysis and life evaluation are specified in Def.Stan.00-970 Chapter 201. This covers techniques for allowing for variances in the data as well as overall requirements and the philosophy to be adopted. Detail requirements of the frequency and magnitude of the repeated loading are given in the particular specification for an aircraft.

10.2.4 United States military aircraft

The United States military aircraft stipulations are to be found in three separate documents. In MIL-A-8866A the emphasis is on the detail of the required magnitude and frequency of the repeated loading rather than on the analysis. Data given cover manoeuvre, gust, ground, and pressurization conditions for fighter. attack, trainer. bomher, patrol, utility, liaison, and transport aircraft. MIL-A-8867 prescribes the ground testing to he undertaken as part of the demonstration of the life of the airframe. MIL-A-8868 paragraphs 3.4 and 3.5 stipulate the information to he provided in the form of reports outlining the analysis and testing undertaken to substantiate the life of the airframe.

10.3 Assumptions made in the analysis of fatigue loading

In order to reduce the problem to one capable of being dealt with in actual design applications it is necessary to make simplifying assumptions. Essentially they are:

(a) A 'linear' damage relation is assumed so that the Miner cumulative damage hypothesis may he applied. This hypothesis is based on the use of fatigue data, essentially that extracted from a stress–repetition curve (S–N curve), for a

given component of the airframe. Figure 10.1 presents a typical S–N curve. If N_i repetitions of a stress, S_i, corresponding to a load, L_i in a given category, are required to cause failure, then the proportion of 'damage' done by n_i repetitions of the stress is assumed to be given by (n_i/N_i) and the total 'damage' done over a given time period which corresponds to the n_i repetitions is:

$$\sum_i (n_i/N_i) \tag{10.1a}$$

where $i = \text{I},\ldots,$ rcovers all the different magnitudes of stress in that category.

Similarly the total 'damage' fraction done in that time period by all categories of load is:

$$\sum_i (n_i/N_i) + \sum_j (n_j/N_j) + \sum_k (n_k/N_k) + \tag{10.1b}$$

where i, j, k, etc. refer to the different load categories, for example manoeuvre, gust and ground loading.

If the time period represents the design life of the vehicle, then the reciprocal of the total 'damage' fraction is the life factor. It may be argued that the fatigue

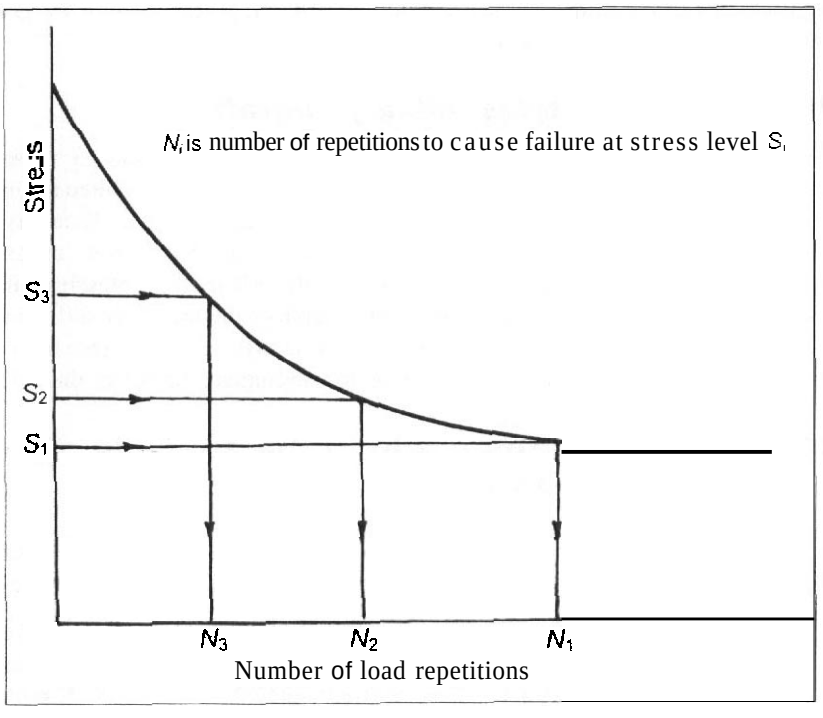

Fig. 10.1 Typical S – N curve

is more closely dependent upon strain, rather than stress, and hence some methods of analysis are based on strain–repetition statistics rather than stress characteristics.

(b) As is implied by (a) above, at the design stage it is usually necessary to ignore the order in which the different magnitudes of loads are applied. However. in service account may he taken of the order of load application in relation to the deployment of the aircraft in different roles. In the special case of the General Dynamics F-111 multi-role aircraft the airframe was subjected to periodic ground loading to a high intensity to relieve local stress concentrations. Related to this was the fact that the initial omission to determine the fatigue effect of the stress concentration at the comers of the pressure cabin windows of the de Havilland Comet airliner was. at least in part, because the fatigue testing was undertaken on a specimen airframe previously subjected to limit loading.

(c) Each load is assumed to be an increment from a datum condition, usually that appropriate to steady level flight.

The first two of these assumptions are justified because of the lack of data on the detailed behaviour of complete structures and the random nature of many causes of fatigue loading. The last is a reasonable representation of the actual conditions found to exist in practice since the majority of loading is incremental to steady level flight or the equivalent ground conditions. Techniques have been developed to assess the life of a structure using this method. Examples are the work of Raithby,[1] ESDU Fatigue Data Sheet 79024,[2] and Def.Stan.00-970 Leaflet 201/3.

10.4 Repeated load data

10.4.1 Presentation of data

It is usual for repeated load data to be presented as load spectra either in diagram or tabular form. The spectra are in terms of a design condition, such as a manoeuvre acceleration or gust velocity, which is reached or exceeded in a given period, specified in terms of number of flights, time, or distance travelled. Some spectra use stress as an alternative to the design condition. Load spectra can be determined by acceleration or strain counters placed in an aircraft, although some means is necessary to distinguish between the consequences of manoeuvres, gusts, and other conditions.

Taylor,[3] collected together a comprehensive set of data relating to repeated loading conditions. The data cover all causes of repeated loads and although biased towards military operations have some information relevant to civil aircraft. His text is a

[1]Raithby. K. D. A method of estimating the permissible fatigue life of the wing structure of a transport aircraft. *Journal of the Royal Aeronautical Society*, 65, November 1961

[2]ESDU Fatigue Data Sheet 79024. The estimation of the endurance of civil aircraft wing structures. ESDU International plc, October 1979.

[3]Taylor, J. *Manual of Aircraft Loads*. AGARDograph 83, Pergamon Press. 1965.

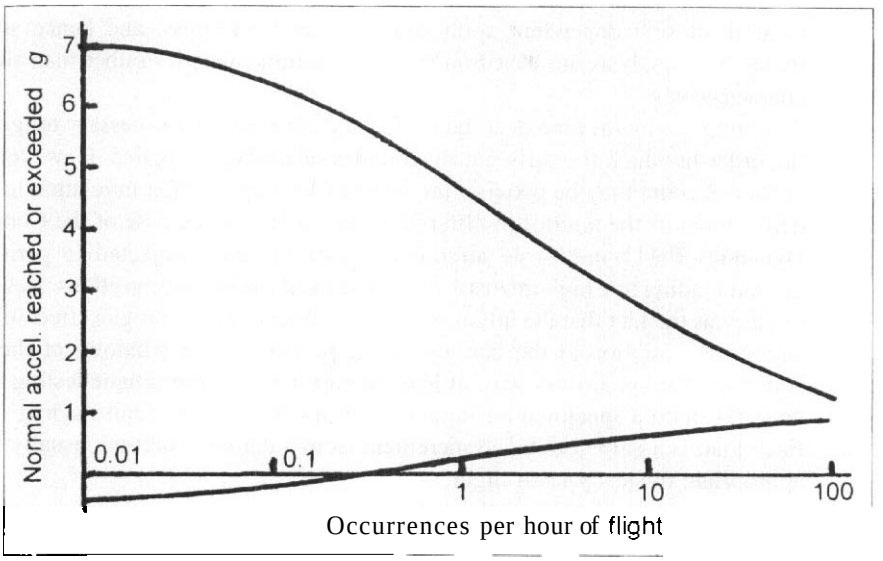

Fig. f0.2 Typical symmetric manoeuvre acceleration *spectrum for a fighter aircraft*

standard reference on the subject. Other reference sources are quoted in the following sections. as appropriate.

10.4.2 Flight manoeuvre cases

10.4.2.1 Symmetric manoeuvres

Extensive information is available in relation to the symmetric manoeuvres of both military and civil aircraft.

An example of a normal manoeuvre acceleration spectrum for an interceptor aircraft is shown in Fig. 10.2. The diagram gives the number of times a given acceleration level is exceeded in each hour of the flight. Thus $4.8g$ is reached or exceeded once in every hour and $6.3g$ once in every 10 hours. That is, one in ten of the $4.8g$ exceedances over a 10 hour period also exceeds $6.3g$. The frequency of a given manoeuvre level may be obtained by tabulating the frequency of each exceedance and successively subtracting from the highest to the lowest. MIL-A-8866A Tables III to VIII give data for fighter/attack, trainers, two classes of bomber, strategic and tactical/assault transports, respectively.

Chapter 5 of Taylor's work presents normal acceleration data derived from flight observations for a large range of military aircraft and also has data applicable to civil transport types. This latter has been extracted and amplified from the work of Buxbaum,[4] to produce Fig. 10.3 and Fig. 10.4. Addendum AD1 gives some data for aerobatic aircraft.

[4]Buxbaum, O. Structure life assessment of the Noratlas transport aircraft. LBF Report FB-71, 1967.

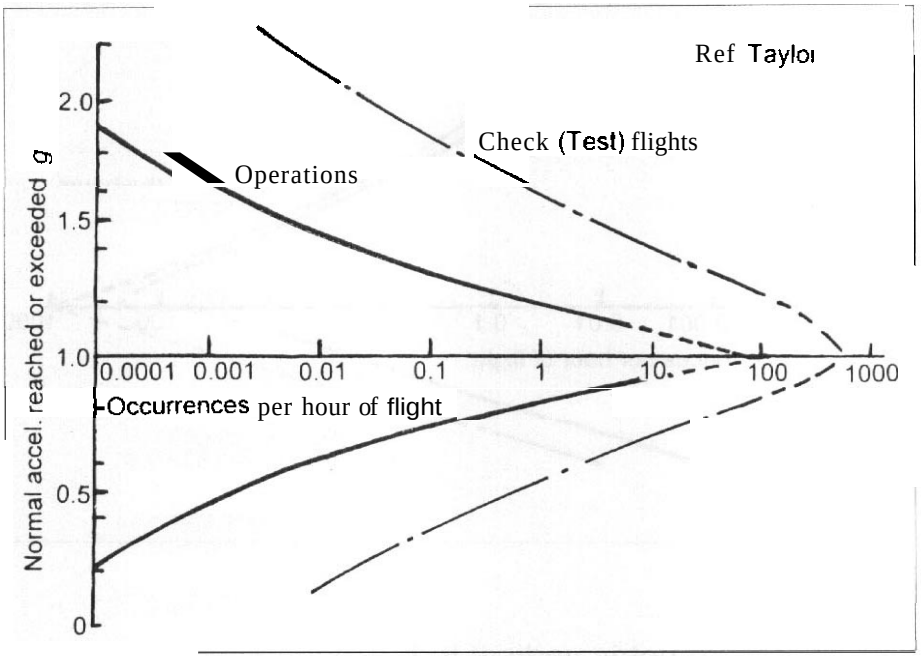

Fig. 10.3 Mission-based manoeuvre spectrum for a civil transport aircraft

Another report of importance is that by Van Dijk and de Jonge.[5] This outlines a fatigue spectrum obtained from flying experience of fighter/attack aircraft which is known as the FALSTAFF spectrum. It is hased on the maximum value *of* peak stress and loading frequency, the peak stress selected being an input parameter.

10.4.2.2 Asymmetric manoeuvres

Fatigue loading data for asymmetric loads is sparse. Chapter 6 of Taylor's text is concerned with asymmetric flight manoeuvres particularly in relation to the movement of the roll and yaw controls. The data given are limited and derived from early jet fighter experience. As far as civil transport aircraft are concerned it would appear that atmospheric turbulence is of much greater significance.

10.4.3 Atmospheric turbulence

10.4.3.1 General

Fatigue loading due to encounters with discrete gusting or the effect of continuous turbulence is of importance for all classes of aircraft, but especially for those where the operational role does not demand substantial manoeuvring in flight.

[5]Van Dijk, G. M. and de Jonge, J. B. Introduction to a fighter aircraft loading standard for fatigue evaluation. National Aerospace Laboratory (Netherlands). NLR Report MP 75071. 1975.

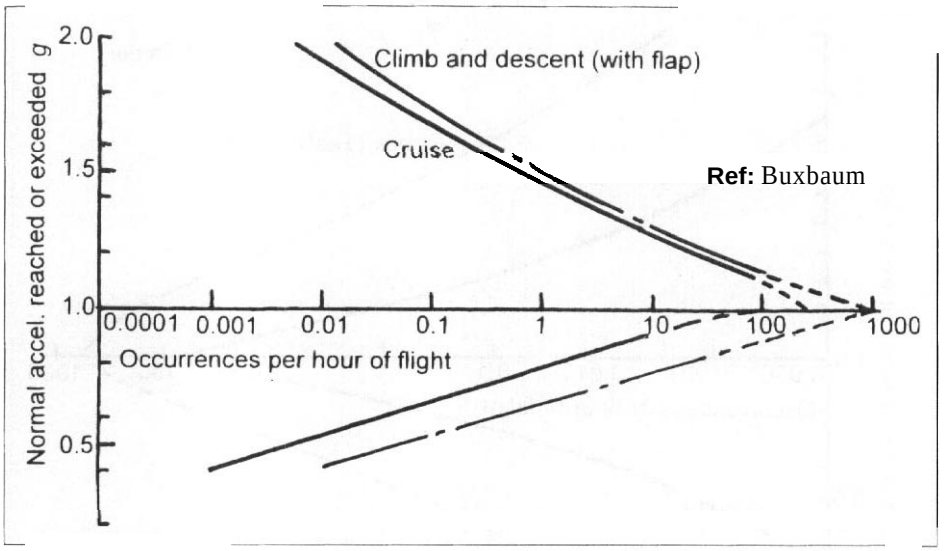

Fig. 10.4 *Flight segment based symmetric manoeuvre spectrum for a civil transport aircraft*

10.4.3.2 Symmetric vertical turbulence

A typical vertical gust spectrum is shown in Fig. 10.5 using data taken from ESDU Data Sheet 69023.[6] This is for a datum altitude of 1527 m (5000 ft) and presents the magnitude of gust velocity levels in terms of distance flown. Gust velocity magnitude is a function of both the flight altitude and the terrain over which the aircraft is flying and at lower altitudes there is a preponderance of up-gusts relative to down-gusts. These effects can be allowed for by using appropriate correction factors, such as are given in Fig. 10.6, which assumes independence of frequency of occurrence with altitude, and Fig. 10.7. It will be noted that it bas been found to be desirable to make a distinction between cruising flight and the climb and descent phases in the same way as for the manoeuvre loading of civil aircraft. This is because the pilot may be able to anticipate and avoid certain turbulent conditions while the aircraft is cruising. Use of an appropriate gust analysis. as outlined in Chapter 6, together with a knowledge of the speed and altitude of the aircraft enables the information of Figs 10.5 to 10.7 to be converted to a normal acceleration spectrum based on hours flown.

A typical discrete vertical gust acceleration spectrum for a fighter aircraft is shown in Fig. 10.8. This may be combined with the symmetric manoeuvre spectrum, Fig. 10.2, to give the total effective normal acceleration pattern, which is illustrated in Fig. 10.9. It will be noted that the lower boundary is determined by the gust effects.

[6]ESDU Data Sheet 69023. **Average** gust **frequencies.** Subsonic transport aircraft. ESDU International plc, May 1989.

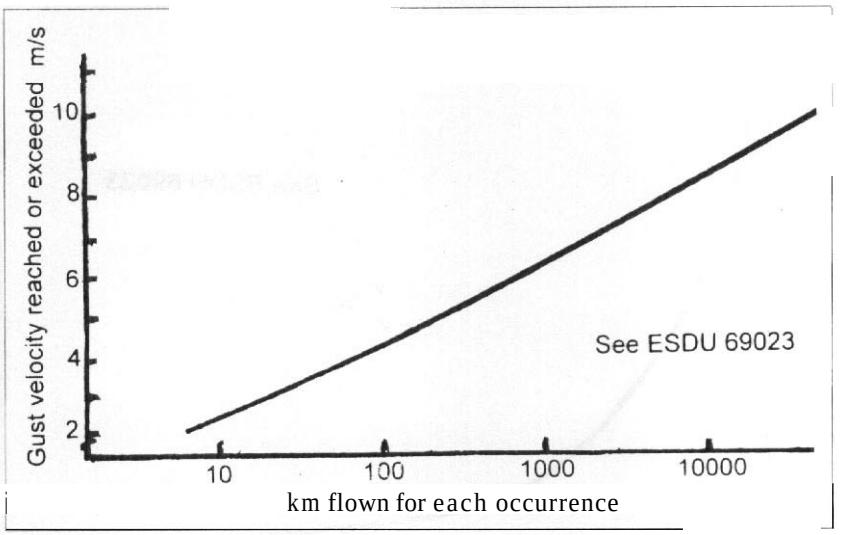

Fig. 10.5 Vertical gust velocity spectrum *at 1527 m (5000 ft) altitude*

assumed here to be symmetric about the $1g$ condition. On the other hand, the top boundary is determined mainly by manoeuvre accelerations, the gusting only having a significant effect at high frequency of occurrences when the manoeuvre acceleration factors are just above unity

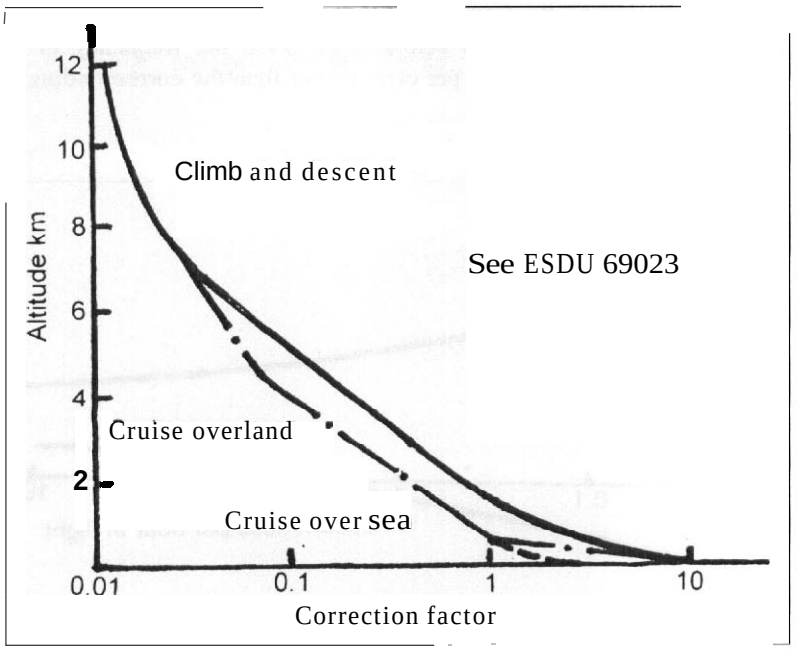

Fig. 10.6 Altitude and terrain correction factor for vertical gusts

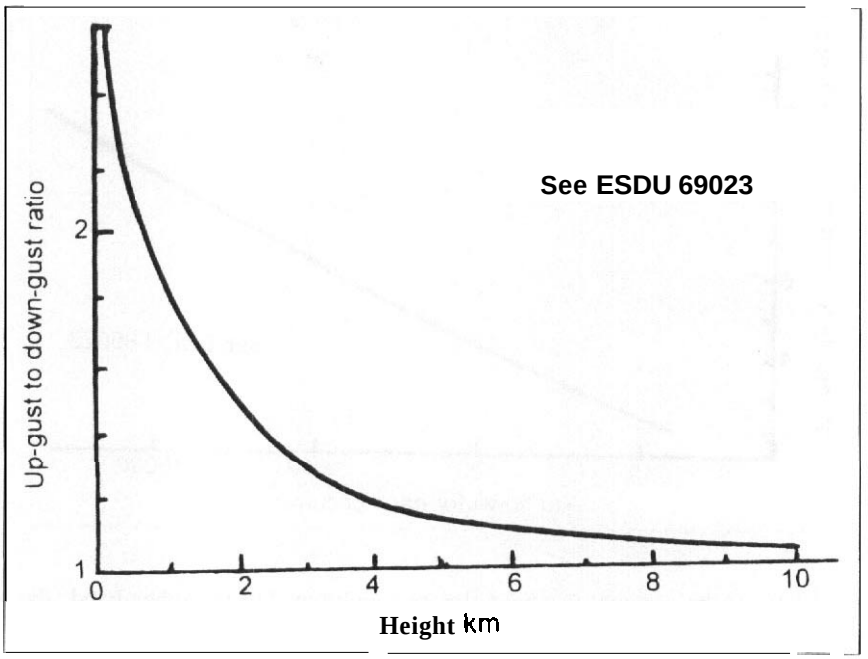

Fig. 10.7 Ratio of up- and down-gusts below 3000 m altitude

10.4.3.3 Lateral turbulence

There is less information on the frequency and magnitude of lateral turbulence but it has been suggested that at altitudes below about 3 km the frequency of a given magnitude of gusting is some 10–15 per cent greater than the corresponding vertical condition.

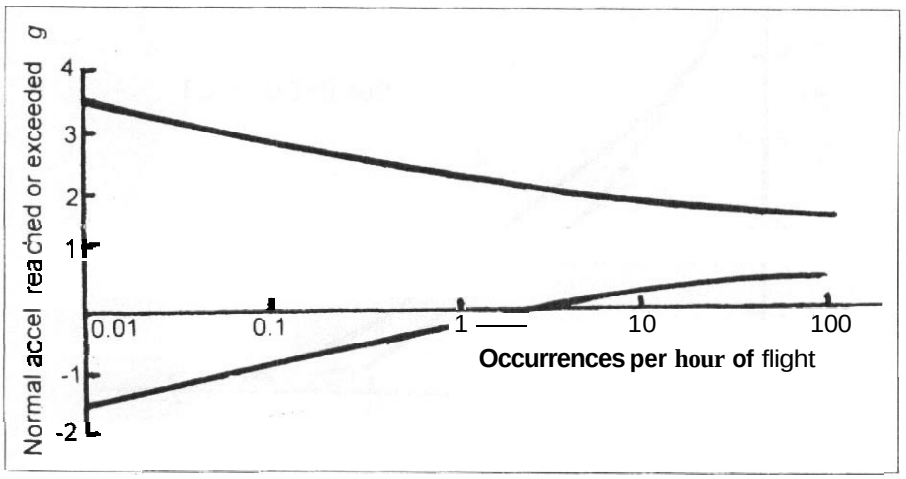

Fig. 70.8 Vertical gust acceleration spectrum for a fighter aircraft

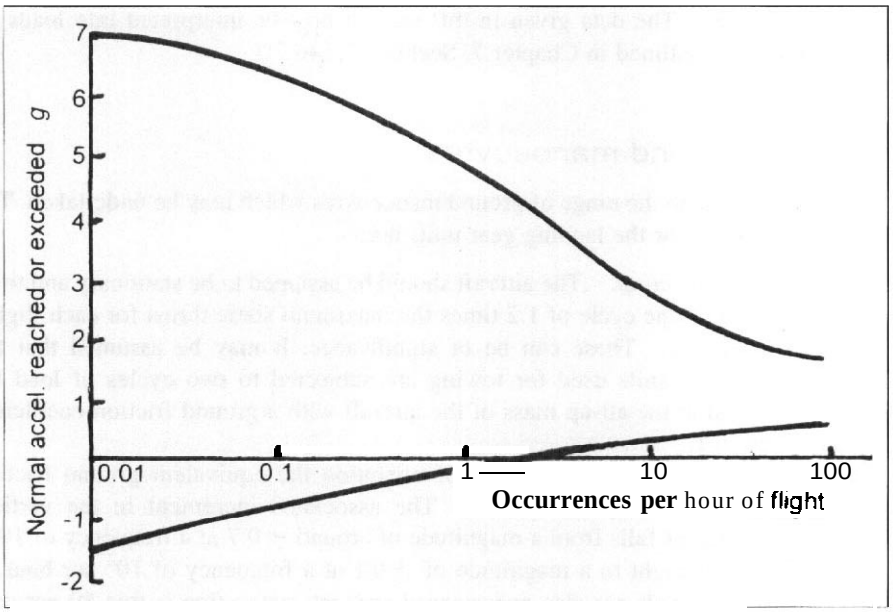

Fig. 10.9 Combined vertical acceleration spectrum for a fighter aircraft

10.4.4 Landing gear loads

10.4.4.1 *General*

The repeated loading of the landing gear and the associated components of the airframe is conveniently discussed under the following headings:

(a) loads due to ground manoeuvring, taxiing.
(b) effect of the unevenness of the ground surface
(c) landing impact conditions.

In addition to MIL-A-8866A useful references include those by McBreaty,[7] Buxbaum and Gassner,[8] Hunter[9] and Hall.[10] Much of this work is summarized in ESDU

[7]McBreaty, I. F. A review of landing gear and ground load problems. AGARD Report 118, May 1957.
[8]Buxbaum, O. and Gassner. E. Cumulative frequency distributions of aircraft landing gear loads. UK Royal Aerospace Establishment Library Translation 1462, June 1970.
[9]Hunter. P. A. Summary of C of G accelerations experienced by commercial transpon aeroplanes in landing impact and ground operations. NASA Technical Note D-6124, April 1971.
[10]Hall, A. W. Landing conditions imposed by ground turning manoeuvres with three jet transport airplanes. NASA Technical Note D-7132, December, 1972.

Data Sheet 75008.[11] The data given in this section may be interpreted into loads by using the analyses outlined in Chapter 7, Sections 7.3 to 7.7.

10.4.4.2 Ground manoeuvres

This is complex due to the range of ground manoeuvres which may be undertaken. The main considerations for the landing gear units are:

(a) Powerplant *run-up.* The aircraft should be assumed to be stationary and to be subjected to one cycle of 1.2 times the maximum static thrust for each flight.

(b) Towing loads. These can be of significance. It may be assumed that the landing gear units used for towing are subjected to two cycles of load for each flight at the all-up mass of the aircraft with a ground friction coefficient of, say, 0.1.

(c) Straight taxiing. In this mode of operation the equivalent ground friction coefficient is likely to be 0.045. The associated increment in the vertical reaction factor falls from a magnitude of around ± 0.7 at a frequency of 10^{-4} per hour of flight to a magnitude of ± 0.1 at a frequency of 10^{1} per hour of flight. Side loads are also experienced and one suggestion is that 50 per cent of the vertical load increments should be associated with side loads of +30 or −30 per cent in equal proportions.

(d) Steering, curved line taxiing. Statistical evidence suggests that for a typical civil transport aircraft steering results in three cycles in each direction at the take-off mass and a similar pattern at the maximum landing mass. Each cycle involves the aircraft being manoeuvred to the equivalent of a centrifugal acceleration of $0.15g$. In the case of military aircraft the equivalent centrifugal acceleration should be taken as $0.4g$ but only the take-off cycles need be considered. The nose-wheel steering mechanism is particularly affected by the taxiing condition and a long taxi may give rise to the equivalent of four applications of the limit load.

(e) Pivoting. This is of special importance for bogie landing gear units. For civil transport aircraft it is suggested that for each flight an allowance should be made of one manoeuvre in each direction with one bogie locked. The pivoting torque should be equivalent to a ground friction coefficient of 0.7 unless limited by the steering torque available. The suggested military aircraft case is less severe and may be taken as one manoeuvre in every ten landings with a torque equivalent to half of that available from the steering unit.

(f) Ground–air–ground *cycle* on landing gear. This case may be covered by assuming that there are three cycles of the vertical load for each flight. The aircraft mass should be the take-off value and the vertical load equivalent to the static condition.

[11] ESDU Data Sheet 75008. **Frequency** of vertical and lateral load factors resulting from ground manoeuvres of aircraft. ESDU International plc, September 1979.

(g) Braking. It has been suggested that braking subsequent to landing can be represented by two applications of the braking force equivalent to a steady ground friction coefficient of 0.4, each application consisting of six cycles of ± 0.1 superimposed on the steady value. Where appropriate the steady value of 0.4 may be replaced by the maximum value allowed by the anti-skid system. Asymmetric braking may be represented by a ground friction coefficient of 0.2 applied to one main gear unit over a period of 0.5 s together with steering at a rate of $10°/s$ into a $30°$ turn.

10.4.4.3 Unevenness of the ground surface

Unevenness of the ground surface over which the aircraft operates gives rise to increments of the vertical reaction together with the associated drag and side loads. Runway characteristics vary enormously and it has been found that typical normal accelerations of $1.2g$ occur on an average runway and $1.5g$ on grass strips. The value depends upon the tyre and shock absorber characteristics as well as the ground surface.

MIL-A-8866A specifies appropriate power density distributions of runway profiles for prepared, semi-prepared, and unprepared surfaces. The equivalent deterministic vertical reactions may be derived from these.

10.4.4.4 Landing impact

Figure 10.10 shows data on the magnitude of the vertical descent velocity reached or exceeded in terms of the frequency of landings for several classes of aircraft. The information relating to the civil types was derived from Chapter 7 of the work of Taylor,[3] and that for military aircraft from MIL-A-8866A. The vertical descent velocity may be used to derive the vertical impact forces together with the associated drag and side forces. The forward speed may be assumed to be 1.25 and 1.4 times the relevant stalling condition for civil aircraft and for military aircraft, respectively.

The spin-up and spring-back case is important and should be allowed for by including two cycles for each flight, the drag load being taken as equivalent to a ground friction coefficient of 0.6. When multiple tyres are used the drag load should be distributed in the ratio 55 to 45 per cent between the tyres, alternating for each cycle.

10.4.5 Other sources of significant repeated loading

10.4.5.1 Buffeting turbulence

Flow over the aircraft may break down at local points and give rise to buffeting. This induces a relatively high-frequency variation in the aerodynamic loads possibly resulting in the fatigue of local airframe components such as skin panels. Sometimes vortices shed from one location on the aircraft flow back and impinge upon another component giving rise to severe high-frequency buffet vibrations.

A significant, overall, buffeting occurs when one aircraft flies in the wake of another. This arises during formation flying and is especially important when the relative

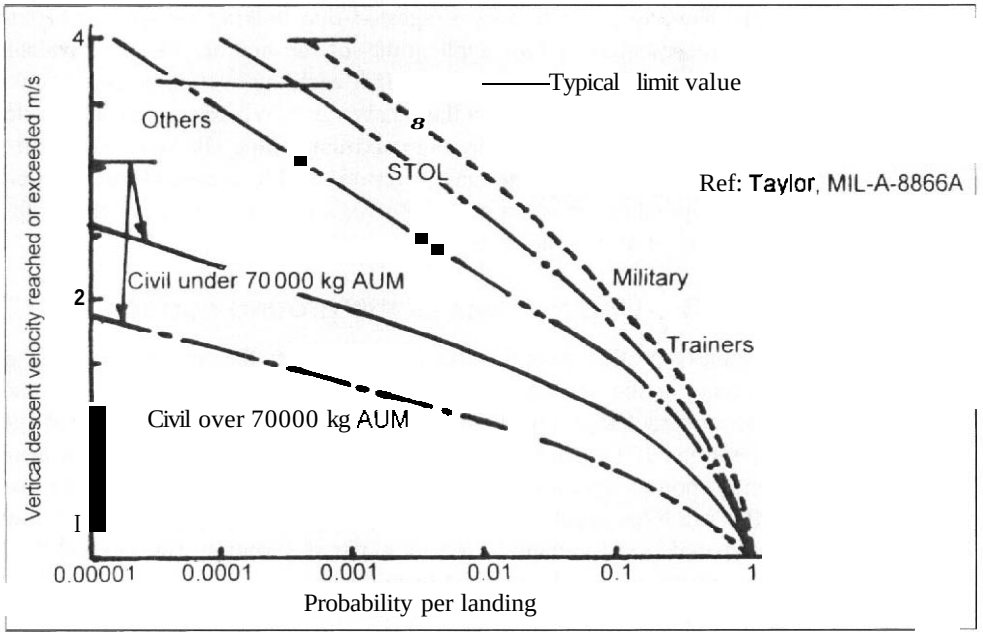

Fig. 10.10 Landing *impact vertical* ***descent*** velocity *spectrum*

positions of the aircraft are held for a considerable time as in flight refuelling. It is of sufficient importance to require a special investigation at the design stage.

It is not easy to generalize these issues, but there are some data in Chapter 11 of Taylor's hook? Local effects may be discovered in flight testing.

10.4.5.2 Noise turbulence

As with buffeting, noise turbulence is usually local in its effect. It may arise in the boundary layer and this is covered in ESDU Data Sheet 75021.[12] More usually the effect is a consequence of powerplant noise. The effect may be eliminated, or at least reduced considerably. by locating the exhaust behind the airframe as far as is possible. See Chapter 12 of Taylor's book[3] and ESDU Data Sheets 74001[13] and 89041.[14]

[12]ESDU DATA Sheet 75021. Estimation of the surface pressure fluctuations in the turbulent boundary layer of a flight vehicle. ESDU International plc, November 1992.

[13]ESDU Data Sheet 74001. An introduction to gas turbine exhaust noise. ESDU International plc, June 1973.

[14]ESDU Data Sheet 89041. Estimation of subsonic far-field jet-mixing noise from single stream circular nozzles. ESDU International plc, February 1990.

10.4.5.3 Wind-milling engine oscillatory loads

An engine suffering a mechanical failure may be out of balance and when wind-milling can induce significant oscillatory loads. Increasingly severe fatigue damage may require the aircraft to land as soon as possible after the failure has occurred.

10.5 Significance of repeated load cases

10.5.1 Introduction

It is instructive to consider the various loads encountered by an aircraft in a typical flight and note their significance with respect to fatigue.

10.5.2 Ground loading

The operation of the aircraft on the ground gives rise to repeated loads which come into the first two categories discussed in Section 10.4.4. Ground manoeuvring loads are likely to he important for the undercarriage itself and possibly some parts of the structure.

10.5.3 Ground–air–ground load

The transfer of the weight of the aircraft from the landing gear to the wing during take-off and the final reversal on landing can be a very important source of fatigue damage. The complete load cycle occurs once per flight and is likely to be most critical when large masses, such as nacelles or fuel tanks, are located in the wing outboard of the main landing gear. The variation in wing bending moment over the cycle may be readily evaluated for a given configuration. This case is one of the significant fatigue conditions for the high aspect ratio wings of transport and similar types of aircraft.

10.5.4 Pressurization

An important consideration from the fatigue aspect is the pressurization of the cabin of a uansport aircraft. This nominally occurs once per flight although it is possible that some low-altitude operations may not require use of the pressurization. The lower differential pressure used in the cabins of combat aircraft is less significant hut must be considered.

10.5.5 Flight manoeuvre loads – symmetric

The flight manoeuvre loads are critical for combat, training. and aerobatic aircraft. Larger, longer range aircraft do not normally manoeuvre at large accelerations except in emergencies. Loads occurring when flaps or airbrakes are deployed are significant in most cases. Section 10.4.2.1 gives some relevant requirements.

10.5.6 Flight manoeuvre loads – asymmetric

In the case of transport aircraft, asymmetric manoeuvre loads are usually of much less importance than the symmetric ones. However, for combat, training, and aerobatic aircraft they must beconsidered. The loads derive directly from operation of the roll and yaw controls so that it is possible to relate the repetition of overall asymmetric loads to these conditions, Section 10.5.7. It has been found that air-to-air refuelling is a dominant condition for both tanker and receiver aircraft. See Section 10.4.2.2.

10.5.7 Control motivator loads

The fatigue loading of control surfaces and related components demands particular consideration. Maximum, or high, control loads do not necessarily coincide with large levels of overall manoeuvre load although, of course, there is a relationship. It is necessary to specify a spectrum for the operation of each control. Chapter 6 of Taylor's work,' has some limited information relevant to military aircraft. See also Addendum AD1 for aerobatic aircraft data.

10.5.8 Flight gust loads

These are likely to be of considerable importance for most large aircraft where the design manoeuvre factors are comparatively low. Thus gusts are a dominant cause of fatigue in civil transport aircraft. In the case of longer range aircraft the gust loads are frequently most severe in the climb and descent phases and this is especially true for aircraft which cruise in the stratosphere where gust intensities are generally low. Military combat aircraft designed for high-speed operations at low level also experience severe fatigue problems due to the high equivalent speeds and high frequency of the turbulence. Actual data are discussed in Section 10.4.3.

10.5.9 Landing loads

Landing loads normally only design the gear itself and the local attachment structure. They may well be more generally critical on unusual layouts such as slender delta configurations. Reference to Section 10.4.4.4 provides relevant data.

10.6 Specification of airframe life

It is common to consider the airframe as having a life of a given number of hours. A typical initial design life for civil transport aircraft may be 40 000 hours although this is frequently extended by in-service upgrades, in some cases up to approaching 100 000 hours. The corresponding figure for a military transport aircraft is likely to be around 20 000 hours. The life of combat types may be as low as 3000 hours although again

there is a tendency to increase this by modifications in service. Other military types have lives between these two values.

However. the life in hours is not necessarily a good criterion. Many of the categories of load causing the fatigue damage are a function of the number of flights rather than time, and this may be considered to he a better basis for comparison. It becomes more appropriate as flight speeds increase and the number of landings for a given total life in hours increases correspondingly. A long-range subsonic jet transport may well have an average flight time of 4–6 hours or. say. 10 000–20 000 flights during its life. A small feeder jet aircraft averages Rights of about 40 minutes duration, or in excess of 60 000 Rights in its life. It is worth noting that in this life period the long-range jet will cover over 30 000 000 km in the air and possibly 300 000 km on the ground. The short-range aircraft may travel rather less in the air. hut more on the ground.

10.7 The fatigue design process

10.7.1 *Introduction*

The fatigue design process is determined by the philosophy adopted to ensure that the life of the airframe is adequate to meet the operational requirement, as outlined in Chapter I, Section 1.3. The design process in the context of the relevant philosophy is outlined in Figs 10.11 to 10.13.

10.7.2 Initial phase of the design to combat fatigue, Fig. 10.11

The first stage in the design procedure is the definition of the relevant fatigue loads, as discussed in the previous sections, and the determination of the response of the aircraft to these loads. The analysis for this follows identically that covered in Chapters 5 to 8 for the limit load conditions, as is relevant. This enables the loading on the individual components of the airframe to be determined.

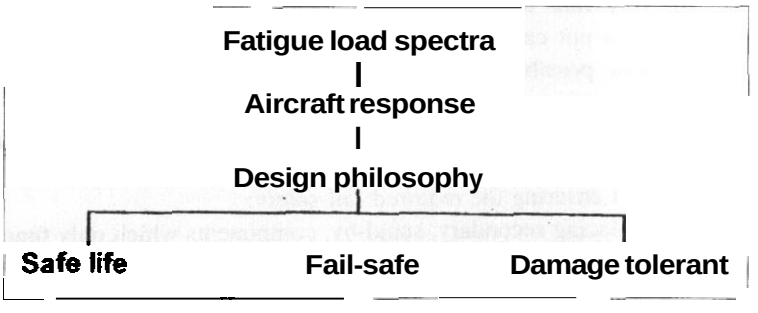

Fig. 70.11 Fatigue design process and philosophies

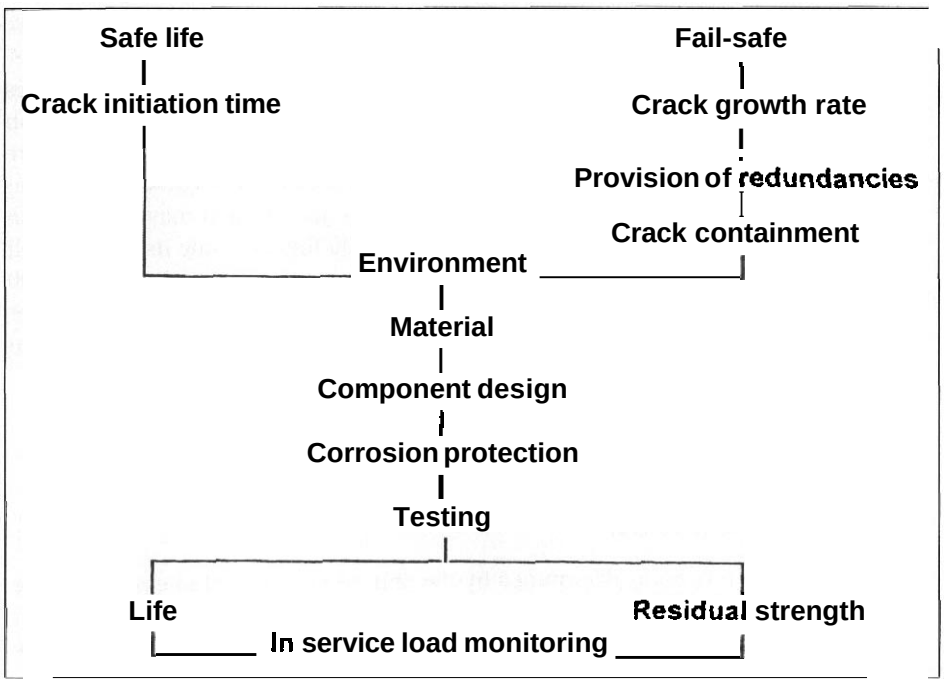

Fig. 10.12 *Application* of the **safe** life *and* fail-safe **philosophies**

10.7.3 Selection of the design philosophy

The next phase in the process is the selection of the overall philosophy to be used in the design of the structure. Although it possible that alternative approaches may be used for particular components of the airframe. as shown in Fig. 10.11 the general concept is chosen from:

(a) Safe life, where the important criterion is the time before a crack is initiated and the subsequent time before it grows to a critical length. It will be seen from Fig. 10.1 that low stress levels, which may be of high frequency. theoretically do not cause any fatigue damage. However, it is necessary to allow for them, possibly by introducing a stress factor such that effectively damage does occur.

(b) Fail-safe, where the dominant features are the crack growth rate and the provision of redundancy in conjunction with appropriate inspection. There are several ways of ensuring the required fail-safety:

(i) By introducing secondary, stand-by, components which only function in the event of a failure of the primary load path. This may consist of a tongue or a stop which is normally just clear of the mating component.

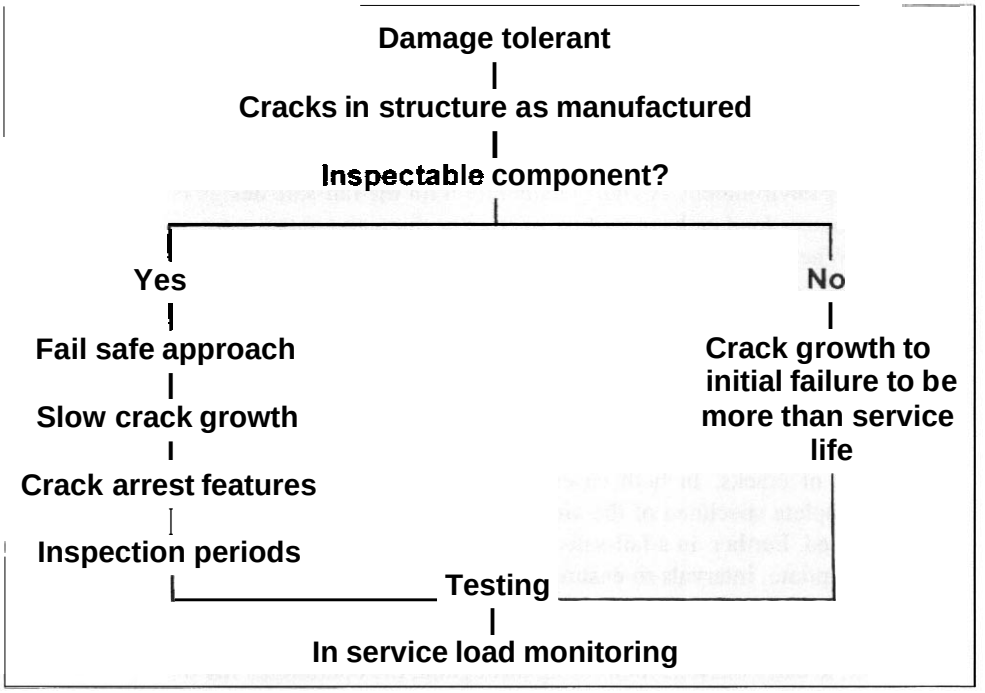

Fig. 10.13 Application of damage tolerant philosophy

A mass penalty may be implied but in some circumstances it is possible to use the secondary items in another role. for example the need for a double pane assembly on cabin windows for thermal insulation purposes.

(ii) By dividing a given load path into a number of separate members so that in the event of the failure of one of them the rest can react the applied load. An example of this is the use of several span-wise planks in the tension surface of a wing box. When the load path is designed to take full advantage of the material strength the use of three separate items enables any two remaining after one has failed to carry the full limit load under ultimate stress. In some instances the 'get home' consideration may enable a less severe approach to be adopted.

(iii) By design for slow crack growth such that in the event of crack initiation there is no danger of a catastrophic failure before it is detected and repaired.

(c) Damage tolerant, where it becomes necessary to distinguish between components that can be inspected and those that cannot. Effectively either the fail-safe or safe life approaches are then applied, respectively, in conjunction with design for slow crack growth and crack stopping.

10.7.4 Design process – safe life and fail-safe, Fig. 10.12

There is a degree of commonality in the design process for the safe life and the fail-safc concepts. The materials to be used for the structure must he selected with a consideration of the critical requirement for crack initiation or crack growth, as relevant, together with the operating environment. A vital consideration for the fail-safe design is the provision of the alternative load paths, possibly together with crack containment or crack arresting features. When these decisions have been made it is possible to complete the design of the individual components of the structure and to define the environmental protection necessary.

In the case of the safe life concept the life, inclusive of an appropriate life factor, follows directly from the time taken from the initiation of the first crack to failure. Inspection is needed to monitor crack growth. In the fail-safe concept the life is determined by the structure possessing adequate residual strength subsequent to the development and growth of cracks. In both cases it is essential to demonstrate by testing, possibly on a complete specimen of the airframe, that the design assumptions and calculations are justified. Further, in a fail-safe design it is necessary to inspect the structure at regular, appropriate, intervals to ensure that any developing cracks do not reach the critical length and are repaired before they do so.

As the design process is critically dependent upon the assumed fatigue loading it is desirable, if not essential, to carry out load monitoring throughout the operational life of the airframe. This is used either to confirm the predicted life or, where necessary, to modify the allowable operational life.

10.7.5 Design process – damage tolerant, Fig. 10.13

The damage tolerant approach commences with the assumption that cracks or faults are present in the airframe as manufactured. Experience suggests that these vary in length from 0.I mm to as much as 1.5 mm.

Those items of the structure which may be readily inspected can be designed by selecting an appropriate material and then applying an essentially fail-safe approach. The working stress level must be selected and used in conjunction with crack stopping features to ensure that any developing cracks grow slowly. Inspection periods must be established to give several opportunities for a crack to be discovered before it attains a critical length.

When it is not possible to inspect a particular component it is essential to design for slow crack growth and to ensure that the time for the initial length to reach its critical failure value is greater than the required life of the whole structure. Since this approach is less satisfactory than that applied to parts that can he inspected it is desirable to design the airframe such that inspection is possible wherever this can he arranged.

As with the safe life and fail-safe philosophies testing is needed to give confidence to the design calculations. Likewise, in-service load monitoring is highly desirable for the same reasons as given in the previous paragraph.

CHAPTER 11

Aeroelastic considerations

11.1 Introduction

The loading design cases are intended to ensure, within the accepted probability of failure, that the aircraft is able to withstand the forces it will encounter during its operational life, whether these arise from the manoeuvres or the environment. As explained in Chapter 1 the magnitude of these forces is to some extent dependent upon the distortion of the airframe under the imposed conditions. Clearly distortion of the airframe under load must not be so great as to adversly affect the performance, but in fact the issue is much more extensive than this. In general it may be stated that the stiffer the airframe the smaller is the change in magnitude of the forces due to structural distortion. The corollary of this is that there must be sufficient stiffness to ensure that the airframe will not become structurally unstable under aerodynamic loading. Interactions between aerodynamic loads and the stiffness, or elasticity, of the structure give rise to aeroelastic requirements. Essentially aeroelasticity covers all interactions of aerodynamics, structure, and inertia including the impact of these interactions on control and stability. The structural deformations may be either static or dynamic and hence it is necessary to consider damping effects as well as the stiffness contributions from the aerodynamic and structural sources. Structural damping effects are small hut beneficial. On the other hand, aerodynamic damping may become negative, that is, have the effect of feeding energy into the system. If the aircraft operates at a sufficientlyhigh speed to he subjected to significant kinetic heating the impact of the increased temperature on the airframe material properties introduces a further parameter.

A comprehensive treatment of aeroelasticity is beyond the scope of this text and the following sections are intended only to illustrate its impact upon the initial structural layout of an aircraft For relevant references see Chapter 17, Appendix A17C.

11.2 Aeroelastic phenomena

11.2.1 Divergence

One form of static aeroelasticity is lifting surface torsional divergence. This can occur when the twisting of a lifting surface results in a change of angle attack of the local aerofoil to the extent that the further induced twisting moment progresses to structural failure. While this is the simplest form of aeroelastic instability an analysis of a uniform. unswept. rectangular wing, as illustrated in Fig. 11.1, serves to illustrate some of the main characteristics of aeroelasticity generally.

The aerodynamic lift is assumed to act along the span-wise lifting line which is located at a distance ***ec*** forward of a structural reference axis. This structural axis, also known as the flexural axis. is the span-wise line about which the airframe twists when the wing is loaded by a torque in the plane of the flight direction. Consider a chord-wise strip located at a distance y out from the root. The strip is assumed to be supported but free to warp. The aerodynamic force on the strip of width δy and of chord, c, is:

$$\rho V_o^2 c \delta y a_1 \theta(y)/2$$

where

p	is air density
V_o	is forward velocity
a_1	is the lift curve slope

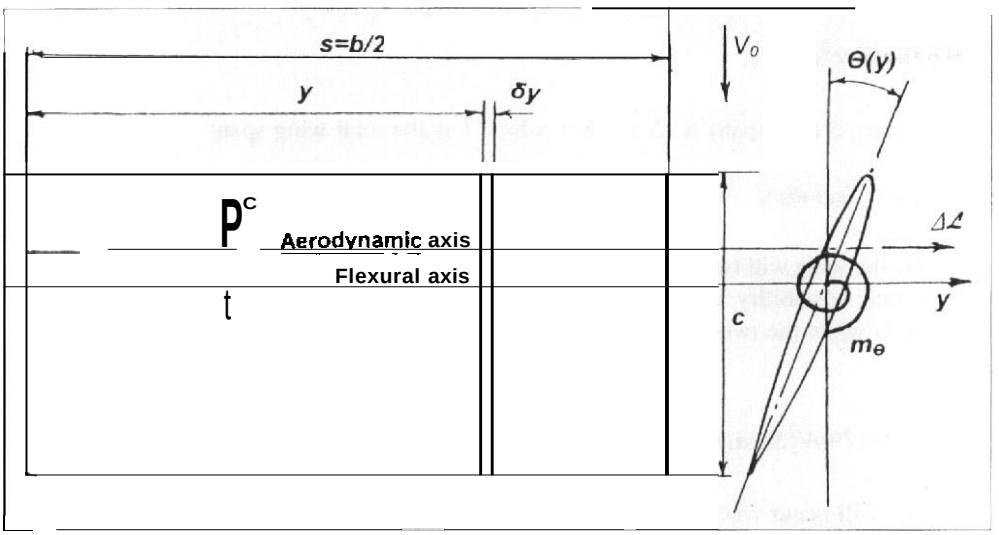

Fig. 71.1 *Wing torsional divergence*

$\theta(y)$ is an incremental change in wing angle of attack, implicitly due to twisting about the flexure axis

The corresponding moment of the aerodynamic force about the flexure axis is:

$$\Delta M_A = \rho V_o^2 e c^2 a_1 \theta(y) \delta y / 2$$

It is usual to specify some span-wise reference for the purpose of defining the torsional stiffness characteristics of the wing, say at 70 per cent of the semi-span, s. If a torque, M_S is applied at this point and gives rise to a twist of θ, then the torsional stiffness is:

$$m_{\theta 0.7s} = M_S / \theta_{0.7s}$$

If the torsional characteristics of the structure are uniform across the span and root constraint is negligible then $d\theta/dy$ may be assumed constant, although it does not meet the tip boundary condition of zero rate of twist. Then:

$$\theta(y) = y\theta_{0.7s}/(0.7s) = 1.43\theta_{0.7s} y/s$$

Thus integrating from zero to $y = 0.7s$ gives, for a uniform lift across the span, an overall value of:

$$M_A = 0.715\rho V_o^2 e c^2 a_1 \int_0^{y/s} \{\theta_{0.7s} y/s\} dy$$
$$= 0.358\rho V_o^2 e c^2 a_1 s \theta_{0.7s}$$

but since the wing area, S (full span) is $(2cs = bc)$, where b is the total wing span:

$$M_A = 0.179\rho V_o^2 S e c a_1 \theta_{0.7s}$$

If M_A is less than M_S the wing will twist, but remain statically stable, but if the reverse is true then there is static instability and the wing will fail, or diverge, in torsion. The neutral, datum case is when the two are equal, that is, when:

$$M_A = M_S$$
$$m_{\theta 0.7s}\theta_{0.7s} = 0.179\rho V_o^2 S e c a_1 \theta_{0.7s}$$

and rearranging, this will occur when the speed is:

$$V_{DIV} = 1.67\{m_{\theta 0.7s}/(\rho V_o^2 b a_1 e c^2/2)\}^{1/2} \qquad (11.1)$$

While the expression for the divergence speed will be different for other wing geometries and structural properties, the form of the equation will be unchanged. The speed at which divergence occurs is proportional to the square root of the torsional stiffness of the wing. The most significant aerodynamic parameter is the location of the local centre of pressure relative to the axis of twist of the structure, the aerodynamic torsional moment being a function of dynamic pressure. The main structural parameter is the torsional stiffness.

A particularly important plan-form parameter is the sweep. The divergence tendency is especially acute on a forward-swept surface of conventional structural form since the coupling between the span-wise bending and twisting is such as to unfavourably increase the angles of attack of the outboard aerofoil sections. The reverse effect occurs on a swept-back lifting surface where torsional divergence is unlikely to be critical.

11.2.2 Reduction of control effect and reversal

Structural distortion can result in a reduction of the effectiveness of controls to the extent that in some cases the forces and moments consequent upon the deflection of a control motivator are opposite in direction to that signalled. For example fuselage vertical bending deformation consequent upon deflection of an elevator will result in a change of effective angle of attack of a fixed, conventional, tail-plane and give rise to loads in the opposite sense to those resulting from the deflection of the elevator. This may be overcome by the use of an all-moving tail-plane for the pitch control. Another possibility is that of aileron reversal, which is shown in Fig. 11.2. In this case the

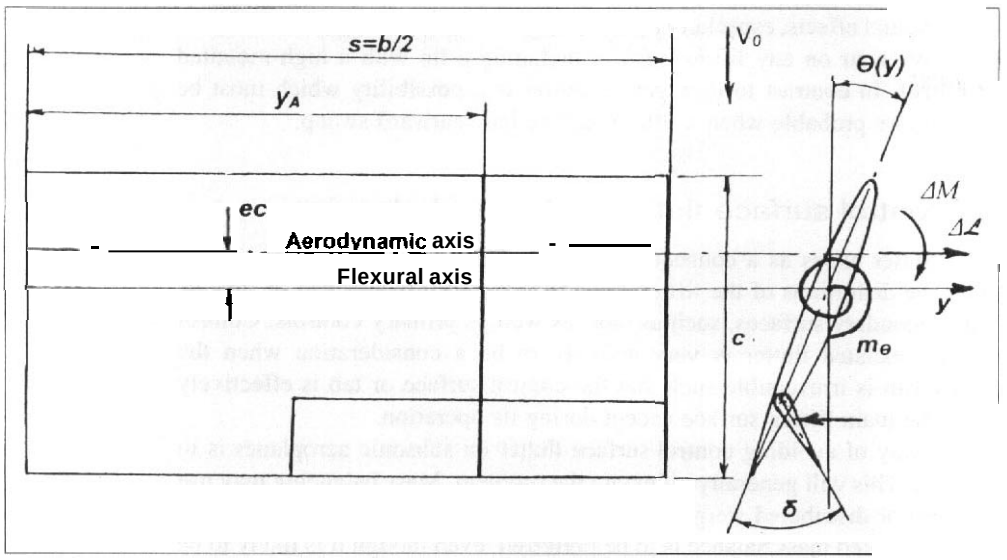

Fig. 11.2 Aileron reversal

adverse twisting of the local aerofoil sections under the chord-wise moments consequent upon an aileron deflection tends to give rise to loads which offset those arising from the aileron effect. In this case also the aerodynamic effects are a function of dynamic pressure and a given speed, known as the aileron reversal speed, may exist at which the aerodynamic and structural effects exactly cancel. At higher speed the aileron effect is the reverse of that intended.

11.2.3 Flutter

11.2.3.1 General

Flutter is a phenomenon where the interaction between the aerodynamic forces, structural characteristics, and inertias results in an oscillation. Flutter may take various forms but unless the structural damping is unusually high the oscillations rapidly diverge and structural failure occurs. There are two main types of flutter.

11.2.3.2 Lifting surface classical bending–torsion flutter

Main lifting surface flutter arises primarily from a combination of dynamic flexural and torsional distortions of the surface hut can also involve body freedoms and other interactions such as servo controls. In this so-called 'classical flutter' the critical speed is primarily dependent upon the frequency of the fundamental torsional vibration mode of the surface. Torsional stiffness plays a large part in determining this but it is also dependent upon inertial effects, especially those of large concentrated masses. Flexure–torsion flutter may occur on any lifting surface including a fin with a high-mounted horizontal stabilizer. In contrast to divergence, flutter is a possibility which must be considered to be more prohahle when a lifting surface has rearward sweep.

11.2.3.3 Control surface flutter and mass balancing

Control surface flutter arises as a consequence of the deflection of a control surface interacting with the distortions of the lifting surface to which it is attached. It may be associated with secondary surfaces, such as tabs, as well as primary controls. Control surface and tab-associated flutter is very unlikely to be a consideration when the operating mechanism is irreversible such that the control surface or tab is effectively fixed relative to the main lifting surface except during its operation.

An alternative way of avoiding control surface flutter on subsonic aeroplanes is to mass balance them. This will generally eliminate the problem. Mass balancing may use either concentrated or distributed weights. Large concentrated weights are not always effective and a distributed mass balance is to be preferred, even though it is likely to be the heavier arrangement. The mass balance requirements for all controls are that at the neutral position and at $\pm$ 10" deflection the product of inertia for the complete control

shall be zero. The product of inertia is defined as:

$$\Sigma mxy$$

where

- m is an element of control surface mass
- x is the distance of m from the hinge-line. measured normal to hinge-line, positive behind hinge-line.
- y is the perpendicular distance of m from a specifically defined fore and aft axis. This is normally the wing root for ailerons (+ve outboard from axis) and the rear fuselage torsion axis for rudders (+ve above axis) and elevators (+ve for each semi-span)

In addition, the centre of gravity of the control surface must fall within $\pm 0.05c_f$ of the hinge-line under the most adverse position where c_f is the mean chord behind the hinge-line of the appropriate surface. When the aerodynamic balance is small the centre of gravity should always be on, or forward of. the hinge-line.

In locating concentrated mass balances care must be taken to ensure that they do not coincide with the nodal line of a critical structural mode. Location of mass balances on control linkages and levers is best avoided and requires careful analysis when used. Control surface tabs can be mass balanced, but this is a complex issue and it may be best not to use mass balance. When spring or servo tabs are fitted to elevators it is recommended that there is no direct interconnection between the two halves of the control. This is to enable the correct frequency ratio to be obtained between the elevator and tab in anti-symmetric modes.

At transonic and supersonic speeds the possibility of negative damping makes the mass balance problem difficult. In most cases irreversible power controls avoid the problem.

High-lift devices should be operated by irreversible units located adjacent to the surface and should be torsionally stiff. It is not normal practice to mass balance flaps.

Mass balance weights may be subjected to substantial dynamic loading and the following ultimate attachment strength conditions can be used as a guide:

$+1.5n_1$g, normal	$-0.75n_1$g, normal
$5.0g$ laterally.	$10.0g$ fore and aft
Angular acceleration	500 rad/s^2 (about control hinge-line)

11.3 Structural response

The dynamic response of a structure is important in two main areas:

(a) The dynamic stress factors which may occur when loads are applied rapidly.
(b) The more general interaction with aerodynamic forces with the possibility of the occurrence of flutter.

Dynamic response is more complex than the static distortion. There are several reasons for this. One obvious point is that, in addition to the stiffness effects. the inertia distribution plays a large part in the response behaviour. Further, although some of the vibration modes and frequencies are determined primarily by overall stiffness and inertia characteristics. they are also influenced by local effects. The higher frequency modes especially may be entirely due to local effects. Methods of analysis are available which idealize the stiffness and inertia characteristics to a relatively simple form, but these are only of sufficient accuracy when the characteristics can so he represented. Now that extensive computation aids are available it is preferable to use a detailed representation of the actual stiffness and inertias by, for example, employing finite element analysis. Large concentrated inertias always have a significant effect upon the dynamic response, both by lowering the frequency and by constraining the mode shapes.

Some comments on dynamic structural response factors are to be found in Chapter 6. Section 6.4.5.

11.4 Specified aeroelastic requirements

The aeroelastic requirements specified in the various airworthiness documents are simply stated in terms of speeds below which catastrophic events must not occur. These events include flutter, loss of control, and aero-servo-elastic instabilities. The speeds are quoted in terms of the design speed, V_D, and vary from $1.15V_D$ for military types to $1.25V_D$ or more for civil aircraft. Some reduction of the margin over the design speed may be possible when an active control system includes flutter suppression. See also Chapter 12, Section 12.2.5.

Civil airliner requirements state that control reversal must not occur below the design speed or design Mach number.

11.5 Stiffness criteria

From the previous paragraphs it can be seen that the torsional stiffness of the lifting surface is the most appropriate criteria to use as a design requirement to ensure adequate wing aeroelastic performance.

Over the years stiffness criteria were evolved to cover the most important geometric, structural and performance parameters. These aimed at providing simple formulae to cover various wing configurations up to transonic and, in a few cases, supersonic speed. One disadvantage of these relatively simple criteria is that it is necessary to include quite large margins of safety to ensure that all of the various conditions are covered, and clearly this may result in an inefficient structure. For this reason the stiffness criteria have fallen into disuse and have been replaced by the simple statement of the aero-elastic requirements covered in the previous section. The only exception is the case of some simple light aircraft. In addition to wing stiffness criteria the requirements for stabilizing, control surfaces, and the fuselage were covered.

However, wing stiffness criteria are sometimes a useful guide for initial design purposes where they may he used to give a first estimate of certain structural properties prior to the undertaking of a more accurate analysis.

The earliest stiffness criteria were concerned solely with torsional characteristics and were aimed at ensuring that classical lifting surface flutter would not occur. They took the form:

$$K = \{m_\theta/(\rho d\bar{c}^2)\}^{1/2}/V_D$$

where

- K is a non-dimensional criteria dependent upon wing density
- V_D is design (diving) speed
- d is 90 per cent of the distance from the root to the tip of the wing, measured along the mid-point of the structure
- $\bar{c}$ is the standard mean chord
- p is the air density
- m_θ is the torsional stiffness measured relative to the wing root at a section 70 per cent of the distance from root to tip

The value of K was arranged to ensure that the flutter speed would be 1.5 to 2 times the design (diving) speed. This simple formula makes no allowance for sweep, compressibility, aspect ratio, taper ratio, and certain other important parameters.

Ultimately more elaborate formulae were developed which included many more of the important design parameters. Such a formula was quoted at one time in the light aircraft requirements of Section K of the British Civil Airworthiness Requirements (BCAR):

$$V_{FLU} = \{2m_\theta/(\rho b\bar{c}^2)\}^{1/2}\left[\frac{(1-0.37\lambda)(1-0.1r)(0.95+1.3/\bar{\sigma}_w)}{\{1.6(f-0.1)(1.3-j)\}}\right] \qquad (11.2)$$

where

- V_{FLU} is the critical flutter speed, taken to be at least $1.25V_D$
- m_θ is the anti-symmetric torsional stiffness at 70 per cent of the semi-span, measured at right angles to the structure, needed to achieve V_{FLU}
- b is the wing span
- c is mean chord
- A is the taper ratio, providing $0.25 < A < 1.0$ where A = tip chord/root chord for straight taper or for, other plan-forms:

$$A = (c_s - 0.6\bar{c})/(1.4\bar{c} - c,)$$

c, being the chord at 70 per cent of semi-span

r is a ratio of the flexural and torsional stiffnesses:

$$r = 5\ell_{\varphi}/(A^2 m_{\theta}) = 0.5/A^2 \qquad \text{approximately}$$

where

A is aspect ratio

ℓ_{φ} is the symmetric flexural stiffness between wing root and 70 per cent semi-span measured at right angles to the structure

f is the fractional position of inertia axis on the chord aft of leading edge providing $0.35 < f < 0.55$

j is the fractional position of the flexural axis aft of the leading edge

$\bar{\sigma}_w$ is relative wing structural density $= \sigma_w/\rho$, and the structural density is:

$$\sigma_w = (W_1 + kW_2)/(S_1 c_1)$$

where

S_1 is the wing area outside the fuselage

c_1 is the corresponding mean chord

W_1 is the corresponding wing structural weight

W_2 is the weight of non-structural loads in the wing

K is a factor which is usually taken to be 0.5

Units in Eqn. (11.2) must be such that the first term in ( ) brackets is (velocity)^2.

The similarity of the first term with that of Eqn. (11.1) is to be noted. A somewhat similar formula was quoted in the previous United Kingdom military requirements, AvP 970, in conjunction with a flutter speed margin of $1.25V_D$:

$$V_{FLU} = \{m_{\theta}/(\rho d\bar{c}^2)\}^{1/2}[(0.9 - 0.33\lambda)(1 - 0.1r)sec^{1.5} \times (\Lambda - \pi/16)/\{0.9(f - 0.1)(1.3 - j)\}]\{f(M_N)\} \qquad (11.3)$$

where

V_{FLU} is the critical flutter speed

$f(M_N)$ is a Mach number correction, where:

$$f(M_N) = (1 - M_N^2)^{1/4} \qquad \text{for } 0 < M_N < 0.8$$
$$= 0.775 \qquad \text{for } 0.8 < M_N \leq 0.95$$

Λ is the sweepback (radians) of a line 5 per cent of chord aft of maximum thickness

The term $(1 - 0.1r)$ is applicable if r, the stiffness ratio, lies between 0.5 and 2.0, but when it is greater than 2.0 it should be replaced hy $(0.77 + 0.1/r)$.

Some idea of the limitations of Eqn. (11.3) can be gained by noting that it does not apply if the flutter is of a type where body freedoms are dominant, as for example on a swept-wing aircraft with a fuselage of low pitching inertia. Nor does it apply for wings of low aspect ratio, wings carrying twin booms. those with large concentrated masses. or those flying at transonic or supersonic speeds. It may be in error if the ratio of the fundamental torsional and flexural wing frequencies is greater than 5.

11.6 Inertia and mass distribution

When the wing is of low structural density the location of inertia loads tends to be more critical than if the reverse is true, but it must be emphasized that this is really only a relative effect.

If concentrated loads such as powerplants, stores. or fuel tanks are housed within or below a wing they should be located so that their individual centres of gravity are as far forward as possible. preferably forward of the wing flexural axis. Should this not be possihle they must be located as near to the root as can be achieved.

In the case of wing fuel tanks the system should be arranged to keep the fuel centre of gravity as far forward as is feasible in all tank conditions. Where external. and especially wing tip, fuel tanks are used it is essential to ensure that the centre of gravity of the fuel does not move either too far forward or too far back.

Very large wing-mounted bodies or inertias, such as large stores, present a particularly difficult problem. Layout restrictions usually dictate their position within closely defined limits. Their effect upon torsional frequency may be so marked as to completely change the vibration characteristics of the wing and cause interactions with body and horizontal stabilizer modes. Reasonable increase of stiffness has only a minor effect upon this and the possibility of flutter is high. The most feasible solution is probably the provision of horizontal rear fins to the wing-mounted body thereby considerably increasing the aerodynamic damping in the torsion modes.

11.7 Structural damping

Although the natural damping inherent in a metallic material is very low, the combination of a large number of components in a complete structure does result in a measurable damping. This effect is due mainly to the joints where energy is dissipated by the small relative motion which occurs. Thus a built-up structure possesses more damping than one using large integrally machined components. Damping may well increase with age as joints loosen up. Also the damping of a given wing, say. may be substantially different to one of nominally identical manufacture and therefore the structural damping effect is sometimes neglected in aeroelastic calculations. However, it is present to some degree and is beneficial. A typical metallic structure may have a damping ratio of between 0.02 and 0.05. the higher value being for a wing with a complex built-up construction. Components using alternative materials, such as wood and fibre-reinforced plastics, have greater structural damping.

11.8 Miscellaneous stiffness and related considerations

This section is concerned with miscellaneous design considerations having a bearing upon aeroelastic and stiffness requirements.

11.8.1 Control surface backlash

The backlash in control surfaces and systems should be as small as possible. As a guide the tolerable values range from no more than *0.0005* rad for surfaces on inherently unstable aircraft up to 0.02 rad for high-lift devices, with normal trailing edge controls at 0.002 rad.

11.8.2 Control surface and shroud distortion

Span-wise distortion of the control surface relative to the wing. due to air-loads on both the wing and the control must not be too great or physical interference may result. As a guide the maximum vertical deflection of the control relative to the main surface should not exceed $0.02d$, where d is the local depth (thickness) of the control surface.

Distortion of the panels of a control surface skin can have a significant effect especially if the result is to change the trailing edge angle since this causes a change in the hinge moment characteristics. The skin must be adequately stabilized. One suggestion is that the $0.02d$ criterion should be applied.

Control surface shrouds must be adequately stiff since distortion is liable to alter the gap, which will also result in a change of the hinge moment characteristics. This is particularly important at speeds when shock waves are formed on or near the shrouds.

11.8.3 Hinged doors, dive brakes, etc.

It is always preferable to hinge a door at the forward edge as the airflow is less likely to cause a tendency for the door to open. The design should be such as to avoid any lip on the leading edge which might serve to trap the air and result in high loads on the door and its attachments. The stiffness required to prevent undue distortion under operating conditions nearly always designs these components.

11.8.4 Overall wing aerofoil contour

Deformation of the local aerofoil section must he kept to an acceptable value to avoid undue drag, loss of lift, or adverse shock formation. The actual magnitude of the allowable waviness and steps will dependupon the chord length and the type of aerofoil, but a limit of *2* mm peak to peak waviness is a guideline for a large aircraft. In general steps down in the airflow are preferable to steps up. The dimension quoted will be much less if laminar flow is a design feature as it is on some advanced aerofoils. including those used for general aviation aircraft such as sailplanes.

CHAPTER 12

Derivation of structural design data

12.1 Introduction

The layout and sizing of the structural components of an airframe is an iterative process. This implies that there must be a synthesis phase to establish overall details before the structural analysis can he undertaken and the design refined. Traditionally the synthesis phase relies upon the experience of the designer in conjunction with the application of simple formulae. Expert programs are becoming available which encapsulate past experience and enable the synthesis/analysis/refinement process to be undertaken in one seamless operation. However, in order to use such programs effectively it is essential to have an understanding of the means by which a structure reacts and transmits loads. All expert programs require an initial input of some kind. In some cases this may be no more than the external geometry of, say, a wing and consequenlly the structural configuration derived will be determined by the historical data built into the program. The ability to input a basic internal configuration for the structure results in more versatility and more rapid convergence to a satisfactory solution. The following chapters outline the primary considerations of structural design and suggest simple techniques which may be used to initiate the structural design procedure. Reference to sophisticated analytical methods is deliberately avoided both because they are not considered to be essential at the initial design phase and because they are adequately dealt with elsewhere.

12.2 Basic aims of structural design

12.2.1 Introduction

The structure of an aircraft must be designed to meet a number of conflicting requirements and it is a measure of the skill of the design organization as to how successful it is in

making the inevitable compromises. The fundamental problem is that of achieving low weight at an acceptable manufacturing cost while at the same time ensuring adequate:

(i) strength:
(ii) stiffness;
(iii) serviceability.

Each of these three characteristics of the structure is time dependent and is affected by the damage caused by deterioration in service and the repetition of loads. The designer must ensure the integrity of the structure with full consideration of both fatigue and corrosion. These effects must be taken into account from the very beginning of the design of the structure to ensure that potential problem areas are avoided and that flight safety-critical structural members can be readily inspected in service or have an adequate safe life.

12.2.2 Strength

Much of the design and analysis of a structure is concemed withensuring that the strength requirements are met both initially and throughout the life of the aircraft. The structural loading cases to be considered are covered fully in Chapters 3 (flight loading cases). 7 (ground loading cases), and 8 (loads on individual airframe components). These are interpreted in Chapters 5 (flight manoeuvre loads), 6 (loads due to atmospheric turbulence), 7, and 8. Chapter 10 deals with the repeated load considerations.

The requirements enable the magnitude of the loading to be evaluated and are expressed initially in terms of the limit conditions which are, to the accepted probability, the most severe load applications of those cases expected to be encountered. As stated in Chapter 1, Section 1.3.4, a proof factor is applied to the limit loads to ensure that there is no unacceptable permanent deformation of the airframe together with the ultimate, or overall safety, factor. The limit requirement is supplemented by a statement of the frequency of occurrence of conditions lower than this maximum in order to enable fatigue evaluation to be undertaken.

The stressing process consists of relating the factored loads to the corresponding material properties and dimensions of the structural members. Therefore it can only he undertaken when the structure has been defined. The result of a stress analysis is stated as a reserve factor, which is the ratio of the potential strength of the given component under the relevant loading condition to the actual load in that condition. Strength is conventionally defined in terms of stress or load. In general it is sufficient for a reserve factor to be quoted to no more than three significant figures.

A summary of the reserve factors is included as part of the type record of the aircraft.

12.2.3 Stiffness

Chapter 11 explains why the overall stiffness of a structure must be sufficient to ensure that during the operation of the aircraft any distortions occurring do not exceed a tolerable magnitude. While there are some purely structural situations, such as cabin floor stiffness, most stiffness effects are concerned with the interaction of the structure

and the aerodynamic characteristics. Unstable aeroelastic effects may be either static or dynamic. From the point of view of structural design the main consideration in both cases is the stiffness, with the torsional stiffness of lifting surfaces being of particular importance. Generally, structural damping is small and not within the control of the designer. Airframe inertias can be important, especially when large concentrated masses are located on lifting surfaces.

While stiffness criteria are no longer specified there are some circumstances where their use for initial work is helpful. Equations (11.2) and (11.3) in Chapter 11 are relevant here but their limitations must be recognized.

12.2.4 Serviceability

From the point of view of overall airframe structural layout the most important serviceability consideration is that which arises from fatigue effects. Chapter 10, Section 10.7 describes the accepted philosophies employed to ensure that the structure continues to retain adequate strength throughout its life, namely safe life, fail-safe, and damage tolerant. The first approach is frequently used for military aircraft, while the last is incorporated in civil transport types as far as is possible. In practice some aspects of all three of the approaches appear together in most practical airframes.

12.2.5 Implication of advanced control systems

Some recent military and civil aircraft incorporate an advanced flying control system employing active technology. This technique is becoming a more usual feature of sophisticated designs. In these cases it is not possible to complete the structural design in isolation since the advanced control system can be used to change the configuration of the aircraft and hence the structural loads during flight. For example the active system may be used in such a way that there is a limitation or an alleviation of the stresses arising from design manoeuvre or gust loading. Alternatively the effects of aeroelastic distortion may be counteracted by appropriate control deflection.

It is difficult to make realistic allowance for the effect of advanced controls at the initial structural design stage. In terms of loads it is necessary to define. or to assume, a realistic reduction in the critical limit loads and the impact on the fatigue spectrum. Some indication of the potential reduction may be obtained by consideration of what can be achieved using the control power available together with the implied performance penalties. As far as aeroelastic effects are concerned the safest approach is to assume that the speed factor applied to these cases can be reduced, possibly to as low as unity.

12.3 Analysis of requirements – structural design data

12.3.1 General procedure

With the exception of certain ground loading conditions an aircraft is effectively a free body in space. The implication of this is that in general the airframe will be in a state of

acceleration in all six degrees of freedom. It is therefore necessary to include all the inertial forces and moments in the analysis used to derive the basic structural design data which may be defined as shear force, bending moment, and torque diagrams. Essentially the procedure consists of:

(a) Interpreting a given loading requirement as stated in the design requirements.
(b) Evaluating the consequent aerodynamic loads. for example the wing–body or tail lift.
(c) Calculating the implied translation and rotational accelerations, using overall moments of inertia consistent with local load distribution (masses and centre of gravity).
(d) Distributing the aerodynamic loads and the local inertia effects appropriately across the airframe. When finite element analysis is used these distributions are allocated as local loads at the structural nodes, see Chapter 15, Section 15.1.2.
(e) When a 'classical' approach is employed, integrating the loads across the airframe with respect to length to obtain shear forces and integrating a second time to get the bending moments or torques. It is usually most satisfactory if the integration commences at the extremities of the aircraft and proceeds towards the centre of gravity. One reason for this is that any accrued errors will be relatively small in comparison with the magnitude of the local data. Also any errors due to inconsistent assumptions are most likely to occur in the wing–body region. It should be noted that when the direction of integration is reversed, as from the rear of the aircraft as opposed to from the nose, the sign of the result is changed.

The process may he applied to overall aircraft components such as wing and fuselage or smaller parts such as control surfaces. Raps, or engine nacelles, but in all cases the forces and moments must be in total equilibrium.

12.3.2 Example of unrestrained beam analysis

In practice the derivation of the structural design data by analysis of the loading requirements consists of calculating the forces and moments on unrestrained beam-like components. Examples are the wing as a span-wise cantilever rotating about the centreline of the aircraft and the fuselage as a longitudinal beam rotating about the centre of gravity. In both instances there is also likely to be translation. A basic example of an unrestrained beam analysis is given in Appendix A12.

12.3.3 Loading conditions in major design cases

12.3.3.1 General

The majority of the major design cases are more complex than that of the simple beam analysis referred to in the previous section although the principles are no different. The primary contributions to the overall loading are considered in the following sections.

12.3.3.2 Symmetric flight cases

Figure 12.1 depicts the loading and corresponding form of the shear force diagram across the span of the wing. Symmetric wing lift is relieved by the inertia of the structure, systems and fuel. The overall loading on the wing is reacted at the side of the fuselage and the bending moment is constant across the width of the fuselage.

The loads on a typical chord-wise section are shown in Fig. 12.2. The sum of the moments of the forces about a given chord-wise reference point yields the torque at that section. Integration of the local values of the torque across the span of the wing yields the overall torque diagram.

Finally Fig. 12.3 illustrates the loading and the form of the shear force diagram along the length of the fuselage. The shear force and bending moment due to the horizontal stabilizer air-load are relieved along the fuselage by the translational and rotational inenia effects. The net fuselage bending moment at the fore and aft centre of gravity position is balanced by the sum of the wing torques at the sides of the fuselage.

An example of the analysis required to derive the longitudinal shear force and bending moment diagrams is given in Addendum AD2.

12.3.3.3 Asymmetric flight cases

The asymmetric flight cases are somewhat more complex than the symmetric ones. Somewhat simplisticly the instantaneous application of aileron control on a wing having

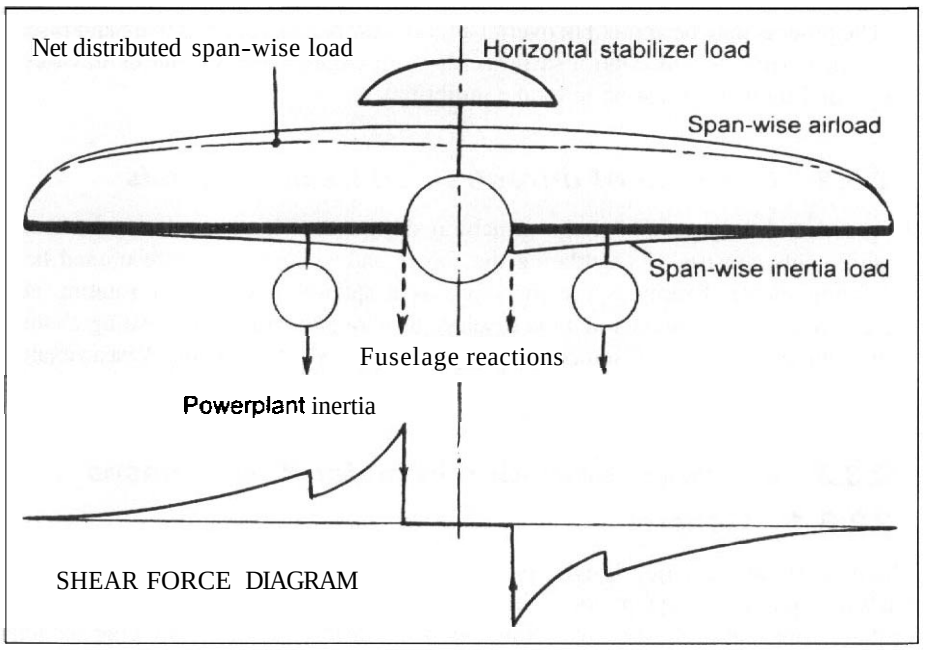

Fig. 12.1 Symmetric loads – span-wise

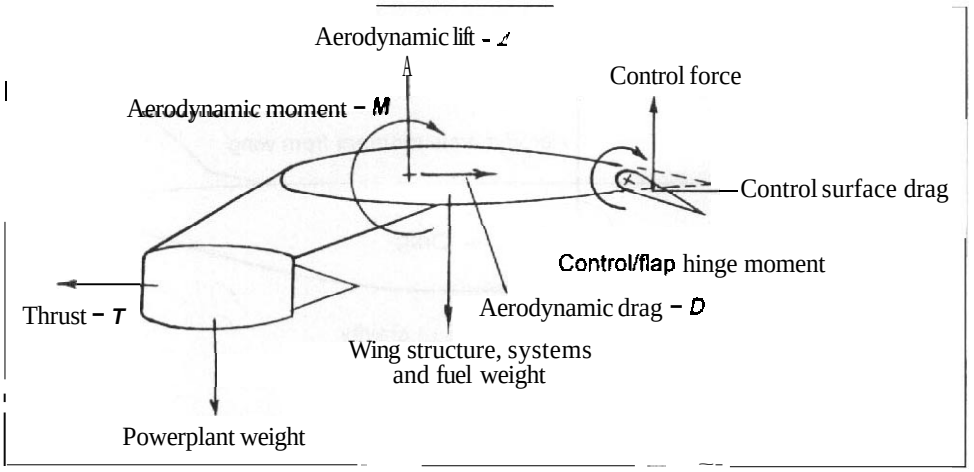

Fig. 12.2 *Symmetric loads – chord-wise torques*

no initial lift results in an anti-symmetric loading. although in practice there is not true symmetry between the up-going and down-going ailerons. A more usual case is when the ailerons are applied as the aircraft is in steady level flight, as is illustrated in Fig. 12.4. The initial steady level flight condition will have a symmetric loading as illustrated in Fig. 12.1. The aileron and the consequent roll effects are approximately anti-symmetric in form. Figure 12.4 shows the shear force distribution due to this anti-symmetric condition as well as the overall result of combining it with the symmetric diagram. In a general rolling motion the couple resulting from the application of the aileron is balanced both by the acceleration effect on the roll inertia and the aerodynamic effect due to the rate of roll. see Chapter 5, Section 5.4.

The torque loading on the rear fuselage as a consequence of the application of rudder control to cause a sideslip motion is shown in Fig. 12.5. The torque due to the fin side load is increased by the effect of the asymmetric distribution of the trimming load on the horizontal stabilizer.

Figure 12.6 is a plan view of the fuselage. This shows how the fin side load is reacted by side forces along the fuselage. The lateral bending along the fuselage is relieved by sideslip and yaw inertial effects and the net value at the junction of the wing and body is balanced by wing aerodynamic forces and yaw inertia. The torque on the fuselage is mainly reacted by the rolling inertia of the wing group.

Addendum **AD3** is an example of the calculation leading to the derivation of the longitudinal stressing data for the asymmetric load cases.

12.3.3.4 Ground **loading cases**

The ground cases differ from the flight cases in that there are local ground forces. The so-called take-off case is effectively a static balance of the aircraft weight by the vertical

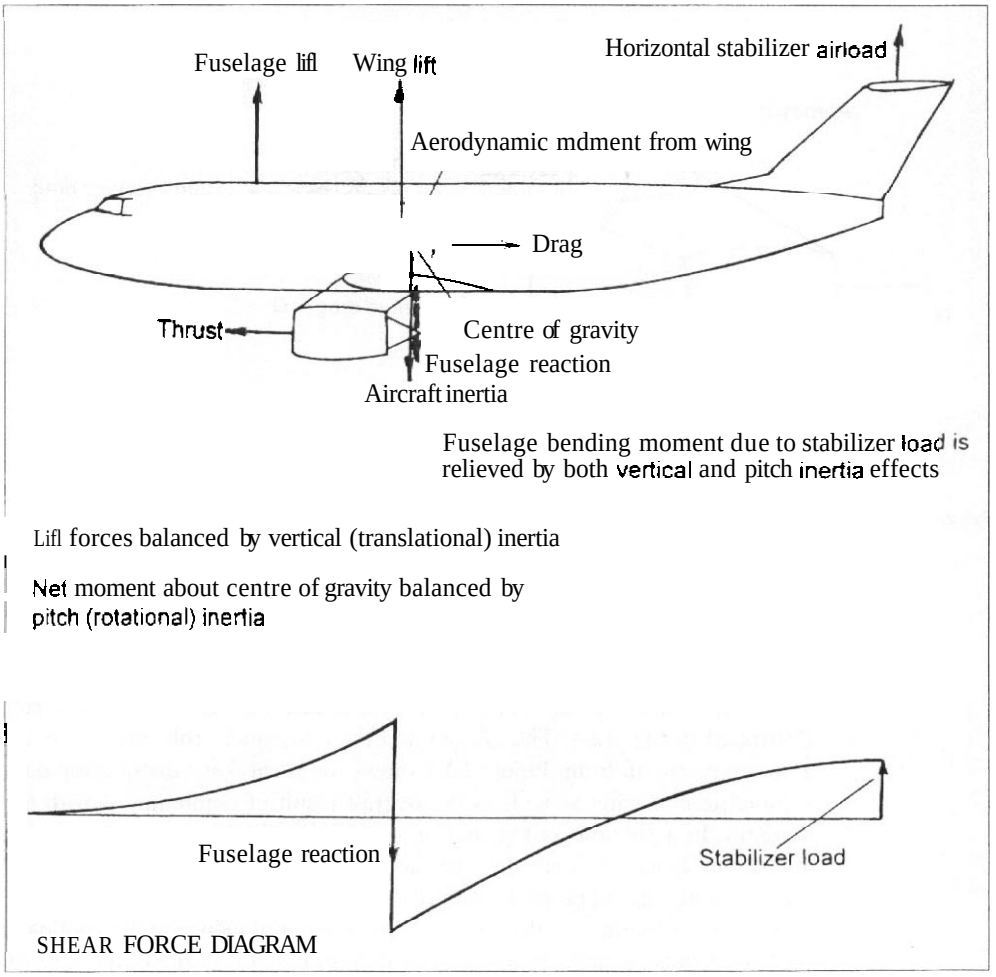

Fig. 12.3 Fuselage loading *in symmetric cases*

loads on the nose- and main-wheels. However, the landing cases are not static in that even after the wheels have made contact with the ground there is a translational motion of the centre of gravity of the aircraft, as well as a rotation in pitch and, possibly, roll. It is also usual for the wing to be providing lift at the time when the wheels contact the ground. Figure 12.7 shows the nature of the landing gear loading in the front view of the aircraft and Fig. 12.8 illustrates the longitudinal situation. The various forces and moments are balanced in the same way as those arising in the flight cases, that is primarily by inertial effects. For this reason it is best to regard the ground contact forces as applied loads rather than as reacting forces.

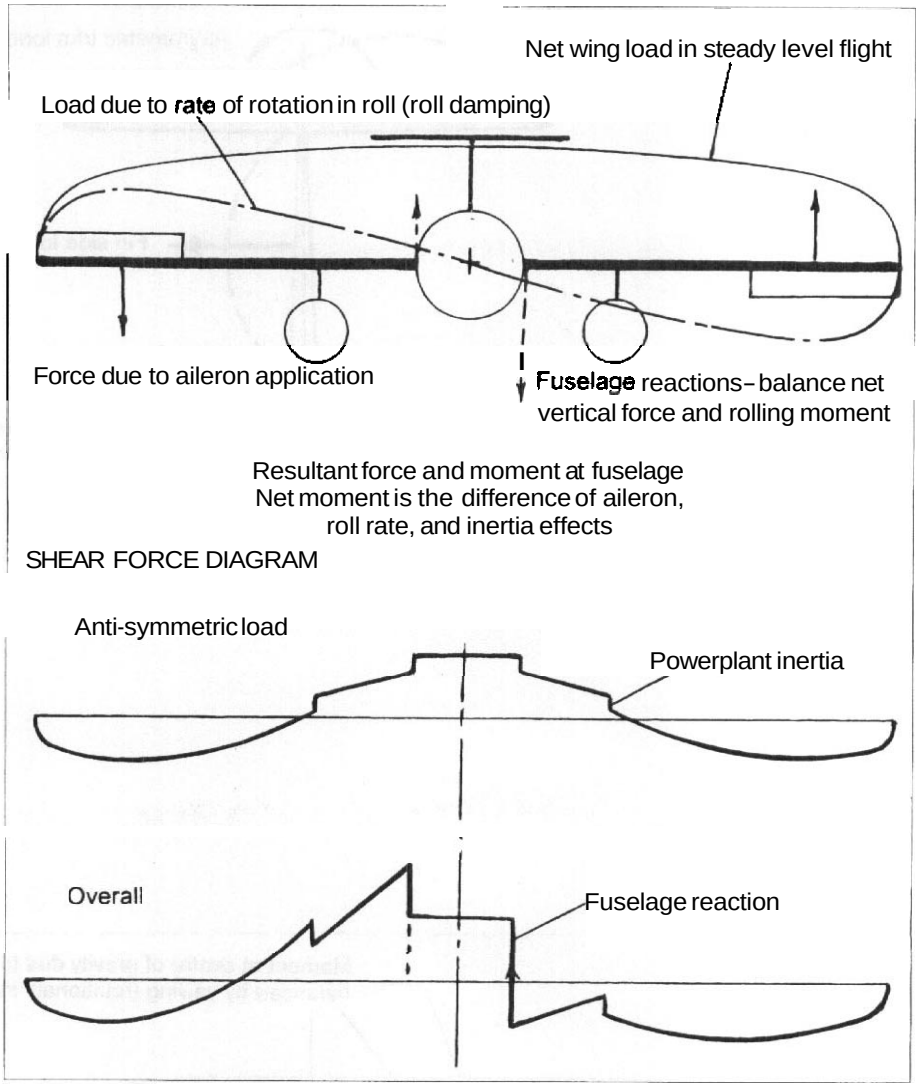

Fig. 12.4 Asymmetric loads (roll) – span-wise

12.4 Sources of load on primary structural components

12.4.1 Introduction

It is useful to review the overall loading arising on the primary structural components as a consequence of the combination of all the cases. The wing may be taken as typical of the lifting surfaces since the horizontal and vertical stabilizing surfaces are subjected to

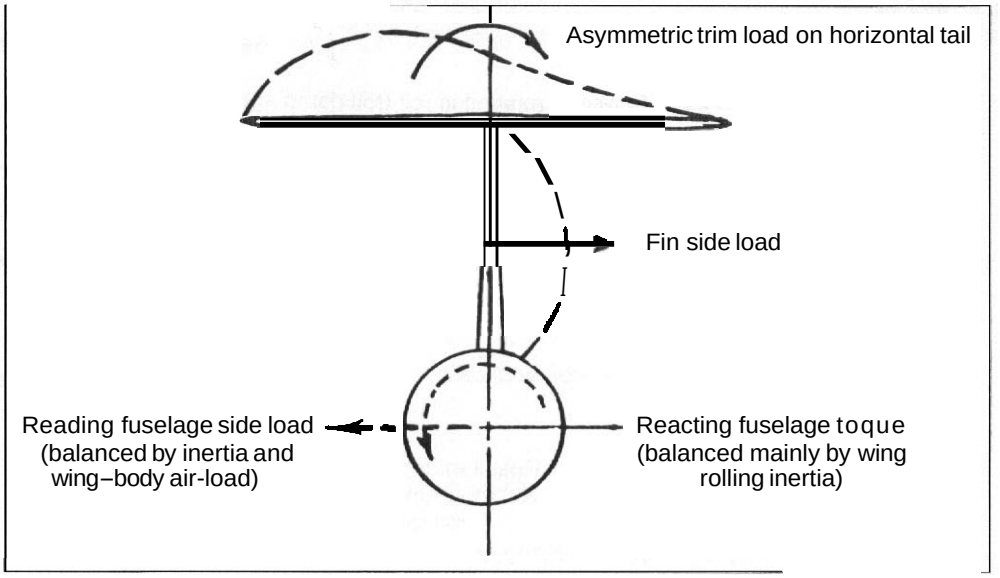

Fig. 12.5 *Asymmetric* loading – fuselage torque

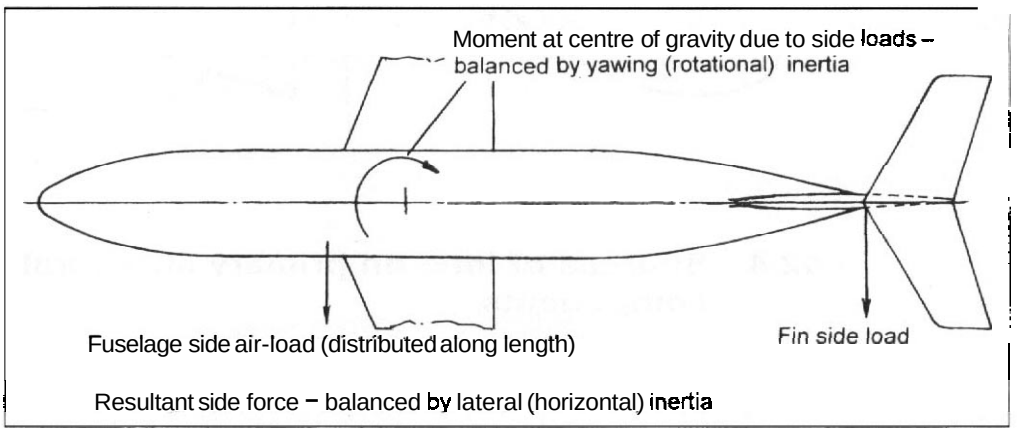

***Fig.* 72.6** Fuselage loading in asymmetric case (sideslip and yaw)

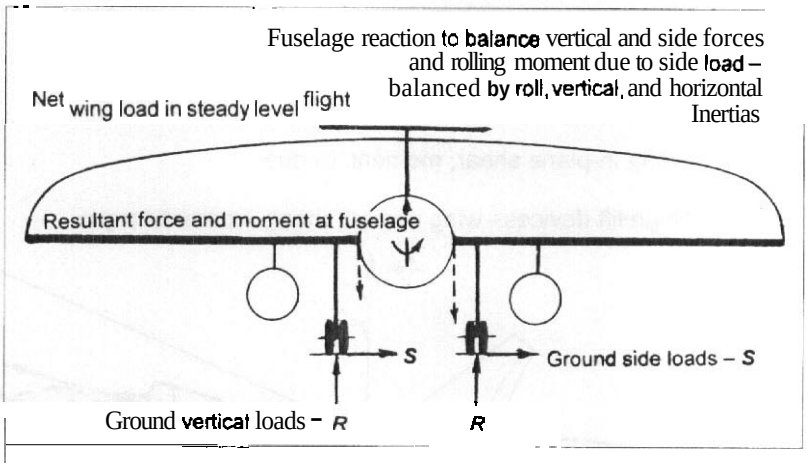

Fig. 12.7 Ground loading – span-wise

similar, but somewhat simpler. loading conditions. The fuselage is in a distinctly different category.

12.4.2 Overall loading on the wing

Figure 12.9 illustrates the set of forces and moments to be considered in wing structural design. The structural role of the wing may include all of the following:

(a) The transmission of the lift force. This is balanced at its root bv the air loads on the fuselage and the stabilizer and by the inertial loads

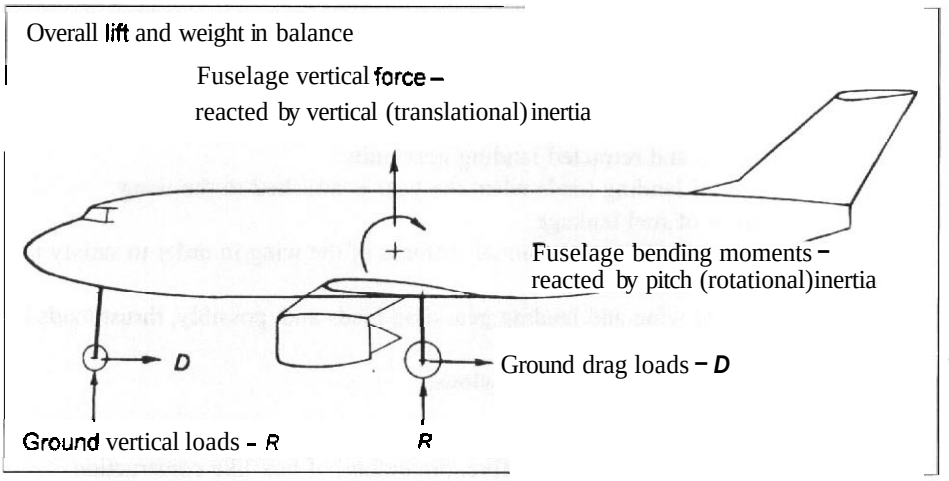

Fig. 12.8 Ground loading – longitudinal

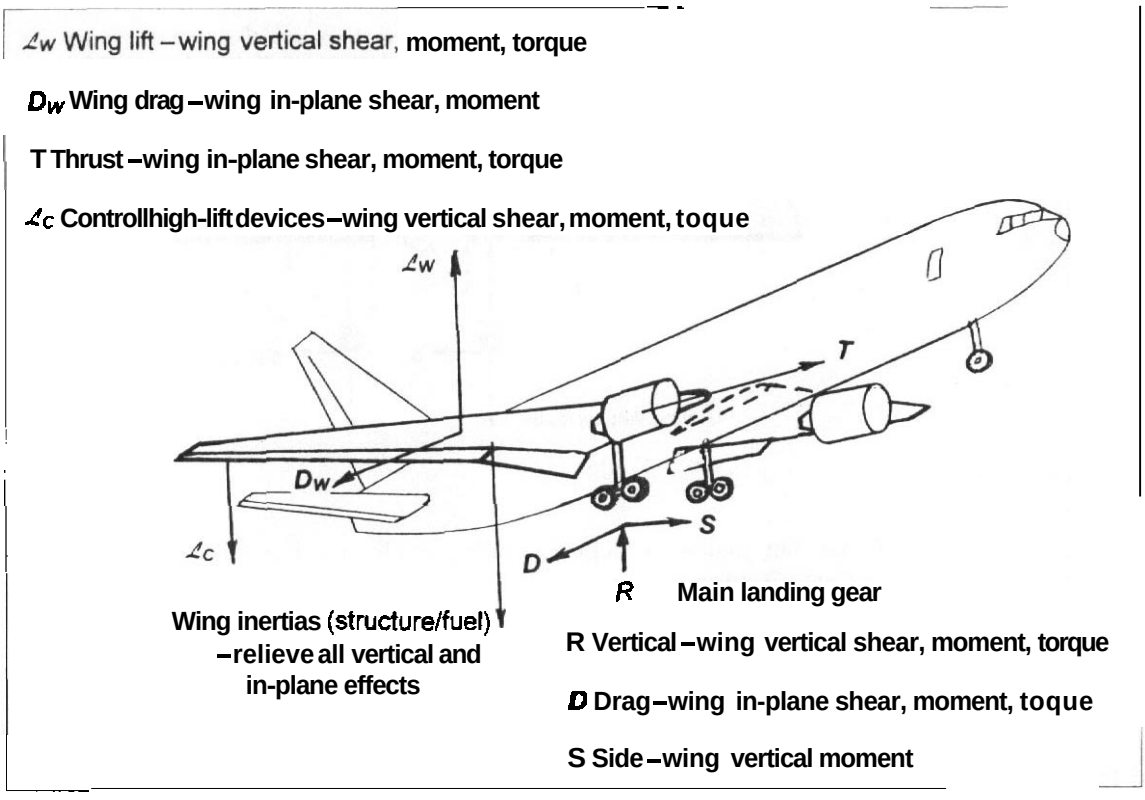

Fig. 72.9 *Overall loading on a lifting* surface

(b) The collection of the chord-wise air-loads and the loads from control surface and high-lift device hinges and the transfer of them to the main span-wise beam structure. This has to be done by a series of chord-wise beams and gives rise to a torque on the span-wise structure as well as contributing to the span-wise bending.
(c) The transfer to the main beam of the local inertia loads from such components as powerplants and retracted landing gear units.
(d) The reaction of landing loads when the gear is attached to the wing.
(e) The provision of fuel tankage.
(f) The provision of adequate torsional stiffness of the wing in order to satisfy the aeroelastic requirements.
(g) The reaction of wing and landing gear drag loads and, possibly, thrust loads in the plane of the wing.
(h) React the loads from stores and pylons.

To perform all these functions the wing has to be both a span-wise and chord-wise beam of significant torsional stiffness and therefore, preferably, of box-like construction.

In addition to the above considerations, high-lift device and control surfaces must provide for the local loads input by the actuation devices. These loads react the aerodynamic hinge moments and determine the hinge reactions.

12.4.3 Fuselage loading

The loading determining the design of the fuselage is shown in Fig. 12.10. The role of the fuselage may include the following:

(a) To provide an envelope and suppon for the payload and crew and, in some cases, the powerplant.
(b) To react landing gear and powerplant loads when these items are located on, or within. the fuselage. The nose gear loads are always present.
(c) To transmit the control and trimming loads from the stabilizing/control surfaces to the centre of the aircraft.
(d) To provide support and volume for equipment and systems.

These requirements imply that to perform its structural role the fuselage has to be a longitudinal beam loaded both vertically and laterally, it also has to react torsion and

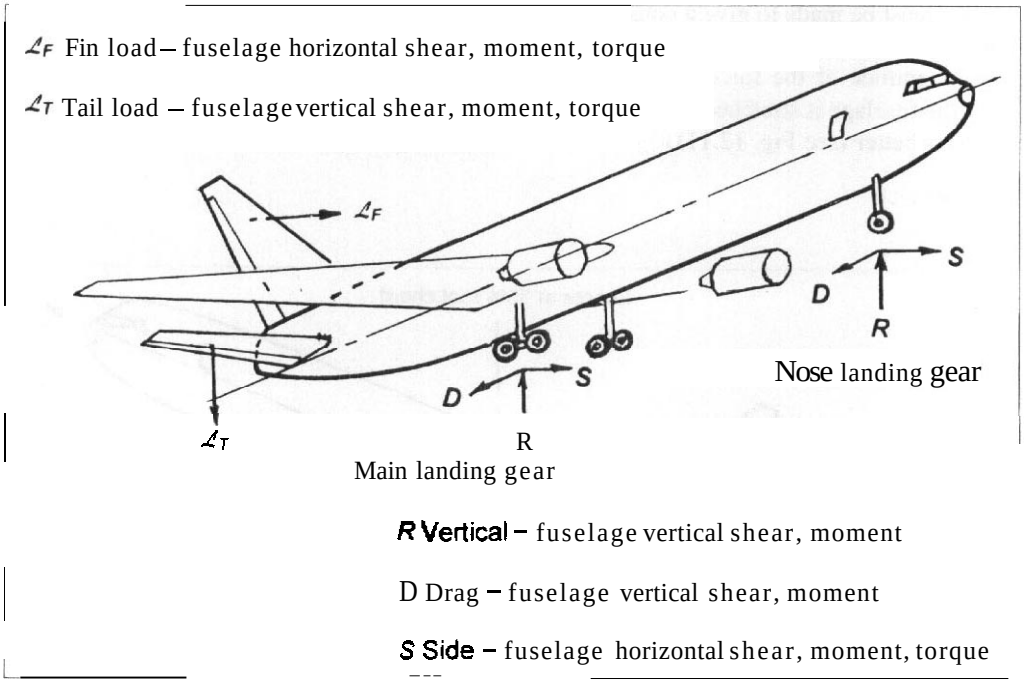

Fig. 12.10 Overall loading on the fuselage

local concentrated loads. The provision of an envelope for the payload implies a box-like construction.

12.4.4 Landing gear

The loads on the landing gear mainly arise due to contact between the wheels and the ground and can be resolved into the three datum directions. There are some cases, for example when a tyre is deflated, which give rise to moments at the axle. The design of the landing gear units is usually such that the bracing struts are only required to react direct loads, whereas the main leg will be subject also to bending and torsion. Unlike the thin, box-like form of construction typical of wings and fuselages. the landing gear components are relatively substantial mechanical items.

12.5 Reference and datum lines

12.5.1 Reference lines

It is important to define reference points and lines at the outset of the structural design. Ideally a set of orthogonal axes passing through the centre of gravity of the aircraft would be used. However, this is not the most convenient since the centre of gravity moves both longitudinally and vertically with differing fuel and payload conditions and so a compromise must be made to give a consistent reference. A fore and aft reference located at the nose of the aircraft is sometimes used but it is not helpful in terms of indicating the magnitude of the forces and moments actually applied, and becomes inconvenient if the fuselage is stretched. A fore and aft datum in the region of the centre of gravity range is better (see Fig. 12.11).

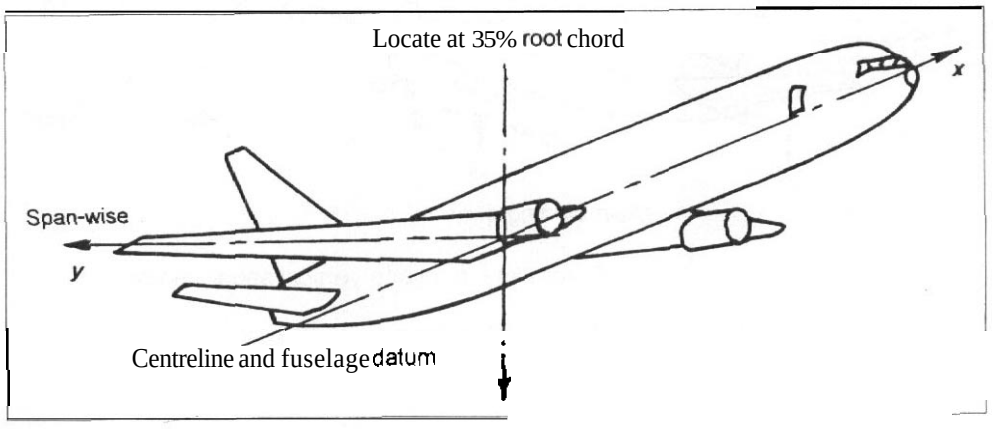

Fig. 12.11 Structural design reference axes — datum lines

Overall the most suitable reference axes are likely to he:

(a) Aircraft ccntreline.
(b) Fuselage horizontal datum in the side elevation unless the mean vertical position of the centre of gravity is significantly removed from it.
(c) Fore and aft axis located at, say. 35–40 per cent of the root chord. This has the advantage that it is in the region of the location of the aft centre of gravity and is close to the local mid-point of the main span-wise structure, especially when the wing is unswept.

12.5.2 Swept lifting surfaces

A particular difficulty arises when the layout of the aircraft uses swept lifting surfaces. as shown in Fig. 12.12. It is logical to treat the outer parts of the surface as an isolated structural member and to fix the span-wise reference axis along the locus of, say, the 40 per cent chord point. The problem arises in the root region where it is necessary to resolve the bending and torsion couples into those appropriate to the overall axis system of the aircraft. Thus what is a convenient definition for the analysis of local structural conditions becomes inconvenient overall. The alternative use of an orthogonal axis across the whole span of a swept wing implies that in the outer region the actual torsion couples are derived as a difference between two relatively large numerical values and it implies the local resolution of couples at each span-wise station. Often the most

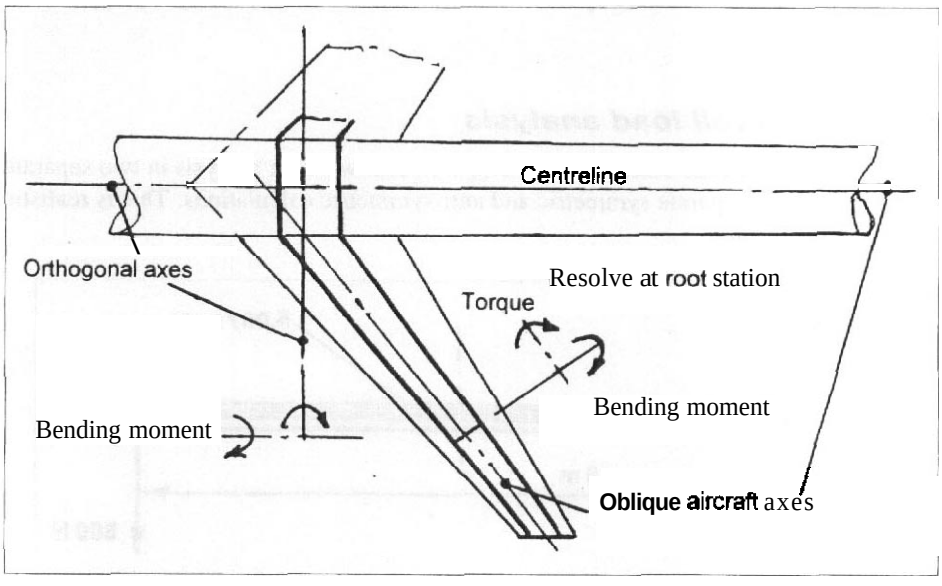

Fig. 12.12 Swept lifting surface datum lines

satisfactory approach is the former with careful thought given to obtain the correct components of couples at the root junction. This problem is dealt with automatically when finite element analysis is used although care must taken in the selection of the element geometries.

In either of the approaches discussed in the previous section, when defining the bending moments and torques it is necessary to identify the load distributions across chord-wise strips. This is straightforward when overall orthogonal axes are used since the chord-wise strips are in the flight direction used conventionally to define the aerodynamic loading. When the wing is treated as an isolated structural member the structural chord-wise strips lie across the stream direction and hence it is necessary to resolve the aerodynamic information appropriately.

Appendix A12 Example of an unrestrained beam analysis

A12.1 Definition of the problem

Figure **A12.1** shows a simple uniform unrestrained beam subjected to both tip loads and a uniformly distributed load which here may represent the mass. It might, therefore, be a simple representation of a wing subjected to vertical inertial forces and tip forces applied by reaction controls.

In order to evaluate the shear force and bending moment distributions along the unrestrained beam it is necessary to invoke d'Alembert's principle. Essentially this allows a dynamic problem to be treated as a quasi-static one by including in the total load that due to the 'internal', or inertial, forces on the beam. These inertial forces are effectively the reactions stated by Newton's third law of motion, derived by application of the second law.

A12.2 Overall load analysis

While it is by no means essential, it is helpful to deal with the analysis in two separate stages, namely as separate symmetric and anti-symmetric calculations. This is realistic

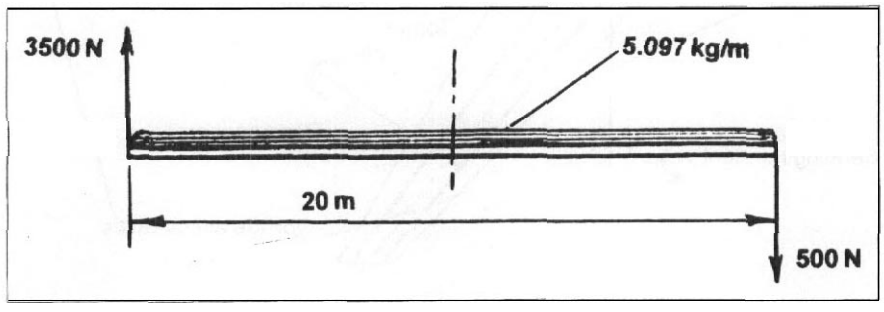

Fig. A12.7 Unrestrained beam example

as in practice aircraft loading cases often effectively consist of symmetric and asymmetric conditions combined together with various individual magnitudes of load.

Assume that the symmetric component of the tip forces is X and the anti-symmetric component is Yas shown in Fig. A12.2. Then:

$$X + Y = 3500\,\text{N}$$
$$X - Y = -500\,\text{N}$$
$$X = 1500\,\text{N} \quad \text{and} \quad Y = 2000\,\text{N}$$

A. *The symmetric condition*

The symmetric loading is shown in Fig. A12.2a and it is noted that the total mass of the beam is 101.94 kg. According to Newton's second law for overall equilibrium:

$$2 \times 1500 = 101.94f$$

where f is the vertical, translational. acceleration of the beam

$$f = 29.43\,\text{m/s} = 3.0g$$

That is, the beam is accelerating upwards with a value equal to three times the gravitational acceleration. For quasi-static equilibrium d'Alembert's principle requires an 'internal' force equivalent to (mass x $3g$), as would be expected.

Using the left-hand end of the beam as a reference the shear force may be written as:

$$1500 - 5.097 \times 9.81 \times 3x = 1500 - 150x\ N$$

which passes through zero at the centre of the beam when $x = 10$ m

Likewise the bending moment is:

$$1500x - 75x^2\ \text{N m}$$

which has a maximum value of 7500 N m at $x = 10$ m, as would be expected since this is the point where the shear force changes sign. The shear force and bending moment diagrams are shown in Fig. A12.2(a)

It should be noted that if the beam was actually pivoted at the centre it would only experience an 'internal' loading equivalent to 1g acceleration, that is 1000 N. The vertical force balance then requires the pivot to react the remaining 2000 N. The new shear force and bending moment relationships are, respectively:

$$1500 - 50x\ \text{N} \quad \text{and} \quad 1500X - 25x^2\ \text{N m}$$

giving a maximum bending moment of 12 500 N m at the centre of the beam.

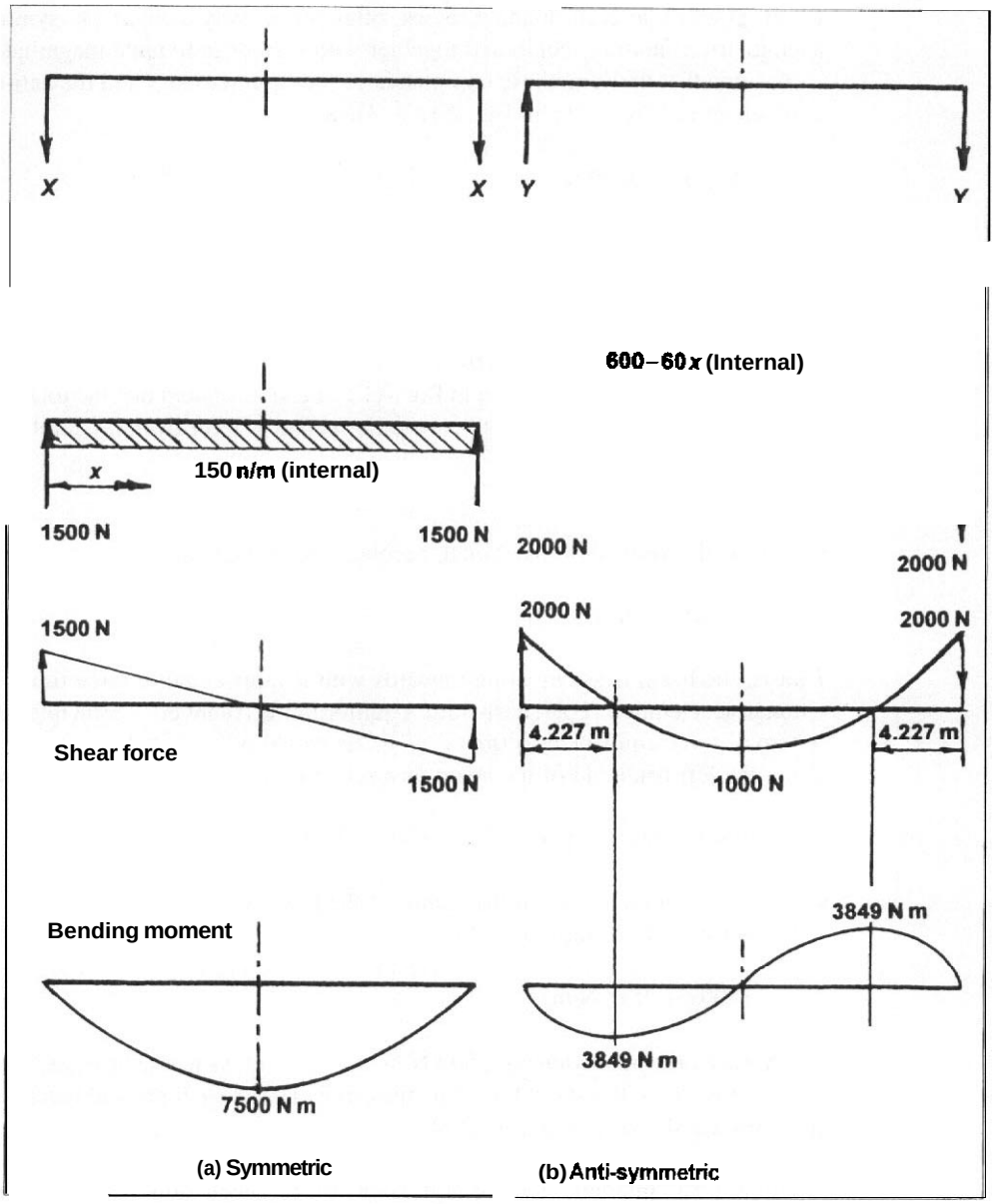

Fig. Ai2.2 Beam example – symmetric and anti-symmetric loadings

B. The anti-symmetric condition

In this case the beam is subject to a couple of value:

$$2000 \times 20 = 40\,000 \text{ N m}$$

and will tend to rotate about a virtual (or actual) point at the centre of the beam.

Newton's second law in angular coordinates can be used to find the angular acceleration of the beam:

$$\alpha = T/I \text{ rad/s}^2$$

where T is the applied torque (couple) and I is the moment of inertia about the point of rotation.

For a long, thin beam rotating about its centre point the moment of inertia is given by $(ml^2/12)$ where m is the mass, and I is the length, that is:

$$I = 101.94 \times 20^2/12 = 3398 \text{ kg m}^2$$

Thus the angular acceleration is:

$$\alpha = 40\,000/3398 = 11.772 \text{ rad/s}^2$$

Again, applying d'Alembert's principle, this acceleration acting on the beam will give rise to an 'internal' couple to balance the applied one. Under the angular acceleration a small segment of the beam located at a distance y from the point of rotation will be subjected to a linear acceleration of $11.772y$ m/s^2. Thus at any point along the beam defined by a distance x from the left-hand end the 'internal' force on the segment of the beam will be:

$$5.097 \times 11.772y = 60y \text{ N/m}$$

or, since $y = (10 - x)$, it will be:

$$60(10 - x) \text{ N/m}$$

The complete anti-symmetric loading on the beam is shown in Fig. A12.2(b)

The 'internal' force distribution is triangular in shape and has a moment of:

$$2 \times (600 \times 10/2) \times 6.667 = 40\,000 \text{ N m}$$

This balances the applied couple as would be expected

The shear force for this case is:

$$2000 - 60\int_0^x (10 - x)dx = 2000 - 600x + 30x^2 \text{ N}$$

The distribution along the beam is shown is Fig. A12.2(b).

The points at which the shear force diagram passes through zero are given by the solution of the shear force equation equated to zero:

$$30x^2 - 600x + 2000 = 0$$

$x = 4.227$ and 15.773 m.

The bending moment for this case is given by:

$$2000x - 300x^2 + 10x^3 \text{ N m}$$

which has maximum values of $\pm$ 3849 N m at $x = 4.227$ and 15.773 m.

The distribution of bending moment is shown in Fig. A12.2(b).

C. Combined case

The complete solution is simply obtained by combining the two separate shear force and bending moment diagrams. A little care is needed in doing this to ensure that all the details are correct. In this problem the combined shear force is given by:

$$1500 - 150x + 2000 - 600x + 30x^2 = 3500 - 750x + 30x^2$$

which has zero values at 6.208 and 18.79 m.

The corresponding two maximum values of bending moment are:

9669 N m at $x = 6.208$ m

and

−293 N m at $x = 18.79$ m

The final shear force and bending moment diagrams are shown in Fig. A12.3

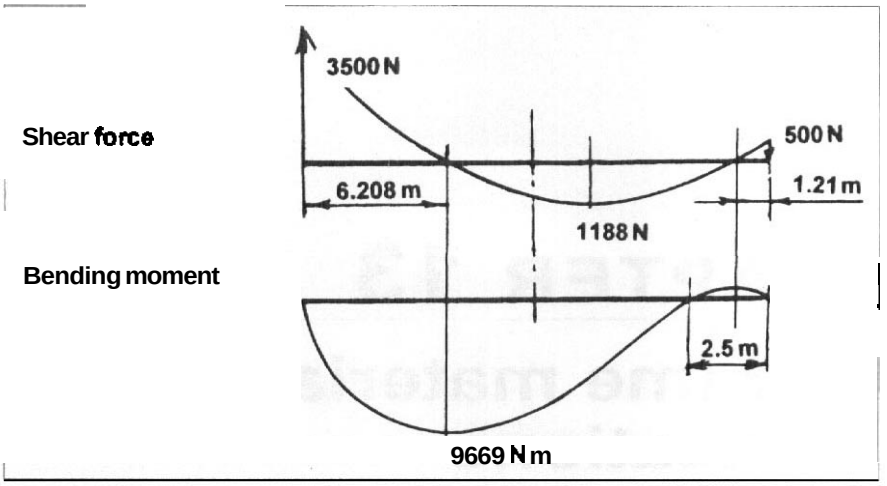

Fig. A12.3 Combined loading *case*

A12.3 Comments

There are some points worthy of note:

(a) While it is not essential to divide the problem into separate symmetric and anti-symmetric cases, it greatly assists in the comprehension of the problem.

(b) A symmetrical load distribution always leads to an anti-symmetric shear force diagram and a symmetric bending moment diagram. The reverse is true for an anti-symmetric loading.

At each stage of the analysis the work should be checked. For example the 'internal' force and moment distributions must balance the external forces and moments. Maximum bending moments must coincide with change in sign of the shear force. The symmetry and anti-symmetry of the diagrams must be appropriate.

CHAPTER 13

Airframe materials and applications

13.1 Introduction

To some extent the structural layout of an airframe is dependent upon the choice of the material of construction. It is necessary to be aware of the available alternatives before the structural design is undertaken. In some circumstances it is desirable to consider different designs employing alternative materials and to compare them before making a final decision on the material to be used. The primary drivers in airframe design are low weight and low cost. These. two criteria have to be balanced in order to achieve an acceptable solution. Both are a function of the material itself and the manufacturing processes used to make the details and assemblies of a structural component. Thus the best solution would be an airframe constructed of an expensive, but low density, material if the associated manufacturing costs are lower than those associated with a cheaper material or the impact of low weight on the life cycle costs of the aircraft is dominant.

13.2 Airframe materials

13.2.1 General

Two fundamentally different classes of material find application in airframes: metals and fibre-reinforced composites. A review of the properties and uses of the actual materials available is given in Section 13.4 but it is useful to list the main types in both classes.

13.2.2 Metallic materials

While many different metals find some application in aircraft as far as the airframe and related components are concerned there are three main groups.

(a) *Aluminium* alloys *(light alloys).* In order to obtain a suitable airframe material aluminium is alloyed with various other metals. such as magnesium, although zinc and copper are the more usual. Developments using lithium as an alloying metal yield lighter, stronger. and stiffer materials but they are much more expensive and not, as yet, so readily available. Aluminium alloys are the most commonly used airframe material because of their low densities, excellent range of properties which can be matched to particular requirements. experience of manufacturing techniques and the known in-service behaviour.

(b) *Titanium* alloys. Titanium has a density about 1.58 times that of aluminium alloys. Some applications use it in pure form but most often it is alloyed with aluminium and vanadium. The strength/density ratio is, if anything, somewhat higher than comparable aluminium alloys hut the elastic modulus/density ratio is rather less. The strength properties are retained at much higher temperatures than light alloy and the metal is less susceptible to corrosion.

(c) Steels. Steel is available with a wide range of properties and can have greater strength than either light alloys or titanium alloys. Its density is some 2.8 times that of aluminium and as a consequence the main use of steels is for highly loaded components where it is desirable to keep the size as compact as possible. Some types of steel are corrosion resistant.

13.2.3 Fibre-reinforced composite materials

A composite consists of two distinct elements which, unlike metal alloys, remain separate within the material. In airframe applications one of the elements is a fibrous material used to reinforce the other, a matrix material. Although the fibres can be short and random they are more usually long and arranged directionally to impart the required strength properties in specific directions. The most frequently used reinforcing fibres are:

(i) carbon (graphite):
(ii) glass;
(iii) aramid, such as Kevlar.

Among other fibres which find some application are boron and silicon carbide.

The matrix material may be a ceramic but for airframe application the usual ones are:

(a) Thermosetting resins, which are by far the most common. They include polyester, polyamide. and epoxy formulations.
(b) Thermoplastic resins, which have some advantages and are finding wider use.
(c) Metal, such as aluminium alloy.

Materials using fibres to reinforce resin matrices are commonly referred to as 'fibre-reinforced plastics' (FRP).

It is worth noting that wood is actually a natural form of fibre-reinforced material. Its use is now limited to small, simple, aircraft because of its relatively low strength, variability. and vulnerability to environmental effects such as moisture.

13.3 Criteria for the selection of materials

13.3.1 General

For airframe application the most important material properties are:

(i) elastic modulus (E) and shear modulus ***(G);***
(ii) ductile yield or proof strength (σ_y) and ultimate tensile strength (UTS);
(iii) fracture toughness, (K_{1C}), which influences the brittle strength;
(iv) density (ρ).

For a given material these properties will vary with environmental conditions. such as operating temperature, and their relative importance depends upon the form of the loading and application. For an airframe the most important loading forms are:

(i) tension, including the effect of pressure in thin shells;
(ii) buckling of slender columns;
(iii) buckling of plate-like components (including reinforced plates);
(iv) bending of plate-like components.

Overall airframe stiffness, especially torsion (shear) stiffness, is also of great importance.

The way in which the basic material characteristics interact with the design considerations is shown in Table 13.1. The selection of a material demands a consideration of all the properties of the material. This includes its cost both in the raw and manufactured condition.

Table 13.1 Material properties for minimum mass

Loading condition	Stiffness	Ductile strength	Brittle strength
Tension (tic rods; tension flange of beams: pressure shells)	E/ρ	σ_y/ρ	K_{1C}/ρ
Torsion (bar; tube; ***box)***	$G^{1/2}/\rho$	$\sigma_y^{2/3}/\rho$	$K_{1C}^{1/3}/\rho$
Compression-buckling (slender struts; thin plates)	$E^{1/2}/\rho$		
Bending – plates	$E^{1/3}/\rho$	$\sigma_y^{1/2}/\rho$	
Bending – bars (bars; rods; tubes)	$E^{1/2}/\rho$	$\sigma_y^{2/3}/\rho$	$K_{1C}^{2/3}\rho$

Notation: ρ, density; E, elastic modulus; G. shear modulus; σ_y, proof stress; K_{1C}, fracture toughness

A comparison of the relative characteristics of usual materials is given in Figs 13.1 to 13.3. These have been derived from Ashby[1] (key to abbreviation in Figs 13.1 to 13.3 is given in Fig. 13.1)

13.3.2 Static (ductile) strength

Figure 13.1 compares the proof (yield) strength of various materials, including those commonly used in airframes, on the basis of density. Proof strength is used in those cases where the material does not exhibit a definite yield and is conveniently taken as the stress causing a permanent residual strain of. say, 0.1 per cent. The materials lying above the constant (σ_y/ρ) line are the most promising for tension applications. On the other hand the performance in the bending of plates is best when the materials lie above the constant $(\sigma_y^{1/2}/\rho)$ line. Ceramic materials look to be promising on the basis of static strength but they are usually mled out by other considerations. Fibre-reinforced plastics are attractive, as is wood parallel to the grain

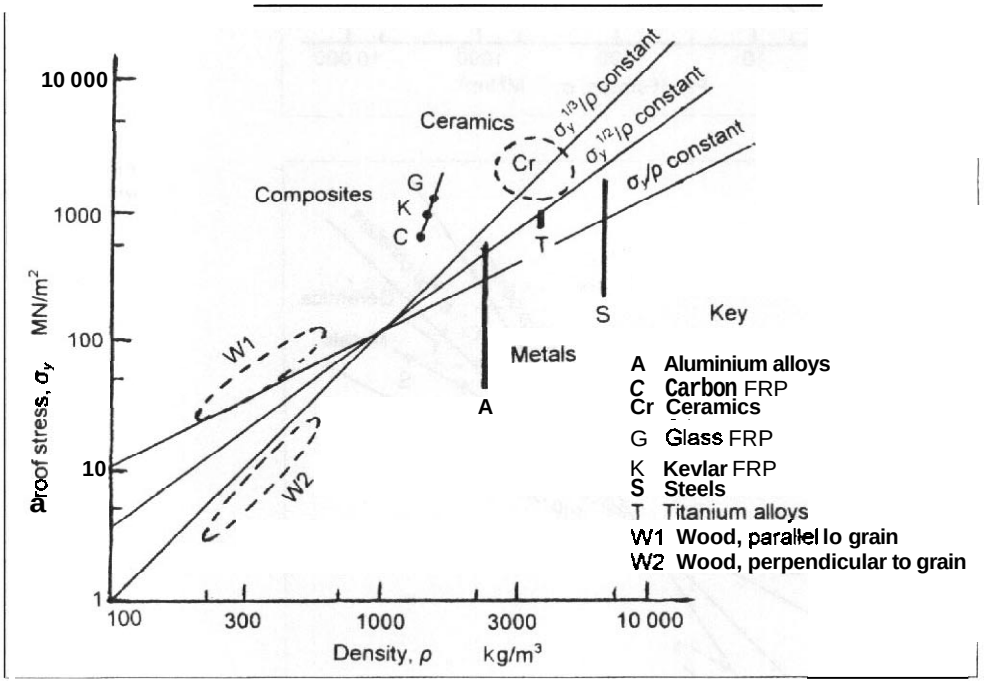

Fig. 13.1 Comparison of material static strengths

[1]Ashby, M. F. Materials selection in conceptual design. *Materials Science and Technology. 5*, June 1989.

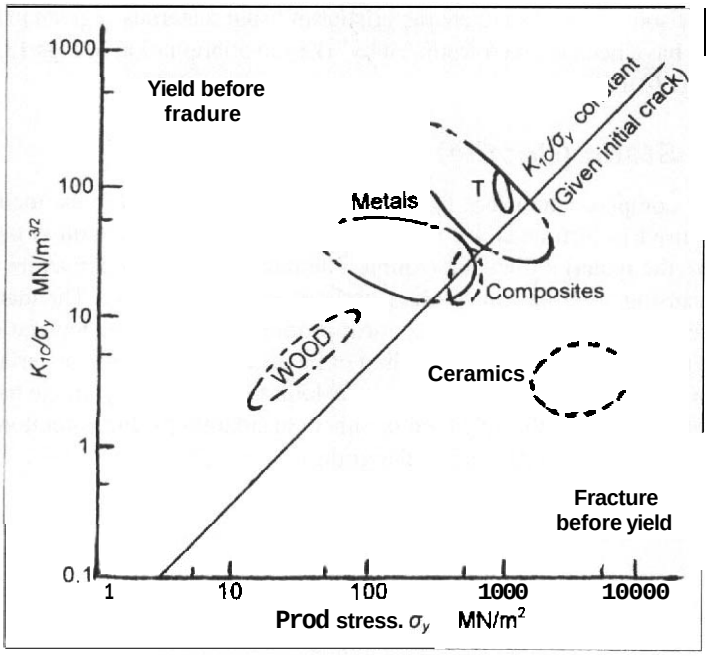

Fig. 73.2 Comparison of material fracture toughness

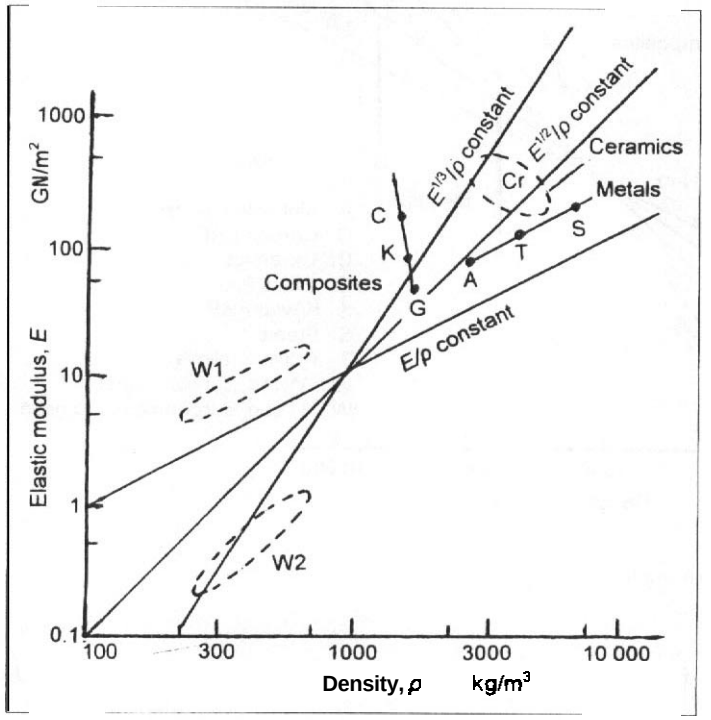

Fig. 73.3 Comparison of material stiffness

13.3.3 Fracture toughness

Figure 13.2 shows a comparison of the fracture toughness of the materials as a function of the proof (yield) strength. The poor characteristics of ceramic materials are apparent. The actual behaviour of a material depends upon the size of the initial flaw, or crack, and the nearer the material is to the upper left-hand comer of the diagram the more tolerant it is.

13.3.4 Stiffness

The comparison of material stiffness in relation to the density is given in Fig. 13.3. Good overall structural stiffness is conferred when the material lies above the constant (E/ρ) line. Those above the constant $(E^{1/2}/\rho)$ line are best for strut and plate compression buckling while plate bending depends upon $(E^{1/3}/\rho)$. The excellent potential of fibre-reinforced plastics and wood parallel to the grain is to he noted.

13.4 Application of aircraft materials

13.4.1 Metals

13.4.1.1 General

Over many years there has been a steady improvement in the properties of metals. Sometimes this has been achieved by improvements in the manufacturing processes and sometimes by the development of new materials. as for example with aluminium–lithium and high-strength iron-based aluminium alloys. The advantages conferred by these developments are significant and the improvements are important since there can be little douht that metals will continue to constitute a major element of airframes for the foreseeable future.

When sheets of metal are subjected to pressure and so-called 'super-plastic' temperatures they may be given very large deformations. This technique is especially valuable in the application of thin material since the shaping possible may be used to confer local stiffness.

Metallic components are commonly joined using mechanical fasteners such as rivets and bolts, but welding and bonding offer alternatives in appropriate circumstances. Bonding may use special glues or a diffusion technique. Diffusion bonding of two components occurs when the temperature is sufficient for diffusion mechanisms to operate across the contact areas. In some cases, for example titanium, the super-plastic and diffusion temperatures are similar such that separate pans may be joined at the same time as the super-plastic forming. When this is the case the process is very efficient and versatile, although the production numbers have to be sufficient to justify the high tooling costs. While aluminium alloys may also be super-plastically formed, diffusion bonding is less readily achieved due to the existence of oxide coatings on the surfaces of the metal. These do not dissolve at high temperature as is the case with titanium.

13.4.1.2 Aluminium alloys

Aluminium alloys are by far the mostly widely used airframe materials and have been developed to meet specific airframe applications. Indeed, until the relatively recent introduction of composites it was true to say that, with very few exceptions, all airframes were mainly of light alloy. Aluminium alloys have very good strength to density ratios. especially in the compression and bending of relatively thin plates and sections. A thin outer cladding of pure aluminium can confer good corrosion resistance but this does have an adverse effect upon fracture toughness and hence it is not now used as much as it was at one time. Low strength aluminium–magnesium alloys can be welded by conventional techniques and higher grade copper-based alloys may be spot-welded. Recent developments in friction-stir welding (FSW) are also finding application in comparatively substantial light alloy assemblies.

The main limitations of aluminium alloys are:

(a) A relatively rapid reduction of properties with temperature even in those alloys specially produced for use at moderately high temperature in excess of, say, 100 "C.

(b) The comparatively large size of sections when the loading intensity is very high. This may have significant disadvantages in some situations, for example joints and shallow beams.

Table 13.2 details some specific uses of particular aluminium alloys. Generally accepted United States specifications are quoted. Zinc-based alloys have higher strength potential but copper-based alloys are preferred where fracture toughness is important, as in primarily tensile loaded components.

Table 13.2 Application of aluminium alloys (typical subsonic transport aircraft)

Component	Item	Alloy	Ageing
Lifting surface	Tension skin	Copper base; 2124, 2324	Natural
	Compressions skin	Zinc base; 7150	Artificial (to high static strength)
	Spars, ribs	Copper base; 7010, 7050	Artificial
Fuselage	Skins	Copper base; 2024	Natural
	Frames		
	Built-up	Copper base; 2024	Natural (may be clad)
	Machined	Zinc base; 7010, 7050. 7175	Artificial

Far the definition of structural components see Chapter 14.

13.4.1.3 Titanium alloys

Although the application of titanium alloys is not extensive, partly because of high cost, they do possess advantages making their choice appropriate in some circumstances:

(a) The retention of properties to comparatively high temperatures, which is useful for engine fire bulkheads and other applications where high temperature is a major consideration.
(b) The coefficient of thermal expansion is low and similar to that of carbon-reinforced plastic material. It is appropriate to use titanium fittings where concentrated loads need to be reacted in carbon-fibre-reinforced structures.
(c) Certain titanium alloys can be super-plastically formed and simultaneously diffusion bonded, see Section 13.4.1.1. This process is suitable for complex components.

Otherwise titanium alloys are mainly used where the high loading intensity and confined space render the use of aluminium alloys inefficient. Titanium bolts are often used.

13.4.1.4 Steels

Usually only high-strength versions of steel are used and like titanium it is particularly applicable when loading intensity is very high. Experience has shown that it is difficult to design a complete airframe in steel efficiently. When loading and high temperature rule out aluminium alloys and composites, titanium is the preferred material. Steel is normally limited in application to detail fittings and components of joints, including bolts, together with large specific items such as landing gear parts.

73.4.2 Composites

13.4.2.1 General

Apart from potentially high material properties an advantage of fibre-reinforced composites is the ability to tailor the properties to meet a given set of requirements. Effectively a specific material can be developed for each application and complex shapes can be readily moulded. However, against these major attributes must be set the more severe quality control considerations and the general problem of joining parts without losing the potential improvements. There is also a need to ensure that the assembly has satisfactory electromagnetic properties, which may mean including conducting fibres or providing an external conducting mesh. The facility for the repair of damage is another issue demanding consideration.

In practice composite materials andcomponents may be formed in a number of ways. In addition to the embedding of fibres in a matrix it is possible to produce 'ply'-type materials consisting of laminates of thin metal and reinforced plastic. Similarly sandwich construction may be employed with metal or fibre-reinforced plastic face-plates and a variety of core materials. Both of these arrangements have advantages in producing stiff materials, often with good acoustic damping and related properties.

A form of composite, applicable to machine parts. is the reinforcement of the matrix with short fihres or particles. Silicon carbide fibres find application in materials intended for high-temperature powerplant applications using melals, such as titanium, or a ceramic as the matrix. The titanium composites are produced by hot isostatic pressing or diffusion bonding of fibres and foil while vapour deposition is used with ceramic matrices.

Boron fihres have found limited application as a consequence of their specific properties but the expense is a severe restriction on their usage. The more commonly used reinforcing fibres are discussed below.

13.4.2.2 Glass-fibre-reinforced plastic (GFRP)

Glass-fibre reinforcement has found widespread application in association with thermosetting resins, primarily because of its low cost and ease of manufacture. Hence it finds application in secondary structure, such as fairings, and primary structure on relatively lightly loaded aircraft in the general aviation and sailplane categories. **A** limitation of glass fibre is its relatively low elastic modulus. see Table 13.3.

Glass reinforcement is used with thin aluminium sheets to form a ply material known as GLARE. This material has considerable potential for application in pressurized fuselages and elsewhere. It overcomes the poor compression properties of earlier materials which used aramid-fibre reinforcement, see Section 13.4.2.4. Fibre-optic glass is also beginning to find special applications in 'smart' components, see Section 13.4.3.

13.4.2.3 Carbon-fibre-reinforced plastics (CFRP)

Carbon fihres are more expensive than glass but offer a better range of material properties. For many applications carbon-fibre-reinforced plastic is the preferred material. The strength and stiffness properties are excellent, but it must be pointed out that the information given in Figs 13.1 to 13.3 refers to properties in the fibre direction,

Table 13.3 Elastic moduli

Material	Tension modulus E_{xo}* (MN/m^2)	Shear modulus G_{xyc}† (MN/m^2)
Conventional light alloy	7.2×10^4	2.9×10^4
Aluminium–lithium alloy	7.9×10^4	3.2×10^4
Titanium	11.6×10^4	4.6×10^4
Carbon/epoxy (GFRP)		
High strength	13×10^4	3.4×10^4
High modulus	$IS \times 10^4$	3.7×10^4
E glass/epoxy (GFRP)	4×10^4	0.9×10^4
Kevlar/epoxy	7.5×10^4	1.7×10^4

*Unidirectional fibres; †45°/45° weave for reinforced plastics.

and typically the properties perpendicular to the fibres are an order of magnitude less. Thus to take full advantage of carbon-reinforced plastics it is necessary to have a situation where there is a high level of loading in a given direction. such as occurs in struts and along the flanges of beams. Thus carbon fibre materials are most suitable for use in components where the primary load direction is well defined. such as in aircraft lifting surfaces, and where the component is of such a size that it can be manufactured in one piece to eliminate joints. While other applications are possible, the advantages are less substantial.

There are other issues to be considered, for example carbon-fibre reinforced plastics can be sensitive to comparatively low levels of impact damage and environmental conditions such as moisture content.

A ply material using titanium outer covers with carbon fibre internal reinforcement. similar in concept to GLARE mentioned in the previous section, is a possibility.

13.4.2.4 Aramid-fibre-reinforced plastics

Aramid fibres, such as Kevlar, produce tough materials, but have low compressive strength. This is a real disadvantage and hence materials with aramid reinforcement tend to be used only where tensile loading is primary or where impact resistance is required. ARALL is an aluminium alloy ply material employing aramid-fibre-reinforced laminates.

13.4.2.5 Matrix materials

The most important matrix materials are:

(a) *Thermosetting* ***resins.*** To date thermosetting matrices have been most widely used. The production of a component depends upon the completion of a curing process involving a chemical change in the matrix polymer. Once curing is complete the shape of the pan is fixed. Effectively both the material and the component are produced at the same time. This can be a difficulty as it is often necessary to use an autoclave process to achieve the desired material properties and thus there is a consequent limitation on the potential size of a component. A significant amount of hand lay-up may be used although automated lay-up procedures are available for quantity production.

(b) *Thermoplastic* ***resins.*** There have been important developments in the application of thermoplastic polymers. In this case the reinforced material reverts to plastic state on heating and may then be reshaped. This offers the possibility of employing an intermediate stage in the manufacture of a component whereby 'standard' items; such as sheets or tubes, may be produced for subsequent reforming and assembly. Apart from the added versatility of this technique it also assists in improving quality control as the standard items may be produced by automated processes. Developments in thermoplastic composites offer considerable potential as experience is gained in their application. In general they are tough and parts can be produced quickly.

(c) Metals. Metal and related materials such as carbon may also be used as a matrix material. The main advantages are the much higher matrix material and temperature properties than is available with polymers. However, at the present time the costs of producing composites with metal matrices is high and application is limited. Metal matrix composites, where properties are enhanced in a preferred direction by incorporating unidirectional fibres, have found some applications, see Section 13.4.2.1

(d) ***Ceramics.*** For some applications the use of a ceramic matrix may be advantageous, especially when high-temperature properties are required. In this case the fibre enhances the basic properties of the ceramic. especially in relation to the fracture behaviour.

13.4.3 Smart materials

There have recently been developments in so-called 'smart' materials. The properties of these materials may vary according to operating conditions so that they can be made to adapt to particular circumstances.

Smart materials may function in a passive manner, that is be able to sense operating conditions and produce appropriate data. Examples of such types are optic fibres incorporated in a reinforced plastic to identify changes in material properties, for example de-lamination. Conducting fibres may be included as aerials or for de-icing.

Smart materials may also be active in that they can respond to changed conditions. Such basic types are the 'memory' metal or electro-rheological fluids which can change form as a function of temperature. Ultimately components built of smart material may be adaptive in nature. Thus a smart leading edge might he designed to automatically vary its camber with aircraft speed. Experience with smart materials is still in its infancy and as yet it is too soon to visualize just how wide the aerospace applications will be eventually.

13.4.4 Other airframe materials

Various other materials find some application in airframes. In most cases they are employed for specific purposes.

(a) Magnesium-based alloys are light, but bulky and prone to corrosion. Their application is very limited but they may sometimes be used in cast form where local stiffness is the main requirement.

(b) Copper-based metals have little application except for some bearing materials and pipe work where the ease of forming is useful.

(c) Nickel alloys are used where temperatures are very high, as in regions of the airframe adjacent to engine exhausts.

(d) Elastomers are used for seals and as inter-layers in transparencies.

(e) Glasses are used for transparencies.

(f) Acrylics and polycarbonates are also used in transparency applications.

(g) Low-density foams are sometimes employed to stiffen thin plate materials. and resin impregnated paper also has a frequent use in honeycomb sandwich construction as an alternative to metal foil.

13.5 Material properties for initial structural design

13.5.1 Introduction

The main material properties required for the initial analysis are:

(a) Elastic moduli:
longitudinal stiffness (E, elastic or. E_t, tangent modulus);
shear stiffness (G).

(b) Allowable stresses:
direct (including bending) stress (σ_b);
shear stress (σ_s);
tensile stress due to pressure, usually based on actual working conditions, (σ_p).

13.5.2 Stiffnesses

Typical values of the elastic moduli for the most commonly used materials, both metals and reinforced plastics, are given in Table 13.3. In the case of metals a given thickness will provide both direct and shear stiffness in the appropriate proportions. However. in the case of a fibre-reinforced plastic composite the values quoted are for a directional laminate or a pure shear lay-up and it is necessary to provide separate laminates to obtain the other required direct and shear properties. see Section 13.5.4.1.

13.5.3 Allowable stresses – metals

13.5.3.1 General

Conventional aluminium alloy of an appropriate specification is the most commonly used metal for the majority of airframe structure, see Table 13.2. The following remarks primarily refer to this class of material, but there is some read across to the alloys of other metals.

13.5.3.2 Direct (bending) stress

The accurate evaluation of the allowable bending stress is complex and requires a knowledge of the detail features of the structure both in the compression and tension surfaces. Experience suggests that if the magnitude of the allowable compression stress in, say. a wing is also used for the tension surface it makes the right order of allowance for fatigue/crack propagation requirements This assumption can only be approximate

and it does result in an overestimate of the allowable tensile stress when the compression stress approaches the 0.2 per cent proof value. Nevertheless. for preliminary design purposes, the use of the same allowable stress level for both surfaces simplifies the calculation without introducing an undue error. The main parameter in the determination of the allowable compression stress is the loading intensity, $\{P/(wL)\}$, see Eqn. (13.1) below.

When sufficient support is provided to compression members to eliminate the possibility of local and overall buckling it is appropriate to assume that under ***ultimate*** bending loads the 0.2 per cent proof stress may be used as the allowable value, see Table 13.3. When this is not the case, as for example if the compression member takes the form of a wide reinforced plate, the allowable bending stress at ***ultimate*** loading may be assumed to be the lesser of the 0.2 per cent proof stress or σ_b, where σ_b may he approximately represented by:

$$\sigma_b = \bar{A} F_B \{P/(wL)\}^{1/2} \tag{13.1}$$

where

$\{P/(wL)\}$	is in the same units as σ_b
L	is the spacing along the axis of the beam of the local supports, see Chapter 16, Fig. **16.1**
w	is the width of the component perpendicular to the bending axis
P	is the effective end load which coincides with the maximum direct stress
$\bar{A}$	is a function of the material
F_B	depends upon the form of construction see Table 13.4 and Fig. 13.4

Suggested values for A are given in Table 13.5 together with the 0.2 per cent proof stress which defines the limit of applicability of Eqn.(13.1). Note that the values of A are appropriate to the allowable stress and $\{P/(wL)\}$ is in MN/m^2 units. In general the

Table 13.4 Buckling **efficiency** factors, F_B

Construction (see **Fig.** 13.4)	F_B
Zed stringer	
Built-up	**0.96**
Machined	**1.02**
Blade stringer	**0.81**
Top hat stringer	**0.96**
Trapezoidal corrugated, semi-sandwich	**0.83**
Triangular corrugated, semi-sandwich	**0.85**
Truss core sandwich	**0.78**

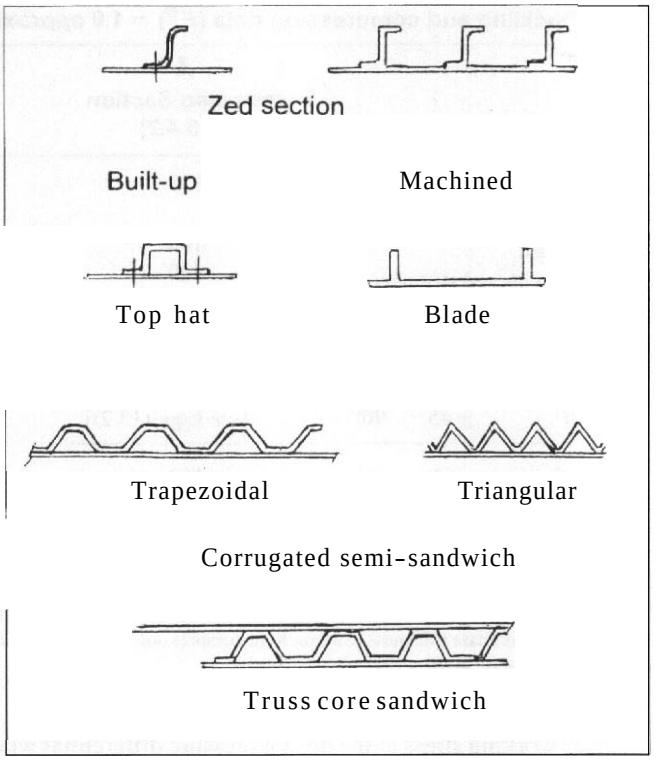

Fig. 13.4 Forms of panel construction

values of A give conservative values for σ_b at stresses below the limiting value, see Fig. 13.5.

13.5.3.3 Shear stress

If it is assumed that the cover skins and internal webs do not buckle in shear, then it is sufficient to assume that at ultimate conditions the allowable shear stress, σ_s, is 50 per cent of the ultimate tensile stress. A different allowable stress applies if the internal wehs are allowed to buckle and become tension field members, see Chapter 16, Section 16.2.4.

13.5.3.4 Allowable tensile stress due to pressure

It is usual for this to be set by the normal working differential pressure, the reduction of allowable stress below the ultimate value allowing for fatigue and crack propagation as well as the ultimate factor. The value chosen does depend upon the design philosophy adopted. In Europe the stress level is often chosen to be such that the critical crack length is that determined by frame spacing. In North America it is more usual to rely upon the crack stopping feature of reinforcing bands. The result of this is that in Europe

Table 13.5 Overall **buckling and** compression data (F^B) = 1.0 approximately)

Construction/material		Plies % at:		A (see also Section 13.5.4.2)	0.2% proof stress (MN/m²)
	0"	±45°	90"	[see Eqn. (13.2)]	
Conventional light alloy with zed or integral blade stringers				138	340
Machined in DTD 5040 plate				180	359
Aluminium–lithium plate with zed stringers				200	365
Titanium with zed stringers (TAIO, 6Al–4Va)				200	830
High-strength CFRP:					
Quasi-isotropic	25	50	25	150	300
Max. Rec. 0°	50	38	12	185	450
Max. Rec. ±45°	12	76	12	150	150
All ±45°	0	100	0	140	100

Note: CRFP buckling stress values allow for the additional thickness of 45" and 90" plies. that is they are allowable stresses based on total laminate thickness. Carbon fibre compression strength is based on I per cent moisture content and a temperature of about 45 °C.

the effective light alloy working stress at the design pressure differential when the frame pitch is typically 0.5 m is less than 100 MN/m², especially for older designs, while in North America it is usually somewhat more. Pending a fracture mechanics analysis it is suggested that an allowable value of no greater than 100 MN/m² at the working

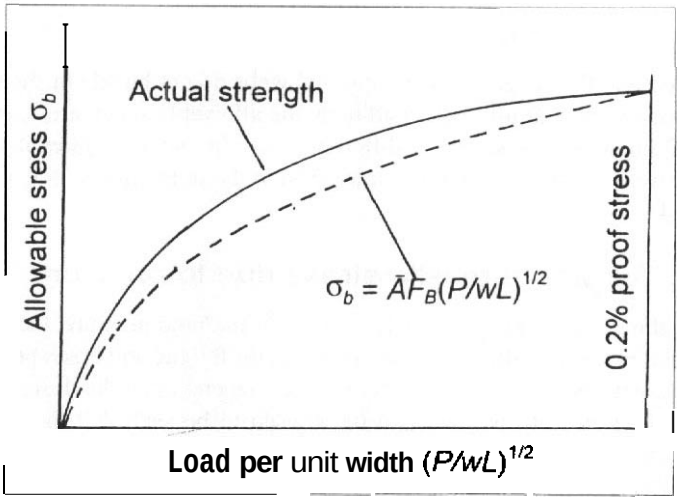

Fig. f3.5 Allowable overall buckling stress

differential pressure he assumed to calculate the first estimate of pressure material thickness for light alloy construction.

13.5.4 Allowable stresses – fibre-reinforced plastic composites

13.5.4.1 General comments – laminate analysis

Estimation of allowable material properties for composite construction is complex due to the need to provide specific directional properties to meet the various load carrying functions. The plies in each direction of the laminate make some contribution to the load carrying capacity in any given direction, and the overall strength is a complex function of the number and direction of the plies as well as the matrix properties. A number of programs have been developed to enable the load carrying capacity of a laminate to be analysed but they are not suitable for use in preliminary design where the problem is to define the numbers and directions of the plies needed to meet the specified loading. One approach is to define and analyse a series of laminate lay-ups from which to choose the most appropriate to meet the given condition.

An alternative is to limit the choice of fibre orientations to four specific directions. namely a datum at 0°, defined by the primary loading. together with 90" and $\pm 45°$, and to use a simple method to make approximate allowance for the directional interactions. A laminate having an equal number of fibres in each of the four directions is known as a quasi-isotropic lay-up. To avoid the possibility of failure of the matrix it is desirable, but not necessarily essential, to incorporate a certain minimum number of fibres in each of the four dircctions. A useful guide and simple method for evaluating laminate strength is the '10 per cent rule' proposed by art-Smith.[2] In this method it is suggested that there should be a minimum of 12 per cent and a maximum of 50 per cent of fibres in each of the 0" and 90" directions. While 50 per cent of $+45°$ with 50 per cent of -45' fibres is feasible it is preferable to limit their total to 76 per cent. Further the laminate should be balanced, that is the arrangement of the plies should be symmetrical about the mid-depth. The predicted strength is based on the assumption that relative to the reference 0° direction each 90, $+45°$ and -45" ply contributes 10 per cent of its directional strength or stiffness. Thus for simple uni-axial loading a quasi-isotropic lay-up has a directional strength of 32.5 per cent of a laminate made up of 100 per cent plies in the 0' orientation, while a laminate with 50 per cent fibres in the 0" direction has a 55 per cent strength ratio. Shear strength is calculated by taking 50 per cent of the directional strength of a complementary lay-up defined as one having the sum of the 0' and 90" disposed equally in the ± 45" directions. This gives a strength ratio of 27.5 per cent for a laminate consisting only of ± 45" plies. Application of the method to shear stiffness yields a value of $0.262E_{xo}$ for the 100 per cent $\pm 45°$ laminate and $0.122E_{xo}$ fur the quasi-isotropic lay-up. where E_{xo} is the directional modulus of elasticity. The 10 per cent rule was used to derive the CFRP values of $\bar{A}$ in Table 13.5, see Section 13.5.4.2.

[2]Hart-Smith, L. I. The Len-per cent rule. *Aerospace Materials*, 5 (2), August/October 1993.

13.5.4.2 Direct (bending) stress

Ultimate direct allowable stresses may be calculated by using the elastic moduli quoted in Table 13.3 with suggested allowable strains of 0.0055 and 0.004 in tension and compression, respectively. Although buckling may be acceptable above limit load for skins less than 3 mm thick it should otherwise be avoided. However, allowable compression may depend upon the buckling characteristics of the component. Tetlow[3] proposes the following for overall buckling:

$$\sigma_b = 0.725F_B\{(E_{xo})^2 Z_o\}^{1/4}\{P/(wL)\}^{1/2} \tag{13.2a}$$

where

w and L	are defined as for metal construction
F_B	is the configuration factor as given in Table 13.4
E_{xo}	is the longitudinal elastic modulus of the covers. given in Table 13.5

The evaluation of Z_o, which is a function of the laminate lay-up, creates a difficulty for design synthesis since it is significantly affected by the angle plies. Tetlow presents a chart for determining Z_o as a function of the lay-up.

An alternative form of Eqn. (13.2a) is:

$$\sigma_b = \bar{A}F_B\{P/(wL)\}^{1/2} \tag{13.2b}$$

where here $\bar{A} = [0.725\{(E_{xo})^2 Z_o\}^{1/4}]$

The 10 per cent rule has been used for the specific high-strength CFRP lay-ups listed in Table 13.5 to enable the evaluation of A, as quoted in the table. The limiting compression stress values are appropriate to environments with about 1 per cent moisture ingress and typical design temperature for subsonic applications.

If it is assumed for initial work that the laminate consists only of the 0" direct stress resistant plies and $\pm 45°$ shear resistant plies then, approximately:

$$Z_o = 0.68sin\{2.244(\bar{R} + 0.3)\} \tag{13.3}$$

Here the angle is radians and $\bar{R}$ is the ratio of the $\pm 45°$ plies to the sum of the 0" and $\pm 45'$ plies.

The difficulty in using Eqn. (13.3) lies in the need to know the value of R, the thickness ratio of the $\pm 45°$ plies. This may be overcome in the design process by analysing the shear stiffness and shear strength requirements before the bending case. Any 90" plies present may be ignored except in as much as they effectively reduce the stress if it is calculated on the total thickness of the laminate.

[3]Tetlow, R. Design charts for carbon-fibre composites. Cranfield Memo No. 9. 1970.

13.5.4.3 Shear stress

In the first instance this is best dealt with by assuming that the total laminate make-up precludes buckling. and using assumed allowed stresses for the $\pm 45'$ plies. Suggested values for initial calculations are:

(a) Glass-fibre laminates, $\mathbf{a}, = 60-80\ \mathrm{MN/m^2}$.
(b) Carbon-fibre laminate. $\sigma_s = 200\ \mathrm{MN/m^2}$ for a quasi-isotropic lay-up to $300\ \mathrm{MN/m^2}$ for all $\pm 45'$ plies.

13.5.4.4 Allowable tensile stress due to pressure

Fibre-reinforced plastic pressure vessels are efficient providing that the reinforcing is continuously, spirally. wound. Such a process is not feasible on the passenger cabin of a large aircraft and in this case the limiting stress is determined by a consideration of the longitudinal and circumferential joints. The stress is determined by the details of the joint and it is not possible to quote a general value although the overall combination of loading due to bending, shear, and pressurization suggest? the use of a quasi-isotropic lay-up. Very careful thought is required if this form of pressure cabin construction is contemplated.

Smaller pressurized fuselages may be made by filament/laminate winding or tape lay-up processes. **A** complete mandrel of, say, a rear fuselage is used to avoid the need for joints in the direction of the hoop stress. Of course there is still a need for joints around the section to assemble the individual longitudinal sections of the fuselage. In these cases the allowable stress due to pressurization may be deduced by the requirement that the pressure cabin must he capable of resisting at least twice the working differential pressure. This implies a strain of, say, no more than 0.002 in the circumferential fibres, see Section 13.5.4.2. This equates to an allowable working stress of about $250\ \mathrm{MN/m^2}$ in the circumferential fibres. or an overall allowable stress of about $140\ \mathrm{MN/m^2}$ for a quasi-isotropic lay-up.

CHAPTER 14

Role and layout of structural members

14.1 Introduction

Chapter 12, Section 12.3.3. outlines the most important loading cases to be considered in the design of an airframe and Section 12.4 summarizes them in the context of the lifting surfaces and the fuselage. Chapter 13 discusses the materials of construction and the next stage of the design process is to determine the location of the main structural members within the major components. This demands an understanding of the role of these structural members.

14.2 Lifting surfaces – wings and stabilizers

14.2.1 Overall requirements

The wing, or main-plane, is typical of the Lifting surfaces and structurally it has to be both a span-wise and chord-wise beam and possess adequate torsional stiffness, as was discussed in Chapter 12, Section 12.4.2.

Figure 14.1 illustrates the plan of the wing of a typical subsonic transport aircraft and shows that the numerous leading and trailing edge devices occupy a significant portion of the chord. The consequence of this is that only about half of the chord is available for the span-wise beam, hut it is the deepest portion and this is preferable for both bending and torsion. Some other classes of aircraft have fewer auxiliary surfaces but other considerations usually lead to a similar situation.

The primary load direction is well defined and is span-wise and therefore a lifting surface is a good candidate for the application of carbon-fibre reinforced plastic providing the overall size is such that it can be built with a minimum number of joints

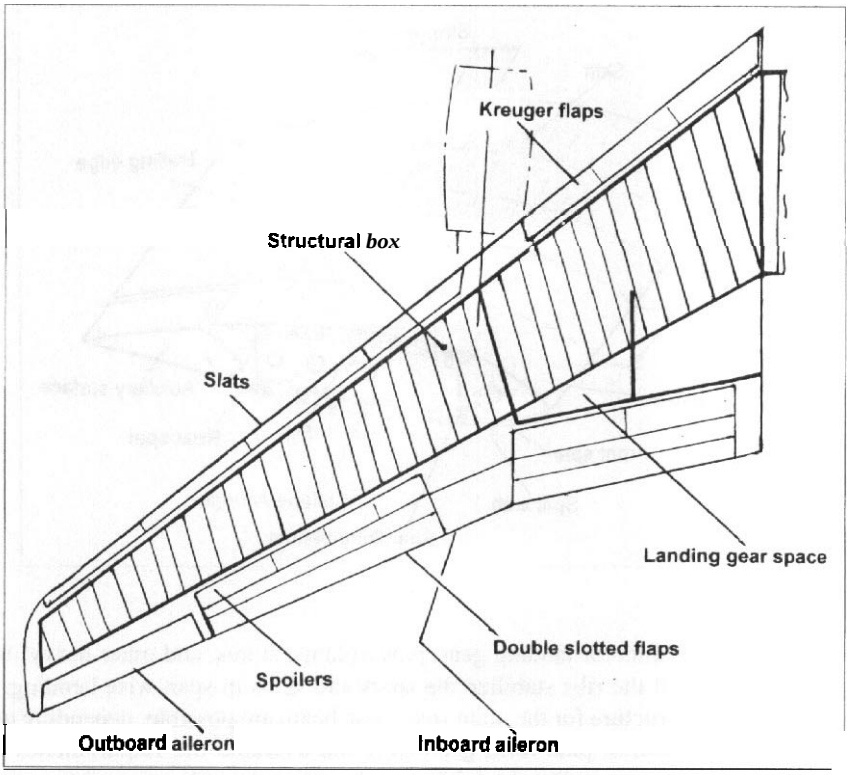

Fig. 14.1 *Plan-form layout of typical subsonic transport*

across the chord. This is especially true of the horizontal and vertical stabilizers which have fewer concentrated load inputs than the wing as well as being of smaller size.

14.2.2 Span-wise beam concepts

14.2.2.1 Main structural components

Figure 14.2 shows the main components used to make up the structure of a lifting surface. Essentially it consists of span-wise beam members. known as spars, chord-wise members, known as ribs, and covering skins which are usually reinforced by span-wise stiffeners.

In conjunction with the stiffened skin the spars transmit bending and torsion loads and form the span-wise beam. Typically the spars consist of a web to react vertical shear and edge flanges or booms. Figure 14.3 illustrates the cross-sections of typical spar flanges and support stiffeners for the cover skins.

The ribs determine the aerodynamic shape of the cross-section and structurally transmit local loads chord-wise across to the span-wise beam. Hinges and supports for secondary lifting surfaces are located at the extremities of relevant ribs. Ribs also

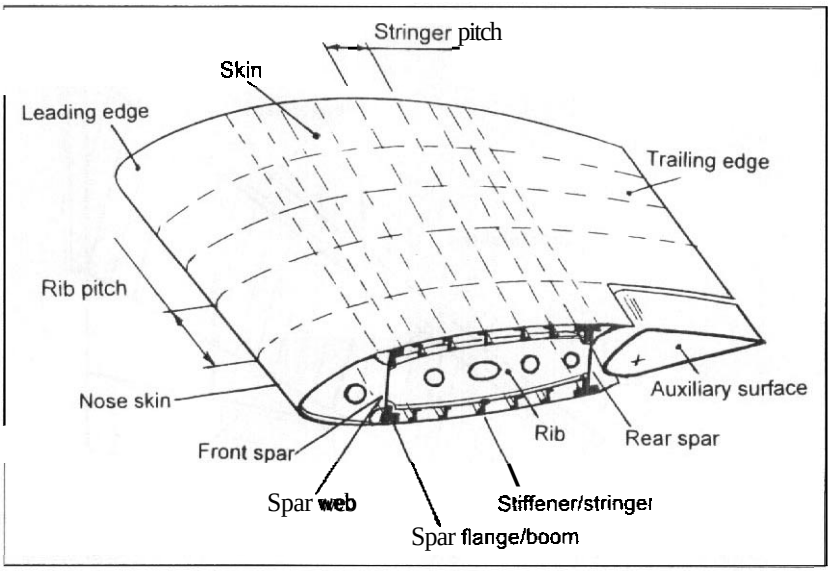

Fig. 14.2 Structural components of a lifting surface

provide attachment points for landing gear. powerplants, stores, and other heavy items as appropriate. Overall the ribs stabilize the spars and skins in span-wise bending.

Various forms of structure for the main span-wise beam are possible, depending upon the overall load intensities, plan-form geometry, and airframe life requirements. The more usual forms are shown in Fig. 14.4. Most are based on the utilization of the vertical webs and outer skins to form the box beam, but there can be exceptions when the loading intensity is low. The span-wise beam is best constructed as one item from wing tip to wing tip, although it may be difficult to achieve this in high-performance combat aircraft having wings of low aspect ratio, see Section 14.5.2.

14.2.2.2 Discrete (mass) booms

In this concept all the span-wise bending load is assumed to be reacted by the flanges, or booms, located at the upper and lower extremities of one or more spars, Figs 14.4(b) and 14.5. Because these discrete flanges are relatively large in cross-section they are sometimes referred to as massive or 'mass' booms. When the torsional and shear loadings are low, as they may be in a light aircraft, they can be reacted by internal cross-bracing. More usually the outer skins are assumed to only react shear loads and the torsion box is formed between the front and rear spars. The 'D' nose is a variation using only a single main spar as shown in Figs 14.4(a) and 14.6. This latter arrangement has some advantages for lightly loaded structures in that the spar may be located at maximum section depth, the thicker nose skin can have a good, smooth, aerodynamic surface, and there is space behind the box for such items as landing gear stowage.

The discrete flange arrangement enables high stresses to be developed in the flanges. It does have a significant problem in that the skins must be stabilized to prevent

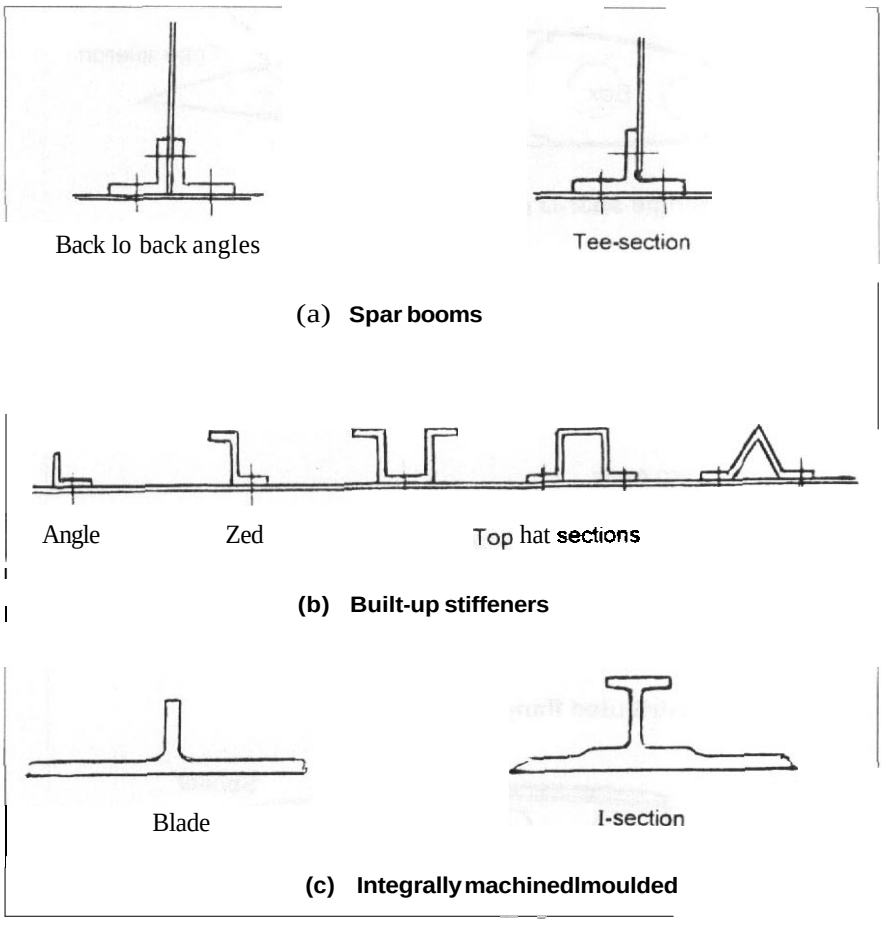

Fig. i4.3 *Cross-sections of* longitudinal ***members***

buckling under shear loads and hence the skins have a tendency to share with the spars in reacting the bending. The skins are stabilized by the introduction of numerous ribs. possibly with a few span-wise stiffeners arranged to be intercostal between the ribs. Further, it is difficult to incorporate damage-tolerant features in the concentrated flanges, although some ptovision is possible with paired, back to back, sections, Fig. 14.3(a).

The spars may be machined as a one-piece item but are more usually built up from a plate web and machined flanges to confer a degree of damage tolerance. The ribs may be assembled as braced frameworks although pressings from sheet material are cheaper.

Summarizing, the discrete flange concept is really only applicable to relatively lightly loaded structures and when used care must be taken to minimize joints and attachments to the boom members. The concept is simple to analyse. The ribs are simple

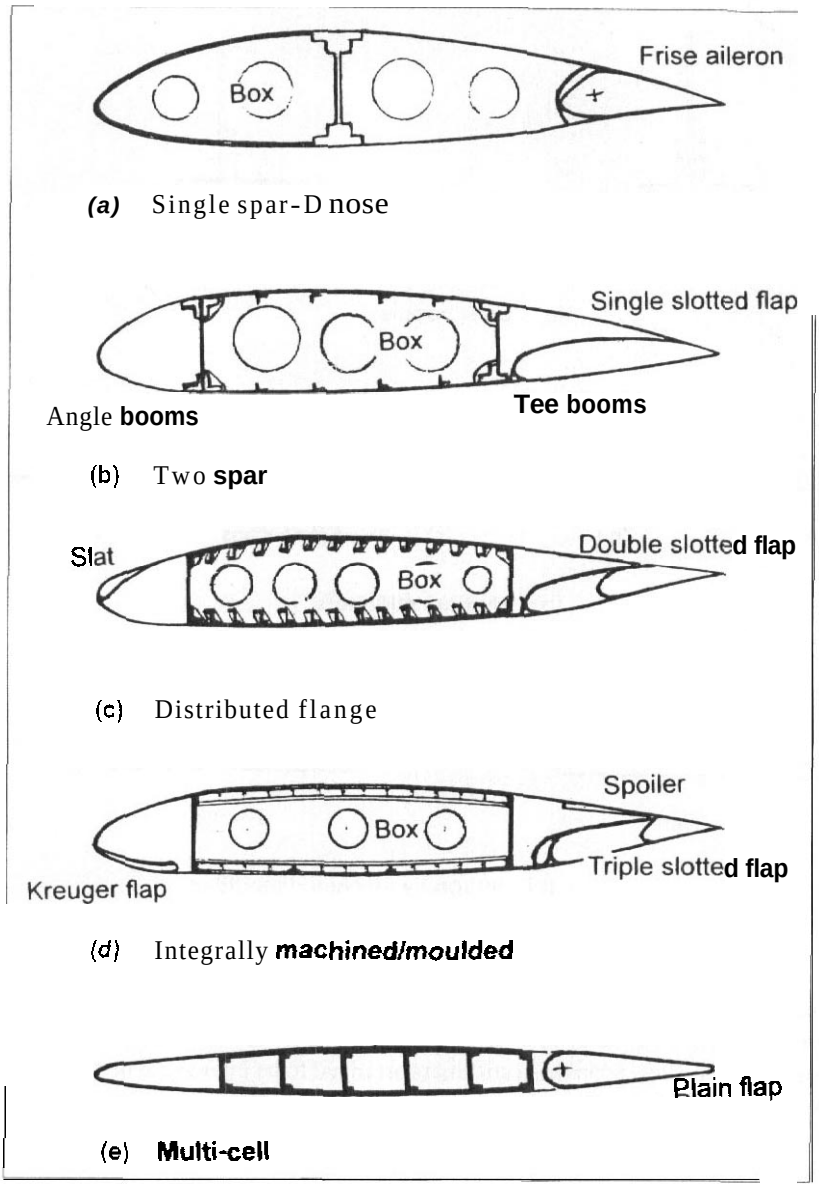

Fig. 74.4 Cross-sections of lifting surface structural beam

to manufacture and only normally need comer cut-outs to clear the spar booms. Cut-outs can be made in the skins of the span-wise beam providing torsional loads are not excessive. ***A*** major cut-out for landing gear stowage inboard of the main leg attachment, as shown in Fig. 14.7, may cause difficulty due to the high load inputs at the outer end of the cut-out.

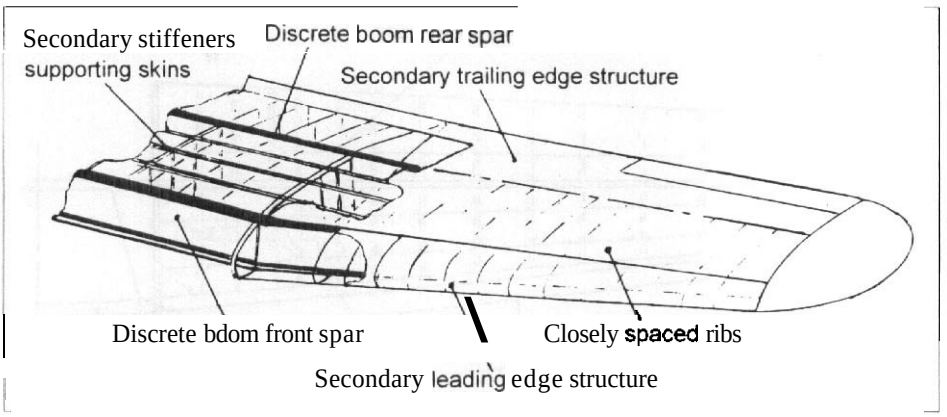

Fig. 14.5 Structural box using discrete flanges

14.2.2.3 Built-up metal skin–stringer construction (distributed flange)

When the load intensity is moderate to high it becomes practical to use the upper and lower skins between the spars to provide the main reaction of the span-wise bending. Thus the skins are made to carry the end load by supporting their cross-section area with span-wise stringers or by some other means such as sandwich construction, Figs 14.4(c) and 14.8. When used. the presence of the relatively large numbers of end load carrying members greatly improves the damage tolerance of the structure. This can be further enhanced in metal construction by dividing the skins into a number of span-wise planks joined by crack stopping joint straps. The stringers may be formed, drawn. extruded, or machined depending upon the section shape and the thickness of the material. Most commonly a Zed-section stringer is preferred.

In the tension surface the stringer size and spacing are likely to be determined by crack stopping requirements, while in the compression surface the design criterion is buckling instability, see Chapter 13, Sections 13.5.3.2 and 13.5.4.2. Thus the

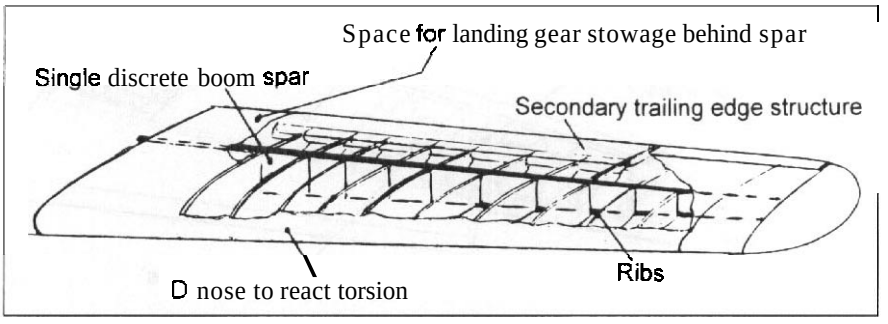

Fig. 14.6 'D' nose structural box

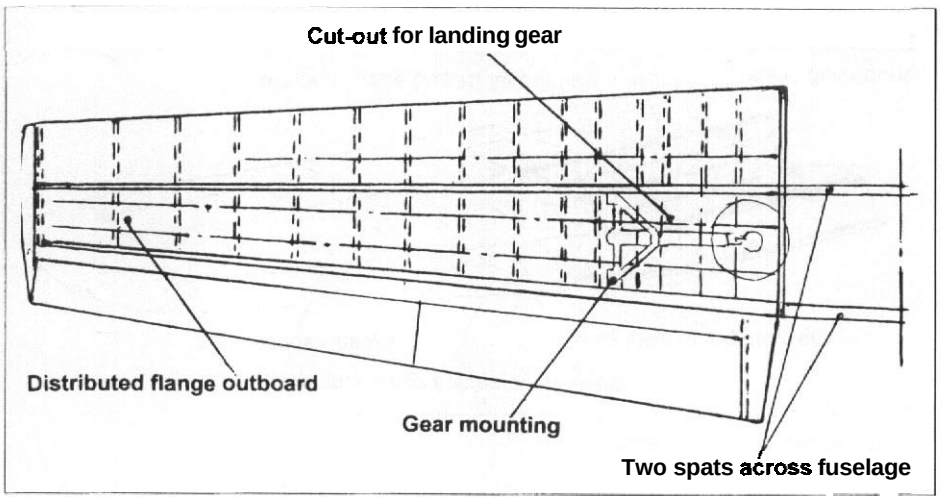

Fig. 74.7 Hybrid discrete boom-distributed flange structural box

compression flange stress level is likely to be restricted by instability considerations. and fatigue requirements often place a similar limit on the tensile working stress.

In a built-up light alloy construction the stress levels tend to be low near to the tips due to restrictions arising from the use of standard thickness sheets. Taper rolled sheets of appropriate thickness graduation can be used to partially overcome this penalty.

The distributed flange form of construction does introduce some design difficulties. The physical interaction between the ribs and the stringers means either that the rib flange has to be passed below the span-wise members or its load path is broken. In either case the use of cleats is likely to be necessary to interconnect and to stabilize the various components. This increases both the complexity and the cost. The spacing between, or pitch of, the ribs is not especially critical structurally and although there is an optimum,

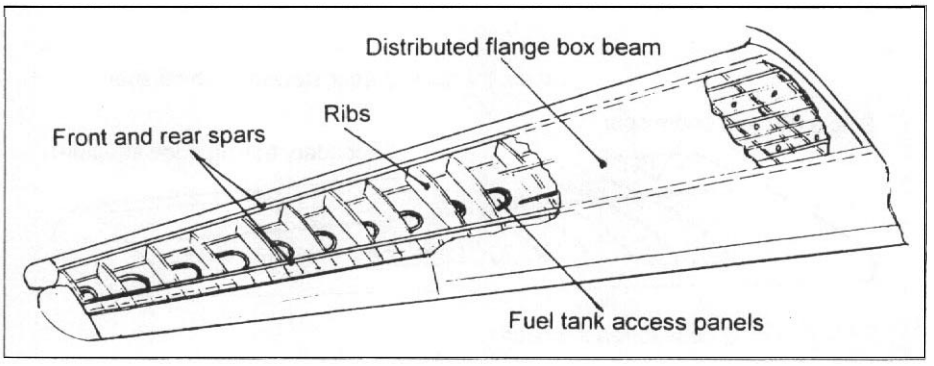

Fig. 14.8 Distributed flange structural box

see Chapter 15, Section 15.2.4, and Chapter 16, Section 16.2.3. It is mainly determined by layout considerations such as control hinge positions and flap supports.

Although the built-up distributed flange, skin–stringer construction can be efficient and is excellent from the point of view of damage tolerance, it is complex and costly to build due to the large number of individual items which go to make up the structure. There are many joints which add weight and create points of high stress where cracking may be initiated.

When integral tanks are used they are difficult to seal, see Section 14.2.3.

14.2.2.4 Integrally machined metal construction

The need to overcome the drawbacks of the separately assembled skin–stringer construction led to the development of integral machining. Fig. 14.4(d). A considerable simplification of manufacture and assembly can be achieved and with the use of numerically controlled machine tools the cost is much less than that of labour intensive hand assemblies. Integrally machined skin panels enable the stringers and skin to be tapered in an optimum way and allowance can be made for reinforcement as needed to meet the local loading. Early designs of integral skins used simple blade stringer cross-sections for ease of machining, see Fig. 14.3(c), but there is now little penalty in using the more nearly optimum Zed- or I-sections. Sealing and joint problems are much reduced. The absence of joint stress concentrations partially compensates for the absence of the crack stopping properties obtained with built-up construction. However, the need to cater for damage tolerance requires the introduction of redundancy in the form of several span-wise skin planks on the tension surface.

Joints must be provided between the spar webs and the covers but the load transfer can be relatively low. Heavily loaded ribs are usually machined as one-piece separate items, but the lightly loaded ones can consist of a sheet web attached to appropriate chord-wise flanges machined on the skin items. Figure 14.9 shows the inboard end of a wing constructed using integral machining techniques.

There is a limit to the technique for large, heavily loaded, aircraft where it becomes impossible to produce the billets of material in a sufficiently large size to enable integral skin panels to be made. This difficulty is overcome by producing separate stringers which are attached by either mechanical fasteners or, possibly, friction-stir-welding,

14.2.2.5 Moulded construction in reinforced plastics

In principle the application of reinforced plastic materials can be made to any of the basic structural configurations described above. However, the most efficient use of reinforced plastics occurs when mechanical joints are minimized so the most likely approach is similar to that of integrally machined construction, Section 14.2.2.4. with moulded assemblies replacing the machined skins, spars, and ribs. The skin and web components are made up from a series of laminations having fibre directions oriented to match the applied loading conditions. Manufacture of moulded components demands

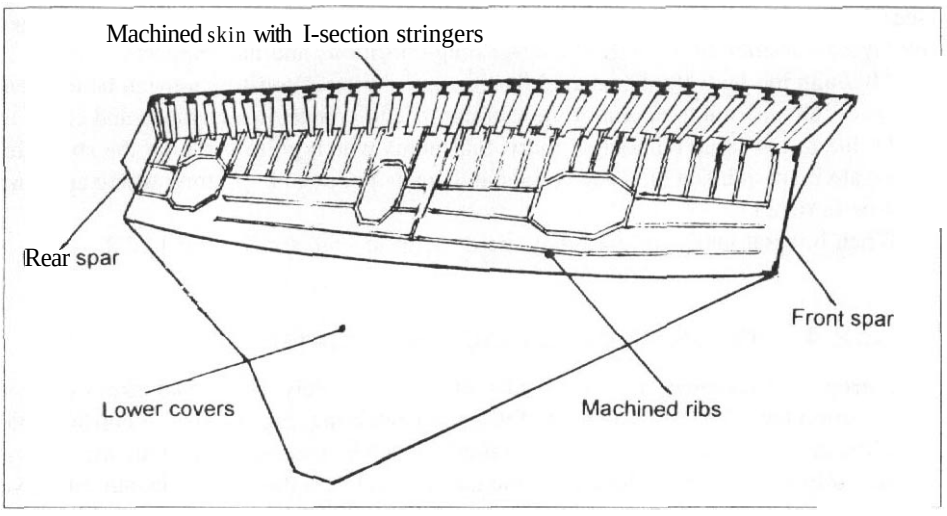

Fig. 14.9 Integrally machined structural box

careful quality control. The means of overall assembly must be carefully planned. It may be possible for some stages of the assembly to be co-cured as the basic components are formed but final assembly often requires the use of cold bonding or mechanical fastening.

14.2.2.6 Multi-cell construction

When the wing is very thin the depth of stringers required to stabilize the skins becomes similar to that of the cross-section and the number of span-wise shear webs has to be increased to enable the vertical shear loads to be reacted, Fig. 14.4(e). This leads to a multi-spar, multi-cell, arrangement, with the spars providing stability to the skins. If the wing is also of low aspect ratio the configuration takes the form of an 'egg box' arrangement with a grillage of relatively closely spaced ribs and spars, see Fig. 14.10.

This form of construction in metal will almost certainly consist of an assembly of machined spars and ribs. In some local regions the ribs may be more heavily loaded than the spars and must be given structural priority at the joints and at the covers.

14.2.3 Wing fuel tanks

In addition to providing the required strength and stiffness, the structural box almost always has to provide fuel space. Integral tanks. as opposed to separate internally supported types, are preferred since their use enables the maximum advantage to be taken of the available volume. Integrally machined or moulded constructions, which use a small number of large components. are obviously an advantage since sealing is reduced to a minimum. The major problem occurs at tank end ribs, particularly in the

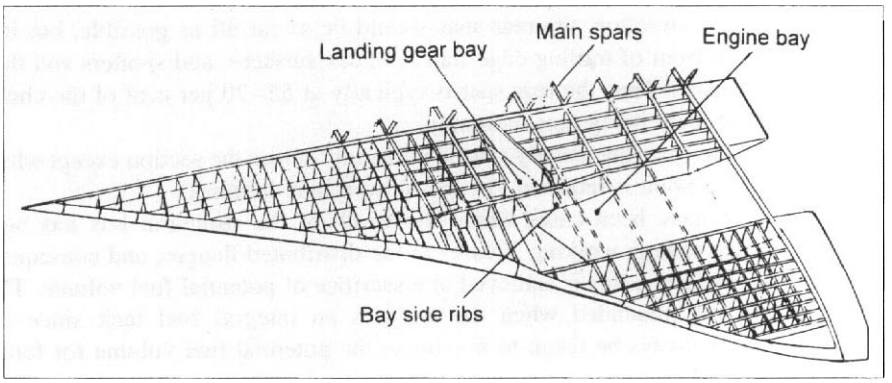

Fig. 14.10 Multi-cell wing construction (Concorde)

comers of the spar web and skins, and at lower surface access panels. The comer difficulty is overcome by using special 'suitcase' comer fittings.

Access panels must be large enough for a person to get through so that the inside can be inspected and resealed if necessary, Fig. 14.8. On shallow section wings the access has to be in the lower surface so that the operator can work in an acceptable way even if the depth is insufficient to climb in completely. Apart from the sealing problems, lower surface access panels are in what is primarily a tension skin and so introduce stress concentrations in an area where crack propagation is a major consideration. The access panels are arranged in a span-wise line so that edge reinforcing can be continuous and minimize stress concentrations due to the cut-outs. see Chapter 16, Section 16.5. Access panels are often designed to carry only shear and pressure loads, the wing bending being reacted by the edge reinforcing members. A deep wing can avoid these problems by using upper surface access panels but this is not a preferred aerodynamic solution.

14.2.4 Chord-wise location of spars

In practice in the majority of designs there is not a great deal of scope for varying the chord-wise locations of the front and rear spars. Generally the front spar should be as far forward as possible subject to:

(a) The local wing depth being adequate to enable vertical shear loads to be reacted efficiently.
(b) There is adequate nose chord space for leading edge devices and their operating mechanisms, de-icing requirements and the like.

Thus the front spar of a two-spar box is usually located in the region of 12–18 per cent of the local chord. A single 'D' nose main spar is likely to be located at the maximum section depth, that is, at 30–40 per cent of chord.

In a two-spar construction, the rear spar should be as far aft as possible, but it is limited to being in front of trailing edge flaps, control surfaces, and spoilers and their operating mechanisms. Thus the rear spar is typically at *55–70* per cent of the chord, with around 65 per cent being most common.

Any intermediate spars are usually spaced uniformly across the section except where a particular pick-up point is required for, say, powerplant or stores.

Although there have been cases where the width of the structural box has been limited to give rise to high working stresses in the distributed flanges, and consequent good structural efficiency, this is achieved at a sacrifice of potential fuel volume. This approach is not recommended when the wing is an integral fuel tank since the opportunity should always be taken to maximize the potential fuel volume for future development.

Spar location should not be stepped in plan layout as this gives rise to offset load paths but a change of sweep at a major rib position is acceptable.

14.2.5 Rib location and direction

The span-wise location of ribs is of some consequence. Ideally the rib spacing should be determined to ensure adequate overall buckling support to the distributed flanges, see Section 14.2.2.3. This requirement may he considered to give a maximum pitch of the ribs. In practice other considerations are likely to determine the actual rib locations such as:

(a) Hinge positions for control surfaces and attachment/operating points for flaps, slats, and spoilers.
(b) Attachment locations of powerplants, stores, and landing gear structure.
(c) A need to prevent or postpone skin local shear or compression buckling, as opposed to overall buckling. This is especially true in a mass boom form of construction.
(d) Ends of integral fuel tanks where a closing rib is required.

When the wing is unswept it is usual for the ribs to be arranged in the flight direction and thereby define the aerofoil section. If the wing is swept there is the option of arranging the ribs aligned with the flight direction, or orthogonal to the spar direction. see **Fig.** 14.1I. While the former does give greater torsional stiffness the ribs are heavier, connections are more complex, and in general the disadvantages outweigh the gains.

Ribs placed at right angles to the rear spar are usually the most satisfactory in facilitating hinge pick-ups, but they do cause layout problems in the root regions, Fig. 14.1. Some designs overcome this by fanning the ribs so that the inclination changes from perpendicular to the spars outboard to stream-wise over the inboard portion of the wing. There is always the possibility of special exceptions. such as powerplant or store mounting ribs, where it may be preferable to locate them in the flight direction.

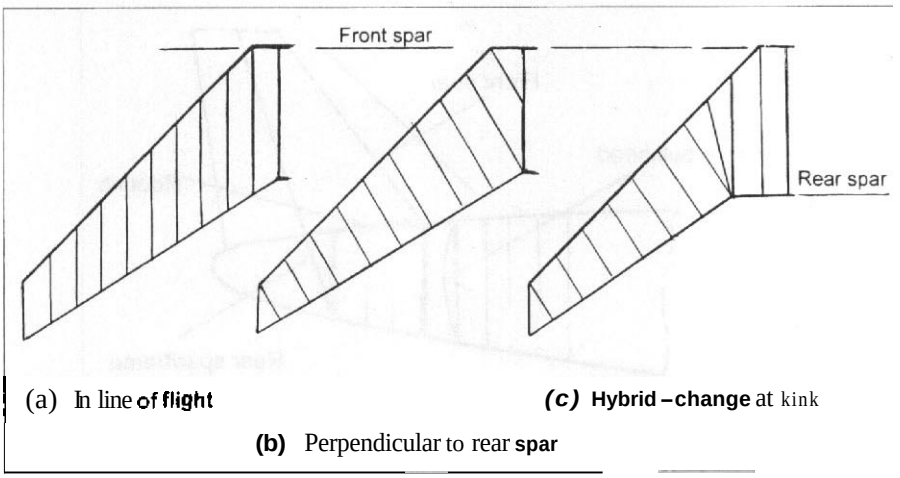

Fig. 14.11 Rib directions on swept lifting surfaces

14.2.6 Fixed secondary structure

A fixed leading edge is often stiffened by a large number of closely pitched ribs, span-wise members being absent. Providing care is taken in the detail design of the skin attachments it is possible to arrange for little span-wise end load to be diffused into the leading edge and buckling of the relatively light structure is avoided. This may imply short span-wise sections. The presence of thermal de-icing, high-lift devices, or other installations in the leading edge also has a considerable influence upon the detail design. Bird strike considerations are likely to be important.

Installations also affect the trailing edge structure where much depends upon the type of flaps, flap gear, controls, and systems. It is always aerodynamically advantageous to keep the upper surfaces as complete and smooth as is possible. Often spoilers can be incorporated in the region above flaps or hinged doors provided for ease of access. The hinges should be flexible and frequently use a continuous. 'piano', type.

14.2.7 Horizontal stabilizer

When the horizontal stabilizer is constructed as a single component across the centreline of the aircraft the basic structural requirements are very similar to those of a wing. see also Section 14.5.1.

14.2.8 Vertical stabilizers

The vertical stabilizer presents a set of issues which are different from those of the main-plane or horizontal stabilizer. Relevant matters are:

(a) It is not unusual to build the vertical stabilizer integrally with the rear fuselage. The spars are extended to form fuselage frames or bulkheads. A 'root' rib is made to coincide with the upper surface of the fuselage and is used to transmit the fin root skin shears directly into the fuselage skin. see Fig. 14.12.

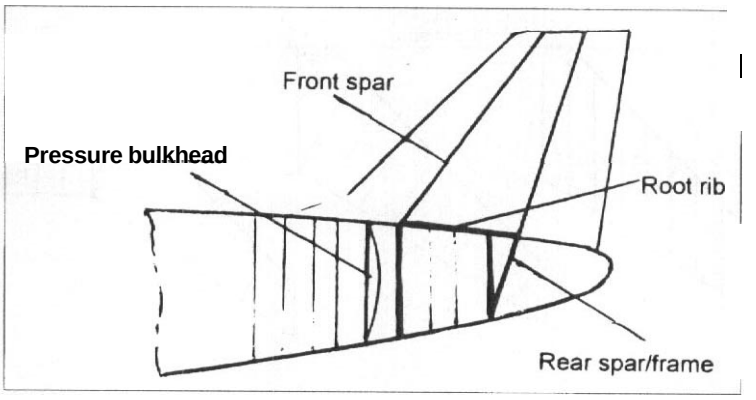

Fig. *74.12* *Vertical stabilizer built* into *rear fuselage*

Fin span-wise bending results in a fuselage torsion. Often it is logical to incline the rear spar bulkhead lo continue the line of the rear spar since it is usually the end of the main fuselage structure. On the other hand, the front spar and any intermediate attachment frames are often best kept perpendicular to the fuselage fore and aft datum, the change in direction being made at the fin root rib. Otherwise the structural form can follow that of a wing.

(b) Sometimes on smaller aircraft the fin is designed as a separate component which may readily be detached, Fig. 14.13. The fin attachment lugs are arranged in both lateral and fore and aft directions so that in addition to vertical loads they react side and drag loads.

(c) There is a special situation when the horizontal stabilizer is attached at some location across the height of the fin. The horizontal stabilizer transmits substantial loads to the fin, usually of the same order of magnitude as the loads on the fin

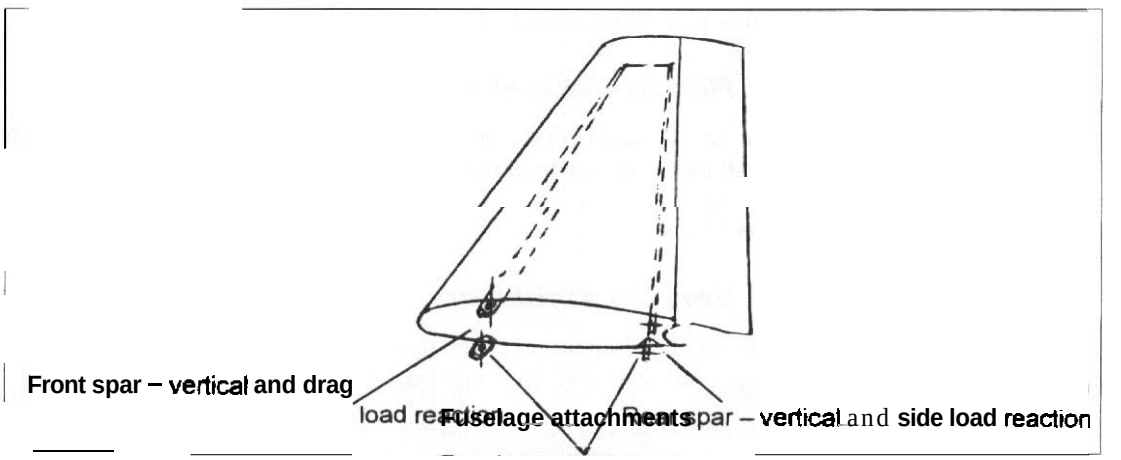

Fig. *14.73* Separate *fin wifh four-point attachment*

itself. A particularly high loading results from the reaction of horizontal stabilizer asymmetric lift case, which always adds to fin lateral air-loads. When full consideration is given to the fin root attachment and the horizontal stabilizer attachment, it is often most satisfactory to employ an essentially discrete boom-type of structural layout, see Fig. 14.14. Any attempt to use a distributed Range concept results in substantial diffusion shears adjacent to the concentrated load points, especially in the root region where it must be recognized that the root rib is flexible in bending in the plane of the fin skin.

14.3 Auxiliary surfaces

14.3.1 General

The structural layout of the auxiliary lifting surfaces is generally similar to that of the wing but there are differences, in pan due to the smaller size and in part due to the need to provide hinges or supports. The latter implies that each auxiliary surface is a well-defined. separate, item. This facilitates the application of fibre-reinforced composite materials when it is appropriate. See Fig. 14.15.

14.3.2 Hinged control surfaces

14.3.2.1 Hinges

Conventional trailing edge control surfaces are almost invariably supported by a number of discrete hinges, although continuous, piano-type, hinges may be used for

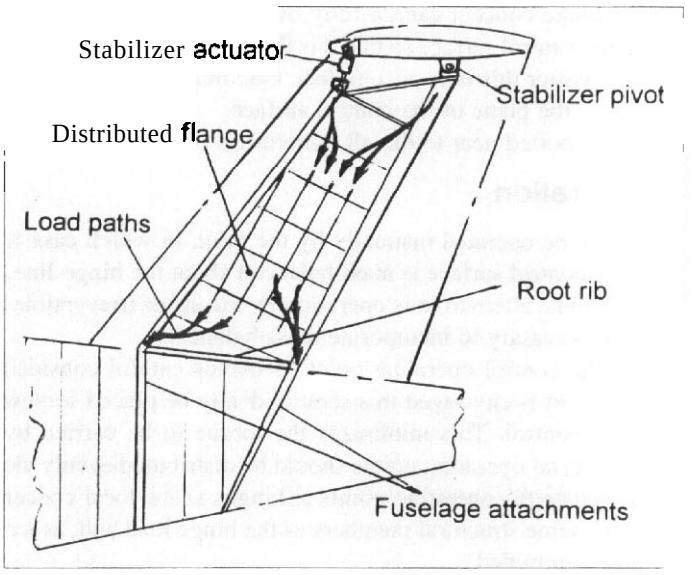

Fig. 14.14 Load paths in fin with a high set horizontal stabilizer

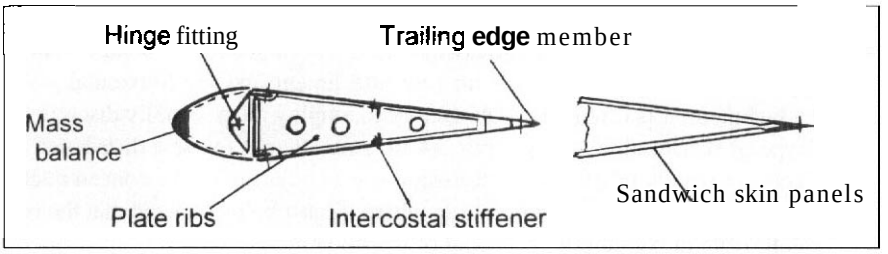

Fig. 14.15 Cross-section of *a typical control surface*

secondary tabs. To some degree the number and location of the discrete hinges depends upon the length of the control. The major points to he considered are:

(a) The bending distortion of the control relative to the fixed surface must be limited so that the nose of the control does not foul the fixed shroud.
(b) The control hinge loads and the resulting shear forces and bending moments should be equalized as far as is possible.
(c) Structural failure of a single hinge should be tolerated unless each hinge is of fail-safe design and can tolerate cracking in one load path.

These points suggest the use of a relatively large number of discrete hinges but there are difficulties associated with this solution. There are the obvious matters of complexity and the possible difficulty of hinge alignment. The loads likely to be induced in the control by the distortion under load of the main surface to which it is attached may be significant. These problems do not arise if only two hinge points are used as any spanwise distortion or misalignment can be accommodated by designing one of the hinges so that it can rotate about a vertical axis, see Fig. 14.16. When more than two hinges are used the 'floating' hinge concept cannot fully overcome the problems. However, it is possible to design the control surface so that it is flexible in bending andindeed the more hinges there are the easier this is to accomplish. One hinge must always be capable of reacting side loads in the plane of the control surface.

The hinges are supported near to the aft extremities of the main surface ribs.

14.3.2.2 Operation

Control surfaces may be operated manually by the pilot, in which case it is usually a requirement that the control surface is mass balanced about the hinge-line. see Chapter 11, Section 11.2.3.3. The alternative is operation by means of irreversible actuators, in which case it is not necessary to incorporate mass balance.

The location of the control operating points demands careful consideration. When only one operating point is envisaged this should ideally be placed somewhere near to the mid-span of the control. This minimizes the torque to be carried by the control surface. Similarly, several operating points should be distributed evenly along the span. It is convenient to locate the operating points at hinges as the local concentrated loads can be carried by the same structural members as the hinge load and, as a consequence, the overall design is simplified.

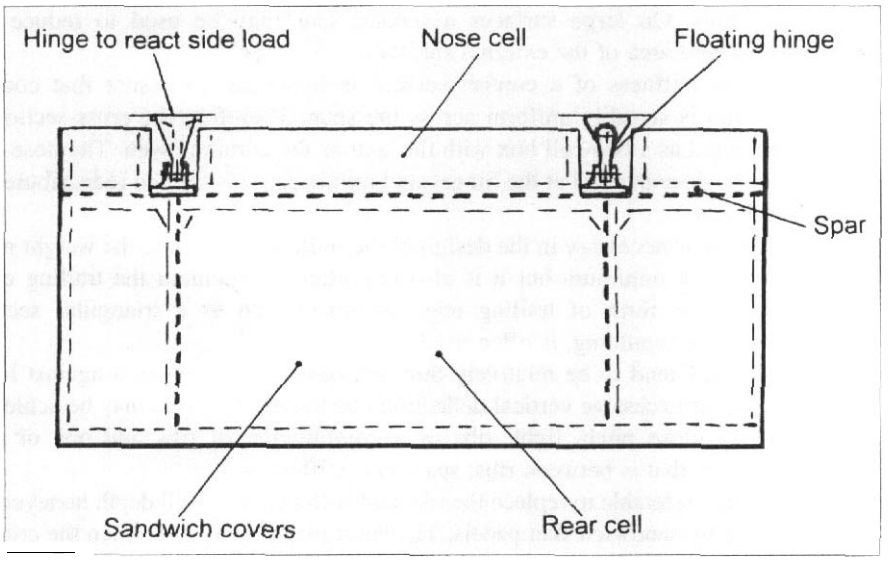

Fig. 14.16 ***Plan*** of *typical control surface*

There are several situations where the operating points might be located other than at the structurally ideal positions. One of these is the space available for the mechanism. Thus it is often preferable to operate rudders from their lower end, the mechanism being in the relatively wide top of the fuselage. The greater lever ratio possible without excursion outside the aerodynamic profile may well offset the higher control surface mass arising from the need to transmit the full aerodynamic torque to the root.

14.3.2.3 Structure

The structural layout of control surfaces is relatively simple and usually it follows a well-established technique. Complications arise when mass balancing is a requirement since then it is essential to minimize the weight of the structure aft of the hinge-line. This is of importance because the arm of a distributed mass balance forward of the hinge-line is relatively small and a penalty will result from small items located in the trailing edge region. Figure 14.15 shows the cross-section of a typical hinged control surface, and Fig. 14.16 is the plan-form. The following comments are particularly relevant to mass balanced surfaces:

(a) Often there is a single span-wise spar which is located behind the hinge-line hut as close to it as possible. The limitation is the size of the hinge fittings which are preferably mounted on the forward face of the spar. Occasionally the spar is located in front of the hinge-line but then access to the hinge fittings is difficult and experience has shown that the overall control surface mass is not likely to be reduced. In the conventional arrangement nose riblets extend forward from the spar to complete the shape, the mass balance weights being attached to their

extremities. On large surfaces a second spar may be used to reduce the unsupported area of the external surfaces.

(b) Torsional stiffness of a control surface is important to ensure that control deflection is sensibly uniform across the span. Therefore the cross-section is constructed as a two-cell box with the spar as the common web. The nose box has to be discontinued at the hinges and reinforcing inserted to redistribute the local loads.

(c) Some care is necessary in the design of the trailing edge. Here the weight must be kept to a minimum but it is also important to maintain the trailing edge angle. Some form of trailing edge member, such as a triangular section extrusion or moulding, is often used.

(d) Metal skins tend to be relatively thin and have to be stabilized against local buckling or excessive vertical deflection due to air-load. This may be achieved by using close pitch, light, ribs or a combination of ribs and one or two intercostal, that is between ribs, span-wise stiffeners.

(e) It may be preferable to replace the ribs and stiffeners by a full depth honeycomb filling or by sandwich skin panels. The latter may be required when the control surface is subjected to an acoustic fatigue environment as light sheet construction fails rapidly in these circumstances. Full depth honeycomh is heavy and should only be contemplated when the section is shallow. When this form of construction is used it is possible to reduce the number of ribs to those at the hinge/operating points and the ends of the surface, as illustrated in Fig. 14.16.

Control surfaces are good candidates for reinforced plastic constmction. Because of their relatively small size it is possible to design them to he made in one piece. One problem is the input of the concentrated hinge and operating loads but this can be overcome by careful detail design.

Local stiffness considerations are often more important than strength as has been indicated above.

14.3.3 Pivoted control surfaces

In certain high-performance aircraft the whole of a stabilizing/control surface on one side of the aircraft may be pivoted about a point on its root chord. Clearly in this case the structural considerations are dominated by the need to react all the forces and moments at the pivot and operating points. Thus the stmctural layout may consist of an integral root rib/pivot/stub spar arrangement to which is attached a number of shear webs fanning out towards the extremities of the surface, possibly in conjunction with full depth honeycomb, Fig. 14.17. High skin shear loading is inevitable due to the need to bring the loads to the two concentrated points. Shearloads due to torsion may belimited by locating the operating point on the root rib some distance away from the pivot.

Some designs incorporate the pivot into the moving surface with the support bearings on the fuselage, while on others, as in Fig. 14.17, the pivot is attached to the fuselage

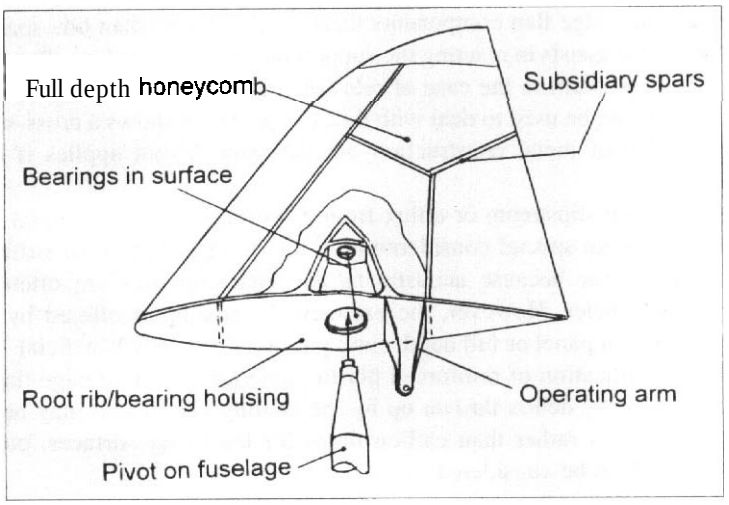

Fig. 14.17 All-moving, pivoted, surface

and the bearings are in the surface. The bearings should be as far apart as local geometry allows to minimize loads resulting from the reaction of the surface bending momenl.

14.3.4 High-lift systems

14.3.4.1 General

There is a wide variety of leading and trailing edge high-lift systems. Some types are simply hinged to the wing. but many require some degree of chord-wise extension. This can be achieved by utilizing a linkage, a mechanism, a pivot located outside the aerofoil contour or, perhaps most commonly, by some form of track. Trailing edge flaps may consist of two or more separate chord-wise segments, or slats, to give a slotted surface and these often move on tracks attached to the main wing structure.

14.3.4.2 Supports

The majority of flaps and slats are split into span-wise segments of no greater length than can he supported at two or three locations. As with control surfaces the locations of the support points are established so as to minimize local deformations since the various slots are critical in determining the aerodynamic performance.

Sometimes the actuation may be located at a different span-wise position from the support points. This is often a matter of convenience, layout clearances. and the like.

14.3.4.3 Flap structure

The structural design of flaps is similar to that of control surfaces but it is simpler as there is no requirement for mass balance, the operating mechanisms normally being irreversible.

On large trailing edge flap components there is often more than one spar member, especially when this assists in reacting the support or operating loading. There may be a bending stiffness problem in the case of relatively small chord slat segments and full depth honeycomb can be used to deal with this. Figure 14.18 shows a cross-section of a typical slotted flap of metal construction hut the same layout applies if composite materials are used.

In many cases the slipstream or efflux from powerplants impinges upon a flap and this is likely to require special consideration in the design. Additional stiffness is not necessarily the answer because acoustic fatigue characteristics are often worse at higher panel frequencies. However, the extensive local support offered by sandwich construction, either in panel or full depth configuration. is usually beneficial. This leads naturally to the application of reinforced plastic materials. Trailing edge flaps tend to be prone to damage by debris thrown up by the landing gear and it may be desirable to use Kevlar or glass rather than carbon fibres for the lower surfaces. but material compatibility needs to he considered.

14.3.4.4 Trailing edge flaps on swept wings

When the flap hinge-line is unswept there is no difficulty in establishing the geometry. Tapered flaps can be dealt with by arranging for the hinge-line to be the axis of a right circular cone whose surface contains the flap movement. Track or link systems may be similarly arranged. A real difficulty arises when the effective hinge-line is swept. It is possible to arrange the geometry so that the flap is deployed at right angles to the hinge-line, that is, along circular arcs on the conical surface. This often implies that any external hinge brackets or tracks are positioned across the airflow with a consequent drag penalty. Alternatively a swept flap may be moved along the line of flight on elliptical paths described on the surface of a circular cone. This results in complex geometry and is best avoided if possible. Practical track contours may well be more complex than circular arcs.

A particular problem arises with variable camber flap systems. it being very difficult to apply this concept efficiently when the basic geometry is swept and tapered.

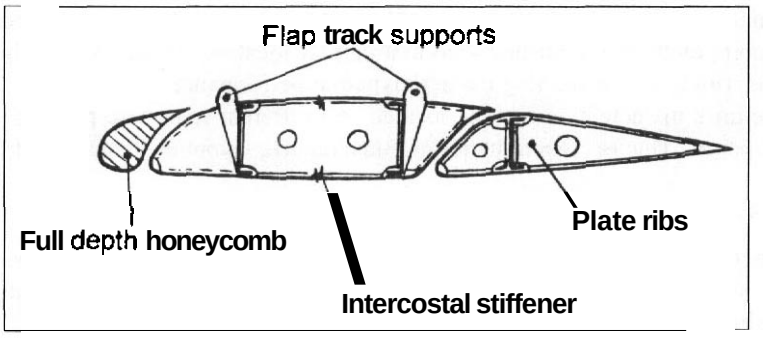

***Fig. 14.18** Cross-section of triple slotted flap structure*

14.3.4.5 Leading edge flaps and slats

Leading edge Raps are usually hinged directly to the front, fixed pan of the aerofoil. Slats move out on circular arc tracks. The track is usually attached to the slat, its support rollers being mounted in the fixed structure. Most designs use a short length of flap or slat, located at two attachments. Actuation is also usually at the track positions, often by means of levers or rack and pinion gears driven by span-wise torque tubes. Bird strike is an important design case and full depth honeycomb is often used, as shown for the nose slat of the trailing edge flap illustrated in Fig. 14.18.

14.4 Fuselage

14.4.1 General considerations

Although there are significant layout differences between the fuselages of various kinds of aircraft, for example airliners and combat types, the primary structural role is similar in all cases. However, one difference is the pressurization requirement of most passenger and freight types as this affects much of the fuselage volume. The lower level pressurization requirement for certain combat types is usually dealt with locally in the crew region.

As a fundamental structural shape the fuselage is close to the ideal. The proportions of depth and width reasonably match those of the vertical and lateral bending and the cross-section shape is appropriate for the reaction of torsion. Unfortunately numerous cut-outs in the primary structure are inevitable and the integrity of the external structural form cannot be maintained. The cut-outs are for such items as passenger and freight doors, windows, canopy, landing gear, powerplant access, weapon stowage and so on.

14.4.2 Cross-section shape

Although a basically rectangular cross-section is advantageous from the point of view of maximum space utilization, and is not infrequently used on combat types and small general aviation aircraft, it is not suitable when a substantial pressure differential is a requirement. Stresses due to internal pressure are minimized by utilizing cross-sections based on the use of circular arcs having as small a radius as possible. A simple circular cross-section is preferable and is often used on low-wing transport aircraft. However, in practice the true circular shape may impose undue restriction on the cross-section layout and the alternative is to use an arrangement with two or more radii to give either a deeper or a shallower section according to the need. An important point is that there should be a tie across the points of intersection of the arcs to balance the skin tension loads at these points, see Fig. 14.19. The shell and its supporting members are subjected to undesirable bending if the tie is not provided.

14.4.3 Basic structural layout – outer shell

14.4.3.1 General

The structural layout of a fuselage may take various forms which, in principle, are not unlike those used for lifting surfaces. the function of the ribs being performed

by frames. The primary components of fuselage construction are illustrated in Fig. 14.20

The structural layout is fundamentally unchanged when composites are used but details must suit the materials employed. Large pressurized fuselage structures are less amenable to the application of composite materials than are lifting surface components. but see Chapter 13, Section 13.5.4.4. There are local exceptions, for example floors. There is more scope in the case of the fuselages of smaller aircraft which can be manufactured in one piece or, at the most, a small number of lengthwise components.

14.4.3.2 Semi-monocoque shell

When the number of large cut-outs is small it is usually preferable to react as much of the loading as possible in the outer shell. This is sometime referred to as a monocoque, or semi-monocoque, design depending upon the degree to which the outer

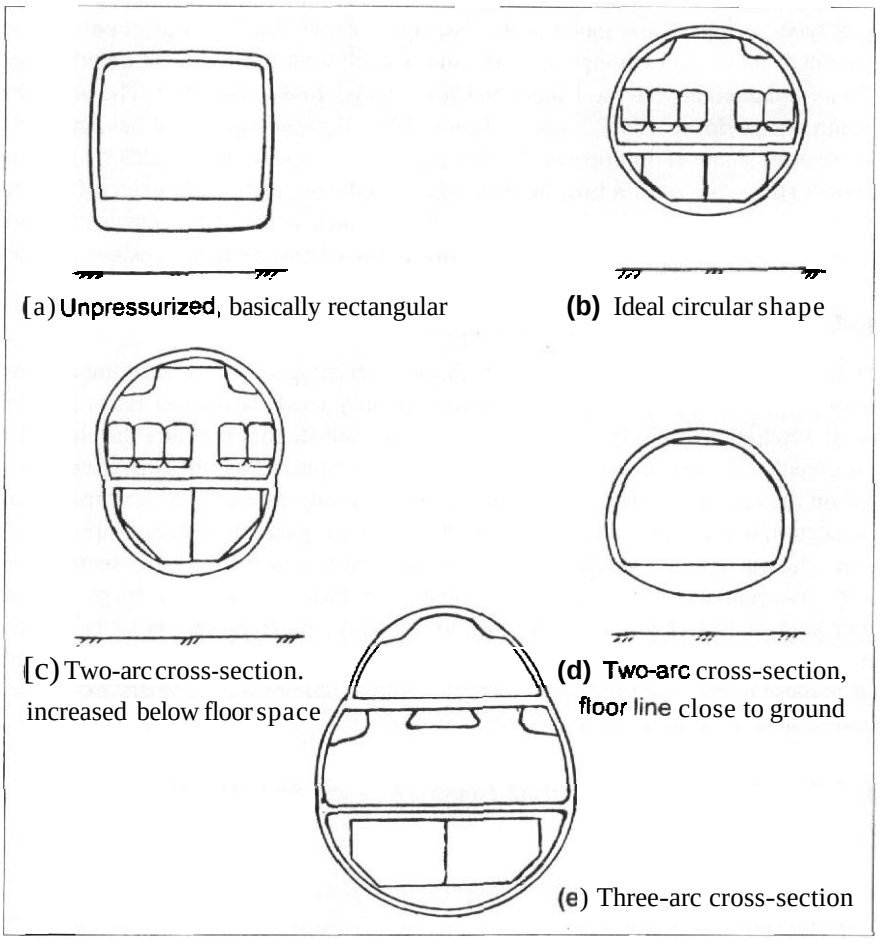

Fig. 14.19 Fuselage cross-sections

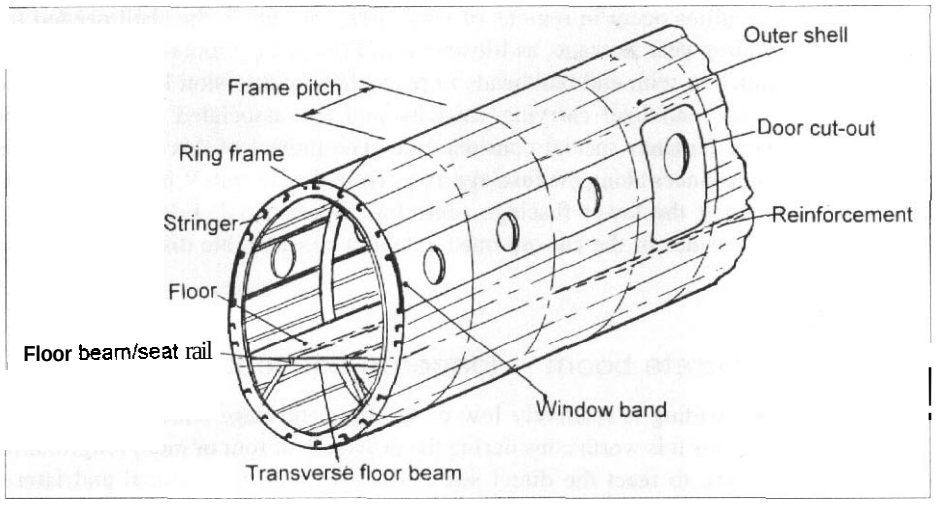

Fig. 14.20 ***Fuselage components***

skin is supported by lengthwise stringers. It is the form of construction shown in Fig. 14.20.

The fuselage skin thickness may be determined by consideration of either pressurization or shear loading, with the former being more critical on designs having a large. deep, cross-section. Skin stabilization is provided by longitudinal stringers and these make a substantial contribution to the overall end load carrying capacity. Jt is usually necessary to incorporate larger cross-section reinforcing members at the edges of discontinuities for doors and the like and in reality these represent the equivalent load carrying capacity of the skin–stringer elements removed by the cut-out, see Chapter 16, Section 16.5. These edge members must extend a substantial distance either side of the cut-out and the skin thickness may have to be increased locally at the comers of the cut-out to handle the high diffusion shear stresses.

Relative to a lifting surface there is usually less scope on a fuselage for tapered skins and integral machining. The cross-section shape and size means that the load levels tend to be lower and they are more uniform in distribution. Some airliner designs do use integrally machined panels along the line of the windows incorporating both the local and the longitudinal reinforcement. Substantially loaded frames are also made up of machined parts.

It is often convenient for the fuselage to be built in a number of lengthwise sections, but as each circumferential joint adds weight the number of components should be as small as possible. Light alloy skins may be either wrapped around the section or laid in lengthwise planks. The former is preferable for parallel section fuselages as it reduces the weight of the skin joints, but the latter is easier for the manufacture of tapered portions since it reduces the necessary pre-forming operations. Skin joints are made on hoth longitudinal stringers and on circumferential frame members. GLARE is a candidate material to replace the light alloy skins, see Chapter 13, Section 13.4.2.2.

Particular difficulties occur in regions of very large cut-outs in the shell needed for such items as landing gear stowage, as illustrated in Fig. 14.21. Floors or decking may be used in conjunction with end bulkheads to react shear and torsion loads. The large discontinuity in the end load carrying capacity and the associated input of major concentrated loads demands special consideration. The impact of this discontinuity is felt at significant distances along the fuselage away from the cut-out. Where possible the use of a 'keel' along the lower fuselage centreline is beneficial. Edge, or coaming, members along the sides of the cut-out must extend a considerable distance both fore and aft of it.

14.4.3.3 Discrete boom – longeron concept

When the overall loading is relatively low or the basic fuselage shell is extensively interrupted by cut-outs it is worth considering the provision of four or more longitudinal booms, or longerons, to react the direct stresses due to both the vertical and lateral bending loads. A typical arrangement is shown in Fig. 14.22. To be effective the longerons must be continuous along the length of the fuselage. It is feasible for them to change direction providing means is provided in the form of a frame or bulkhead to react the kink loads.

The residue of the outer shell is used to support the longerons against overall compression buckling and to provide shear carrying capacity. The structural cross-section shape should be maintained as a closed section by incorporating floors or decking in locations where the upper or lower shell is cutaway, but large cut-outs in the decking are feasible. The basic shape is formed and the skins are stabilized against shear buckling by utilizing closely spaced frames with, if necessary, intercostal stiffeners between them. Bulkheads, as opposed to open frames, are preferred to transmit shear

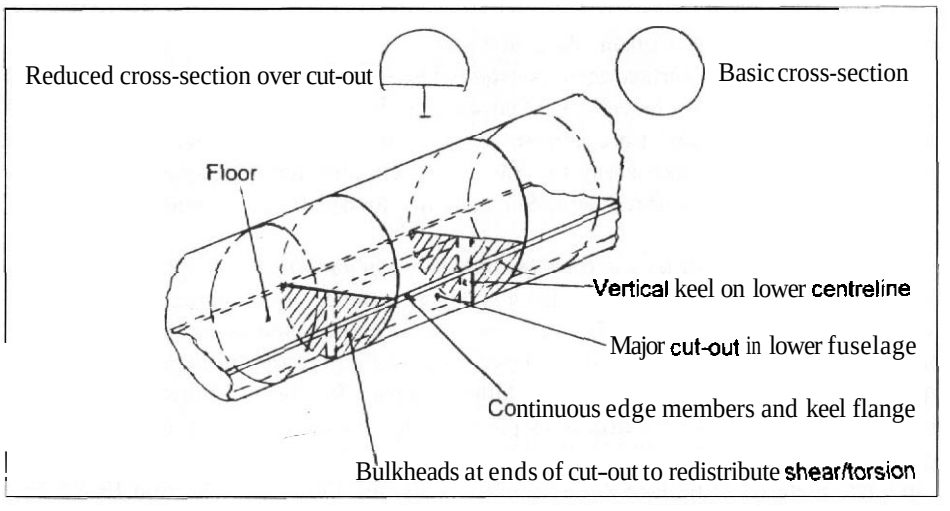

Fig. 14.21 Large cut-out in pressurized fuselage

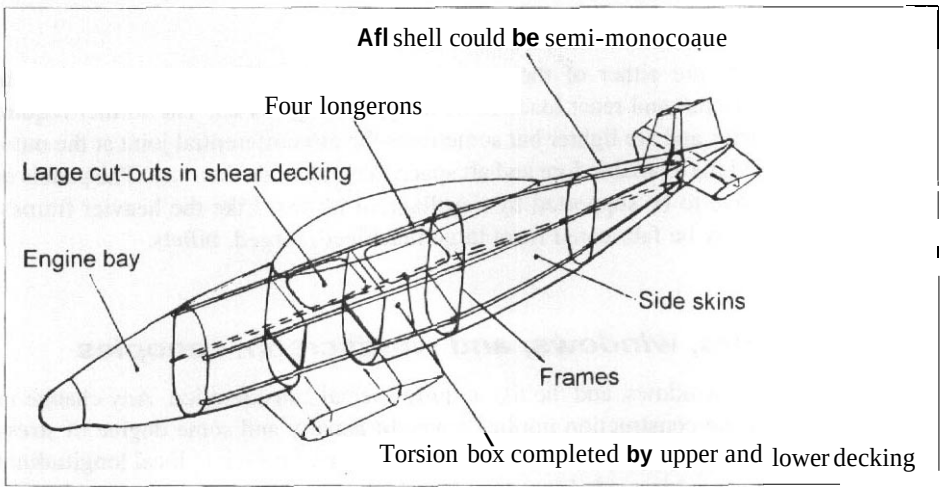

Fig. 14.22 Discrete longeron fuselage construction

loads and maintain torsional integrity where the cross-section has major changes in shape.

14.4.4 Frames

14.4.4.1 General

Relatively lightly loaded frames are used to stabilize the skin–stringer elements and transmit local shear loads into the structure. They may also help to react the pressurization loads where this is relevant. These light frames are usually manufactured as pressings, possibly with reinforced edges. Their spacing is often not critical from overall considerations and, in the case of airliners, was once determined by window positions. It is now more likely that crack stopping requirements will be critical. To act as a crack stopper a frame must have continuous direct contact with the skin, the stringers passing through and being cleated to it. An alternative is to use 'floating' frames which are attached only to the stringers. These reduce manufacturing costs but when used in transport aircraft it is necessary to introduce bands inside the skin to act as crack stoppers under pressure loading.

14.4.4.2 Heavily loaded frames and bulkheads

Large concentrated load inputs require the use of more substantial frames or bulkheads. Basically the latter close the whole cross-section and naturally occur at the end of a pressure cabin or fuel tank. Heavily loaded frames are often built up by using sheet metal components, in conjunction with forged or extruded fittings, but they may be totally forged in combat aircraft.

14.4.4.3 Pressure bulkheads

Pressure bulkheads are either of the curved, membrane, type which react loads in tension, or they are flat and react loads in bending, see Fig. 14.23. The former require crack stopping strips and are lighter but sometimes the circumferential joint at the outer skin is difficult and the available fore and aft space may preclude their use. The panels of a flat bulkhead have to be supported by a grillage of beams. Like the heavier frames, some bulkheads may be fabricated from large machined, forged. billets.

14.4.5 Doors, windows, and windscreen/canopies

Cut-outs for doors, windows, and the like require special consideration. Any change in the basic form of the construction implies a weight penalty and some degree of stress concentration. Door openings must be of adequate size, and sufficient local longitudinal and shear reinforcement is needed to ensure that the local stress level is acceptable. The problem is most severe when the fuselage is pressurized, in which case the door is best designed to act as a 'plug' in the cut-out, the initial opening movement being inwards.

Generally it is best to keep windows to a narrow longitudinal band reinforced above and below by longerons, see Section 14.4.3.2. Usually the frames of glazed windscreen area. are only designed to react local loads and reinforcing around the cut-out is required.

14.4.6 Floors

Floors give rise to both a local and an overall problem. Floor beams are usually designed hy emergency alighting (crash) cases and the floor panels by local loads. These may be sufficiently high to require a heavy construction, especially for freighter aircraft. Heavy floors constructed mainly from fore and aft members tend to pick up loads in the

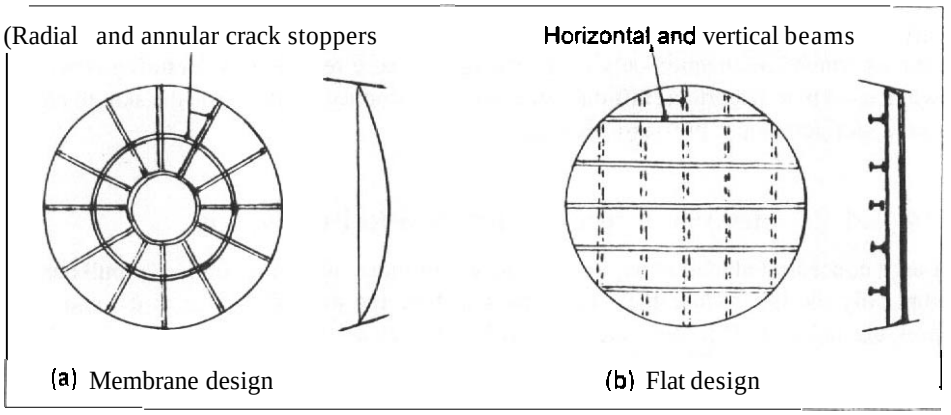

Fig. 14.23 Pressure bulkheads

longitudinal direction under fuselage bending and if they are below the neutral axis cause an undesirable increase of stresses in the upper skin. Hence. frequently the floor is designed in short longitudinal portions and is supported laterally off the frames. Frame stress and frame weight are increased hut this has to be accepted to yield the best overall design.

The floor panels and support beams need to be locally stiff to avoid undue vertical deflection and may well use a reinforced plastic construction.

14.5 Attachment of lifting surfaces

14.5.1 Continuous carry-through structure

The joint of the fuselage with the wing is subjected to heavy load inputs and there is a potential for considerable relative distortion. This distortion is usually accepted and the wing centre box is built completely into the fuselage, the resulting constraint stresses being allowed for, see Fig. 14.24. It is usual for the wing structure of large aircraft to include a production joint at the side of the fuselage and this is virtually essential when the wing is swept. see Chapter 16. Section 16.4.

It is sometimes possible and profitable to arrange the wing pick-ups as pivots on the wing neutral axis, or set them on swinging links as shown in Fig. 14.25. In this case the relative motion is allowed to take place and there are no induced stresses. Structural assembly of the wing to the fuselage is relatively simple.

Similar remarks also apply to the attachment of the horizontal stabilizer when the incidence setting is fixed. If the surface is also used for trimming or control some special consideration is necessary in the location of the pivot and actuation fittings. These usually require a relatively heavily loaded rib. or pair of ribs. and where possible at least one of the attachment points should be close to the rib/spar intersection, see Figs 14.26

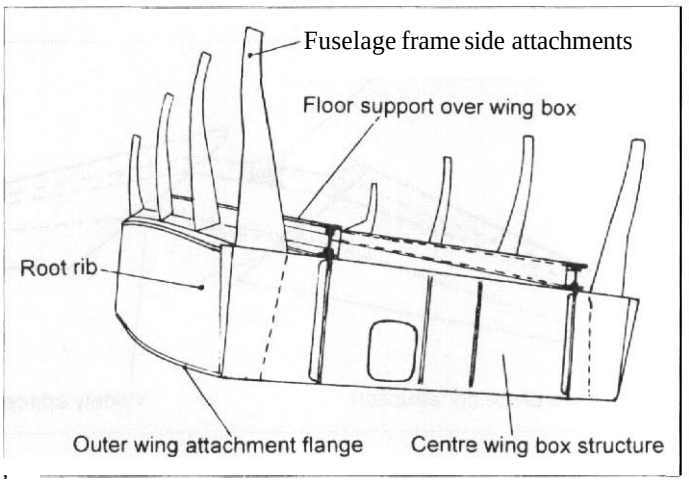

Fig. 14.24 *Built-in* ***centre*** *wing/fuselage* component

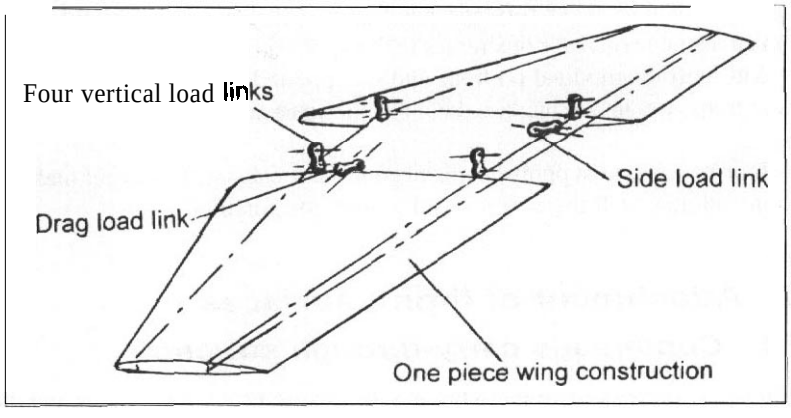

Fig. 14.25 Wing attached lo fuselage by links

and L4.27. It is desirable to arrange for the lateral distance between the pivots to be as great as possible to minimize pivot loads resulting from asymmetric span-wise loading. When the controls are manually operated it is simplest if the elevator hinge-line and pivot coincide.

Fins are often built integrally with the rear fuselage. This is mainly due to the different form of loading associated with the geometric asymmetry, see Section 14.2.8.

14.5.2 Wing loads passed round fuselage

In the case of high-performance combat aircraft it is important to minimize the fuselage cross-section area and it is common in this class of aircraft for the wing bending loads to be passed into frames for transmission around the fuselage, as in the example shown in Fig. 14.28.

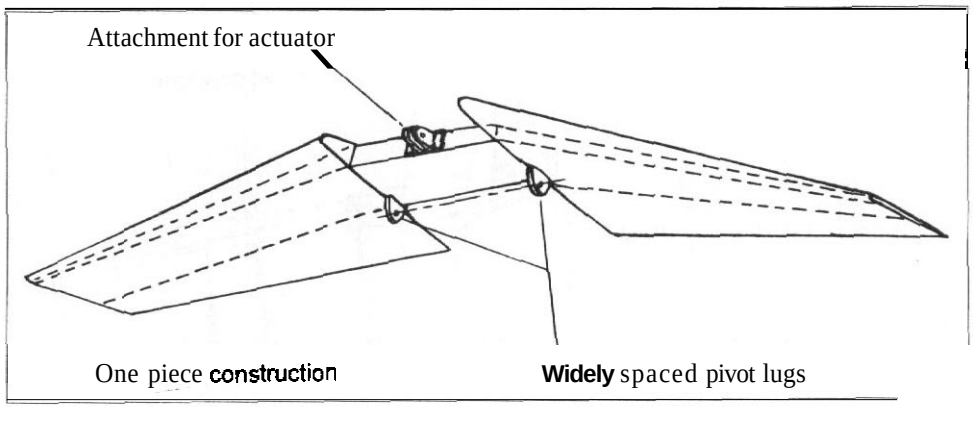

Fig. 14.26 All-moving stabilizer surface

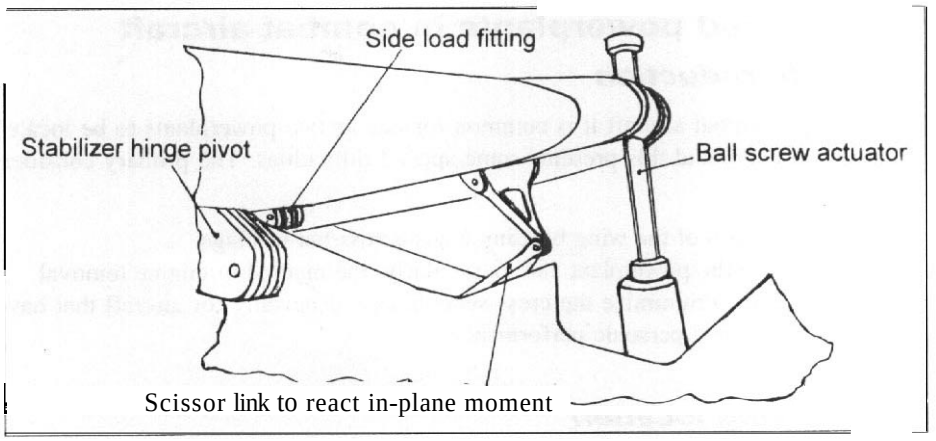

Fig. 14.27 All-moving *surface installation*

The implied mass penalty is reduced by the fact that these aircraft have wings of low aspect ratio enabling a multi-spar/frame layout to be adopted. It is important that the frames should be complete, that is not having any discontinuities around the circumference. Engine removal requires careful consideration. a frequent solution being to locate it behind the wing structure and to lower it through doors in the fuselage.

The implications of buried powerplants are discussed in Section 14.6.

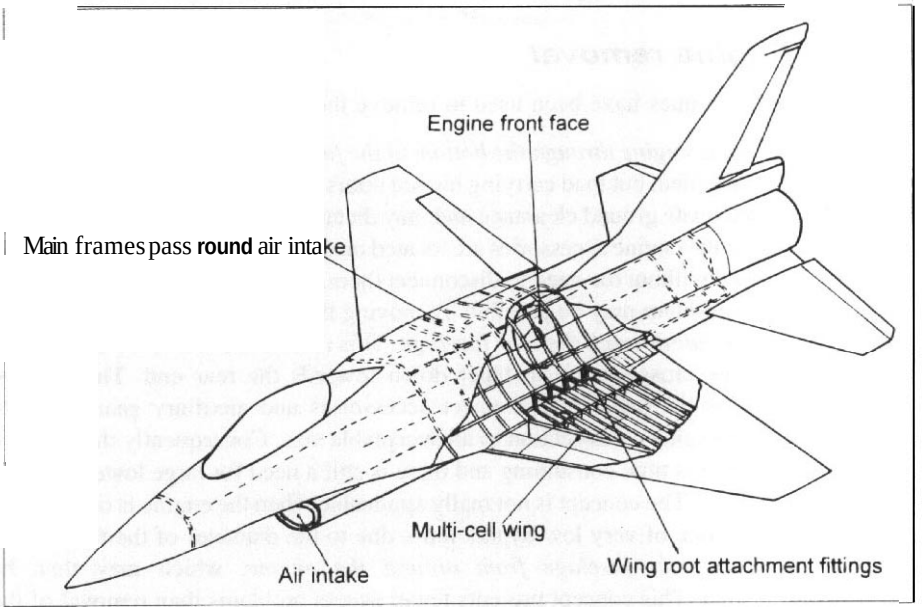

Fig. 14.28 ***Low*** aspect ratio wing loads passed *around fuselage (F-16)*

14.6 Buried powerplants in combat aircraft

14.6.1 Introduction

In the case of combat aircraft it is common for one or two powerplants to be located within the fuselage and this presents some special difficulties. The primary considerations are:

(a) The reaction of the wing bending loads across the fuselage.
(b) Access to the powerplant and, particularly, the method of engine removal.
(c) The need to minimize the cross-section area, especially for aircraft that have transonic or supersonic performance.

14.6.2 Wing location

Ideally the wing structure should be continuous across the fuselage to avoid the necessity of transferring symmetric wing bending moments through the fuselage structure When this is precluded by the layout it is necessary to recognize that substantial, deep, fuselage frames are required as an alternative. These are inevitably heavily loaded in bending and any proposal to incorporate a removable segment for access to the engine will involve severe and probably unacceptable weight penalties. It may be concluded, therefore, that the wing location should be either above or below the powerplant vertically, or that in the fore and aft sense the wing structure does not coincide with the engine. The former situation must imply a penalty in terms of cross-section area and the latter almost certainly means that the engine must he behind the wing structure, the bending loads being reacted by frames located around the air intake system.

14.6.3 Engine removal

The following techniques have been used to remove the engine:

(a) ***Lowering rhe engine through the bottom of the fuselage***. Sometimes a removable panel is provided, but load carrying hinged doors are preferred. This method does require adequate ground clearance and may dictate the length of the landing gear. As most of the engine accessories are located on the lower pan of the engine it can be removed without the need to disconnect them. Some alleviation of the ground clearance problem may be possible by moving the engine aft as it is lowered.
(b) ***Withdrawal aft through the rear fuselage.*** This is difficultdue to the usual trend for fuselage cross-section to taper down towards the rear end. The greatest drawback is the need to disconnect accessories and auxiliary gear boxes to reduce the engine cross-section to an acceptable size. Consequently the removal of the engine is time consuming and there is still a need for large lower fuselage access panels. The concept is not really applicable when the engine is other than a pure jet, or one of very low bypass ratio, due to the diameter of the fan.
(c) ***Removal of rear fuselage from around the engine,*** which may then be disconnected. This concept presents fewer access problems than removal of the

engine rearwards, and can be used with fan engines. There is clearly a structural penalty and the technique can only he applied when the engine is located in the rear fuselage, aft of the wing. It also requires disconnection of primary flight control and other systems.

(d) ***Upward removal through the top of the fuselage.*** In layout terms this is similar to downward removal. The main advantage is that it removes the need to provide additional ground clearance which is especially important when the engine is large in diameter. The primary disadvantage is the requirement for a crane or other special lifting gear which may not be readily available in some operational circumstances.

14.6.4 Special problem of vertical take-off and landing designs

Vertical take-off and landing aircraft introduce an additional constraint which further complicates the issue. Clearly the overall vertical thrust must pass through the centre of gravity and it is most efficient when the vertical deflection of the cruise propulsion thrust provides the greatest possible proportion of the vertical thrust. Therefore, regardless of the actual lift system used, there is a general tendency for the deflected thrust of the main cruise engine to pass comparatively close to the centre oigravity. This implies that the main cruise engine is likely to be located somewhere near to the centre of gravity. Regardless of the lifting surface layout the wing must also be located in the same fore and aft region. This conflict is aggravated by the need for the engine exhaust to pass through the lower fuselage of the aircraft in the vertical flight mode.

It may be concluded that for this class of aircraft the wing should be located above the powerplant since the low- or mid-wing positions are most likely to be excluded by the fore and aft location of the main vertical thrust nozzle.

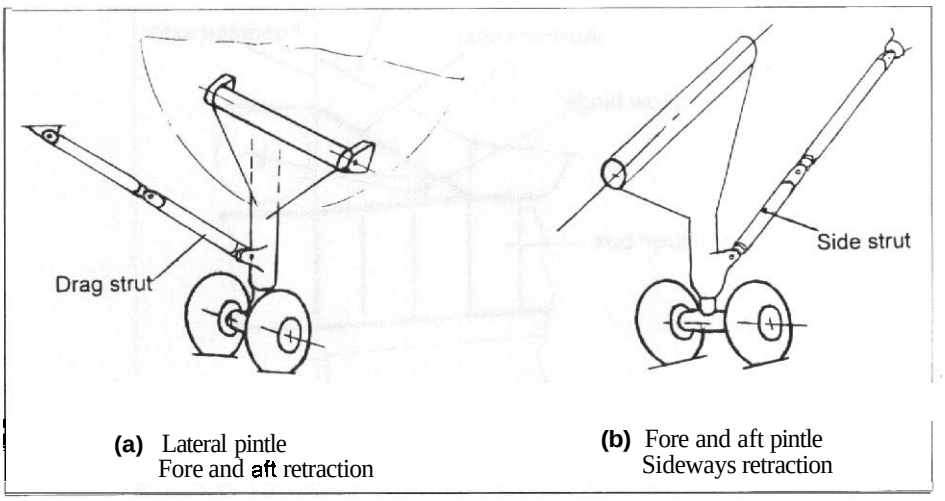

Fig. 14.29 Landing ***gear*** retraction ***layouts***

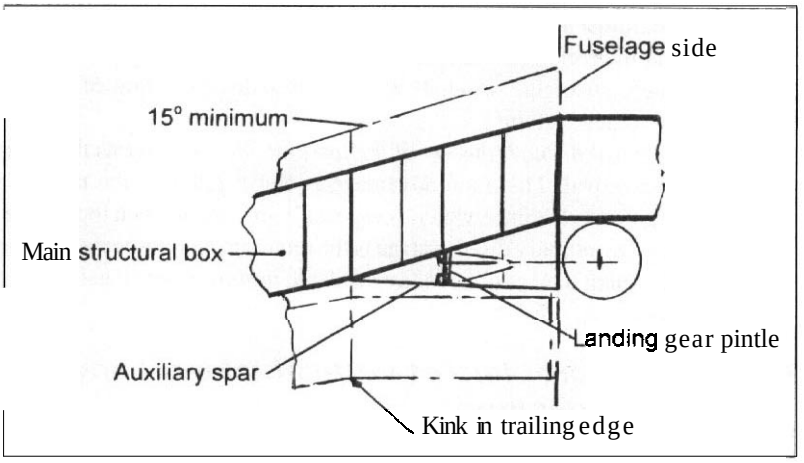

Fig. 74.30 Main landing gear retraction into swept wing

14.7 Landing *gear*

14.7.1 Landing gear mechanical layout

In general the layout of the landing gear structure is a straightforward arrangement of beams and struts. Often the hinge pivot of a retractable landing gear is extended in length to form a 'pintle', see Fig. 14.29. The pintle can then be used to react the moments which result from the drag or side loads applied at the wheel. For example a lateral

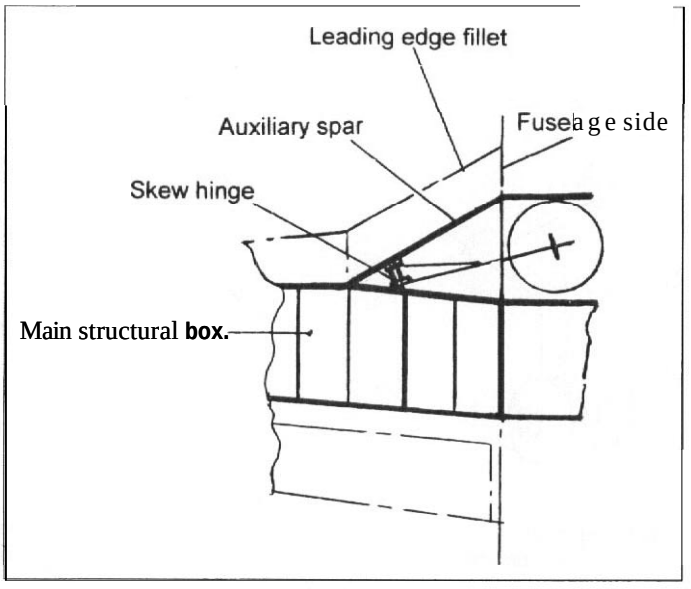

Fig. 14.31 Main landing gear retraction into an unswept wing

pintle used to give fore and aft retraction will react the moments due to side load. Similarly a fore and aft pintle reacts the moments due to drag loads. Ideally the main leg should be supported by a single drag or side strut attached as low as possible on the leg. A lateral pintle usually requires a folding or telescopic drag strut although in this case it sometimes may he possible to lock the leg by means of a down-lock directly located on primary structure.

14.7.2 Landing gear retraction

An important structural layout consideration is the provision of adequate internal space for the retracted landing gear units. The structural problem associated with fuselage stowage is discussed in Section 14.4.3.2.

The use of a kinked trailing edge on a swept-back wing to create a stowage volume in the wing is illustrated in Fig. 14.30, and is also to he seen in Fig. 14.1. When the wing is unswept it may be possible to provide stowage space forward of the structural box as is shown in Fig. 14.31. The solution shown in Fig. 14.7, where the gear is retracted between the spars, is not recommended, except possibly on relatively small aircraft having a low structural loading.

CHAPTER 15

Synthesis procedure – initial sizing of members

15.1 Introduction

15.1.1 Basic data

The initial sizing of the main structural members may be accomplished in one of two ways. The first of these may be regarded as the 'classical' approach where use is made of the loading data obtained from the kind of analyses outlined in Chapters 5 to 10 to derive shear force, bending moment, and torque diagrams and then to employ these to evaluate the initial sizes of the main members of the airframe.

Alternatively, it is possible to use a seamless process, commencing with the determination of the load distribution and directly proceeding to a first sizing using, for example, a finite element technique. This approach is often based on an initial definition of the structural layout but it may use an 'expert' concept derived from past experience of similar aircraft. It may also be iterative in that the initial sizing is used to calculate the static and dynamic distortions of the airframe, compensate for these in the loading analysis, and recalculate the sizes of the members.

The actual design procedure is similar in both approaches and requires a knowledge of, or a determination of, the following:

(a) Reasonably comprehensive load distributions, which may be used to derive the shear force, bending moment, and torque diagrams, together with any particular concentrated load inputs, see Chapter 12.

(b) Any relevant airframe life requirements and, if appropriate, stiffness criteria, refer to Chapters 10 and 11, respectively.

(c) An initial definition of the location of the main stmctural members, although there must always be an acceptance of the possible need for revision as the design process becomes more refined, see Chapter 14.

(d) An initial choice of the main materials of construction. However, it is often desirable to investigate more than one alternative before a final decision is reached. In terms of the initial sizing of the mcmbcrs the main distinction is between metals and composites. Chapter 13 covers the materials aspect of the design.

The procedure outlined in this chapter is the classical approach. Section 15.1.2.2, although reference is made to the use of more advanced techniques where these are relevant.

15.1.2 Distribution of loads

15.1.2.1 Advanced computational techniques

When a finite element, or similar, approach is used for the structural design process it is necessary to distribute the air and inertial loads across the airframe in such a way as to ensure that the overall balance is maintained. To achieve this there must be a definition of the location of the main structural members whether this is derived from an expert program or by using information such as that given in Chapter 14. This structural layout is used to define the airframe as a set of elements, the detail of which is dependent upon the capacity of the computational process and the local complexity of the structure. The distributed loadings are idealized as sets of point loads applied at the nodes of the elements used to define the airframe, a procedure which may conveniently be achieved by the use of a pre-processor before the actual finite element analysis. It will be noted that the derivation of the shear force, bending moment, and torque diagrams is not strictly necessary since the analysis effectively performs the integrations needed to obtain them from the local load distributions

15.1.2.2 Classical technique

As stated above, the classical technique is based on the direct use of the shear force, bending moment, and torque diagrams together with concentrated local load inputs.

The form of the basic shear force, bending moment, and torque diagrams is outlined in Chapter 12, Section 12.3. It is necessary to adapt them to allow for the way in which the loads are reacted from one primary structural component to another. For example the longitudinal shear forces are reacted at the wing root spar attachment points although the initial diagram is usually related to the centre of gravity of the aircraft.

The span-wise symmetric and asymmetric loadings are straightforward. These are illustrated in Figs 12.1, 12.4, and 12.7 where, as is shown, it is normal for the loads to he reacted at attachments located at the sides of the fuselage.

The situation is more complex in the longitudinal sense where the distribution of load between the spar attachments is a function of the stiffness of the root section of the wing and of the fuselage pick-up frames. As a first approximation, to enable the design process to be stated, it may he assumed that the front and rear spar loads can be estimated by a simple static analysis of the wing root section. Each spar will have two components of load:

(a) The load due to the effective vertical shear force which may he assumed to be acting at the 'centroid' of the second moment of area of the front and rear spars, see Section 15.2.1, Eqns (15.2). The front and rear spar loads are inversely proportional to their distances from the point of action of the load.

(b) The load arising from the overall torsion moment about the centroid referred to in (a) above.

An analysis similar to that given in Section 15.2.6 may be used. If the box beam is of rectangular cross-section and the structural parameters arc symmetric about the mid-point of the width, so that the centroid is at that mid-point, the loads on the spar attachments due to the vertical shear only. (a) above, are equal. It must be noted that in the case of a swept wing the torsion moment referred to in (b) is the resultant of the bending and torsion couples resolved in the flight direction at the root section, see Chapter 12, Section 12.5.2.

The effect of including the front and rear spar reactions on the longitudinal shear force and bending moment diagrams is shown in Fig. 15.1. The significant result is a reduction of both the shear force and the bending moment in the region between the spars.

15.1.3 Synthesis technique

As noted in the previous sections the more advanced methods of structural analysis require a specification of the structural details, achieved by using an expert program or by using as an input an initial structural layout with arbitrary sizes for the members. Unless a design closely resembles a predecessor this is not necessarily the most efficient process. It is often more satisfactory to use elementary theory to provide a first indication of the dimensions of the main structural items. This provides a good basis for input to an advanced analytical treatment which may then be used for refinement and the investigation of problem areas. The simple approach enables understanding of the way in which the structure functions, it also provides a validation of the concept and is a datum against which to check the output of a more advanced analysis.

When using elementary theory it is important to recognize that there are limitations in its application and to make some allowance for these wherever possible. The limitations are discussed in more detail in Chapter 16, and, in practice, are often best treated by the use of a finite element or similar technique.

Throughout the subsequent paragraphs it is assumed that all the loads are the ultimate values except for those concerning pressure cabin tensile stresses which are based on the actual working differential pressure.

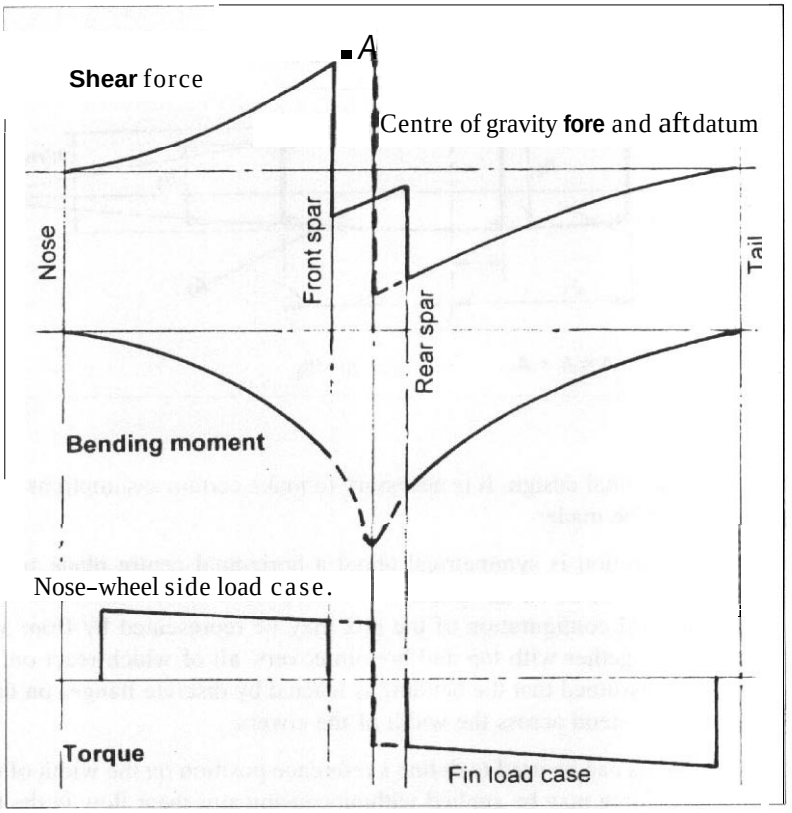

Fig. 15.1 The effect of front and rear spar root reactions on the longitudinal shear force, bending moment, and torque diagrams

15.2 Box beam of lifting surfaces

15.2.1 Cross-section of the structural box

The relevant dimensions are defined in Fig. 15.2, which shows the true shape of the structural box as determined by the aerofoil section. An intermediate spar is included to illustrate how the effect of such a member may be allowed for.

An important property of the structural cross-section is the shear centre, which is also known as the centre of twist. No twisting of the section occurs when a force is applied at this point, the location of which is a function of both the geometry and the structural configuration. The locus of the shear centres of the individual cross-sections across the span is known as the flexural axis., Since the shear centre is a function of the structural configuration it is not possible to specify its position until the sizes of the structural elements have been determined. On the other hand a reasonably accurate prediction of the location is desirable to ensure that the reaction of the applied loading is adequately

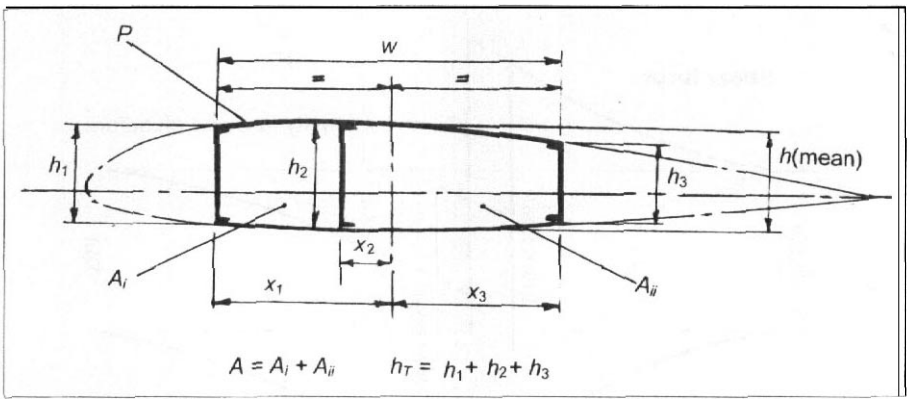

Fig. **15.2** *Dimensions of a lifting surface structural box*

representative of the final design. It is necessary to make certain assumptions to enable such a prediction to be made:

(a) The cross-section is symmetrical about a horizontal centre plane so that the shear centre will he on this plane.

(b) The structural configuration of the box may be represented by front and rear spar webs together with top and bottom covers, all of which react only shear loads. It is assumed that the bending is reacted by discrete flanges on the spars which may extend across the width of the covers.

These assumptions can he used to define a reference position on the width of the box at which a vertical force may be applied without causing any shear flow in the top and bottom covers:

$$e = w/(1 + h_3/h_1) \tag{15.1}$$

where

e is the location of the reference point as a fraction of the width of the box, w, forward of the rear spar

h_1 and h_3 are the depths of the front and rear spars, respectively

For initial design work it is often adequate to assume that the structural box may be idealized to a rectangular cross-section having a mean depth, h. If the structural configuration is also assumed to he symmetric about the horizontal mid-point of the width the shear centre is located at that mid-point.

Section 15.1.2 comments upon the need to correct the longitudinal stressing data for the position of the root attachments. Reference is made to the centroid of the second moment of area of the spars, which is proportional to the square of their respective depths. When the cross-section is truly doubly symmetric the centroid is clearly at the mid-point of the width and the spar reactions of the vertical load are equal. If this is not

the case it is suggested that, for initial work, it is assumed that the centroid is then given by:

$$e_c = h_1^2/(h_1^2 + h_3^2) \tag{15.2a}$$

where e_c is the position of the centroid forward of the rear spar as a fraction of the width of the box, w.

The corresponding ultimate front spar and rear spar reactions are:

$$\begin{aligned} &\text{Front spar,} \quad F = Vh_1^2/(h_1^2 + h_3^2) \\ &\text{Rear spar.} \quad R = Vh_3^2/(h_1^2 + h_3^2) \end{aligned} \tag{15.2b}$$

where V is the applied ultimate vertical shear load.

15.2.2 Torsional stiffness requirement

As explained in Chapter 11, Section 11.5, stiffness criteria are now rarely used for final design purposes. Nevertheless, it is advantageous at the initial design phase to employ a relevant criterion to give a guide to the likely impact of the torsional stiffness requirement. The stiffness criterion is used to establish a minimum average value of the thickness of the shear material for the vertical webs and covers of the primary structural box. While in many cases this may not be critical it is useful in providing a first value for comparison with later work. Examples of situations when torsional stiffness is likely to be critical are a fin with a high-mounted stabilizer and the outer portion of a wing of relatively high aspect ratio.

An approximate, but usually adequate procedure, is as follows:

(a) Estimate the enclosed area. A, and perimeter, P_r, of the structural box at several positions across the wing span.

(b) Use the Bredt–Batho theory to calculate the rate of twist at each section due to a concentrated torque, T_C, applied at a defined location on the semi-span and with a mean thickness of shear material, t_θ, then:

$$d\theta/d\ell = \{P_r/(4GA^2)\}(T_C/t_\theta)$$

or

$$\theta = \{(T_C/t_\theta)\int(P_r/A^2)d\ell\}/4G \tag{15.3}$$

where

G	is the shear modulus of the material
$d\theta/d\ell$	is the rate of twist along the length of the box, ℓ

The notional concentrated torque, T_C, is usually applied at 0.7 semi-span and θ is measured at this point.

(c) Plot P_r/A^2 against ℓ up to the reference point given in the stiffness requirement, for example 0.7 semi-span, as illustrated in Fig. 15.3. Integrate by using the area under the curve to give θ in terms of (T_C/t) and hence:

$$T_C/\theta = kfg = m_\theta$$

where k is a constant derived from the integration and m_θ is the specified stiffness requirement, examples of which are to he found in Chapter 11, Section 11.5.

The ***average*** value of the thickness of the vertical webs and the cover skins needed to meet the torsional stiffness requirement is then given by:

$$t_\theta = m_\theta/k \tag{15.4}$$

15.2.3 Overall torsion moment

The overall torsion moment at any given cross-section is used to check the shear thickness of the outer surfaces and spar webs required to react the torsion loading. The procedure is:

(a) Estimate the enclosed area, A, of the primary structural box at representative sections across the span, as in the previous section.

(b) The corresponding shear flow in the covers and webs is approximately:

$$Q_T = T/2A \tag{15.5}$$

where T is the magnitude of the ultimate applied, distributed, torsion, and Q_T will be nose-up or nose-down and hence positive or negative depending upon the sign convention.

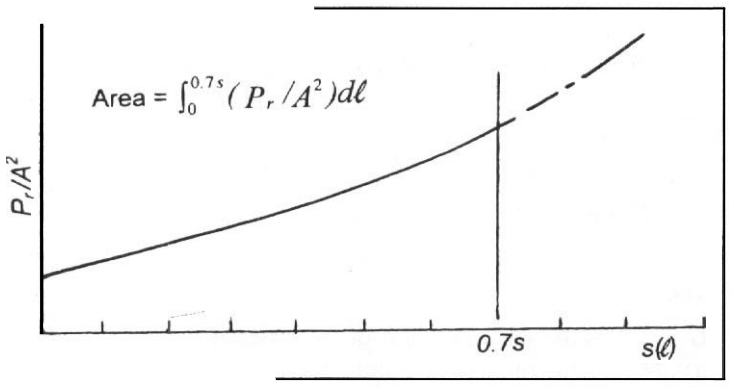

Fig. 15.3 *Integration of section properties for torsional stiffness evaluation*

(c) Select the allowable shear stress, σ_s, from Chapter 13, Sections 13.5.3.3 for metal construction or 13.5.4.3 for composite construction, as appropriate.

(d) The mean material thickness needed to react the torsion moment is then:

$$t_q = T/2A\sigma_s \tag{15.6}$$

15.2.4 Overall bending moment

The bending moment at a given cross-section is used to establish the approximate value of the effective end load material of the top and bottom spar booms or distributed flanges of the primary structural box.

The procedure is as follows:

(a) At various points across the span evaluate the idealized (mean) depth of the primary structural box, ***h***.

(b) Calculate the effective direct loads. P, in the top and bottom surfaces required to react the appropriate ultimate bending moment, M, at each section:

$$P = M/h \tag{15.7}$$

(c) Evaluate the allowable stress, σ_b. Reference should be made to Chapter 13, Section? 13.5.3.2 or **13.5.4.2** as appropriate for the material of construction. Where required the value of the rib pitch, L, is given by Eqn. (15.10) below and in the case of a composite material the thickness of the $\pm$ **45°** plies implied by $\bar{R}$ in Eqn.(13.3) is taken as the greatest of t_q from Eqn. (15.4) and t_q from Eqn. (15.6).

(d) Evaluate the cross-section area required to meet the bending condition, A_b, by dividing the load P by the allowable stress σ_b. A_b is the total flange/boom area on one side of the neutral axis of the box beam.

(i) For a discrete boom design. where all the bending moment is reacted by the spar caps:

$$A_b = P/\sigma_b = M/(h\sigma_b) \tag{15.8}$$

σ_b is the allowable proof stress in this case.

Initially assume A„ is divided equally between all the spar caps on one side of the hox.

(ii) For a distributed flange initially assume a uniform effective thickness, t_e, across the width of the box, ***w***, to give:

$$t_e = M/(h\sigma_b) \tag{15.9}$$

In this case σ_b is given by Eqns (13.1) and (13.2) as appropriate. In order to apply these equations it is necessary to know a value for L, the rib pitch. needed to ensure overall compression stability. The derivation of the optimum

rib pitch is discussed in Chapter 16, Section 16.2.3. L may increase outboard along a lifting surface as the load intensity decreases. If some form of sandwichconstruction is used L can be relatively large. An analysis of typical designs of conventional metal construction, interpreted in the context of optimization theory, suggests that at the root of a lifting surface, in the absence of better information, it may be assumed that:

$$L = 0.55(d_r)^{1/2} \quad \text{m} \tag{15.10}$$

where d_r is the maximum depth of the wing chord at the side of the fuselage (m). (Note that both d_r and L are dimensional.)

The thickness, t_e, is an equivalent value derived from that of the skin and the area of the stringers. Typically the effective thickness due to the stringers is between 50 and 100 per cent of that of the skin, depending upon the form of construction and the load intensity. Assuming the lower value, the actual skin thickness needed in the bending case, t_b, is approximately:

$$t_b = 0.65M/(hw\sigma_b) \tag{15.11}$$

Clearly the 0.65 reduces to 0.5 when the skin and stringers contribute equally to the effective area. The design of the stringers is further discussed in Section 15.2.7.

15.2.5 Thickness of upper and lower box surfaces

15.2.5.1 Metal construction

When metal construction is used the cover thickness may initially be assumed to be the greatest of that given by the conditions of Sections 15.2.2, 15.2.3, or 15.2.4 in Eqns (15.4). (15.6). and (15.11), respectively. The critical condition may well vary across the span, but that given by Eqn. (15.11) is most often dominant except when discrete booms are used.

15.2.5.2 Composite construction

In the case of composite construction it is necessary to provide sufficient separate directional fibres to meet the stiffness and various loading conditions. Thus span-wise, 0°, fibre thickness will be determined primarily by the condition of Section 15.2.4 while the shear, $\pm 45'$ fibre, thickness will derive from either Sections 15.2.2 or 15.2.3.

There will also be a need for fibres in the 90" direction to react loads input by the ribs and give a satisfactory laminate, see Chapter 13, Section 13.5.4.1. These must be dealt with in subsequent design but for initial calculations an allowance of, say, 25 per cent of the 0° fibres should he made. The contribution of fibres in a given direction to the strength in other directions may be neglected initially, but see Chapter 13, Section 13.5.4.1.

15.2.6 Spar webs

While the condition of Section 15.2.3 gives an adequate initial estimate of the shear thickness required in the upper and lower covers, it is necessary to add the effect of the vertical shear loads to those of the torsion loads to obtain the required thicknesses of the spar webs. To do this:

(a) Evaluate the total effective depth of all the spars, h_T, see Fig. 15.2. For initial purposes the depth of each spar may he taken as the actual depth of the aerofoil section at the relevant sparposition rather than the idealized, rectangular box value.

(b) The shear flow in the webs due to the ultimate vertical shear force, V, is:

$$Q_v = V/h_T \tag{15.12}$$

When this analysis is used to evaluate the front and rear spar reactions at the root attachment, reference should be made to Section 15.2.1, Eqns (15.2).

(c) The net shear flow in the webs is then approximately given by:

$$Q_w = Q_v + 2xQ_T/w \tag{15.13}$$

where x is the chord-wise location of a particular web relative to the mid-point of the box, see Figs 15.2 and 15.4. The sign of **x** is important. heing positive forward for a positive nose-down torsion and a positive downward vertical force. Q_T may be derived from Eqn. (15.5) which neglects, for simplicity, the effect of any intermediate webs.

The web thickness is then:

$$t_w = Q_w/\sigma_s \tag{15.14}$$

See Section 15.2.3 for reference to the value of σ_s

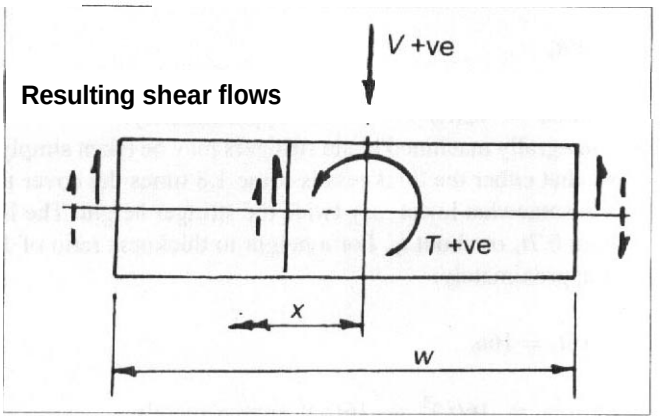

Fig. 15.4 *Reaction of vertical shear and torsion in spar webs*

15.2.7 Stringer configuration

Section 15.2.4 suggests that as an initial estimate the total stringer area can be assumed to be 0.35 of the total area of the distributed flange, although it recognizes that this may be somewhat low for some designs. Eventually it is necessary to undertake a more precise optimization, see Chapter 16, Section 16.2.3. It is useful, however, to make a first estimate of stringer configuration. Stringer sections are illustrated in Chapter 14, Fig. 14.3. The most common stringer shapes are Zed and blade, the latterbeing especially associated with simple integrally machined panels. Enclosed top-hat section stringers, tending to corrugated reinforcement may be used, particularly with composite materials.

(a) Stringer pitch is often between 1.5 and 5 times the stringer height, the lower values being associated with blade stringers. It is determined by practical considerations as optimum design usually gives an impractical low pitch. For initial work assume a value of 3.5.

(b) In the case of separate Zed-section stringers the width of each of the shorter flanges is often about 40 per cent of stringer height, giving a total cross-section area of $(1.8h_s t_s)$ where h_s and t_s are the stringer height and thickness, respectively. The assumption that the total stringer area is 35 per cent of the cover effective area leads to:

$$0.35t_e \times 3.5h_s = 1.8h_s t_s \tag{15.15a}$$

so that approximately:

$$t_s = 0.68t_e \tag{15.15b}$$

This suggests that the stringer thickness should be about the same as the cover skin thickness, t_b, see Eqn. (15.11). Further the width to thickness ratio of the free flange is typically about 16 to match the local and overall buckling. Thus $0.4h_s$ is equal to $16t_s$ and:

$$h_s = 40t_s \tag{15.15c}$$

The stringer area $= 72(t_s)^2 = 70(t_b)^2$ approximately.

(c) The area of integrally machined blade stringers may be taken simply as $h_s t_s$, and this suggests that either the thickness is some 1.8 times the cover thickness, t_b, or the pitch is somewhat lower, say twice the stringer height. The latter gives t_s as being about 0.71, or about t_b. For a height to thickness ratio of 16 this latter value gives approximately:

$$h_s = 16t_s = 16t_b \tag{15.16}$$

The stringer area $= 16(t_s)^2 = 16(t_b)^2$ approximately

Interestingly. the implication that the thicknesses of the skin and stringer are likely to be similar also applies to cases where the ratio of the stringer to skin areas is around unity since this geometry tends to he associated with a relatively lower stringer pitch.

When the aerofoil is thin the effective height of the stringer is limited by the depth of the box. In extreme circumstances the stringers are replaced by full depth webs.

15.3 Ribs

Ribs may be designed using a similar technique to that used for the primary span-wise box, assuming that the rib flanges act as discrete booms. In general ribs react the local distributed air-load, inertial and any concentrated loads and, acting as beams, transmit them in the chord-wise direction to the spars. Rib equilibrium is maintained by the change in shears in the box covers which are input at the rib. The greatest difficulty is the evaluation of the chord-wise rib bending moments, which requires a detailed knowledge of the actual skin–stringer configuration. For initial design work it is simplest to consider only those ribs subjected to concentrated load inputs, such as control hinge ribs or ribs reacting engine, or landing gear loads. The calculation can be based on the assumption that the vertical load on the rib is reacted only at the front and/or rear spars, the contribution of the covers being neglected. It must he remembered that a wing torsion couple, which is effectively a rib bending moment, may be associated with the vertical load.

Thus, for example, a hinge rib for a trailing edge control surface or flap can he taken as a cantilever beam loaded by a vertical shear force equal to the hinge reaction and a bending couple due to the chord-wise offset of the hinge from the rear spar location, see Fig. 15.5. The spar web will react most of the vertical shear, and in practice if the hinge fitting is perpendicular to the rear spar, the rib flanges at the spar will be loaded by direct

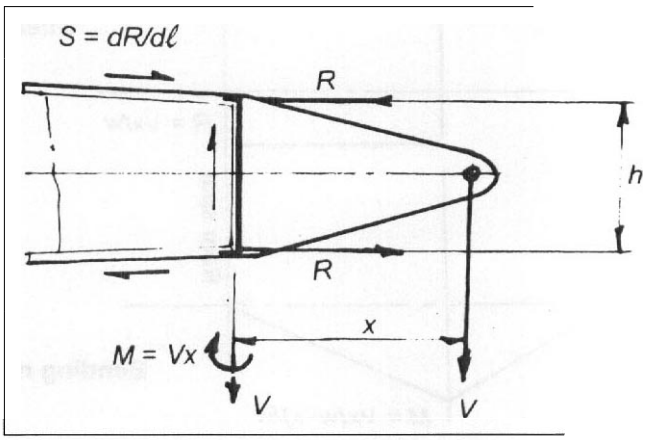

Fig. 15.5 Cantilever hinge rib

forces given by:

$$R = \pm Vx/h \tag{15.17}$$

where

- V is the hinge reaction
- x is the offset of the hinge from the spar
- h is the depth of the rib at the spar

If the rib is not perpendicular to the rear spar a component of the load R will act along the spar boom.

The rib Range area at the rear spar is the load R divided by the allowable bending stress, as discussed in paragraph 15.2.4(c). The load decreases forwards along the main box rib as it is balanced by the reacting torsional shear in the skin. For simplicity this shear may be assumed to be constant across the width of the box, so that the load R falls linearly to zero at the front spar.

When there is a concentrated load applied at a point along the length of a rib between the front and rear spars it can be treated as a chord-wise beam simply supported at those spars, see Fig. 15.6. The load must be transferred to the local shear centre and any consequent torsion moment dealt with. If the rib Range is in contact with the cover skin the latter makes a contribution to the area of the flange. This is usually taken to be 20 times the cover thickness when the attachment is simply supported as in a single row of

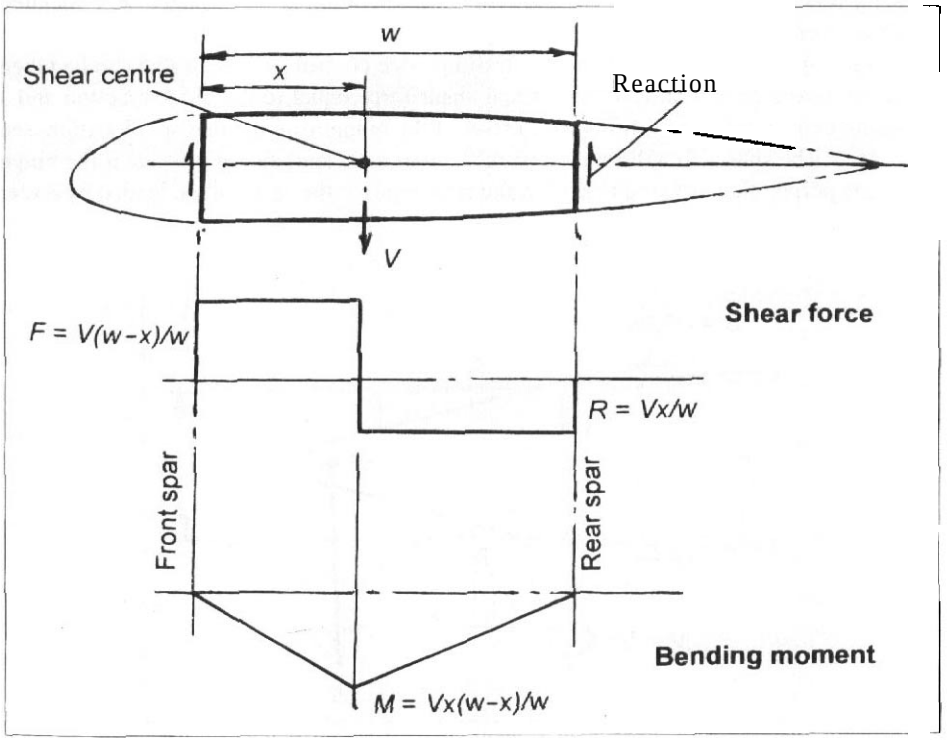

Fig. 15.6 Inter-spar rib with concentrated load input

fasteners, hut it may be as much as 40 times the cover thickness when there is effective clamping, as with a double row of fasteners or bonding.

The thickness of the web of a rib is given by dividing the vertical component of the applied load by the product of the local rib depth and the allowable shear stress.

Ribs also experience a so-called 'Brazier' load, which is a load normal to the wing surface caused by the direct skin stresses acting along the curvature of the aerofoil. It is only significant when the outer surface has a relatively small radius of curvature.

Fuel tank end ribs are required to withstand pressure loads due to rolling and similar manoeuvres. These may be treated as flat pressure bulkheads, see Section 15.7.2. The pressure varies over the area of the rib due to hydrostatic and aircraft acceleration effects hut a maximum value may be used for initial design purposes.

15.4 Auxiliary surfaces (controls, flaps, slats, and spoilers)

15.4.1 Hinge/support positions

The first task in the design of an auxiliary surface is the determination of the location of the hinges/supports. Indeed, the rib positions in the main lifting surfaces are considerably influenced by this although the initial sizing of the primary box may not be greatly affected. In some cases the number of segments of an auxiliary surface and the number of hinge/support points on the individual segments may be readily established. More often, however, these decisions form an important part of the overall structural design. To begin this process the following assumptions may be made:

(a) The effective spar boom area of the auxiliary surface in bending is constant so that the second moment of area is proportional to the square of the local depth at the chord-wise position of the hinge or the main spar.
(b) The air loading either is constant along the length of the surface, or varies linearly with length along the hinge-line.
(c) The effect of bending of the main surface is negligible.

Usually the hinge positions are chosen to reduce auxiliary surface deflections to an acceptable value without causing unduly high bending moments. The effect of the number and the position of the hinges may be evaluated by using continuous beam analysis.

As a guide, for a two-hinge arrangement on a uniform beam with uniform loading the minimum deflection occurs when the hinges are spaced equally about the centre and 55 per cent of the overall length apart. The tip deflection of the beam then equals that at its centre. This results in a maximum bending moment which is some 15 per cent greater than the lowest value achieved when the hinges are 59 per cent of thc length apart. Clearly in a practical situation with a tapering cross-section and varying load the optimum values will be different. As a first adjustment the inner hinge may be left in the same place, but the outer one should he moved out to about 35 per cent of the half-length from the centre.

It is not possible to give specific guidelines when there are more than two hinges due to the additional parameters which must he considered. Some indication of the effect of

using three or more hinges may be gained by applying the three moments equation to a simply supported continuous beam of uniform cross-section and uniform loading, u, per unit length. In this case:

$$M_{n-1} + 4M_n + M_{n+1} = -u\ell^2/2 \tag{15.18}$$

where here

ℓ is the spacing between the hinges, assumed to be equal
M_n is the additional moment applied at support n because of continuity

In the case of an auxiliary surface it is likely that there will be an overhang at each end of, say, ℓ_h, and the moment at the adjacent hinge may be derived in terms of the deflection of the free end, δ:

$$\delta = u\ell_h^4/8EI$$

and

$$M_\delta = u\ell_h^2/2$$

thus

$$M_\delta = 4EI\delta/\ell_h^2 \tag{15.19}$$

where

M_δ is the moment at the first binge due to the overhang
I is the second moment of area
E is the elastic modulus of the cross-section

A value may be allocated to δ to ensure that there is adequate clearance between the surface and the fixed structure. Chapter 11, Section 11.8.2 suggests that an appropriate value is 0.02 of the local depth of the spar of the auxiliary surface. Thus a value for M_δ may be determined in terms E, I, and ℓ_h and this is the value of the additional moment at the two end hinges corresponding to Eqn. (15.18). For example if there are five hinges $M_1 = M_5 = M_\delta$. Table 15.1 summarizes the values of the additional moments for the cases of three. four, and five hinges.

The total moment distribution along the beam is the sum of the additional moments as given in Table 15.1 and the simply supported moment, M_{SS}, on each intermediate section of the span:

$$M_{SS} = u\ell^2/8 \tag{15.20}$$

Further the total length of the surface having n supports, b_S, is:

$$\begin{aligned} b_S &= (n-1)\ell + 2\ell_h \\ \ell_h &= \{b_S - (n-1)\ell\}/2 \end{aligned} \tag{15.21}$$

Table 15.1 Additional moments for multi-hinge surfaces

Hinges	M_1	M_2	M_3	M_4	M_5
3	M_δ	$-(M_\delta/2 + u\ell^2/8)$	M_δ		
4	M_δ	$-(M_\delta/5 + u\ell^2/10)$	$-(M_\delta/5 + u\ell^2/10)$	M_δ	
5	M_δ	$-(2M_\delta/7 + 3u\ell^2/28)$	$(M_\delta/7 - u\ell^2/14)$	$-(2M_\delta/7 + 3u\ell^2/28)$	M_δ

If it is further assumed that a first estimate of the spacing to minimize the bending moments is obtained by equating the overhang moment to that of the simply supported beam section then:

$$4EI\delta = \ell_h^2/8$$

and substituting for ℓ_h from Eqns (15.21):

$$(n-1)\ell^2 - b_S\ell + 8(2EI\delta/u)^{1/2} = 0 \qquad (15.22)$$

which may be solved for ℓ.

Associated with the hinge/support locations is the actuation point. Whereas the hinge/support points determine the form of the vertical shear force and bending moment diagrams, the actuation point determines the form of the torsion moment diagram since the whole torque on the surface is reacted by the actuation system. The maximum value of torque can he kept low by locating the actuation at. or near to, the centre, see Fig. 15.7, but as noted in Chapter 14, Section 14.3.2.2 other practical considerations may override this.

15.4.2 Sizing of the main elements

Once the shear force, bending moment, and torque diagrams have been adapted to allow for the hinge/supports and actuation, as shown in Fig. 15.7, it is possible to proceed with the sizing of the main members. In general this can follow the procedure suggested for a lifting surface in Section 15.2. The differences to note are:

(a) Because auxiliary surfaces usually lie at the extremities of the chord of the wing the cross-section varies considerably. For example trailing edge surfaces are close to triangular in shape. For this reason it is usual to assume that all the vertical shear and bending is reacted by a single discrete boom spar configuration, the covers being used only to react local air-loads and shear. One exception to this may be the front or centre segment of a multi-slotted flap system which can be nearer to rectangular shape and could have both front and rear spars. In assessing the effective spar boom area an allowance should be made for the contribution from the cover skins, say 20 times skin thickness.

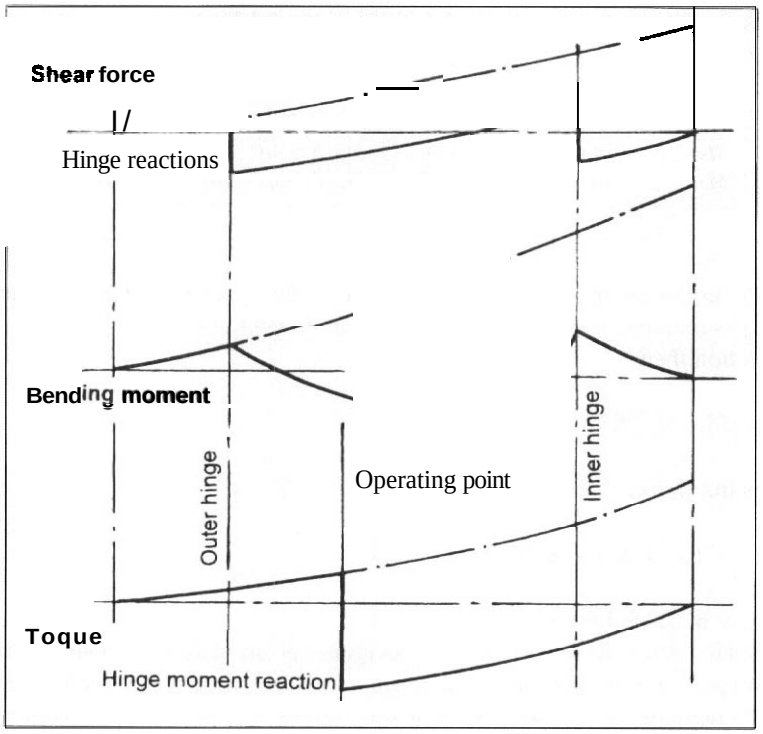

Fig. 75.7 Corrected auxiliary surface structural design data

(b) Because it is necessary to avoid undue twist along the length of an auxiliary surface, there is an implied torsional stiffness requirement even if a specific one is not stated. As an approximate guide the twist from one end to the other should not exceed about 10 per cent of the overall angular control deflection. It is often desirable to use as much of the cross-section area as possible to react the torsional shears to achieve this. This includes the nose region of a flap or trailing edge control as far as is possible, bearing in mind the need for cut-outs in the hinge regions. Equation (15.3) may be adapted to check this condition.

(c) It is not normally desirable for the outer covers of auxiliary surfaces, especially controls, to buckle below the limit load.

(d) The effectiveness of a control surface is critically dependent upon its aerodynamic shape, especially the effective trailing edge angle. Thus the outer covers must not deflect unduly under air-load and it is suggested that the normal deflection of a panel should not exceed about 2 per cent of the local depth. The deflection at the centre of a rectangular panel of isotropic properties subjected to uniform pressure may he found from ESDU Data Sheet 71013.[1]

[1] ESDU Data Sheet 71013. Elastic direct stressses and deflectionsfor flat rectangular plates under uniformly distributed normal pressure. ESDU International plc, August 1982.

For simply supported edges the deflection, δ, is approximately:

$$\delta = 0.143\{pa^4/(Et^3)\}\{n^3/(n^3 + 2.2)\} \quad (15.23)$$

where

- p is the uniform pressure
- a is the length of the shorter side
- n is the ratio of longer to shorter side
- E is the modulus of elasticity
- t is the thickness of the plate

This, together with the need to prevent shear buckling, leads to one of two design solutions. The first is to use closely spaced ribs to minimize side length a, possibly with small intercostal stiffeners between them to reduce n. The other is to use some form of stiff sandwich skin to effectively increase the cover thickness, t, or to use full depth support. The latter is associated with a minimum number of ribs.

15.5 Fuselage

15.5.1 Pressurization

The first distinction to make is between pressurized and non-pressurized fuselages. If the former is the case, and the pressure differential is significant, then the analysis should commence by evaluating the skin thickness needed to meet this condition. Unless the pressure differential is less than about 0.3 bar (4.4 lb/in^2) the fuselage cross-section should consist of circular arcs when a complete circle is not feasible. There should be ties across the points where the curvature changes, see Chapter 14, Section 14.4.2, otherwise undesirable bending loads are introduced.

The skin thickness required to limit the hoop tensile stress to an acceptable value is given by:

$$t_p = \Delta pR/\sigma_p \quad (15.24)$$

where

- Δp is the maximum *working* differential pressure
- R is the local radius of the shell
- σ_p is the allowable tensile *working* stress. The establishment of the allowable stress is discussed in Chapter **13,** Sections **13.5.3.4** and 13.5.4.4

In some military and general aviation aircraft a relatively low pressure differential is used with non-circular section fuselages. In these cases the design to meet the pressure requirement is best left until after other loading cases have been analysed.

15.5.2 Torsion shear requirement

For most aircraft the critical torsion cases are effectively the fin root bending moment, including the tail-plane rolling moment, aft of the wing and the torque due to nose-wheel side load forward of the wing. These torques can be used to establish the appropriate skin thickness required to react the implied shear loads using Eqn. (15.6). It should be noted that the enclosed torsion box area may well not be that of the whole cross-section. For example, in a four longeron construction the box may be completed by the decking and floor, as is shown in Chapter 14, Fig. 14.22. Where large cut-outs occur on a basically circular cross-section there should be internal webs or walls to close the box, as indicated in Fig. 14.21

15.5.3 Overall bending

In the case of the fuselage, both vertical and horizontal bending moments must be considered, although as a first estimate it may be assumed that the respective wont cases apply in isolation from one another.

(a) Considering the vertical bending moment first, a procedure similar to that outlined above in Section 15.2.4 may be followed by using a number of stations along the fuselage length to evaluate stresses.

(b) When discrete longerons are used it is a simple matter to evaluate the value of h at each station and hence the required longeron cross-section area using an assumption for allowable stress as for the wing, Eqn. (15.8).

(c) The analysis has to be dealt with differently when the bending moment is reacted by the whole cross-section of the fuselage. The bending section modulus of a thin shell is approximately given by the product of the enclosed area A, and the equivalent skin thickness, t_e, so the required equivalent skin thickness to resist a bending moment, M. is:

$$t_e = M/(\sigma_a A) \tag{15.25}$$

where σ_a is the allowable stress.

Now $(\sigma_a \times t_e)$ is the effective load per unit width at the maximum distance from the neutral axis. That is, from Eqns (13.1) and (15.25):

$$\sigma_a t_e = P/w = M/A \tag{15.26}$$

Hence the allowable stress is:

$$\sigma = F_B \bar{A}\{M/(AL)\}^{1/2} \tag{15.27}$$

where in this case L is the frame pitch, see Section 15.6. The construction and material properties F_B and A are defined in Chapter 13, Sections 13.5.3.2 and 13.5.4.2.

As with the design of the wing. the actual skin thickness, t_b, needed to react the bending is likely to he about 65 per cent of the value given by Eqn. (15.26). the rest of the magnitude of t_c being made of stringer reinforcing. that is:

$$t_b = 0.65M/(\sigma_a A) \tag{15.28}$$

The same analysis is then undertaken for horizontal bending which may, or may not, yield a greater value of t_b at some longitudinal stations.

15.5.4 Determination of the skin thickness

The actual skin thickness at the various stations is thus the greatest of t_s from Eqn. (15.24) where relevant, the torsion shear value from Section 15.5.2 above, or t_b from Eqn. (15.28). The value of t_p may well prove to be greater than t_b, or even t_c, for a large-diameter pressurized fuselage, but it is still necessary to make allowance for longitudinal reinforcing equivalent to about 0.351, to stabilize the outer skin, possibly in the form of intercostals between frames. The pitch of these longitudinal reinforcing memhers may be determined by optimization considerations, but the ideal will vary round the cross-section as the local end loading varies. Initially it is reasonable to assume a constant pitch of about three to four times the stringer depth. It is thus possible to make a first design of the stringer, assuming its thickness is similar to that of the skin. as described in Section 15.2.7.

Should composite construction be employed it is clearly necessary to include directional fibres to meet all the load conditions, including the longitudinal pressure stress, which is half the hoop value. In this case it is often found that, away from joints. the required design is close to an isotropic lay-up.

15.6 Fuselage shell support frames

In the pressurized fuselages of transport aircraft the frame pitch is typically around 0.5 m, see Chapter 14, Section 14.4.4.1. Where bending loads reduce and the overall cross-section diameter reduces, as in the nose and tail regions. it may be preferable for the purposes of manufacturing to use more closely pitched frames and eliminate the longitudinal stiffening.

For other fuselages the frame pitch will vary according to the critical loading case and local attachment requirements. As a first guide a spacing of around 25 per cent of the overall depth of the structure may be assumed for relatively heavily loaded areas, but increasing as loading decreases to be as much as the local structural depth.

Frame width is likely to be constrained by internal layout considerations, but may typically be around *3–5* per cent of the overall fuselage width. Shell support frames must be adequately stiff to support the shell in overall bending and this requirement is likely to determine the thickness of the material used. Usually the thickness will be similar to that of the skin. In a pressurized fuselage of small to moderate diameter it is often found that the skin contributes about 50 per cent of the shell material and the basic frames and longitudinal stringers *25* per cent each.

15.7 Main attachment frames and bulkheads

15.7.1 Heavily loaded frames

The heavily loaded frames are effectively curved beams designed by the local input loads and it is necessary to evaluate the frame shear force and bending moment distributions in order to determine the required cross-sections. Once the distribution of the shear forces and bending moments round the frame are known the thickness of the web and the area of the flanges can be estimated by a similar technique to that quoted for mass boom spars in Sections 15.2.4 and 15.2.6. Many frames are of shallow depth to make available the maximum internal cross-section. Bulkheads are effectively deep frames where, in the limit, the whole makes up a deep shear web and shear stresses become critical.

Fuselage frames are often of circular shape, or approximately so. **A** first indication of the required cross-sectional area may be obtained by assuming that there is a constant stiffness around the frame, that EI is constant, where E is the modulus of elasticity and **I** is the second moment of area of the frame cross-section. For this case the bending moment, shear force, and end loads in the frame section due to the input of radial and tangential loads and couples are known. Thus the required frame cross-sections for any given set of loading may be obtained by resolving the applied direct loads into their radial and tangential components and using the principle of superposition to combine the basic conditions in the appropriate proportions. Table 15.2 together with Fig. *15.8* summarizes the maximum frame loading for the basic conditions. It should be noted that the maximum bending moment, end load, and shear force actually occur at different locations around the frame.

This approach is also adequate for the initial sizing of frames which approximate to a circular shape.

Table 15.2 Maximum load conditions in ring frames supported in a fuselage shell (see Fig. 15.8)

Loading case	Radial load, P_n	Tangential load, P_t	Couple, M_c
Bending moment	$-0.24P_nr$	$\pm 0.063P_tr$	$\pm 0.5M_c$
End load	$+0.433P_n$	$\pm 0.5P_t$	$\pm 0.318M_c/r$
Shear force	$\pm 0.5P_n$	$+0.232P_t$	$+0.478M_c$

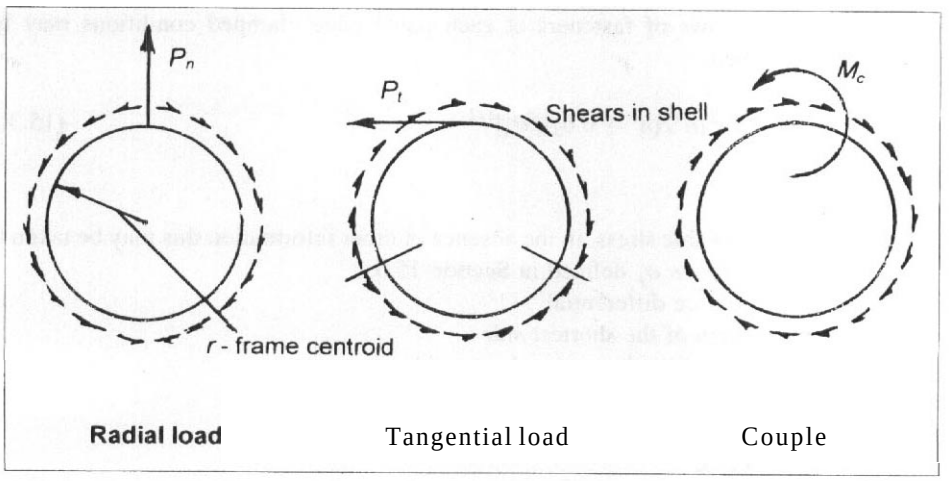

Fig. 15.8 Loading cases for fuselage rings

It should be noted that when calculating the areas of the outer flanges of frames and bulkheads, credit should be taken for the contribution made by the outer skin, say equivalent in area to 20–40 times the skin thickness depending upon whether the attachment is effectively simply supported or built-in, respectively, see Section 15.3.

15.7.2 Pressurebulkheads

15.7.2.1 Domed pressure bulkheads

Pressure bulkheads of a domed shape may be treated in the same way as the outer, pressurized, skin. The tensile stress due to pressure in a hemi-spherical shell is equal to the longitudinal stress in a cylinder, that is half of the value given by Eqn. (15.24), except that in this case the radius. R, is that of the hemi-sphere rather than that of the cylinder.

15.7.2.2 Flat pressure bulkheads

Flat pressure bulkheads consist of a series of beams and intermediate flat panels. As a first guide to the size of the vertical beams they may be assumed toconsist of individual items supported at a number of points along their length by the beams in the transverse direction, and vice versa. The loading may be approximated by taking the pressure on a width of the bulkhead equal to the spacing of the beams and using the three-moment equation discussed in Section 15.4.1 to obtain an indication of the moments at the supports.

The required thickness of a flat rectangular panel having isotropic material properties and simply supported edges under pressure load is given by ESDU Data Sheet 71013.[1] It is approximately:

$$t = [0.71\Delta p a^2\{n^3/(n^3 + 1.5)\}/\sigma_a]^{1/2} \qquad (15.29)$$

If there are two rows of fasteners at each panel edge clamped conditions may be approximated when:

$$t = [0.5\Delta p a^2 \{n^4/(n^4 + 0.6)\}/\sigma_a]^{1/2} \tag{15.30}$$

where

- σ_a is the allowable stress, in the absence of other information this may be taken to be the same as σ_p defined in Section 15.5.1
- Δp is the pressure differential
- a is the length of the shortest side
- n is the ratio of the longer to shorter side

15.8 Floors

Floor dimensions may well be determined by stiffness rather than strength although, where they are relevant, the emergency alighting cases are likely to be significant. Floors are usually supported by lateral beams which transmit the loads to the fuselage frames, the design of which must make an appropriate allowance. Longitudinal beams, which may well incorporate seat rails or other load attachment points, are used to transfer the normal floor loads to the lateral beams. As a whole the floor and its beams may be treated in the same way as a flat pressure bulkhead, see Section 15.7.2, but one difference is that there are effectively external concentrated loads at the intersections of the longitudinal and lateral beams.

For the purpose of initial design the lateral beams can be assumed to be simply supported at the frame attachments although in practice there is likely to be some fixation and they may also be propped, see Fig. 14.20. The loading on a lateral beam element may be taken as an effective uniform pressure applied over a frame pitch, equivalent to that given by Eqn. (15.20), together with the concentrated load inputs. Should the floor be propped the continuous beam analysis of Section 15.4.1 is appropriate.

When a floor is used as a tie across kinks in a pressure shell, or as part of a torsion box, allowance must be made for the additional loads.

CHAPTER 16

Important departures from elementary theory

16.1 Introduction

There are many situations where the elementary theory used in Chapter 15 is not valid and some are of sufficient importance to demand consideration at the initial design stage. Advanced methods of analysis may automatically handle these conditions, see Chapter 15, Section 15.1.2.

16.2 Buckling considerations

16.2.1 Introduction

16.2.1.1 Causes of buckling

The majority of aircraft structural components are subjected to compression or shear under some loading conditions. Because many of these components include relatively thin sections there is a strong likelihood of buckling being a major consideration. This has already been considered to some extent in the definition of the allowable overall bending stress proposed in Chapter 13, Section 13.5. However, because of the importance of the subject a more extensive review of the issues involved is desirable.

The comments made below are intended as a general guide for initial design work.

16.2.1.2 Compression buckling – skin buckling

Many configurations of compression structures can contribute to the reaction of increasing load after skin huckling has taken place. While outer skin buckling is not desirable under conditions of normal level flight, and small departures from it, its onset under higher load conditions is usually acceptable in metal construction. Therefore, especially in the case of relatively lightly loaded metal structures, local skin buckling should be allowed to occur if the consequence is a lighter, more efficient, configuration. The allowable stress defined in Chapter 13, Section 13.5.3.2, can imply compression skin buckling in some circumstances and it is suggested that it represents a good approach for the initial design of light alloy shells and related components. When a skin buckles the stiffness of the skin–stringer combination is reduced. For example if the attachments of the stringers effectively provide simple support to the cover skin the post-buckled stiffness is about one-third of the unbuckled value. It may be as high as one-half when clamped edge conditions apply. Skin buckling is less likely to he a consideration when high loading intensity results in high working stress.

In the case of composite components the limited evidence available suggests that the use of a buckled design may be acceptable in some circumstances. However, it is probable that in many applications the loading intensity is such that skin buckling will not occur. The allowable stress suggested in Chapter 13. Section 13.5.4.2, is essentially based on the assumption that local buckling is precluded.

16.2.1.3 Shear buckling

The allowable shear stresses quoted in Chapter 13, Section 13.5.3.3 and 13.5.4.3, are based on the assumption that shear buckling is prevented by the provision of adequate local support. That is, the dimensions required to react the shear stresses are based simply on the allowable material shear stress. Such shear members are sometimes called 'shear resistant' This may be unduly conservative in some circumstances, but it is a safe starting assumption. The load carrying capacity of buckled shear members is dealt with in Section 16.2.4.

16.2.2 Struts

Individual struts are often used in aircraft structures, especially when there is an input of a concentrated load as in landing gear components, control linkages, and powerplant mountings. These may be designed using the simple strut relation:

$$P = \pi^2 EI/\ell^2$$

or

$$P/A = \sigma = \pi^2 E/(\ell/\kappa)^2 \qquad (16.1)$$

where

- P is the applied load and σ the corresponding stress
- E is the modulus of elasticity

I is the second moment of area of the section of area **A**
ℓ is the effective length of the strut
K is the radius of gyration, (ℓ/κ) being the slenderness ratio

The simplest situation is when the strut is pin jointed at both ends, as is often the case in a truss structure, when ℓ is the actual length between the end attachments. The other extreme is when the ends are fully built in, in which case ℓ is half the actual length between the ends. The latter case is rarely met in practice, although frequently some degree of fixation is present. For initial work it is preferable to be conservative in the assumption of fixing effect. Even when a strut is apparently well built-in at its ends the effective length may still he as much as 90 per cent of the actual value.

Equation (16.1) is applicable up to the 0.2 per cent proof stress.

16.2.3 Optimization of distributed flange–stringer designs

16.2.3.1 Introduction

Distributed flange, skin–stringer, components form a large part of the structure of most aircraft. It is important to ensure that the design of these components is as near to optimum as possible in order that the structure weight is as low as can be practically achieved. While Chapter 15, Section 15.2.7 suggests that a typical ratio of the skin to stringer area is two to one it is desirable to be more precise as the design is developed. It is possible to undertake an optimization study to decide the lightest compression structure as defined by:

(a) Rib or frame pitch.
(b) Stringer pitch.
(c) Stringer type and properties.
(d) Relative areas of stringer and skin,

The absolute optimum occurs at, or near to, the condition when the design is such that the various failure modes occur simultaneously. However, the ideal optimum may not be practically achievable. Further such an ideal optimum is likely to be dangerously susceptible to the effect of imperfections and measures should he taken to avoid this even though a theoretical penalty has to be accepted.

16.2.3.2 Modes of failure

The primary modes of failure of a panel in compression, as illustrated in Fig. 16.1, are overall and local buckling.

(a) Overall buckling is determined primarily by rib pitch and the second moment of area of a skin–stringer element, and is effectively given by Eqn. (16.1). Using

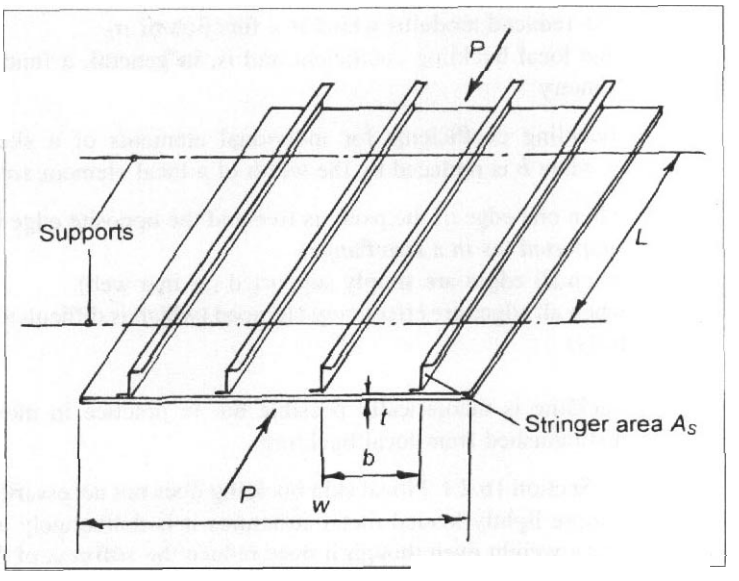

Fig. 16.1 Skin–stringer panel in compression

the suffix 'E' to indicate overall buckling Eqn. (16.1) may be rewritten as:

$$\sigma_E = K_E E_E b^2 / L^2 \tag{16.2}$$

where

K_E is the overall buckling coefficient and is equal to $(\pi\kappa/b)^2$
σ_E is the overall huckling stress
b is the stringer pitch
L is the rib or frame pitch
κ is now the bending radius of gyration of a skin–stringer element
E_E is, generally, a reduced elastic modulus and is a function of σ_E

(b) Local instability of the stringer elements, that is the webs or flanges. This depends upon the local stringer geometry and the support provided by the skins. The local instability stress is given by:

$$\sigma_L = K_L E_L t^2 / b^2 \tag{16.3}$$

where

σ_L is the stress at which local buckling occurs
t is the thickness of the skin

E_L is the reduced modulus which is a function of σ_L
K_L is the local buckling coefficient and is, in general, a function of the geometry

The local buckling coefficients for individual elements of a skin–stringer combination when b is replaced by the width of a local element are:

0.58 when one edge of the panel is free and the opposite edge is simply supported (as in a free flange)
3.62 when all edges are simply supported (as in a web)
6.32 when all edges are effectively clamped (which is difficult to achieve fully)

(c) Torsional buckling is theoretically possible but in practice in most cases it cannot be distinguished from local buckling.

As is mentioned in Section 16.2.1.2 local skin buckling does not necessarily result in failure and in some more lightly loaded metal structures it is deliberately allowed to occur in order to reduce weight even though it does reduce the stiffness of the panel.

16.2.3.3 Optimization in elastic conditions

In the case of metal construction the values of the elastic modulus for the skin and stringers may be taken to be the same and for elastic conditions they are equal to the modulus of elasticity, E. The same is true of composite construction provided the laminate lay-up of the skin and stringers is identical. Then:

$$E_E = E_L = E \tag{16.4}$$

It is convenient to write:

$$f(\sigma) = \sigma / E_T(\sigma) \tag{16.5}$$

where $E_T(\sigma)$ is the reduced modulus, equal to E in elastic conditions.

The panel working stress is:

$$\sigma = P/(wtk_t) \tag{16.6a}$$

where

P is applied compressive load
w is the overall width of the panel
t is the skin thickness

$$k_t = 1 + A_S/bt \tag{16.6b}$$

where A_S is the stringer area

It is usual to introduce safety factors to cover the possibility of imperfections and to separate the overall and the local buckling modes. Defining these as λ_E and λ_L respectively, and using suffix 'a' to indicate allowable gives:

$$\sigma_E = \lambda_E \sigma_{aE} = K_E E b^2/L^2$$
$$\sigma_L = \lambda_L \sigma_{aL} = K_L E t^2/b^2 \tag{16.7}$$

It is now acceptable to assume that the maximum allowable stress occurs when σ_{aE} is equal to σ_{aL}. Further the minimum panel weight coincides with the lowest value of the skin thickness for a given value of k_t. Using Eqn. (16.5) it is possible to write Eqn. (16.7) as:

$$f(\sigma) = \sigma/E$$
$$f(\lambda_E \sigma) = K_E b^2/L^2 \tag{16.8}$$
$$f(\lambda_L \sigma) = K_L t^2/b^2$$

Thus

$$\sigma/E = P/(wEtk_t) = K_E b^2/(\lambda_E L^2) = K_L t^2/(\lambda_L b^2) \tag{16.9}$$

from where

$$b = [PL^3/(wE)]^{1/4}/[K_L \lambda_E^3/(K_E^3 \lambda_L k_t^2)]^{1/8} \tag{16.10}$$

$$t = [K_E \lambda_L/(K_L \lambda_E)]^{1/2}(b^2/L) \tag{16.11a}$$

$$t = [PL/(wE)]^{1/2}/[k_t^2 K_E K_L/(\lambda_E \lambda_L)]^{1/4} \tag{16.11b}$$

$$\sigma = [K_E K_L/(k_t^2 \lambda_E \lambda_L)]^{1/4}[PE/(wL)]^{1/2} \tag{16.12}$$

Equations (16.10) and (16.11) indicate the relative properties of the panel required to achieve the same working stress in the skin and stringers, as given by Eqn. (16.12). Equation (16.12) may be written as:

$$\sigma = [F_B/(\lambda_E \lambda_L)^{1/4}][PE/(wL)]^{1/2} \tag{16.13a}$$

$$F_B = (K_E K_L/k_t^2)^{1/4} \tag{16.13b}$$

F_B is dependent upon the type of stringer and typical values are given in Chapter 13, Table 13.4.

If values are allocated to λ_E and λ_L, Eqn. (16.13a) can be used to express the panel working stress. σ, as a function of the pitch of the supports, L, σ being inversely proportional to the square root of L.

Clearly it is desirable to use the highest working stress which is practically feasible. In the case of composite construction it may be assumed that the allowable compression stress in the laminate is within the elastic range so that this value may be used as a starting point. However, in the case of metal construction the loading intensity is likely to be such that the panel stress is beyond the elastic range and Eqns (16.10) to (16.13) do not, by themselves. indicate the likely value of the achievable stress.

A significant stress in the evaluation of the buckling characteristics of light alloy construction is that at which the tangent modulus, E_T, is half that of the elastic modulus, E. This stress, σ_n, is typically about 10 per cent less than the 0.1 per cent proof stress and hence it is a feasible value to use as a design target for optimization. It is usual to define:

$$\varepsilon_n = \sigma_n/E \tag{16.14}$$

where ε_n is the elastic portion of the strain when σ is equal to σ_n.

For most light alloys $0.003 \leqslant \varepsilon_n \leqslant 0.005$ and the latter value may he taken as typical for the class of light alloy used in heavily loaded compression components. Equations (16.10). (16.11), and (16.13) may be written in terms of ε_n:

$$b = \varepsilon_n^{1/2} BL(\lambda_E^3/\lambda_L)^{1/8}[P/(wL\varepsilon_n f_n)]^{1/4} \tag{16.15}$$

$$t = \varepsilon_n TL(\lambda_E\lambda_L)^{1/4}[P(wL\varepsilon_n\sigma_n)]^{1/2} \tag{16.16}$$

$$\sigma = [\sigma_n F_B/(\lambda_E\lambda_L)^{1/4}][P/(wL\varepsilon_n\sigma_n)]^{1/2} \tag{16.17}$$

where

$$B = [K_L/(K_E^3 k_t^2)]^{0.125}$$
$$T = 1/(K_E K_L k_t^2)^{1/4} \tag{16.18}$$

Typical values have been deduced for B and T for various forms of construction. For example in the case of Zed-section stringers B and Tare 0.95 and 0.44, respectively, while for blade stringers the values are 1.4 and 0.52.

Equations (16.15) to (16.18) can he used to estimate the likely levels of achievable load intensity and the corresponding dimensions of the elements of the panel. For a light

alloy construction having $\varepsilon_n = 0.005$. $\sigma_n = 350$ MN/m, $\lambda_E = 1.2$, and $\lambda_L = 1.0$ the following approximate values may be derived:

(a) Zed stringers:

$$\sigma = 230[P/(wL)]^{1/2} \tag{16.19a}$$

$$\begin{aligned} t &= 0.0017L[P/(wL)]^{1/2} \\ &= 0.0066L \quad \text{when} \quad \sigma = \sigma_n \end{aligned} \tag{16.19b}$$

$$\begin{aligned} b &= 0.063L[P/(wL)]^{1/4} \\ &= 0.077L \quad \text{when} \quad \sigma = \sigma_n \end{aligned} \tag{16.19c}$$

(b) Blade stringers:

$$\sigma = 200[P/(wL)]^{1/2} \tag{16.20a}$$

$$\begin{aligned} t &= 0.0026L[P/(wL)]^{1/2} \\ &= 0.0046L \quad \text{when} \quad \sigma = \sigma_n \end{aligned} \tag{16.20b}$$

$$\begin{aligned} b &= 0.092L[P/(wL)]^{1/4} \\ &= 0.12L \quad \text{when} \quad \sigma = \sigma_n \end{aligned} \tag{16.20c}$$

As a first approximation the optimum rib pitch for lifting surfaces of light alloy construction can be taken as:

$$L_{opt} = 0.9d_r[1 - 0.5(0.3P/w)^{1/2}] \tag{16.21}$$

where

d_r is the depth of the rib (m)
P is in MN/m and w in m

This may be compared with the expression given in Chapter 15, Eqn. (15.10).

In many cases the optimization process results in a large number of closely spaced stringers, and this is not likely to be practical. Typically the optimum stringer pitch is about the same as the stringer depth. Moving somewhat off optimum does not usually

introduce significant penalties and it is suggested that in practice the stringer pitch should not be less than about three times the stringer depth.

16.2.3.4 Optimum design in plastic conditions

It should be pointed out that the analysis which leads to Eqns (16.15) to (16.20) is an adapted elastic solution which does not adequately represent the conditions which apply when the panel is loaded outside the elastic range. Optimum design in the plastic range is complicated by the non-linear form of the stress–strain curve although a representation, such as that of Ramberg and Osgood, see ESDU Data sheet 76016,[1] may be used to define the problem mathematically.

Even so it is not possible to make general conclusions except when the material has a definite yield point followed by a more or less constant stress as the strain increases. This behaviour is not typical of light alloys but it may be used to indicate the trend of plasticity effects. For example when $\sigma = \sigma_n$ and $\lambda_E = \lambda_L = 1$, in the adapted elastic analysis the parameter:

$$[P/(wL)]/(\varepsilon_n \sigma_n) = (1/F_B^2)$$

approximately. In the fully yielded plastic analysis it is found to equal $(2/F_B^2)$. A similar factor is found in the expressions for t and in the case of b the factor is $2^{\frac{1}{3}}$. Thus it may be concluded that the adapted elastic analysis underestimates the extent of the load carrying capacity of the panel when plastic conditions are present. The degree of the underestimation is dependent upon the shape of the stress–strain curve of a particular material. Generally graphical or computational analysis is needed for the optimum design in non-elastic conditions.

16.2.4 Buckled shear webs

16.2.4.1 General

Internal shear webs may be allowed to buckle provided that the consequent overall shear deflection is acceptable. Buckled webs fall into two categories, namely those where there is a pure tension field effect, see next section. and those where the conditions lie between the tension field case and a shear-resistant, unbuckled, condition.

16.2.4.2 Tension field web

In the case of a pure tension field web the shear stresses are wholly reacted by the development of buckles in the web. The shear is reacted by tension forces along the line of the buckles, as shown in Fig. 16.2. The simplest case is that of a beam of constant depth. If it is assumed that the flanges do not contribute to the reaction of the shear and

[1] ESDU Data Sheet 76016. Generalization of smooth continuous stress–strain curves for metallic materials. ESDU International plc, September 1991.

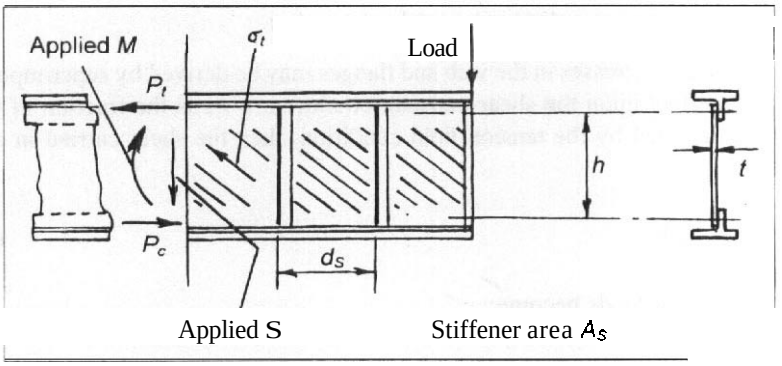

Fig. 16.2 Tension field shear web

the buckles develop at 45' to the flanges:

$$\sigma_t = 2V/ht \tag{16.22}$$

where

, is the tensile stress
V is the applied shear force
t is the thickness of the web
h is the nominal depth **of** the web between the centroids of the flanges

The presence of the stress σ_t in the webs results in a change in the end load in the flanges:

$$P_T = M/h - V/2$$
$$P_C = M/h + V/2 \tag{16.23}$$

where

M is the applied bending moment
P and P_C are the flange tension and compression loads, respectively

When the beam is tapered the tensile stress in the webs is less than that given by Eqn. (16.22) but the flange end loads are increased.

Stiffeners are usually required to support the flanges. The end load in the stiffener is:

$$P_S = Vb/(hA_S) \tag{16.24}$$

where

b is the stiffener pitch along the web
A_S is the cross-section area of the stiffener

16.2.4.3 Intermediate buckled webs

In this situation the stresses in the web and flanges may be derived by superimposing the tension field effect upon the shear-resistant condition. If k_V is the fraction of the total shear that is reacted by the tension field condition, then the shear carried in diagonal tension is:

$$V_{DT} = k_V V \tag{16.25a}$$

and the flange end loads become:

$$\begin{aligned} P_T &= M/h - k_V V/2 \\ P_C &= M/h + k_V V/2 \end{aligned} \tag{16.25b}$$

approximately:

$$k_V = (1 - \sigma_b/\sigma_s)^n \tag{16.26a}$$

where:

$$n = 1 + 5P_S/(A_S\sigma_s)$$

and σ_s is the shear stress in the web:

$$\sigma_s = V/ht \tag{16.26b}$$

In the case of a panel with simply supported edges and having a depth h and width b the stress at which shear buckling, σ_b, occurs is:

$$\sigma_b = k_S(t/h)^2 \tag{16.26c}$$

k_S is a function of b/h and for simply supported edges has the values given in Table 16.1

Table 16.1 Values of shear buckling coefficient for simply supported panel edges

	b/h					
	1	2	3	4	6	10
k_S	8	5.75	5.3	5.1	4.9	4.8

16.3 Cut-out, constraint, and sweep effects in box beams

16.3.1 Introduction

The elementary theories of bending and torsion are hased on assumptions which are not correct in certain circumstances. For example simple beam theory assumes that plane sections remain plane. that is, they do not distort in the span-wise or length-wise sense. Likewise, the torsion theory assumes that the cross-sections are free to distort out of plane.

16.3.2 Bredt–Batho torsion – cut-outs and constraint effects

16.3.2.1 General

The simple Bredt–Batho torsion theory is based on the assumption that the torsion moment is reacted in a closed box and that there is no constraint on shear distortion. The box may consist of more than one cell and when this is the case the additional internal members do make a contribution to reacting the moment. There are two main departures from the theory which demand consideration, these being the effects of cut-outs and constraints at a built-end.

16.3.2.2 Cut-outs

Cut-outs are discussed in more detail in Section 16.5.1 hut their presence in a torsion box is worthy of comment here:

(a) If at all possible additional structural members should be included to keep the box of closed section, albeit of reduced enclosed area. This may be done by introducing a roof, floor, or sidewall within the overall cross-section, and joining it to the outer shell by bulkheads located at the ends of the cut-outs. These latter should have shear stiffness in their own plane but small sdffness out of plane. They act to collect the shell shears and redistribute them into the changed cross-section. refer to Chapter 14, Figs 14.21 and 14.22. Clearly the shear stresses in the box are increased in the region of the smaller structural cross-section, due to the reduced enclosed area, see Chapter 15, Eqn. (15.5).

(b) If it is impossible to use a closed section the applied torsion moment can be reacted by diffcrcntial bending providing that one end of the component is effectively restrained. This implies a need for substantial end load carrying edge memhers located along the length of the cut-out. as is illustrated in Fig. 16.3. Together with the sides of the shell these effectively act as cantilever beams. Torsional stiffness is inevitably significantly reduced in the cut-out region and it is always beneficial to incorporate an enclosed section even if it is of small cross-section area.

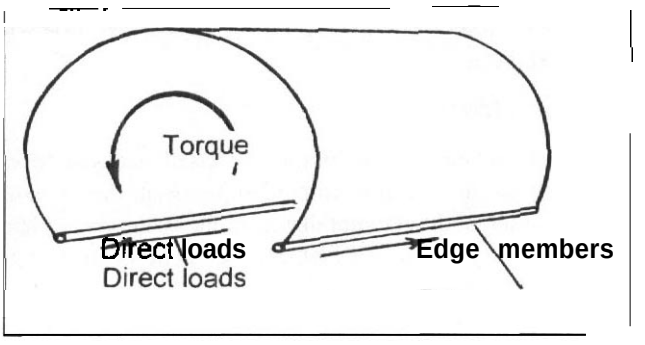

Fig. 16.3 Reaction of torsion by differenfial bending

16.3.2.3 End constraints and concentrated shear inputs

When it is subjected to shearing stress a rectangular plate distorts into a trapezoidal shape as is shown in Fig. 16.4. In a box of rectangular cross-section the distortion of adjacent sides is compatible so that there is a tendency for one comer to move longitudinally in one direction, while the adjacent ones move in the opposite direction. This is known as warping and it will occur in all cross-section shapes except circular ones and special cases. If an unswept box is built-in at one end these longitudinal distortions are prevented from occurring and corresponding longitudinal strains are introduced to give compatibility. The consequence is the introduction of longitudinal constraint forces which have a maximum value at the comers of the built-in end and which die away to zero along the length of the box. **A** built-in situation is often encountered, as for example at the centreline of a wing box loaded by torsion moments symmetric about the centreline of the aircraft.

The analysis of constraint effects involves some complexity. Figure 16.5 illustrates the form of this effect for a typical box geometry having a width to depth ratio of 2.5.

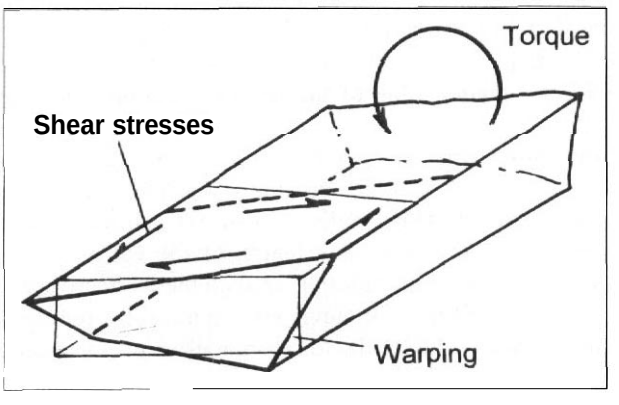

Fig. *16.4* Warping *of* a torsion box

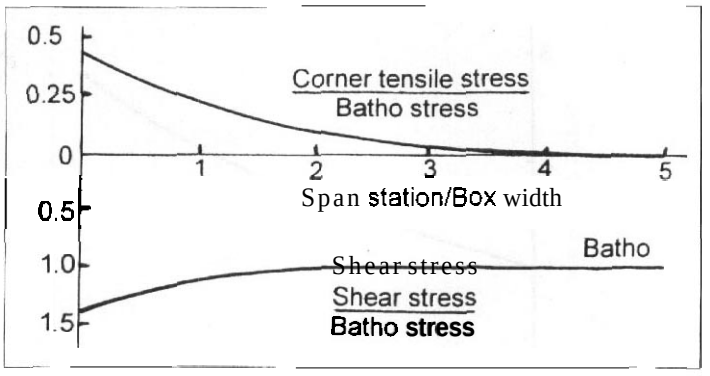

Fig. 16.5 **Stresses** *due to the end constraint of a torsion box*

The direct stresses in the comers are shown as a ratio of the Batho shear stress. The actual shear stress is also increased in the constraint region.

Large end loads may also be introduced in the boom at the comers of a box or, for that matter, an isolated spar when there is a large local input of shear force. In this latter case the additional concentrated load implies a sudden change in the shear strain as it is brought to a compatible situation by the inducing of local boom end loads.

16.3.3 Constraint effects in swept-wing boxes

The problem of swept boxes is similar in certain respects to the end constraints of a built-in unswept torsion box, but it is complicated by the effect of sweep at the built-in end.

When a symmetrical unswept rectangular box is loaded in bending the assumption that plane sections remain plane applies and the direct stresses in the covers resulting from the reaction of the bending moment are uniformly distributed across the width of the box. However, when the box is swept the root section is not plane with respect to the longitudinal structural axis of the box and hence the direct stresses are not uniform across the root width of the box. As a general principle the greatest loads are reacted by the stiffest load path. This is often, although not invariably, the shortest one. Thus there is a tendency for the direct stresses to be highest at the rear of a swept-back box, and correspondingly at the front of a swept-forward box. In practice in the case of a swept-back box the usual chord-wise air-load distribution is such as to tend to counteract this effect, but the basic tendency is present. Figure 16.6 shows this effect for the simple case of a swept rectangular box loaded by a tip bending couple.

Unfortunately the analysis of the magnitude of this modified root constraint problem is complex and in a practical case requires a finite element solution. A simple, first, approach is to assume that the wing is rigid and undertake a simple static analysis of the wing vertical shear forces at the fuselage attachment points. To do this it is necessary to resolve the wing bending and torsional moments into the plane of the root cross-section and to use Chapter 15, Section 15.2, Eqns (15.1) and (15.2) to determine the vertical

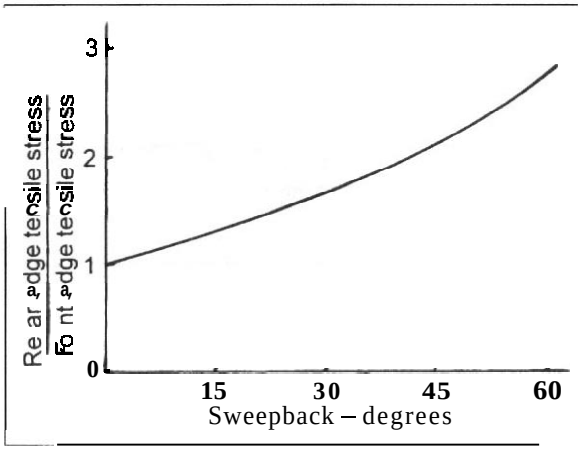

Fig. 76.6 Constraint effect at the *mot* of swept boxes due to a bending *couple*

web shear forces due to both effects. The resulting total vertical shears may then be used as a guide to the corresponding end loads in the appropriate spar booms, since the rate of change of the end load along the spar is equal to the shear force. Such an approach will tend to overestimate the constraint effect since the wing is not rigid, but it may be used to give a first estimate. Before the advent of computational techniques an analytical procedure was developed by Hemp[2] using oblique co-ordinates. This is complex to use in a practical case but applied to an idealized box geometry can rapidly yield an indication of the magnitude of the constraint effect. Howe[3] extended the method to cover the case of boxes having concentrated booms at the junctions of the covers and spar webs.

16.4 Joints

16.4.1 General

Structural joints should be avoided wherever possible but some are inevitable. Major structural joints may he placed into one of two categories. namely transport and production joints.

16.4.2 Transport joints

Transport joints include those that may be required for major maintenance, such as a separable rear fuselage to gain access for powerplant removal.

[2]Hemp, W. S. On the application of oblique co-ordinates to the problems of plane elasticity and swept wing structures, ARC R and M 2754, January 1950.

[3]Howe, D. An approximate solution to the swept wing root constraint problem. College of Aeronautics Report No. 98. February 1956.

Inevitably joints of this kind must be capable of reasonably rapid dismantling and hence load paths have to be concentrated into a small number of connections. When the primary structure is of semi-monocoque form a significant mass penalty may be anticipated. An exception to this generalization is the attachment of a one-piece lifting surface to a fuselage, providing that the primary structural box is continuous, see Chapter 14, Section 14.5.1.

16.4.3 Production joints

Rapid dismantling of production joints is not required. On the contrary their purpose is to enable the airframe to be built of individual components of acceptable size. Thus the fuselage of a large aircraft may be conveniently constructed as three or more major subassemblies. with the main-plane panels attached to either side of the centre section. Joint loads may be distributed across the whole of the load carrying region and when correctly designed the mass penalty is small.

16.4.4 Joint details

It is preferable for the connecting components of any type of joint to carry the load in shear or compression. rather than in tension. Thus fuselage production joints can consist of riveted or bonded shear butt-straps to transmit skin loads together with stringerjoint cleats which employ bolts or similar fasteners in shear.

An area of particular difficulty is the joint of a wing to a carry-through box located within the fuselage where, because of the relative shallowness of the aerofoil, it is desirable to make full use of the available depth. Joining the box covers at a rib with a large number of span-wise tension/compression fasteners located across the chord, just within the aerofoil contour. can provide the lightest solution and enables relatively easy access for assembly. The joint is usually located within the wing–body fairing.

16.5 Cut-outs and load diffusion

16.5.1 Cut-outs

16.5.1.1 General

The presence of cut-outs in a structure is one of the major difficulties of structural design. Large cut-outs should he avoided wherever possible by appropriate structural layout. but there are circumstances. especially in fuselages. where they are inevitable. If a cut-out is basically rectangular in shape the comer radii must be as large as possible.

16.5.1.2 Minor cut-outs – local reinforcement

As a general statement a minor cut-out may be defined as one whose dimensions are of an order of magnitude less than. those of the overall cross-section. Items such as windows in cabins and wing fuel tank inspection holes come into this category. Such cut-outs require local reinforcing but for initial structural design it is adequate to assume that they do not significantly change the overall load paths and structural dimensions.

A special case of what is effectively a minor cut-out in this context is that of a circular hole of comparable diameter to the width of a shear web where local reinforcement around the edges of the hole can deal with the redistribution of the stresses.

16.5.1.3 Major cut-outs

The presence of major cut-outs for doors. landing gear bays, weapon bays, cockpit enclosures, and the like presents a serious difficulty. Essentially all such cut-outs require substantial end load carrying members to be located along the edges parallel to the spanwise/longitudinal loading as well as torsion and shearreinforcing of the skins around all sides. It is essential to recognize that the loads in the edge booms have to be distributed into the rest of the structure over a considerable length either side of the cut-out, see Section 16.5.2. Thus the effect of the cut-out impacts over a much greater length of the fuselage or the lifting surface than the cut-out itself.

Where a number of cut-outs occur along the length of, say. a fuselage it is important to note the following:

(a) If the cut-outs are in the same surface of a component, for example side, top, or bottom, the edge members should be continuous across all of them even if it is necessary to introduce changes in direction of an edge member at frame or bulkhead positions.

(b) When cut-outs are required in opposite surfaces, for example right- and left-hand sides of a fuselage, where possible the cut-outs should be staggered to minimize the reduction of the load carrying material of the shell at any given cross-section location.

At the initial design stage it is important to recognize the effect of a cut-out. As a first estimate the area of an edge member required may he calculated as that needed to maintain the overall section area or bending modulus at the 'uncut' value. The estimate of shear reinforcing round the cut-out necessitates some level of more detailed analysis. In general a finite element analysis is essential, but a simpler approach can sometimes be used to obtain a first approximation of what is required.

Useful references for cut-out analysis can be found in the works of Kuhn[4] and Niu[5] among others. These references are not intended for initial design, but analysis. To overcome this difficulty one of the methods covered by Niu (Chapter 6. Section 6.4) has been applied, with some approximations, to the cut-out geometry shown in Fig. 16.7 to produce the design curves of Figs 16.8 and 16.9.

These refer to the case of a cut-out in a panel uniformly loaded across its width by a direct stress, such as an idealized wing skin or the relevant side of a rectangular section fuselage.

---

[4]Kuhn P, *Stresses* in *Aircraft* and Shell Structures. McGraw-Hill, 1956

[5]Niu C.Y, *Airframe Structural* Design. Conmilit Press. 1988.

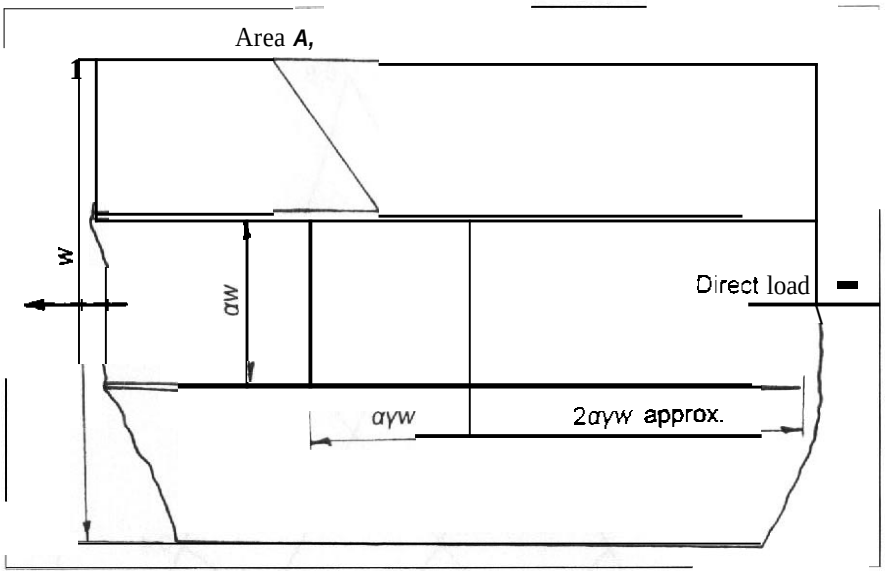

Fig. 16.7 Cut-out in a uniformly loaded panel

The average direct stress, σ_0, in the absence of a cut-out is:

$$\sigma_0 = P/(\delta wt) \tag{16.27a}$$

where

- P is the effective end load
- *w* is the width of the panel perpendicular to the load
- *t* is the skin thickness
- δ is a measure of the effective end load material

$$\delta = [\eta + \Sigma A_S/(wt)] \tag{16.27b}$$

where

- ΣA_S is the total stringer cross-section area
- η is the skin effectiveness, being unity if the skin is unbuckled and about 0.10 when fully buckled.

The cut-out has a width (αw) across the panel and a length $(\alpha\gamma w)$, and is reinforced by edge members which have a cross-section area ***(A,)*** along the length of the cut-out. This latter is conveniently described non-dimensionally as:

$$\beta = 2A_e/(wt) \tag{16.28}$$

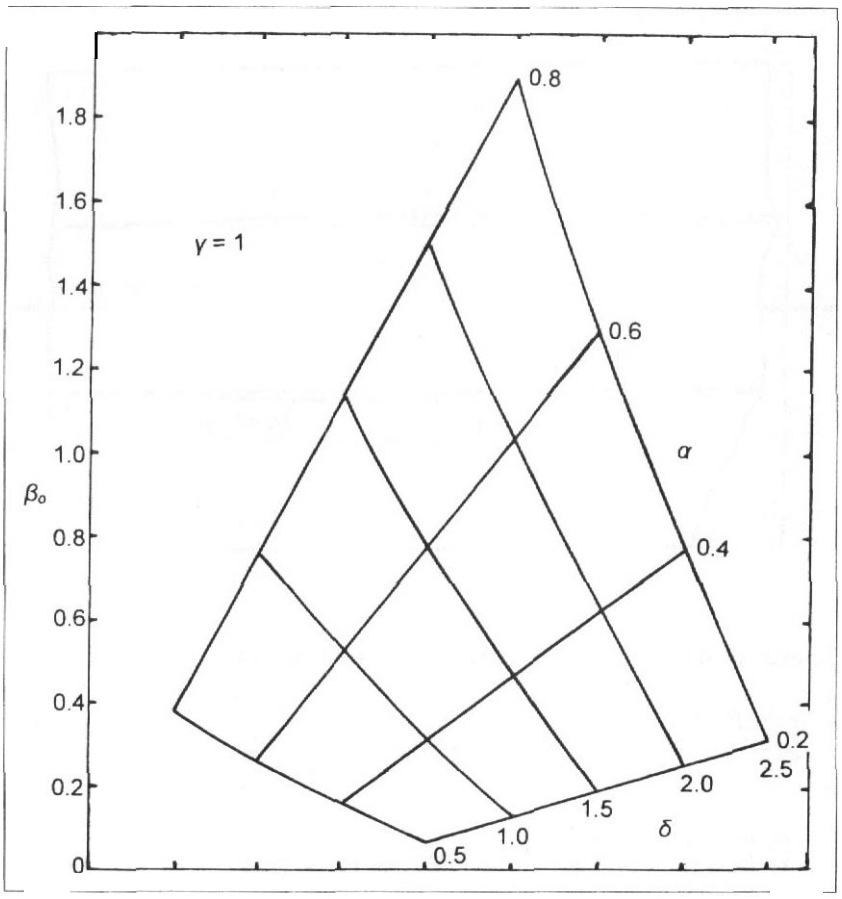

Fig. 16.8 Required edge member area for maintaining the stress in a cut-out panel

The method has been used to estimate the cross-section area of the edge member needed to maintain the stress at the same value as that in the uncut panel given by Eqn. (16.27a). This is defined non-dimensionally as β_0, and gives the required value of A_e at the comer of the cut-out, see Eqn. (16.28). β_0 is shown in Fig. 16.8 as a function of α and δ for the case of γ equal to unity, that is a square cut-out. Figure 16.9 shows the corresponding critical direct and shear stresses in the comer region for a material having a ratio of shear to direct modulus of 0.38. The stresses are given in normalized form f_E and q_E where:

$$\sigma_e = f_E \sigma_0 \qquad \text{and} \qquad \sigma_{sM} = q_E \sigma_0 \tag{16.29}$$

where

σ_e is the maximum direct stress in the edge member
σ_{sM} is the maximum shear stress in the skin at the comer of the cut-out.

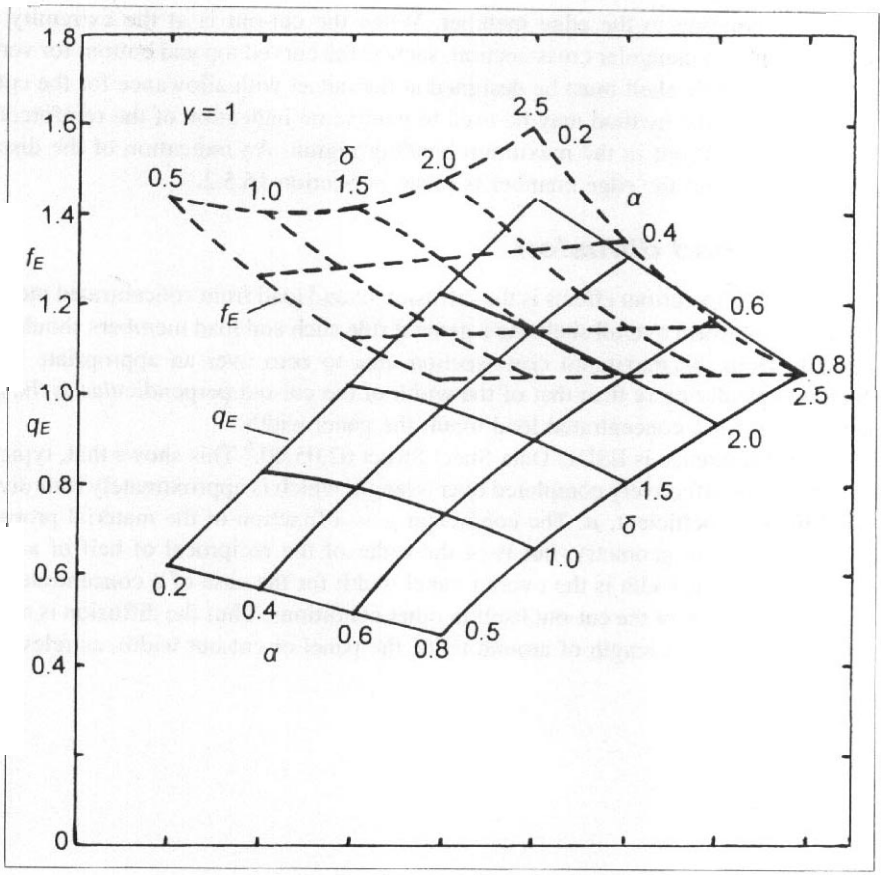

Fig. 76.9 Stresses at the corner of a *cut-out* in *a panel*

The effect of change in cut-out aspect ratio is not great in the range $0.5 \leqslant y \leqslant 2.0$; as shown in Table 16.2.

While they provide only a guide, Figs 16.7 and 16.8 might also be applied to the case of a cut-out in a shell in bending when the cut-out is located across the neutral axis. In this case the datum stress level. σ_0, of Eqn. (16.27a) is that at the depth in the uncut

Table 16.2 Effect of the aspect ratio of the cut-out

Y	0.5	1.0	2.0
β_o factor	0.97	1.0	1.02
f_E factor	0.98	1.0	1.02
q_E factor	1.02	1.0	**0.98**

shell corresponding to the edge member. When the cut-out is at the extremity of a fuselage of non-rectangular cross-section, such as the curved top and bottom for vertical bending, the whole shell must be designed at the outset with allowance for the cut-out region. Even so the method may be used to gain some indication of the reinforcement required for a cut-out in the maximum bending region. An indication of the distance required to run out the edge member is given in Section 16.5.2.

16.5.2 Load diffusion

Closely related to cut-out effects is the diffusion of end load from concentrated members into a more uniform overall shell. As a general rule such end load members should taper gradually from the maximum cross-section area to zero over an appropriate length, which is typically more than that of the width of the cut-out perpendicular to the main load path or, for a concentrated load input, the panel width.

A useful reference is ESDU Data Sheet Struct 02.05.00.[6] This shows that, typically, the diffusion is effectively completed over a length which is approximately four divided by a diffusion coefficient, μ. The coefficient μ is a function of the material properties and local structure geometry, but is of the order of the reciprocal of half of a datum width. This datum width is the overall panel width for the case of a concentrated load input and the width of the cut-out itself in other conditions. Thus the diffusion is more or less complete over a length of around twice the panel or cut-out width, as relevant.

[6] ESDU Data Sheet *Struct* 02.05.00 Diffusion of loads into flat uniform panels. ESDU International plc **February** 1983.

CHAPTER 17

Conclusions

17.1 Review and analysis

The procedures outlined in the previous chapters are intended to provide a method for the first evaluation of the loading actions and the definition of the layout and sizing of the structure of an aircraft. Of necessity in most respects the procedure has been restricted to aircraft of conventional layout. Having reached this stage in the design process it is necessary to review the assumptions made and to use the derived information as a basis for a more detailed and precise analysis.

17.2 Loading calculations

The loading analysis covered in Chapters 4 to 6 was largely based on the assumption that the airframe is rigid. This assumption was made to illustrate how a first calculation of the loads is made so that the initial layout of the structure and the preliminary sizing of the members can be undertaken. It is clear that the fact that in practice the airframe is not rigid has a potentially significant impact upon the distribution of the loads and hence upon the structural design. The initial sizing of the structural members may be used to estimate the extent of the distortion of the structure under load and thus its effect, where relevant, upon the sizes of the members. That is, if becomes possible to undertake the next phase of the iteration in the design process.

As was pointed out at the beginning of the text the availability of powerful computational facilities enables the loading analysis. initial structural design, and the input of static and dynamic distortion to be handled as a seamless process. Such a technique is almost invariably used for the design of advanced aircraft. Intentionally this text does not cover the detail of such programs but it does form a basis for the

understanding of their outputs and. more importantly, a means of interpreting and checking those outputs.

17.3 Structural design

17.3.1 Introduction

The procedure for the initial layout and sizing of the structure outlined in the later chapters is intended only to provide a starting point for the structural analysis. Having obtained a first indication of the sizes of the main structural members, corrected if necessary using the revised loads commented upon in Section 17.2, it is possible to proceed with an analysis based on more accurate analytical or computational methods. At the very least it is necessary to undertake a stress analysis of the derived structure to establish the reserve factors. This process is beyond the scope of this work and Appendix A17 lists a selection of relevant standard texts.

However, before embarking upon more precise calculations it is valuable to undertake a check of the features of the structural design in order to ensure that any possible detail design problems have either been eliminated or. at least, have been anticipated.

17.3.2 Structural design check list

17.3.2.1 Layout/geometry

(a) Keep load paths straight wherever possible.
(b) Keep load paths as short as possible, the load will always take the stiffest route and this is often the shortest.
(c) Where load paths intersect, maintain orthogonality whenever possible. This minimizes the effect of offset moments.
(d) Ensure that load paths intersect at the point defined by the intersection of the lines of centroids of area of the members at the joint.
(e) Avoid offsets as far as is possible but where an offset is inevitable arrange for a structural member to react the offset moment or provide sufficient local reinforcing.
(f) Identify the most highly loaded load path at an intersection and, when required. discontinue the other member.

17.3.2.2 Reaction of applied loads

(a) Identify the most severe loading situation in terms of the geometric configuration of the structure.
(b) Avoid reacting loads by bending structure when an alternative. for example shear, is available.
(c) In a non-circular shell avoid the bending of the cross-section due to pressure by using circular arcs for the cross-section with ties across the kinks formed at the intersection of the. arcs.

(d) Where tensile loading is inevitable incorporate redundant load paths and crack stopping features.
(e) Ensure that there is adequate local and overall support to avoid premature buckling of compression members.
(f) When a box beam is used it is structurally desirable to make it as deep as possible. The width depends upon a compromise between reduction of stress levels and avoidance of buckling. However, in the case of a wing box the width should always be made as large as possible to ensure the potential for maximum fuel capacity.
(g) React torques with a closed section wherever possible, providing it is not very shallow compared with the width. Relatively large cut-outs in one side of a box loaded only in torsion can be tolerated provided appropriate reinforcement is provided
(h) Heavily loaded members having connection to a comparable member must be tapered towards the unconnected end as the load in the member is diffused into the local structure.
(i) Ensure that there is adequate backup structure to react locally applied concentrated loads in order to distribute them into the major load carrying members.

17.3.2.3 Joints and cut-outs

(a) Joints always cause problems and they should be avoided wherever possible.
(b) As far as possible avoid cut-outs in primary load carrying structure. When a cut-out is inevitable the maximum possible comer radii must be used.
(c) If a cut-out is filled by a load carrying panel it is easier to design the panel to resist compression or shear loading rather than tension. This may influence the location of access panels.
(d) Cut-outs in shear members are less of a problem than those in directly loaded ones.

Appendix A17 – Bibliography

Selection of relevant literature generally available

Where appropriate the information is given in the format:
Author Title Publisher Date

A. Airworthiness requirements

1. Federal Aviation Administration – Federal Aviation Regulations:
FAR-23: Utility, Aerobatic and Commuter Category Airplanes
FAR-25: Transport Category Airplanes.

2. Joint Airworthiness Authorities – Joint Aviation Requirements:
JAR-22: Sailplanes and Powered Sailplanes.
JAR-23: Utility, Aerobatic and Commuter Aeroplanes.
JAR-25: Large Aeroplanes.
3. UK Ministry of Defence – Design Requirements for Service Aircraft, Def.Stan.00-970. Vol. 1 Aeroplanes.

B. Loading and general texts

1.	Rabister. A. W.	*Aircraft Dynamic Stability and Response*	Pergamon Press	1980
2.	Cook, M. V.	*Fight Dynamics Principles*	Arnold	1997
3.	Hoblit, F. M.	*Gust Loads on Aircraft: Concepts and Applications*	AIAA	1988
4.	Howe, D.	*Aircraft Conceptual Design Synthesis*	Professional Engineering Publications	2000
5.	Lomas, E.	*Structural Load Analysis for Commercial Aircraft*	AIAA	
6.	Taylor, J.	*Manual of Aircraft Loads*	Pergamon Press	1965

C. Aeroelasticity

1.	Bishplinghoff. R. L. and Ashley. H.	*Principles of Aeroelasticity*	Dover	1975
2.	Bishplinghoff, R. L., Ashley, H. and Halfman, R. L	*Aeroelasticity*	Addison-Wesley	1955
3.	Fung, Y. C.	*An Introduction to the Theory of Aeroelasticity*	Dover	1995
4.	Hodges, D. H. and Pierce, G. A.	*Introduction to Structural Dynamics and Aeroelasticity*	Cambridge University Press	2002

D. Selection of materials

I.	Crane, F. A. and Charles, J. A.	*Selection and Use of Materials*	Butterworths	1984
2.	Farag, M.	*Selection of Materials and Manufacturing Procedures*	Prentice-Hall	1989

E. Strength of materials

1.	Murdi, B. B.	*Engrneering Mechanics of Materials*	Collier-Macmillan	*1980*
2.	Timoshenko. S. P. and Gere, J. M.	*Mechanics of Materials*	Van Nostrand Reinhold	1969

F. Structures and stressing

1.	Bruhn, F. E.	*Analysis and Design of Flight Vehicle Structures*	Tristate Offset Co.	
2.	Coates, R. C. *et al*	*Structural Analysis*	Nelson	1980
3.	Curtis, M.	*Aircraft Structural Analysis*	McGraw-Hill	1997
4.	Donaldson, B. K.	*Analvsis of Aircraft Structures*	McGraw-Hill	1993
5.	Anon	*Structurers Data Sheet Series*	ESDU International plc.	
6.	Megson, T. H. G.	*Aircraft Structures for Engineering Students*	Arnold	1999
7.	Niu, C. Y.	*Airframe Structural Design*	Conmilit Press	1988
8.	Niu, C. Y.	*Airframe Stress Analysis and Sizing*	Conmilit Press	2001
9.	Peery, D. J. and Azar, J. J.	*Aircraft Structures*	McGraw-Hill	1982
10.	Roark, R. J.	*Formulae for Stress and Strain*	McGraw-Hill	1975
11.	Sun. C. T.	*Mechanics of Aircraft Structures*	Wiley	1998

G. Finite element analysis

1.	Brown, D. K.	*An Introduction to Finite Element Methods Using Basic programs*	Surrey University Press	
2.	Cheung, Y. K. and Yeo, M. F.	*A Practical Introduction to Finite Element Analysis*	Pitman	1970

H. Composite construction

1.	Agarwal. B. D. and Broutman, L. J.	*Analysis and Performance of Fibre Composites*	Wiley	1980
2.	Decolon, C.	*Analysis of Composite Structures*	Hermes Penton Science	2002
3.	Hoskins, R. C. and Baker, A. A.	*Composite Materials for Aircraft Structures*	AIAA	1986
4.	Jones, R. M.	*Mechanics of Composite Materials*	McGraw-Hill	1975
5.	Middleton. D. H.	*Composite Materials in Aircraft Design*	Longmans	1990
6.	Niu. C. Y.	*Composite Aircraft Structures*	Conmilit Press	1992
7.	Tsai, S. W. and Hahn, H. T.	*Introduction to Composite Materials*	Technical Publishing Co	1980

I. Landing gear design

1.	Conway, H. G.	*Landing Gear Design*	Chapman and Hall	1958
2.	Curry, N. S.	*Aircraft Landing Gear Design*	AIAA	1988

J. Aerodynamic data and derivatives

1.	Anon	Aerodynamic Data Sheet Series	ESDU International plc.	
2.	Hoerner, S. F.	*Fluid Dynamic Lift*	Hoerner	1985
3.	Hoerner, S. F.	*Fluid Dynamic Drag*	Hoerner	1965
4.	Torenbeek, E.	*Synthesis of Subronic Aircraft Design*	Delft University	1982
5.	Smetna, F. O.	*Computer Assisted Analysis of Aircraft Performance, Stability and Control*	McGraw Hill	1984

ADDENDUM AD1

Example application of flight loading cases

AD1.1 Scope of example

This addendum is concerned with the application of certain of the loading cases to an actual aircraft. The example selected is the Cranfield A1 aerobatic aircraft, G-BCIT, which is illustrated in the frontispiece. It is a simple design with a single piston engine and a fixed tail-wheel landing gear. This particular aircraft has been chosen as the example partly because the simplicity of the design enables the relevant loading cases to he readily selected and partly because of the availability of a comprehensive set of data. The data were derived by calculation backed up by wind tunnel testing and by flight testing. The data have also been used as inputs for the Cranfield Flight Simulator.[1] Thus it is possible to compare the aircraft dynamic behaviour derived from the simulation with that obtained from the analysis outlined in Chapters 4 and 5.

The loading cases considered are:

(a) Symmetric flight manoeuvres and atmospheric turbulence.
(b) Roll manoeuvres consequent upon aileron application.
(c) Directional manoeuvres resulting from the application of the rudder.

[1] Allerton, D. J. The design of a real-time engineering flight simulator for the rapid prototyping of avionics and flight systems. Transactions of the Institute of Measurement and Control, 21 (2/3), 1999.

AD1.2 Cranfield A1 aerobatic aircraft

Although only one prototype of the aircraft was built it has been the subject of research and development over a period of time. As a consequence it has flown in several configurations. Originally designed as a tandem, two-seat, layout only the rear cockpit was equipped when the aircraft first flew in August 1976.

After some flight development the aircraft received a special category certificate of airworthiness as a single-seat aircraft in August 1978 and carried the type designation A1-100. It was cleared for symmetric manoeuvres of $+7g$ and -5g at a maximum take-off mass of 876 kg.

Subsequently the aircraft was flown in various aerobatic competitions with moderate success and frequenlly appeared in air shows. After some 10 years in this role it was used for flight research. Some modifications were made to the aircraft during these phases of the life of the aircraft including the installation of an electrical system enabling the aircraft to operate independently of ground starting facilities. Around 1990 consideration was given to the conversion of the aircraft to the originally envisaged two-seat configuration. In order to provide a basis for this a series of flight tests was undertaken at a single-seat take-off mass of 945 kg. As a result of this initiative the aircraft was modified to the two-seat role, given the designation AI-200. re-registered as G-BCOA, and was first flown in this configuration in 1995. Later a new design of fin and rudder was incorporated and the designation changed to A1-400.

The version of the aircraft used in this example is the single-seat A1-100 in its final form as flown in 1990.

AD1.3 Aircraft data

AD1.3.1 General

The following data apply to the single-seat A1-100 as at 1990 with a maximum take-off mass of 945 kg. The data required for the loading actions calculations and also used in the Cranfield Flight Simulator study are outlined below. The aircraft is powered by a single Lycoming IO-540D piston engine driving a three-bladed propeller of 2.0 m diameter. Tbe fuselage datum is aligned along the thrust line. There are no high-lift devices. A general arrangement drawing is shown in Fig. ADI.1.

AD1.3.2 Inertial characteristics

Take-off mass, m, 945 kg
Pitch moment of inertia, I_y, 2800 kg m^2
Roll moment of inertia, I_x, 1310 kg m^2
Yaw moment of inertia, I_z, 3850 kg m^2

Flight centre of gravity range, 0.21 to 0.25 of the aerodynamic mean chord (MAC)

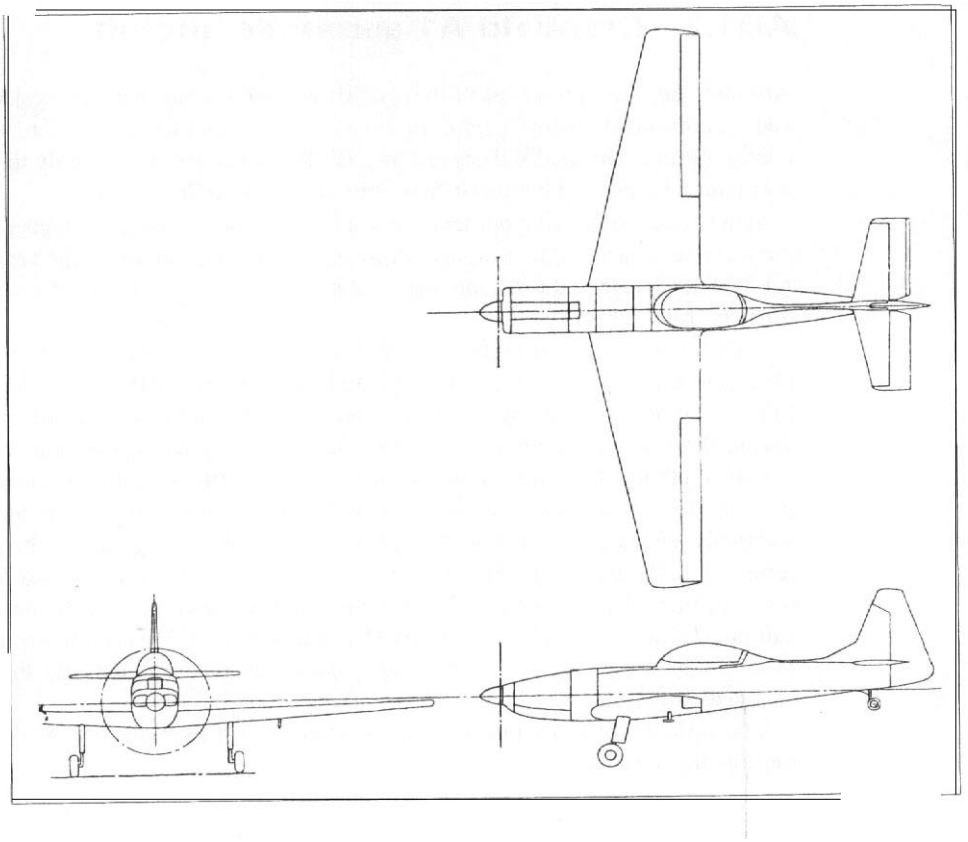

Fig. AD1.1 General arrangement of the A1 aircraft

AD1.3.3 Geometry

Wing

Span, b	10.1 m	Area, S	15.08 m^2
Sweep of 0.25 c line, $\Lambda_{\frac{1}{4}}$	9.58"	Taper ratio, A	0.44
Standard mean chord (SMC)	1.492 m	Aerodynamic mean chord (MAC)	1.576 m
Dihedral. Γ	3"	Washout (tip-down)	2°
Centreline aerofoil section	NACA 23015	Tip aerofoil section	NACA 23012

(Linear variation of aerofoil across wing span)

Setting of root chord to body datum, a_r.	1"
Location of 0.25 MAC forward of the unswept trailing edge	1.176 m
Location of nominal centreline wailing edge below body datum	0.46 m

Aileron span	2.95 m	Aileron chord aft of hinge-line	0.327 m
Aileron movement, up	19'	Aileron movement, down	15°
Location of inboard end of aileron from centreline			1.95 m
Aileron balance chord, forward of hinge-line			0.128 m

Horizontal stabilizer

Span. b_T	3.096 m	Area , S_T	2.72 m^2
Sweep of 0.25 chord line. $\Lambda_{\frac{1}{4}T}$	10.4'	Taper ratio. λ_T	0.643
Standard mean chord	0.875 m	Aerodvnamic mean chord	0.892 m
Centreline aerofoil section	NACA 0010	Tip aerofoil section	NACA 0012
(Linear variation across span)			
Setting of centreline chord to body datum, α_T			+1°
Location of 0.25 MAC forward of unswept trailing edge			0.669 m
Location of unswept trailing edge aft of wing trailing edge			3.574 m
Location of 0.25 chord at centreline above body datum			0.53 m

Elevator span	3.11 m	Elevator chord aft of hinge-line	0.354 m
Elevator movement, up	28'	Elevator movement, down	27"
Width (span) of horn balance.	0.076 m	Area of horn balance (per side)	0.026 m^2
(A trim tab of 0.037 m^2 area is fitted to the right-hand elevator)			
Elevator balance chord forward of hinge-line			0.037 m
Location of inboard end of elevator from centreline			0.106 m

Vertical stabilizer

Overall fin height, b_F	1.775 m	Area (including fuselage), S_F	2 m^2
Effective aspect ratio	1.58	Nominal mean chord	1.12 m
Chord at lower rudder hinge	1.57 m	Nominal tip chord	0.43 m
Aerofoil section	NACA 0010	Rudder movement	±25°
Sweepback of 0.25 chord line, $\Lambda_{\frac{1}{4}F}$, (0.5 chord line is unswept)			11.47°
Ratio of rudder chord aft of hinge-line to overall chord			0.44
Rudder tip horn balance area (basic rudder has round nose)			0.12 m^2
Height of lower rudder hinge above body datum			0.41 m
Total height above lower rudder hinge			1.42 m
Location of 0.5 chord line aft of wing trailing edge			3.35 m

Fuselage

Overall length	8.14 m		
Maximum depth	1.27 m	Maximum width	0.85 m
Location of unswept wing trailing edge aft of fuselage nose			3.985 m

AD1.3.4 Aerodynamic data

Wing–body

Wing–body lift curve slope, a_{1WB}	4.3/rad
Wing no lift angle relative to the centreline chord, α_0	−0.72"
Maximum lift coefficient. C_{LMAX}:	
Upright	1.42
Inverted	1.oo
Lift coefficient at zero wing–body angle	0.13
Wing–body aerodynamic centre position on MAC. H_a	0.19
Zero-lift pitching moment coefficient, C_{M_0}	−0.032
Wing–body pitch damping coefficient, $C_{M\theta}$	0
Rate of change of downwash at tail due to wing incidence, $d\varepsilon/d\alpha$	0.38

Aileron

Aileron two-dimensional lift curve slope	2.5/rad
Rolling moment coefficient due to aileron application, L_ξ	−0.3/rad
Aileron hinge moment coefficient due to wing incidence, b_1	0
Aileron hinge moment coefficient due to aileron deflection. b_2	−0.18/rad
Effective mean aileron angle at full deflection	0.28 rad

Horizontal stabilizer

Horizontal stabilizer lift curve slope, a_{1T}	2.7/rad
Elevator lift curve dope, a_{2T}	1.7/rad
Elevator hinge moment coefficient due to stabilizer incidence, b_{1T}	−0.13/rad
Elevator hinge moment coefficient due to elevator deflection, b_{2T}	−0.43/rad
Effective up-elevator angle at full deflection	−0.4 rad
Effective down-elevator angle at full deflection	0.4 rad
Proportion of air-load on elevator due to stabilizer incidence, S_{1T}	0.08
Proportion of air-load on elevator due to elevator deflection, S_{2T}	0.20
Tail-plane rolling moment coefficient due to sideslip, K_β	0.12

Vertical stabilizer

Fin lift curve slope, a_{1F}	1.7/rad
Rudder lift curve slope, a_{2F}	1.0/rad
Rudder hinge moment coefficient due to fin incidence, b_{1F}	+0.3/rad
Rudder hinge moment coefficient due to rudder deflection, b_{2F}	−0.33/rad
Effective rudder angle at full deflection	0.37rad
Proponion of air-load on rudder due to fin incidence, S_{1F}	0.10
Proportion of air-load on rudder due to rudder deflection, S_{2F}	0.25

Lateral/directional stability coefficients

Rolling moment coefficient due to:
- roll, L_p -0.20/rad
- yaw, L_r $+(0.03 + 0.12C_L)$/rad
- sideslip, L_v $-(0.025 + 0.04C_L)$/rad

Yawing moment coefficient due to:
- roll, N_p -0.017/rad
- yaw, N_r $(0.05 + 0.08C_L^2)$/rad
- sideslip, N_v 0.05/rad

sideslip coefficient due to:
- roll, Y_p 0.035/rad
- yaw, Y_r 0.10/rad
- sideslip, Y_v -0.52/rad

Drag

Zero-lift drag coefficient, C_{dc}	0.038
Induced drag factor, K	0.065

$(C_d = C_{dc} + KC_L^2)$

AD1.4 Definition of design loading conditions

AD1.4.1 General – applicable requirements

The Cranfield A1 was originally designed to meet the provisions of British Civil Airworthiness Requirements. (BCAR), Section K. supplemented where it was considered to be necessary to cover the anticipated aerobatic manoeuvres. The additional provisions included the extension of the normal acceleration design limits as mentioned in Section **AD1.2.** The pitching acceleration cases were based on those suggested in BCAR Section D and outlined in Chapter 5, Sections 5.3.3 and 5.3.4. An analysis of experimental flight test results was used to estimate the loads in the more unusual aerobatic manoeuvres, such as lomcovàks and flick rolls.

BCAR Section K has now been superseded by JAR-23 and this latter document will be used as the basis for the load calculations outlined in this example. The main provisions of JAR-23 are referred to in the relevant sections of Chapter 3. However, by way of example. the scope of this calculation will be extended by applying the more comprehensive pitching acceleration analysis. as used for the original A1 load analysis, and the directional loading analysis based on the former United Kingdom military requirements covered in Chapter 5, Sections 5.5.2 and 5.5.3. In addition. for completeness, a design envelope analysis of the pitch/heave response of the aircraft to continuous turbulence is included.

AD1.4.2 Specification of design normal manoeuvres and speeds

The design normal manoeuvres and speeds are based on JAR-23 paragraphs 23.333 and 23.335. The specified limit normal acceleration factors, as given in Chapter 3, Table 3.1, are +6.0 and −3.0. The Cranfield A1 was originally cleared to effective values of $(n_1 m)$ of 6132 kg and $(n_2 m)$ of −4380 kg. The increase in mass to 945 kg during development up to 1990 implies that the strength of the airframe limits the acceptable normal limit acceleration factors to nominally 6.5 and −4.6. These values are used for design purposes rather than the somewhat lesser ones specified in JAR-23.333.

The manoeuvre speed, V_A, is based on the level flight stalling speed of the aircraft, V_S, see Chapter 2, Eqns (2.1) and (2.2). Using the data given in Section AD1.3 V_S is calculated to he 26.66 m/s with the C_{LMAX} value of 1.42. As the speed presented to the pilot of an aircraft is in knots this is approximately equivalent to 52 knots (26.8 m/s). Thus:

$$V_A = V_S(n_1)^{1/2} = 68 \text{ m/s} = 132 \text{ knots}$$

JAR-23.335 specifies that the minimum value for the cruising speed, V_C, may he evaluated from $V_C = 36(W/S)^{\frac{1}{2}}$ knots where Wand Sare the weight of the aircraft in lb and the wing area in ft^2, respectively, see Chapter 2 Section 2.6.2.3. For this case the equation yields 130 knots (66.9 m/s) as the minimum value for V_C. This is less than the calculated value for V_A. An alternative definition for V_C is that it need not exceed $0.9V_H$, where V_H is the maximum speed in level flight, see Section 2.6.2.4. Calculation, simulator studies, and flight tests show that the value of V_H at low altitude is 146.5 knots so that $0.9V_H$ is 132 knots (68 m/s). This is the same as the manoeuvre speed V_A. Therefore, in this instance, V_C is taken to be the same as V_A.

JAR-23.335 specifies that the design speed V_D should be at least $1.55V_{CMIN}$, see Chapter 2 Section 2.6.2.5. Using 130 knots as the minimum value of V_C yields V_D equal to 202 knots (104 m/s).

The gust speed V_B, Chapter 2 Section 2.6.2.6, is not applicable to this class of aircraft, see Chapter 3 Section 3.5.3.4.

The summary of the above is:

$n_1 = +6.5$
$n_2 = -4.6$
$V_A = V_C = 68$ m/s (132 knots) EAS
$V_D = 104$ m/s (202 knots) EAS

AD1.4.3 Manoeuvre diagram

The manoeuvre flight envelope follows directly from the summarized data given at the end of the previous section in conjunction with the information contained in Chapter 3, Section 3.2.3. It is shown in Fig. AD1.2. The chain dotted horizontal lines indicate the usual JAR-23 aerobatic aircraft limits.

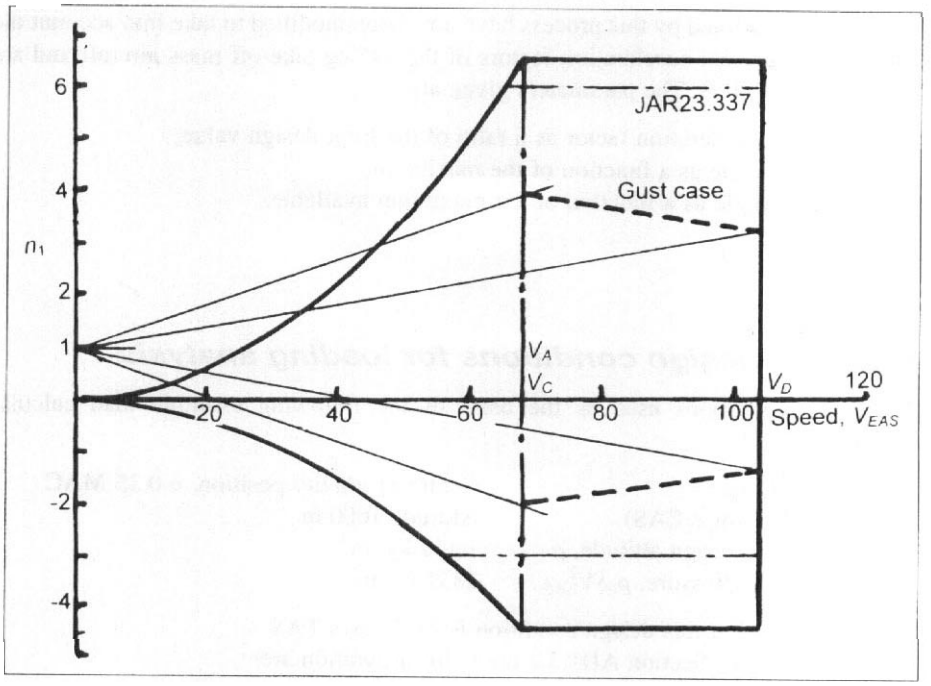

Fig. AD1.2 Flight envelope

Also shown in Fig. AD1.2 as dotted lines are the alleviated sharp-edged gust conditions at speeds V_C and V_D. These are for flight at 1000 m altitude, see Section AD1.4.5. The derivation is covered in Section AD1.9.2.

AD1.4.4 Load spectra

Normal acceleration load spectra exist for light aircraft designed to meet the standard aerobatic conditions. Many such aircraft are only used in a training role and the manoeuvres performed are not representative of those experienced in competition flying. In particular most of the normal acceleration events are positive whereas competition flying involves a significant number of negative events. In order to derive valid data for use in the fatigue design of the Cranfield A1, typical competition aerobatic routines and relevant data for military aircraft given by Taylor,[2] were analysed in conjunction with aerobatic pilots. Examples of such routines may be found in ***Aerobatics*** by Williams.[3] A typical competition routine lasts some 10 to 15 minutes and, since the competition manoeuvres dominate the load spectra, it was assumed that each flight hour included one competition flight.

[2]Taylor, J. ***Manual*** of Aircraft ***Loads***. AGARDograph 83. Pergamon Press. 1965,
[3]Williams, N. *Aerobatics*. Airlife Publications 1975.

The spectra derived by this process have now been modified to take into account the reduced limit normal acceleration factors of the 945 kg take-off mass aircraft and are shown in Fig. AD1.3. The parameters given are:

$\bar{g}$ normal acceleration factor as a ratio of the limit design value;
ξ_a aileron angle as a function of the maximum;
rudder angle as a function of the maximum available.

AD1.4.5 Design conditions for loading analysis

The design conditions used as the basis of the following example load calculations are:

Mass, m 945 kg	Centre of gravity position. h 0.25 MAC
Speed, V_C (68 m/s EAS)	Altitude 1000 m
Air density at design altitude, p	1.112 kg/m^3
Case dynamic pressure, $\rho_0 SV_{EAS}^2$	2632 N/m^2

The true airspeed at this design condition is 71.37 m/s TAS

From the data in Section AD1.3.2 the radii of gyration are:

Roll, k_x	1.177 m
Pitch, k_y	1.721 m
Yaw, k_z	2.018 m

The maximum available control angles are those given in Section AD1.3.4. All the loads auoted in the succeeding sections are limit loads, that is, the ultimate factor has not been applied.

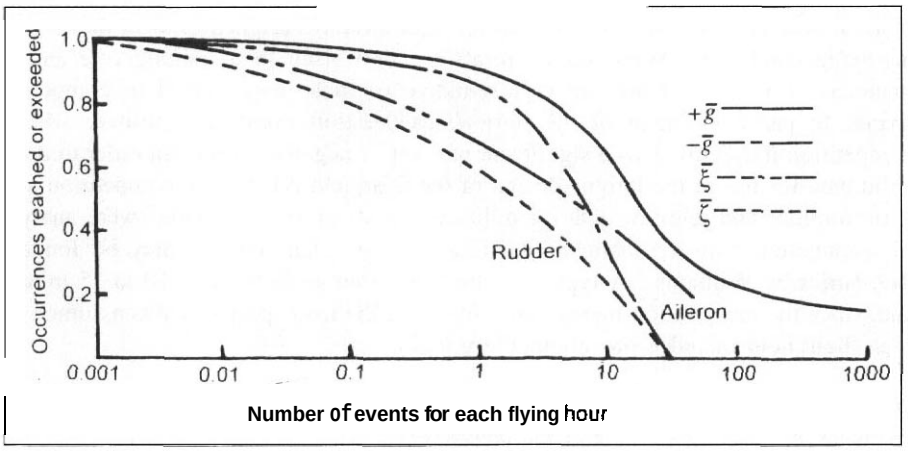

Fig. AD7.3 Load spectra

AD1.5 Symmetric manoeuvres – elevator deflection

AD1.5.1 Introduction

The symmetric manoeuvre conditions are outlined in Chapter 3, Section 3.2, and amplified in terms of the actual loading requirements in Chapter 5. Section 5.3. The calculation of the loading on the lifting surfaces utilizes the equations derived in Chapter 4, Section 4.2. 4.3. and 4.6, especially Section 4.6.3.

The conditions covered at the selected speed of V_C are:

(a) The application of the elevator to result in the nose-up and nose-down pitching accelerations specified in JAR-23.423.

(b) The unchecked movement of the elevator to the limit $\pm ng$ condition using a step input.

(c) The unchecked movement of the elevator to the limit $\pm ng$ condition and from the $\pm ng$ condition back to level flight using the reduced rate of elevator application given by Eqn. (5.23b).

(d) The sinusoidal application of elevator to pitch from 1g to $+n_1 g$ and to pitch back from $+n_1 g$ to $1g$.

There is also a requirement for the full, unchecked, application of the available elevator angle at speed V_A. Since V_A is equal to V_C in this instance it could well give the critical load case and hence this will also be evaluated. The analysis procedure is outlined in more detail in Addenda AD2. Section AD2.3.

ADI.5.2 Calculation of aircraft characteristics

It is convenient to calculate the relevant aircraft characteristics in the pitching mode as a precursor to the derivation of the loads. This is done by using the data presented in Section AD1.3 in the appropriate equations, as outlined below.

Non-dimensional time constant, Eqn. (4.61b), τ	0.6332
Longitudinal relative density, Eqn. (4.61d), μ_1	71.515
Tail arm. Eqn. (4.5), ℓ_T,	4.081
Tail volume coefficient, Eqn. (4.24), $\bar{V}$	0.468
Stick-fixed static margin. Eqn. (4.30). K_n	0.123
Stick-fixed manoeuvre margin. Eqn. (4.37c), H_m	0.169
Damping coefficient, Eqn. (4.82b), R_1	4.040
Damped natural frequency, Eqn. (4.82c), J_1	5.212
Undamped natural frequency, Eqn. (4.83a), ω_1	6.594
Elevator application function, Eqn. (4.82e and f), δ_1	−48.48
Approximate elevator application function. Eqn. (4.82g), δ_1 approx.	−47.65
Damping ratio, Eqn. (4.83b), ζ_{D1}	0.613
$\mathrm{Exp}(-\pi R_1/J_1)$,	0.0876
Elevator step input over-swing factor, Eqn. (5.16d), Σ	0.9194

Unchecked elevator application function, k	24.89
Sinusoidal elevator input frequency, Eqn. (5.29a), φ_1	6.594
Sinusoidal elevator input frequency, Eqn. (5.29b), φ_2	2.481
Sinusoidal elevator input term, Eqn. (5.27c), Γ	0
Sinusoidal elevator input magnitude parameter. Eqn. (5.31d), Y_1	55.80
Sinusoidal elevator input magnitude parameter. Eqn. (5.31e), Y_2	26.94
Sinusoidal elevator input magnitude parameter, Eqn. (5.31c), y	−2.071
$\mathrm{Tan}^{-1}y$	2.021

AD1.5.3 Evaluation of the datum flight conditions

AD1.5.3.1 Introduction

The level flight trim condition is the baseline upon which the manoeuvre loads are superimposed. The relevant equations are to be found in Chapter 4, Eqns (4.9) and (4.10). The elevator angle required to trim the aircraft is given by Eqn. (4.19).

The nose-down pitch condition from $n_1 g$ to $1g$ assumes that before the application of the required down-elevator the aircraft is in a quasi-trimmed condition at zero pitching velocity. That is, the loads on the aircraft are the sum of the level flight trim condition and the steady rotation loading corresponding to An $=$ (6.5−1). Likewise the nose-up pitchcase from $n_2 g$ to $1g$ is the sum of the level flight trim loading and that arising in the steady rotation with An $=$ (−4.6 − 1). The steady rotation conditions are evaluated in Section AD1.5.4.

AD1.5.3.2 Level flight trim, zero pitching condition

In the first case referred to above it is usual to make the initial assumption that the body angle, α_B, is zero to obtain a first estimate of the trimming tail load and the corresponding wing–body load. This latter is then used in Eqn. (4.14d) to derive a first estimate of the body angle to be used for a second evaluation of the trimming load.

It is further assumed in this analysis that the local moment on the tail due to the chord-wise displacement of the incidence and control centres of pressure, M_T, is negligible in comparison with the other moment terms.

The zero-lift pitching moment, Eqn. (4.20), is found to be −2154 N m and the moment due to the vertical offset of the thrust from the centre of gravity is − 10.6 N m.

First estimate of trim condition, a, assumed zero, Eqn. (4.10):

Tail load to trim, $\mathcal{L}_T$	− 316.4 N
Wing–body load, $\mathcal{L}_{WB}$	9587 N
Corresponding body angle, α_B	0.02220 rad

Second estimate of trim condition, $\alpha_B = 0.0222$ rad, Eqn. (4.9):

Tail load to trim, $\mathcal{L}_T$	− 319.1 N
Wing–body load, $\mathcal{L}_{WB}$	9590 N
Corresponding body angle, a,	0.022 22 rad

Thus the second estimate is acceptable.

The elevator angle to trim, Eqn. (4.19). η_{Trim}, is calculated as -0.0559 rad (up) and the load just due to this elevator deflection, $\mathcal{L}_{T\eta}$, is -732.6 N. The corresponding load due to the incidence of the tail-plane is the algebraic sum of this value and the total trim tail load, that is $+413.4$ N.

AD1.5.3.3 Quasi-steady flight at 6.5*g* with constant pitching velocity

Section AD1.5.4 gives the incremental tail loads due to elevator deflection and incidence for this case as -3318 N and 4479.2 N. respectively. Thus, using the level flight trim values derived in the previous section, the total loading is made up as follows:

Tail load due to incidence in trimmed level flight	413.4 N
Tail load due to elevator deflection in trimmed level flight	732.6 N
Increment in incidence tail load due to the steady manoeuvre	4479.2 N
Increment in elevator load due to the steady manoeuvre	-3318 N
Total tail load due to incidence	4892.6 N
Total tail load due to elevator deflection	-4050.6 N
Total tail load	842 N
Wing–body load in trimmed level flight	9590 N
Incremental wing–body load due to manoeuvre	50 978 N
Total wing–body load	60 577 N
Corresponding wing–body angle of attack	0.2993 rad
Corresponding wing–body lift coefficient	1.418

The total load due to the deflection of the elevator is within the limiting value stated in SectionAD1.5.4.The trimmed lift coefficient for the case is just within the maximum value of 1.42. The case drag coefficient of 0.1685 implies that if it is required to maintain a steady flight condition the thrust would need to be 3.5 times the maximum available.

AD1.5.3.4 Quasi-steady flight at $-4.6g$ with constant pitching velocity

Although there is no stipulated case in the requirements for the entry and exit from negative, nose-down, manoeuvres for comparative purposes this condition will also be evaluated. The nominal conditions for a constant pitching velocity at $-4.6g$ are stated in Section AD1.5.4 which gives the incremental tail loads due to elevator deflection and incidence as 3380 and -4560.6 N, respectively. The overall loading is thus:

Tail load due to incidence in trimmed level flight	413.4 N
Tail load due to elevator deflection in trimmed level flight	-732.6 N
Increment in incidence tail load due to the steady manoeuvre	4560.6 N
Increment in elevator load due to the steady manoeuvre	3380 N
Total tail load due to incidence	-4147.2 N
Total tail load due to elevator deflection	2647.4 N

Total tail load	−1499.8 N
Wing–body load in trimmed level flight	9590 N
Incremental wing–body load due to manoeuvre	−51 915 N
Total wing–body load	−42 325 N
Corresponding wing–body angle of attack	−0.2615 rad
Corresponding wing–body lift coefficient	−0.991

The total elevator load is well within the limiting value quoted in the next section. The trimmed lift coefficient for the case is −0.991, just within the maximum negative value of 1.0. The case drag coefficient of 0.101 implies that if it is required to maintain a steady flight condition the thrust would need to be about twice the maximum available.

AD1.5.4 Steady rotary motion

The idealized steady rotary motion condition is a datum for the determination of the required elevator deflection in both constant and variable pitching velocity conditions.

The elevator angle, η_{SS}, needed to maintain the aircraft at a constant pitching velocity, corresponding to a given normal acceleration, is derived at Eqn. (5.11a) and the corresponding tail load due only to the deflection of the elevator, is given by Eqn. (5.12a). The incidence contribution to the tail load derives from Eqn. (5.20). The relevant values are as follows.

Steady $6.5g$ (An = 5.5):	
Incremental elevator angle, η_{SS}	− 0.2534 rad
Tail load due to elevator deflection, $\mathcal{L}_{\eta SS}$	− 3318 N
Tail load due to incidence, $\mathcal{L}_{T\alpha SS}$	4479.2 N
Pitch rate, θ	0.794 rad/s
Steady $-4.6g$ (An = −5.6):	
Incremental elevator angle, η_{SS}	0.2580 rad
Tail load due to elevator deflection. $\mathcal{L}_{\eta SS}$	3380 N
Tail load due to incidence, $\mathcal{L}_{T\alpha SS}$	− 4560.6 N
Pitch rate, $\dot{\theta}$	− 0.808 rad/s

In this context it may be noted that the maximum available load as a consequence of the deflection of the elevator is ±5242 N.

AD1.5.5 Unchecked manoeuvres

AD1.5.5.1 Pitching acceleration as specified by JAR-23 at speed V_C

The design pitching accelerations for light aircraft are specified in JAR-23.423 and are quoted in Chapter 5, Section 5.3.2.2. Although the implication of the requirement is that the elevator angle is removed as soon as the desired normal acceleration is achieved, effectively a checked manoeuvre, this case is included here since the derived tail loads are comparable to the unchecked cases.

In this case for n_1 of $+6.5$ the nose-up pitching acceleration from $1g$ to $6.5g$ is found to be 9.614 rad/s^2 and that for nose-down pitch from $6.5g$ to 1g $-9.614 rad/s^2$. Use of Eqn. (5.13b) gives the incremental tail loads needed to achieve these accelerations as -6596 and $+6596$ N, respectively. These, being entirely due to the deflection of the elevator, are, by themselves, greater than the maximum value quoted in Section AD1.5.4. However, the total loading is obtained by superimposing these loads on those on the appropriate initial condition as derived in Section AD1.5.3:

Nose-up pitch:	
Incidence tail load	413.4 N
Load doe to elevator deflection	– 7328 N
Total load	– 6915 N

However, the elevator load cannot exceed -5242 N which implies that only -4510 N is available for the manoeuvre. Thus the maximum nose-up pitch acceleration that can be physically achieved is 6.565 rad/s^2 and the final loads become:

Nose-up pitch:	
Incidence tail load	413.4 N
Load due to elevator deflection	-5242 N
Total load	-4829 N
Nose-down pitch:	
Incidence tail load	$+4893$ N
Load due to elevator deflection	2455.5 N
Total load	7348 N

The elevator load in the nose-down case is within the available magnitude and so the prescribed pitching acceleration can be obtained. In passing it is worthy of note that in FAR-25.331 the given nose-down acceleration is only two-thirds of that in the light aircraft requirements resulting in an incremental load due to elevator deflection of 4397 N and a total tail load of 5239 N

AD1.5.5.2 Step input of elevator deflection to give the required normal acceleration at speed V_C

Chapter 5, Section 5.3.3.2, outlines the analysis for this condition. When allowance is made for the over-swing factor, Σ, the step elevator inputs required to pitch the aircraft nose-up to $+6.5g$ and to pitch nose-down to $-4.6g$ are found to be -0.233 and $+0.237$ rad, respectively. The corresponding tail loads due to the deflection of the elevator, given by Eqn. (5.18a), are -3054 and $+3110$ N. If it is assumed that the elevator deflections are held until the end of the first half cycle of the motion. the maximum angle of attack, the tail incidence loads, $\mathcal{L}_{T\alpha}$, are $+4483$ and -4564 N, giving total tail load increments due to the manoeuvre of $+1429$ and -1454 N.

Superimposing these loads upon the initial trim values gives:

Nose-up pitch, $1g$ *to* $6.5g$:	
Incidence tail load	+4896 N
Load due to elevator deflection	−3787 N
Total load	+1109 N
Nose-down pitch. $1g$ *to* $-4.6g$:	
Incidence tail load	−4151 N
Load due to elevator deflection	+2377 N
Total load	−1773 N

AD1.5.5.3 Exponential unchecked manoeuvre at speed V_C

This case is covered by Chapter 5, Section 5.3.3.3. The analysis quoted by Richards,[4] provides for the calculation of the loads both to initiate the unchecked motion and to return the aircraft back to level flight at some later time. A summary of the results of applying the method follows

Nose-up from $1g$ *to* $+6.5g$:	
Elevator deflection, Eqn. (5.24a), η_1	+ 0.188 rad
Load due to elevator deflection, Eqn. (5.25a)	−2465 N
Corresponding total manoeuvre tail load, Eqn. (5.26)	−1886 N
Load due to incidence in manoeuvre (Eqn. (5.26)−Eqn.(5.25a)}	+579 N
Total incidence load including trim loads, see Section AD1.5.3.2	+992 N
Total loads due to elevator deflection, including trim	−3197 N
Total tail load	−2205 N
Nose-down from $+6.5g$ *to* $1g$:	
Elevator deflection, Eqn. (5.24b), η_2	−0.0654 rad
Load due to elevator deflection, Eqn. (5.25b)	−857 N
Corresponding total manoeuvre tail load. Eqn. (5.26)	+1886 N
Load due to incidence in manoeuvre, (Eqn. (5.26)−Eqn.(5.25b)}	+2742 N
Total incidence load including mm loads, see Section AD1.5.3.3	+7634.5 N
Total loads due to elevator deflection, including trim	−4907.5 N
Total tail load	+2727 N
Nose-down from $1g$ *to* $-4.6g$:	
Elevator deflection, Eqn. (5.24a), η_1	+0.191 rad
Load due to elevator deflection, Eqn. (5.25a)	+2509 N
Corresponding total manoeuvre tail load, Eqn. (5.26)	+1920 N
Load due to incidence in manoeuvre. {Eqn. (5.26)−Eqn. (5.25a)}	−589 N
Total incidence load including trim loads, see Section AD1.5.3.2	−176 N
Total loads due to elevator deflection, including trim	+1776 N
Total tail load	+1601 N

[4] Richards *L.W. Aircraft Engineering.* January, Febmary, March, 1960.

Nose-up from $-4.6g$ to $1g$:

Elevator deflection, Eqn. (5.24b), η_2	+0.0666 rad
Load due to elevator deflection, Eqn. (5.25b)	+873 N
Corresponding total manoeuvre tail load, Eqn. (5.26)	−1920 N
Load due to incidence in manoeuvre. {Eqn. (5.26)−Eqn. (5.25b)}	−2792 N
Total incidence load including trim loads. see Section AD1.5.3.4	−6939.2 N
Total loads due to elevator deflection. including trim	+3520.4 N
Total tail load	−3419 N

AD1.5.5.4 Movement of the elevator to maximum available angle at speed V_A

This case is referred to in Chapter 3. Section 3.2.4. It is similar to the case covered in Section AD1.5.5.2except that the criterion is the maximum elevator deflection rather than a given pitching acceleration. Thus the analysis follows that of Section AD1.5.5.1. In the evaluation of the available elevator force it is necessary to make allowance for the $1g$ trim condition applying at the instant the control is moved.

Nose-up pitch movement of *the* elevator *from* $1g$:
In the case of elevator motion to pitch nose-up from level flight the trim situation requires an elevator load of −732 N (up) so that the net load available for the manoeuvre is −(5242 − 732) N or −4510 N. At the instant of the application of the elevator the only incidence load on the tail-plane is the trim force of 413.4 N. The resulting loading is:

Total incidence load	+413.4 N
Total load due to elevator deflection	−5242 N
Total tail load	−4828.6 N

Nose-down pitch movement of *the* elevatorfrom $1g$:
When the control is moved to give a nose-down pitching the load arising from the elevator deflection is now in the opposite sense to the trim case and is {5242−(−732)} N or 5955 N. The loading on the tail-plane is:

Total incidence load	+413.4 N
Total load due to elevator deflection	+5242 N
Total tail load	+5655.6 N

AD1.5.6 The checked manoeuvre at speed V_C

The analysis of the checked manoeuvre is based on that derived by Richards? and described in Chapter *5*, Section 5.3.4. The calculation proceeds in the same way as that for the unchecked exponential elevator application covered in Section AD1.5.5.3. The physical difference is that in the checked case the deflection of the elevator follows a continuous sinusoidal shape rather than being in two discrete, exponentially defined, stages. The critical frequency of application of the control in this case is found to be that

of the undamped pitching motion of the aircraft, see Chapter 5, Section 5.3.4.2 and also Section AD1.5.2, so that the Γ term in Eqns. (5.27) is zero. The analysis below covers only the positive normal manoeuvre. A summary of the results follows.

Nose-up from $1g$ ***to*** $+6.5g$:	
Maximum change in elevator angle during the manoeuvre, Eqn. (5.30), η_C	−0.3234 rad
Elevator deflection to pitch nose up, Eqn. (5.31a), η_1	−0.2640 rad
Load due to elevator deflection, Eqn. (5.33a)	−3225 N
Corresponding total manoeuvre tail load, Eqn. (5.32a)	−2109 N
Load due to incidence in manoeuvre, {Eqn. (5.32a) − Eqn. (5.33a)}	+1116 N
Total incidence load including trim loads, see Section AD1.5.3.2	+1529 N
Total loads due to elevator deflection, including trim	−3957 N
Total tail load	−2428 N
Nose-down from $6.5g$ ***to*** $1g$:	
Elevator deflection, Eqns (5.31b) to (5.31e), η_2	+0.1410 rad
Load due to elevator deflection, Eqn. (5.33b)	+1848 N
Corresponding total manoeuvre tail load, Eqn. (5.32b)	+3312 N
Load due to incidence in manoeuvre, {Eqn. (5.32b) − Eqn. (5.33b)}	+1464 N
Total incidence load including trim loads. see Section AD1.5.3.3	6356.5 N
Total loads due to elevator deflection, including trim	−2202.5 N
Total tail load	+4154 N

AD1.5.7 Maximum design tail loads

AD1.5.7.1 Introduction

The maximum, or design, tail load is found by a comparison of the various cases investigated. As would be expected, since the conditions of Chapter 5, Section 5.3.5 have been met, the checked manoeuvre gives higher loads that those in the unchecked, exponential, elevator movement case.

AD1.5.7.2 Speed V_C

The maximum checked manoeuvre loads are:

Nose-up $1g$ to $6.5g$	−2428 N
Nose-down $6.5g$ to $1g$	+4154 N

Although the step input of control demand yields a higher load due to the deflection of the elevator than in the exponential input case, the total load at the end of the first half cycle of the consequent motion is less than the critical load derived for the latter case. This implies that the critical load occurs at some point before the maximum angle of attack is reached.

The exponential input applied to the negative normal manoeuvre results in the development of lower loads than in the positive normal manoeuvre situation, hut the reverse is true of the step input. Nevertheless, all the negative unchecked manoeuvre loads are less than the checked ones quoted above.

It is useful to compare the initial tail loads with those derived by application of the pitching accelerations specified in JAR-23.423 and stated in Section AD1.5.5.1. These loads are seen to be significantly higher than those derived from the more rational approach of the sinusoidal checked manoeuvre:

Nose-up case, limited by the available elevator angle	−4828 N
Nose-down case, JAR-23.423 (light aircraft)	7348 N
Nose-down case, FAR-25.331 (transport aircraft)	5239 N

AD1.5.7.3 Speed V_A

For most aircraft the manoeuvre speed. V_A, is less than the cruise speed, V_C, and thus it is not immediately clear whether the elevator deflection conditions at V_C will give greater loads than the V_A case of step movement of the elevator to the maximum available up and down limits. In this case it happens that V_A has the same value as V_C so that it may be expected that the V_A case could yield greater loads than those determined by the unchecked exponential and checked sinusoidal elevator motions at V_C. This is found to be the case, the total tail loads for the V_A requirement being:

Nose-up case	−4828 N
Nose-down case	+5656 N

It will be noticed that the nose-up load is the same as that derived due to the application of the JAR-23.423 pitching acceleration formula since the latter is limited by the available elevator angle and the speeds are the same. However, the nose-down case is less than the corresponding load from the JAR-23.423 analysis since the V_A case is associated with the $1g$ trim condition rather than the $6.5g$ trim condition. Nevertheless the V_A case does give a higher load than the nose-down FAR-25.331 pitching acceleration requirement for a transport aircraft.

AD1.5.7.4 Design loads

From the foregoing it is deduced that the deign maximum loads are:

Up load (JAR-23.423 case)	7348 N
Down load (JAR-23.423 case and V_A case)	−4828 N

The severe upload condition suggests that further investigation should be made to determine whether or not it would be justified to reduce the magnitude to the FAR-25 V_A case value of 5239 N.

AD1.5.8 Loads on the elevator

The values of S_{1T} and S_{2T} indicate that of the incidence-dependent load only some 8 per cent is located over the elevator itself while for the elevator-dependent load the value is 20 per cent, see Chapter 5, Section 5.3.7. The load on the elevator follows from these values as given by Eqn. (5.35).

Examination of the various load cases reveals that the highest load on the elevator arises in the nose-up and nose-down conditions at speed V_A. The nose-up case gives a load of -1107 N on the elevator itself, this being marginally greater than the nose-down load of $+1081$ N. Interestingly the JAR-23.423 nose-down case is not critical for the elevator, the relevant load being $+1011$ N.

AD1.5.9 Tail-plane torques

The method of evaluation of the design torque on the tail-plane is outlined in Chapter 5, Section 5.3.6.3. In structural terms the torque is the chord-wise moment about the local centre of twist of the section, hut as this is likely to be unknown at the initial loading phase it is more convenient to select a suitable reference point. This chord-wise location should preferably be close to the anticipated centre of twist, see Chapter 12, Section 12.5.

In the present case it will be assumed that the chord-wise centre of pressure of the tail-plane load due to incidence lies at the 0.25 chord location and that due to the deflection of the elevator at the 0.41 chord position. For simplicity the torque will be evaluated about the tail-plane 0.33 mean aerodynamic chord point which, it is anticipated, will lie close to the actual local centre of twist. Thus in this analysis the incidence load is taken to be 0.0714 m ahead of the reference point and the load due to elevator deflection 0.0714 m aft of it.

It is necessary to calculate the torques for all of the loading cases considered in Sections AD1.5.3, AD1.5.5, and AD1.5.6; in addition, as stated in Chapter 5, Section 5.3.6.3, there are two further considerations:

(a) ***Unchecked exponential manoeuvre.*** The combination of the incidence load coinciding with the maximum angle of attack, $\mathcal{L}_{T\alpha}$, see Section AD1.5.5.2, and the elevator load corresponding to the angle needed to maintain the steady rotary motion, see Section AD1.5.4. These loads are $+4483$ and -3318 N, respectively, for the nose-up pitch case to $+6.5g$ and -4564 and $+3382$ N. respectively, for the pitch down to $-4.6g$ case. Since these loads are manoeuvre increments the torques derived from them must be added to the level flight trim value.

(b) ***Checked sinusoidal manoeuvre.*** The combination of an incidence load of 1.2 times $\mathcal{L}_{T\alpha}$, and the load due to the deflection of the elevator to the maximum value reached in the manoeuvre, η_C, see Section AD1.5.6. These two loads are found to be $+5380$ and -4235 N, respectively, and, as in (a) above, must be added to the level flight trim case.

As an example of the calculation, the torque in the level flight trim condition may be cited. From Section AD1.5.3.2 the tail-plane incidence load is +413.4 N and that due to the trimming elevator deflection is −732.6 N. Thus the torque is:

$$413.4 \times 0.0714 - (-732.6) \times 0.0714 = 81.6\,\text{N} \cdot \text{m}$$

When all the cases are examined a maximum nose-up torque of 774 N . m is found to occur in the unchecked exponential nose-down pitch from $+6.5g$ back to level flight. This is marginally greater than the 770 N . m derived from the additional checked manoeuvre case of (b) ahove. The maximum nose-down torque of −502 N . m derives from the quasi-steady case at $+6.5g$ normal acceleration.

ADI.5.10 Derivation of stressing data

Although it is beyond the scope of this example the next stage of the loading analysis is the distribution of the calculated design air-loads across the appropriate lifting surfaces as described in Chapter 9. These air-load distributions must he combined with the inertia distributions resulting from the action of the relevant normal and pitching accelerations on the local masses before undertaking span-wise integration to obtain the shear force, bending moment, and torque diagrams. This procedure is outlined in Chapter 12, Section 12.3, and reference may also be made to Addenda AD2.

Note that although the tail-plane loads derived in the previous sections are distributed symmetrically across the span there is also the asymmetric case, this being dealt with in Section AD1.8.

AD1.6 Lateral manoeuvres − aileron deflection

In terms of loading cases the consequences of deflection of the ailerons to initiate a rolling motion is relatively straightfonvard, as is outlined in Chapter 3, Section 3.3.2, and amplified in Chapter 5, Section 5.4. The analysis is dependent upon the equations developed in Chapter 4, especially Section 4.7.4. The calculations involved consist of:

(a) Evaluating the initial rolling acceleration consequent upon the step deflection of the aileron to the prescribed value using Eqn. (5.36b).
(b) Calculating the maximum, steady, rate of roll achieved as aconscquence of that aileron deflection, Eqn. (5.37).

When the ailerons are moved to the effective maximum deflection of 0.28 rad at speed V_C the initial rolling acceleration is found to be $-27.66\,\text{rad/s}^2$ and the steady rate of roll 2.828 rad/s (162 deg/s). These results are used with the appropriate aerodynamic load distributions covered in Chapter 9, especially Section 9.3.3, and the relevant inertial relief effects to derive the stressing data, see Section AD1.5.10. The load increments due to the rolling manoeuvre must be superimposed upon the initial flight conditions as relevant.

AD1.7 Directional manoeuvres – rudder deflection

AD1.7.7 General remarks

The requirements associated with the deflection of the rudder to initiate yawing and sideslipping motion are specified in Chapter **3,** Section 3.3.3, and amplified in Chapter **5,** Section **5.5.** The analysis of the loads uses the equations developed in Chapter 4. especially Section 4.7.5.

While there are some similarities with the symmetric manoeuvre requirements there are also differences:

(a) It is usual that in steady level flight there is no loading on the vertical stabilizer and control surface as a consequence of the overall symmetry of the aircraft. Therefore there is no equivalent of the basic trim condition.

(b) When a step, unchecked, rudder deflection is applied the aircraft is considered to reach a steady, equilibrium, sideslip condition before the rudder is returned to the neutral position and the aircraft restored to normal flight. This is comparable to the idealized steady pitch rotary motion but unlike that case it is a practical possibility.

(c) Where it is relevant the sinusoidal application of rudder is allowed to continue for I or **1.5** cycles rather than being terminated at the end of the first half cycle as is the case for the elevator application.

(d) In the elevator-induced pitching motion the normal and pitching accelerations are effectively specified by the requirements. In the directional case they are less obvious due to the interaction between the yawing and sideslipping modes and have to be specifically calculated for each design condition. See Chapter **5,** Section 5.5.5.

The analysis procedure is outlined in Addendum AD3, Section AD3.4

AD1.7.2 Calculation of aircraft characteristics

In addition to the relevant numerical characteristics already derived for symmetric calculation in Section **AD1.5.2,** the following data are needed in the asymmetric analysis. These have been calculated from the data presented in Section AD1.3.

Non-dimensional roll inertia constant, Eqn. (4.61e), i_x	0.01359
Non-dimensional yaw inertia constant, Eqn. (4.61e), i_z	0.03994
Directional relative density. Eqn. (4.61d), μ_2	11.16
Fin volume coefficient, Eqn. (4.94b), $\bar{V}_1$	0.0565
Damping coefficient, Eqn. (4.100b), R_2	0.8709
Damped natural frequency, Eqn. (4.100c), J_2	3.702
Undamped natural frequency. Eqn. (4.101b), ω_2	3.802
Application function due to rate of rudder movement, Eqn. (4.100f), F_{21}	0.133
Application function due to rudder movement. Eqn. (4.100f), F_{22}	15.82

Damping ratio, Eqn. (4.101c), ζ_{D2}	0.229
$\text{Exp}(-\pi R_2/J_2)$	0.4776
$\text{Exp}(-2\pi R_2/J_2)$	0.2281
$\text{Exp}(-3\pi R_2/J_2)$	0.1089
Product of fin reference area and dynamic pressure, $\rho V_C^2 S_F/2$	5664 N

AD7.7.3 Unchecked directional manoeuvre – step input to rudder

AD1.7.3.1 General remarks

It is assumed that the rudder is moved abruptly to a specific deflection and held at that position until the aircraft has reached an equilibrium sideslip angle. Subsequently it is moved back to the neutral position and the aircraft returns to straight flight. At speed V_C the design rudder deflection is the maximum available, that is 0.37 rad.

AD1.7.3.2 Design sideslip angles

The major parameters in the determination of the design loads on the fin and rudder are the maximum, or over-swing. angle achieved at the end of the first half cycle of the motion and the eventual steady, equilibrium, sideslip angle. It follows from the data given in Sections AD1.3 and AD1.7.2 that for a step rudder deflection of 0.37 rad these sideslip angles are:

Equilibrium angle. Eqn. (5.45a), β_E	0.405 rad
Over-swing angle. Eqn. (5.46b), β_π	0.598 rad
Over-swing ratio	1.477

Even under dynamic conditions the second of these two angles is very high and stalling of the fin might be expected. Nevertheless, it will be retained here as the design value for the purpose of loading calculations.

AD1.7.3.3 Fin and rudder design loads

There are four combinations of the loads due to the fin incidence and the deflection of the rudder:

(a) Aircraft in initial straight flight. rudder suddenly deflected to 0.37 rad:

Load due to fin incidence	0 N
Load due to rudder deflection, Eqn. (5.48a)	2096 N
Total load	2096 N

(b) Aircraft at over-swing sideslip angle, rudder deflection maintained:

Load due to fin incidence, Eqn. (5.48b)	−5868 N
Load due to rudder deflection, Eqn. (5.48a)	2096 N
Total load	−3772 N

(c) Aircraft at the equilibrium sideslip angle, rudder deflection maintained:

Load due to fin incidence, Eqn. (5.48c)	–3971 N
Load due to rudder deflection. Eqn. (5.48a)	2096 N
Total load	– 1875 N

(d) Aircraft at the equilibrium sideslip angle, rudder returned to neutral:

Load due to fin incidence, Eqn. (5.48b)	–3971 N
Load due to rudder deflection, Eqn. (5.48c)	0 N
Total load	–3971 N

The greatest total load on the fin and rudder is seen to arise when the rudder angle is removed at the equilibrium condition, although this is only marginally higher than in the over-swing case.

AD1.7.3.4 Accelerations at the centre of gravity due to the manoeuvres

The lateral acceleration factors at the centre of gravity of the aircraft are directly related to the four phases of the manoeuvre outlined in the previous section. They are found to he:

Condition (a). Eqn. (5.57b)	0.226
Condition (b), Eqn. (5.59a)	– 1.149
Condition (c), Eqn. (5.60)	– 0.705
Condition (d), Eqn. (5.61a)	– 0.931

AD1.7.4 Sinusoidal application of the rudder

AD1.7.4.1 Introduction

Although the sinusoidal movement of the rudder is a military rather than civil requirement it is applied here to the A1 aircraft by way of example and for the purpose of comparison with the step input case covered in Section AD1.7.3.

AD1.7.4.2 Design rudder deflection

As stated in Chapter 3. Section 3.3.3.4(c), for a military aircraft the rudder deflection, ζ_e, to be used for the sinusoidal analysis is taken to be two-thirds of the angle used for the step calculations. This is 0.247 rad for the present example.

AD1.7.4.3 Design sideslip angles

The requirements for a combat aircraft are that the oscillation of the rudder should continue for 1.5 cycles, that is up to $(3\pi R_2/J_2)$ in non-dimensional time units. Non-combat aircraft are only required to maintain the oscillation to the end of the first

cycle of the motion, up to $(2\pi R_2/J_2)$. Both situations will be examined in this example. The resulting sideslip angles reached are found to be:

(a) Sideslip angle at the end of the first cycle, $\beta_{2\pi}$ – 0.467 rad
(b) Sideslip angle at the end of 1.5 cycles, $\beta_{3\pi}$ 0.539 rad

The comments made in Section AD1.7.3.2 concerning the stalling of the fin are relevant here also.

AD1.7.4.4 Fin and rudder loads

The load due to the deflection of the rudder to the design angle, ζ_c, of 0.247 rad is given by Eqn. (5.50d) as 1397 N. However, at the critical sideslip conditions at the end of 1 and 1.5 cycles the rudder is in the neutral position by definition so that there is no load from this source. The fin loads, entirely due to the incidence contribution, are calculated to be:

(a) After 1 cycle, Eqn. (5.50b) 4584 N
Associated with this condition, but not occurring at the same time, the approximate value of the load on the rudder itself is given by Eqn. (5.50c). This is further referred to in Section AD1.7.6.
(b) After 1.5 cycles, Eqn. (5.51b) –5292 N
The corresponding load on the rudder in this condition is given by Eqn. (5.51c)

AD1.7.4.5 Accelerations at the centre of gravity of the aircraft

The lateral acceleration factors at the centre of gravity in this manoeuvre are:

(a) After 1 cycle. Eqn. (5.63b) 0.503
(b) After 1.5 cycles, Eqn. (5.65b) –0.670

AD1.7.5 Design total fin and rudder loads

The maximum fin and rudder load resulting from the step input of the control is 3971 N which arises when the aircraft is in the equilibrium sideslip condition and the rudder is returned to the neutral position. As could be expected. in spite of the application of a lower rudder angle, the loads resulting from the sinnsoidal mode are higher being 4584 N at the end of the first cycle and –5992 N after 1.5 cycles. It is not unreasonable to consider that the combat aircraft requirement, which gives the latter of these two values, is representative of competition aerobatic flying and may be taken as the fin and rudder design load for the A1 aircraft.

AD1.7.6 Loads on the rudder

The loading on the rudder itself is evaluated in accordance with Chapter 5, Section 5.3.7 and the calculation procedure is the same as that used for the elevator in

Section AD1.5.8. The maximum load on the rudder in the unchecked, step, case arises at the instant that the rudder is moved to initiate the manoeuvre. The magnitude is 524 N. Use of Eqns. (5.50c) and (5.51c) for the loads at 1 and 1.5 cycles of the sinusoidal motion gives rudder loads of 696 N and 745 N. respectively. Use of the same argument as in the total fin and rudder load case of the previous section leads to the conclusion that the last value should he taken as the rudder design load.

AD1.7.7 Fin torque

The fin torque is calculated in the same way as the tail-plane torque in Section AD1.5.9. The application of the unchecked, step, input case is straightforward and the critical condition is invariably found to he the over-swing case. If it is assumed that the fin incidence load acts at the 0.25 chord location, the load due to the deflection of the rudder acts at 0.39 chord, and the torque reference axis is at the 0.32 fin mean chord point then the moment arm of the loads about the reference point is 0.0784 m. In the over-swing case the fin torque is found to he 624 N . m.

No torque design case is specified for the sinusoidal rudder case. However, by comparison with the comparable elevator case it is possible to calculate an overriding value using a factor of 1.2 applied to the incidence load combined with the load due to the maximum deflection of the rudder, ζ_e. Section AD1.7.4.4 quotes the latter as 1397 N. Using this in conjunction with the loads due to incidence, also given in Section AD1.7.4.4, results in torques of 541 and 607 N . m for the 1 and 1.5 cycle cases respectively. It will he noted that these are lower than the design value from the step input analysis.

ADI.7.8 Derivation of stressing data

The information needed for the structural design process is derived for the fin and rudder loads in the same manner as that used for the tail-plane and elevator and described in Section AD1.5.10. Reference may also be made to Addendum AD3.

AD1.8 Asymmetric tail-plane loads due to sideslip

This case is introduced in Chapter 3, Section 3.3.3.5, and the analysis is covered in Chapter 5, Section 5.6. The level flight trim load on the tail-plane, which may have been increased to allow for the effect of asymmetry on the zero-lift pitching moment, has to be distributed across the span to give the rolling moment defined by Eqn. (5.66). The value of the rolling moment coefficient, K_β, is given as 0.12 in Section AD1.3.4 and this leads to the distribution of the tail-plane lift such as to give a rolling moment of 2864β N . m. For the three possible design sideslip cases it becomes:

(a) Step rudder input, over-swing condition 1713 N . m
(b) Sinusoidal I cycle case -1338 N . m
(c) Sinusoidal 1.5 cycle case 1544 N . m

AD1.9 Gust and continuous turbulence considerations

AD7.9.7 Introduction

Although it is unlikely that atmospheric turbulence will provide critical loading cases for the A1 aircraft due to the high design normal manoeuvres it must he considered. The JAR-23 requirements for this class of aircraft specify only discrete gust cases at design speeds V_C and V_D. The details can be found in Chapter 3, Sections 3.5.2 and 3.5.3.4. The application to design is further dealt with in Chapter 6, Section 6.2.

Continuous turbulence analysis is not required for aircraft in the JAR-23 category However, by way of an example a design envelope analysis of the vertical air turbulence is undertaken and compared with the discrete gust results.

AD1.9.2 Discrete gust analysis–symmetric flight

This is based on the application of the alleviating factor, F_1, Eqn. (3.3) which is itself dependent upon the value of the gust relative density parameter, μ_{G1}, Eqn. (3.2). For the A1 aircraft at the design condition specified in Section AD1.4.5 the value of μ_{G1} is found to be 17.57 and the corresponding value of F_1 is 0.676. The design gust velocities. U_{de}, are 15.2 and 7.6 m/s at speeds V_C and V_D, respectively. Application of Eqn. (6.3) gives the following increments of normal acceleration factor due to aircraft encountering the alleviated sharp-edged gust:

At speed V_C ± 2.99
At speed V_D ± 2.28

The above increments have to be superimposed upon the level flight condition to give the following total normal acceleration factors:

At speed V_C:
positive $+3.99$
negative -1.99
At speed V_D:
positive $+3.28$
negative -1.28

These normal acceleration factors have been included in Fig. AD1.2 to provide comparison with the manoeuvre envelope. They lie well within the manoeuvre envelope.

AD1.9.3 Design envelope analysis

Continuous turbulence representation is introduced in Chapter 3, Section 3.5.2.3. It is further considered in Chapter 6, Section 6.4. and the application is in Sections 6.4.3 and 6.4.4, especially 6.4.4.3. The twodegree of freedom 'Peele' analysis considered in this latter section is applied here. At the V_C design speed of 68 m/s EAS the true speed is

71.37 m/s TAS at the 1000 m altitude design condition. The required pitch dynamic factors have already been evaluated for the manoeuvre analysis in Section AD1.5.2, namely:

Non-dimensional time constant, τ	0.633
Damping coefficient. R_1	4.040
Damped natural frequency, J_1	5.212
Undamped natural frequency, ω_1	6.594
Damping ratio, ζ_{D1}	0.613

The following analysis is needed, see Section 6.4.4.3(a) to (1). The gust scale factor, L, is taken to be 762 m.

Translational response distance constant, Eqn. (6.29a), δ_1	2635 m
Translational time response, Eqn. (6.29b), τ_1	0.369 s
Undamped natural frequency, real time, Eqn. (6.29c), f_{o1}	0.664 Hz
Relative gust scale, Eqn. (6.29e), s	967
Reduced frequency, Eqn. (6.290, k_{o1}	0.046
Product of gust scale and reduced frequency, Eqn. (6.29g), sk_{o1}	44.48
Kussner attenuation factor, $M_N = 0.2$, Fig. 6.6, $\bar{a}$	1.35
Product of reduced frequency and $\bar{a}$, $\bar{a}k_{o1}$	0.062

The non-dimensional response integrals for $sk_{o1} = 44.48$, $\bar{a}k_{o1} = 0.066$, and $\zeta_{D1} = 0.613$ are obtained from Figs 6.7(a) to (b) by extrapolation to the required ζ_{D1}.

$(\bar{R})_{01}$	0.94
$(\bar{R})_{21}$	0.04
$(\bar{R})_{41}$	0.05
$(\bar{R})_{61}$	0.35
Coefficient B_{11}, Eqn. (6.29k)	0.331
Coefficient B_{21}, Eqn. (6.29k)	−0.627

Dynamic response factors:

Heave load factor, Eqn. (6.30a), $(\bar{A})_{\Delta n}$	0.0694
Pitch angle, Eqn. (6.30b), $(\bar{A})_\theta$	−0.00852
Pitch rate, Eqn. (6.30c), $(\bar{A})_{\dot{\theta}}$	−0.00732
Pitch acceleration, Eqn. (6.30d), $(\bar{A})_{\ddot{\theta}}$	−0.034

The actual values of the response of the aircraft are obtained by multiplying the above response factors by the datum gust velocity. U_σ. Refemng to Chapter 3, Section 3.5.2.3, this is given as 25.91 m/s, hence:

Normal, heave, acceleration factor	1.8
Pitch angle	0.221 rad
Pitch rate	−0.19 rad/s
Pitch acceleration	−0.881 rad/s^2

There is a significant difference between the continuous turbulence normal acceleration factor of 1.8 and the equivalent alleviated sharp-edged value of 2.99 derived in the previous section. This is worthy of comment. The discrete gust analysis is based upon a single degree of freedom. heave, response of the aircraft, see Chapter 6, Section 6.4.4.2. The design envelope analysis includes the pitch response of the aircraft and reference to Figs 6.7(a) to (d) clearly shows the dependence of the response integrals on the pitch damping ratio. ζ_{D1}. It happens that the value of ζ_{D1} in this calculation is relatively high. primarily because the flight design condition is at low altitude. If. by way of comparison, an arbitrary value of ζ_{D1} equal to 0.2 is taken instead of 0.613 the relevant response integrals become:

$(\bar{R})_{21}$	0.14
$(\bar{R})_{41}$	0.13
and the coefficient B_{11}	0.0156

These values lead to $(\bar{A})_{\Delta n} = 0.104$ and a normal acceleration factor of 2.69 which is much closer to the discrete gust value.

AD1.10 Simulation

AD1.10.1 Introduction – scope of simulation

The Cranfield Flight Simulator,' is a real time, fixed base, representation of an aircraft and is primarily intended for the development of avionics and flight systems. The flight dynamics is based on the standard equations of motion of the aircraft as developed in Chapter 4, Sections 4.4 to 4.8. The coupling between all six degrees of motion is retained so that the behaviour of the simulation is representative of the aircraft being modelled.

The direct use of the simulator for the investigation of loading conditions is inconvenient and therefore for the present purposes the dynamic equations have been extracted to enable numerical simulation to be undertaken on a personal computer. This has necessitated the introduction of some limitations in the application of control demands which have to be selected from a menu of limited possibilities. The basic characteristics of this numerical simulation, as relevant to loading investigations, are:

(a) A facility to set a range of flight conditions:
- Airspeed (knots)
- Heading (deg)
- Altitude (ft)
- Rate of climb (ft/s)
- Landing gear position?
- Flap position*
- Engine lever setting (%)
- Elevator angle initial setting (deg)

Aileron angle initial setting (deg)
Rudder angle initial setting (deg)
* Not relevant to A1 aircraft

(b) An auto-trim capability which balances the normal and horizontal forces and pitching moments by adjustmenl of elevator angle and engine setting.

(c) The ability to input a single increment of elevator, aileron, and rudder deflection described by:
Continuous sinusoidal motion
Ramp
Doublet
Pulse
Step

(d) The ability to output. as a function of time, the following parameters:
Airspeed
Altitude
Rate of climb
Engine lever setting, %
Normal acceleration factor, G
Pitch angle (deg), θ
Pitch rate (deg/s), $d\theta/dt$
Roll angle (deg), φ
Roll rate (deg/s), $d\varphi/dt$
Yaw angle (deg), ψ
Yaw rate (deg/s), $d\psi/dt$
Body angle of attack (deg), α_B, Alpha
Rate of change of body angle (deg/s), $d\alpha_B/dt$, Alpha rate
Sideslip angle (deg), β, Beta
Rate of change of sideslip angle (deg/s), $d\beta/dt$, Beta rate
Elevator angle (deg), η
Aileron angle (deg), ξ
Rudder angle (deg), ζ

There are also facilities for the input of autopilot settings and weather variations not relevant to the present purposes except, possibly, for a turbulence feature.

Within the limitations of the equations of motion the aircraft characteristics used to represent the A1 aircraft were identical to those given in Section AD1.3. The simulations have all been performed for the design condition specified in Section AD1.4.5.

AD1.10.2 Trim conditions

The simulation was run with the aircraft in steady level flight at the design speed and altitude; the auto-trim function was used to establish the trim settings of the elevator and engine lever, together with the corresponding body angle of attack. The trim

elevator setting was found to be −4.184" (0.073 rad) and the body angle of attack +1.339" (0.0234 rad). The engine lever setting was 96.61 per cent of the maximum available.

The two former values may be compared with those derived by calculation in Section AD 1.5.3.2 which were a trim elevatorangle of −3.203' (0.0559 rad) and a body angle of +1.273° (0.0222 rad), respectively. The elevator angle derived from the simulation represents an additional elevator down load of about −230 N and a corresponding nose-up trimming moment of rather less than 1000 N . m. The variation of the body angle simply compensates for the increased elevator down load. The explanation for this discrepancy in the trimming moment lies in the representation in the simulation of the pitching moment due to the change in angle of attack. effectively the derivative M_{α} defined in Chapter 4, Section 4.6.2. Implicitly this assumes that the angles of attack of the wing and the horizontal stabilizer are identical. This is correct for changes from a datum condition but erroneous for the datum, that is the trim, case. In the A1 design the tail-plane is set at an angle of +1.72° relative to the wing–body no-lift condition and thus the simulation overestimates the tail-plane incidence load. the difference having to be offset by an increased elevator setting. It effectively means that the simulation introduces an additional pitching moment which is of the same order as that due to the zero-lift term but of opposite sign. This discrepancy has no effect upon the incremental conditions due to manoeuvres except that the maximum elevator angle available has to he compensated for the 0.984" (0.017 rad) difference in the trim angle Thus the elevator travel available in the simulation must be taken as −0.417 rad (−23.9") up and 0.383 rad (21.9") down.

As a matter of interest the simulation was run with the auto-trim facility off but with initial settings for the elevator angle and engine lever at −4.184°and 96.61 per cent. respectively. The output, as would be expected, was identical to the auto-trim case after a settling time of about 1 s.

AD1.10.3 Pitching manoeuvres

AD1.10.3.1 Introduction

The comparison of the simulation outputs with the analysis used to derive the loads in Section AD1.5 is of interest. The analysis is based on a number of assumptions, of which possibly the most important are:

(a) Manoeuvre loads are effectively assumed to be superimposed upon level Right conditions. This arises from the use of the 'steady rotary' motion of Chapter 5, Section 5.3.1.4, as the datum for establishing the deflection of the elevator needed to initiate a given manoeuvre.

(b) The forward speed is constant. This is clearly not true in practice as there is a tendency for the speed to fall as the aircraft pitches nose-up, due both to increased drag and the component of gravity acting along the flight path. In a pitch-down manoeuvre the speed variation may be less since the gravitational component tends to offset the increase of drag.

Recapitulating from Chapter 4, Section 4.2.1.1, the normal acceleration factor. Eqn. (4.4a) is:

$$cosy + An$$

where **An** is the increment due to the manoeuvre and γ is the angle of the flight path relative to the horizontal. Reference to Fig. 4.1 shows that γ is equal to $(\theta - \alpha_B)$ where θ is the pitch angle and α_B the body angle relative to the flight path direction. Thus, for those cases where $(\alpha)_B$ is zero, such as when α_B is constant or has reached a maximum value, in a manoeuvre:

$$\Delta n = \dot{\theta} V/g$$

The assumption that the flight path is level leads to:

$$\dot{\theta} = (n - 1)g/V$$

where n is the total normal acceleration factor. However, in practice:

$$a = (n - \cos\gamma)g/V$$

Thus in making comparisons between the analysis and the simulation the valid parameter is the pitching velocity, $\dot{\theta}$. In comparing the normal acceleration factors it is necessary to allow for both the change in flight path angle and the forward speed. In the simulation the pitch angle is defined in terms of the stability, that is the flight path, axes so that the change in γ is equal to the pitch angle. $(\theta)_s$ Hence:

$$G = (n)_s = cos(\theta)_s + \Delta n \qquad \text{(AD1.1)}$$

$$= cos(\theta)_s + (\theta)_s(V)_s/g \qquad \text{(AD1.2)}$$

where suffix 's' refers to the output from the simulator.

Further, it should be noted that in the analysis the times of the critical manoeuvre conditions are defined in terms of the displacement of the body angle, α_B, (Alpha).

AD1.10.3.2 Step elevator input. see Section AD1.5.5

A. Nose-up pitch, 1g to 6.5g at design speed V_C

The calculated elevator input for this case is given in Section AD1.5.5.2 as −0.233 rad (−13.35°). Figures AD1.4 and AD1.5 show the simulation outputs for:

(a) Auto-trim off.
(b) Elevator initial setting −4.184" (trim condition).
(c) Engine setting 96.61 per cent (trim condition).
(d) Elevator step input −13.35" (−0.234 rad) after 1 s and held there.

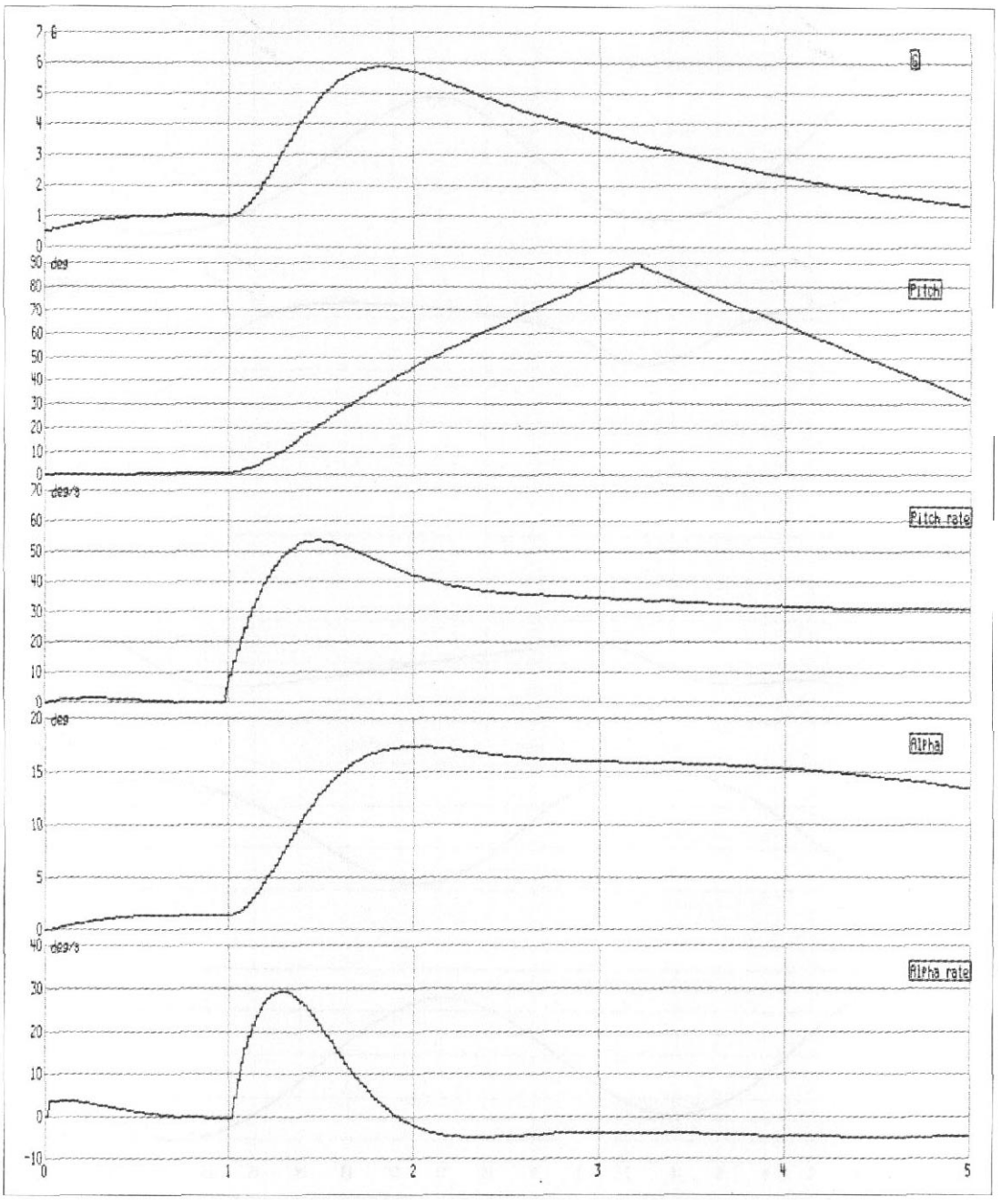

Fig. **AD1.4** **Nose-up pitch from level flight due to** -13.35° *elevator step input at* V_C

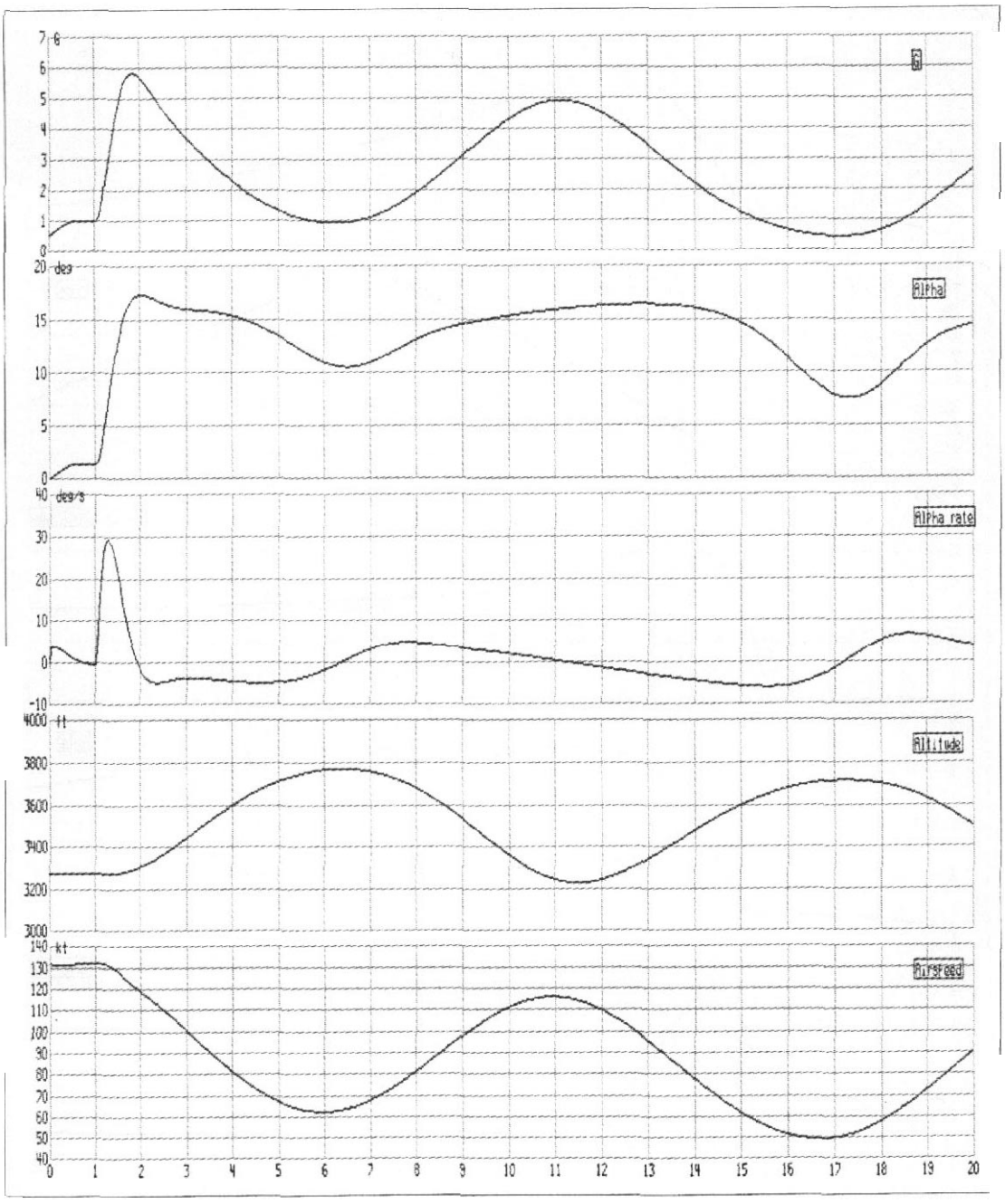

Fig. AD1.5 *Nose-up pitch from level flight due to* $-13.35°$ *elevator step input at* V_C

From Fig. AD1.4 it will be seen that Alpha, the body angle $(\alpha_B)_s$, reaches a maximum, as defined by the Alpha rate passing through zero. 0.9 s after the deflection of the control. This maximum value is 17.4" (0.304 rad) and coincides with a pitch rate, $(\theta)_s$, of 45°/s (0.785 rad/s) and a pitch angle, $(\theta)_s$, of 42" (0.733 rad). Figure AD1.5 is the output for same condition but over a 20 s timescale and shows alternative parameters. By the time Alpha has reached the first maximum value the forward speed has dropped from 132 knots (68 m/s) to 121 knots (62.3 m/s). Hence the simulator normal acceleration factor will not be 6.5, as used as the basis for calculating the elevator input quoted above, but from Eqn. (AD1.2):

$$(n)_s = cos(0.733) + 0.785 \times 62.3/9.81$$
$$= 0.743 + 4.988 = 5.72$$

The simulation output shows the maximum value of G, the normal acceleration factor, $(n)_s$ = 5.83, which falls to 5.75 at the time Alpha is a maximum, and so accounts for the difference in the values of n and $(n)_s$. In passing it may be noted that in order for the simulation to show a normal acceleration factor of 6.5 the elevator step input must be increased to − 15.3".

Since the body angle reaches the maximum value at the end of the first half cycle, that is 0.9 s after the elevator input, the period of the Alpha motion is 1.8 s. This is related to the non-dimensional natural damped frequency in radians, J_1, by:

$$(J_1)_s = 2\pi/(\tau \times \text{period}) \qquad \text{(AD1.3)}$$

where τ is the non-dimensional time constant, in this case 0.633, so that $(J_1)_s$ is equal to 5.51. This may be compared with the calculated value of 5.22.

The damping ratio in the motion may be deduced from the overshoot of Alpha relative to the eventual steady slate value. This latter is seen to be about 16° before other effects occur. Thus the overshoot ratio is:

$$(17.4^\circ - 16^\circ)/16^\circ = 0.088$$

In terms of the damping ratio, ζ_D, the overshoot ratio is:

$$[\exp\{\pi\zeta_D/(1-\zeta_D^2)^{1/2}\}]^{-1} \qquad \text{(AD1.4)}$$

which in this case gives $(\zeta_{D1})_s$ equal to 0.61 compared to a calculated value of 0.612.

The non-dimensional undamped natural frequency is related to the damped natural frequency and the damping ratio by:

$$(\omega_1)_s = (J_1)_s/(1-\zeta_{D1}^2)^{1/2} \qquad \text{(AD1.5)}$$

and in this case:

$$(\omega_1)_s = 5.51/(1 - 0.61^2)^{1/2} = 6.95$$

which compares with the calculated value of 6.59.

The simulation value of the damping coefficient, $(R_1)_s$, is the product of the damping ratio and the undamped natural frequency and is 4.24 compared to the calculated value of 4.04.

Overall, therefore. there are some small discrepancies between the analytical and simulated results, but see also Table ADI.1.

Figure AD1.5 also shows the effect of keeping the step elevator input in place thus introducing an out of trim condition. It will be seen that this results in a longer period, phugoid type, motion superimposed upon the short-period disturbance. The aircraft experiences significant changes in both altitude and forward speed. Figure **AD1.6** shows the same output parameters for the case when the elevator step input is replaced by a pulse of $-20°$ amplitude and 0.02 s width. The true phugoid motion resulting is confirmed by the fact that Alpha is effectively constant after the initial disturbance. The variations in both speed and altitude are relatively small.

B. Nose-down pitch, 6.5g to 1g at design speed V_C

Analytically this case assumes that the aircraft is in the quasi-steady condition at $6.5g$ normal acceleration and the elevator is moved to return it to $1g$ level flight. In order to try to reproduce this in the simulation the following procedure was adopted:

(a) Auto-trim set to off.

(b) Initial elevator setting at $-23.13°$ (-0.4 rad), to induce the pitching manoeuvre, the angle being that required to trim in this case.

(c) At time 7.7 s, when the pitch angle indicates that the aircraft is passing through upright level Bight. input a step elevator angle of $+18.95°$ (0.331 rad) to bring the elevator angle back to the $1g$ level flight trim value.

The simulation output for an initial forward speed of 132 knots (68 m/s) is shown in Fig. AD1.7. It will be noticed that following the step input of control at 7.7 s the aircraft does return to the desired condition except for a small nose-down pitch angle, but the value of the normal acceleration factor at the instant the elevator deflection is changed is only 4.9 rather than the required value of 6.5. This has arisen because the forward speed has dropped to 80 knots (41.2 m/s) by 7.7 s. However, the pitch rate of about 45°/s (0.785 rad/s) is consistent with the required value of 0.794 rad/s, see Section AD1.5.3.

Figure AD1.8 shows the output parameters for the same condition except that the entry speed to the manoeuvre has been increased to 198 knots (102 m/s). The aircraft returns to upright level flight within 5.6 s but by this time the forward speed has still fallen to as low as 112 knots (57.7 m/s). The normal acceleration factor is the required value of 6.5 which is achieved by vinue of the fact that the instantaneous pitching rate is about 53°/s, but it is still decreasing. Extension of the simulation

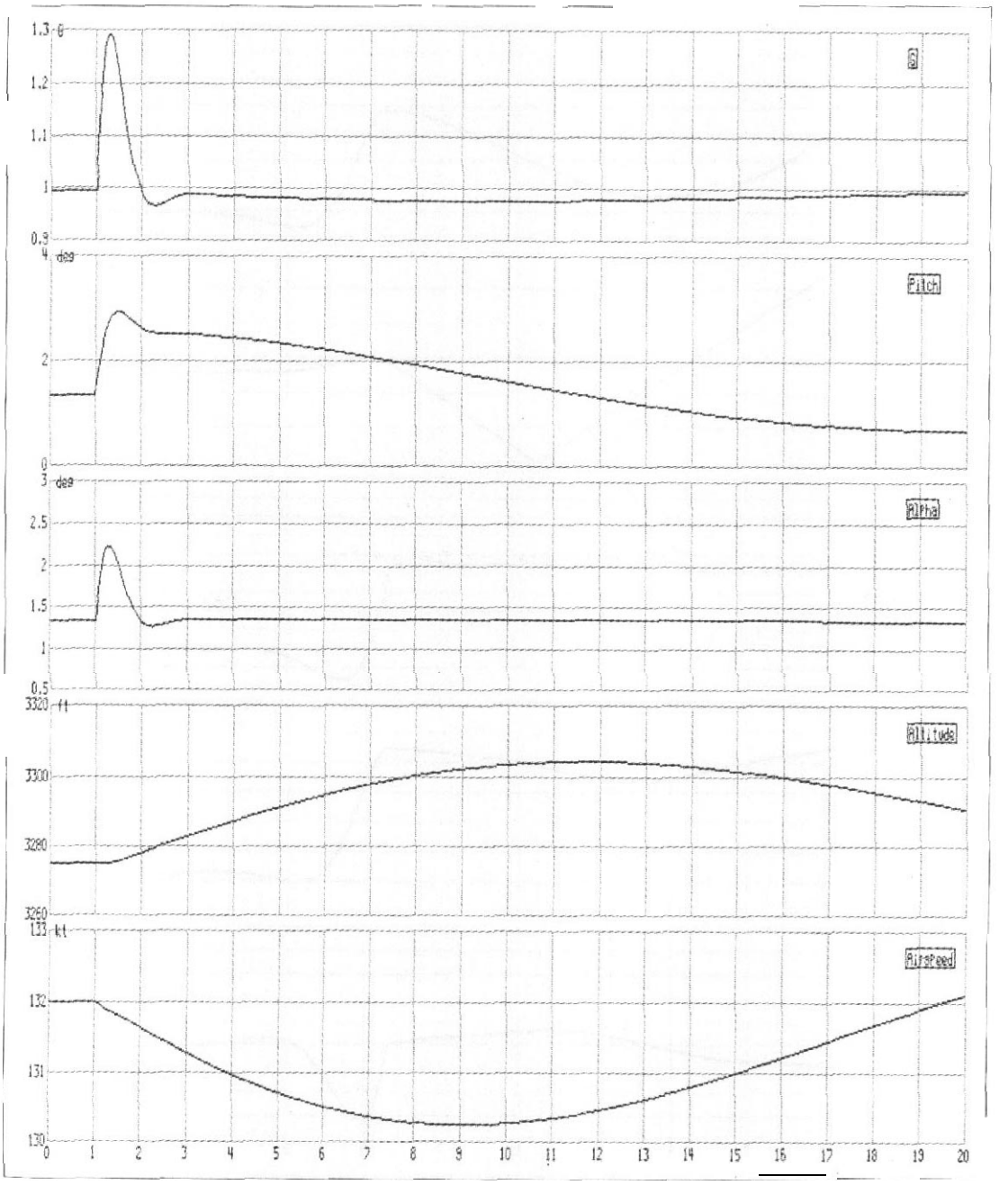

Fig. AD1.6 ***Consequence*** *of a* 20 . *0 02 s width elevator pulse input at* V_C

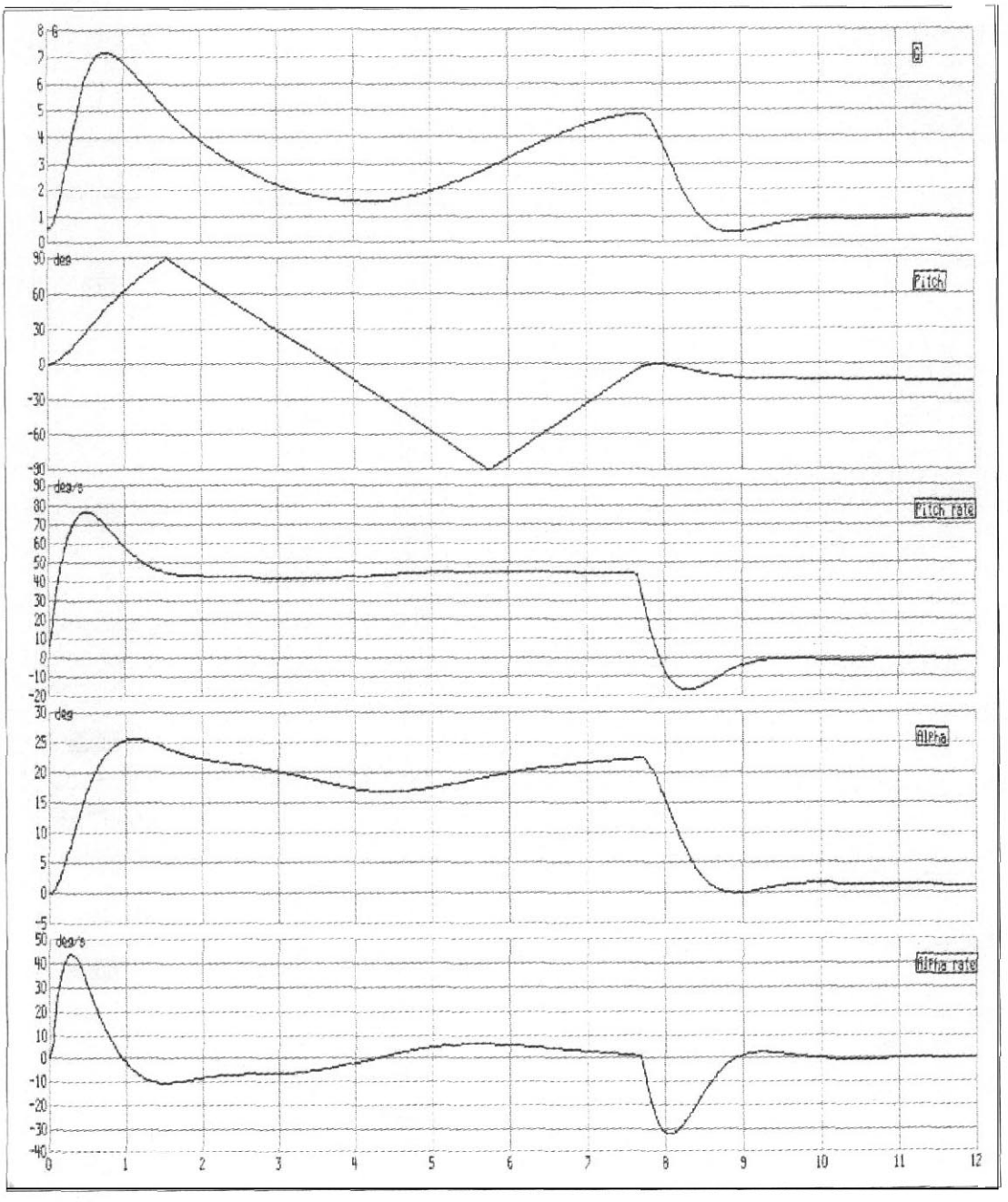

Fig. AD1.7 ***Nose-down*** *pitch from* 6.5*g* ***to level flight due to*** $+18.96^{\circ}$ ***elevator step input at*** V_C

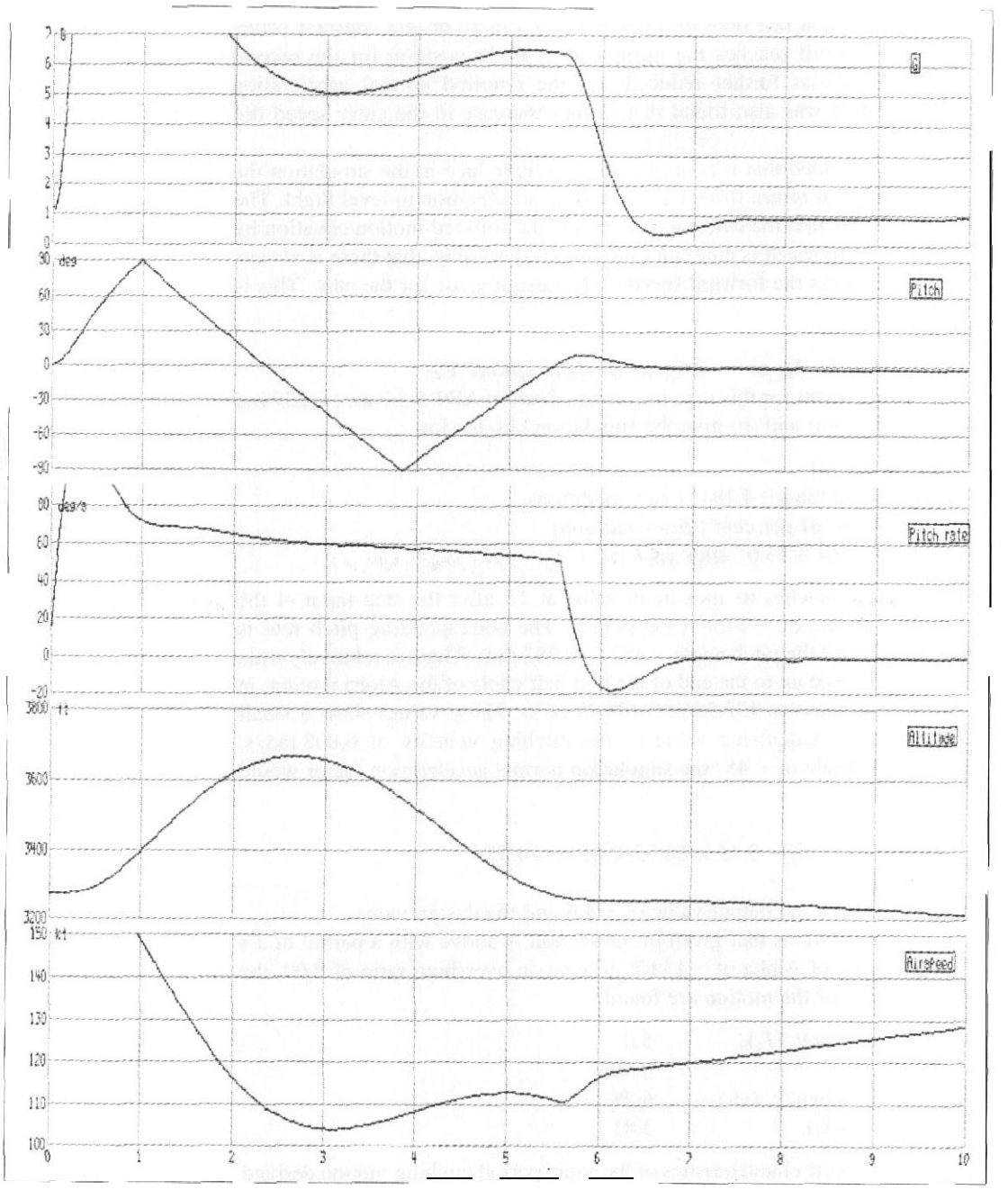

Fig. *ADI.8* ***Nose-down pitch from 6 5g to level flight due to +18 95 elevator step Input at 198 knots entry speed***

time indicated that the pitch rate does eventually reach a more or less constant value, but by the time the aircraft reaches the upright level flight position for the second time the forward speed has further reduced and the required normal acceleration factor is not achieved. It was also found that further increase in the entry speed did not resolve the issue.

Thus it must be concluded that it is not possible to reproduce in the simulation the idealized analytical case of return from a given normal acceleration to level Right. The primary reason for this is that the calculations neglect the forward motion equation by assuming that the forward speed is constant implying, erroneously. that there is always sufficient thrust to maintain the forward speed at the design value for the case. This is clearly not so.

C. Nose-down pitch, 1g to −4.6g at design speed V_C

The calculated elevator input for this case is given in Section AD1.5.5.2 as +0.237 rad (+13.6°). Figures AD1.9(a) and (b) give the simulation outputs for:

(a) Auto-trim set to off.
(b) Elevator initial setting −4.184" (trim condition).
(c) Engine setting 96.61 per cent (trim condition).
(d) Elevator step input +13.6° after 1 s.

The body angle, Alpha, reaches its maximum value at 1 s after the step input of the elevator and it has a value of −14.9" (−0.26 rad). The corresponding pitch rate is −43°/s (−0.75 rad/s) and the pitch angle −45" (−0.785 rad). There is relatively little change in the forward speed up to the end of the first half cycle of the Alpha motion, in fact there is a slight increase to 133.5 knots (68.75 m/s). These values show a small difference relative to the calculated value of the pitching velocity of 0.808 rad/s. Allowing for the pitch angle of −45" the simulation normal acceleration factor would be expected to be:

$$(n)_z = cos(-0.785\ \text{rad}) - 0.75 \times 68.75/9.81 = -4.55$$

which is very close to both the output value of −4.6 and the design value.

Using the same procedure as that given in Subsection A above with a period of 2 s and an equilibrium value of Alpha of −13.67" to give an overshoot ratio of 0.09, the following characteristics of the motion arc found:

Damped natural frequency, $(J_1)_s$	5.0
Damping ratio, $(\zeta_{D1})_s$	0.606
Undamped natural frequency, $(\omega_1)_s$	6.28
Damping coefficient, $(R_1)_s$	3.81

Table AD1.l summarizes the characteristics of the short-period pitching motion derived from the calculations and the-simulation. The reasons for the differences between the nose-up and nose-down simulation results are not immediately obvious hut there is good agreement between the mean values and those calculated.

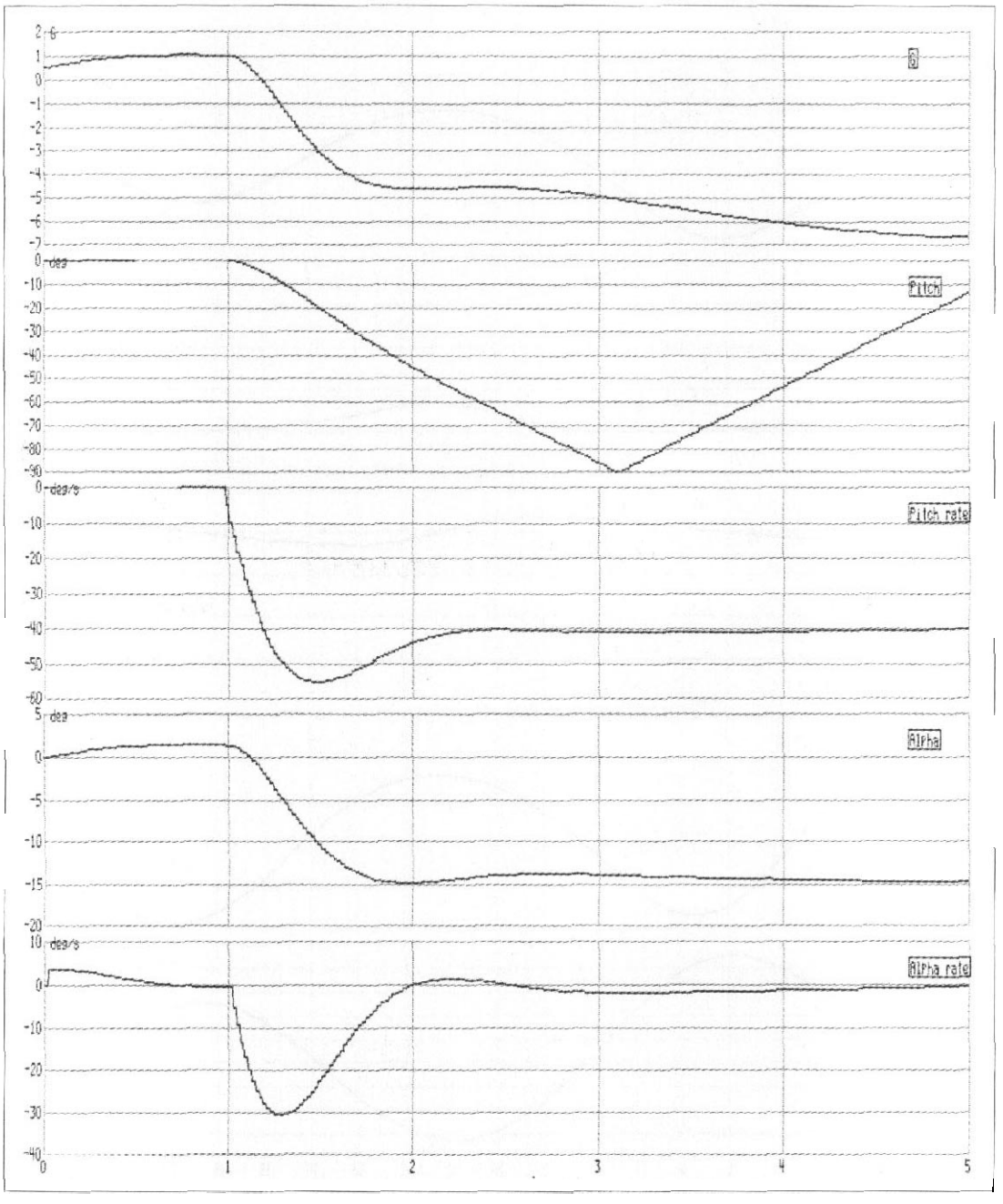

Fig. *AD1.9(a)* ***Nose-down pitch from level flight*** *due to* +13.6° ***elevator step*** *input at* V_C

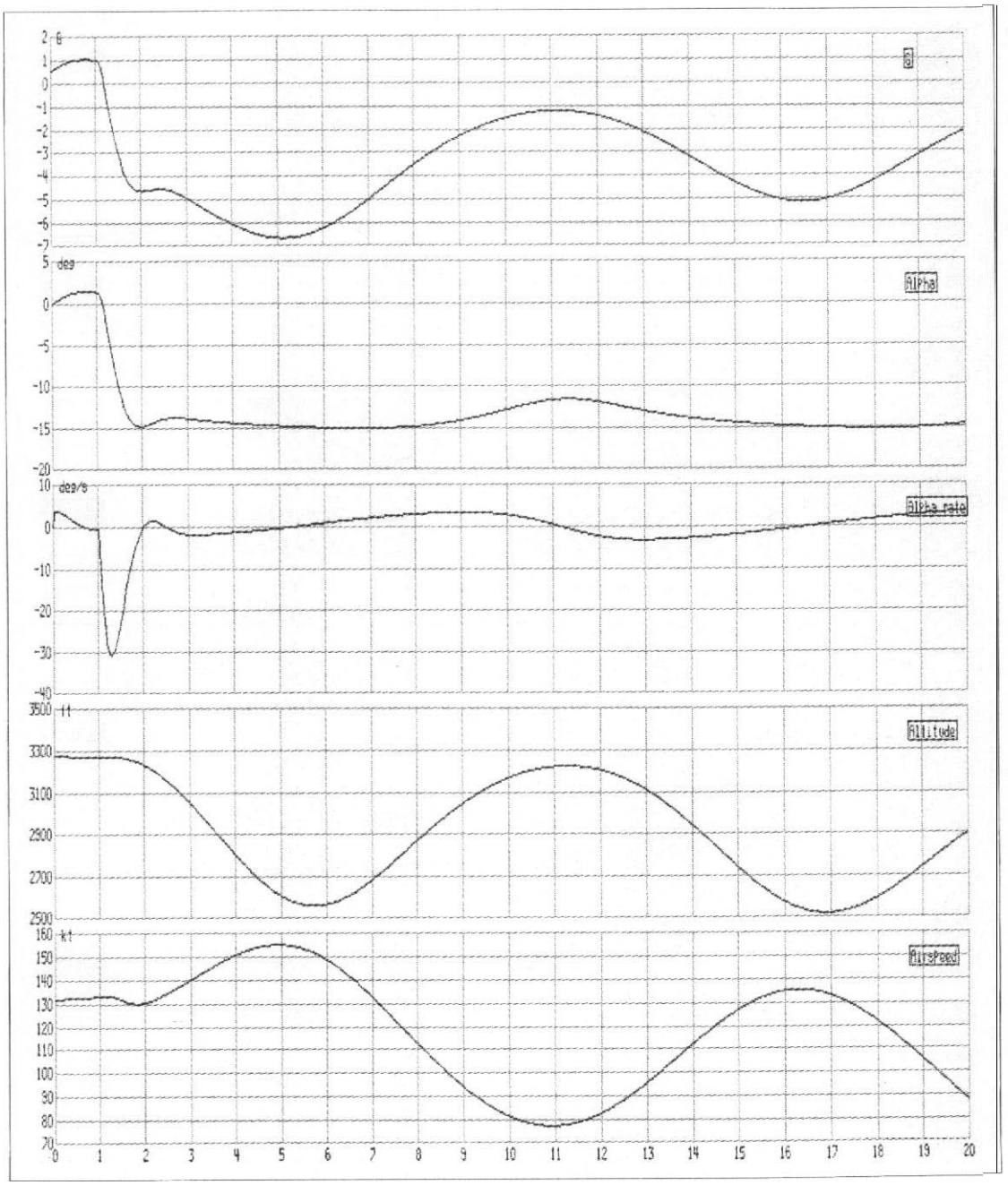

Fig. AD1.9(b) *Nose-down pitch from level flight due to* $+13.6°$ *elevator step input at* V_C

Table AD1.I Short-period pitching motion characteristics

Parameter	Simulation			Calculation
	Nose-up	Nose-down	Mean	
Dimensional:				
Damped period	1.8 s	2.0 s	1.9 s	1.90 s
Undamped period	1.41 s	1.58 s	1.5 s	1.51 s
Nun-dimensional:				
Damped natural frequency. J_1	5.51	5.0	5.25	5.22
Damping coefficient, R_1	4.24	3.81	4.02	4.04
Damping ratio, ζ_{D1}	0.61	0.606	0.608	0.612
Undamped natural frequency. ω_1	6.95	6.28	6.62	6.59

D. Nose-up pitch, −4.6g to 1g at design speed V_C

For this case the same procedure as outlined in Subsection B above was followed:

(a) Auto-trim set to off.
(b) Initial elevator setting at +7.19° (0.1254 rad), to induce the pitching manoeuvre, the angle being that required to trim the aircraft at −4.6*g*.
(c) At time 11.5 s, when the aircraft reaches upright level flight, input a step elevator movement of −11.37° (−0.198 rad) to bring the elevator angle back to the 1*g* level flight trim value.

Figure AD1.10 shows the simulation outputs for this case. It will be noted that the aircraft more or less returns to the required level flight condition after the step input of the elevator hut that at 11.5 s the normal acceleration factor is only −1 rather than the design value of −4.6. The pitch rate of 38°/s (0.663 rad/s) is less than the calculated value of 0.808 rad/s (46.3°/s) and it was also found that the forward speed had fallen from the input value of 132 knots (68 m/s) to 80 knots (41.2 m/s) at 11.5 s.

In an attempt to correct these discrepancies thc entry speed was increased to 250 knots (128.7 m/s) which is actually outside the design limits of the aircraft. The consequences of doing this are given in Fig. AD1.11, the aircraft now reaching the upright level flight condition after 8 s. At 8 s the speed is close to the required 132 knots, but the pitch rate at 35°/s (0.611 rad/s) is lower than the calculated value and as a result of this the normal acceleration factor is only −3.2. In order to achieve a compatibility of pitch rate with the calculated value it would be necessary to increase the initial setting angle of the elevator but this would result in a lower speed at the time upright level flight is reached. Again it must be concluded that the simplified analysis is not reprcscntative of actual flight conditions, but from the simulation outputs it may be concluded that it yields conservative loads.

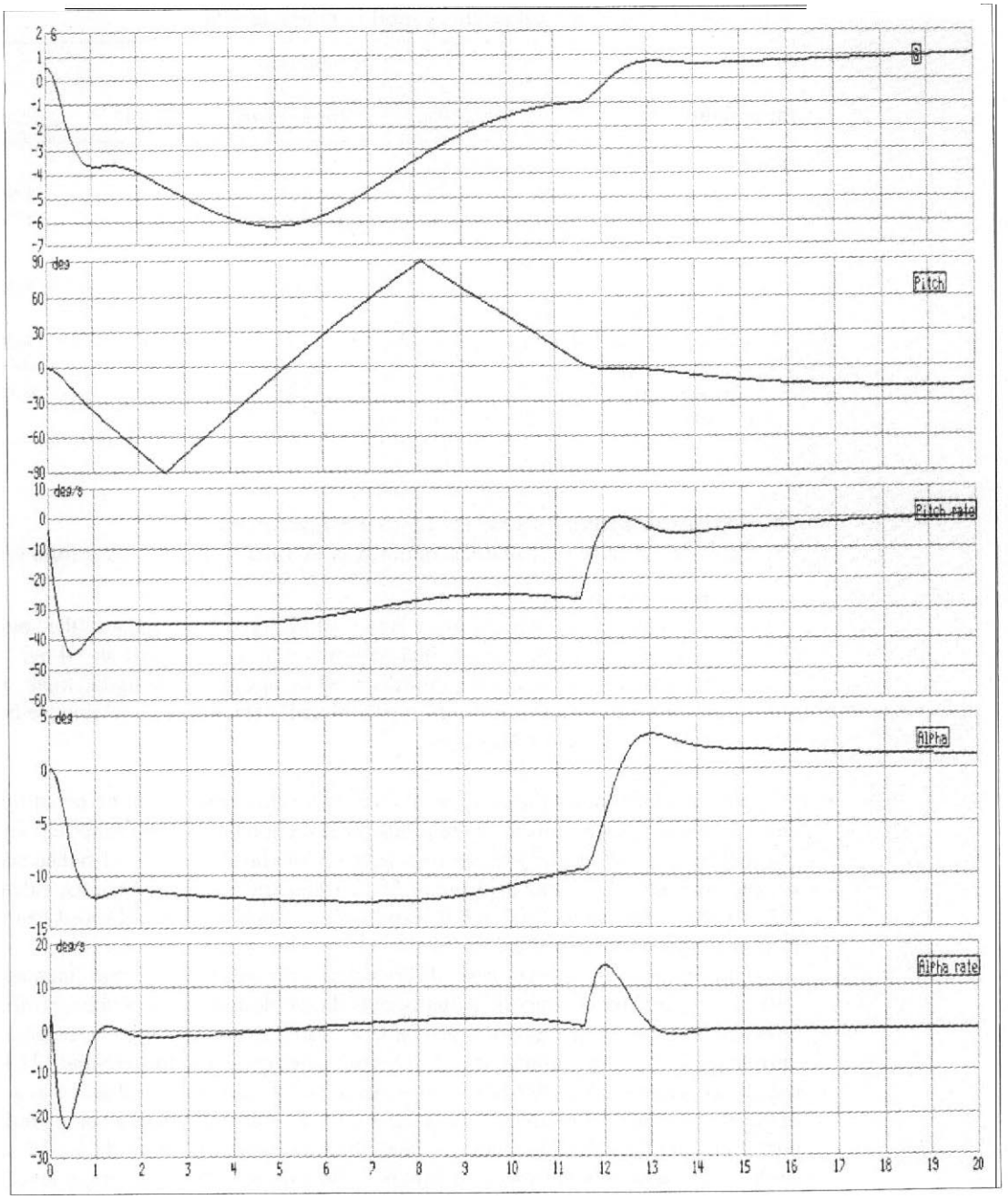

Fig. *AD1.10* *Nose-up pitch from* $-4.6g$ *to level flight due to* $-11.37°$ *elevator step input at* V_C

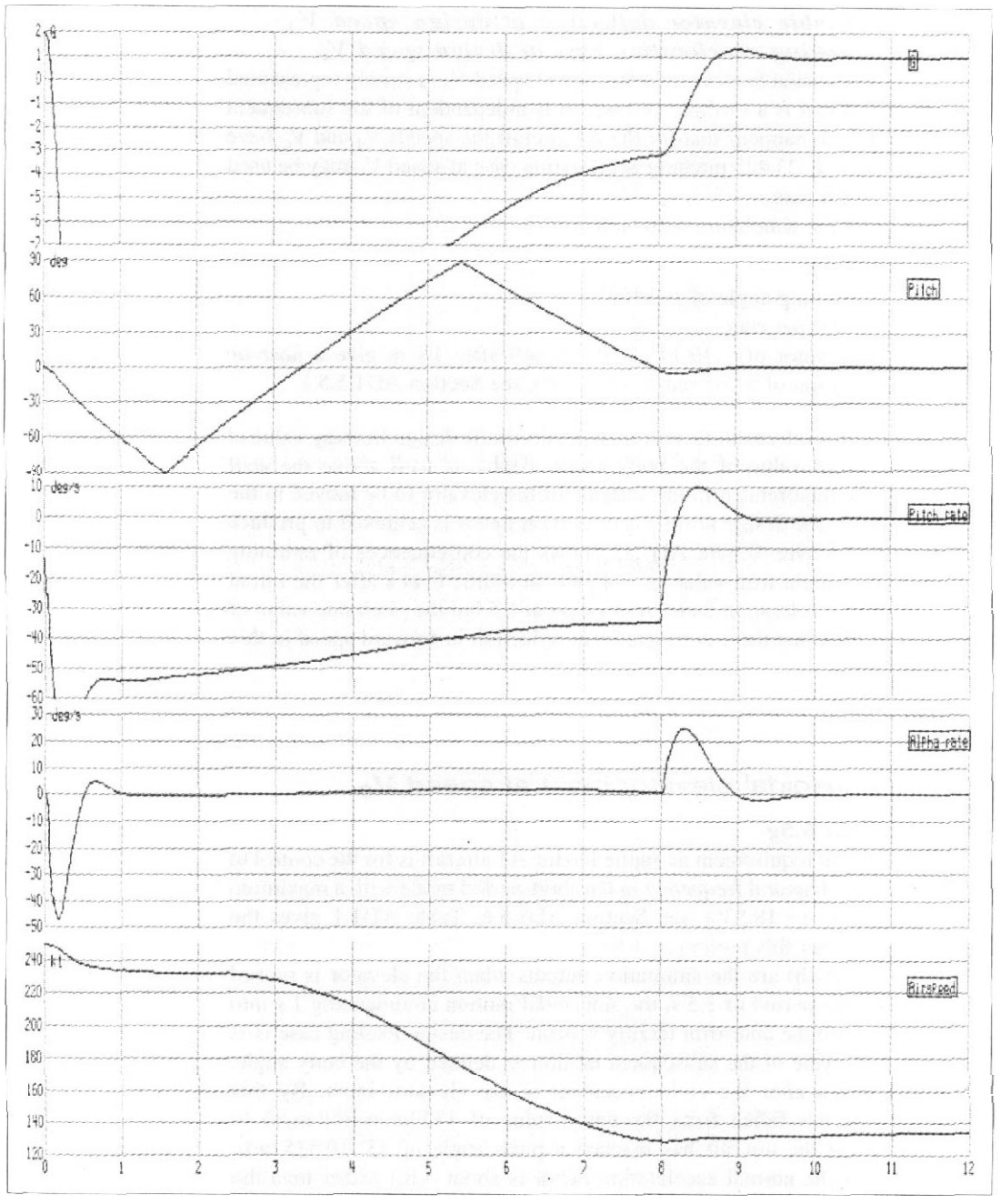

Fig. AD1.11 *Nose-up pitch from* −4 6*g lo level flight due to* −11 37 ***elevator step*** *input at* 250 ***knots entry speed***

E. Maximum available elevator deflection at design speed V_A and JAR-23 pitching acceleration case at design speed V_C

The requirement for full available elevator deflection at speed V_A is simply represented in the simulation and in fact is a loading case which is independent of the subsequent motion of the aucraft. It so happens that for the A1 aircraft the speeds V_A and V_C have the same value and the JAR-23.423 pitching acceleration case at speed V_C may be used to represent the V_A design case.

Figure AD1.12 gives the simulation outputs for:

(a) Auto-trim set to off.
(b) Elevator initial setting angle of −4.184".
(c) Engine setting 100 per cent.
(d) Step input of elevator of −19.74" (−0.345 rad) after 1 s to give a nose-up pitching acceleration of 6.565 rad/s^2 (376°/s^2), see Section AD1.5.5.1.

It is seen that the normal acceleration factor rapidly exceeds the design limiting value of 6.5 and the corresponding value of the body angle. Alpha, is well above the stall condition. However, the requirement in this case is for the elevator to be moved in the opposite sense as soon as the design normal acceleration factor is achieved to produce a form of checked manoeuvre. Figure AD1.13 shows the consequences of returning the elevator to the level flight trim value of −4.184" at a time 0.44 s after the initial application. The normal acceleration factor now peaks at 6.5 but the pitch rate value of 80°/s (1.4 rad/s) indicates that there is a significant reduction in forward speed in this short time.

AD1.10.3.3 Sinusoidal **elevator input** at **speed V_C**

A. Nose-up pitch to 6.5g

The checked elevator input requirement as applied to the A1 aircraft is for the control to be moved at the undamped natural frequency in the short-period mode with a maximum amplitude of −0.3234 rad (−18.53"). see Section AD1.5.6. Table AD1.l gives the mean value of the period for this motion as 1.5 s.

Figures AD1.14(a) and (b) are the simulation outputs when the elevator is moved through ± 18.53" with the period of 1.5 s, the sinusoidal motion commencing 1 s into the simulation. In this case the auto-trim facility was on. The design loading case is at the end of the first half cycle of the subsequent motion as defined by the body angle, Alpha. This occurs 0.75 s after the commencement of the elevator input. By this time the forward speed has fallen from the entry value of 132 knots (68 m/s) to 122 knots (62.8 m/s) and the aircraft has reached a pitch angle of 33' (0.575 rad). Because of these effects the normal acceleration factor is about +6.1 rather than the design value of +6.5.

This result again suggests that the analytical assumptions lead to somewhat conservative loads.

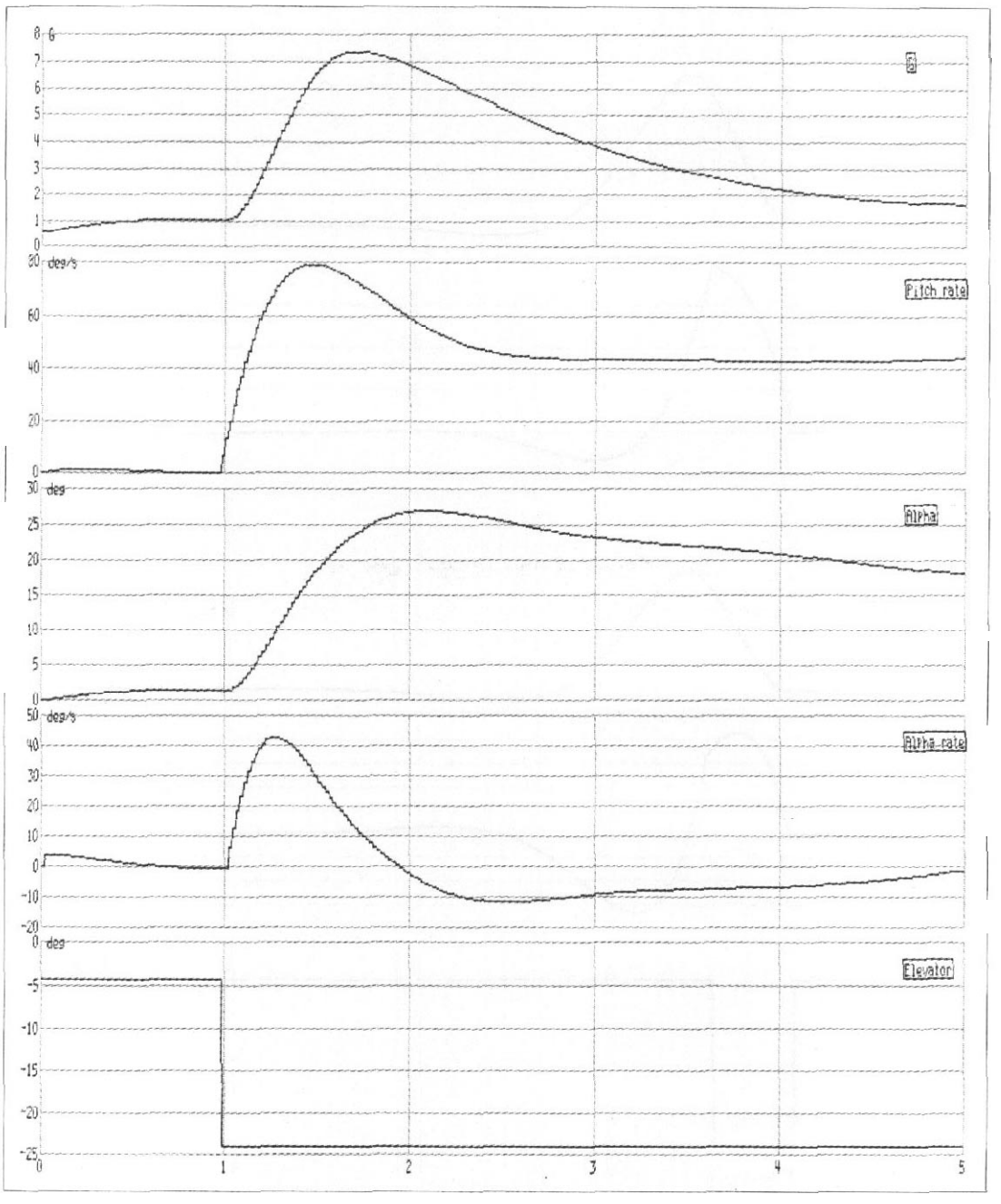

Fig. AD1.72 Maximum available up-elevatordeflection, -19.74°, at V_C

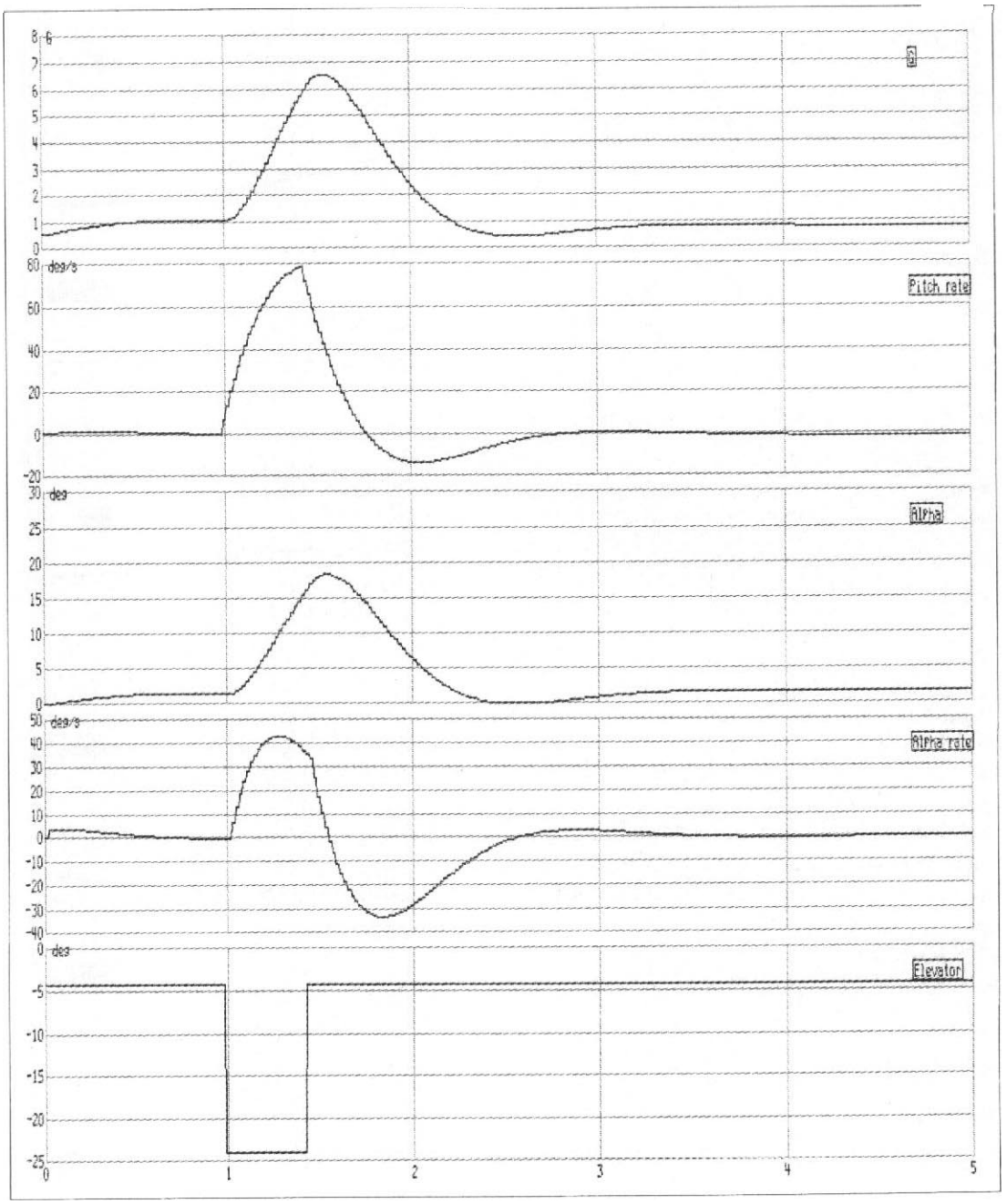

Fig. AD1.13 *Checked motion due to −19.74° elevator input for 0.44 s at* V_C

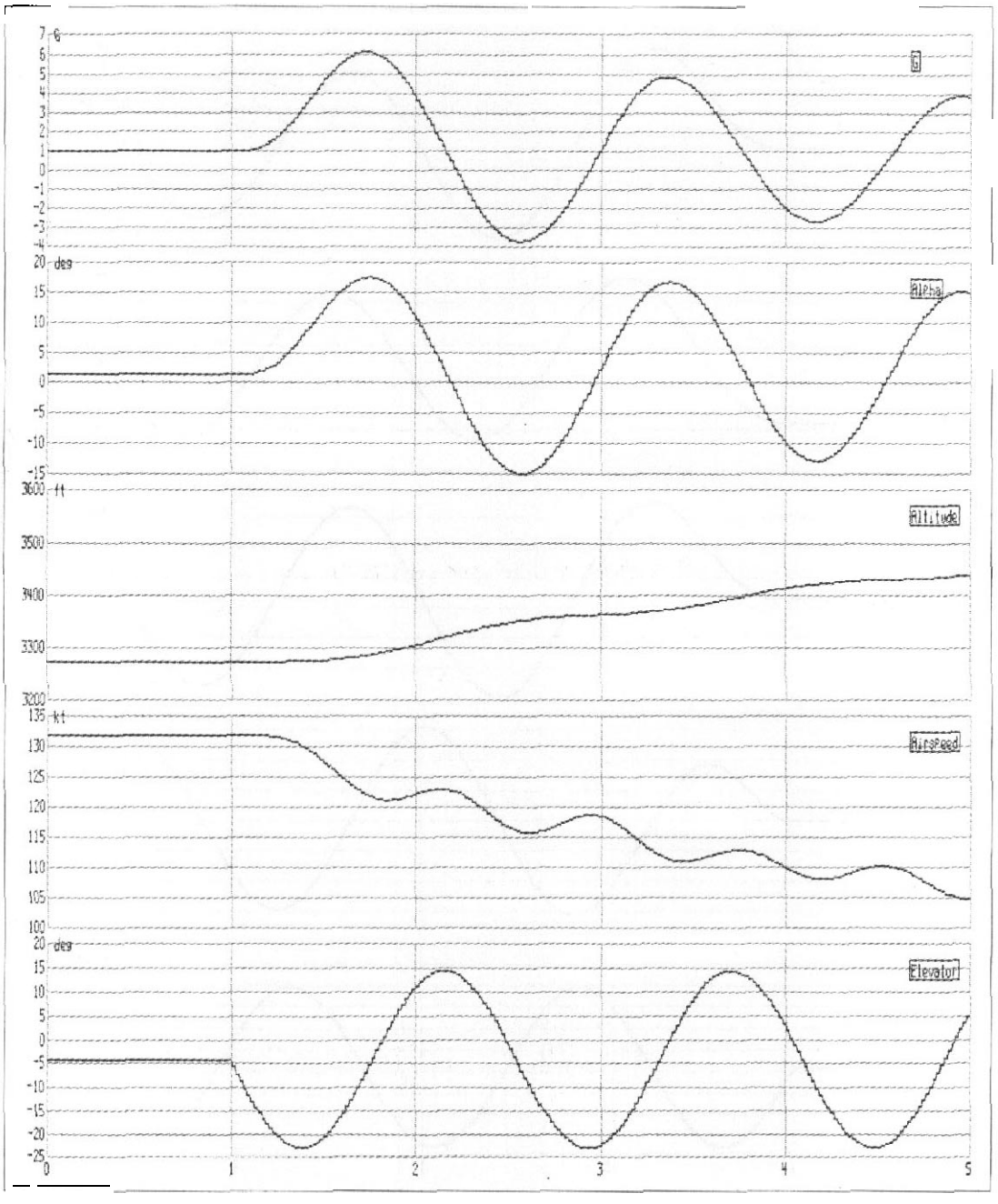

Fig. AD1.14 (a) **and** (b) Sinusoidal application **of** $\pm$ **18.53 elevator** input **at** V_C

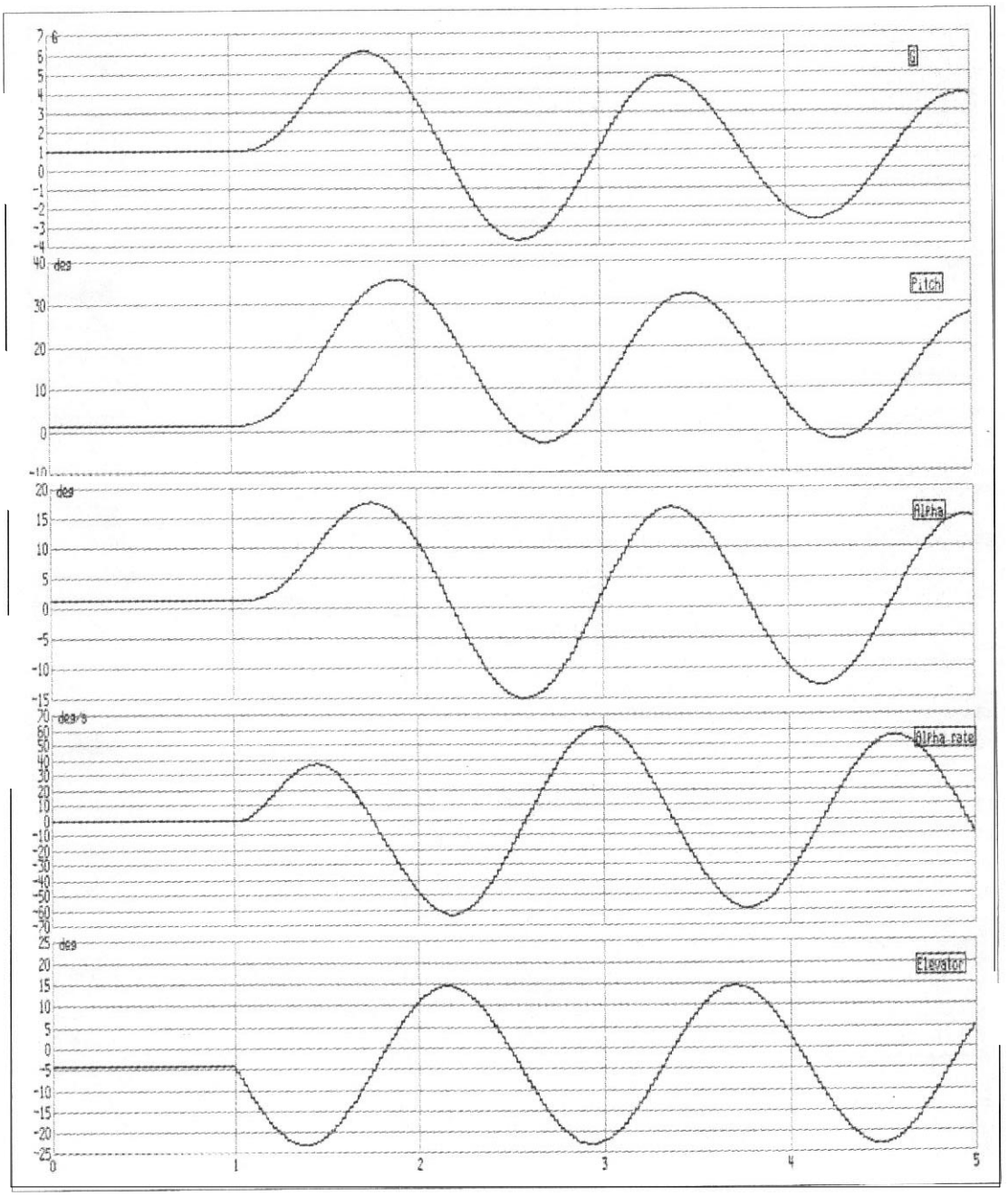

Fig. AD1.14 Continued

B. *Return to level flight*

The limitations of the simulation model imply that it is not possible to introduce a second sinusoidal input or to stop the first one. Thus the return of the aircraft from the sinusoidal excitation to steady level flight cannot be directly simulated. However. in an attempt to reproduce the assumptions made in the analysis, the simulation outlined below was undertaken.

(a) Auto-trim set to off.
(b) The elevator was set to an initial value of $-18.53'$ (-0.3234 rad) to represent the maximum elevator angle in the sinusoidal motion. see Subsection A above.
(c) Engine setting 100 per cent.
(d) A sinusoidal elevator input of $\pm 18.53''$ maximum amplitude and having a period of 1.5 s was introduced at time 6.6 s, by which time the aircraft had reached upright level flight after the initial disturbance.
(e) An entry speed *of* 200 knots (103 m/s) was used to give a speed of about 132 knots at the initiation time of the sinusoidal elevator motion at 6.6 s.

The outputs for this case are given in Figs AD1.15(a) and (b). The normal acceleration factor and the pitch rate are close to the required values of 6.5 and 45.5°/s (0.794 rad/s), respectively. see Section AD1.5.4. By the end of the first half cycle of the motion resulting from the sinusoidal application of the elevator the body angle. Alpha, has a value consistent with the 1*g* level flight case. The limitations of the simulation preclude any further detailed comments.

AD1.10. 4 Rolling manoeuvres, see Section AD1.6

Providing that the aircraft remains in the vertical plane of symmetry there is no coupling between the rolling and pitching motions. Thus the complexity associated with the gravitational forces is not present. However, there is a coupling between the rolling and the yawing motions which was neglected in the simple analysis used in Section AD1.6.

With theauto-trim facility on, Figs AD1.16(a) and (b) show the simulation outputs fur the case at speed V_C when the ailerons are given a step input of $+16''$ (0.279 rad) at time 1 s. The points marked by 'x' on the first of these figures are the calculated values of the roll rate during the initial disturbed motion. A number of observations may be made:

(a) The steady rate of roll of 160°/s agrees closely with the analytical value of 162°/s but the rate of build-up is more rapid than calculated.
(b) During the rolling motion the aircraft oscillates in yaw through about $\pm 10''$ (0.175 rad).
(c) The sideslip angle. Beta, both oscillates and tends to diverge.
(d) Significantly, there is also a tendency for the pitch angle to oscillate and diverge.

Thus the basic assumption of the analysis neglecting the pitch and yaw coupling is questionable. However. the requirements implicitly allow the use of the elevator and rudder control to offset the pitch and yaw effects.

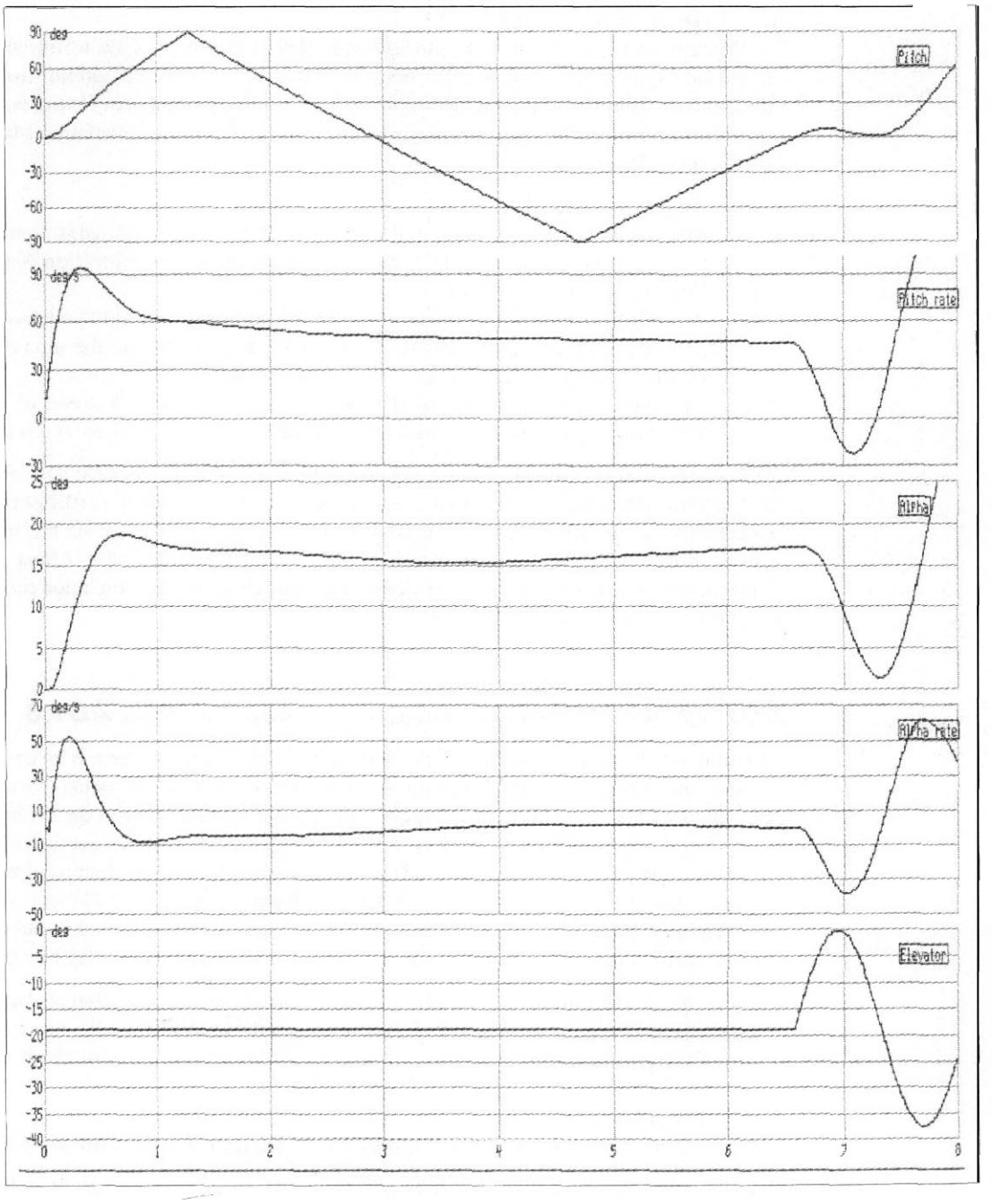

Fig. AD1.15 *(a) and (b)* ***Return to level*** *flight* ***from*** *sinusoidal* ***elevator input at*** V_C

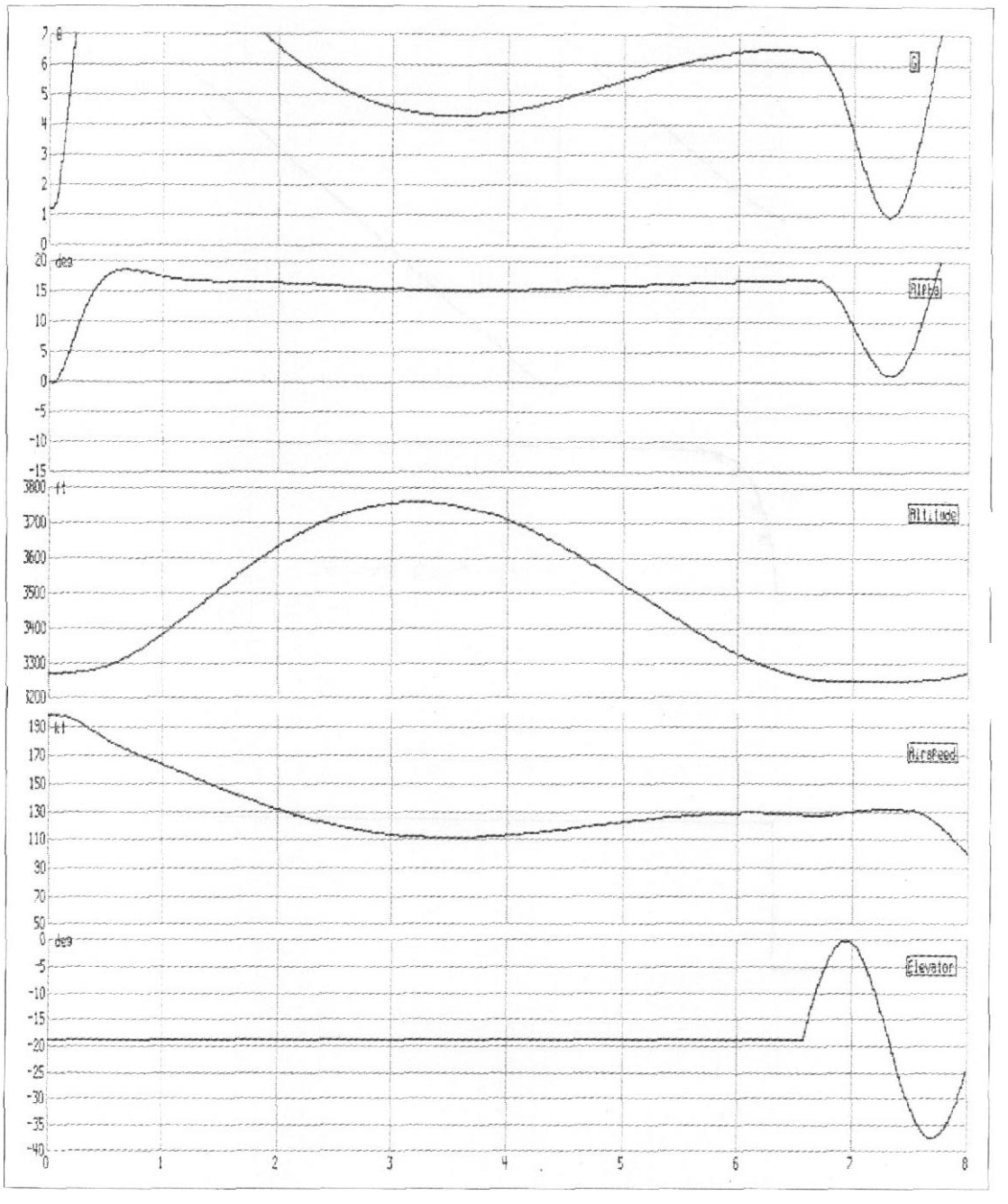

Fig. **AD1.15** *Continued*

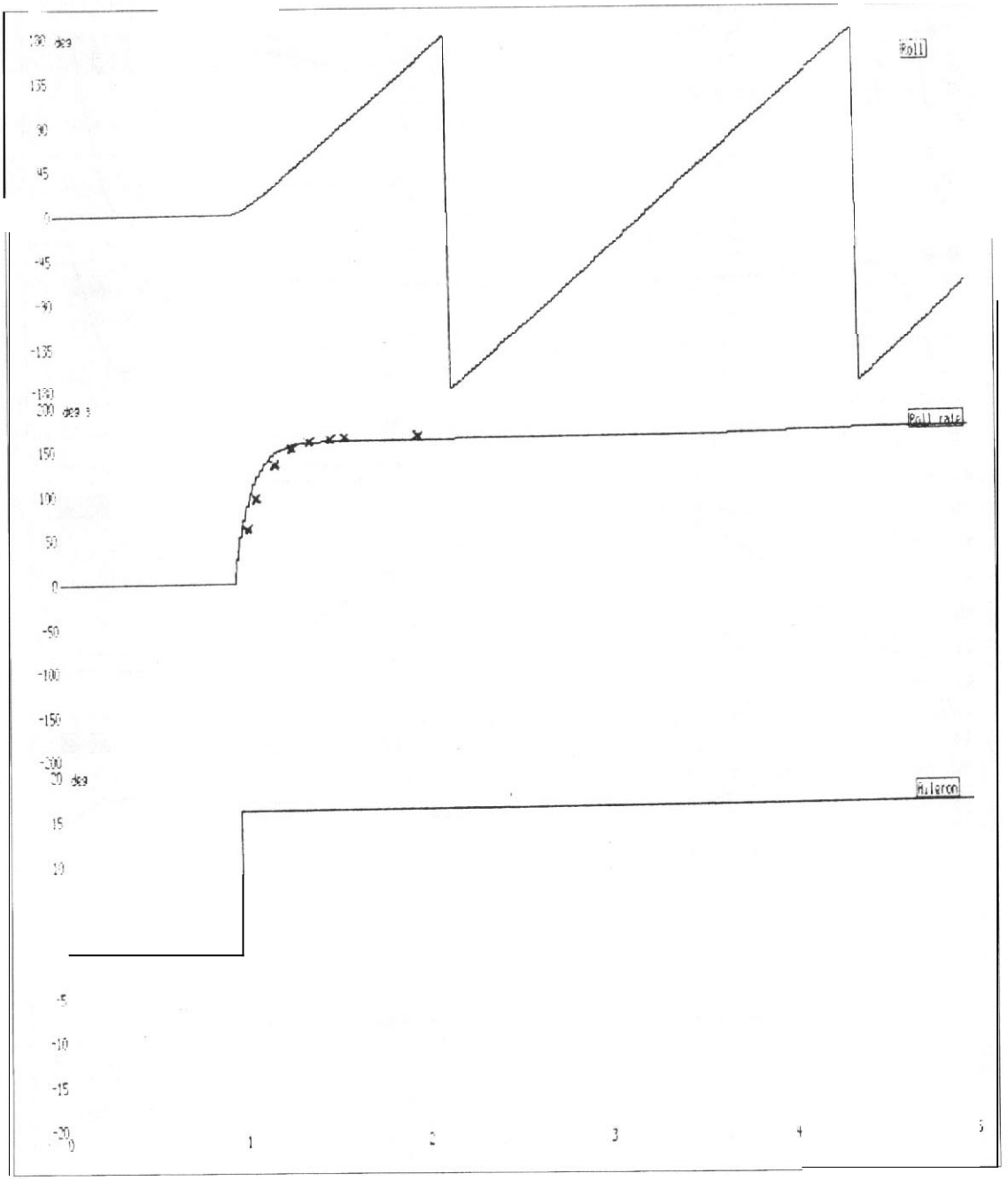

Fig. AD1.16 *(a) and* **(b)** ***Rolling*** *motion due to* 16° *aileron step #"putat* V_C*, rudder neutral*

Fig. AD1.16 Continued

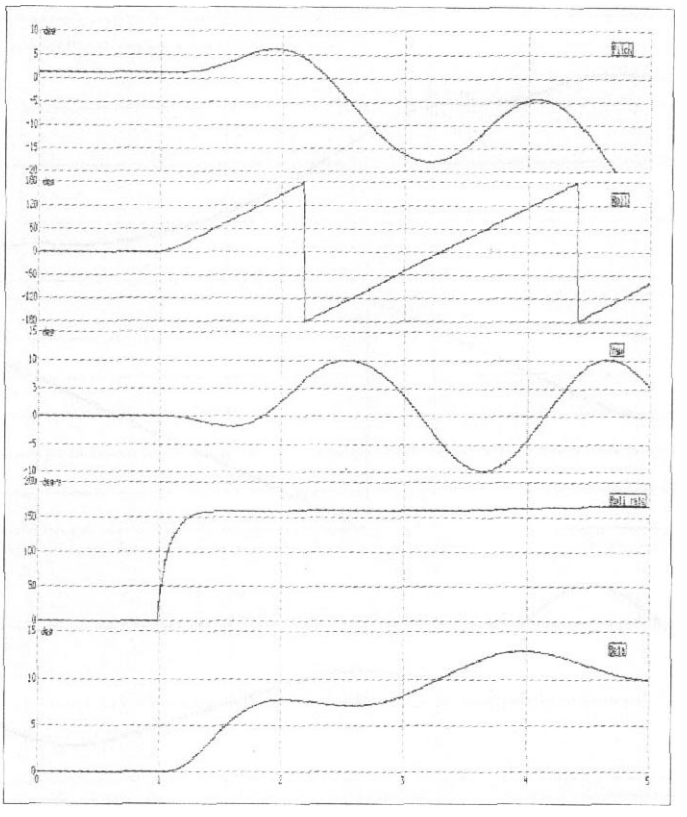

Figure AD1.17 is the simulation output when the rudder is initially set at −8" (−0.14 rad). Comparison with Fig. AD1.16 shows that for this condition:

(a) There is a slight reduction in the steady rate of roll.
(b) After the initial disturbance the yaw oscillation is reduced to about ±2.5" (0.044 rad).
(c) The sideslip oscillation is also only about ±2.5" and the divergence tendency is virtually eliminated.
(d) The amplitude of the pitching motion is much reduced, but there is still a tendency for it to diverge.

It will he noted that at time 2 s, that is 1 s after the application of the ailerons. when the roll has stabilized at its maximum value, there is no pitch or sideslip divergence and the yaw angle is more or less constant for a short time at about 7° (0.122 rad). From this it may be reasonably concluded that in this instance the simple analytical assumption of a single degree of freedom rolling motion is justified and tends to lead to somewhat conservatively high values of roll rate. The assumption may not be justified for a low aspect ratio wing configuration.

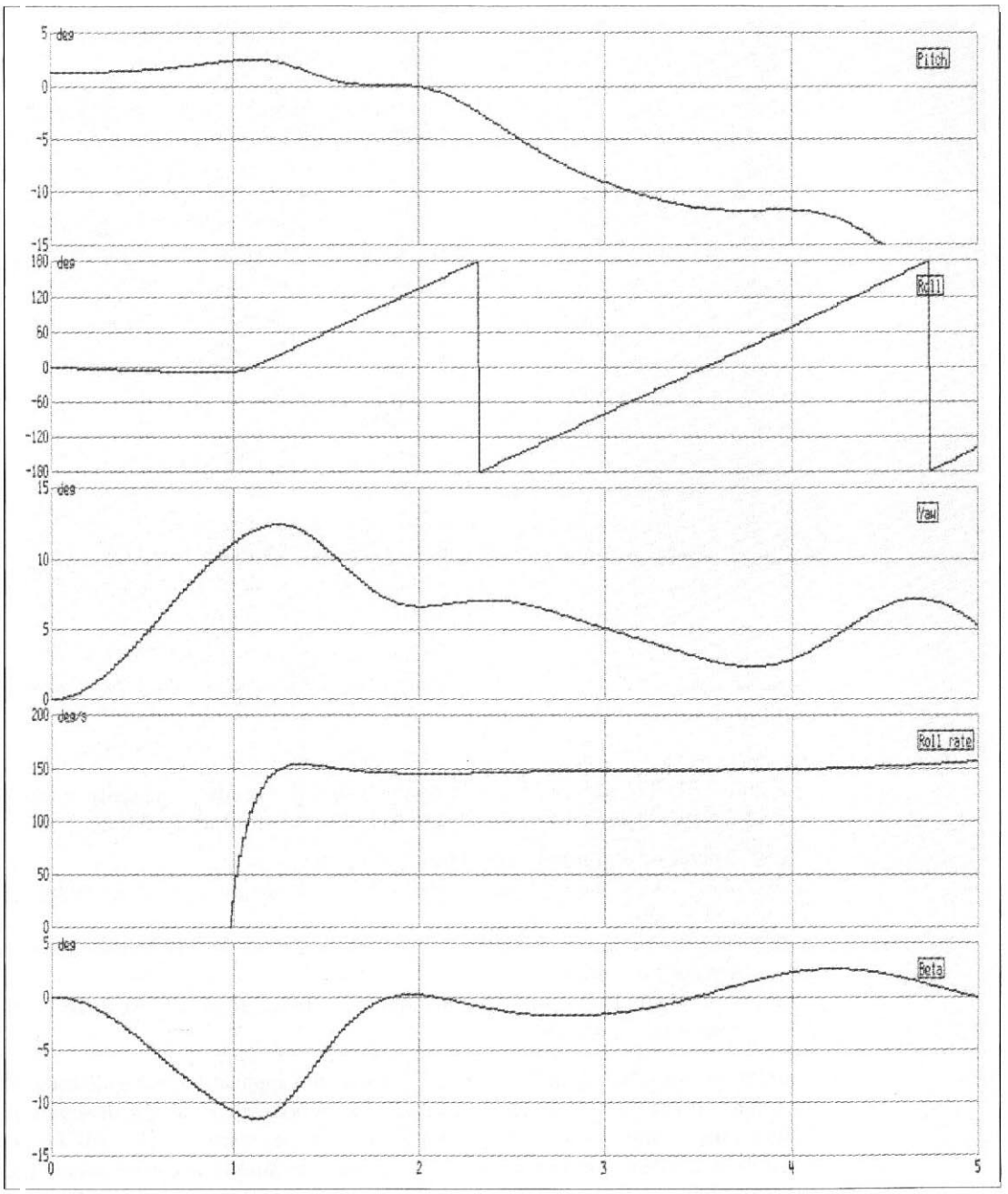

Fig. AD1.17 *Rolling motion due to 16' aileron step input at V_C – 8' rudder setting*

AD1.10.5 Yawing and sideslipping motions

AD1.10.5.1 Introduction

The yawing and sideslipping motions are coupled with the rolling as discussed in the previous section, but it is assumed for analytical purposes that the ailerons are used to keep the wings level during directional manoeuvres. Further, at least for aircraft with moderate to high aspect ratio wings, it is assumed that there is no coupling with the pitching motion and thus the complication of gravitational forces is not present.

AD1.10.5.2 Step input of rudder angle, see Section AD1.7.3

Figure AD1.18 gives the simulator output5 for the condition when the rudder is deflected instantaneously through an angle of 21.1° (0.37 rad) at time 1 s. The ailerons were not deflected but the auto-trim facility was on:

(a) There is some oscillation in the pitch angle and a tendency for it to diverge after about 7 s.
(b) There is also a steady increase in the roll displacement.
(c) After the initial disturbance the yaw angle increases steadily.
(d) As expected there is an oscillation of the sideslip angle. Beta. which tends to an equilibrium value by the end of the simulation.

The consequences of initially setting the aileron angle to −1.5" (0.026 rad) are shown in Fig. AD1.19. After the initial disturbance the following observations may be made:

(a) The pitch angle becomes more or less constant at −5" (−0.087 radj indicating that the aircraft has entered a shallow dive.
(b) The roll displacement is zero for a period of about 2 s before diverging.
(cj The variation of yaw angle is less marked and it is more or less constant at about −46" (−0.803rad) during the time that the aircraft is not rolling.
(d) There is a slight reduction in the magnitudes of both the maximum and equilibrium sideslip angles, Beta.

Finally Fig. AD1.20 is a 20 s simulation output with the initial aileron setting of −1.5" (−0.026rad) and the rudder step input of 21.2" (0.37 rad) held for a period of 11 s before being returned to neutral position. The first part of the output is as in Fig. AD1.19 but it shows theretum of the aircraft to straight flight and other parameters.

The simulation outputs have been used to derive the characteristics of the directional motion both with and without the initial setting of the ailerons. The procedure of Subsection AD1.10.3.2(A) was employed and the results are compared with the calculated values in Table AD1.2:

It will be seen that the sideslip angles predicted by the calculation agree well with those derived from the simulation when there is no aileron deflection but that the damping ratio is somewhat higher and the natural frequency somewhat less. The

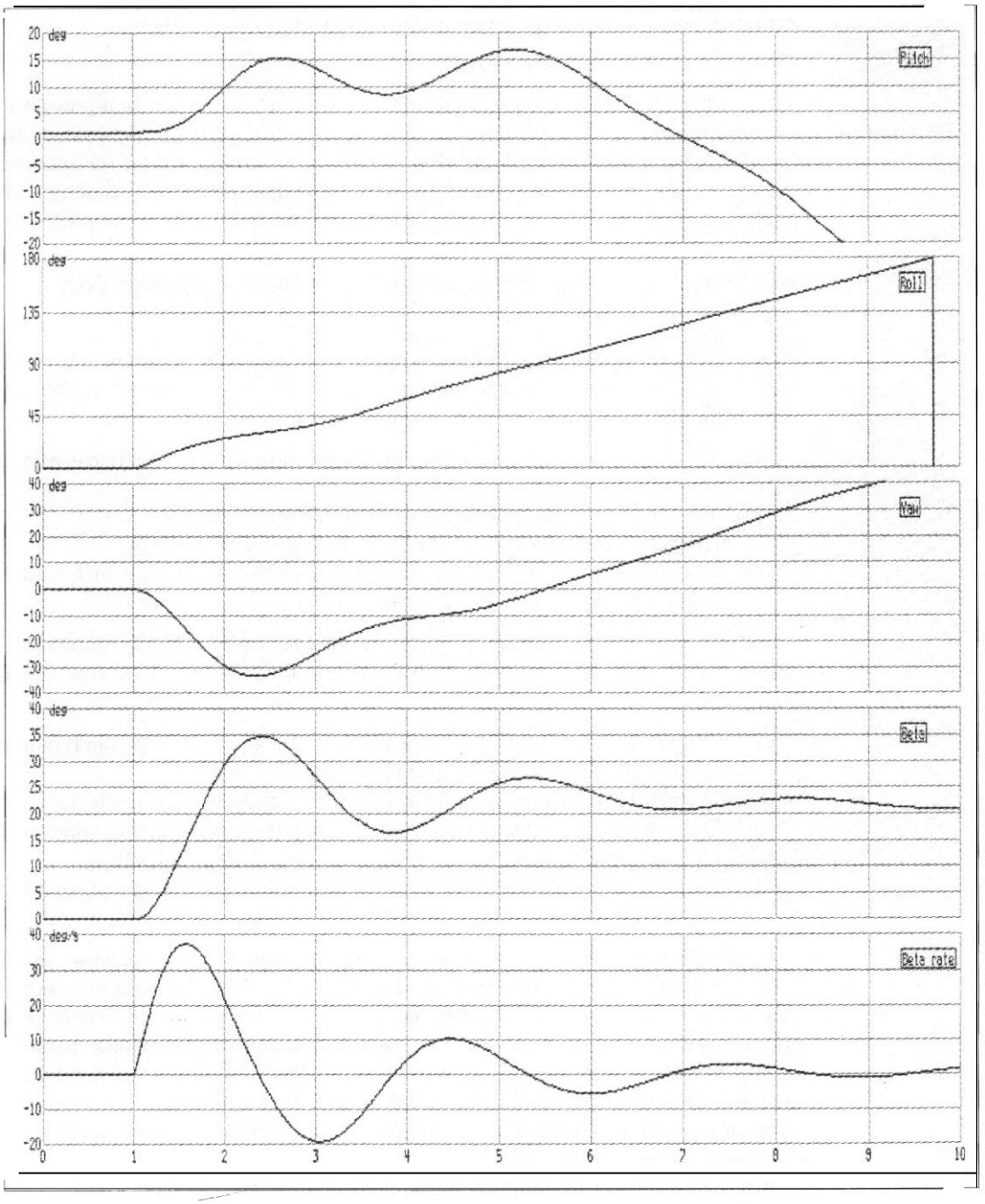

Fig. AD7.78 *Directional motion due to* $+21.1^{\circ}$ *rudder step input at* V_C, *ailerons* **neutral**

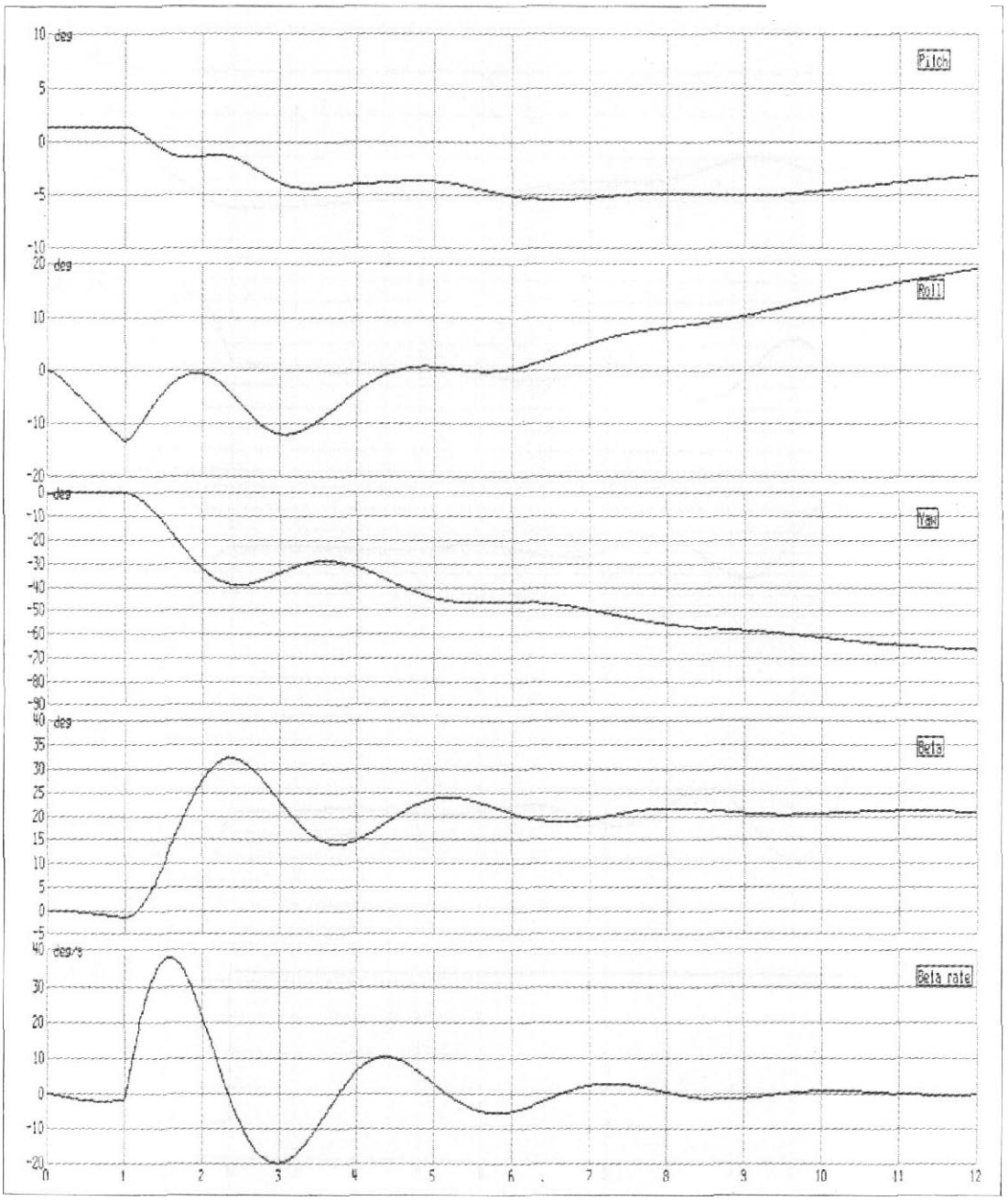

Fig. AD7.19 ***Directional*** *motion* ***due to +21*** *.1°* ***rudder step input at*** V_C, ***−1.5' aileron*** *setting*

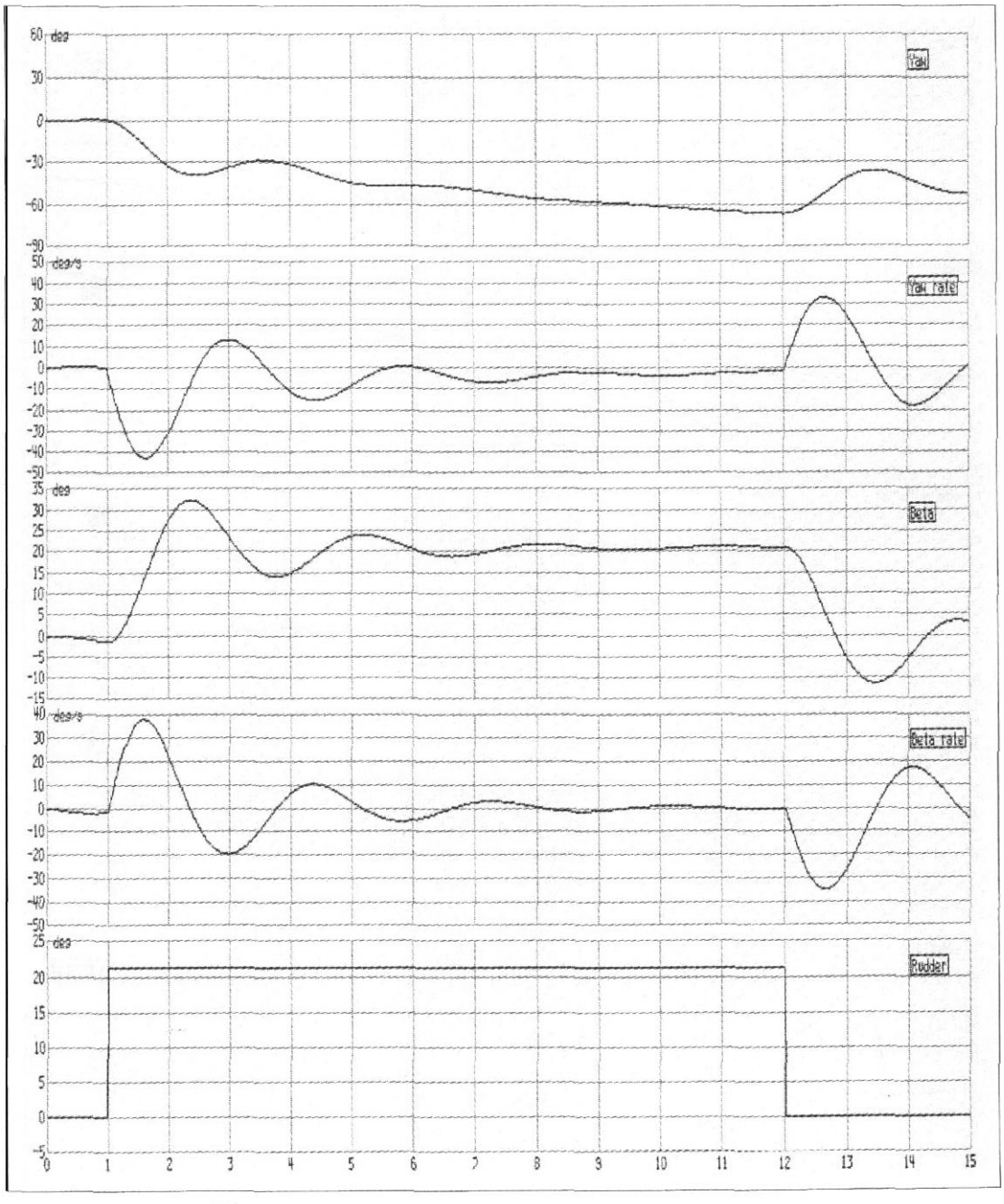

Fig. *A07.20* ***Directional motion doe to*** $+21.1^{\circ}$ ***rudder step input at*** V_C, -1.5° *aileron setting,* ***return to straight*** *flight*

Table AD1.2 Characteristics of the directional motion

Parameter	Simulation Aileron angle		Calculation
	Zero	−1.5	
Dimensional:			
Over-swing sideslip angle, β_{MAX}, deg	34.8	32.5	34.3
Equilibrium sideslip angle, β_E, deg	23.0	22.0	23.2
Over-swing ratio	1.51	1.48	1.477
Period of oscillation, s	2.90	2.80	2.68
Nan-dimensional:			
Damped natural frequency, J_2	3.42	3.54	3.70
Damping coefficient, R_2	0.735	0.818	0.871
Damping ratio, ζ_{D2}	0.21	0.225	0.229
Undamped natural frequency, ω_2	3.50	3.63	3.80

inclusion of the −1.5" of aileron deflection to compensate for the rolling tendency goes some way to the removal of these discrepancies but the sideslip angles are rather lower. Nevertheless, the uncouplcd. two degree of freedom motion assumed for the calculations does give an adequate representation being, if anything. slightly conservative in terms of the parameters from which the loads are derived.

AD1.10.5.3 Sinusoidal input of rudder, see Section AD1.7.4

Figures AD 1.21(a) and (b) are the simulator outputs for the case when the rudder input is a sinusoidal oscillation of $\pm 14.13^{\circ}$ (± 0.247 rad) maximum amplitude at the damped natural frequency of the directional motion. taken to have period of 2.9 s, see Table AD1.2. In this case there was no initial setting of the ailerons. The two figures are for the same conditions but show diffcrcnt output parameters. It is seen that over the first 1.5 cycles of the motion:

(a) Although there is an oscillation of pitch angle the amplitude is not large.
(b) As would be expected there is a roll coupling which is oscillatory but again the amplitude is not large.
(c) At the end of the first cycle of the motion the sideslip angle reaches about −27" (−0.471 rad). This compares well with the calculated value of −0.467 rad (−26.8").
(d) At the end of the first 1.5 cycles the sideslip angle is $+31.5^{\circ}$ (+0.55 rad), the corresponding calculated value being +0.539 rad ($+30.9^{\circ}$).

There is thus good agreement between the simulation and calculated results for this case.

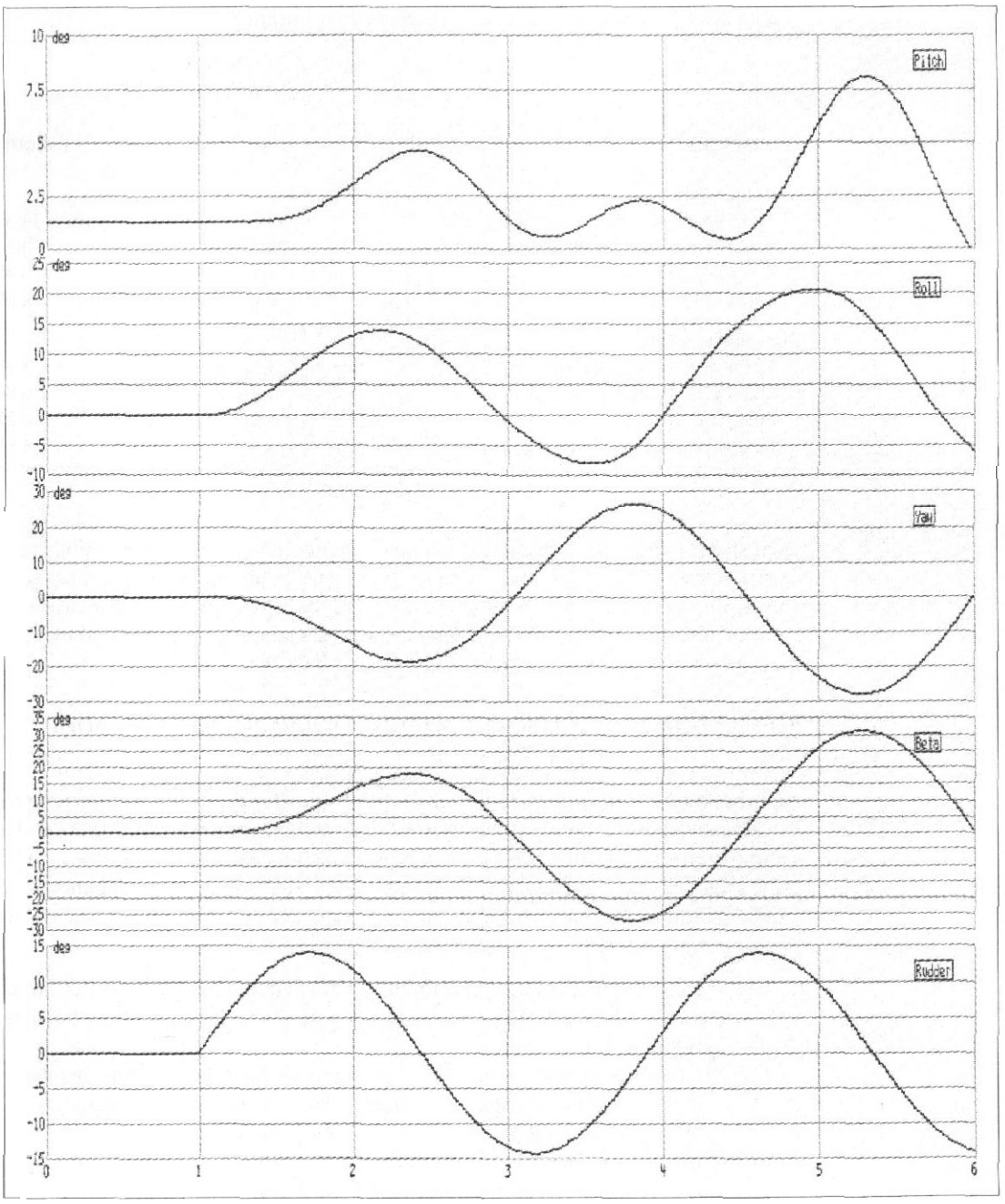

Fig. AD1.21 *(a) and (b) Sinusoidal application of* $\pm 14.13^{\circ}$ *rudder input at speed* V_C*, ailerons neutral*

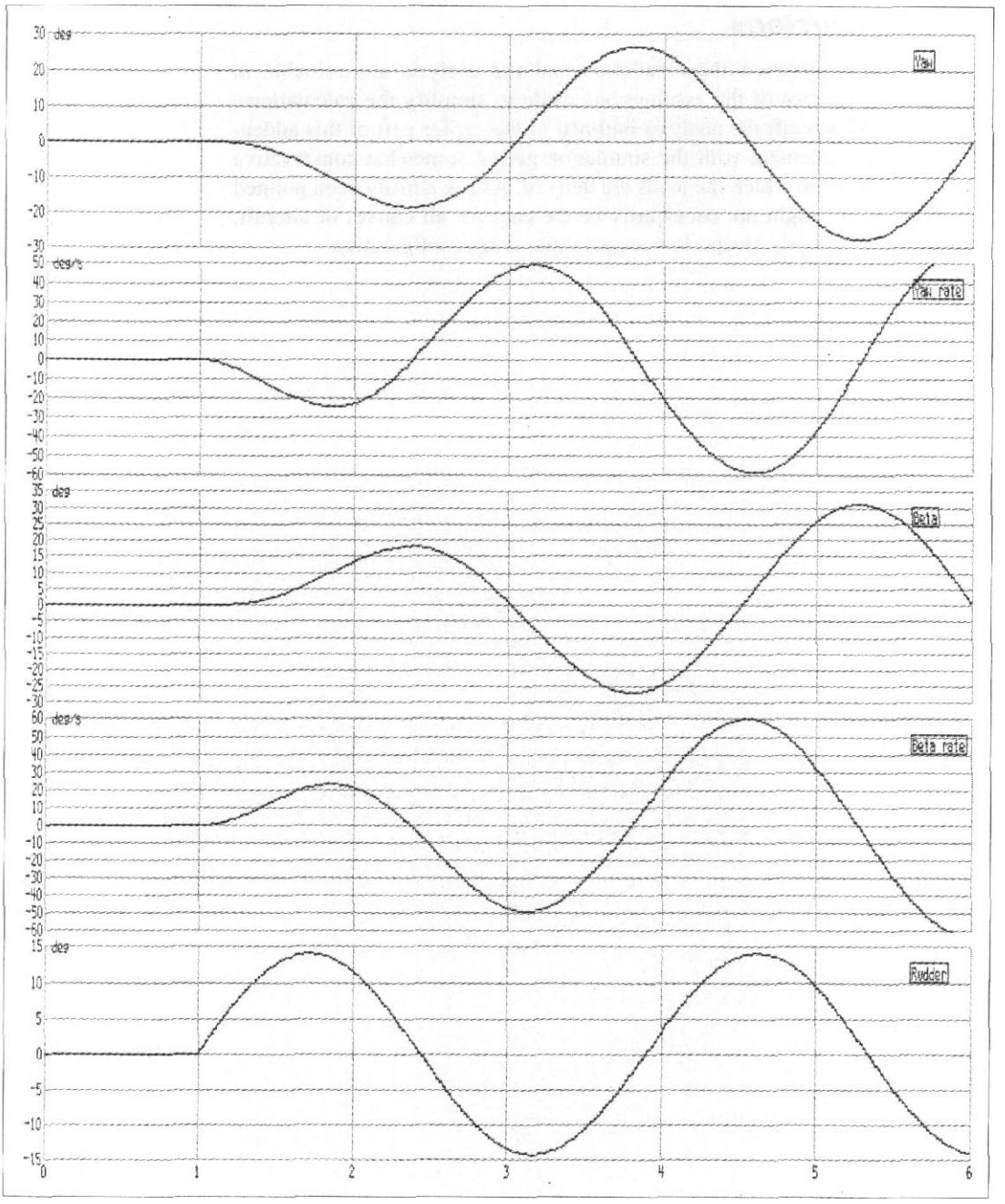

Fig. AD1.21 Continued

AD1.10.6 Conclusions

The overall comparisons between the simulation and the analysis are valuable in emphasizing the consequences of the assumptions made to simplify the calculations. Nevertheless, for the A1 aircraft the analysis outlined in the earlier part of this addendum shows reasonable agreement with the simulation giving somewhat conservative values of the parameters from which the loads are derived. As has already been pointed out this satisfactory result might not necessarily he the case for all classes of aircraft. especially those having a highly swept, low aspect ratio, wing configuration.

ADDENDUM AD2

Symmetric flight – balance procedure

AD2.1 Introduction

The procedure outlined in this addendum is based on the symmetric flight equations coveredin Chapter 4, Sections 4.2 and 4.6, and Chapter 5, Sections 5.2 and 5.3, to which reference should be made as necessary. The notation is that of those chapters.

The equations of motion in symmetric flight are expressed in terms of aerodynamic derivatives that. for the most part, can he clearly identified as describing a discrete load or moment. The main exceptions to this are:

(a) Wing–body contribution to damping in pitch, M_θ Eqns (4.22). which is usually negligible except for tailless aircraft.

(b) Contribution of the lift on the body, both to the total wing–body lift and especially its impact upon the location of the overall aerodynamic centre and the zero-lift pitching moment. It is essential to ensure consistency in this respect. That is, the body lift distribution must be such as to bring the overall aerodynamic centre to the correct position, or alternatively used to define it, and give the correct fuselage lift contribution to the zero-lift pitching moment.

It is reasonable to relate all the forces and moments to the centre of gravity in a given case and to subsequently make local corrections to transfer them to the wing–fuselage attachment locations, seehapter 15, Section 15.1.2.

When deriving the shear force and bending moments by integration of the load distribution along the length of the body it is usually best to work from both extremities

towards the centre of gravity. There are three reasons for this:

(a) Any errors arising due to slight inaccuracies in the specification of load arc minimized by keeping moment arms to the lowest possible value.
(b) It is most likely that any discrepancies, such as between hody lift distribution and the associated aerodynamic derivatives, occur in the central region of the aircraft.
(c) The shear force and bending moment values are highest in the wing–fuselage intersection region, so any discrepancies hcrc are of less relative significance.

However, in the example given here this procedure has not been followed and in all cases the integration is undertaken from the tail through to the nose. This has been done to simplify the expressions for shear force and bending moment which in this case can bc integrated analytically. It does result in minor discrepancies which, finally, have to be transferred back to the location of wing lift or the centre of gravity.

AD2.2 Basic conditions

In the longitudinal balance of the aircraft the manoeuvre conditions are superimposed upon datum initial conditions. The cases are:

(a) ***Steady** level flight **trimmed case.*** This is a very important datum condition and it is essential that the distrihuted forces and moments are in exact balance. With the usual assumption that thrust is not changed during a manoeuvre, this case takes care of thrust forces and moments, zero-lift pitching moment. and any other conditions that are assumed to remain constant in the manoeuvre. The relevant equations are to be found in Chapter 4, Section 4.2, and Chapter 5, Section 5.3.1.2.
(b) ***Steady** rotary flight at the **design manoeuvre acceleration.*** This is used with (a) above as a datum for evaluating the conditions associated with a manoeuvring back to level flight. see Chapter 5, Section 5.3.1.4.
(c) ***Pitching accelerarion cases,*** which result from a movement of the pitch control motivator to cause the aircraft to depart from either condition (a) or (b) above. An appropriate definition of the motivator movement is required. This is covered in Chapter 5, Section 5.3.2.

AD2.3 Summary of analysis procedure

The first stages in the analysis are outlined in Addendum ADI. For completeness they are summarized here:

(a) Specify the case conditions for a given set of aircraft data.
(b) Calculate the basic terms needed for the analysis:

$$\bar{V}, \mu_1, H_m, R_1, J_1, \Sigma, \delta_n, \varphi, M_o$$

In order to assure a correct balance of the forces and moments it is necessary to use the complete definition of δ_n, Eqn. (4.82f), not the approximate one given by Eqn. (4.82g).

(c) Calculate the wing–body and tail lifts in the level flight trimmed condition, together with the corresponding body angle. Distribute the wing–body lift on the wing and along the body. Calculate the associated moments and check the overall force and moment balance.

(d) Calculate the elevator angle to maintain the aircraft in the steady rotary manoeuvre condition and the associated pitching velocity. Use the latter to evaluate the change in body angle and wing–body lift. Evaluate total tail lift. Distribute the lift forces appropriately and the aerodynamic moment balance. Balance the lift force increments by the increments of the inertial forces. As the pitching velocity is constant there is no increment in the inertial moment.

(e) Determine the method for specifying pitching acceleration. Establish the design load condition and the load conditions to ensure that there is overall force and moment balance.

(f) In summary for each design condition:

(i) state the wing lift and its point of application;
(ii) state the body lift and distribute it along the body length as defined;
(iii) state the tail lift and its location;
(iv) evaluate the inertial relief due to the translational acceleration and distribute it appropriately between the wing and along the body;
(v) where appropriate evaluate the inertia relief due to the rotational acceleration; distribute it appropriately between the wing and along the body making allowance for any contributions from masses located vertically from the reference body axis;
(vi) where appropriate state the vertical thrust component and its location;
(vii) state the zero-lift pitching and thrust moments and points of application.

(g) In any given condition, derive the load distribution along the length of the aircraft and integrate it to obtain the shear force distribution, including concentrated forces at the appropriate locations.

(h) Integrate the shear force along the aircraft to obtain the bending moment distribution, adding the discrete couples at appropriate points. It is important to correct any discrepancy back to the centre of gravity.

(i) Combine the shear force and bending moments from the various conditions to obtain the design cases:

(i) trim in level flight;
(ii) trim plus steady rotary manoeuvre;
(iii) trim plus initiation of manoeuvre;
(iv) trim plus steady rotary manoeuvre plus departure from manoeuvre.

(j) Construct the shear force and bending moment diagrams along the length of the aircraft. When the wing attachment locations, defined by the spar positions, become available the diagrams can be corrected to allow for the way in which the shear forces are reacted at the wing–body attachment.

AD2.4 Example

AD2.4.1 Introduction

The example is based on a project design for a freight aircraft powered by four turbo-fan engines. The data have been modified somewhat to give an idealized mass and body lift distribution to eliminate the need for numerical integration. For the purposes of the example the checked manoeuvre case covered here is based upon the approach given in Chapter 5. Section 5.3.4.2. Shear forces and bending moments are derived for the flight conditions outlined, see Section AD2.2.

AD2.4.2 Basic aircraft data

(a) Mass. m, 101 500 kg. The mass of the fuselage items, totalling 31 200 kg, is assumed to he uniformly distributed at 800 kg/m over the 39 m length of the fuselage. The fuselage and the overall aircraft centre of gravity are thus at the mid-point of thc length. Tail masses are included in the fuselage mass distribution.

(b) Pitch moment of inertia, I_y, 4 319 000 kg m^2, giving an overall pitch radius of gyration, k_y, of 6.523 m. The total conmbution from the wing items is 244 400 kg m^2. By assumption the wing centre of gravity coincides with the overall aircraft centre of gravity so there is no contribution to the pitch moment of inertia from the offset of the wing centre of gravity. The total contribution from the fuselage items is 4 075 000 kg m^2. This is made up of two effects:

(i) 3 954 600 kg m^2 due to the uniform mass distribution along the length of the fuselage;

(ii) 120 000 kg m^2 due to the vertical location of individual items:

- horizontal and vertical tail 100 000 kg m^2 (located at thc rear of fuselage);
- main landing gear 15 000 kg m^2 (located at the centre of gravity);
- nose landing gear 5 000 kg m^2 (located at the front of fuselage).

(c)

Wing span, b	46.1 m	Wing area, S	193.3 m^2
Tailplane area, S_T	48 m^2	Tail arm, ℓ'_T	19.5 m
Wing aerodynamic mean chord. c			4.70 m
Location of 0.25 aerodynamic mean chord aft of nose			18.8 m

(d)

Powerplant thrust at design condition	90 000 N
Distance of thrust from centre of gravity, z_T	−0.06 m

(e) Distribution of wing–body lift, $\mathcal{L}_{WB}$:

Wing lift 0.94 $\mathcal{L}_{WB}$

Body lift 0.06 $\mathcal{L}_{WB}$

The body lift is distrihuled linearly along the length with the maximum value at the nose decreasing to −0.3167 of the nosc value at the tail. This gives the centre of pressure at 6.975 m aft of the nose and a datum lift of 13.325 N for 1 N/m at the nose.

(f) The design manoeuvre speed, V_A, is 134 m/s (EAS).

AD2.4.3 Design case

Mass: 101 500 kg
Speed: V_D at sea level, 180 m/s (EAS) ($M_N = 0.77$). Aft centre of gravity: h = 0.4c.
(This happens to coincide with the mid-point of the fuselage length.)

Checked elevator motion as defined in Chapter 5, Section 5.3.4.2:

(a) Nose-up, level flight to 3g manoeuvre.
(h) Nose-down, 3g steady rotary motion to 1g level flight.

AD2.4.4 Trim case

The application of the relevant conditions for the design case leads to the following loads and moments acting on the aircraft when it is in steady level. flight:

Zero-lift pitching moment. M_o	– 1 096 186 N · m
Tail load. $\mathcal{L}_T$	12 373 N
Wing–body lift, $\mathcal{L}_{WB}$	987 914 N

The summary of the vertical loads, which are in balance, is:

Wing lift (987 914 x 0.94)	928 639 N
Body lift (987 914 x 0.06)	59 275 N
Tail lift	12 373 N
Vertical thrust component	– 4 572 N
Inertia force	– 995 715 N

The summary of the moments about the centre of gravity is:

Moment due to wing lift (928 639 x 0.15 x 4.7 x 0.9987	653 839 N . m
Moment due to body lift (59 275(19.5 – 6.975) x 0.9987)	741 454 N . m
Tail moment (– 12 373 x 19.5 x 0.9987)	– 240 960 N · m
Thrust moment (90 000 x (– 0.6))	– 54000 N . m
Zero-lift pitching moment	– 1 096 186 N · m

These moments summate to +4147 N m, or a discrepancy of some 0.3 per cent. This is acceptable and is probably due to a small error in the correlation of the zero-lift pitching moment. M_o, and the body lift distribution.

AD2.4.5 Steady rotary condition at 3g normal acceleration (constant pitch velocity)

This is an important datum condition. It is the basis for calculating the loads required to initiate the manoeuvre and is the initial condition for the return from a steady manoeuvre to level flight. For the latter reason it is necessary to use the exact value of the pitch forcing function, δ_n, which makes allowance for the effect of the tail load. see paragraph AD2.3(b).

The application of the analysis outlined in Chapter 5, Section 5.3.1.4 yields the following data:

(a)	Elevator angle required, η_{SS}	−0.0367 rad
(b)	Steady pitching velocity, $\dot{\theta}$	0.2596 rad/s
(c)	The increment in tail load due to the elevator deflt, $\Delta\mathcal{L}_{T\eta}$	−132741 N
(d)	The wing–body angle of attack? α_{WB}	0.0692 rad
(e)	Corresponding increment in wing–body lift, $\Delta\mathcal{L}_{WB}$	1 857 102 N
(f)	The increment of load on the tail due to the body angle and the pitch velocity, $\Delta\mathcal{L}_{T\alpha}$	276 062 N
	The total increment in tail load is therefore: (267 062 − 132 741)	34 321 N

Therefore the summary of the incremental vertical loads is:

Wing lift (1 857 102 x 0.94)	1 745 676 N
Body lift (1 857 102 x 0.06)	111 416 N
Tail lift	134 321 N
Incremental inertia force = 2 x 995 715	1 991 430 N

These vertical loads are in balance within about 7 N and are clearly acceptahle.

The summary of the incremental moments about the centre of gravity is:

Moment due to wing lift (1 745 676 x 4.7 x 0.15)	1 230 702 N · m
Moment due to body lift (111 426(19.5 − 6.975))	1 395 611 N · m
Moment due to tail lift (134 321 x (−19.5))	− 2 619 260 N . m

There is a discrepancy in the moment balance of 7 034 N . m, which is some 0.27 per cent. This is of the same order as that found in the level flight trimmed case and is acceptable.

AD2.4.6 Pitching acceleration conditions

These are based on the semi-empirical method given in Chapter 5, Section 5.3.4.2 for a pilot-operated control system with no other limits. The relevant calculations lead to:

(a) Datum manoeuvring tail load, using the more exact expression, $\mathcal{L}_{T0}$ − 130 729 N (Note the approximate expression for δ_n gives $\mathcal{L}_{T0}$ as −136 162 N.)

(b) The total increment of tail load required to pitch towards the 3g manoeuvre, $\mathcal{L}_{T1}$ 82 177 *N*

(c) The corresponding total tail load increment to pitch out of a steady 3g manoeuvre, $\mathcal{L}_{T2}$ 123 051 N

(d) The maximum change in elevator angle, η_C −0.0545 rad

(e) The design elevator angle required to pitch from level flight to $3g$, η_1 −0.0371 rad

(f) The corresponding elevator angle required to pitch out of the 3g manoeuvre, η_2 +0.0131 rad

(g) Increment of elevator load to pitch nose-up to $3g$, $\Delta\mathcal{L}_{T1\eta}$ $-134\,312$ N (Note if this elevator load is applied as a step function, the instantaneous nose-up angular acceleration would be -0.606 rad/s^2).

(h) Increment of elevator load when pitching nose-down from $3g$, $\Delta\mathcal{L}_{T2\eta}$ $+47\,514\,N$ (Note if applied as a step function this would result in a nose-down pitching acceleration of 0.2145 rad/s^2. However, this is not meaningful as the reduction of wing–body lift as the motion proceeds results in a reduction of the implied nose-up moment and hence a greater nose-down pitching acceleration.)

AD2.4.7 Analysis of the condition when the aircraft pitches nose-up towards 3g from level flight

The conditions for this case are given in Section AD2.4.6. The basic loads derived using the method of Chapter 5, Section 5.3.4.2 can be added directly to the trim flight condition at $1g$ and the normal acceleration may be artificially adjusted to give vertical balance. Here, however, the analysis will be taken further to derive the condition when the total tail load is at its maximum value, as might be derived from a response calculation or simulation, see comments in Section **AD2.4.8.**

To initiate the manoeuvre from steady level flight the elevator is moved to cause a nose-up pitching acceleration. Section AD2.4.6 derives the following information:

Incremental design total tail load, $\mathcal{L}_{T1}$	$-82\,177$ N
Incremental elevator load at design condition, $\mathcal{L}_{T1\eta}$	$-134\,312$ N

From this it can be deduced that the tail load due to the change in body angle relative to the initial trimmed condition is:

$$\{-82\,177 - (-134\,312)\} = 52\,135\,\text{N}$$

This implies that the change in body angle; $\Delta\alpha_B$ is:

$$\Delta\alpha_B = 52\,135/\{2\rho V^2 S_T a_{1T}(1 - d\varepsilon/d\alpha)\}$$
$$= 0.0171\,\text{rad}(0.98°)$$

where the tail-plane lift curve slope, a_{1T} is 5.0/rad and the rate of change of downwash, $d\varepsilon/d\alpha$, is 0.36. Since the wing–body lift curve slope is 7.0/rad the corresponding change in wing–body lift is:

$$\Delta\mathcal{L}_{WB} = 0.5\rho V^2 S a_1 \Delta\alpha_B = 459\,174\,\text{N}$$

At the design condition the total increment in vertical load is:

$$459\,174 - 82\,177 = 376\,997\,\text{N}$$

This is equivalent to an increment in the normal acceleration of:

$$376\,997/(101\,500 \times 9.81)g = 0.3786g$$

The design tail load case is equivalent to an overall normal acceleration factor of 1.3786. The increment in pitching moment due to the additional wing–body and tail loads is:

$$\Delta\mathcal{L}_{WB}(h - H_o)c - \mathcal{L}_{T1}\ell'_T$$

where the aerodynamic centre position on the chord, H_o, is 0.1 and the tail arm, ℓ'_T is 19.5 m. Thus the incremental pitching moment is:

$$459\,174(0.4 - 0.1) \times 4.7 - 82\,177(-19.5) = 2\,249\,887\,\text{N}\cdot\text{m}$$

This corresponds to a nose-up angular acceleration of:

$$2\,249\,887/4\,319\,000 = 0.5209\,\text{rad/s}^2$$

(Note this value is, as would be expected, less than the equivalent instantaneous value of 0.606 rad/s^2 calculated previously, since it allows for the actual rate of application of the elevator and the response of the aircraft to it.)

Thus in the design condition the summary of the incremental loads, which are in balance, is:

Wing lift (459 174 x 0.94)	431 624 N
Body lift (459 174 x 0.06)	27 550 N
Tail lift	−82 177 N
Inertial force (0.37826 x 995 715)	−376 998 N

The summary of the incremental moments is:

Moment due to wing lift (431 634 x 0.15 x 4.7)	304 295 N . m
Moment due to body lift [27 550(19.5 – 6.975)]	345 063 N . m
Moment due to tail lift [−82 177(−19.5)]	1 602 452 N . m
Inertial relief moment (0.5209 × 4 319 000)	−2 249 887 N · m

There is a moment discrepancy of 1913 N · m, or some 0.085 per cent, which is acceptable.

AD2.4.8 Analysis of the condition when the aircraft pitches nose-down from a 3g manoeuvre

The conditions for this case are given in Section AD2.4.6. As with the loads occurring during the initiation of the manoeuvre from level flight the loads must be added directly to the initial condition, which in this case is the steady 3g rotary motion. It should be pointed out that the semi-empirical method of Chapter 5, Section 5.3.4.2 is based on this assumption and if the loads are used with the procedure of Section AD2.4.7 an unrealistically high value of nose-down pitching acceleration results. However, if the loads are determined by some other technique, for example a simulation, the method of Section AD2.4.7 can be applied here.

The increments in the tail load to initiate the return to level flight, as given in Section AD2.4.6, are:

$$\mathcal{L}_{T2} = +123\,051\ \text{N}$$
$$\mathcal{L}_{T2\eta} = +47\,514\ \text{N}$$

The method states that it should be assumed that the aircraft remains in the 3g manoeuvre condition. To achieve this the wing–body lift must be reduced by the same amount as the tail lift has increased, that is, by 123 051 N. The resulting total change in pitching moment about the centre of gravity is then:

$$\{(-123\,051 \times 0.3 \times 4.7) + (123\,051(-19.5))\} \qquad 2\,572\,996\ \text{N/m}$$

and the corresponding nose-down angular acceleration is:

$$\{-2\,572\,996/4\,319\,000\} \qquad -0.5957\ \text{rad/s}^2$$

The summary of the balanced incremental loads relative to the 3g condition is thus:

$\Delta\mathcal{L}_{WB}(-123\,051 \times 0.94)$	$-115\,668$ N
$\Delta\mathcal{L}_{B}(-123\,051 \times 0.06)$	-7383 N
$\Delta\mathcal{L}_{T}$	$+123\,051$ N

The corresponding moments are:

Due to wing lift $(-115\,668 \times 0.15 \times 4.7)$	$-81\,546$ N
Due to body lift $\{7383(19.5 - 6.975))$	$-92\,472$ N
Due to tail lift $(123\,051(-19.5))$	$-2\,399\,495$ N
Inertial relief moment $(0.595\,74 \times 4\,319\,000)$	$+2\,573\,001$ N . m

There is a discrepancy of -512 N . m, or 0.02 per cent, in the moment balance.

AD2.5 Shear force and bending moment calculations

AD2.5.1 Level flight trimmed case

The loads and moments are those calculated in Section AD2.4.4. The loads were calculated relative to the flight direction, that is, at an angle of $-2.91°$ to the body datum. It is convenient to evaluate shear forces and bending moments along the body datum, so the forces must be resolved to the component perpendicular to this datum.

(a) Component of $\mathcal{L}_W$: (928 639 x 0.9987) = 927 432 N acting at $0.25c$, or 18.795 m aft of the nose.

(b) Component of $\mathcal{L}_B$: (59 275 x 0.9987) = 59.198 N located at 6.975 m aft of the nose but distributed along the length:
Local load at nose = 59 198/13.325 = 4442.6 N
Local load at tail = −0.3167 x 4442.6 = −1407 N
Thus the load distribution = $-1407 + 150X$
where X is the distance forward of the tail, see Fig. AD2.1

(c) Component of $\mathcal{L}_T$: 12 373 x 0.9987 = 12 357 N acting at 39 m from nose.

(d) Inertia force component: −995 715 x 0.9987 = −994 421 N. Of this (−70 300 x 9.81) x 0.9987 = −688 746 N is due to wing inertia and is located, by definition, at 19.5 m aft of the nose. The remaining −305 675 N is due to the body inertia, distributed uniformly along its length as:

$$-305\,675/39 = -7837.8\ \text{N/m}$$

(e) The thrust component = −90 000 x 0.0508 = −4572 N assumed to act at the same location as the wing lift.

(f) The zero-lift pitching moment is 1 096 186 N . m and the thrust moment 54 000 N . m. both nose-down.

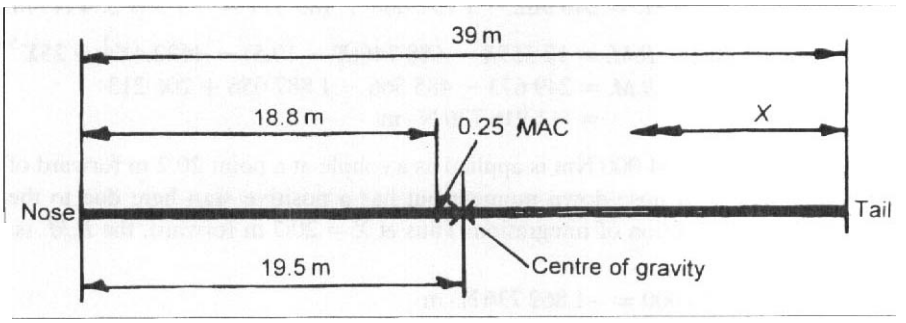

Fig. AD2.1 Notation used *for defining the shear force and bending moments*

Shear force distribution

The shear force (*S.F.*) is the integration of the load distribution. It is convenient to integrate from the tail forwards to the nose, any error indicated by a non-zero value at the nose should then be transferred hack to the centre of gravity or location of the wing lift.

$$S.F. = 12\,357 + \int_0^x (-7837.8 - 1407 + 150X)\mathrm{d}X$$

For $0 \leqslant X < 19.5$: $S.F. = 12\,357 - 9244.8X + 75X^2$
At $X = 0$: $S.F. = 12\,357$ N
At $X = 19.5$: $S.F. = 12357 - 180\,274 + 28\,519 = -139\,398$ N

For $19.5 < X < 20.2$: $S.F. = (12\,357 - 688\,746) - 9244.8X + 75X^2$
At $X = 19.5$: $S.F. = 828\,165$ N
At $X = 20.2$: $S.F. = -676\,389 - 186\,791 + 30\,618 = -832\,568$ N

For $20.205 < X \leq 39$: $S.F. = (-676\,389 + 927\,432 - 4572) - 9\,244.8X + 75X^2$
At $X = 20.2$: $S.F. = 94\,870$ N
At $X = 39$: $S.F. = 246471 - 360547 + 114075 = -1$ N

Moment distribution

The bending moment (*B.M.*) is the integration of the shear force distribution. Integrating from the tail forwards, as for the shear force:

$$\text{B.M.} = \int_0^x (12.357 - 9244.8X + 75X^2)\mathrm{d}X$$

For $0 \leqslant X < 19.5$: $\text{B.M.} = 12\,357\,X - 4622.4X^2 + 25X^3$
At $X = 0$: $\text{B.M.} = 0$
AT $X = 19.5$: $\text{B.M.} = 240\,962 - 1\,757\,668 + 185\,371 = -1\,331\,334$ N . m

For $19.5 < X < 20.2$: $B.M. = 12\,357X - 688\,746(X - 19.5) - 4622.4X^2 + 25X^3$
At $X = 20.2$: $\text{B.M.} = 249\,673 - 485\,566 - 1\,887\,056 + 206\,213$
$= -1\,916\,736$ N . m

The thrust moment of 54 000 Nm is applied as a couple at a point 20.2 m forward of the tail datum. This is a nose-down moment but has a positive sign here due to the effectively negative direction of integration. Thus at $X = 20.2$ m forward, the B.M. is:

$$-1\,916\,736 + 54\,000 = -1\,862\,736\,\mathrm{N \cdot m}$$

Also acting at station 20.2 is the vertical force due to the difference between the wing lift and the vertical component of the thrust:

$$927\,432 - 4572 = 922\,860\ \text{N}$$

The zero-lift pitching moment is also effectively positive and acts at the overall aerodynamic centre, which is at 18.09 m aft of the nose. Therefore:

For $20.2 < X < 20.91$: $B.M. = 12\,357X - 688\,746(X - 19.5) + 922\,860(X - 20.2) + 54\,000 - 4622.4X^2 + 25X^3$

At $X = 20.91$: $B.M. = 258\,385 - 971\,132 + 650\,616 + 54\,000 - 2021043 + 228\,560 = -1\,800\,614\ \text{N} \cdot \text{m}$

and at $X = 20.91$ forwards: $B.M. = -1\,800\,614 + 1\,096\,186 = -704\,428\ \text{N . m}$

For $20.91 < X < 39$: $B.M. = 12\,357X - 688\,746(X - 19.5) + 922\,860(X - 20.2) + 1\,150\,186 - 4622.4X + 25X^3$

At $X = 39$: $B.M. = 481\,923 - 13\,430\,547 + 17\,349\,768\ \text{N} + 1\,150\,186 - 7\,030\,670 + 1\,482\,975 = -979\ \text{N . m}$

The value at the nose should he zero. However, the error is small. It is some 0.052 per cent of the maximum bending moment and is acceptable.

AD2.5.2 3g steady manoeuvre condition

In this case the loads and moments are the incremental ones calculated in Section AD2.4.5. As in the trimmed flight condition covered in the previous section?allowance should be made for the inclination of the body axis. In this case the body angle is 3.96" relative to the trimmed condition, or overall:

$$3.96 - 2.91 = 1.05^\circ (0.019\ \text{rad})$$

This is sufficiently small to be neglected.

(a) $\Delta\mathcal{L}_W$: 1 745 676 N located at 18.795 m aft of the nose

(b) $\Delta\mathcal{L}_B$: 111 416 N distributed along the body:
Local load at nose = 111 426/13.325 = 8362.2 N
Local load at tail = −0.3167 × 8362.2 = −2648.3 N
The load distribution = $-2648.3 + 282.3X$

(c) $\Delta\mathcal{L}_T$: 134 321 N

(d) Inertial force: − 1991 430N
Of this − 1 379 286 N is due to the wing and is located at the mid-point of the body. The remaining −612 144 N is distributed uniformly along the body:

$$-612\,144/39 = -15\,696\ \text{N/m}$$

(e) There are no other contributions since the thrust is not changed relative to the trim condition and the pitching velocity is constant.

Shear force distribution

$$S.F. = 134\,321 + \int_0^X (-15\,696 - 2648 + 282.3X)\mathrm{d}X$$

For $0 \leqslant X < 19.5$: $S.F. = 134\,321 - 18\,344X + 141.15X^2$

At $X = 0$: $S.F. = 134\,321$ N

At X = 19.5: $S.F. = 134\,321 - 357\,708 + 53\,672 = -169\,715$ N

For $19.5 < X < 20.2$: $S.F. = 134\,321 - 1\,379\,286 - 18\,344X + 141.5X^2$

At $X = 19.5$ forwards: $S.F. = -169\,175 - 1379\,286 = -1549001$ N

At X = 20.2: $S\,F = -1\,244\,965 - 370\,641 + 57\,623 = 1\,557\,983$ N

For $20.2 < X \leqslant 39$: $S.F. = -1\,244\,965 + 1745\,676 - 18\,344X + 141.15X^2$

At X = 20.2 forwards: $S.F. = -1\,557\,983 + 1\,745\,676 = 187.693$ N

At X = 39: S.F. = 500 711 – 715 416 + 214 689 = −16 N

The small error is similar to that of the load calculation in Section AD2.4.5.

Moment distribution

Integrating the shear force from the tail, the bending moment is:

$$B.M. = \int_0^X (134321 - 18\,344X + 141.15X^2)\mathrm{d}X$$

For $0 \leqslant X \leqslant 19.5$: $B.M. = 134\,321X - 9172X^2 + 47.05X^3$

At $X = 0$: $B.M. = 0$

At X = 19.5: $B.M. = 2\,619\,260 - 3\,487\,653 + 348\,870 = -519\,523$ N · m

For $19.5 < X < 20.2$: $B.M. = 134\,321X - 1\,379\,286(X - 19.5) - 9172X^2 + 47.05X^3$

At X = 20.2: $B.M. = 2\,713\,956 - 972\,397 - 3\,744\,396 + 388\,093$
$= 1\,614\,744$ N · m

For $20.2 < X \leqslant 39$: $B.M. = 134\,321X - 1\,379\,286(X - 19.5) + 1\,745\,676$ (X – 20.2) $- 9172X^2 + 47.05X^3$

At $X = 39$: $B.M. = 5\,238\,519 - 26\,896\,077 + 32\,809\,980 - 13\,950\,612 + 2\,790\,959$
$= 7321$ N . m

The error of 7321 N . m is similar to the overall moment balance in Section AD2.4.5 and it is therefore acceptable.

Total shear forces and bending moments

To obtain the total shear force and bending moments in the steady rotary 3g manoeuvre it is necessary to add the incremental values derived above to those calculated for the level flight trim condition of Section AD2.4.5.

AD2.5.3 Nose-up initiation of 3g manoeuvre

The loads and moments for the condition are derived in Section **AD2.4.7**. The change in body angle relative to the trimmed condition was found to be 0.98°. That is the actual total body angle is:

$$0.98 - 2.91 = -1.93°(0.0337\ \text{rad})$$

This is sufficiently small to be neglected.

(a) $\Delta\mathcal{L}_W$: 431 624 N, located at 18.795 m aft of the nose.

(b) $\Delta\mathcal{L}_B$: 27 550 N, distributed along the body:

Local load at nose = 27 550/13.325 = 2067.5 N

Local load at tail = 0.3167 × 20 675 = −654.8 N

The distribution = $-654.8 + 69.8X$

(c) $\Delta\mathcal{L}_T$: − 82 177 N

(d) Inertial relief due to vertical acceleration: − 376 998 N

Of this −261 113 N is due to wing effects and is located at the mid-point of the body. The other −115 885 N is distributed uniformly along the body:

$$-115\,885/39 = -2971.4\ \text{N/m}$$

(e) Inertial relief due to angular acceleration: 2 249 897 N · m

Of this the wing accounts for:

$$-244\,400 \times 2\,249\,897/4\,319\,000 = -127\,315\ \text{N} \cdot \text{m}$$

assumed to act at the centre of gravity.

The uniform distribution of mass along the iuselage accounts for:

$$-3\,954\,600 \times 2\,249\,897/4\,319\,000 = -2\,060\,070\ \text{N} \cdot \text{m}$$

This varies linearly along the fuselage length. The local force at the nose is:

$$-800 \times 19.5 \times 0.52093 = -8126.5\ \text{N}$$

Thus, using the tail as the rcfcrence point, the distribution is:

$$8126.5 - 416.74X$$

The rest is due to the vertical location of individual items:

$$120\,000 \times 2\,249\,897/4\,319\,000 = 62\,512\ \text{N} \cdot \text{m}$$

made up of:

(i) −52 094 N . m due to tail, assumed to act as a couple at rear of body;

(ii) −7814 N . m due to main landing gear, assurncd to act at body mid-point;

(iii) − 2604 N . m due to nose landing gear. assumed to act at body nose.

Thus the total inertial relief moment acting about the centre of gravity is:

$$-127\,315 - 7814 = -135\,129\ \text{N} \cdot \text{m}$$

(f) There are no other changes relative to the initial, trimmed condition

Shear force distribution

$$S.F. = -82\,177 + \int_0^x (-2971.4 - 654.8 + 69.8X + 8126.5 - 416.74X)dX$$

For $0 \leqslant X < 19.5$: $S.F. = -82\,177 + 4500.3X - 173.47X^2$

At $X = 0$: $S.F. = -82\,177$ N

At $X = 19.5$: $S.F. = -82\,177 + 87\,756 - 65\,962 = -60\,383$ N

For $19.5 < X < 20.2$: $S.F. = -82\,177 - 261\,113 + 4500.3X - 173.47X^2$

At $X = 19.5$ forwards: $S.F. = -60\,383 - 261\,113 = 321\,416$ N

At $X = 20.2$: $S.F. = -343\,290 + 90\,929 - 70\,818 = -323\,179$ N

For $20.2 < X \leq 39$: $S.F. = -343\,290 = 431\,624 + 4500.3X - 173.47X^2$

At $X = 20.2$ forwards: $S.F. = 431\,624 - 323\,179 = 108\,445$ N

At $X = 39$: $S.F. = 88\,334 + 175\,512 - 263\,848 = -112$ N

This discrepancy is 0.035 per cent of the maximum shear force and is acceptable

Moment distribution

The bending moment distribution is determined by integrating the shear force and adding in the couples at the appropriate locations (nose-down couples are positive, see above).

$$B.M. = 52904 \int_0^x (-82\,177 + 4500.3X - 173.47X^2)dX$$

For $0 \leqslant X < 19.5$: $B.M. = 52\,094 - 82\,177X + 2250.15X^2 - 57.82X^3$

At $X = 0$: $B.M. = 52\,094$ N · m

At $X = 19.5$: $B.M. = 52\,094 - 1\,602\,451 + 855\,620 - 428\,728$
$= -1\,123\,465$ N · m

At $X = 19.5$, forward: $B.M. = -1\,123\,465 + 135\,129 = -988\,336$ N . m

For $19.5 < X < 20.2$: $B.M. = 187\,223 - 82\,117X - 261\,113(X - 19.5)$
$+ 2\,250.15X^2 - 57.82X^3$

At X = 20.2: $B.M. = 187\,223 - 1\,660\,386 - 184\,065 + 918\,606 - 476\,930 = -121\,552\ \text{N} \cdot \text{m}$

For $20.2 < X < 39$: $B.M. = 187\,223 - 82\,177X - 261\,113(X - 19.5) + 431\,624(X - 20.2) + 2\,250.15X^2 - 57.82X^3$

At X = 39: $B.M. = 187\,223 - 3\,204\,903 - 5\,091\,704 + 8\,112\,373 + 3\,422\,478 - 3\,429\,825 = -4358\ \text{N} \cdot \text{m}$

There should be a value of +2604 N . m here because of the vertical location of the nose-wheel. Thus the error is:

$$-4358 - 2604 = -6963\ \text{N} \cdot \text{m}$$

This is some 0.57 per cent of the maximum bending moment and is acceptable. It might have been less had the integration been undertaken from both extremities of the aircraft to the centre of gravity. Nearly one-third of the error was present in the initial calculation.

Total shear forces and bending moments

The total shear forces and bending moments for this case are ohtained by combining the above values with those for the level flight trimmed case of Section AD2.5.1.

AD2.5.4 Nose-down pitch from 3g condition to level flight

The relevant loads and moments are calculated in Section AD2.4.8.The change of wing-body lift at the design condition is small and hence the body angle of attack is similar to that in the steady 3g manoeuvre and may he neglected in the balance calculations.

(a) $\Delta\mathcal{L}_W$: −115.668 N, located at 18.795 m aft of the nose.

(b) $\Delta\mathcal{L}_B$: −7383 N. located at 6.975 m aft of the nose and distributed along the body:

Local load at nose = −7383/13.325 = −554 N

Local load at tail = −0.3167 x −554 = 175 N

The load distribution = 175 − 18 75X

(c) $\Delta\mathcal{L}_T$: +123 051 N

(d) Inertial relief due to vertical acceleration. This has no effect here, since there is no change in the normal acceleration by definition.

(e) Inertial relief due to angular acceleration: +2 573 001 N · m

Of this the wing accounts for:

$$244\,400 \times 2\,573\,001/4\,319\,000 = 145\,599\ \text{N} \cdot \text{m}$$

acting at the centre of gravity

The uniform mass distribution along the body accounts for:

$$3\,954\,600 \times 2\,573\,001/4\,319\,000 = 2\,355\,913\ \text{N} \cdot \text{m}$$

This varies linearly along the fuselage. The local force at the nose is:

$$+800 \times 19.5 \times 0.595\,74 = +9293.5\ \text{N}$$

and using the tail reference the distribution is:

$$-9293.5 + 476.6X$$

The remainder is due to the vertical location of the individual items:

$$120000 \times 2\,573\,001/4\,319\,000 = 71\,489\ \text{N} \cdot \text{m}$$

This is made up of:

(i) 59 574 N . m due to the tail, assumed to act at the tail;
(ii) 8936 N . m due to the main landing gear, assumed to act at body mid-point;

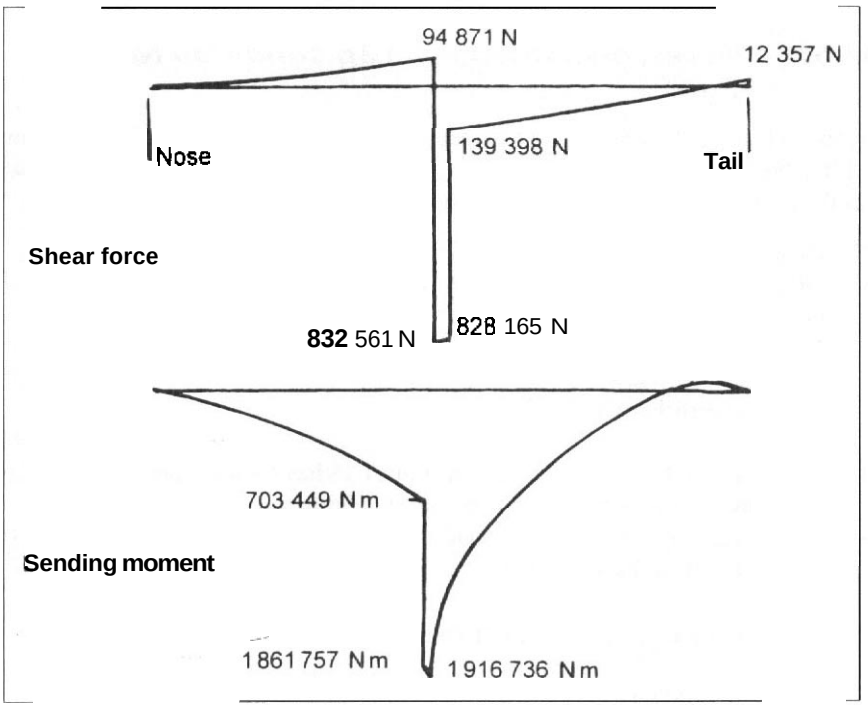

Fig. AD2.2 Shear force and bending moment distribution in trimmed level flight

(iii) 2979 N · m due to the nose landing gear, assumed to act at body nose.

Thus the total incremental relief moment acting about the centre of gravity is:

$$+145\,599 + 8936 = 154\,535\ \text{N} \cdot \text{m}$$

(f) There are no other changes.

Shear force distribution

$$S.F. = 123\,051 + \int_0^X (-9293.5 + 476.6X + 175 - 18.7X)\,dX$$

For $0 \leqslant X = 19.5$: $S.F. = 123\,051 - 9118.5X + 229X^2$

At $X = 0$: S.F. $= 123\,051$

$X = 19.5$: $S.F. = 123051 - 177811 + 87\,077 = 32\,317$ N

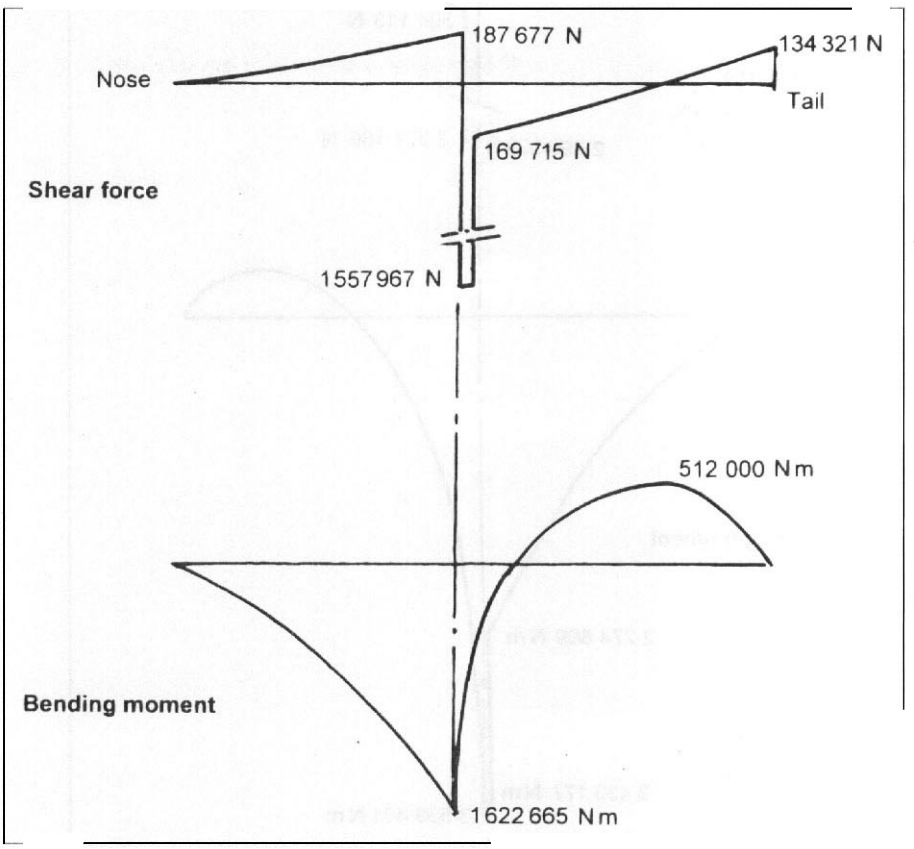

Fig. AD2.3 Incremental shear force and bending moment diagrams in steady 3g manoeuvre

In this case there is no additional force at the centre of gravity, so the above relationship for shear force also applies up to X = 20.2 m.

At X = 20.2: $S.F. = 123\,051 - 184\,239 + 93\,487 = 32\,299$ N

For $20.2 < X \leqslant 39$: $\text{S.F.} = 123051 - 115668 - 9118.5X + 229X^2$
$= 7\,383 - 9118.5X + 229X^2$

At X = 20.2 forwards: $S.F. = 32\,299 - 115\,668 = -83\,369$ N

At X = 39: $\text{S.F.} = 7383 - 355\,622 + 348\,309 = 70$ N

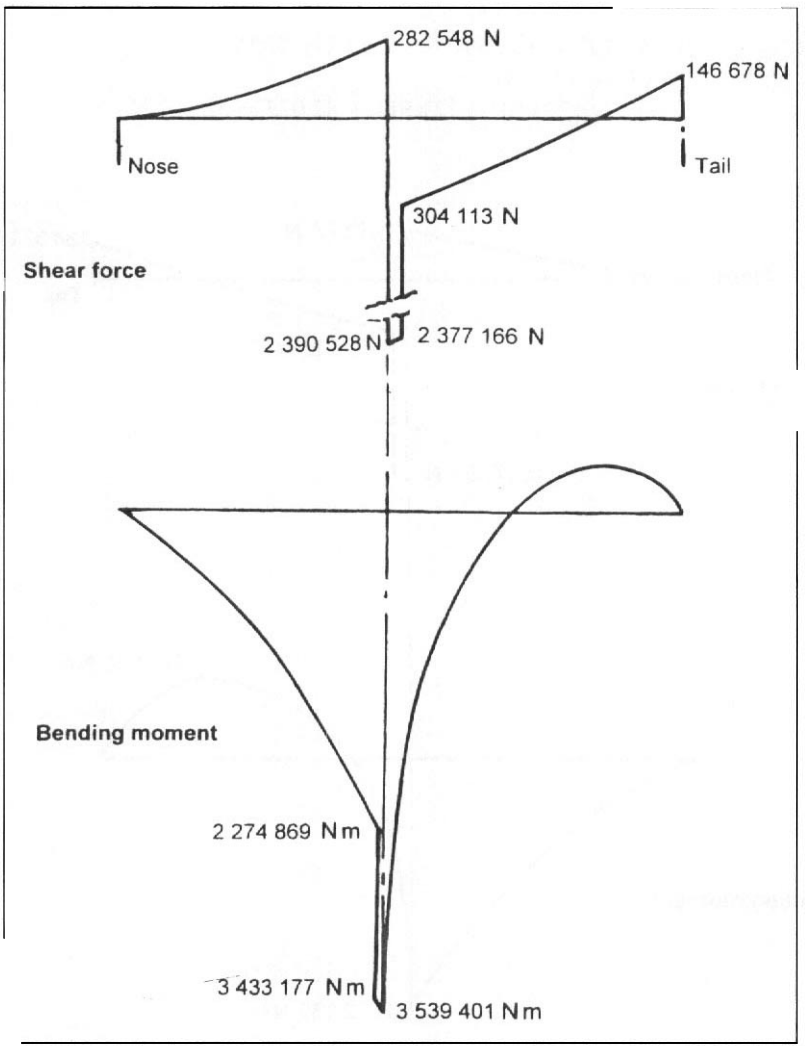

Fig. AD2.4 Total shear force and bending moment diagrams in steady 3g manoeuvre

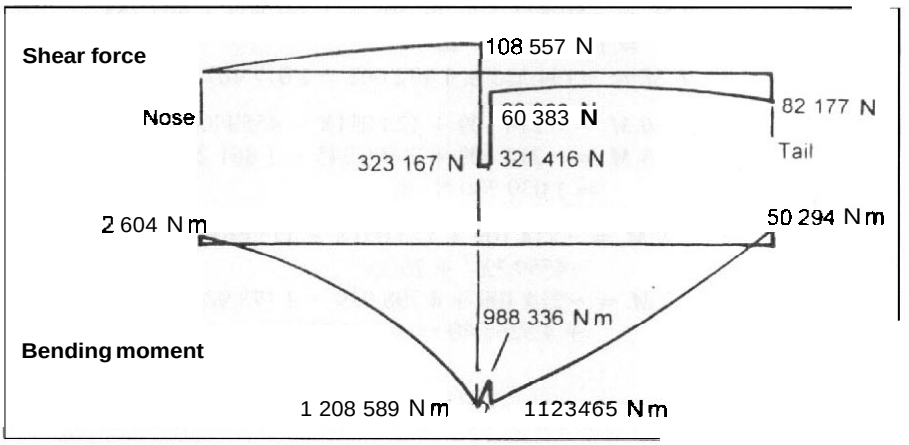

Fig. AD2.5 *Incremental* ***shear*** *force* ***and bending moments*** *pitching* ***nose-up*** *towards* ***3g***

The discrepancy, which is some 0.08 per cent of the maximum shear force, is due to small errors in the integration of the distributed forces.

Moment distribution

Integration of the shear fnrces and addition of the concentrated couples at the appropriate locations gives:

$$B.M. = -59\,574 + \int_0^X (123\,051 - 9118.5X + 229X^2)\,dX$$

For $0 \leqslant X \leqslant 19.5$ $B.M. = 59\,574 + 123\,051X - 4559.3X^2 + 76.3X^3$

At $X = 0$: $B.M. = -59\,574$ N . m

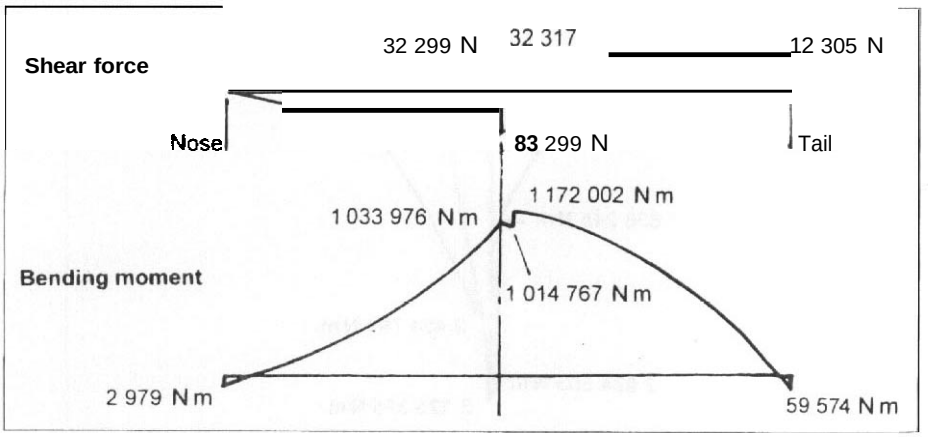

Fig. AD2.6 ***incremental shear force and bending moment diagrams*** *pitching* ***nose-down from*** *3g*

At X = 19.5 $B.M. = -59574 + 2\,399\,495 - 1\,733\,674 + 565\,755$
$= 1\,172\,002\ \text{N} \cdot \text{m}$

At X = 19.5 forward: $B.M. = -154\,535 + 1\,172\,002 = 1\,017\,467\ \text{N} \cdot \text{m}$

For $19.5 < X < 20.2$: $\boldsymbol{B.M.} = -214\,109 + 123\,051X - 4559.3X^2 + 76.3X^3$

At X = 20.2: $\boldsymbol{B.M.} = -214\,109 + 2\,486\,245 - 1\,861\,298 + 629.362$
$= 1\,039\,200\ \text{N} \cdot \text{m}$

For $20.2 < X \leqslant 39$: $\boldsymbol{B.M.} = -214\,109 + 123\,051X - 115\,668(X - 20.2)$
$-4559.3X^2 + 76.3X^3$

At $X = 39$: $\text{B.M.} = -214\,109 + 4\,798\,989 - 2\,173\,980 - 6\,934\,695$
$+ 4\,526\,040 = +2245\ \text{N} \cdot \text{m}$

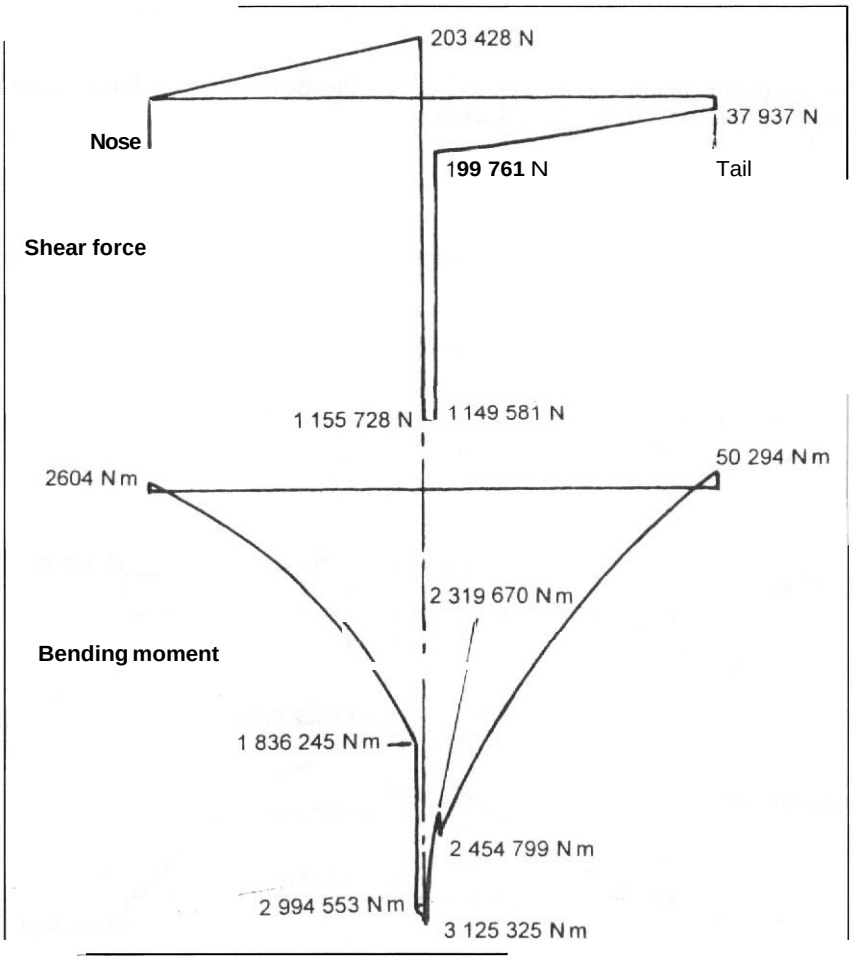

Fig. AD2.7 *Total shear force and bending moment diagrams pitching nose-up towards 3g*

At the nose the moment should have been $-2979\,\mathrm{N \cdot m}$ and so the discrepancy is:

$$2245 - (-2979) = 5224\,\mathrm{N \cdot m}$$

This is 0.5 per cent of the maximum bending moment, and as in the previous section is primarily due to numerical error compounded by integrating to the nose from the tail, rather than from either end of the centre of gravity.

Total shear forces and bending moments

In this case the total shear forces and bending moments are derived by the algebraic summation of three components:

(a) The trimmed level flight values of Section AD2.5.1.
(b) The incremental values in steady 3g flight from Section AD2.5.2
(c) The additional incremental values derived in this section.

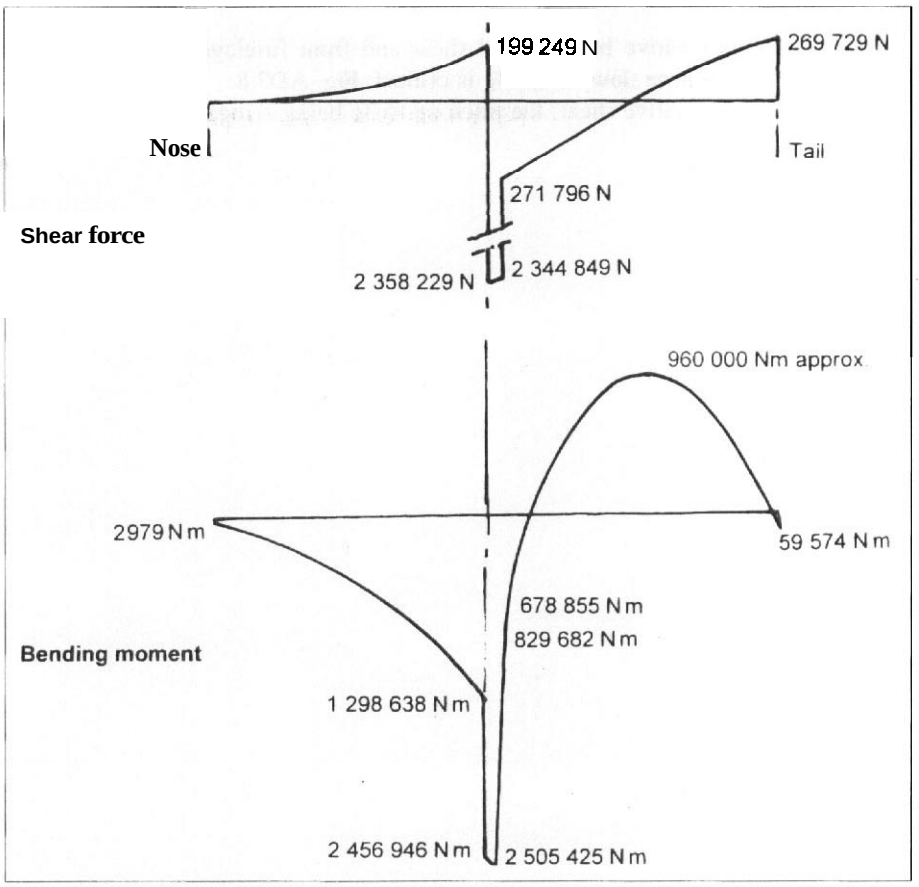

Fig. AD2.8 Total shear force and bending moment diagrams pitching nose-down from 3g

AD2.6. Shear force and bending moment diagrams

The derived shear force and bending moment diagrams are shown in Figs **AD2.2** to AD2.8. In all cases any discrepancy in shear force or bending moment at the nose has been transferred back to the point of wing lift application of the wing lift.

Fig. **AD2.2:** Trimmed level Hight.
Fig. **AD2.3:** Incremental conditions in steady 3*g* manoeuvre.
Fig. AD2.4: Total steady 3*g*, manoeuvre condition.
Fig. **AD2.5:** Incremental condition, pitching nose-up towards *3g*
Fig. **AD2.6:** Incremental condition pitching nose-down from *3g.*
Fig. **AD2.7:** Total condition pitching towards 3g.
Fig. **AD2.8:** Total condition pitching nose-down from 3*g*.

Inspection of the diagrams shows that the total loads in the *3g* steady rotation case. Fig. **AD2.4,** give the most severe conditions except for:

(a) Rear fuselage positive bending and shear and front fuselage negative shear, where the pitch nose down from *3g* is critical, Fig. AD2.8.
(b) Rear fuselage negative shear, the pitch up to *3g* being critical, Fig. **AD2.7.**

ADDENDUM AD3

Asymmetric flight – balance procedure

AD3.1 Introduction

The procedure outlined here is based on the equations developed in Chapter 4, Section 4.7. and Chapter 5, Section 5.5, concerned with the asymmetric flight dynamics and loading cases. The notation used here follows that of those chapters and reference should be made to them as necessary.

In comparison with the longitudinal balance of the aircraft the lateral balance is simpler in that there are no initial loads or moments. However, the way in which derivatives are used to express the forces consequent upon the initiation of a manoeuvre, or the encountering of a gust, does introduce some difficulty. If it is assumed that the prime purpose of the lateral balance is to derive fuselage shear forces and bending moments it is possible to introduce some simplification. In the first instance the wing forces and moments may be taken as acting at the centre of gravity and subsequently transferred to the wing–fuselage attachment points by undertaking a local calculation. This is a reasonable assumption since as far as the wing is concerned the effects are primarily in the chord-wise plane and the primary structural influence is at the attachments.

AD3.2 Assumptions

In undertaking the balance calculations it is helpful to make the following assumptions:

(a) Vertical stabilizer, that is the fin, forces act at a point a numerical distance ℓ_F aft of the centre of gravity.

(b) The fin inertial effects may be combined with the fuselage inertia distribution.

(c) Wing aerodynamic forces and moments act at. or about, the centre of gravity as discussed in Section AD3.1
(d) Wing inertial forces and moments also act at, or about, the centre of gravity.
(e) Fuselage air-loads are distributed to ensure that there is consistency with the aerodynamic moments on the fuselage, see Section AD3.3.

The assumptions imply that inertial forces and moments can be conveniently divided between the fuselage and the wing.

AD3.3 Consistency of derivatives

It is essential that there is consistency between the individual contributions of the fin, fuselage, and wing to the force and moment derivatives. Thus it is necessary to know the relative proportions resulting from the fin, fuselage, and wing contributions to all the aerodynamic derivatives:

(a) N_ζ and Y_ζ. These terms are both solely fin effects and it is only necessary to ensure that the definitions used are consistent with those given in Chapter 4, Section 4.7.2. It is to be noted that the rudder arm, taken to be the same as the fin arm from the centre of gravity, is negative for the conventional tail arrangement.
(b) N„ and Y_v. All three components contribute to these terms. The assumption made concerning wing effects in paragraph AD3.2(c) implies that there is no difficulty in this respect however:
  (i) $(Y_v)_F$ (due to fin) must equal $\{(N_v)_F \times b/_{\ell F}\}$, which it will do if the usual method of calculating derivatives is used; his wing span.
  (ii) $(Y_v)_B$ (due to fuselage) must he located at a point along the fuselage consistent with the value of $(N_v)_B$. That is:

$$(Y_v)_B = (N_v)_B \times b/\ell_o \qquad \text{(AD3.1)}$$

  where ℓ_o is the position of the centre of pressure of the fuselage side force forward of the centre of gravity. If there is no better information concerning the distribution of this force it is suggested that a triangular distribution should be assumed with the maximum value at the nose of the aircraft. The length of this distribution along the fuselage will then he $\{3 \times (\ell_n - \ell_o)\}$ aft of the nose, where ℓ_n is the distance from the nose to the centre of gravity. The maximum value of the force is then simply:

$$2(\bar{Y})_v/\{3(\ell_n - \ell_o)\} \qquad \text{(AD3.2)}$$

  where $(\bar{Y})_v$ is the actual fuselage force.
  (iii) N_r and Y_r. Generally N_r is small in comparison with N„ and the contributions of the fuselage and wing to Y_r are small in comparison with the fin contribution. Thus it is usually adequate to assume that wing and

fuselage contributions to N_r can he taken as couples about the centre of gravity. There will, however, bc a fin side force which gives rise to the fin contribution to N,, defined by:

$$(Y_r)_F = (N_r)_F \times b/\ell_F \qquad \text{(AD3.3)}$$

It is suggested that it is assumed that $(Y_r)_F$ is balanced by an appropriate modification to the lateral acceleration, and hence inertial force. This is best done during the detail calculations rather than initially to avoid the implication of modification to the basic equations.

AD3.4 Analysis procedure

(a) Specify the case conditions and calculate the applied fin/rudder force and moments.

(b) Calculate the sideslip angle, β, the rate of change of sideslip, $\dot{\beta}$, the yaw rate, r, the yaw acceleration, $\dot{r}$, and the lateral acceleration at the centre of gravity, ***o,*** from Chapter 5, Eqns (5.38) to (5.41), (5.45) to (5.47), (5.49) , (5.53) and (5.57) to (5.65) as relevant. These need to be converted to real time using Chapter 4, Eqn. (4.61b).

Use β and r to evaluate the overall values of the aerodynamic forces and moments.

(d) Use o and $\dot{r}$ to calculate the translational and rotational inertia effects.

(e) Check that there is an overall balance of forces and moments before proceeding.

(f) Allocate the aerodynamic forces and moments to the fin, fuselage, and wing. Evaluate the fin side force corresponding to $(N_r)_F$ and the fuselage air-load distribution corresponding to $(N_v)_B$ and $(Y_v)_B$ using, if necessary, Eqn. **(AD3.2).**

(g) Correct the lateral inertial force for the $(Y_r)_F$ effect and distribute both translational and rotational inertial effects between the wing and fuselage.

(h) Evaluate the total loads on the fin and at centre of gravity due to the wing effects. Use these in conjunction with the distribution of aerodynamic force, (Y_v) effect, and the inertial force along the fuselage to produce the shear force diagram.

(i) Evaluate the total couple acting at the centre of gravity due to the wing effects and use this in conjunction with the shear forces to produce the bending moment diagram.

It must he noted that:

(i) It may be useful to deduce the shear force and bending moment distributions for the fuselage air-load at stage (f) above and those for the fuselage inertial forces at stage (g) above.

(ii) It is usually best to integrate the shear force and bending moments from the extremities of the aircraft to the centre of gravity. This may not always be convenient, and it may be preferable to work forwards from the rear. In this case the sign of the wing couples at the centre of gravity must be changed and any final out of balance shear force or bending moment should he transferred back to the centre of gravity.

AD3.5 Example of a lateral balance

AD3.5.1 Introduction

This example of a lateral balance analysis is based on the same freight aircraft study as that used in Addendum AD2. As there, the data have been modified somewhat for simplicity to give an idealized mass distribution. The example analyses a manoeuvre initiated hy a step input to the rudder. Shear forces and bending moments are derived for:

Initiation condition
Sideslip equilibrium condition
Sideslip over-swing condition

AD3.5.2 Basic aircraft data

(a) Mass, m 101 500 kg
Mass of the fuselage items, of 31 200 kg, is assumed lo be uniformly distributed at 800 kg/m over the 39 m fuselage length. Thus the overall centre of gravity is at the mid-point of the length.

(b) Yaw moment of inertia, I_z, is 7 978 000 kg m^2 giving an overall radius of gyration. k_z, of 8.866 m. The individual contributions are:
Wing items 4 023 000 kg m^2
Fuselage items 3 955 000 kg m^2

(c) Wing span, b 46.1 m Wing area, S 193.3 m^2
Fin area, S_F 33 m^2 Fin (rudder) arm, l_F 19 m

(d) Fin lift curve slope due to rudder deflection, α_{2F} 1.9/rad
Derivatives:

(i) Side force due to sideslip Y_v:

Wing items	−0.305
Fuselage items	−0.33
Fin	−0.375*
Total	**−1.01**

(ii) Yawing moment due to sideslip. N_v:

Wing item	−0.012
Fuselage items	−0.080

Fin	+0.155*
Total	**+0.063**

(iii) Yawing moment due to rate of yaw, N_r:

Wing items	$-(0.003 + 0.004C_L^2)$
Fuselage items	0 . 0 0 6
Fin	−0.051
Total	$-(0.06 + 0.004C_L^2)$

(iv) Y_r and all the rolling derivatives are assumed to be negligible for the purpose of the analysis.

'In order to achieve moment balance it is essential that the fin contributions to Y_v and N_v are consistent. That is $(Y_v)_F = \{(N_v)_F \times b/l_F\}$.

AD3.5.3 Design case

Mass 101 500 kg — Speed, V_A, 180 m/s (TAS)
Altitude. — 6 km where the air density. ρ, is 0.66 kg/m^3

Aft centre of gravity, at the mid-point of the fuselage length.
Step rudder input of 0.1 rad (5.73")

AD3.5.4 Relevant data

Application of the aircraft data and the design case results in the following information:

Lateral relative density, μ_2	34.52
Non-dimensional time constant, τ	0.1131
Fin volume coefficient. $\bar{V}_v$	0.0704
Flight case lift coefficient, C_L	0.48
Rudder force derivative, Y_ζ	0.3244
Rudder moment derivative. N_ζ	−0.1338
Yawing moment due to yawing derivative, N_r	−0.061
Parameter, $\{b/k_z\}^2$	27.04
Non-dimensional damping coefficient, R_2	1.330
Non-dimensional damped natural frequency, J_2	7.662
Rudder forcing function, F_ζ	$125.4\zeta + 0.3321$
Lateral force due to rudder deflection, $\mathcal{L}_{Fo}$	67 040 N
Yawing moment due to rudder deflection, N_{Fo}	− 1273 760 N · m

AD3.5.5 Basic equations and datum sideslip values

The equations of motion. Eqns (5.38), yield the following expressions when the case data are used:

From Eqn. (5.38a):

$$\hat{\beta} + 1.01\beta + \hat{r} = 0.032\,44 \qquad \text{(AD3.4)}$$

Differentiating Eqn. (5.38a) with a constant rudder deflection:

$$\ddot{\hat{\beta}} + 1.01\dot{\hat{\beta}} + \dot{\hat{r}} = 0 \qquad \text{(AD3.5)}$$

From Eqn. (5.38b):

$$\dot{r} = -12.49 - 1.649\hat{r} + 58.81\beta \qquad \text{(AD3.6)}$$

Equations (5.45a) and (5.47) give the datum sideslip angles for the instantaneous rudder application condition as:

equilibrium angle. $\beta_E = 0.2073$ rad (11.88")
over-swing angle. $\beta_{MAX} = 0.3275$ rad (18.77°)
over-swing ratio $= 0.3275/0.2073 = 1.5797$

AD3.5.6 Accelerations and rates of motion

(a) ***Case 1.*** Initiation of manoeuvre, $\beta = r = 0$ initially.
- (i) from Eqn. (AD3.4), the sideslip rate, $\dot{\beta}$, is 0.0324 rad (non-dimensional) (in real time $\dot{\beta} = 0.003\,67$ rad/s);
- (ii) from Eqn. (AD3.6) the yawing acceleration. r, is −12.49 rad (non-dimensional) (in real time $\dot{r} = 0.1597$ rad/s^2);
- (iii) Equation (5.53b) for a point at the centre of gravity defines the lateral acceleration, o, as $\{(\dot{\beta} + r)V\}$ which in this case is, since r = 0 initially: $(0.00367 \times 180) = 0.6606$ m/s.

(b) ***Case 2.*** Equilibrium condition, $\ddot{\beta} = \dot{\beta} = 0$ and $\beta = 0.2073$ rad.
- (i) from Eqn. (AD3.4) the yaw rate. 7, is −0.1770 rad (non-dimensional) (in real time $r = -0.020$ rad/s);
- (ii) From Eqn. (5.53b) the lateral acceleration at the centre of gravity. o, is, as $\dot{\beta}$ is zero: $(r \times 180) = -3.6$ m/s.

(c) *Case* ***3.*** Over-swing condition, $\dot{\beta} = 0$ and $\beta = 0.3275$ rad.
- (i) from Eqn. (AD3.4) the yaw rale, $\hat{r}$, is −0.2983 rad (nun-dimensional) (in real time $r = -0.0337$ rad/s);
- (ii) from Eqn. (AD3.6) the yawing acceleration, $\dot{\hat{r}}$, is 7.26 rad (non-dimensional) (in real time $\dot{r} = 0.0930$ rad/s^2);
- (iii) from Eqn. (AD3.5) the sideslip acceleration, $\ddot{\beta} = -\dot{r}$ for this condition:
- (iv) from Eqn. (5.53b) the lateral acceleration at the centre of gravity, o, is, since $\dot{\beta}$ is zero: $(r \times 180) = -6.075$ m/s^2.

AD3.5.7 Balance, shear forces, and bending moments

AD3.5.7.1 Case 1 – Initiation of manoeuvre

Lateral acceleration $= 0.6605$ m/s^2
Angular acceleration $= -0.1597$ rad/s^2

Aerodynamic force due to rudder movement. $= \mathcal{L}_{Fo} = 67\,040$ N
Moment due to rudder increment, $N_{Fo} = -1\,273\,760$ N . m

(a) Lateral translation:
Inertial relief due to fuselage mass
$= -800 \times 0.6605 = -528.4$ N/m
Inertial relief due to wing mass
$= -(101\,500 - 31\,200) \times 0.6605 = -46433$ N
Check force balance:
Total inertia relief
$= -46\,433 + 528.4 \times 39 = -67\,040$ N
which balances applied load of 67 040 N.

(b) Rotational motion:
Inertial relief due to fuselage mass
$= -3955\,000 \times (-0.1597) = 631\,613$ N
distributed as:
$-800(X - 19.5)(-0.1597) = 127.76(X - 19.5)$ N/m
where X is measured forward from the rear end of the aircraft, see Fig. AD2.1.
Thus the inertial distribution varies linearly from -2491 N/m at the rear end to $+2491$ N/m at the nose.
The moment due to this distribution about the centre of gravity is:
$= 2\int_0^{19.5} 127.76(X - 19.5)(X - 19.5)dX$
$= 631\,550$ N · m
Moment at centre of gravity due to the wing inertia relief:
$= -4\,023\,000 \times (-0.1597) = 642\,473$ N . m
Check moment balance:
Total inertia relief
$= 631\,550 + 642\,473 = 1\,274\,023$ N · m
which is within 0.02 per cent of the applied moment of $-1\,273\,760$ N . m.

(c) Total inertial distribution
$= -528.4 + 127.76(X - 19.5)$
Integrating, the shear force due to the inertial distribution
$= -528.4X + 127.76(X^2/2 - 19.5X)$
$= -3019.7X + 63.88X^2$
Integrating again the bending moment due to the inertial distribution
$= -3019.7X^2/2 + 63.88X^3/3$
$= -1509.9X^2 + 21.293\sim'$.

(d) Total shear force diagram. The total shear force diagram is obtained by superimposing the concentrated forces due to the rudder deflection at station, X = 0.5 m, and the wing inertial relief at station, X = 19.5, as shown in Fig. AD3.1.

(e) Total bending moment diagram, see Fig. AD3.1. The overall bending moment diagram is obtained by superimposing upon the fuselage inertial moment:
(i) the wing inertial relief moment of 642 473 N · m assumed to act as a couple at the centre of gravity, X = 19.5;

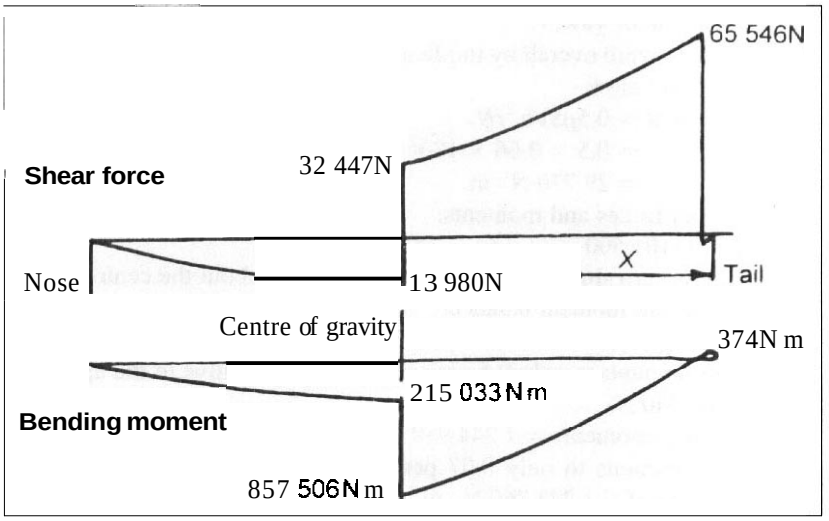

Fig. AD3.1 Shear force and bending moment diagrams at start of manoeuvre

(ii) the bending moment due to the fin force, which is $67\,040(X - 0.5)$ N · m for $X \geqslant 0.5$;

(iii) The bending moment due to the wing translational inertial relief, which is $46\,433(X - 19.5)$ N . m for $X \geqslant 19.5$.

AD3.5.7.2 **Case 2** – Equilibrium condition

In this case there is no angular acceleration and hence no direct rotational relief forces or moments. However, although $\dot{\beta}$ is zero, r is not and hence there are translational relief forces and moments resulting from the implied lateral acceleration:

Lateral acceleration $= -3.6$ m/s^2
Sideslip angle, $\beta_E = 0.2073$ rad
Rate of yaw, $r = -0.02$ rad/s

(a) Aerodynamic forces and moments:

(i) due to rudder angle:

force = 67 040 N

moment = − 1 273 760 N . m

(ii) due to sideslip angle, that is side velocity, $v = \beta V$:

force $= 0.5\rho SV^2\beta Y_v$

$= 0.5 \times 0.66 \times 193.3 \times 180^2 \times 0.0273 \times (-1.01)$

$= -432324$ N

moment $= 0.5\rho SV^2 b\beta N_v$

$= 0.5 \times 0.06 \times 193.3 \times 180^2 \times 46.1 \times 0.2073 \times 0.063$

$= 1\,244\,919$ N · m

(iii) due to rate of yaw, r:

force is zero overall by implication of the assumption that Y_r is zero. hut see (e) below.

moment $= 0.5\rho SVb^2 rN_r$

$= 0.5 \times 0.66 \times 180^2 \times 193.3 \times 46.1^2 \times (-0.061)(-0.02)$

$= 29\,770$ N · m.

(b) Inertial relief forces and moments:

force $= -101\,500 \times (-3.6) = 365\,400$ N.

moment is zero since there is no overall rotation about the centre of gravity.

(c) Check force and moment balance:

(i) reacting forces $= -432\,724 + 365\,400 = -67\,324$ N

This amounts to only 0.4 per cent unbalance relative to the applied force of 67 040 N.

(ii) reacting moments $= 1\,244\,919 + 29\,770 = 1\,274\,689$ N . m

This amounts to only 0.07 per cent imbalance relative to the applied moment of $-1\,273\,760$ N . m.

(d) Allocation of aerodynamic forces and moments to fin, fuselage, and wing:

(i) Fin:

The fin carries +246 per cent of the N_v effect and 83.6 per cent of the N_r effect, that is a moment of:

$2.46 \times 1\,244\,919 + 0.836 \times 29\,770$

$= 3\,062\,500 + 24\,888 = 3\,087\,388$ N . m

This acts at a point 19 m aft of the centre of gravity, X = 0.5 m, and is equivalent to a force of:

$3\,087\,388/-19 = -162\,494$ N

However, the calculated force on the fin due to the reaction of the aerodynamic effect is due only to 37.3 per cent of Y_v, that is $-161\,184$ N. The difference of -1310 N results from the assumption that Y_r is zero as no force allocation was made. It is suggested that this discrepancy is balanced by increasing the inertial relief by this amount, see (e) below.

(ii) Fuselage:

The fuselage carries -127 per cent of the N_v effect and 9.8 per cent of the N_r effect, that is a moment of:

$-1.27 \times 1\,244\,919 + 0.098 \times 29\,770$

$= -1\,581\,047 + 2917 = -1\,578\,130$ N . m

The N_r effect is so small that it can be regarded as a couple about the mid-point of the fuselage. However, the N_v contribution must be distributed so as to give a side force corresponding to that of the fuselage effect due to Y_v. This latter is 32.7 per cent of the total Y_v term or $-141\,500$ N. That is the moment arm of the fuselage side force due to β has to be:

$-1\,581\,047/-141\,500 = +11.17$ m (relative to centre of gravity)

The simplest way of representing this distribution is a triangular shape with the peak at the nose of the aircraft, falling to zero at a point 5.5 m aft

of the centre of gravity, X = 14 m, see Eqn. (AD3.2). When this representation is used the load at the nose is $-11\,320$ N/m and the distribution is described by $-453Y$ where $Y = X - 14$. The corresponding shear force is then $-226.5Y^2$ and the bending moment $-75.5Y^3$.

(iii) Wing:

The moment on the wing, assumed to act about the centre of gravity, is 19 per cent of the N_v effect and 6.6 per cent of the N, effect. That is:

$$-0.19 \times 1\,244\,919 + 0.066 \times 29\,770$$
$$= -236\,535 + 1965 = -234\,570 \text{ N} \cdot \text{m}$$

Assuming that the N_r effect is a couple, the aerodynamic force on the wing, acting at the centre of gravity, is 30 per cent of the Y_r term, and has a value of $-129\,817$ N.

(e) Inertial force distribution:

The modified inertial force, which allows for the reaction of the Y_r effect on the fin side force is:

$$365\,400 + 1\,310 = 366\,710 \text{ N}$$

Of this 253 987N is due to wing items and 112723 N is due to fuselage items assumed to be uniformly distributed aver its length at 2890 N/m. The corresponding shear force is $2890X$ and bending moment is $1445X^2$.

(f) Total shear force diagram:

The net load on the fin ($X = 0.5$) from the rudder, sideslip. and Y, effect is:

$$67040 - 161\,184 - 1310 = -95\,454 \text{ N}$$

The net load on the wing comes from the sideslip and inertial effects and is:

$$-129\,817 + 253\,987 = +124\,170 \text{ N}$$

These discrete forces are superimposed upon the shear forces resulting the distributed fuselage Y_v and inertial effects. The resulting shear force diagram is shown in Fig. AD3.2. Integrating from rear to front using the above figures gives a shear force out of balance of about -140 N at the nose. some 0.14 per cent of the maximum value.

(g) Total bending moment diagram:

The bending moment is derived by integrating the shear force diagram and superimposing upon it the wing couple of $-234\,570$ N · m at the centre of gravity. It should be noted that since the integration will proceed from the rear towards the nose, because of the definition of X, then the sign of this couple has to be reversed and it becomes positive. As an alternative to direct integration of the shear forces, the moments may be calculated by superimposing upon the wing couple the individual moment contributions from:

(i) fin and wing discrete forces;
(ii) fuselage inertial and air load distributions.

Figure AD3.2 shows the final bending moment. When constructed by the latter process the moment out of balance at the nose is found to be about 2000 N . m, or 0.14 per cent of the maximum bending moment.

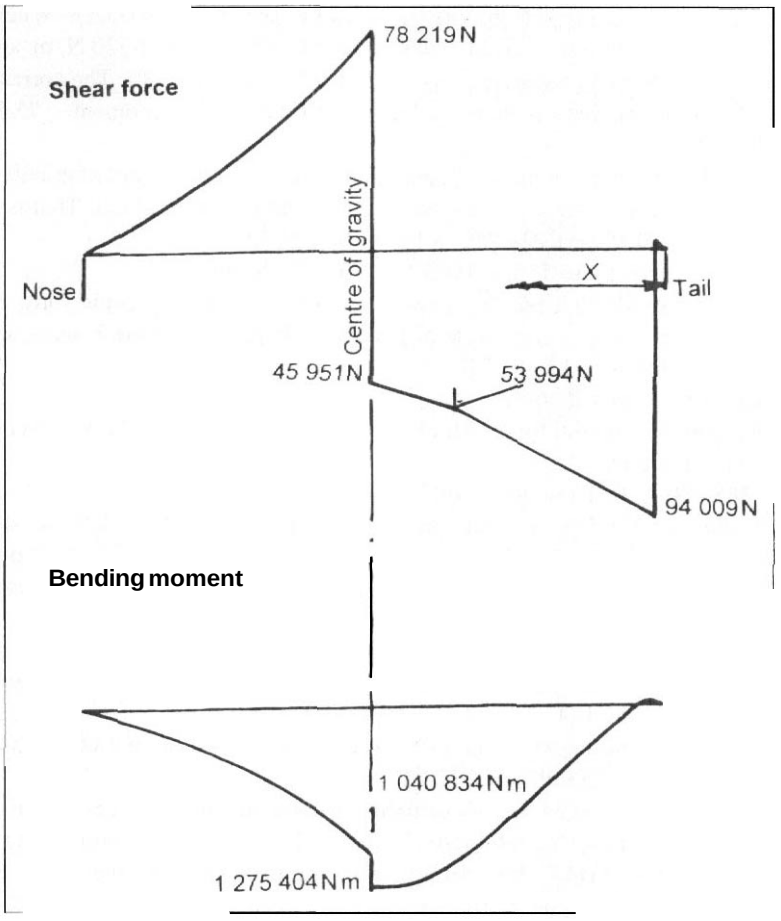

Fig. *AD3.2* ***Shear force and bending moment diagrams at the equilibrium sideslip condition***

AD3.5.7.3 **Case** *3* – **Over-swing condition**

In this case there are both lateral and rotational accelerations in spite of the fact that $\dot{\beta}$ is zero. Otherwise the forces and moments involved are as for Case 2. dealt with in the previous section, but of different magnitude due to the different values of β and r.

Sideslip angle, β_{MAX}, $(1.5797\beta_E)$	0.3275 rad
Rate of change of sideslip angle, $\dot{\beta}$	0
Rate of yaw, r, (1.685 that of Case 2)	-0.0337 rad/s
Yaw acceleration, $\dot{r}$	0.0926 rad/s^2
Lateral acceleration, ***o,***	-6.075 m/s^2

(a) *Aerodynamic forces* and *moments.*

(i) due to rudder angle:

force = 67 040 N

moment = – 1 273 760 N

(ii) due to sideslip angle. β:

The force and moment arc those of Case 2 multiplied by the overswing ratio, 1.5797, that is:

force $-432\,724 \times 1.5797 = -683\,574$ N

moment $1244919 \times 1.5797 = 1966599$ N · m

(iii) due to ratc of yaw, ***r:***

Here the multiplying factor is the ratio of the yaw rates, that is:

$-0.337/16.85-0.020 = 1.685$

from where the moment = 29 770 x 1.685 = 50 162 N . m

(b) *Inertial* ***relief of forces and moments.***

force = $-101\,500 \times (-6.075) =$ 616 613 N

moment = $-7\,978\,000 \times 0.0926 =$ $-738\,763$ N . m

(c) ***Check overall force*** *and moment* ***balance.***

(i) Reacting forces = $-683\,574 + 616\,613 =$ -66961 N

This amounts to about 0.12 per cent imbalance relative to the applied force of 67 040 N

(ii) Reacting moments = 1 996 599 + 50 162 – 738 763 = 1 277 998 N · m This is about 0.33 per cent imbalance relative to applied moment of – 1 273 760 N . m.

(d) *Allocation* ***of*** *aerodynamic forces* ***and moments*** to fin, fuselage, and wing. Use factored values from Case 2. see paragraph AD3.5.7.2(d).

(i) ***Fin***

N_v effect = 1.5797 x 3 062 500 = 4837831 N . m

N, effect = 1.685 x 24 888 = 41 936 N . m

Total = 4 879 767 N . m

This gives an effective fin force of $4\,879\,767/(-19) = -256\,830$ N

The fin force from the Y_v effect is:

$-1.5797 \times 161\,184 =$ – 254 622 N

Thus the additional allowance to be made on inertial relief to compensate for the Y_r effect is:

$-256\,830 + 254\,622 =$ – 2208 N

(ii) *Fuselage*

From Case 2:

N_v effect = $-1\,581\,047 \times 1.5797 =$ – 2 497 580 N · m

N_r effect = 2917 x 1.685 = 4915 N m

Total = $-2497\,580 + 4\,915 =$ – 2 492 665 N . m

The fuselage force is obtained by factoring the distribution of Case 2 hy 1.5797. That is:

$-453 \times 1.5797Y = -715.6Y$

where Y = (X – 14)

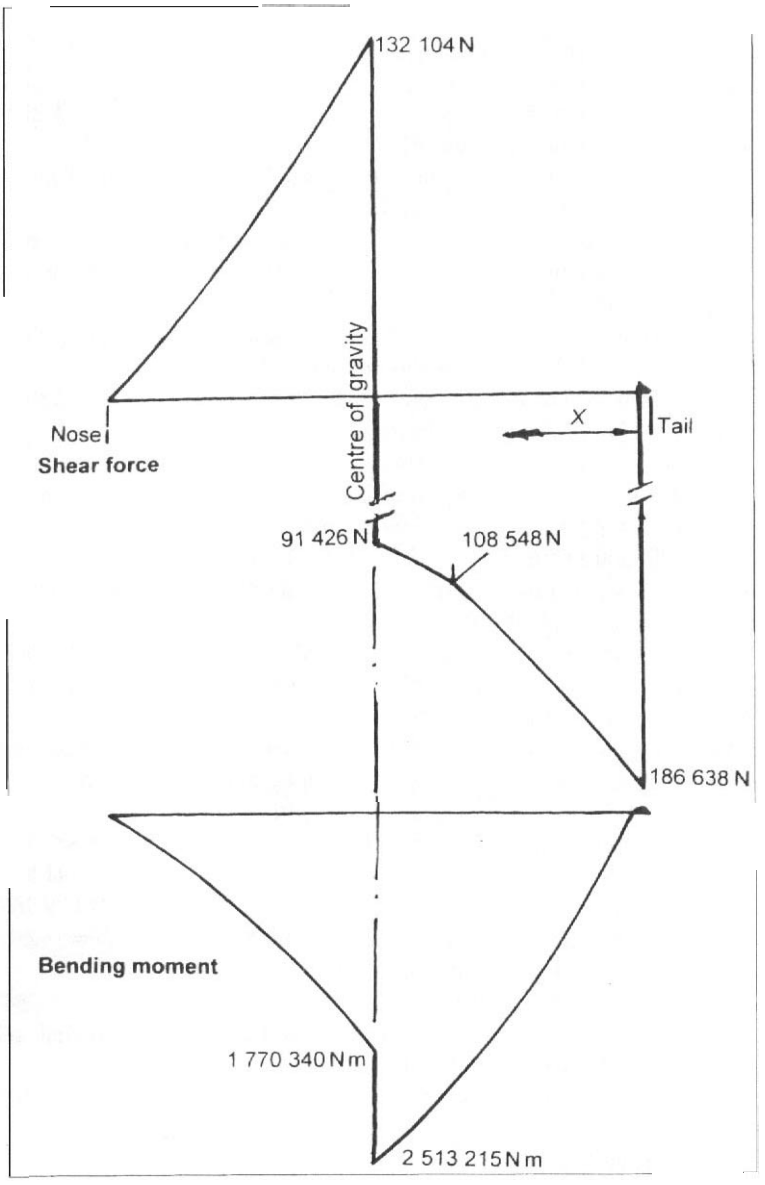

Fig. AD3.3 ***Shear force and bending*** *moment* ***diagrams at the over-swing*** *sideslip condition*

The corresponding shear force is $-357.8Y^2$ and the bending moment is $119.3Y^3$.

(iii) ***Wing***

Factoring the aerodynamic moments **on** the wing from Case 2 gives:

N_v effect = −236 535 x 1.5797 = − 373 654 N.m

N_r effect = 1965 x 1.685 = 3311 N · m

Total $= -373\,654 + 3\,311 =$ $-370\,343$ N · m
Y_r effect $= -129\,817 \times 1.5797 =$ $-205\,072$ N

(e) ***Inertial force** distribution.*

The modified translational force, accounting for reacting of the fin Y_r effect is:

$616\,613 + 2\,208 = 618\,821$ N

Of this 428 602 N is reacted on the wing and 190 219 N along the fuselage distributed uniformly as 4 877 N/m. This has to be combined with the distribution due to the inertial moment.

The total inertial moment is $-738\,763$ N . m, of which $-372\,530$ N . m is accounted for by the wing and $-366\,233$ N . m by the fuselage. Comparison with the corresponding distrihution from Case 1 shows that this can be represented by:

$-127.76 \times 366\,233(X - 19.5)/631\,613 = -74.08(X - 19.5)$

The overall fuselage inertial distribution is thus:

$4877 - 74.08\,(X - 19.5) = 6321.6 - 74.08X$

The corresponding shear force is $(6321.6X - 37.04X^2)$ and the bending moment is $(3160.9X^2 - 12.36X^3)$.

(f) ***Total shear force diagram.***

The net load on the fin $(X = 0.5)$ is given by:

$67\,040 - 256\,830 =$ $-189\,790$ N

The net load on the wing is:

$-205\,072 + 428\,602 =$ $223\,530$ N

As in Case 2, these forces are superimposed upon the shear forces derived from the aerodynamic and inertial distributions along the fuselage. The resulting shear force diagram is shown in Fig. AD3.3. The out of balance force at the nose is some 14 N or only 0.07 per cent of the maximum shear force.

(g) ***Total bending moment.***

The bending may bc derived directly from the shear force diagram. making allowance for the couple to be input at the wing which is:

$-370\,343 - 372\,530 = -742\,873$ N . m

which becomes positive when allowance is made for the direction of integration, as explained in Case 2. Alternatively the bending moment diagram may hc derived by superimposing the moments due to the distrihuted forces and the wing couple.

The resulting bending moment diagram is shown in Fig. AD3.3. The moment out of balance at the nose is about 5000 N · m or 0.2 per cent of the maximum bending moment.

ADDENDUM AD4

Landing gear – load analysis

AD4.1 Introduction

The purpose of this addendum is to outline the procedure used to derive the loading on a landing gear unit occurring as a consequence of the specified landing cases. In particular the roles of the shock absorber and tyre characteristics are explained and the opportunity is taken to cover the determination of the spin-up and spring-hack loads. The analysis is based on the material presented in Chapter 7. The load cases dealt with are those given in Table 7.1 and the supporting Section 7.4, interpreted by use of the energy absorption requirements stated in Section 7.3.

AD4.2 Design example

The aircraft selected for the example is a military combat type designed to meet the United Kingdom requirements contained in Def.Stan.00-970. The design take-off mass of the aircraft is 10 000 kg and the maximum landing mass is 9000 kg. There are two main landing gear units, each fitted with a single wheel/brake/tyre assembly. The layout of a main landing gear unit is illustrated in Fig. **AD4.1.**

The shock absorber load–deflection characteristics, as derived from a drop test, are given in Fig. AD4.2, the maximum deflection being 0.4 m.

The tyre specification is 32 in (0.814 m) diameter x 11.5 in (0.293 m) width with a 15 in (0.382 m) diameter rim. Inflation pressure is 150 lb/in^2 (10.2 bar). The maximum tyre deflection is 7.47 in (0.19 m) and the load–deflection characteristics may be

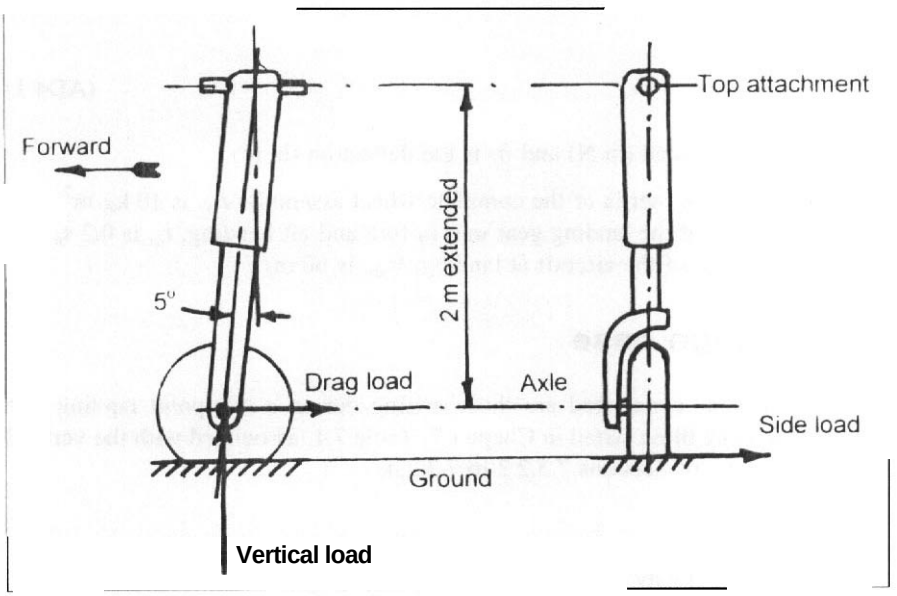

Fig. AD4.1 Layout of landing gear leg

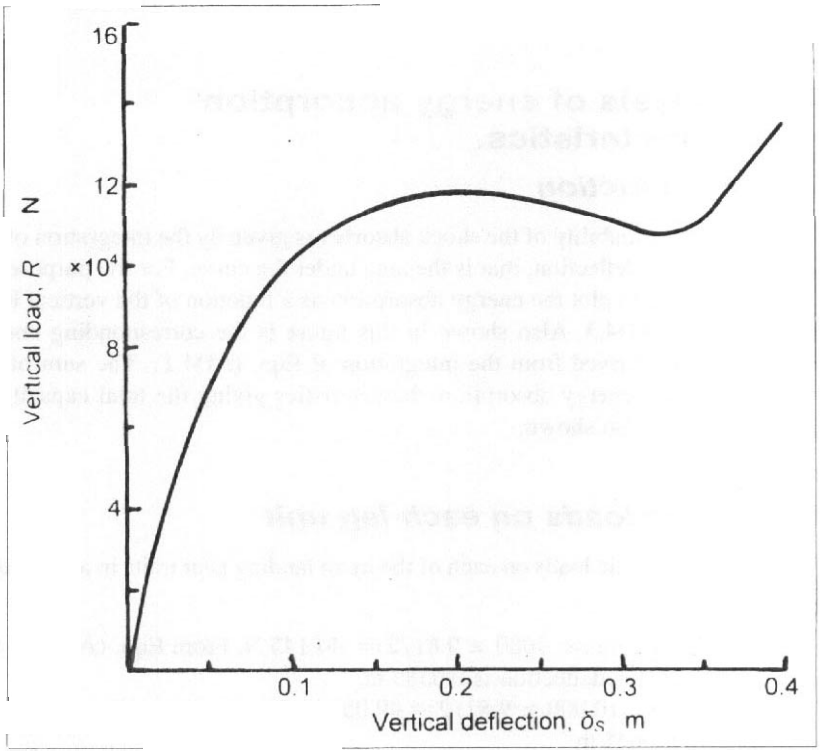

Fig. AD4.2 Shock absorber curve

represented by:

$$R = 10^6 \delta_T \qquad \text{(AD4.1)}$$

where R is the vertical load (in N) and δ_T is the deflection (in m).

The polar moment of inertia of the complete wheel assembly, I_W, is 10 kg m^2
The natural period of the landing gear unit in fore and aft bending, t_n, is 0.2 s
The approach speed of the aircraft at landing, V_{ap}, is 60 m/s

AD4.3 Design case

The design conditions considered are those arising during a two-point landing, the individual cases being those stated in Chapter 7, Table 7.1, associated with the vertical velocity requirements of Sections 7.3.2.2 to 7.3.2.4:
At design landing mass:

Limit vertical velocity = 3.66 m/s (12 ft/s)
Ultimate vertical velocity = 4.40 m/s (14.4 ft/s)

At take-off mass:

limit vertical velocity = 2.93 m/s (9.6 ft/s)

AD4.4 Analysis of energy absorption characteristics.

AD4.4.1 Introduction

The energy absorption capability of the shock absorber is given by the integration of the load as a function of the deflection, that is the area under the curve. For the purposes of analysis it is convenient to plot the energy absorption as a function of the vertical load. This is shown in Fig. AD4.3. Also shown in this figure is the corresponding energy absorption of the tyre, derived from the integration of **Eqn.** (AD4.1). The sum of the shack absorber and tyre energy absorption characteristics giving the total capacity of the landing gear unit is also shown.

AD4.4.2 Static loads on each leg unit

The equivalent vertical static loads on each of the main landing gear units in a two-point landing case are:

(a) At design landing mass: 9000 x 9.81/2 = 44 145 N. From Eqn. (AD4.1), the corresponding tyre deflection is 0.0586 m.
(b) At take-off mass: 10000 x 9.81/2 = 49 050 N. The corresponding static tyre deflection is 0.0645 m.

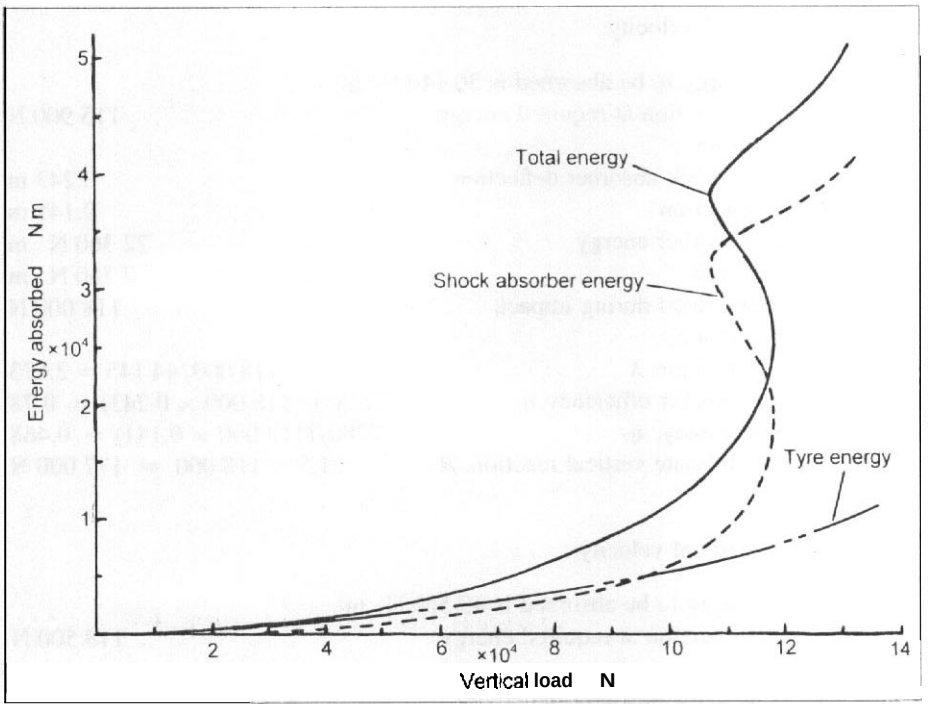

*Fig. **AD4.3** Energy absorbed as a function of the vertical load*

AD4.4.3 Energy requirements for each landing gear unit

The energies to be absorbed by each of the main units in the two-point case are:

(a) Design landing mass. limit vertical velocity: $9000 \times 3.66^2/4 = 30\,140$ N . m
(b) Design landing mass, ultimate vertical velocity: $9000 \times 4.40^2/4 = 43\,560$ N . m
(c) Take-off mass, limit vertical velocity: $10\,000 \times 2.93^2/4 = 21\,462$ N · m

Thus the take-off mass condition does not represent a critical design case

AD4.4.4 Vertical reactions at the design landing mass

Reference to Fig. AD4.3 enables. the vertical reactions corresponding to the required energy absorptions to be evaluated. Having determined the reaction in a given case the shock absorber deflection may he ascertained by reference to Fig. **AD4.2** and the tyre deflection from Eqn. (AD.I).

fa) Limit vertical velocity:

Vertical energy to be absorbed is 30 140 N . m	
Vertical reaction at required energy condition	115 900 N
Vertical shock absorber deflection	0.243 m
Tyre deflection	0.141 m
Shock absorber energy	22 360 N · m
Tyre energy	7 780 N · m
Maximum load during impact, Fig. AD4.2	118 000 N
Reaction factor, A	118 000/44 145 = 2.673
Shock absorber efficiency, η_S	22 360/(118 000 × 0.243) = 0.78
Tyre efficiency, η_T	7780/(118 000 × 0.141) = 0.468
Design ultimate vertical reaction, *R*	1.5 × 118 000 = 177 000 N

(b) Ultimate vertical velocity:

Vertical energy to be absorbed is 43 560 N . m	
Vertical reaction at required energy absorption	118 500 N
Vertical shock absorber deflection	0.365 m
Tyre deflection	0.144 m
Shock absorber energy	35 425 N · m
Tyre energy	8 135 N · m
Maximum load during impact, Fig. AD4.2	118500 N
Reaction factor, A	118 500/44.145 = 2.684
Shock absorber efficiency, η_S	35 425/(118 500 x 0.365) = 0.82
Tyre efficiency, η_T	8 135/(118 500 x 0.144) = 0.477
Design ultimate vertical reaction, *R*	1.0 × 118 500 = 118 500 N

Therefore the ultimate energy case does not give rise to a critical ultimate load condition, this being determined by the factored load in the limit vertical velocity case.

AD4.5 Derivation of design loads

AD4.5.1 Introduction

Chapter 7, Section 7.4 and Table 7.1, outline the loading cases to be associated with the maximum factored verticalreaction, *R*, derived in Section AD4.4.4. For convenience, with the exception of Section AD4.5.5, all the loads quoted below are ultimate values. The ultimate value of R is 177 000 N.

AD4.5.2 Landing with drag and side load – Chapter 7 Section 7.4.2.2, Case(1c)

From Table 7.1, the summary of the ultimate loads for this case is:

Vertical load	177 000 N
Drag (fore and aft) load	0.4 x 177 000 = 70 800 N
Side load, inwards	0.25 x 177 000 = 44 250 N
Side load, outwards	0.25 x 177 000 = 44 250 N

The shock absorber vertical closure is assumed to be $0.3\delta_S$ for the case, that is (0.3 x 0.243 = 0.0729 m). Thus the vertical distance between the axle, where the drag load is assumed to act. and the top gear attachment is (2 – 0.0729 = 1.927 m). The tyre deflection is 0.141 m and hence the vertical distance from the ground, at which point the side load in assumed to act, to the axle is (0.814/2 – 0.141 = 0.266 m), or 2.193 m vertically below the attachment. For the purposes of structural design it is necessary to resolve the vertical and drag forces parallel and normal to the leg, see Section AD4.5.4.

AD4.5.3 Side load – Chapter 7 Section 7.4.3, Case (2)

From Table 7.1, the summary of the ultimate loads for this case is:

Vertical load	0.5 × 177 000 = 88 500 N
Drag (fore and aft) load	0
Side load, inwards.	0.4 × 177 000 = 70 800 N
Side load, outwards	0.3 × 177 000 = 53 100 N

With the limit vertical load of (88 500/1.5) N the shock ahsorber deflection is 0.04 m. The shock absorber vertical closure is assumed to he $0.5\delta_S$ for the case. (0.5 x 0.04 = 0.02 m). Thus the vertical distance between the axle, where the drag load is applied, and the top gear attachment is (2 – 0.02 = 1.98 m). The tyre deflection in this case is 0.085 m and hence the vertical distance from the ground, where the side load is assumed to act, to the axle is (0.814/2 – 0.085 = 0.322 m), or 2.302 m vertically below the attachment. An example of the resolution of the forces parallel and normal to the landing gear leg is given in Section AD4.5.4.

AD4.5.4 High-drag landing and spring-back – Chapter 7 Section 7.4.4, Case (3)

Direct application of the information given in Table 7.1 leads to the following ultimate loads:

Vertical load	0.8 × 177 000 = 141 600 N
Drag (fore and aft) load	±0.64 × 177 000 = ± 113 280 N
Side load, inwards	0
Side load. outwards	0

The shock absorber vertical closure is assumed to he $0.15\delta_S$ for the case. At the limit load of 94 400 N, δ_S is 0.085 m (0.15 x 0.085 = 0.0128 m). Thus the vertical distance between the axle, the assumed point of action of the drag load, and the top gear attachment is (2 – 0.0128 = 1.987 m).

For the spin-up case the drag load is positive, that is aft, and hence referring to Fig. AD4.1 the ultimate load normal to the landing gear leg is:

$$113\,280 \cos 5^\circ - 141\,600 \sin 5^\circ = 100\,517 \text{ N}$$

Likewise the ultimate load parallel to the leg is:

$$141\,600 \cos 5^\circ + 113\,280 \sin 5^\circ = 150\,929 \text{ N}$$

For the spring-back condition the fore and aft load acts in the forward, or negative. direction and thus in this instance the ultimate load normal to the leg is:

$$-(113\,280 \cos 5^\circ + 141\,600 \sin 5^\circ) = -125\,183 \text{ N}$$

while the ultimate load parallel to the leg is:

$$141\,600 \cos 5^\circ - 113\,280 \sin 5^\circ = 131\,190 \text{ N}$$

AD4.5.5 High-drag landing and spring-back analysed by the method of MIL-A-8862

The United States military requirements for the determination of the loads on the landing gear present a more precise method for the analysis of the high-drag landing and spring-hack case, see Chapter 7, Section 7.4.4.2. It must be noted that in the MIL-Spec. this case also covers the landing with drag case, similar to Case (1c) of Table 7.1 and is therefore based on the full value of the vertical reaction, R. In order to compare the results with those of the previous section based on the application of Table 7.1 Case (3), it is necessary to use the same vertical load, that is $0.8R$. Thus an ultimate load of 141 600 N is the datum value, R_{MAX}. For this case the following parameters apply, all values being based on limit loads unless otherwise stated:

Reaction factor	(141 600/1.5)/44 145 = 2.138
Vertical shock absorber deflection at 94 400 N	0.086 m
Corresponding tyre deflection	0.117 m
Total effective deflection. δ_V	(0.5 x 0.086 + 0.117) = 0.16 m
Tyre rolling radius, r	(0.5 x 0.814 – 0.117) = 0.29 m

(a) ***Spin-up condition.***
The time after the initial contact with the ground for the vertical reaction to reach its maximum value, t_R, is given by Eqn. (7.10). Hence, using the appropriate values with a descent velocity of 3.66 m/s yields:

$$t_R = [3.66 - \{3.66^2 - 9.08 \times 0.16 \times 2.183\}^{1/2}]/(4.54 \times 2.138)$$
$$= 0.0464 \text{ s}$$

Equations (7.11) give the time, t_{SU}, for the spin-up to he complete. As t_R is low in this instance assume, initially, that $t_{SU} > t_R$ so that using the data from Section AD4.2 and Eqn. (7.11b):

$$t_{SU} = 60 \times 10/(0.55 \times 94\,400 \times 0.29^2) + 0.363 \times 0.0464 = 0.1542 \text{ s}$$

which confirms that $t_{SU} > t_R$.

The ratio of the spin-up time, t_{SU}, to the natural fore and bending period of the leg, t,,, is therefore (0.1542/0.2 = 0.771). and from Fig. 7.5 the spin-up factor, K_{SU}, is 1.51.

Equation (7.9b) gives the limit loads at time t_{SU}:

$$R_{SU} = 94\,400 \text{ N}$$
$$D_{SU} = 0.55 \times 94\,400 = 51\,920 \text{ N}$$

From Eqn. (7.12a) the limit load normal to the leg in the spin-up condition is:

$$1.51(51\,920 \cos 5^\circ - 94\,400 \sin 5^\circ) = 65\,686 \text{ N}$$

and the limit load parallel to the leg is:

$$(94\,400 \cos 5^\circ + 51\,920 \sin 5^\circ) = 98\,563 \text{ N}$$

Fsctnring these values hy 1.5 to ohtain the ultimate loads gives 98 529 and 147 845 N, respectively, which may be compared with the corresponding values from Section AD4.5.4 of 100 517 and 150 929 N.

(b) ***Spring-back condition.***
From Fig. 7.5 the spring-hack dynamic factor, K_{SB}, is 1.39, and thus from

Eqn. (7.14a) the limit load normal to the leg, forward, is:

$$-[1.39(51\,920\cos 5" - 94\,400\sin 5") + 94\,400(0.9$$
$$+ 94\,400/94\,400)\sin 5°]$$
$$= -76\,087\ \text{N}$$

and the limit load parallel to the leg. Eqn. (7.14b) is:

$$94\,400\cos 5° = 94\,041\ \text{N}$$

Applying the 1.5 factor gives the ultimate values of these loads as – 114 131 and 141 062 N, respectively. These may be compared with the equivalent values from Section AD4.5.4 which are – 125 183 and 131 196 N.

It can be seen that, with the exception of the load parallel to the leg in the spring-back case. the loads derived from the MIL-A-8862 method are lower than those obtained by application of Table 7.1 Case (3). The one instance of a higher load is due to the assumption, implied by the MIL-Spec., that the fore and aft load is zero at the moment the maximum reaction is developed during the spring-back process. This is a conservative, but reasonable, assumption and if applied to Table 7.1 Case (3) the corresponding load becomes identical.

AD4.5.6 One wheel landing – Chapter 7 Section 7.4.5, Case (4)

As far as the landing gear is concerned for this aircraft the loads in a one wheel landing are identical to those given by Case (1c), see Section AD4.5.2.

Index